Outer Continental Shelf Environmental Assessment Program

Final Reports of Principal Investigators

Volume 41 **June 1986**

U.S. DEPARTMENT OF COMMERCE
National Oceanic and Atmospheric Administration
National Ocean Service
Office of Oceanography and Marine Assessment
Ocean Assessments Division
Alaska Office

U.S. DEPARTMENT OF THE INTERIOR
Minerals Management Service
OCS Study, MMS 86-0055

"Outer Continental Shelf Environmental Assessment Program Final Reports of Principal Investigators" ("OCSEAP Final Reports") continues the series entitled "Environmental Assessment of the Alaskan Continental Shelf Final Reports of Principal Investigators."

It is suggested that sections of this publication be cited as follows:

Feely, R. A., G. J. Massoth, A. J. Paulson, and M. F. Lamb. 1980. Distribution and elemental composition of suspended matter in Alaskan coastal waters. U.S. Dep. Commer., NOAA, OSCEAP Final Rep. 41(1986):1-207.

Pitman, R. W. 1984. Tidal data from the Bering, Chukchi, and Beaufort Seas. U.S. Dep. Commer., NOAA, OSCEAP Final Rep. 41(1986):147-207.

Wilson, D. E., S. D. Pace, P. D. Carpenter, H. Teas, T. Goddard, P. Wilde, and P. Kinney. 1982. Nearshore coastal currents--Chukchi Sea, Summer 1981. U.S. Dep. Commer., NOAA, OSCEAP Final Rep. 41(1986):209-519.

Requests for receipt of OCSEAP Final Reports on a continuing basis should be addressed to:

NOAA-OMA-OAD
Alaska Office
701 C Street
P.O. Box 56
Anchorage, AK 99513

OUTER CONTINENTAL SHELF

ENVIRONMENTAL ASSESSMENT PROGRAM

FINAL REPORTS OF PRINCIPAL INVESTIGATORS

Volume 41

June 1986

U.S. DEPARTMENT OF COMMERCE
National Oceanic and Atmospheric Administration
National Ocean Service
Office of Oceanography and Marine Assessment
Ocean Assessments Division
Alaska Office

U.S. DEPARTMENT OF THE INTERIOR
Minerals Management Service
Alaska OCS Region
OCS Study, MMS 86-0055

Anchorage, Alaska

The facts, conclusions, and issues appearing in these reports are based on research results of the Outer Continental Shelf Environmental Assessment Program (OCSEAP), which is managed by the National Oceanic and Atmospheric Administration, U.S. Department of Commerce, and funded (wholly or in part) by the Minerals Management Service, U.S. Department of the Interior, through an Interagency Agreement.

Mention of a commercial company or product does not constitute endorsement by the National Oceanic and Atmospheric Administration. Use for publicity or advertising purposes of information from this publication concerning proprietary products or the tests of such products is not authorized.

Content of these reports has not been altered from that submitted by the Principal Investigators. In some instances, minor grammatical, spelling, and punctuation errors have been corrected to improve readability; some figures, charts, and tables have been enhanced to improve clarity in reproduction.

Outer Continental Shelf Environmental Assessment Program

Final Reports of Principal Investigators

VOLUME 41 JUNE 1986

CONTENTS

DISTRIBUTION AND ELEMENTAL COMPOSITION OF SUSPENDED MATTER IN ALASKAN COASTAL WATERS

by

Richard A. Feely, Gary J. Massoth,
Anthony J. Paulson, and Marilyn F. Lamb

Pacific Marine Environmental Laboratory
National Oceanographic and Atmospheric Administration

Final Report
Outer Continental Shelf Environmental Assessment Program
Research Unit 152

September 1980

DISCLAIMER

The NOAA Environmental Research Laboratories does not approve, recommend, or endorse any proprietary product or proprietary material mentioned in this publication. No reference shall be made to the NOAA Environmental Research Laboratories, or to this publication furnished by the NOAA Environmental Research Laboratories, in any advertising or sales promotion which would indicate or imply that the NOAA Environmental Research Laboratories approves, recommends, or endorses any proprietary product or proprietary material mentioned herein, or which has as its purpose an intent to cause directly or indirectly the advertised product to be used or purchased because of this NOAA Environmental Research Laboratories publication.

TABLE OF CONTENTS

LIST OF FIGURES

LIST OF FIGURES (Continued)

LIST OF FIGURES (Continued)

LIST OF FIGURES (Continued)

LIST OF TABLES

LIST OF TABLES (Continued)

1. SUMMARY

1.1 Northeast Gulf of Alaska

The distribution of suspended matter in the northeastern Gulf of Alaska is affected by a number of parameters which combine to form a unique distribution pattern. East of Kayak Island the surface particulate matter distributions are dominated by the discharge of sedimentary material from the coastal streams which drain the Bering, Guyot and Malaspina Glaciers. As this material is discharged into the Gulf, the westward flowing currents quickly deflect it to the west along the coast until it reaches Kayak Island where it is deflected to the southwest and is trapped by a clockwise gyre.

The major source of sedimentary material to the Gulf of Alaska is the Copper River. Once discharged into the Gulf, the suspended material from the Copper River is carried to the northwest along the coast until it reaches Hinchinbrook Island where a portion of the material passes into Prince William Sound and the remaining material is carried to the southwest along the coast of Montague Island.

In general, concentrations of suspended matter in the northeast Gulf of Alaska are high at the surface with an average concentration of approximately 1.0 mg/L. Beneath the surface, concentrations generally decrease with depth until the sea floor is approached. Close to the sea floor suspended matter concentrations increase sharply and the highest concentrations are found within 5 meters of the seawater-sediment interface. Studies of the temporal variability of suspended matter near the bottom show evidence for resuspension and redistribution of bottom sediments. These processes have occurred as a result of interactions between tidal and storm-induced bottom currents and the surficial sediments.

Studies of the chemical composition of the suspended matter show significant spatial and seasonal variations which have been correlated with seasonal variations in primary productivity, variations in the supply and transport of terrestrially derived suspended matter from the coastal rivers, and resuspension of bottom sediments.

1.2 Lower Cook Inlet

The seasonal distributions and elemental compositions of suspended particulate matter in lower Cook Inlet were studied and compared with current patterns and bottom sediment distributions. In general, the suspended matter distributions appear to follow the pattern of circulation in lower Cook Inlet and Shelikof Strait. The inflowing clear saline Gulf of Alaska water, which is enriched in biogenic particles of marine origin, flows northward along the eastern coast until it reaches the region near Cape Ninilchik where it mixes with the outflowing brackish water. The outflowing turbid water, which contains terrigenous particles derived primarily from the Susitna, Matanuska, and Knik Rivers, moves seaward along the western side of the inlet past Augustine Island and Cape Douglas into Shelikof Strait where it mixes with the oceanic water and is dispersed. Chemical analysis of the particulate matter reveals that: (1) fine-grained aluminosilicate minerals generally comprise about 80-95% of the suspended matter with biogenic material making up the rest; (2) Kachemak Bay is characterized by trace element enrichments in the organic phases of the particulate matter; (3) Kalgin Island region is characterized by trace element enrichments in the Fe-Mn oxyhydroxide phases; and (4) lower Cook Inlet and Shelikof Strait are linked by biogeochemical processes involving Mn and organic matter. These studies lead to the speculation that bioaccumulation of certain trace elements could occur in Kachemak Bay if it were to receive a sudden massive insult of these dissolved trace elements.

1.3 The Southeastern Bering Sea Shelf

The distribution of suspended matter at the surface in the southeastern Bering Sea Shelf is controlled by the discharge of sedimentary material from the coastal rivers and the semi-permanent counterclockwise currents which dominate the water circulation in Bristol Bay. A large plume of suspended matter extends to the southwest from Cape Newenham. Suspended matter originating from the Kvichak and Nushagak Rivers is carried to the west until it reaches Cape Newenham where it combines with a portion of the material discharged from the Kuskokwim River and is deflected to the southwest. Chemical analysis of suspended matter from the plume indicates that it is essentially of terrestrial origin.

A second plume extends to the southwest from Kuskokwim Bay. High concentrations of suspended matter extend as far west as Nunivak Island. This material is derived from the Kuskokwim River.

Along the Alaska Peninsula surface suspended matter concentrations decrease rapidly away from the coast. As the Pacific Ocean water passes through Unimak Pass and is deflected to the northeast along the coast of the Alaska Peninsula, suspended matter of marine origin is carried into Bristol Bay. When this water mixes with the highly turbid Shelf water, it is rapidly diluted producing the sharp gradients in the suspended matter distributions near the coast.

In the region north of Unimak Pass large suspended matter plumes appear to be the result of increased productivity during the summer months.

Below the surface, the particulate matter distributions follow the same distribution pattern as at the surface. However, suspended matter concentrations increase sharply near the bottom indicating that resuspension of bottom sediments is occurring.

Studies of the major and trace element composition of the suspended matter show significant spatial variations which are directly related to the supply of terrestrially derived suspended matter from coastal rivers and local variations in primary productivity.

1.4 Norton Sound

The distributions and elemental compositions of suspended particulate matter in Norton Sound were studied and compared with current patterns and sediment distributions. The suspended matter distributions appear to follow the general pattern of cyclonic circulation in the Sound. The inflowing water picks up terrigenous aluminosilicate material from the Yukon River and transports it to the north and northeast around the inside periphery of the Sound, with some material settling to the bottom and the remaining material being transported to the northwest through the Bering Strait into the Chukchi Sea. Chemical analysis of the suspended material from Norton Sound reveals that: (1) aluminosilicate material from the Yukon River comprises about 88-92% of the suspended matter, with biogenic matter making up the rest; (2) organic matter of terrestrial origin dominates the organic phase in the Yukon River Estuary; and (3) Mn and Zn are enriched in an oxyhydroxide phase of the surface and near-bottom suspended matter in Norton Sound.

2. INTRODUCTION

The development of petroleum and natural gas resources on the Alaskan outer continental shelf will undoubtedly result in an increased potential for crude oil contamination of its coastal waters. Of particular concern are the major accidents which cause massive oil spills, such as the ARGO MERCHANT oil spill on Fishing Rip near Nantucket (NOAA Special Report, 1977). However, chronic release of oil through minor spills and localized transfer operations may be more important over the long term.

Oil spilled onto the surface of the ocean is acted upon by several physical processes, including evaporation, solution, emulsification, and injection into the atmosphere (Kreider, 1971; McAuliffe, 1966, 1969, and Baier, 1970). With respect to the oceanic environment, only the solution and emulsification processes represent important mechanisms by which spilled oil becomes entrained in the water column, thus increasing its potential for impacting marine organisms.

Since crude oil is sparingly soluble in seawater, it tends to form emulsions when introduced into marine waters, especially under intense wave action. The emulsions have a high affinity for particles and tend to be adsorbed rapidly. Recent studies of oil spills in coastal waters containing high suspended loads have indicated rapid dispersal and removal of the oil by sorption onto particles along frontal zones (Forrester, 1971; Kolpack, 1971; and Klemas and Polis, 1977). These zones are regions where turbid brackish water contacts seawater. At the interface downwelling occurs in most cases, causing the inorganic material from the rivers and any associated contaminants to be carried down into the water column. Similarly, laboratory studies involving the interaction between Prudhoe Bay and Cook Inlet crude oils and river-derived inorganic suspended matter have indicated that significant amounts of oil may be accommodated by suspended material, and that the quantity of oil retained on the particles is dependent upon the isoelectric point of oil and sediment particles, particle size, temperature, and the concentration of oil relative to that of the suspended material (Feely et al., 1978). Since these processes play a major role in the dispersal and deposition of petroleum hydrocarbons, this report addresses the spatial and temporal variations of the distribution, chemical composition, and dispersal of suspended material in several continental shelf regions of Alaska.

3. CURRENT STATE OF KNOWLEDGE

3.1 Northeast Gulf of Alaska

Reimnitz (1966) studied the sedimentation history and lithology of sediments from the Copper River Delta. He estimated the particulate matter supply of the Copper River to be 107×10^6 tons/yr which mostly consists of fine-grained sands and silt.

Sharma et al. (1974) compared some surface particulate matter distributions taken during February 24-28, 1973, between Kenai Peninsula and Kayak Island with ERTS multispectral scanner images of the same region which were obtained on October 12, 1972, and August 14, 1973. The ERTS images show that the Copper River and Bering Glacier provide most of the sediment load to this region. The westward flowing current deflects a portion of the Copper River plume to the west. The suspended matter moves along the coast with some material entering Prince William Sound through the passages on either side of Hinchinbrook Island and the remaining material is carried along the southeast shore of Montague Island.

Carlson et al. (1975) used ERTS imagery to study the transport of suspended material in nearshore surface waters of the Gulf of Alaska. During the late summer and early fall months large quantities of fine-grained silt and clay-sized material from the Bering, Guyot and Malaspina Glaciers are discharged into the Gulf between Kayak Island and Yakutat Bay. This material is carried to the west by the Alaska current until it reaches Kayak Island where it is deflected to the south.

El Wardani (1960) studied the distribution of organic P in the Bering Sea, Aleutian trench and the Gulf of Alaska. He demonstrated that particulate organic P in the upper 200 meters of the water column bears an inverse relationship to inorganic P. Below 200 meters no detectable particulate organic P was found.

3.2 Lower Cook Inlet

Previous studies of suspended material in lower Cook Inlet have been limited to observations of LANDSAT satellite and aircraft photographs, augmented with sea-truth measurements in some places. These studies have provided useful information about near-surface suspended matter dispersal patterns, particularly in the Kalgin Island region where concentration gradients have been observed to be extremely high. Sharma, Wright, Burns, and Burbank (1974) used these techniques to study suspended matter distributions in Cook Inlet during late summer of 1972 and early spring of 1973. Suspended matter concentrations ranged from 100 mg/L near the Forelands to 1-2 mg/L near the entrance of the inlet. Large temporal variations were related to tidal variations in water circulation.

Gatto (1976) studied the dispersal of sediment plumes from coastal rivers as affected by tidal currents in the inlet. Turbid plumes from the Tuxedni, Drift, Big, and McArthur Rivers on the west side formed distinct surface layers, riding over and mixing with the saline water from the south. During flood tide, the plumes flowed northward along the coast. On ebb tide, the plumes migrated back to the south and west. Occasionally, the relict plumes were observed far offshore, which indicated that at least some plumes of sediment-laden water were capable of maintaining their identity for several tidal cycles.

Burbank (1977) used LANDSAT imagery to study suspended matter dispersal patterns in Kachemak Bay. Suspended material in Kachemak Bay is derived from the inorganic and biogenic materials residing in the inflowing saline Gulf of Alaska water, in situ production, and suspended material discharged from the Fox and other local rivers. Sediment plumes were observed along the northwest shore of inner Kachemak Bay. These plumes were diverted around Homer Spit and into outer Kachemak Bay by a counter-clockwise rotating gyre. In the outer bay, the plumes moved to the west and north under the influence of a second counterclockwise gyre.

3.3 Southeastern Bering Sea Shelf

There is very little published information about the distribution and composition of suspended particulate matter in the southeastern Bering Sea Shelf.

Sharma et al. (1974) compared some particulate matter distributions taken during June-July 1973 in the southern Bering Sea and Bristol Bay region with ERTS multi-spectral scanner images of the same area which were obtained on October 2, 1972. The surface contours of suspended load distributions indicate several regions of relatively turbid water which originate from a variety of sources. These turbid regions include:

(1) A region of turbid water which is north of the Aleutian Islands. This is probably due to the high level of primary productivity that is the result of the mixing of nutrient-rich deep water with the Alaskan Stream which flows into the Bering Sea from the south.

(2) A region of turbid water which extends south from Kuskokwim Bay and west from northern Bristol Bay. This plume probably represents sus-

pended sediments derived from the Kuskokwim River from the north and the Kvichak and Nushagak Rivers from the east.

(3) A region of slightly turbid water extending to the southwest from Bristol Bay which probably represents suspended matter derived from the Kvichak and Nushagak Rivers.

The ERTS imagery indicates that the Nushagak River is a major source for particulate matter in the Bristol Bay area. The suspended particles from Kvichak and Nushagak Rivers are carried to the west by the prevailing counter-clockwise current. Sharma et al. (1974) state that although the river plumes remain close to shore, offshore transport of material in suspension is probably brought about by tidal currents.

There is only a small amount of information about the chemical composition of the suspended matter in the southeastern Bering Shelf. Loder (1971) studied the distribution of particulate organic carbon (POC) north of Unimak Pass and found high POC concentrations (221-811 μgC/L) in the thermally stabilized upwelled water north of Unalaska Island. Lower POC concentrations were found north of Unimak Island and west of Akutan Pass which presumably were due to current mixing.

Tsunogai et al. (1974) studied the distribution and composition of particulate matter from six stations in the south central and southeastern Bering Sea and northern North Pacific Ocean. They found the highest concentrations of particulate matter occurred at 20 to 30 meters depth which appeared to be due to the high productivity and the slow decomposition of organic matter just below the surface. The organic portion of the suspended matter was about 67 percent for the samples from the Bering Sea and 80 percent for the samples south of the Aleutian Islands in the northern North Pacific.

3.4 Norton Sound

Previous work on suspended matter in Norton Sound has been limited to studies of LANDSAT photographs and suspended matter distributions. Sharma et al. (1974) used density-sliced LANDSAT photographs and sea truth measurements to study suspended matter distributions in Norton Sound during the late summer of 1973. Suspended matter concentrations were highest near the mouth of the Yukon River (range: 2-8 mg/L) and in Norton Bay (range: 3-4 mg/L), located in the northeast corner of the Sound. The authors postulated that the general pattern of cyclonic circulation in the Sound caused suspended material to be transported to the north and northeast along the coast. The authors also noted that unusually high particulate matter concentrations (>9.0 mg/L) were observed throughout the water column in the region approximately 30 km south-southwest of Nome. They suggested that this plume could have been a detached portion of the Yukon River plume which was isolated by tidal pulsation.

Cacchione and Drake (1979) combined suspended matter surveys during September - October 1976 and July 1977 with deployments of a tripod (GEOPROBE) containing instruments designed to measure bottom currents, pressure, temperature, and light transmission and scattering to study suspended matter dispersal patterns in Norton Sound. They described the transport of suspended materials as dominated by distinctly different quiescent and storm regimes. The quiescent regime was characterized by relatively low levels of sediment transport caused by tides and mean flow to the north and northeast, which was augmented by surface waves during spring tides. The authors stated that during this period much of the fine-grained suspended matter present over the prodelta was resuspended at shallow depths during spring tide and transported northward with the mean current. The storm regime, which occurs during the months of September through November, was characterized by strong southerly and southwesterly winds which generate waves with heights of 1-3 m and periods of 8-11 sec. The storm events cause near-bottom shear velocities which are in excess of that required for resuspension of bottom sediments, and, as a result, more than 50% of the sediment transport occurs during this regime.

Although there is no background information on the chemistry of suspended matter in Norton Sound, extensive studies of trace metal partitioning in various phases of Yukon River materials were conducted by Gibbs (1973; 1977). He concluded that transition metals associated with oxhydroxide coatings and crystalline phases comprised the major fraction (72-91%) of riverine transition metal transport to the sea. Particulate organic phases contained the next largest fraction (3-16% of the total). Metals in solution and metals sorbed to particulate materials made up the remainder (5-15% of the total).

4. THE STUDY REGIONS

4.1 Northeast Gulf of Alaska

The northeast Gulf of Alaska is bordered by a mountainous coastline containing numerous glaciers which deliver large quantities of suspended material to the Gulf during the summer months when maximum discharge occurs (fig. 1). The major sediment discharge is from the Copper River. Reimnitz (1966) estimates that approximately 107 x 10^6 tons of fine-grained material are delivered annually to the Gulf by way of the Copper River system. The maximum discharge of the Copper River occurs during the months of June through September.

Additional inputs into the Gulf occur along the coastline east of Kayak Island where coastal streams containing high sediment concentrations drain the Bering, Guyot and Malaspina Glaciers. Since there are no permanent gauging stations on these streams, there is no information about the quantities of materials that are discharged into the Gulf from these sources.

The current systems in the Gulf are dominated by the large counterclockwise gyre of the Alaska Current. It is usually characterized by a core of relatively warm (5.5° - 6.2°C) water at about 130 meters (Galt and Royer, 1975). The Alaskan Stream comes in contact with the shelf just east of Icy Bay where it is turned to the west and appears to follow the 150 meter isobath.

West of Kayak Island the Alaska Current is deflected to the southwest, leaving the large shelf area between Middleton Island and the Copper River Delta relatively free of its influence. In this region the circulation is affected by seasonal wind patterns. In the summer, the winds are predominantly from the southwest. This produces an Ekman drift of surface waters offshore. During the winter, the winds are from the southeast which results in an Ekman drift onshore and downwelling in subsurface waters.

4.2 Lower Cook Inlet

Cook Inlet is a large tidal estuary in south central Alaska. It lies on a northeast-southwest axis and is about 150 nautical miles long and 50 nautical miles wide at the mouth (fig. 10). Physiographically, the inlet is divided into three sections. At the head of the inlet, it separates into Knik and Turnagain Arms. Near the middle, upper Cook Inlet is separated from lower Cook Inlet by two geographic constrictions, the East and West Forelands.

The inlet receives fresh water from four major rivers: the Matanuska and Knik Rivers at the head of Knik Arm and the Susitna and Beluga Rivers to the northwest. These rivers supply about 70% to 80% of the freshwater input (Rosenberg and Hood, 1967). In addition, numerous streams containing large concentrations of glacial flour drain into the lower inlet from both sides. Included in this category are the Kenai, Kalisof, Nihilchik, and Anchor Rivers on the eastside and the McArthur, Big, Drift, and Tuxedni Rivers which discharge into the inlet from the west.

Water circulation in lower Cook Inlet has been described by several authors (Kinney et al., 1970; Wright et al., 1973; Gatto, 1976; Burbank, 1977; and Muench et al., 1978). The last reference provides the most completed description of water circulation in lower Cook Inlet. Circulation in the inlet is characterized by a net inward movement of oceanic water up the eastern shore and a net outward movement of a mixture of oceanic water and runoff water along the western shore. In the vicinity of the Forelands, the water masses are vertically mixed due to the turbulent action of tidal currents. However, lateral separation of the water masses is apparent, resulting in a shear zone between the incoming saline water on the east-side and the outgoing less saline water on the west. Coastal upwelling occurs in the vicinity of the Chugach Islands, from the region west of Elizabeth Island to Cape Starichkof.

The distribution and composition of bottom sediments in lower Cook Inlet have been studied (Sharma and Burrell, 1970; Bouma and Hampton, 1976; Hein et al., 1979). The sediments are primarily composed of medium-to-fine grained sands; however, occasional silt and clay-sized sediments have been observed. The deposits in the northern part of the inlet are winnowed Pleistocene-early Holocene gravels, with many of the sand-sized and smaller particles being removed and redeposited to the south. In addition to the relict sands and gravels, the sediments also contain a very thin cover of fine-grained silts and clays which are modern. Hein et al. (1979) state that the clay mineral deposits in lower Cook Inlet are dominated by clay mineral suites from two distinct sources. A chlorite-rich suite dominates the clay mineral fraction in deposits from the region around the Barren Islands in Kachemak Bay. The

Copper River appears to be the major source of this material as it discharges chlorite-rich fine-grained material into the northeast Gulf of Alaska which is diverted to the west and southwest by the coastal alongshore currents (Feely et al., 1979). Apparently, some of this material reaches Kennedy Entrance and is transported into lower Cook Inlet along with the inflowing Gulf of Alaska water.

The region to the west and north of Kachemak Bay is dominated by an illite-rich suite; the Susitna River in upper Cook Inlet being its major source. These authors further state that the distribution of clay minerals in the bottom sediments in lower Cook Inlet reflects the dispersal routes for suspended material in the overlaying water. Thus, fine-grained particles from these two sources follow the general pattern of water circulation in the inlet and form the bulk of the mud deposits in the quiet embayments along the shore and throughout Shelikof Strait.

4.3 Southeastern Bering Sea Shelf

The southeastern Bering Shelf is a relatively shallow embayment which is bounded by the Kilbuk Mountains to the north and east, and the Alaska Peninsula to the south (fig. 8). Except for some small depressions near the Alaska Peninsula, the shelf floor is extremely smooth with an average slope of about 0.0003 (Sharma, 1974).

The region receives sedimentary material from the Kuskokwim, Kvichak, and Nushagak rivers. The largest river, the Kuskokwim, discharges approximately 4.0×10^6 tons of sediments annually (Nelson, 1974). The maximum discharge occurs during the months of May through September.

A counterclockwise movement generally dominates the water motion in the Bristol Bay region. Pacific Ocean water enters the Bering Sea through the

Aleutian Island passes and flows to the northeast along the coast of the Alaska Peninsula. The water moves along the northern coastline by tidal and wind-driven currents until it reaches Nunivak Island where it is turned to the north.

The permanent currents in the southeastern Bering Shelf appear to be somewhat sluggish. Current velocities ranging from 2.0 to 5.0 cm sec^{-1} have been observed north of the Alaska Peninsula (Hebard, 1959). However, tidal currents are dominant in northeastern Bristol Bay where tidal velocities of up to 125 cm sec have been observed in Nushagak Bay (U.S. National Ocean Survey, 1973).

4.4 Norton Sound

Norton Sound is a shallow embayment located in the central region of the west coast of Alaska (fig. 9). Relative to the Bering Sea, it is an east-west extending embayment which is about 200 km long in the east-west direction and about 150 km wide in the north-south direction. The Yukon River, which flows into the southwest quadrant of the embayment, is the major source of freshwater and suspended matter to the Sound as well as to the entire eastern Bering Sea Shelf. Its annual suspended matter load of 88 x 10^6 tons ranks 18th among the major rivers of the world (Inman and Nordstrom, 1971). The annual discharge curve for the Yukon River is unimodal with peak flow occurring during June and low flow conditions persisting throughout the winter months. Additional smaller freshwater inputs into the Sound occur along the coastline east of the Yukon River Delta and along the northern coast.

Water circulation in the vicinity of Norton Sound has been described by several authors (Coachman et al., 1975; Muench and Ahlnäs, 1976; Muench et al., 1981). The shelf water west of Norton Sound, the Alaska Coastal water, has a net northward flow of about 1.5 x 10^6 m^3 sec^{-1}. About one-third of this flow passes between St. Lawrence Island and the mouth of Norton Sound. The intensity of the cyclonic flow appears to be affected by local winds and by freshwater runoff. The eastern half of the Sound is characterized by two vertically well-mixed layers. The lower layer contains cold, dense residual water formed during the previous winter. Both water masses follow the general pattern of cyclonic flow in the region, although much more sluggishly than surface and bottom waters further to the west.

The distribution of sediments in Norton Sound has been summarized (McManus et al., 1974; Sharma, 1974; Nelson and Creager, 1977; and McManus et al., 1977). In the central and southern regions, the sediments consist of very fine-grained sands and silts which are modern. In the northern region, silty sands predominate everywhere except for a narrow strip along the coast between Cape Nome and Cape Douglas. Here, coarse sands and gravels predominate because bottom currents have caused almost complete erosion of the fine-grained sediments. Approximately one-half to two-thirds of the sediment load of the Yukon River is deposited as a bank of sediments extending from the Yukon River Delta northward and eastward around the inside periphery of the Sound. The remaining sediment load of the Yukon River is transported to the north through the Bering Strait and deposited in the Chukchi Sea.

5. SOURCES, METHODS AND RATIONALE OF DATA COLLECTION

In order to obtain information about the distribution and composition of suspended matter in the various study areas, we have conducted three cruises in the northeast Gulf of Alaska (Cruise RP-4-Di-75C-I, 21 October-10 November 1975; Cruise RP-4-Di-76A-III, 13-30 April 1976; and Cruise RP-4-Di-76B-I, 19-31 July 1976), six cruises in lower Cook Inlet (Cruise RP-4-Di-77A-IV, 4-16 April 1977; Cruise Acona-245, 28 June-12 July 1977; Cruise RP-4-Di-77C-II, 3-12 October 1977; Cruise RP-4-Di-78A-III, 4-17 May 1978; Cruise RP-4-Di-78B-II, 22 August-6 September 1978; and Cruise RP-4-Di-79A-II, 7-20 May 1979), two cruises in the northeastern Bering Sea Shelf (Cruise RP-4-Di-75B-III, 12 September-5 October 1975 and Cruise RP-4-MW-76B-VII, 24 June-9 July 1976), and one cruise to Norton Sound (Cruise RP-4-Di-79A-VI, 7-18 July 1979). Figures 1 through 9 show the locations of the sampling stations for the various cruises.

5.1 Sampling Methods

5.1.1 Particulate Matter

Water samples were collected from preselected depths in General Oceanics 1070 10-L PVC Top-Drop Niskin bottles. Nominally these depths included: 0-2 m, 10 m, 20 m, 40 m, 60 m, 80 m, and 5 meters above the bottom. Aliquots were drawn within 10-15 minutes after collection from each sample and vacuum filtered through preweighed 0.4 μm pore diameter Nuclepore polycarbonate filters (47 mm) for total suspended matter concentration determinations and 25 mm for multi-element particulate composition analyses. Samples were also filtered through 25 mm, 0.45 μm pore diameter Selas silver filters for particulate C and N analyses. All samples were rinsed with three 10mL aliquots of deionized and membrane filtered water, placed in individual petri dishes with lids slightly ajar for a 24-hour desiccation period over sodium hydroxide, and then sealed and stored (silver filters frozen) for subsequent laboratory analysis.

5.1.2 Nephelometry

The vertical distribution of suspended matter was determined with a continuously recording integrating analog nephelometer. The instrument was interfaced with the ship's CTD system using the sound velocity channel (14-16 KHz). Continuous vertical profiles of forward light scattering were obtained in analog form on a Hewlett Packard 7044 X-Y recorder.

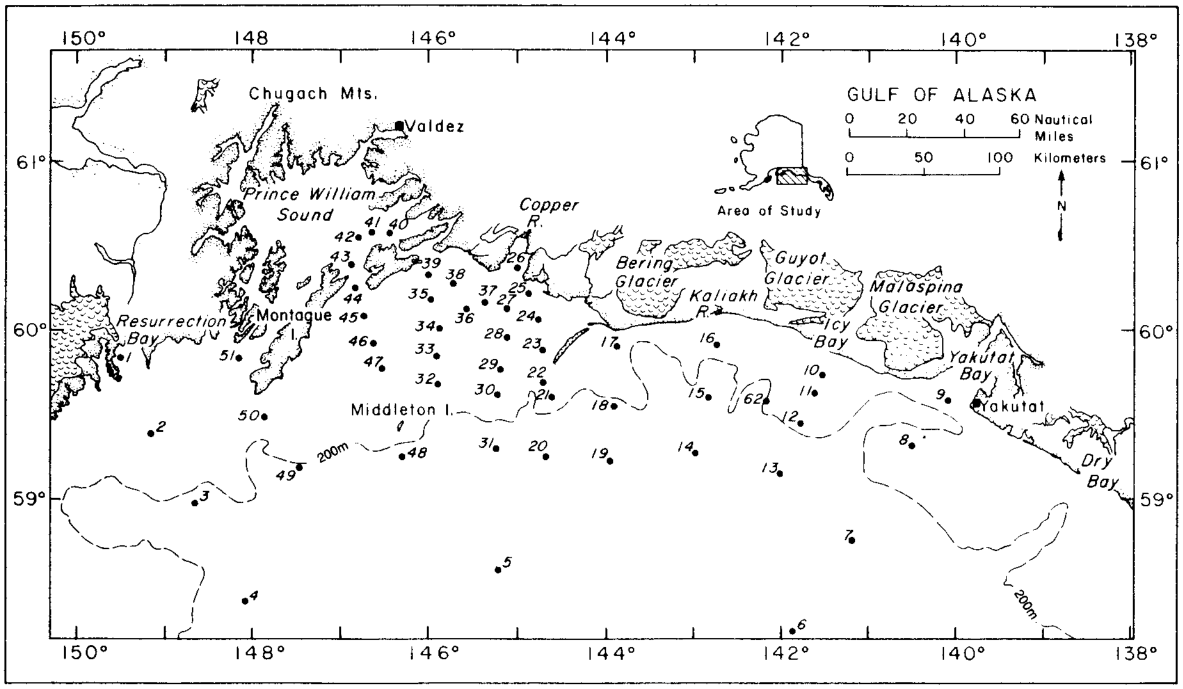

Figure 1. Locations of suspended matter stations in the northeastern Gulf of Alaska (Cruise RP-4-Di-75-C-I, 21 October-10 November 1975).

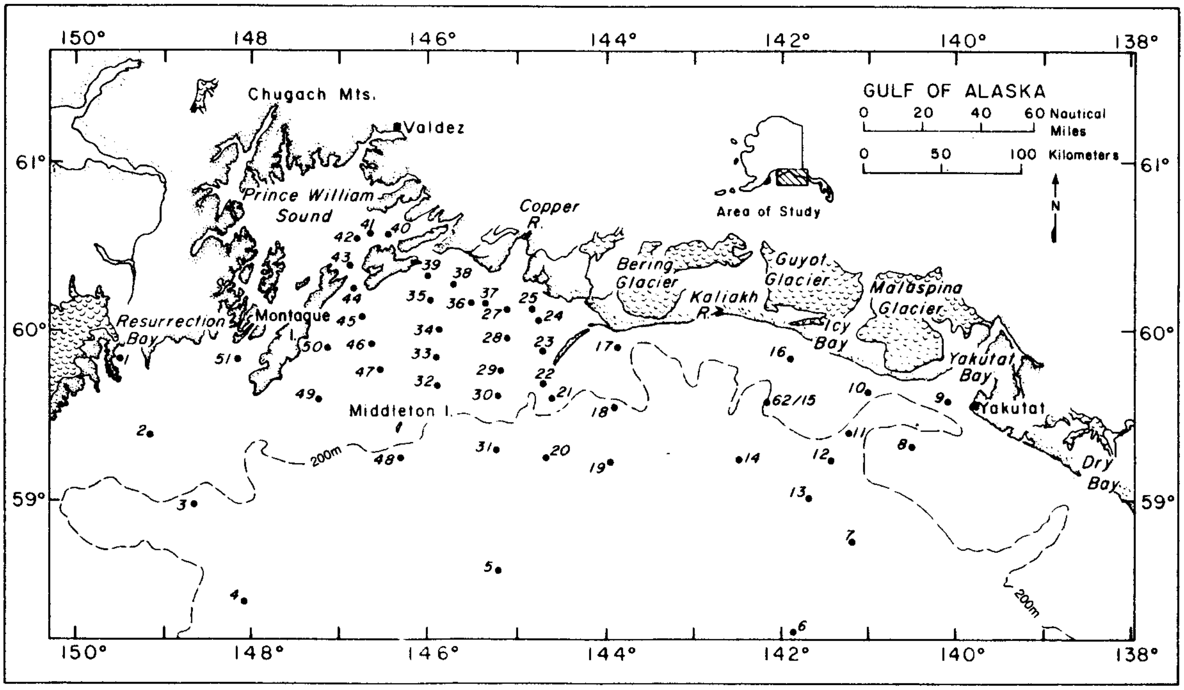

Figure 2. Locations of suspended matter stations in the northeastern Gulf of Alaska (Cruises RP-4-Di-76A-III, 13-30 April 1976 and RP-4-Di-76B-I, 19-31 July 1976).

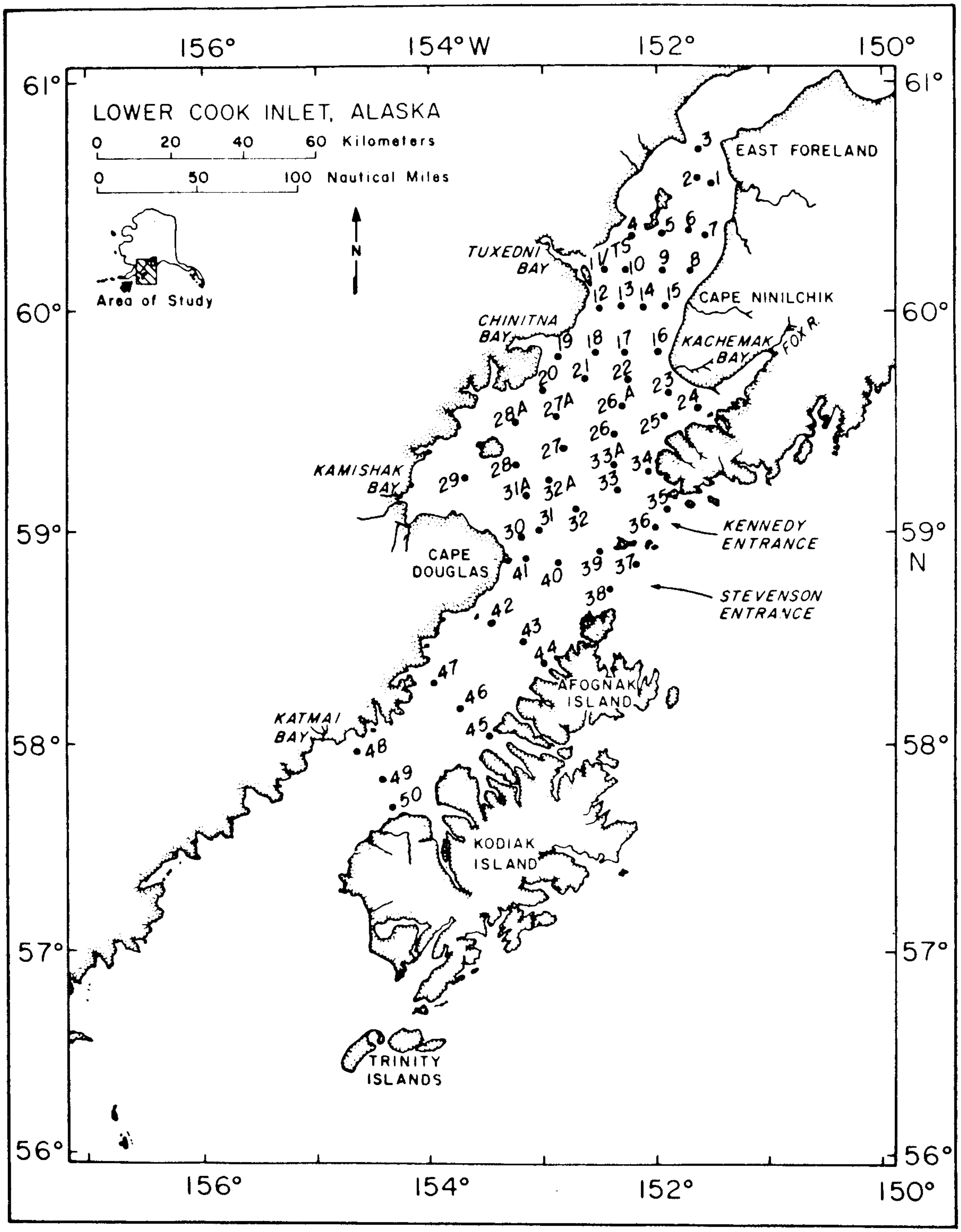

Figure 3. Locations of suspended matter stations in lower Cook Inlet and Shelikof Strait (Cruise RP-4-Di-77A-IV, 4-16 April 1977).

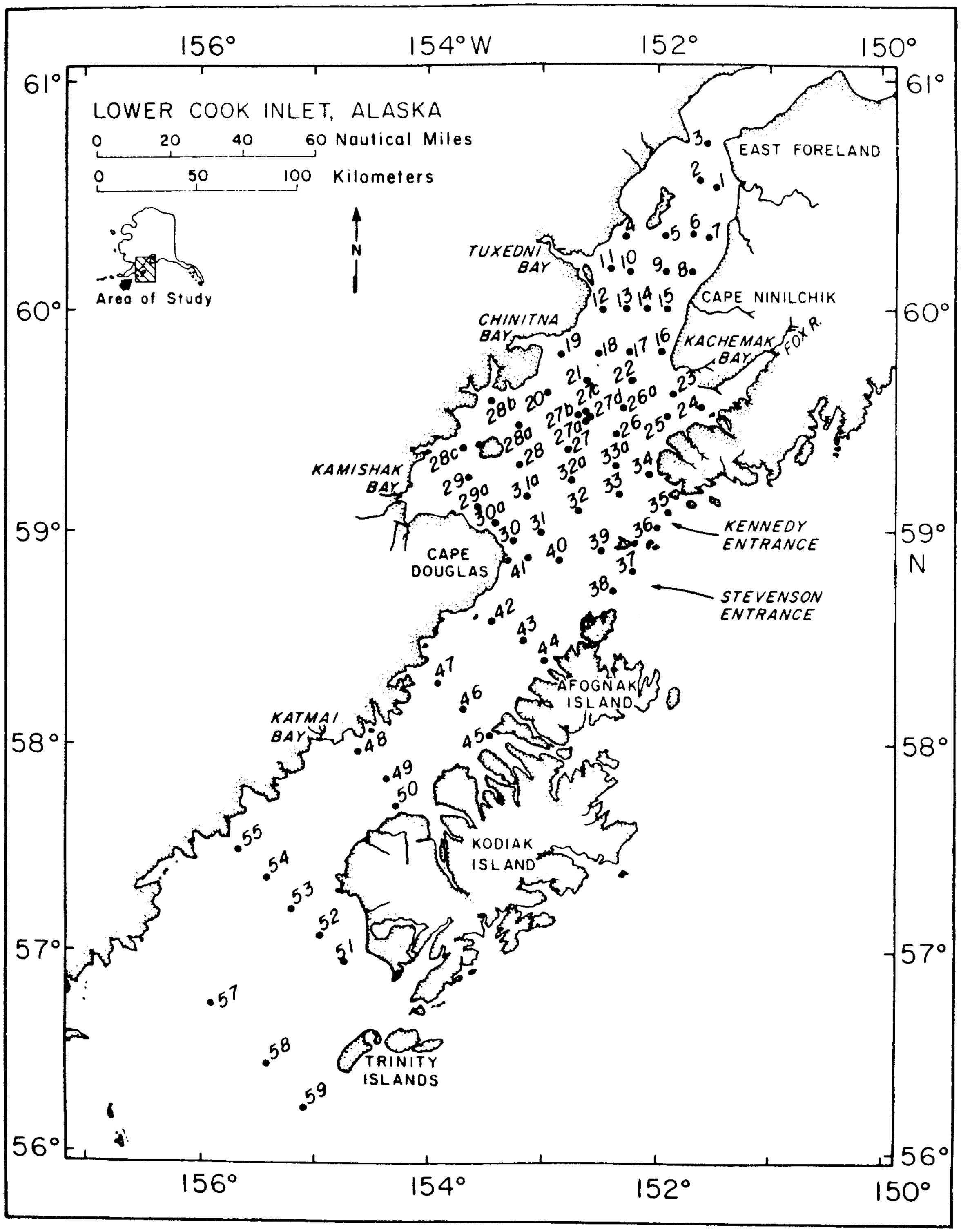

Figure 4. Locations of suspended matter stations in lower Cook Inlet and Shelikof Strait (Cruise Acona-245, 28 June - 12 July 1977).

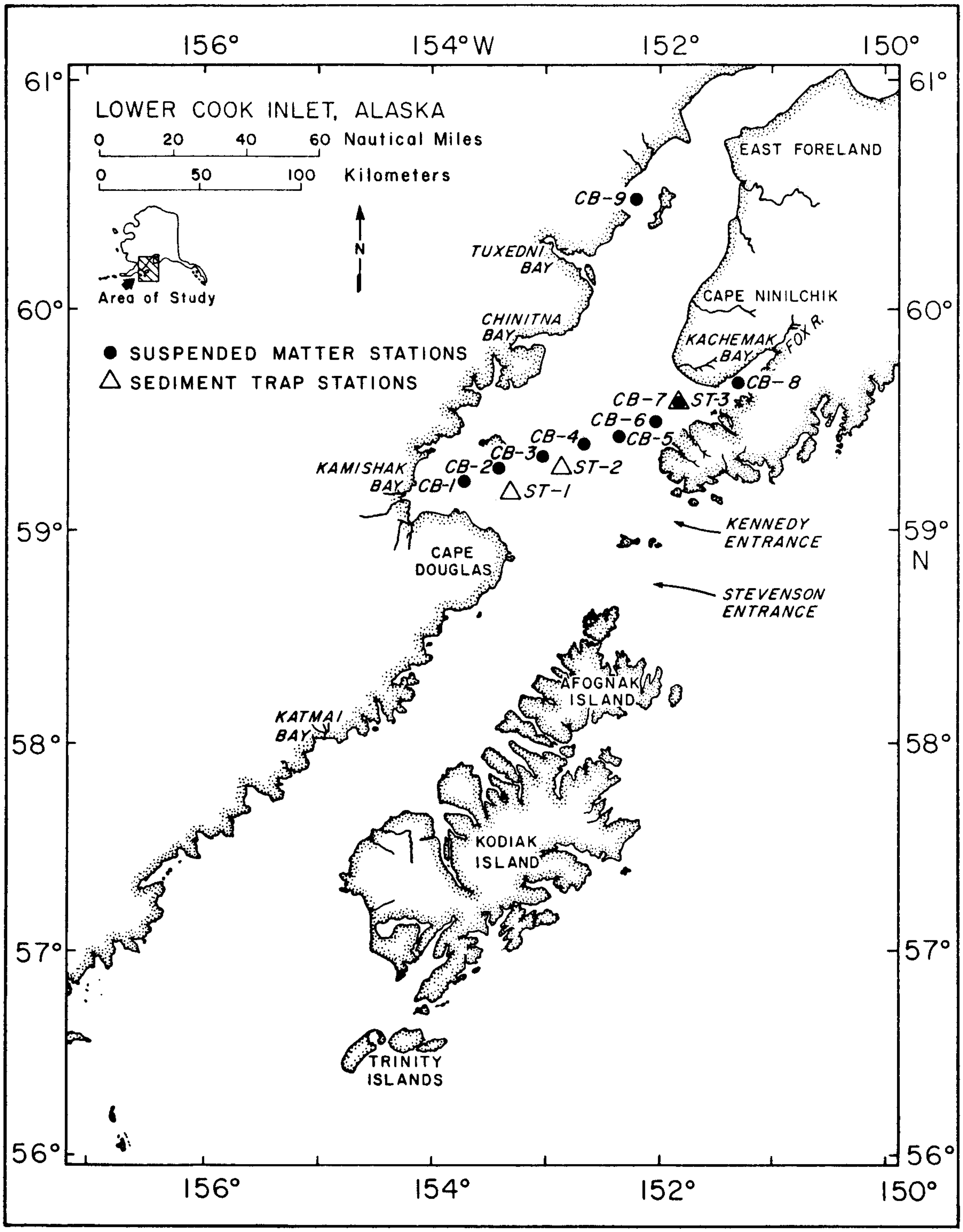

Figure 5. Locations of suspended matter and sediment trap stations in lower Cook Inlet (Cruise RP-4-Di-78A-III, 4-17 May 1978).

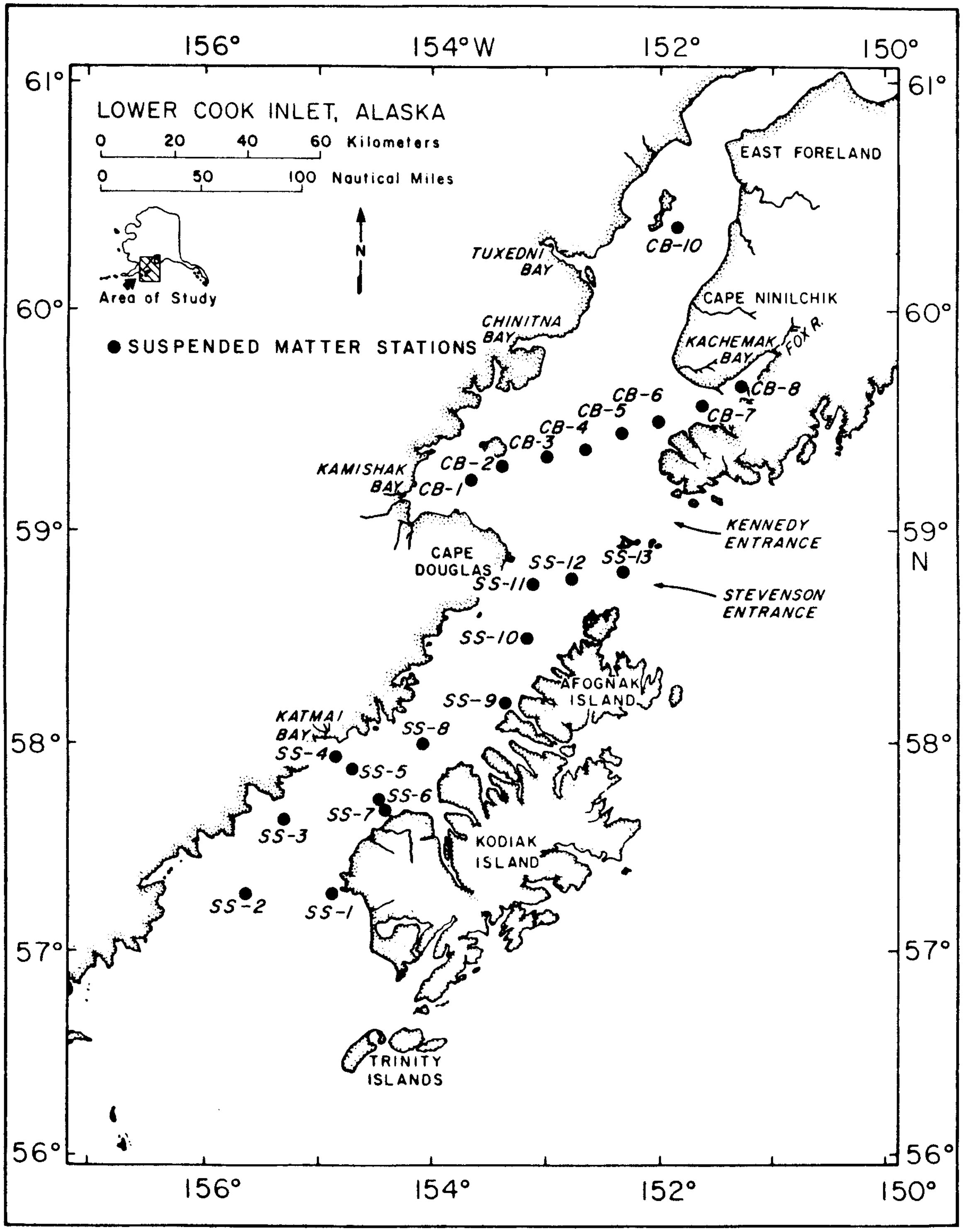

Figure 6. Locations of suspended matter stations in lower Cook Inlet and Shelikof Strait (Cruise RP-4-Di-78B-II, 22 August - 6 September 1978).

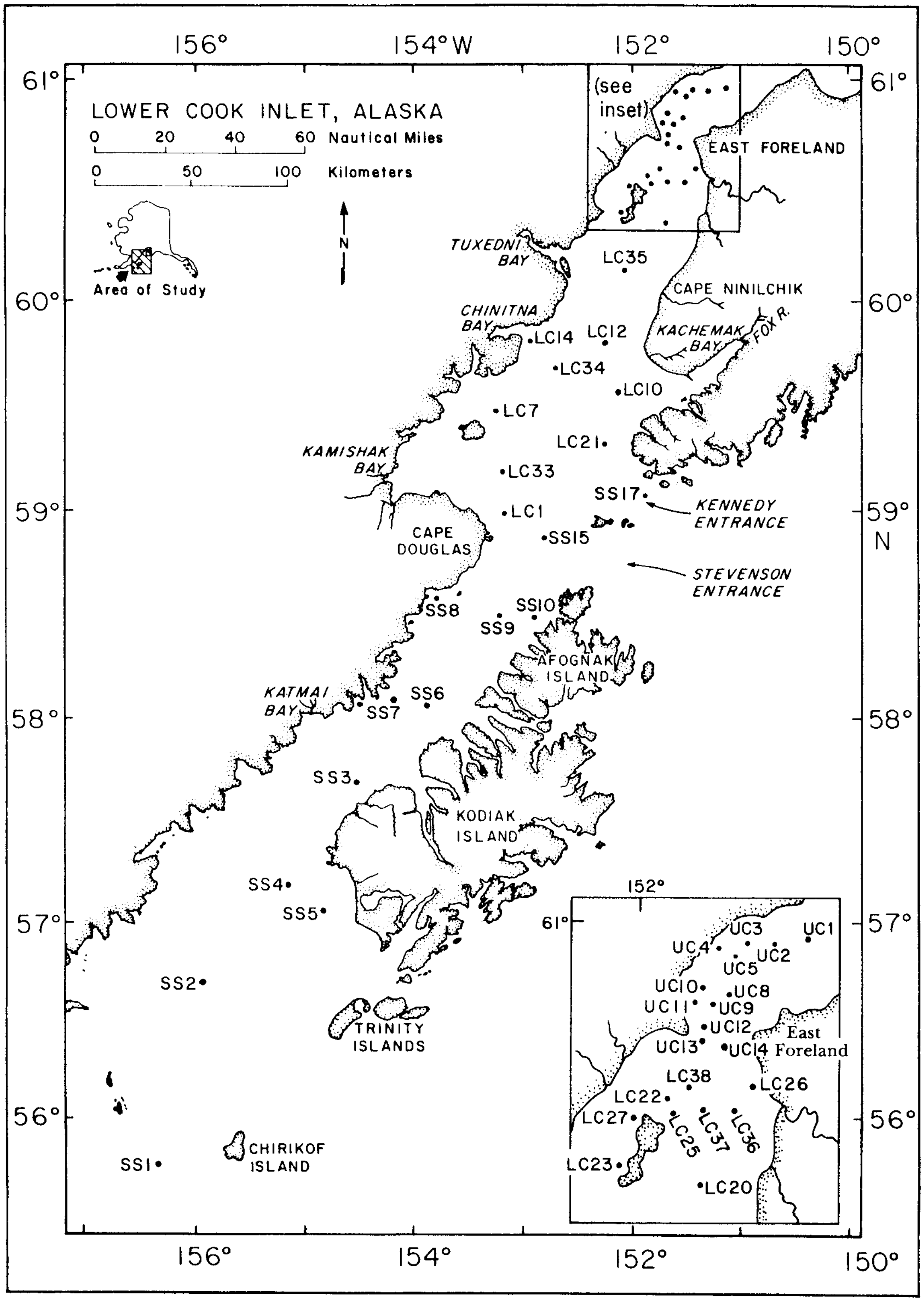

Figure 7. Locations of suspended matter stations in lower Cook Inlet and Shelikof Strait (Cruise RP-4-Di-79A-II, 7 - 20 May 1979).

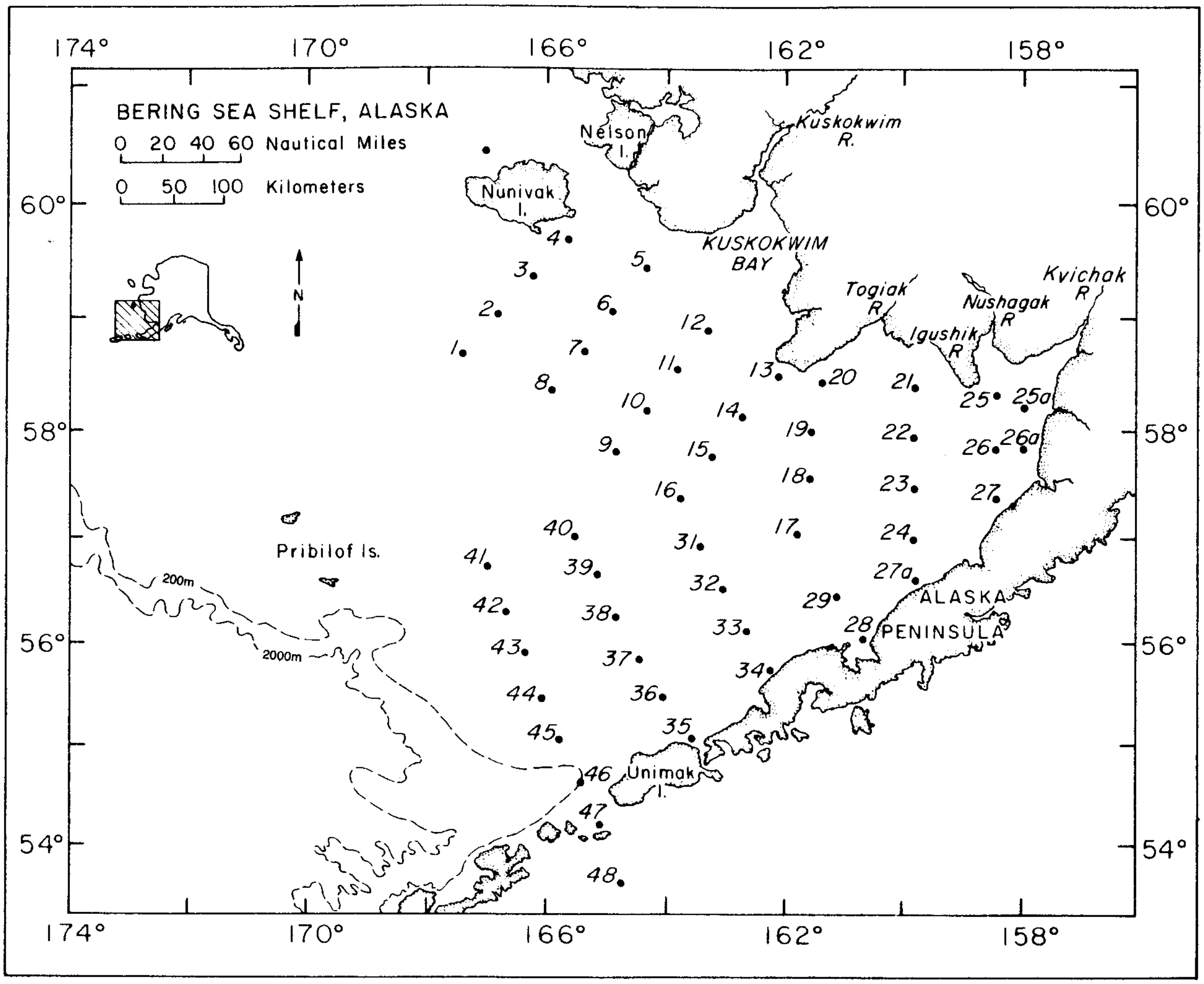

Figure 8. Locations of suspended matter stations in the southeastern Bering Shelf (Cruises RP-4-Di-75B-III, 12 September - 5 October 1975, and RP-4-MW-76B-VIII, 24 June - 9 July 1976).

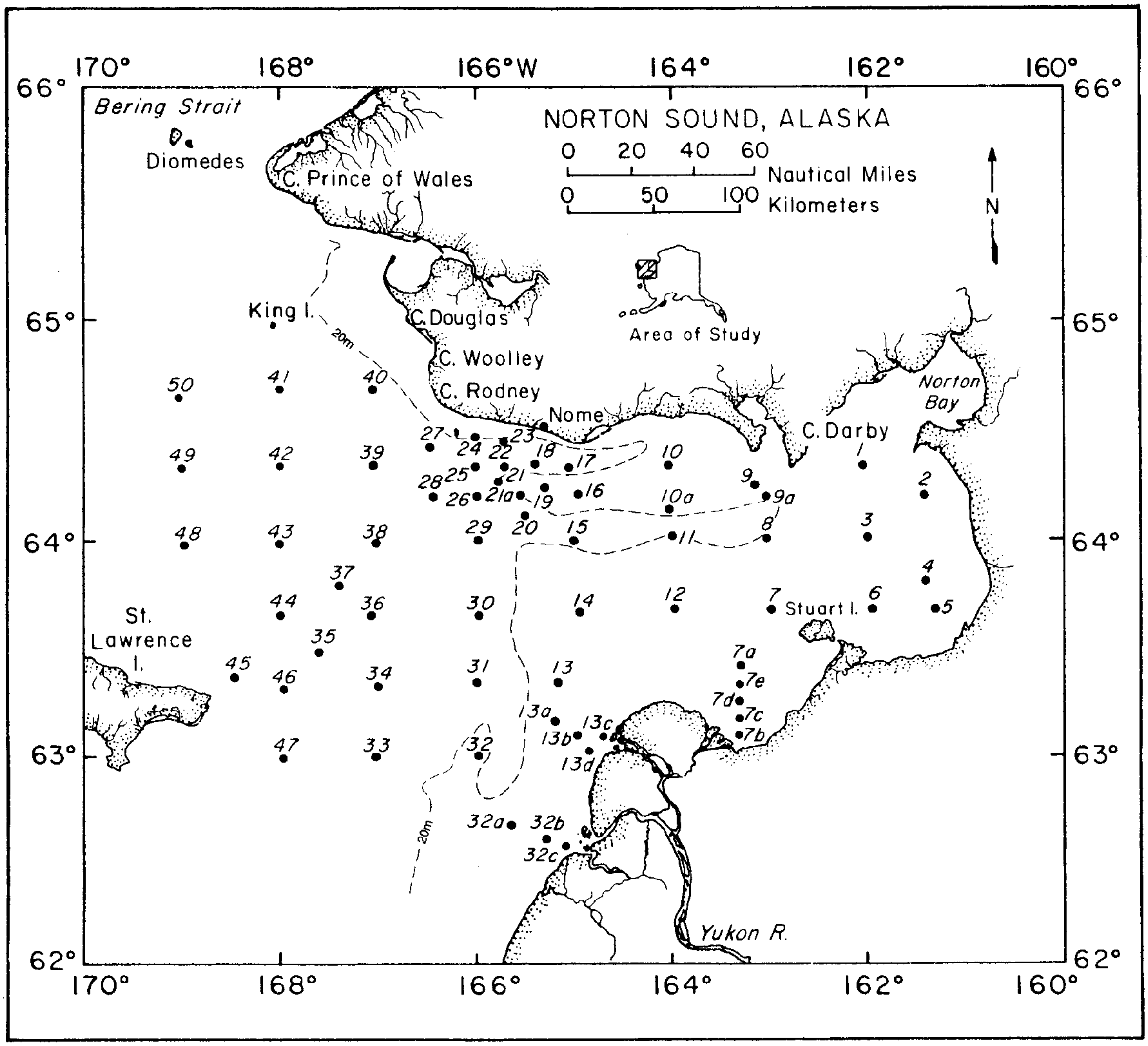

Figure 9. Locations of suspended matter stations in Norton Sound (Cruise RP-4-Di-79A-VI, 7-18 July 1979).

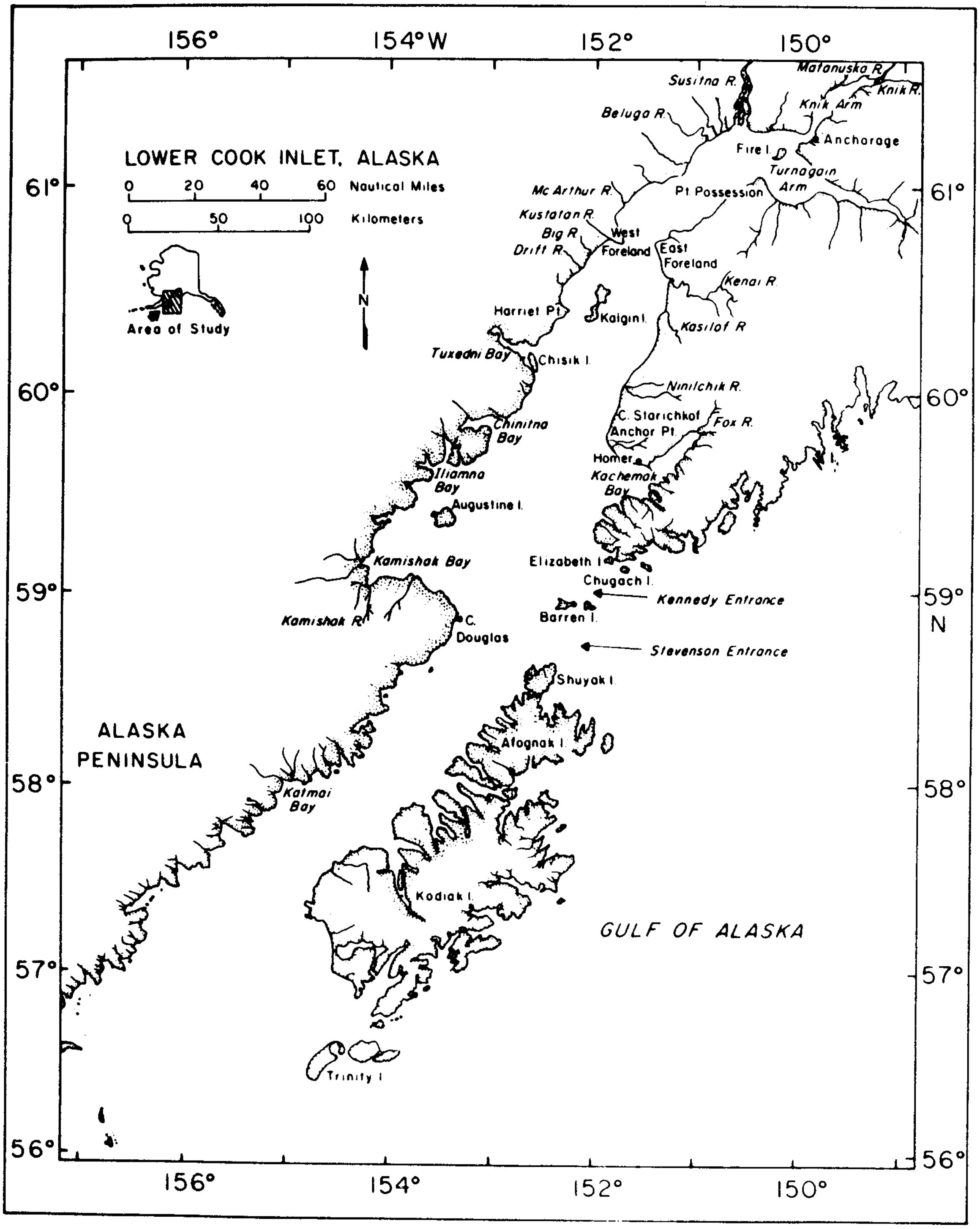

Figure 10. Physiographic setting of lower Cook Inlet, Alaska.

5.1.3 Conductivity (Salinity), Temperature, and Depth

These standard hydrographic data were acquired with a Plessy Model 9040 Environmental Profiling System (CTD probe) and a Model 8400 digital data logger using 7-track, 200 B.P.I. magnetic tape. Temperature and salinity calibration data were provided by ship personnel from discrete water samples utilizing reversing thermometers and a bench salinometer, respectively. Signals from the CTD system and the nephelometer were also simultaneously interfaced with the ship's data acquisition system. This resulted in computer listings of continuous (uncorrected) data for conductivity, temperature, depth, salinity, sigma-t, and light scattering for all vertical sampling stations.

5.2 Analytical Methods

5.2.1 Gravimetry

Total suspended matter concentrations were determined gravimetrically. Volumetric total suspended matter samples were collected on 47 mm, 0.4 μm pore diameter Nuclepore filters which were weighed on a Cahn Model 4700 Electrobalance before and after filtration. The suspended matter loadings were then determined by difference. The weighing precision ($2\ \sigma = \pm .011$ mg) and volume reading error (± 10 mL) yield a combined coefficient of variation in suspended matter concentration (mg/L) at mean sample loading and volume (2.057 mg and 2 L, respectively) of approximately 1%. However, preliminary investigations of sampling precision (coef. of var.: 25%) suggest that the actual variability in the particulate matter concentrations of these waters is much greater than the above analytical precision.

5.2.2 Gas Chromatography

Analysis of total particulate C and N in suspended matter was performed with a Hewlett Packard Model 185B C-H-N analyzer. In this procedure, particulate C and N compounds are combusted to CO_2 and N_2 (micro Pregl-Dumas method), chromatographed on Poropak Q, and detected sequentially with a thermal conductivity detector. NBS acetanilide is used for standardization. Analyses of replicate surface samples yield coefficients of variation ranging from 2% to 10% for C and 7% to 14% for N.

5.2.3 X-ray Secondary Emission Spectrometry

The major (Mg, Al, Si, K, Ca, Ti, and Fe) and trace (Cr, Mn, Ni, Cu, Zn, and Pb) element chemistry of the suspended particulate matter samples was determined by x-ray secondary emission (fluorescence) spectrometry utilizing a Kevex Model 0810A-5100 x-ray energy spectrometer and the thin-film technique (Baker and Piper, 1976). The inherent broad band of radiation from a Ag x-ray tube was used to obtain a series of characteristic emission lines from a single element secondary target which then more efficiently excited the thin-film sample. Fe, Se and Zr secondary targets were used to analyze the samples for both major and trace elements. Standards were prepared by passing suspensions of finely ground USGS standard rocks (W1, G-2, GSP-1, AGV-1, BCR-1, PCC-1) and NBS trace element standards through a 37 μm mesh polyethylene screen followed by collection of the size fractionated suspensates on Nuclepore filters identical to those used for sample acquisition. The coefficient of variation for 10 replicate analyses of a largely inorganic sample of approximately mean mass was less than 3% for the major constituents and as high as 5% for the trace elements. However, when sampling precision is considered, the coefficients of variation increase, averaging 12% and 24% for major and trace elements, respectively.

5.2.4 Atomic Absorption Spectrophotometry

The suspended matter samples from lower Cook Inlet and Norton Sound were analyzed for Al, Fe, Mn, Cr, Cu, Ni, Zn and Pb by means of several extraction procedures. The first extraction procedure involves the use of hydrogen peroxide (H_2O_2) to release organically-bound trace metals. The second treatment utilizes 0.3 N hydrochloric acid (HCl) to release trace metals which are weakly bound to inorganic phases. The third procedure involves the use of 25% acetic acid (CH_3COOH) to remove amorphous Fe and Mn oxides. The details and validity of these procedures are outlined below.

5.2.4.1 H_2O_2 Treatment

Crecelius et al. (1974) have demonstrated that 30% H_2O_2 efficiently oxidizes particulate organic matter and thus removes certain trace metals from sediments. Landing (1978) had shown that the modification of this procedure, as described below, efficiently removes organic C and N from suspended matter. The release of trace metals from suspended matter during this procedure is attributed to the dissolution of organically bound trace metals.

> Procedure. Dilute 30% ULTREX (J.T. Baker) H_2O_2 to 10% with the addition of quartz distilled water (Q-H_2O). Combine 5 mLs of 10% H_2O_2 with 100-500 mg of sample material in a precleaned centrifuge tube equipped with a nonsealing cap. The volume and mass of extractant and sample, respectively, may vary within the above limits depending on the relative magnitude of the organic fraction in the sample. We are currently using polypropylene centifuge tubes and caps. Heat the extractant-sediment solution in a water bath at approximately 50°C for 48 hours. During the final 24 hours of heating, vigorously sonicate the solution to assist in dispersal and breakdown of the organic matter. Centrifuge the tube contents at 2000 rpm for 1 hour. Decant the supernate into a precleaned and tared polyethylene (CPE) bottle. Rinse the residual particulate matter with one 10 mL aliquot of quartz-distilled water. Centrifuge, as above, after the rinse and combine all supernates in the polyethylene bottle. Since the centrifugation separation is not complete, filter the samples through a 0.4 μm Nuclepore filter. Determine the weight of the supernate by difference.

5.2.4.2 0.3 N HCl Treatment

Malo (1977) has shown that leaching with hot 0.3 N HCl is the most effective method for dissolving trace metals associated with surface coatings. In this study, this method was modified by heating the sediment-0.3 N HCl mixture to 75°C instead of 100°C. The time required for completion of the reaction was determined by leaching subsamples for different lengths of time. The results of this kinetic study (fig. 11) indicate that no additional Cu is released after the first 2 hours while Ni and Zn continue to be leached for 12 hours. Therefore, the sediment-acid mixture was heated for 24 hours to insure that the reaction was complete. A high efficiency for this reaction was confirmed by analyzing the amount of Cu and Mn released on a subsequent 0.3 N HCl leach (table 1).

Procedure. Dilute ULTREX (J.T. Baker) HCl to 0.3N with Q-H_2O. Add 8 mLs of 0.3 N HCl to 100-500 mg of sample which has been treated with H_2O_2. Heat the mixture to 75°C for 24 hours while sonicating. Centrifuge the mixture at 2000 rpm for 1 hour. Decant the supernate into a precleaned and tared polyethylene bottle. Add 8 mLs of 0.3 N HCl to the residual sediment. Shake this mixture, then centrifuge as above and decant the supernate into the bottle. Repeat the rinsing of the residual sediment once. Filter the combined supernates through a 0.4 μm Nuclepore filter. Determine the weight of the final supernate by difference.

Table 1. Efficiency of Successive 0.3 N HCl Treatments

	Mn (ppm)	Cu (ppm)
First Treatment (n = 3)	911 ± 78	49.3 ± 2.5
Second Treatment (n = 3)	6.7 ± 0.3	0.7 ± 0.1

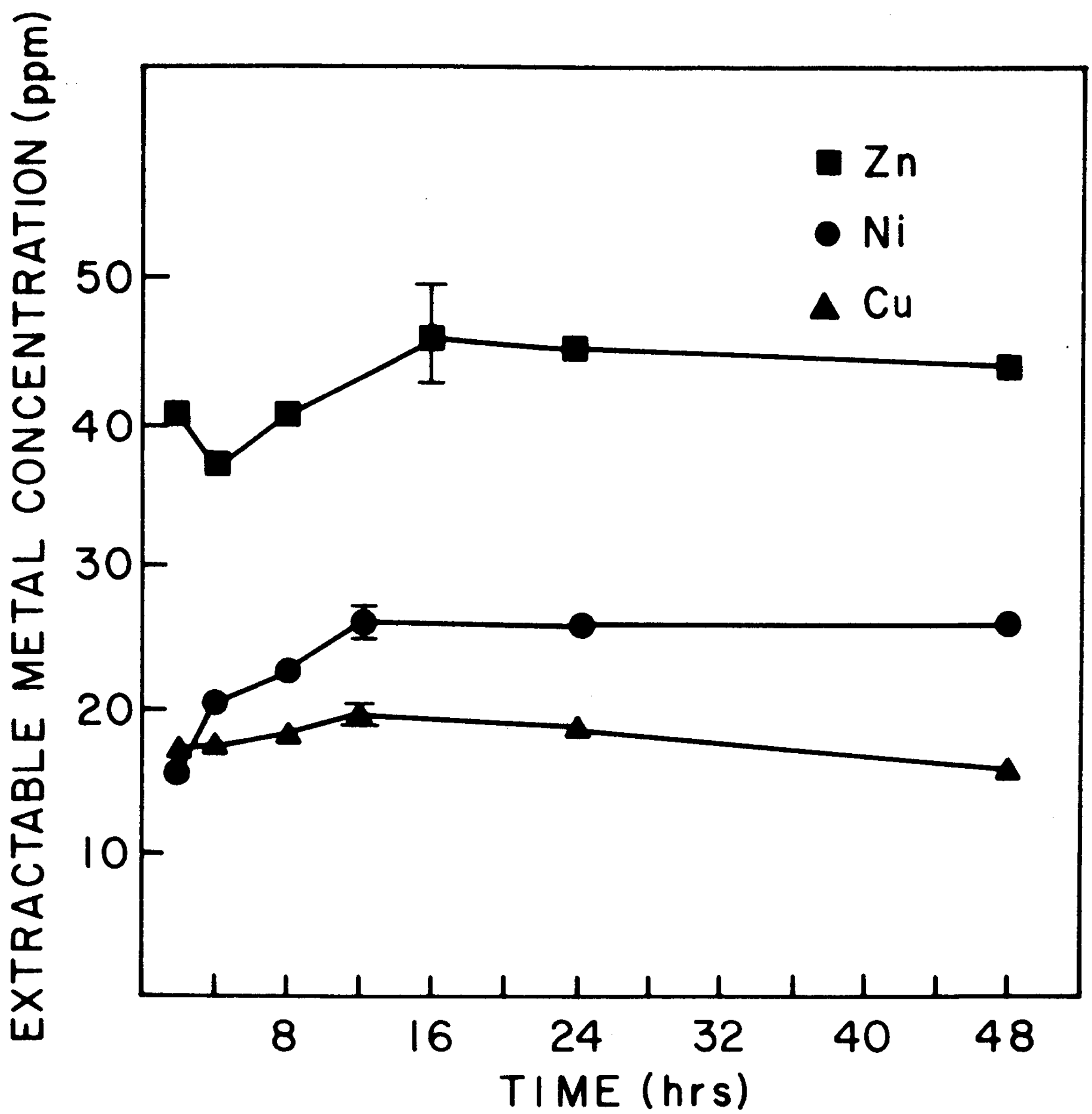

Figure 11. Extractable metal concentrations versus time in contact with 0.3 N HCl for Zn, Ni, and Cu. The range of values is given for duplicate samples at 12 hours.

5.2.4.3 25% Acetic Acid

The amorphous Mn and Zn in the poorly structured oxyhydroxide phase of selected suspended matter samples were determined by the method of Bolger et al. (1978). Desiccated samples were leached with 5 mL of 25% (v/v) Ultrex acetic acid at room temperature for 2 hours. The resulting supernate was filtered through an acid-cleaned polypropylene-glass apparatus containing a 0.4 µm Nuclepore filter. The residue was rinsed with quartz-distilled water, then filtered; and the supernate was combined with the original supernate, acidified with 0.5 mL of concentrated Ultrex HCl, and stored in an acid cleaned polyethylene bottle. The Mn and Zn in this solution (weak-acid soluble) were analyzed by flameless atomic absorption procedures using addition methods. The remaining solid suspended matter (weak-acid insoluble) was dissolved in an Ultrex HCl - HNO_3 - HF matrix according to Eggiman and Betzer (1976) and analyzed for Mn and Zn in a similar manner.

5.2.4.4 Bulk Elemental Analysis

Elemental composition of suspended matter was determined using a modification of the method of Eggiman and Betzer (1976).

> Procedure. If the sediment is refractory, grind the dry sediment in a boron carbide mortar and pestle. Weigh out approximately 2 mg and place in a digestion bomb (Bombco, Inc.). Add 0.75 mL of 12 N HCl (ULTREX) and seal the bomb tightly and place in boiling water for 45 minutes. Cool for 45 minutes in a freezer. Add 0.25 mL of 16 N HNO_3 (ULTREX), seal, and place in boiling water for 45 minutes. Cool for 45 minutes in freezer. Add .05 mL of concentrated HF (ULTREX), seal, and place in boiling water for 90 minutes. Cool for 90 minutes. Quantitatively transfer the contents of the digestion bomb to a wide mouth bottle and rinse the bomb with Q-H_2O. Dilute the sample to 20 gm with Q-H_2O.

5.2.4.5 Instrumental Procedures

Flameless atomic absorption measurements were made using a Perkin-Elmer 603 spectrophotometer equipped with an HGA-2200 furnace control, deuterium arc background corrector, AS-1 automatic sampler and a Model 54 recorder. The normal instrument parameters are listed in table 2. Baker AAS standards are

Table 2. Summary of the analytical parameters utilized in the flameless atomic absorption determinations. Analyses conducted with a Perkin-Elmer 603 AAS, D-2 Arc Background Corrector, HGA-2200 Flameless Atomizer, AS-1 Automatic Sampler. Pyrolitically coated tubes used for all elements. Std. Add. = Standard Additions.

Element	Wavelength (nm)	Slit (nm)	Volume (μl)	Dry Cycle (Time/Temp	Ash Cycle Time/Temp	Atomize Cycle Time/Temp	Gas	Flow Units	Bkg. Cor.	Comments
Al	257	0.2	10	30/100	22/1300	5/2600	Ar	40	No	Std. Add.
Fe	347	0.2	10	30/100	22/1050	5/2600	N_2	40	No	
Mn	280	0.2	10	30/100	22/1000	5/2600	N_2	55	No	
Cr	358	0.7	10	30/100	22/1000	5/2600	Ar	45	No	
Cu	325	0.7	10	30/100	22/ 800	5/2500	Ar	35	No	
Ni	232	0.2	20	40/100	32/ 900	5/2500	Ar	35	Yes	
Pb	217	0.7	20	40/100	32/ 600	5/2500	Ar	35	Yes	
Zn	214	0.7	10	30/100	22/ 500	5/2500	Ar	40	Yes	

6. RESULTS AND DISCUSSIONS

6.1 Northeast Gulf of Alaska

6.1.1 Particulate Matter Distributions and Transport

Figures 12 thru 17 show the distributions of suspended matter at the surface and 5 m above the bottom for the fall, spring, and summer cruises, respectively. The surface distributions showed significant variations which can be related to fluctuations in sediment flux from coastal rivers, formation of eddies, and local variations in current patterns and transport processes; whereas near-bottom distributions appeared to be affected primarily by local variations in bottom currents and secondarily by regional sources.

East of Kayak Island, surface particulate matter distributions were dominated by the discharge of sedimentary material from the coastal streams which drain the Bering, Guyot, and Malaspina glaciers. As this material was discharged into the Gulf, coastal along-shelf currents quickly advected it to the west along the coast. Comprehensive analyses of LANDSAT imagery for this region (Sharma et al., 1974 and Carlson et al., 1975) have indicated that most of the material discharged from the rivers east of Kayak Island remains relatively close to the coast (within 40 km) until it reaches Kayak Island, where it is deflected offshore. Surface particulate matter distributions for the cruises in October and April (figs. 12 and 13) followed this pattern. Along the transect southeast of Icy Bay (stations 10-13), particulate matter concentrations in fall and spring decreased from >1.0 mg/L near the coast to >0.5 mg/L approximately 40 km off the coast. During July, however, a plume of turbid water was observed extending outward from the coast (fig. 14). From careful analysis of LANDSAT imagery for this area, Burbank (1974) observed that occasionally counterclockwise eddies were formed which transported plumes of terrigenous material offshore. Similar low frequency motions were observed in current meter records from stations located southwest of Icy Bay (Hayes and Schumacher, 1976).

During fall and spring, plumes of turbid water (>1.0 mg/L) extended to the southwest from Kayak Island. From an analysis of LANDSAT-1 satellite photographs taken on August 14, 1973, Sharma et al., (1974) postulated that terrigenous debris discharged from the coastal rivers east of Kayak Island is carried to the west around the island's southern tip (Cape St. Elias) and trapped by a quasi-permanent anticyclonic gyre. Our data from the October and April cruises support their hypothesis (figs. 12 and 13). During October, a turbid plume extended to the west about 100 km from Kayak Island to station 33 (fig. 12). Particulate concentrations within the plume were high, averaging about 1.5 mg/L. North and south of station 33, particulate concentrations dropped below 1.0 mg/L, suggesting that the plume had an eastern origin. In April, a similar plume extended 50 km southwest of Kayak Island (fig. 13), with particulate concentrations decreasing from east to west. These similarities in the suspended matter distribution patterns suggest that, at the time of the cruises, similar hydrographic processes were operating to cause offshore transport of suspended matter.

In July, particulate distributions were significantly different from the preceding cruises. Near Kayak Island, there was no evidence of plumes extending offshore (fig. 14). A zone of turbid water extended only about 4 km from the eastern coast of Kayak Island, around the southern tip of the island and northward along the western coast. Near the mouth of the Copper River a plume of highly turbid water extended as far as 40 km offshore. Suspended matter concentrations within the plume were the highest of the three cruises, averaging 6.7 mg/L, reflecting the increased sediment discharge during July. As with the previous two cruises, sedimentary material from the Copper River was carried west along the coast until it reached Hinchinbrook Island. A portion of the material passed into Prince William Sound from either side of the island and the remaining material was carried southwest along the southern coast of Montague Island.

The distribution of suspended matter 5 m above the bottom for the three cruises is shown in figures 15, 16, and 17. The concentration data must be considered with some caution because the sampling was conducted with respect to the bottom and actual depths vary with the topography. Nevertheless, the data show a consistent pattern of decreasing concentrations away from the coast. Near-bottom concentrations were highest in the region south of the Copper River Delta and on either side of Kayak Island, where particulate concentrations ranged between 1.1 and 10.4 mg/L. At the edge of the continental shelf, near-bottom distributional patterns have been described previously for the continental shelf of the United States (Meade et al., 1975; Biscaye and Olsen, 1976) and have been attributed to resuspension of fine-grained sediments. The near-bottom turbid plumes in the northeast Gulf were primarily located over regions dominated by modern accumulations of clayey silts and silty clays (Carlson et al., 1977) and showed little resemblance to the surface plumes in space and time. These data suggest that bottom sediments were being resuspended locally to form near-bottom nepheloid layers in the Gulf, either by the actions of bottom currents, waves, or benthic organisms.

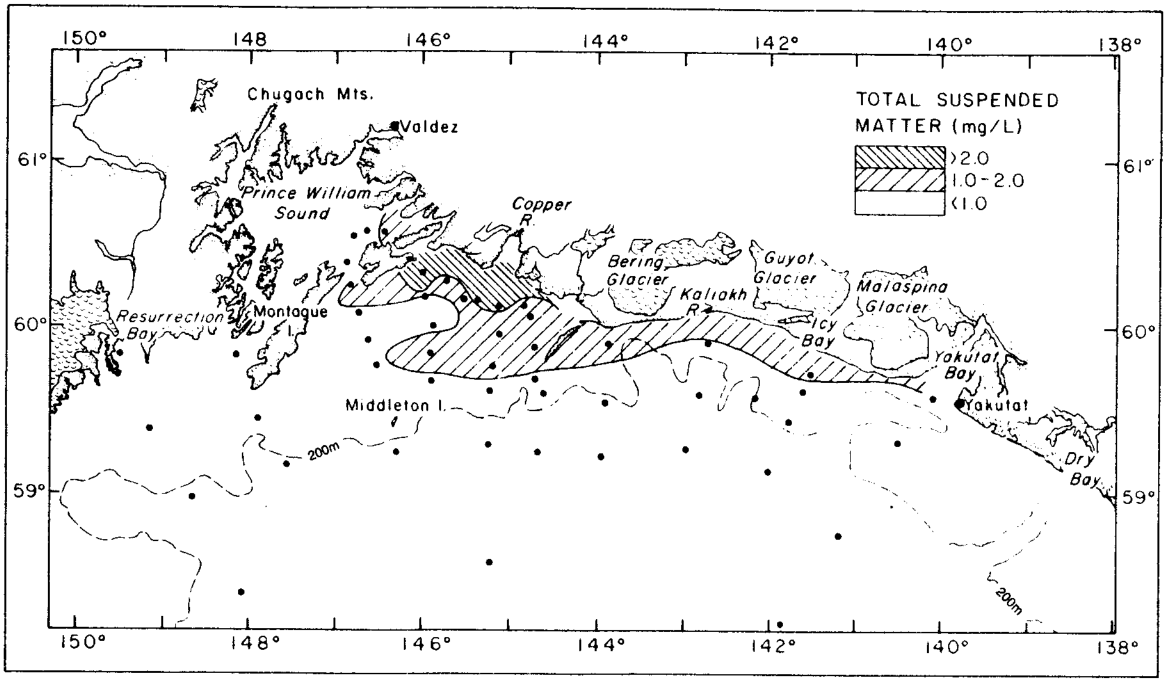

Figure 12. Distribution of total suspended matter at the surface in the northeastern Gulf of Alaska (Cruise RP-4-Di-75C-I, 21 October - 10 November 1975).

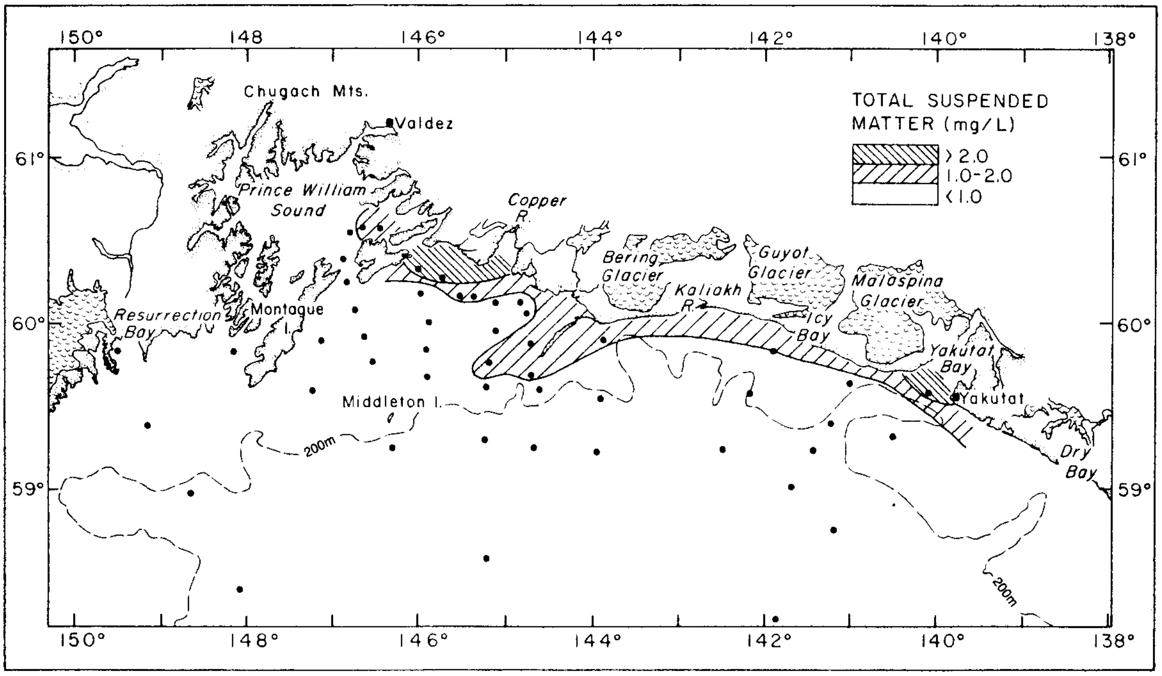

Figure 13. Distribution of total suspended matter at the surface in the northeastern Gulf of Alaska (Cruise RP-4-DI-76A-III, 13-30 April 1976).

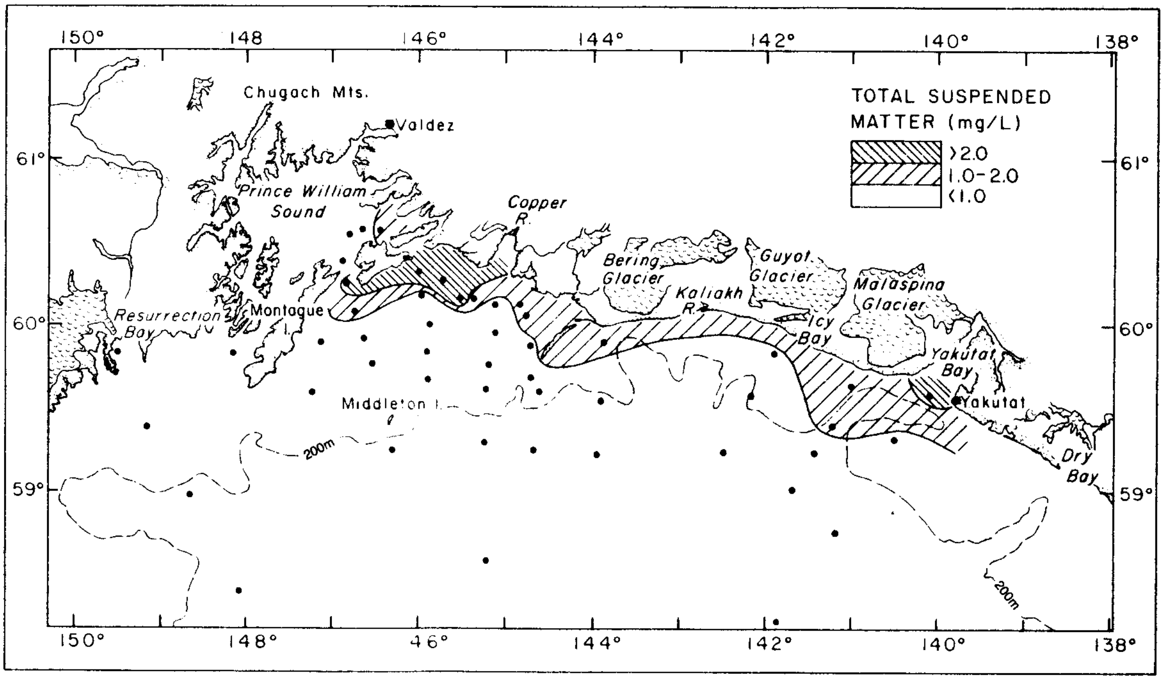

Figure 14. Distribution of total suspended matter at the surface in the northeastern Gulf of Alaska (Cruise RP-4-Di-76B-I, 19-31 July 1976).

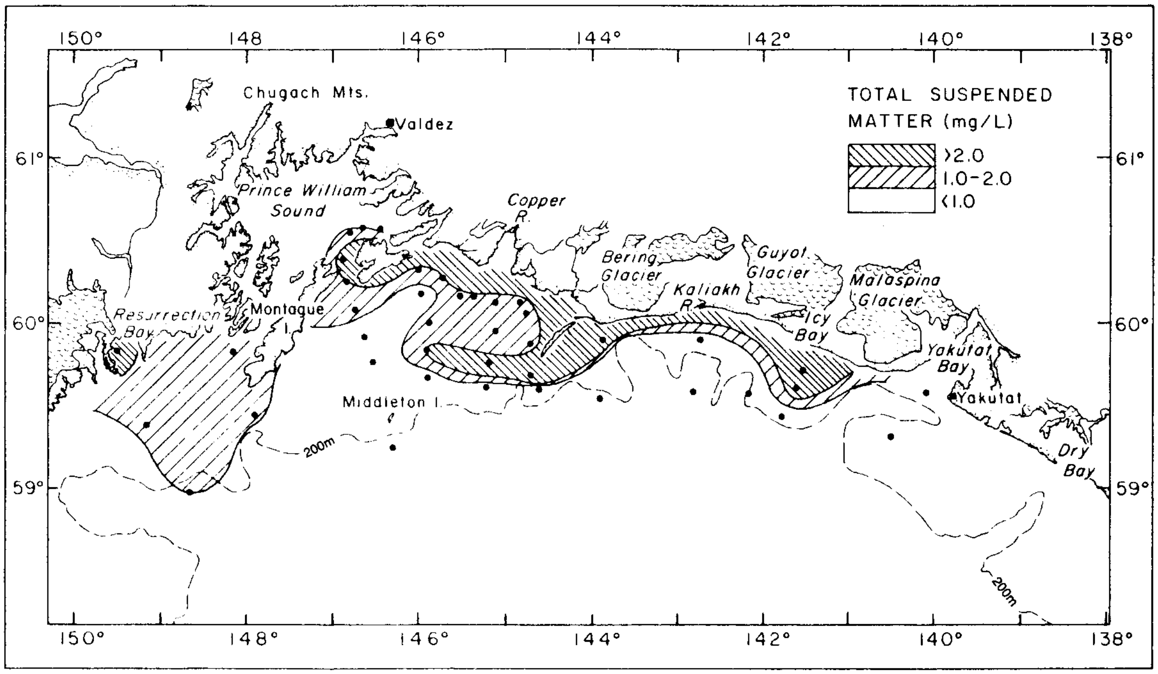

Figure 15. Distribution of total suspended matter at 5 meters above the bottom in the northeastern Gulf of Alaska (Cruise RP-4-Di-76B-I, 21 October - 10 November 1975).

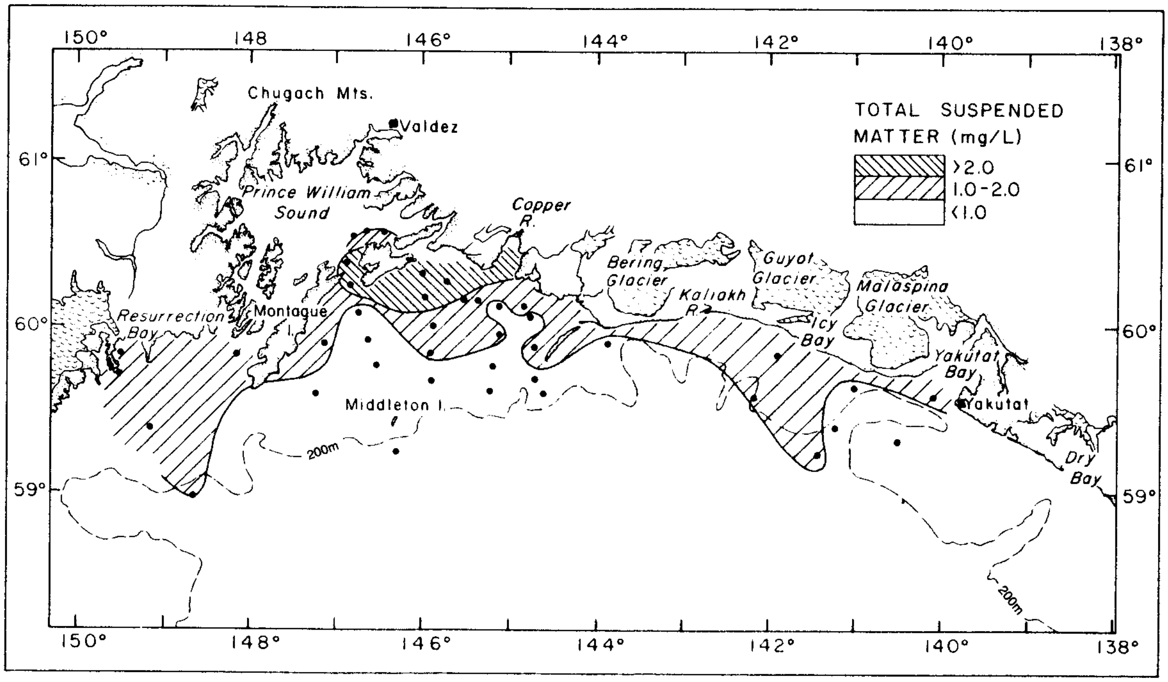

Figure 16. Distribution of total suspended matter at 5 meters above the bottom in the northeastern Gulf of Alaska (Cruise RP-4-Di-76A-III, 13-30 April 1976).

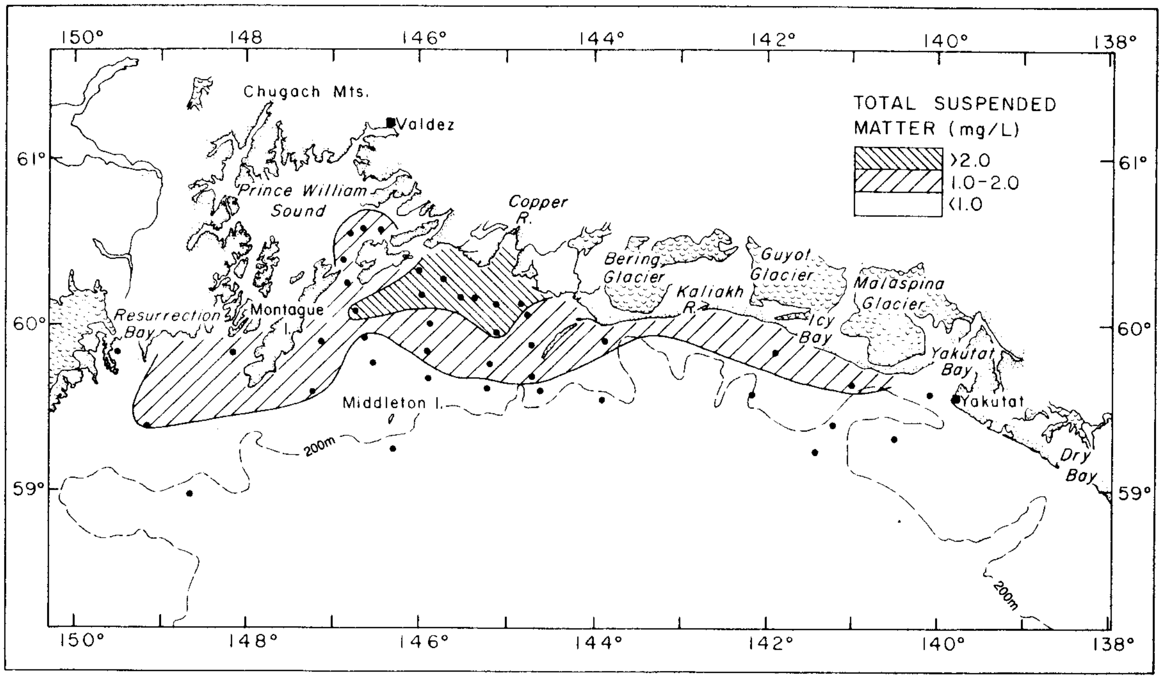

Figure 17. Distribution of total suspended matter at 5 meters above the bottom in the northeastern Gulf of Alaska (Cruise RP-4-Di-76B-I, 19-31 July 1976).

6.1.2 Elemental Composition of the Suspended Matter

Table 3 compares summaries of the data on the elemental composition of suspended matter from the Copper River with summaries of the surface and near-bottom suspended matter from the Gulf of Alaska. The data for the underlying sediments are given in table 4 and average element/Al ratios for the three cruises are given in table 5. The data for the Gulf surface suspended matter samples have been arranged into three groups. Group I contains all samples in which the sum of the major inorganic element concentrations (expressed as oxides) is greater than 75% of the total suspended load; samples containing inorganic sums ranging between 31% and 75% comprise Group II, and samples containing less than 31% inorganic sum are in Group III. In general, Group I samples are primarily composed of clay-sized terrestrial particles from the coastal rivers and are located in the nearshore stations and offshore from Kayak Island. Group II samples are composed of mixtures of terrestrial and biogenic matter and are located near the shelf break; and Group III samples are primarily composed of biogenic particles of marine origin and are found seaward of the shelf break.

The elemental compositions and element/Al ratios illustrate some compositional differences between near-shore (Group I) and offshore (Group III) suspended matter. Since most of the Al in marine particulate matter is located in aluminosilicate material (Sackett and Arrhenius, 1962) and because marine plankton contains only about 500 ppm Al by weight (Martin and Knauer, 1973), the Al concentrations in the suspended matter can be used to estimate aluminosilicate percentages in the particulate matter (Al x 10). Similarly, Gordon (1970) suggested that particulate C may also be used to estimate the amount of organic matter in the suspended matter by multiplying the particulate C content by a factor 1.8. Based on the particulate Al and particu-

TABLE 3

Summary of the elemental composition of particulate matter collected from the Copper River and the northeast Gulf of Alaska. The Copper River particulate matter was collected during high discharge conditions (June 1976) from a position 10 km landward of the river mouth. The 1σ precision values are from replicate analyses of a near surface sample. For the northeast Gulf of Alaska data groups, the 1σ averaging precision is given. Superscripts indicate the number of elemental values averaged when different from the number of samples in the respective group.

Sample Location	No. of samples	C Wt. %	N Wt. %	Al Wt. %	Si Wt. %	K Wt. %	Ca Wt. %	Ti Wt. %	Cr ppm	Mn ppm	Fe Wt. %	Ni ppm	Cu ppm	Zn ppm
Copper River	1	1.0 ± .5	.1 ± .1	9.3 ± .2	27.9 ± .5	1.8 ± .1	4.4 ± .1	.64 ± .01	126 ±13	1210 ± 50	6.7 ± .2	61 ± 5	63 ± 2	133 ± 5
October-November 1975														
Surface (Group I)	11	11.4[9] ±4.7	1.6[9] ± .8	10.2 ±1.3	29.7 ±2.1	1.5 ± .2	3.3 ±1.3	.57 ± .06	119 ±18	1200 ±120	6.5 ± .8	81 ±19	109 ±20	210 ±58
Surface (Group II)	6	33.8[5] ±5.9	4.7[5] ±1.2	4.1 ±1.7	18.0 ±5.6	0.6 ± .2	2.1 ± .9	.27 ± .07	75 ±30	660 ±140	3.1 ± .7	62 ±23	195 ±67	270 ±60
Surface (Group III)	2	48.8 ±8.1	6.2 ±1.6	1.5 ± .7	13.9 ±1.0	0.4 ± .3	2.4 ±1.1	.16 ± .13	47 ± 6	410 ±113	2.0 ± .7	58 ±20	116 ± 4	172 -
5 m above	12	11.3[10] ±5.8	1.4[10] ± .7	9.4 ±1.7	30.7 ±3.6	1.3 ± .3	2.3 ± .7	.50 ± .10	104 ±16	1170 ±210	6.1 ±1.2	79 ±22	100 ±18	184 ±30
April 1976														
Surface (Group I)	11	6.9 ±3.3	1.2[10] ± .7	10.3 ±1.3	30.8 ±2.2	1.5 ± .2	2.5 ± .8	.54 ± .08	113 ±20	1180 ± 80	6.3 ± .9	78 ±14	55[10] ±11	292 ±154
Surface (Group II)	6	18.3[5] ±6.9	3.4[5] ±1.0	4.8 ±1.9	19.0 ±7.2	0.6 ± .3	1.1 ± .3	.28 ± .09	67 ±14	740 ±180	3.1 ± .9	46 ±11	26 ±10	307 ±154

TABLE 3 (Continued)

Sample Location	No. of samples	C Wt. %	N Wt. %	Al Wt. %	Si Wt. %	K Wt. %	Ca Wt. %	Ti Wt. %	Cr ppm	Mn ppm	Fe Wt. %	Ni ppm	Cu ppm	Zn ppm
Surface (Group III)	6	23.7[5] ±2.1	4.3[4] ± .4	0.5[4] ± .3	19.0 ±14.0	0.1 ± .1	0.5 ± .3	.80 ± .06	35[4] ±14	260 ±210	1.3 ± .8	39[3] ± 7	30[3] ±4	237 ± 67
5 m above the bottom	11	4.8[10] ±1.7	0.8[10] ± .4	10.2 ± .6	30.6 ±1.5	1.5 ± .1	2.9 ± .5	.58 ± .04	116 ± 8	1160 ± 70	6.6 ± .3	79 ±16	56[10] ± 9	194 ± 36
<u>July 1976</u>														
Surface (Group I)	3	5.5 ±2.2	1.0 ± .5	10.3 ±1.0	31.3 ±1.0	1.7 ± .2	3.1 ± .7	.59 ± .10	103 ±18	1260 ± 81	6.5 ±1.0	65 ± 9	97 ± 6	248 ±51
Surface (Group II)	7	21.4 ±6.8	3.8[6] ±1.8	5.5 ±1.3	28.4 ±7.1	0.9 ± .2	1.3 ± .3	.28 ± .05	78 ±24	930 ±160	3.7 ± .5	55 ±12	125 ±38	264 ±152
Surface (Group III)	10	28.5 ±7.7	4.6[9] ±2.0	1.1[9] ± .7	15.8 ±6.7	0.4[9] ± .5	0.4 ± .2	.10 ± .03	68[7] ±45	340 ±200	1.4 ± .6	57[3] ±20	87 ±23	232 ±112
5 m above the bottom	15	4.8 ±3.6	0.7[14] ± .6	10.8 ± .7	31.3 ±1.6	1.6 ± .2	2.8 ± .6	.58 ± .05	119 ±15	1330 ±180	6.8 ± .6	67 ±15	95 ±18	214 ±56

TABLE 4

Summary of the elemental composition of sediment samples from the northeast Gulf of Alaska*

Sample Description	No of Samples	Al Wt. %	Ca Wt. %	Fe Wt. %	Mn ppm	Cr ppm	Ba ppm
	15	7.24 ±0.85	4.10 ±2.20	4.64 ±0.88	813 ±111	126 ±22	503 ±118

*Data from Robertson and Abel as reported in Burrell (1977).

TABLE 5

Summary of elemental ratios to aluminum for particulate matter samples from the Copper River and the Northeast Gulf of Alaska. The 1σ precision values were determined by propagation of errors from data given in table 3.

Sample Description	C/Al	N/Al	Si/Al	K/Al	Ca/Al	Ti/Al	Cr/Al $\times 10^{-3}$	Mn/Al $\times 10^{-3}$	Fe/Al	Ni/Al $\times 10^{-3}$	Cu/Al $\times 10^{-3}$	Zn/Al $\times 10^{-3}$
Copper River	.11 ±.05	.01 ±.01	3.0 ±.1	.19 ±.01	.48 ±.01	.07 ±.01	1.3 ±.1	13 ±1	.72 ±.03	.66 ±.02	.68 ±.03	1.4 ± -
October-November 1975												
Surface (Group I)	1.1 ±.5	.16 ±.08	2.9 ±.4	.15 ±.03	.32 ±.13	.06 ±.01	1.2 ±.2	12 ±2	.64 ±.11	.79 ±.21	1.1 ±.2	2.1 ±.6
Surface (Group II)	8.7 ±3.7	1.2 ±.6	4.4 ±2.3	.15 ±.08	.51 ±.31	.07 ±.03	1.8 ±1.1	16 ±8	.76 ±.36	1.5 ±.8	4.8 ±2.6	6.6 ±3.1
Surface (Group III)	33 ±16	4.1 ±2.2	9.3 ±4.4	.23 ±.23	1.6 ±1.1	.11 ±.10	3.1 ±1.5	27 ±15	1.3 ±.8	3.9 ±2.2	7.7 ±3.6	11 ± -
5 m above the bottom	1.2 ±.7	.15 ±.08	3.3 ±.7	.14 ±.04	.24 ±.09	.05 ±.01	1.1 ±.3	13 ±3	.65 ±.17	.84 ±.28	1.1 ±.3	2.0 ±.5
April 1976												
Surface (Group I)	.67 ±.33	.12 ±.07	3.0 ±.4	.15 ±.03	.24 ±.08	.05 ±.01	1.1 ±.2	12 ±2	.61 ±.12	.76 ±.17	.53 ±.13	2.8 ±1.5
Surface (Group II)	3.8 ±2.1	.71 ±.35	4.0 ±2.2	.13 ±.07	.23 ±.11	.06 ±.03	1.4 ±.6	15 ±7	.65 ±.32	.96 ±.44	.65 ±.44	6.4 ±4.1
Surface (Group III)	47 ±29	8.6 ±5.2	38 ±36	.22 ±.21	1.00 ±.81	.16 ±.15	7.0 ±5.1	52 ± 52	2.6 ±2.2	7.8 ±4.8	6.0 ±3.7	47 ±31

TABLE 5 (Continued)

Sample Description	C/Al	N/Al	Si/Al	K/Al	Ca/Al	Ti/Al	Cr/Al $\times 10^{-3}$	Mn/Al $\times 10^{-3}$	Fe/Al	Ni/Al $\times 10^{-3}$	Cu/Al $\times 10^{-3}$	Zn/Al $\times 10^{-3}$
5 m above the bottom	.47 ±.17	.08 ±.14	3.0 ±.2	.15 ±.01	.28 ±.06	.06 ±.01	1.1 ±.1	11 ±1	.65 ±.05	.77 ±.16	.55 ±.09	1.9 ±.4
<u>July 1976</u>												
Surface (Group I)	.53 ±.22	.10 ±.05	3.0 ±.3	.17 ±.03	.30 ±.07	.06 ±.01	1.0 ±.2	12 ±1	.63 ±.11	.63 ±.11	.94 ±.11	2.4 ± 1.06
Surface (Group II)	3.9 ±1.5	.69 ±.37	5.2 ±1.8	.16 ±.05	.24 ±.08	.05 ±.02	1.4 ±.6	17 ±5	.67 ±.18	1.0 ±.3	2.3 ±.9	4.8 ±3.0
Surface (Group III)	25 ±18	4.2 ±3.2	14 ± 11	.34 ±.49	.40 ±.34	.09 ±.06	6.2 ±5.7	31 ±27	1.3 ±1.0	5.2 ±3.8	7.9 ±5.6	21 ±17
5 m above the bottom	.44 ±.33	.06 ±.06	2.9 ±.2	.15 ±.02	.26 ±.06	.05 ±.01	1.1 ±.2	12 ±2	.63 ±.07	.62 ±.14	.88 ±.18	2.0 ±.5

late C concentrations, approximately 103 (±13)% and 15 (±6)%, respectively, of the suspended matter from Group I is aluminosilicate material and organic matter. Within the statistical limits of the measurements, nearly all the elemental concentrations of the Group I samples are the same as the river samples, indicating that the coastal rivers are the major source of the inorganic material. Only particulate C and N show significant enrichments over the river suspended matter; this is probably due to production of organic matter in near-shore waters (Larrance et al., 1977).

In contrast to the near-shore samples, the offshore samples (Groups II and III) are significantly depleted in particulate Al, Si, K, Ti, Cr, Mn, Fe, Ni, and Zn; and are enriched in particulate C and N. These depletions are attributed to a drop in the relative amount of aluminosilicate material in the suspended matter (<15% by weight for the Group III samples) and an increase in the proportion of organic matter (>40% by weight), which is depleted in these elements relative to aluminosilicate material (Martin and Knauer, 1973). Particulate Cu is relatively depleted in the samples taken during the spring cruise and enriched in the samples taken during the summer cruise. This may be due to selective uptake of Cu by some planktonic organisms during a particular phase of their growth cycle, as suggested by the data of Morris (1971) and again by Martin and Knauer (1973).

Table 5 shows the average elemental concentration ratios to Al for the samples from the various groups. The Si/Al and C/Al ratios from Group III are considerably elevated over ratios for the river samples. This is due to the presence of biogenic Si and biogenic C in the suspended matter. Price and Calvert (1973) and Feely (1975) demonstrated that the amount of biogenic Si and biogenic C can be estimated by assuming a constant Si/Al and C/Al ratio due to suspended aluminosilicates and terrestrial C, respectively. Any excess Si and

C is assumed to be of biogenic origin. Using the Si/Al and C/Al of the suspended material from the Copper River, values of approximately 14 (±12)% and 29 (±19)% by weight of the Group III samples are estimated to be composed of biogenic Si and biogenic C, respectively. In contrast, it is estimated that on the average, the Group I samples only contain about 8% by weight biogenic C and < 1% biogenic Si.

In similar fashion, examination of the element/Al ratios for the other elements reveal that: N/Al, Ni/Al, Cu/Al, and Zn/Al ratios from Group III are considerably elevated (> 2X) over ratios for the river samples; Ca/Al, Cr/Al, Mn/Al, and Fe/Al ratios are moderately (1-2X) elevated over ratios for the river samples; and K/Al and Ti/Al ratios are virtually the same as the ratios for the river samples. These data are taken as evidence for concentration of N, Ca, Cr, Mn, Fe, Ni, Cu, and Zn in biogenic phases in offshore waters. These results are consistent with the general conclusion of Wallace et al., (1977) that biogenic matter regulates the concentrations of particulate metals in offshore surface waters where aluminosilicate concentrations are low.

Table 3 also summarizes the elemental composition of suspended matter samples taken from 5 m above the bottom. With the exception of particulate C and N, the major and trace elements in the near-bottom suspended matter have about the same concentration as the river samples. These data suggest that the coastal rivers, which are the major source of the near-shore surface suspended matter, are also the major source for the near-bottom material. As stated by Feely et al., (1979), this is caused by a number of processes, including: offshore transport and subsequent sinking of near-shore surface material captured by gyres; downwelling and offshore transport of near-shore surface material in winter; and resuspension and offshore transport of previously deposited sediments.

6.2 Lower Cook Inlet

6.2.1 Particulate Matter Distribution and Transport

Figures 18 through 22 show the distribution of suspended matter at the surface and 5 m above the bottom for the April and July 1977 cruises in lower Cook Inlet and Shelikof Strait. As shown in figures 18, 20, and 22, the surface particulate matter distributions are characterized by unusually high horizontal gradients. On the eastern side particulate concentrations were relatively low, ranging from 0.5 mg/L near Cape Elizabeth to about 5.0 mg/L near Cape Ninilchik. On the western side suspended loads increased rapidly from concentrations around 5.0 mg/L in the vicinity of Kamishak Bay to concentrations greater than 100 mg/L north of Tuxedni Bay. The salinity and temperature data for these cruises show very similar horizontal distribution patterns, illustrating the predominance of the inflowing relatively clear saline Gulf of Alaska water on the eastern side and the outflowing turbid low salinity water from upper Cook Inlet on the western side. The outflowing turbid water is transported to the southwest past Augustine Island and Cape Douglas into Shelikof Strait where it continues to mix with the oceanic water and the suspended matter is dispersed. The near-bottom suspended matter distributions (figs. 19 and 21) are very similar to the surface distributions, suggesting that cross-channel gradients in the suspended matter distributions exist throughout the water column.

The seasonal data show some characteristic patterns which apparently are consistent from year to year. First, the outward-flowing brackish water on the western side is colder in May 1978 and warmer in August-September than the inward-flowing Gulf of Alaska water (Feely and Massoth, in press). This feature is consistent with data obtained in April and July 1977 (figs. 18 and 20) and May 1979, and appears to be related to the temperature of the

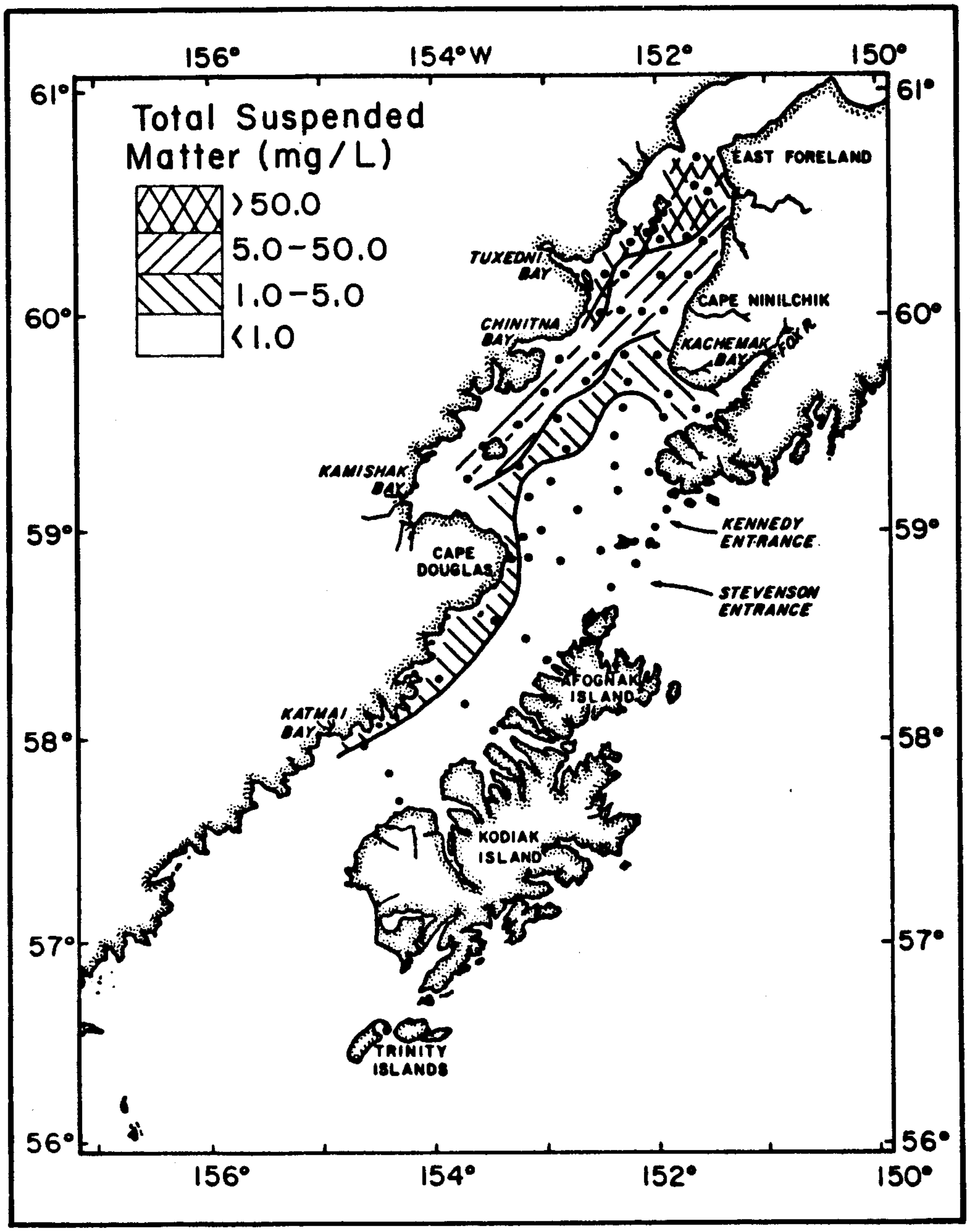

Figure 18. Distribution of total suspended matter at the surface (Cruise RP-4-Di-77A-IV, 4-16 April 1977).

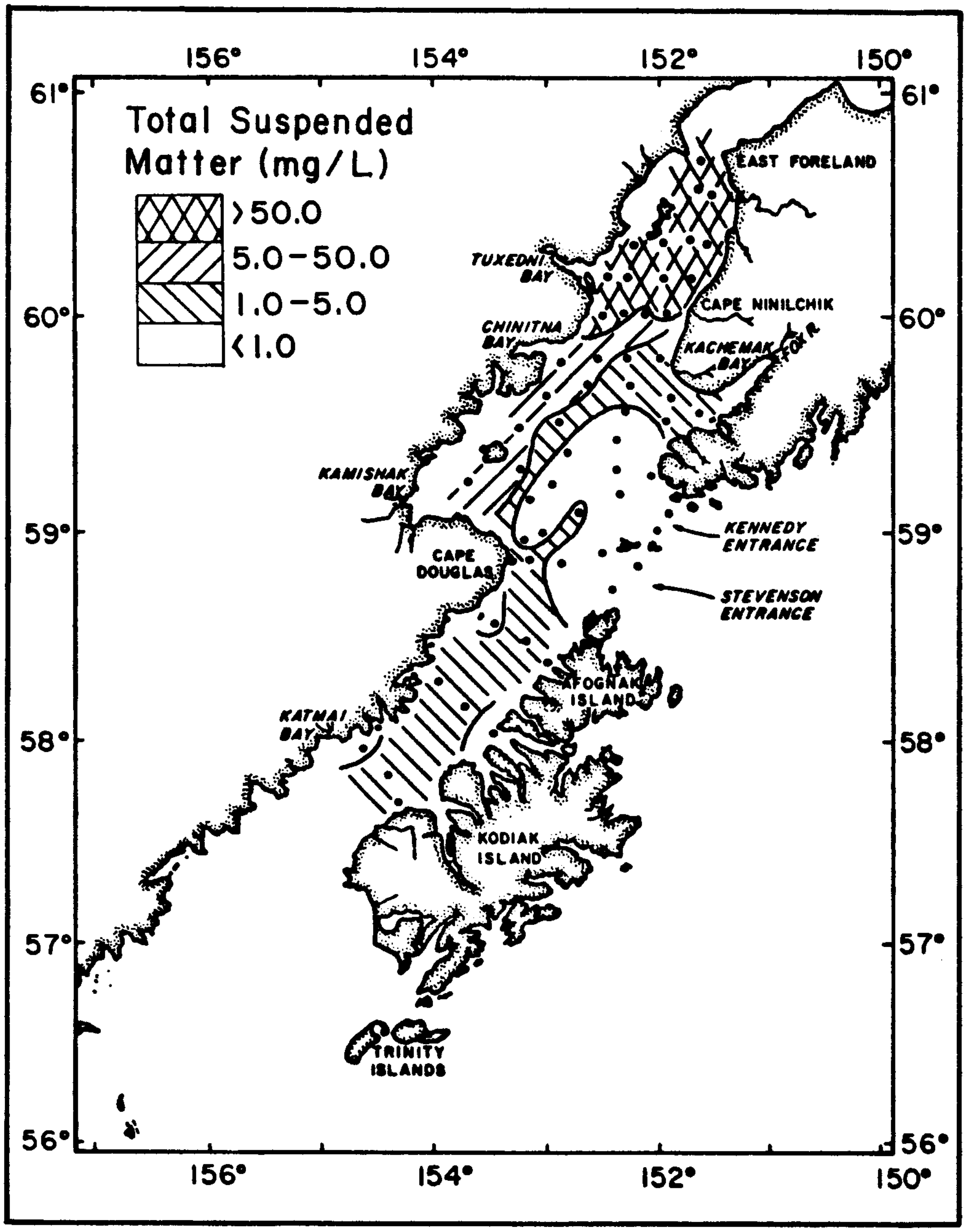

Figure 19. Distribution of total suspended matter at 5 m above the bottom (Cruise RP-4-Di-77A-IV, 4-16 April 1977).

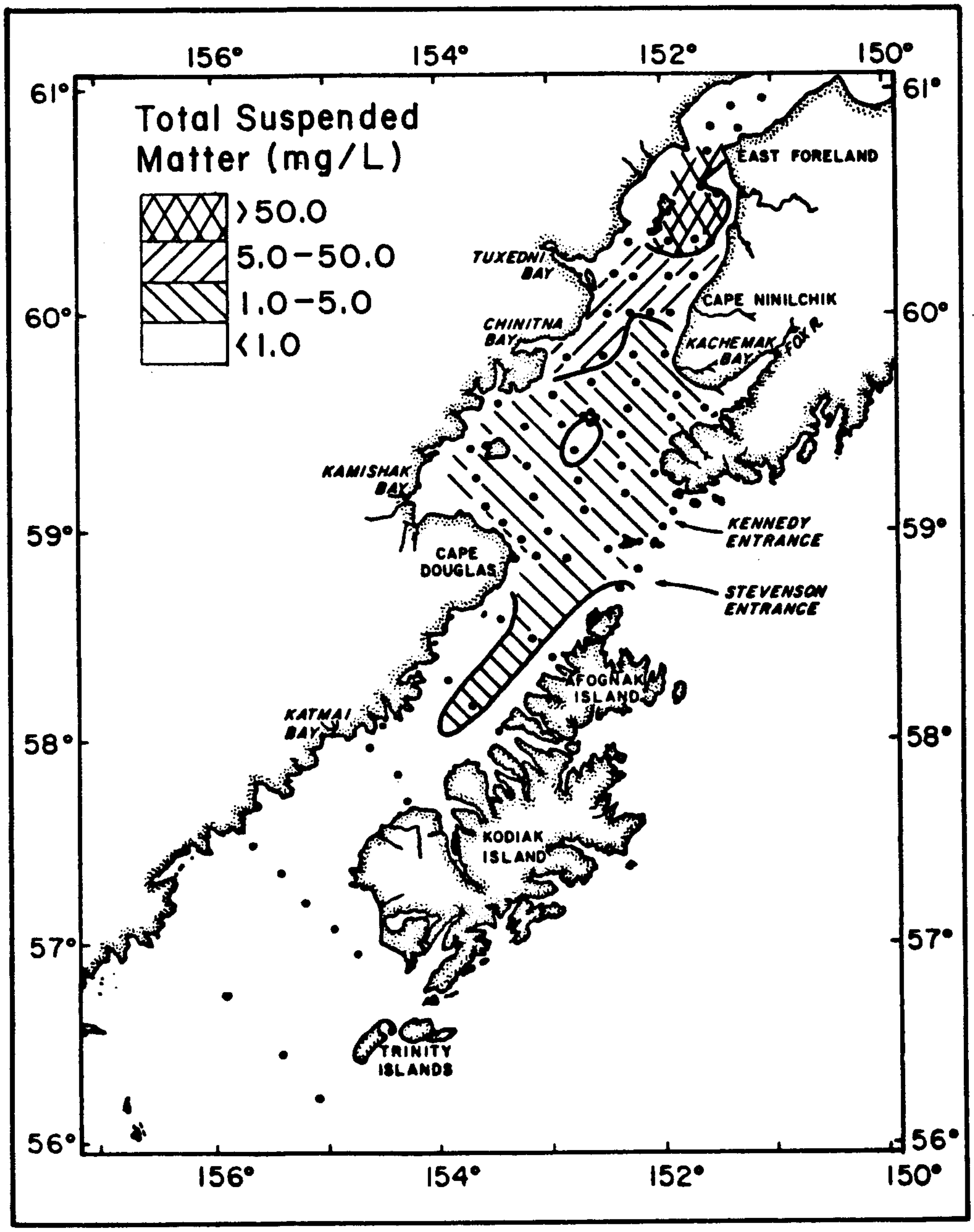

Figure 20. Distribution of total suspended matter at the surface (Cruise Acona-245, 28 June - 12 July 1977).

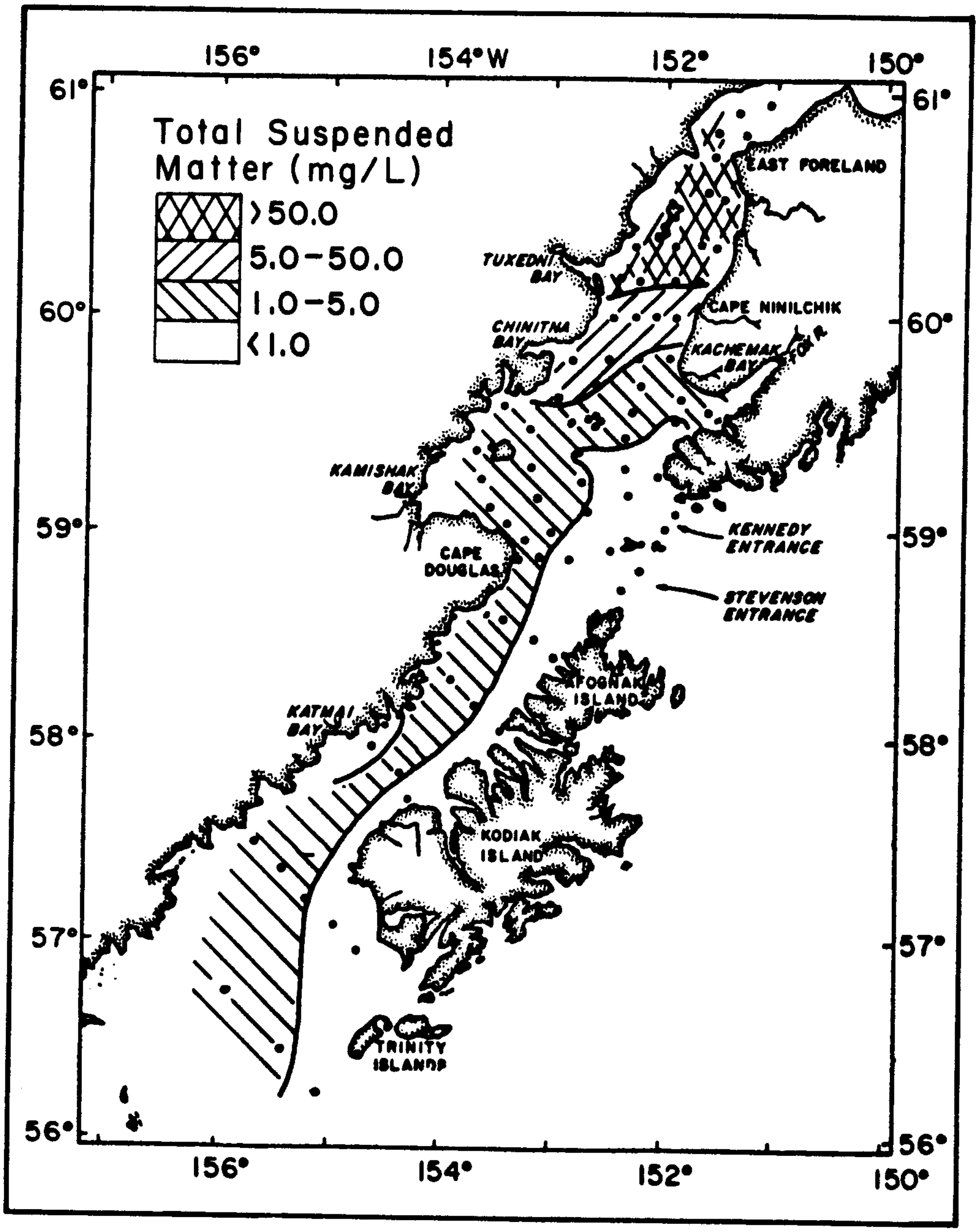

Figure 21. Distribution of total suspended matter at 5 m above the bottom (Cruise Acona-245, 28 June - 12 July 1977).

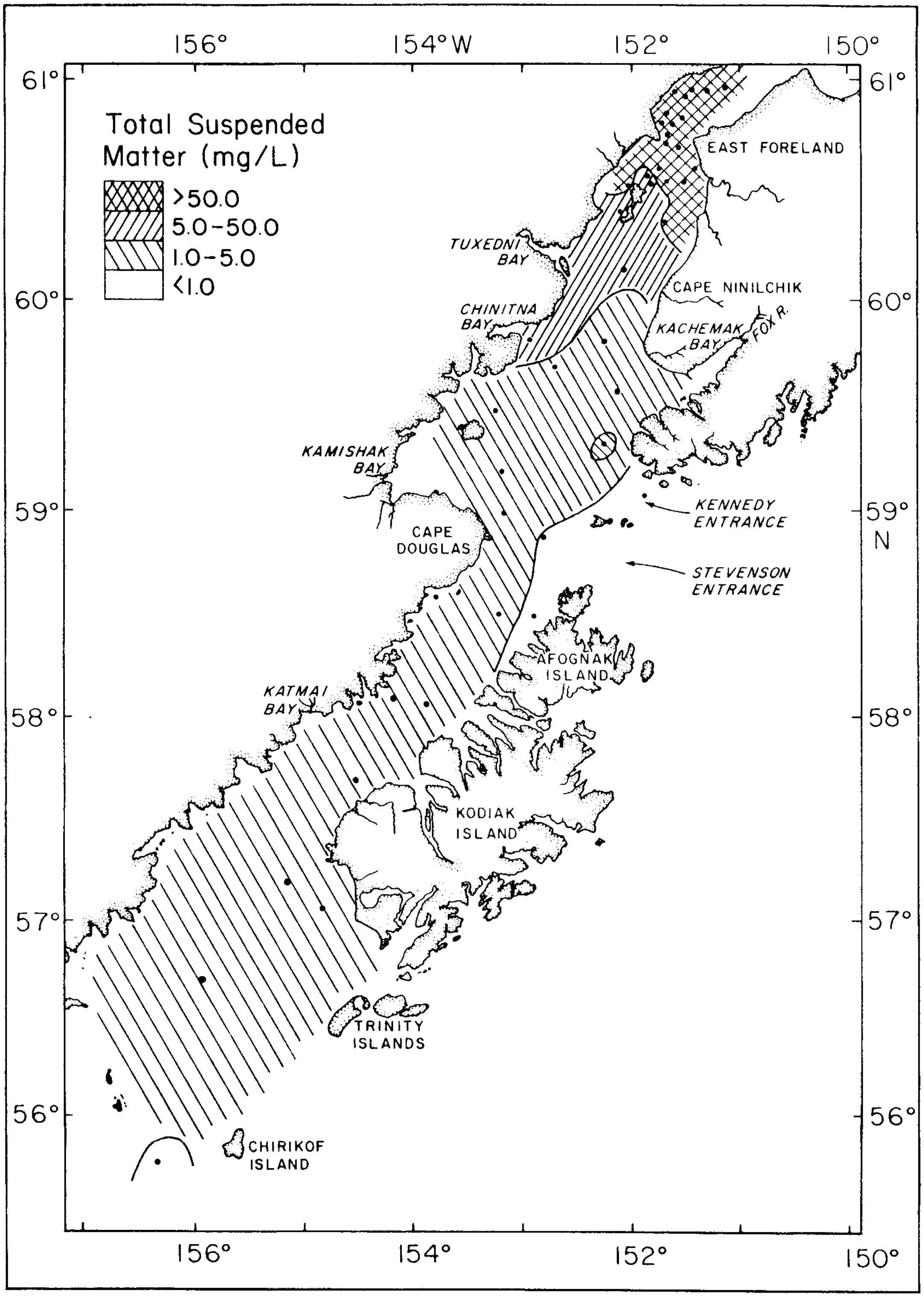

Figure 22. Distribution of total suspended matter at the surface (Cruise RP-4-Di-79A-II, 7-20 May 1979).

the in-flowing river water and shows larger seasonal variations due to the larger fluctuations of temperature over the continental land masses. Furthermore, suspended-matter concentrations in the Kamishak Bay region are higher in early spring than in late summer even though there is more freshwater input into Cook Inlet during late summer (Gatto, 1976). A possible explanation for this phenomenon is that early spring is usually the time when most of the ice breakup occurs in upper Cook Inlet. Resuspension and transport of previously deposited sediments may result from the ice movement. Another possibility is that if the currents are strong, there is less time for mixing and dilution of ambient suspended matter. This probably is true to some degree as the April 1977 data show higher suspended matter concentrations and lower salinities than the May 1978 data (Feely and Massoth, in press). However, this cannot be the only explanation because the July and October 1977 data show relatively low suspended matter concentrations (<2.0 mg/L) in Kamishak Bay waters without extensive mixing with seawater (i.e., salinity $\cong 30^{o}/oo$). Nevertheless, the data suggest that more river-borne suspended matter is transported out of the inlet and into Shelikof Strait during early spring than during the summer.

Above the Forelands, suspended matter concentrations range from 120 mg/L starting at about the Forelands (fig. 22) to values greater than 1000 mg/L near the mouths of the Susitna River and Knik Arm (Sharma et al., 1974). Suspended matter distributions in this region are totally dependent upon input from the rivers and tidal mixing. Sharma (1979) states that the amount of suspended matter varies considerably throughout the Foreland region during each tidal cycle, with significant quantities of suspended material being carried south of the Forelands during ebb tide.

Since suspended matter may play an important role in scavenging and transporting contaminants from the study region, the question of where the large amount of suspended materials that pass into lower Cook Inlet ultimately reside becomes important. The dramatic decrease in suspended loads from > 100 mg/L near the Forelands to < 1.0 mg/L near the inlet's mouth may be an indication of particulate settling. However, recent studies of major sediment types in lower Cook Inlet indicate that the sediments in the central part of the inlet consist primarily of unconsolidated coarse-grained sands deposited during the retreat of the Pleistocene glaciers (Bouma and Hampton, 1976). Another possibility is that the suspended matter gradients are the result of dilution of the brackish water by the less turbid oceanic water. Figure 23 shows a scatter plot of the relationship between total suspended matter and salinity for the surface samples from the central region of lower Cook Inlet, where the cross-channel gradients are highest. The data, which were from the April 1977 cruise, show that the suspended loads are linearly correlated with salinity, indicating that dilution is the major process controlling suspended matter concentrations in the central portion of the inlet. A scatter plot for the July 1977 data shows similar results. These results suggest that the central part of lower Cook Inlet acts like a conduit, allowing large amounts of suspended material to pass through the system with little net sedimentation. Sedimentation of suspended matter is occurring in the numerous small embayments along the coast.

Figures 24 and 25 show vertical cross-sections of temperature, salinity, total suspended matter, and sigma-t for stations located in Shelikof Strait. The data were obtained on the August-September cruise. Stations SS2, SS5, SS6, SS8, SS9, SS10, and SS12 represent a longitudinal cross-section along the axis of the Strait. Stations SS4 through SS6 and SS11 through SS13 represent transverse cross-sections at midchannel and at the upper mouth, respectively. The data show cross-channel gradients of temperature, salinity, and suspended matter which are consistent with the cross-channel gradients in lower Cook Inlet. This is the strongest evidence to date which suggests that riverborne suspended matter from Cook Inlet is transported into Shelikof Strait. There is also evidence for a near-bottom nepheloid layer in the strait which exists in the lower 50-60 m of the water column. Since there are no corresponding large changes in temperature and salinity which would tend to buoy up suspended material, the bottom nepheloid layer in this region is probably due to resuspension of bottom sediments. This suggests that sediments and/or contaminants probably get redistributed in the strait before final deposition occurs.

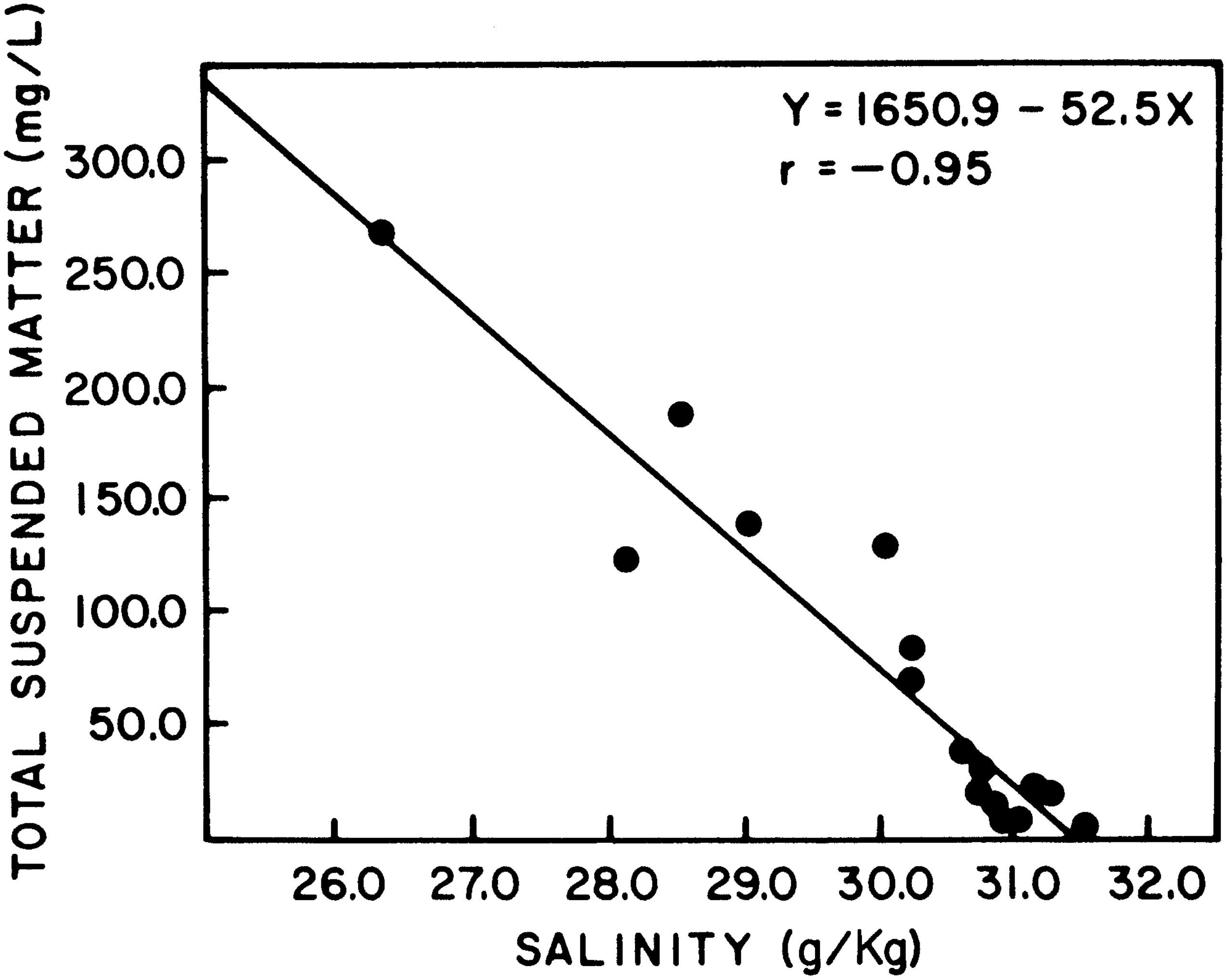

Figure 23. Scatter plot of the relationship between total suspended matter and salinity for surface samples from lower Cook Inlet (Cruise RP-4-Di-77A-IV, 4-16 April 1977).

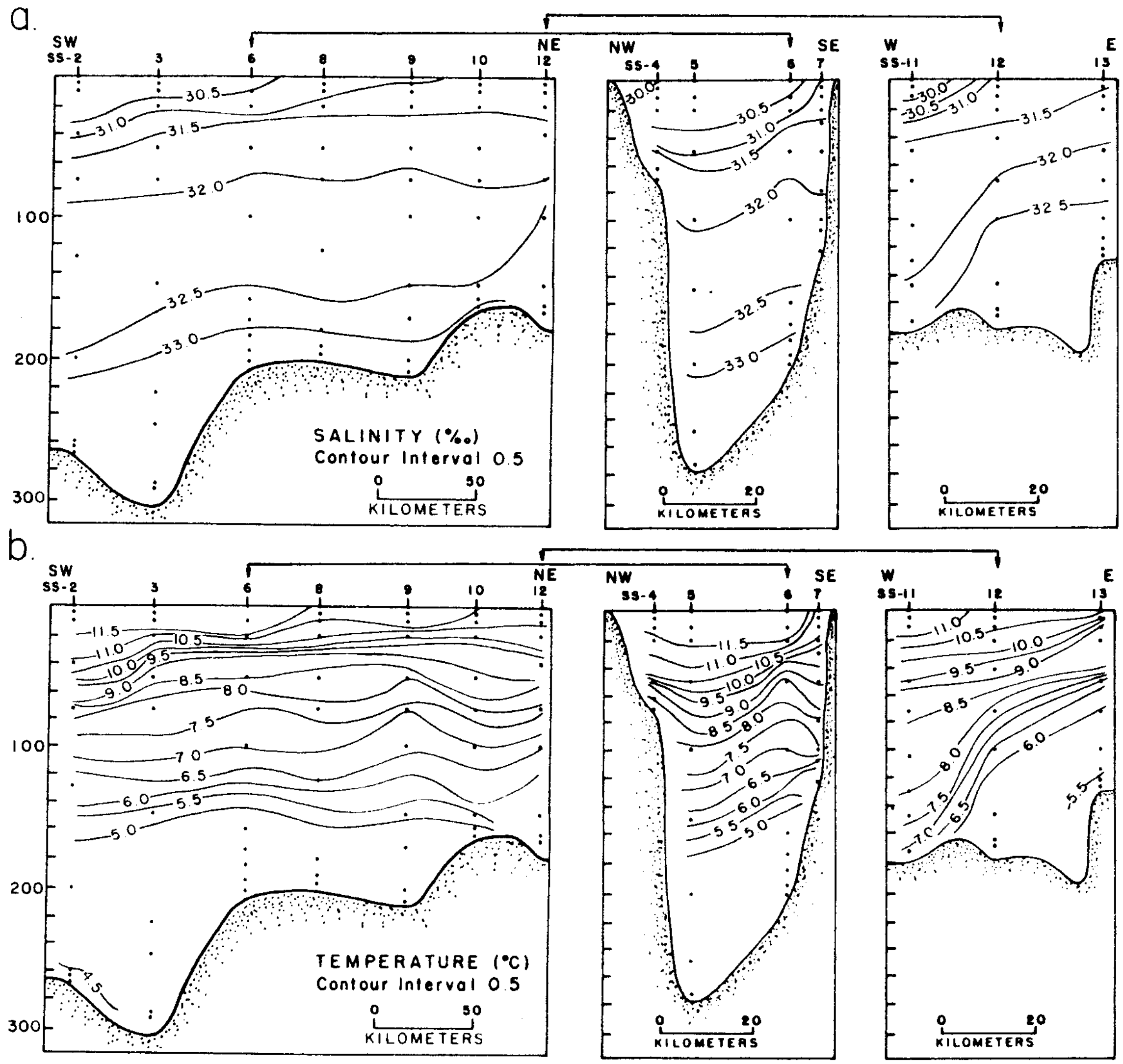

Figure 24. Vertical cross-sections of the distributions of: a. salinity; and b. temperature for stations SS-2 thru SS-13 in Shelikof Strait (Cruise RP-4-Di-78B-II, 22 August - 6 September 1978).

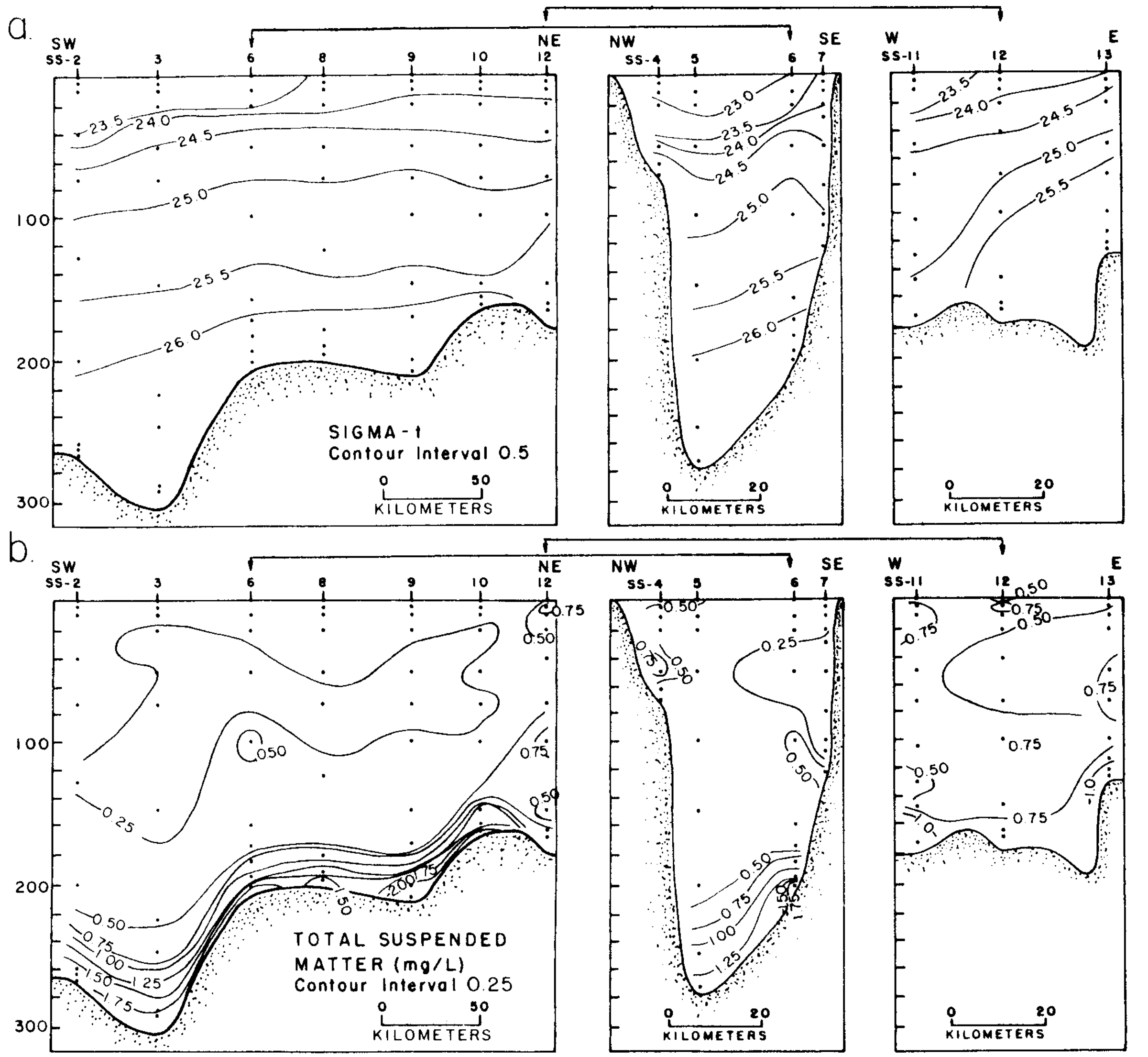

Figure 25. Vertical cross-sections for the distributions of: a. sigma-t; and b. total suspended matter for stations SS-2 thru SS-13 in Shelikof Strait (Cruise RP-4-Di-78B-II, 22 August - 6 September 1978).

6.2.2 Sedimentation Studies

During Cruise RP-4-MF-78A-11 (19 May-4 June 1978), three moorings, each supporting one set of tandem sediment traps located 10 m above the bottom, were deployed along a transect line extending from Kamishak Bay to Kachemak Bay in lower Cook Inlet (fig. 5). The purpose of the traps was to obtain long-term averages of the vertical fluxes of suspended matter in selected regions of lower Cook Inlet. The sediment trap capture period was set for closure approximately 85 days after deployment, which occurred on 27 May 1978. Of the six sediment traps deployed, four were recovered. The two sediment traps from station ST-3 were accidentally dredged up by the fishing vessel, Columbian, and the samples were lost. In addition, one sample from the sediment traps at ST-2 was also lost due to breakage of the sodium azide diffusion cup during recovery. Table 6 summarizes the particulate matter fluxes obtained by gravimetric analysis of the material captured by the traps. Also included are the mean particulate fluxes obtained by Larrance (1978) for short-term sediment trap deployments at CB-1, CB-4, and CB-7. The long-term flux at ST-1 is about the same as the mean value obtained by Larrance for traps deployed at CB-1 (20.8 g m^{-2} d^{-1} vs. 22.0 g m^{-2} d^{-1}). This suggests that the two locations are very similar in their sedimentation characteristics and the data from the two sets of traps can be intercompared. The long-term sediment flux at ST-2 was 2.4 times greater than the mean of the sediment fluxes at CB-4 (28.5 g m^{-2} d^{-1} vs. 12.0 g m^{-2} d^{-1}). While these stations were less than 15 nautical miles apart (fig. 5), these differences are probably real because station ST-2 is within the region dominated by the outward-flowing brackish water and station CB-4 is in the region influenced by the inward-flowing Gulf of Alaska water. Presumably, a significant fraction of the suspended matter in the outward-

TABLE 6. Comparison of sedimentation rates of suspended materials collected by sediment traps deployed on moorings approximately 10 m above the bottom at selected locations in lower Cook Inlet with average accumulation rates of the underlying sediments as determined by ^{210}Pb geochronology.

Location	Station No.	Average Sedimentation Rate of Suspended Matter ($g\ m^{-2}\ d^{-1}$)	Average Accumulation Rate of Sediments ($g\ m^{-2}\ d^{-1}$)
Kamishak Bay	CB-1*	22.0 ± 25	27.1
	ST-1	20.8 ± 7	2.2
Central Inlet	CB-4*	12.0 ± 8	no data
	ST-2	28.5	no data
Kachemak Bay	CB-7*	18.8 ± 2	10.5

*After Larrance and Chester (1979).

flowing brackish water settles out in Kamishak Bay. These data are consistent with the ^{210}Pb sediment accumulation rates for the underlying sediment cores (table 6). The good agreement between the sedimentation rate and the sediment accumulation rate for CB-1 in Kamishak Bay indicates that this region is a depositional environment for the fine-grained material that originates from upper Cook Inlet.

In order to obtain a more detailed picture of the long-term sedimentation history of fine-grained sediments in lower Cook Inlet and Shelikof Strait, sediment cores were collected during three of the cruises for ^{210}Pb geochronological studies. The locations of the gravity cores obtained are illustrated in fig. 26. The cores were cut into 2-cm sections and delivered to C.W. Holmes and E.A. Martin (U.S. Geological Survey, Corpus Christi, Texas) who performed the ^{210}Pb analyses. No cores were collected from the central basin of lower Cook Inlet although numerous attempts were made. The sediments there are primarily composed of relict sands and gravels (Bouma and Hampton, 1976) which did not remain intact during recovery of the gravity corer. The results of the ^{210}Pb radiometric analyses are given in table 7. The data show that the major regions of sedimentation in decreasing order of importance are: Shelikof Strait, Kamishak Bay, and Kachemak Bay. Using the sediment distribution map of Bouma and Hampton (1976) for lower Cook Inlet, it is estimated that the areas of active sedimentation are 750 km^2 in Kamishak Bay and 60 km^2 in Kachemak Bay. Averaging the ^{210}Pb sediment accumulation rates for these two regions (i.e., 0.66 g cm^{-2} y^{-1} in Kamishak Bay and 0.38 g cm^{-2} y^{-1} in Kachemak Bay) and multiplying by the area of active sedimentation yield estimates of annual sediment accumulations of 4.9×10^{12} g y^{-1} and 2.3×10^{11} g y^{-1}, respectively, for these two regions. This represents only about 18% of the total annual input of fine-grained sediments to Cook Inlet from the rivers

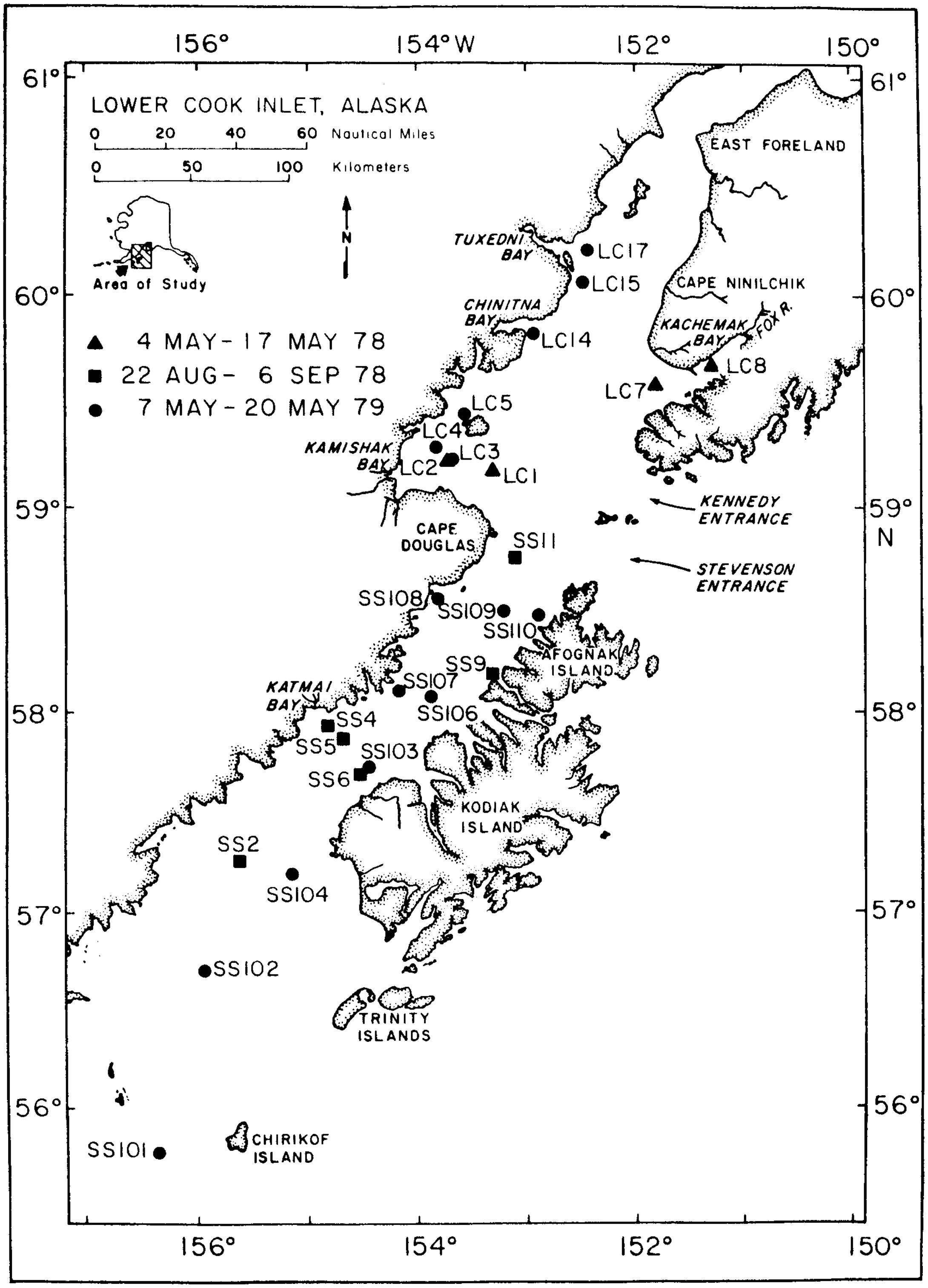

Figure 26. Locations of stations where gravity cores have been collected for the determination of excess ^{210}Pb activity.

estimated to be approximately 2.8×10^{13} g y^{-1}, Gatto, 1976; Sharma, 1979). The remaining 82% must either be deposited in upper Cook Inlet or transported in Shelikof Strait. Since the sediments of upper Cook Inlet also consist primarily of relict sands and gravels (Sharma and Burrell, 1970; Sharma et al., 1979), we believe that the major fraction of fine-grained sediments that originates in Cook Inlet is transported to Shelikof Strait where it is deposited. This conclusion is supported by ^{210}Pb data for Shelikof Strait. Using the 100 m contour as the upper limit of the region of active sedimentation in the upper third of the Strait and the 200 m contour as the upper limit of the region of active sedimentation in the lower Strait, an area of 9200 km^2 is estimated to be the region of active sedimentation. This region was divided into three sections and average accumulation rates were computed for each (i.e., 0.8 g cm^{-2} y^{-1} for the upper third; 0.7 g cm^{-2} y^{-1}; for the middle third; and 0.6 g cm^{-2} y^{-1} for the bottom third). Multiplying the sediment accumulation rates by the respective areas and obtaining the sum yields an estimate of the annual sediment accumulation rate of 6.2×10^{13} g y^{-1} for Shelikof Strait between Cape Douglas and the Trinity Islands. This value is approximately 220% of the annual input of fine-grained sediments from the rivers discharging into Cook Inlet. This suggests that additional sources of fine-grained sediments are required to balance this accumulation rate. The recent findings of Feely and Massoth (in press) indicate that suspended sediments in Shelikof Strait consist of a mixture of clay-sized suspended material from Cook Inlet, terrigenous sediments from the Copper River in the northeast Gulf of Alaska, and biogenic material produced in the water column. If these materials form the bulk of the fine-grained sediments in Shelikof Strait then the sedimentological data presented here would indicate that the sediments of Shelikof Strait are probably composed of nearly a 40:60 mixture of Cook Inlet-derived material and Copper River-derived material.

Table 7. Sediment accumulation rates for sediment cores collected from lower Cook Inlet and Shelikof Strait. Accumulation rates were determined by the excess ^{210}Pb method.[1]

Station No.	Position	Depth (m)	Core Acquired Month/Year	Accumulation Rate ($g\ m^{-2}\ d^{-1}$)
SS101	55°46.8'N, 156°22.1'W	245	May 1979	DNA[2]
SS102	56°42.8'N, 155°56.7'W	292	May 1979	16.7
SS104	57°11.2'N, 155°07.8'W	225	May 1979	DNA
SS2	57°17.1'N, 155°37.0'W	278	Sept.1978	DNA
SS4	57°55.3'N, 154°48.4'W	152	Sept.1978	DNA
SS5	57°52.1'N, 154°42.9'W	273	Sept.1978	17.8
SS6	57°42.4'N, 154°29.1'W	208	Sept.1978	20.3
SS103	57°43.0'N, 154°26.7'W	208	May 1979	16.7
SS106	58°03.5'N, 153°51.7'W	194	May 1979	37.2
SS107	58°05.2'N, 154°09.2'W	285	May 1979	DNA
SS9	58°11.3'N, 153°21.1'W	210	Sept.1978	DNA
SS108	58°32.9'N, 153°47.2'W	51	May 1979	22.5
SS109	58°28.9'N, 153°12.9'W	168	May 1979	8.8
SS110	58°28.2'N, 152°53.6'W	192	May 1979	DNA
SS11	58°46.4'N, 153°08.3'W	186	Sept.1978	NA[3]
LC1	59°11.5'N, 153°19.2'W	38	May 1978	2.2
LC2	59°14.4'N, 153°40.9'W	33	May 1978	27.1
LC3	59°13.4'N, 153°40.7'W	35	May 1979	DNA
LC4	59°16.4'N, 153°50.6'W	24	May 1979	9.3
LC5	59°25.6'N, 153°35.5'W	26	May 1979	DNA
LC7	59°34.1'N, 151°37.1'W	79	May 1978	10.4
LC8	59°39.3'N, 151°16.7'W	30	May 1978	5.2
LC14	59°46.9'N, 152°55.5'W	27	May 1979	DNA
LC15	60°03.5'N, 152°28.4'W	30	May 1979	DNA
LC17	60°14.2'N, 152°23.6'W	48	May 1979	NA

[1] Data prepared by C. W. Holmes and E. A. Martin, U.S.G.S., Corpus Christi, Texas

[2] DNA - data not available

[3] NA - no excess ^{210}Pb detected

6.2.3 Elemental Composition of the Particulate Matter

The particulate matter collected during the six cruises in lower Cook Inlet have been analyzed using a variety of methods to determine how the elements are distributed in the particles. Total elemental composition of the particulate matter was determined by the x-ray fluorescence and atomic absorption techniques described in section 5 of this report. Trace elements associated with the easily oxidizable organic matter and manganese oxyhydroxide coatings were determined on selected samples from 1978 time series stations at CB-7, CB-9, and CB-10. The results of these studies are described below.

Tables 8 through 10 compare summaries of the data on the total elemental composition of suspended matter from the Susitna, Knik, and Matanuska Rivers with summaries of the surface and near-bottom data for the April and July 1977 cruises in lower Cook Inlet. Within the statistical limits of the measurements, the samples from lower Cook Inlet have very nearly the same major element composition as the samples from the rivers. This is especially true for Al, K, Ti, and Fe which have been shown to be almost exclusively associated with aluminosilicate minerals of terrestrial origin (Price and Calvert, 1973). The high concentrations of these elements in the surface and near-bottom samples from lower Cook Inlet indicate that aluminosilicate minerals are the most dominant (80-95%) solid phase in the particulate matter.

These results are not surprising since the Susitna, Matanuska and Knik Rivers supply about $15\text{-}20\times10^6$ tons of sediment annually to the inlet (Rosenberg and Hood, 1967).

Table 8. Summary of the elemental composition of particulate matter samples from the major rivers discharging into Cook Inlet. (Surface samples were obtained with a precleaned 4-L polyethylene bottle extended from a bridge 26 June 1977.)

Element	Susitna River	Matanuska River	Knik River
C (Wt.%)	1.04	0.55	0.75
N (Wt.%)	0.06	0.03	0.05
Mg (Wt.%)	4.28	3.02	4.30
Al (Wt.%)	10.39	8.57	12.90
Si (Wt.%)	36.12	28.53	36.32
K (Wt.%)	2.62	1.54	2.73
Ca (Wt.%)	2.33	2.37	1.33
Ti (Wt.%)	0.63	0.55	0.67
Cr (ppm)	172	112	182
Mn (ppm)	1308	1157	1206
Fe (Wt.%)	6.45	6.07	6.90
Ni (ppm)	94	43	70
Cu (ppm)	71	49	61
Zn (ppm)	186	106	152
Pb (ppm)	56	25	51

Table 9. Summary of the elemental composition of particulate matter samples from lower Cook Inlet (Cruise RP-4-Di-77A-IV, 4-16 April 1977).

Element	Average of 50 surface samples	Average of 50 samples from 5 m from the bottom
C (Wt.%)	4.01 ± 4.0	2.72 ± 2.5
N (Wt.%)	0.65 ± 0.5	0.41 ± 0.4
Mg (Wt.%)	3.54 ± 0.6	3.47 ± 0.9
Al (Wt.%)	3.64 ± 1.6	8.70 ± 1.6
Si (Wt.%)	31.04 ± 3.4	30.20 ± 4.3
K (Wt.%)	2.15 ± 0.4	2.24 ± 0.4
Ca (Wt.%)	2.20 ± 0.4	2.23 ± 0.3
Ti (Wt.%)	0.55 ± 0.1	0.58 ± .07
Cr (ppm)	95 ± 15	99 ± 16
Mn (ppm)	1313 ± 113	1326 ± 159
Fe (Wt.%)	6.22 ± 1.0	6.42 ± 0.8
Ni (ppm)	61 ± 10	63 ± 10
Cu (ppm)	71 ± 15	76 ± 17
Zn (ppm)	165 ± 32	176 ± 34
Pb (ppm)	56 ± 13	56 ± 12

Tables 9 and 10 also summarize the elemental composition of 50 samples taken 5 m above the bottom. In general, the major element concentrations of the near-bottom samples are similar to the surface samples. This is especially true for the April 1977 cruise and in the northern part of the inlet where the water column is well mixed. However, during the July 1977 cruise and in the southern part of the inlet the water column was vertically stratified and the elemental composition of the suspended matter showed some differences between the surface and 5 m above the bottom. For example, figure 27 shows vertical cross-sections of particulate C and C/N ratios for the May and August-September 1978 cruises. The August-September data show higher particulate C concentrations at the surface than at the bottom, indicating a vertical stratification of the particulate organic matter. Similar vertical gradients are not easily discernible in the May 1978 or April 1977 data which suggests that in early spring the waters are extremely well-mixed with respect to water properties and suspended matter.

The vertical cross sections of particulate C also show significant cross channel gradients in both spring and summer data, with the highest concentrations and vertical gradients occurring at stations located in Kachemak Bay. Larrance et al. (1977) state that phytoplankton productivity and standing stocks of chlorophyll a are highest in Kachemak Bay and decrease steadily to low values in the middle of the inlet. These data suggest that the observed variations of particulate C are directly related to production of marine organic matter in the inlet, with Kachemak Bay being the most productive. This is probably the result of a number of factors, including: (1) upwelling of nutrient-rich subsurface waters in the region northwest of the Chugach Islands (Burbank, 1977); (2) stratification and stabilization of the surface waters due to formation of two gyre systems (Burbank, 1977 and Larrance et

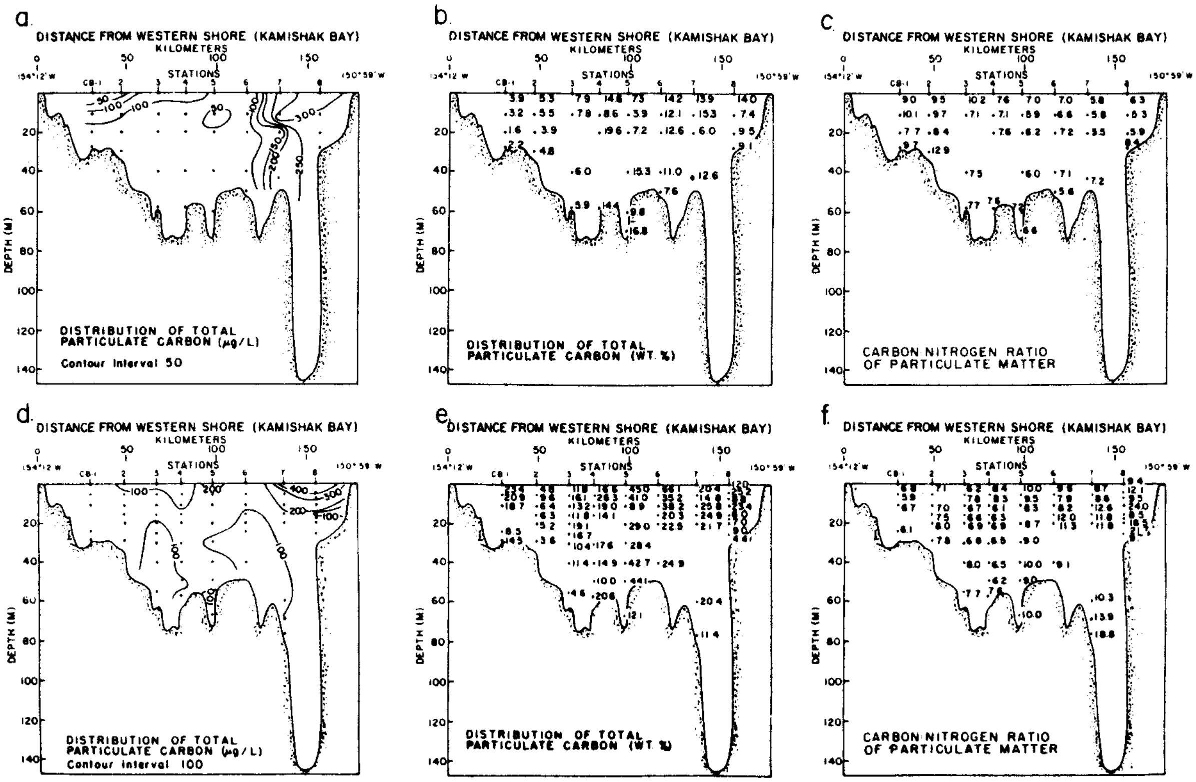

Figure 27. Vertical cross-sections of the distributions of: a. particulate carbon in units of μg/L; b. particulate carbon in weight percent of the suspended matter; and c. carbon to nitrogen atom ratios for stations CB-1 thru CB-8 in lower Cook Inlet (Cruise RP-4-Di-78A-III, 4-17 May 1978).

Table 10. Summary of the elemental composition of particulate matter from lower Cook Inlet and Shelikof Strait (Acona-245, 28 June - 12 July 1977).

Element	Lower Cook Inlet: Average of 50 Surface Samples	Lower Cook Inlet: Average of 51 Samples from 5 m above the Bottom	Shelikof Strait: Average of 17 Surface Samples	Shelikof Strait: Average of 16 Samples from 5 m above the Bottom
C (Wt.%)	10.77 ± 11.0	6.18 ± 9.0	31.17 ± 11.2	8.40 ± 5.8
N (Wt.%)	1.98 ± 2.0	0.99 ± 1.4	4.89 ± 1.5	1.24 ± 0.8
Mg (Wt.%)	2.86 ± 1.41	3.59 ± 0.82	1.89 ± 0.91	4.01 ± 1.22
Al (Wt.%)	6.98 ± 4.24	8.88 ± 2.34	3.72 ± 2.46	9.49 ± 3.20
Si (Wt.%)	35.75 ± 5.56	38.09 ± 4.92	28.67 ± 10.10	44.71 ± 3.60
K (Wt.%)	1.86 ± 0.86	2.24 ± 0.45	0.89 ± 0.43	2.19 ± 0.63
Ca (Wt.%)	1.84 ± 0.63	2.23 ± 0.32	1.53 ± 0.35	2.08 ± 0.33
Ti (Wt.%)	0.46 ± 0.20	0.58 ± 0.10	0.27 ± .09	0.53 ± 0.12
Cr (ppm)	99 ± 30	115 ± 24	75 ± 36	116 ± 29
Mn (ppm)	1138 ± 574	1460 ± 362	981 ± 709	4174 ± 7642
Fe (Wt.%)	5.14 ± 2.11	6.50 ± 0.95	3.15 ± 1.14	6.39 ± 1.71
Ni (ppm)	70 ± 25	81 ± 16	59 ± 19	77 ± 13
Cu (ppm)	99 ± 33	100 ± 31	94 ± 27	112 ± 30
Zn (ppm)	352 ± 158	343 ± 194		
Pb (ppm)	65 ± 19	69 ± 13	60 ± 10	76 ± 22

al., 1977); and (3) deeper light penetration due to input of relatively non-turbid oceanic water from the Gulf of Alaska.

Undoubtedly, some of the organic matter that is produced in the Kachemak Bay region settles to the bottom and gets buried within the sediments. However, since the net circulation is to the north and back again to the southwest into Shelikof Strait, a significant fraction of the organic matter produced in Kachemak Bay probably gets deposited in Shelikof Strait. This means that the two regions are linked by physical, chemical, and biological processes. While detailed information on chemical and biological processes in Shelikof Strait are unavailable at this time, data from the August-September cruise are available which tend to support the hypothesis that the two regions are linked by chemical processes. Figure 28 shows the distributions of particulate C and particulate Mn in Shelikof Strait. The enrichment of particulate Mn in the near-bottom waters is probably due to release of reduced Mn from the sediments. This process occurs in regions of high productivity and high sedimentation (Graham et al., 1976). While data on regional productivity in Shelikof Strait are unavailable at this time, the data suggest that there is a positive correlation between particulate C and Mn in the near-bottom waters and that lower Cook Inlet is probably a major source for the organic matter. Although limited to a great extent, these data indicate that physical and chemical processes occurring in dynamic environments in lower Cook Inlet directly affect bottom water chemistry in the less dynamic environments of Shelikof Strait. If any of these processes are altered, either by natural or artificial means, the major effect might be observed in Shelikof Strait. If this is the case, then environmental parameters monitored in Shelikof Strait may be sensitive indicators of subtle changes occurring in the inlet.

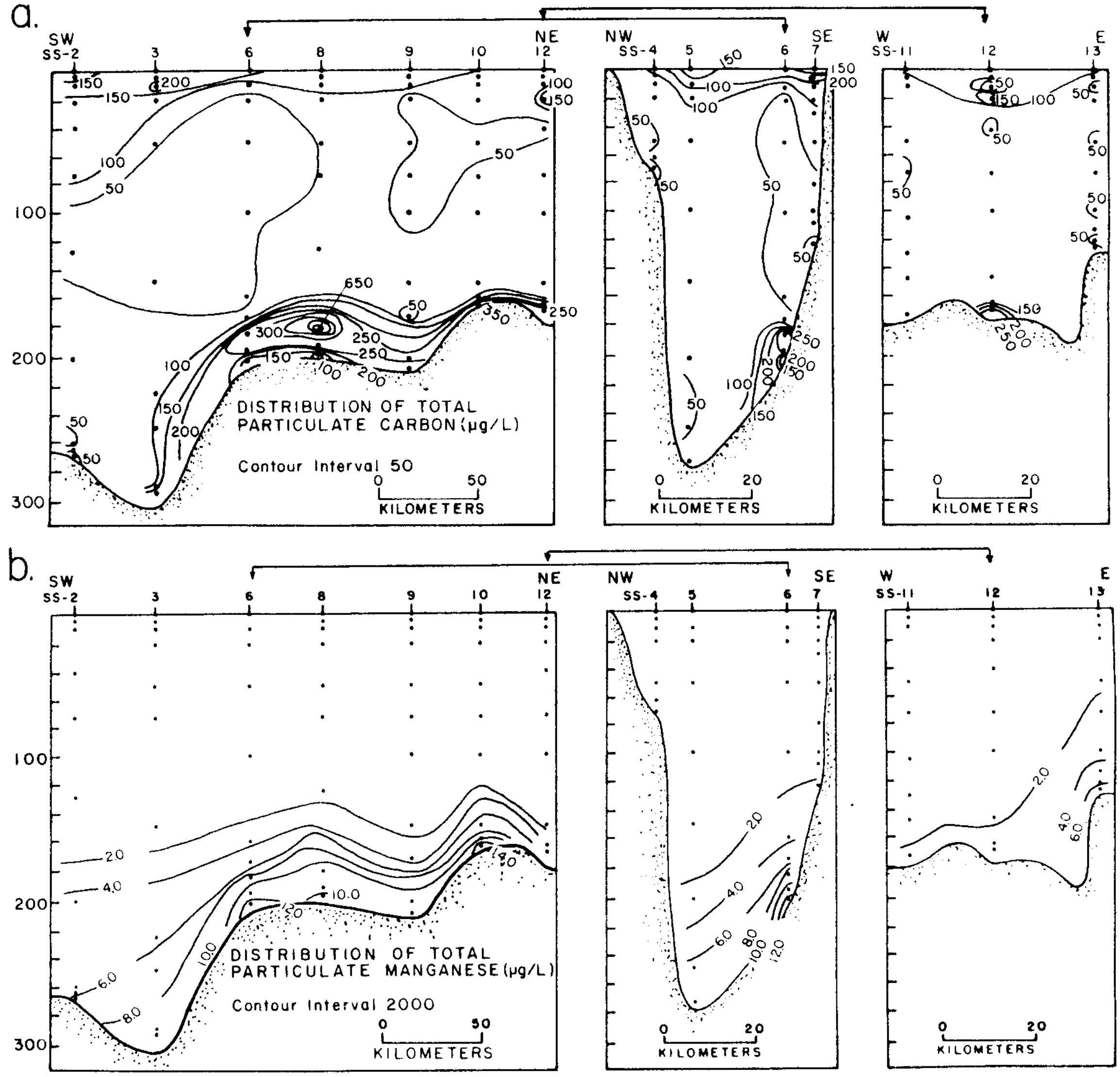

Figure 28. Vertical cross-sections of the distribution of: a. total particulate carbon; and b. total particulate manganese for stations SS-2 thru SS-13 in Shelikof Strait (Cruise RP-4-Di-78B-II, 22 August - 6 September 1978).

6.2.4 Extractable Elements in the Particulate Matter

During the May and August-September 1978 cruises, large volume particulate samples were collected on 142 mm Nuclepore filters for the purpose of providing information on the potential availability of trace elements to organisms. Water was collected at the surface and 5 m above the bottom every 12 hours for 48 hours in Kachemak Bay (CB-7) and west of Kalgin Island (CB-9) in May (fig. 5), and east of Kalgin Island (CB-10) in August-September (fig. 6). In addition, a single surface sample was collected in May at CB-1 in Kamishak Bay (fig. 5). The samples were subjected to: (1) a peroxide treatment to release organically bound trace elements; (2) a 0.3 N HCl treatment to release elements associated with Fe-Mn oxyhydroxide coatings on particles; and (3) a total element analysis of untreated samples. A full description of the procedures is provided in section 5.

In contrast to the high degree of temporal variations of particulate material in the water column at CB-9 (Feely and Massoth, in press), the trace element content of the surface particulate material remained fairly constant (fig. 29). The average total elemental composition and the partitioning between organic and oxyhydroxide phase are listed in table 11. The major cation content of the particulate matter from CB-9 suggests that the source of this material was the illite-rich suspended material of the rivers flowing into upper Cook Inlet. The small amount of trace metals present in the peroxide extractable phase reflects the concentration and character of the particulate organic matter. Due to the turbidity associated with the high suspended matter concentrations, the biological productivity in this region is low (Larrance et al., 1977), resulting in organic matter comprising only 2% of the total weight of suspended material. This organic matter has a C/N ratio of 11.3 indicative of a terrestrial origin (Loder and Hood, 1972). Cu showed the highest degree of organic association with 1.7% of the total Cu being present in peroxide extractable phase, followed by Mn and Cr each with 0.5%. The weak acid extraction released a major portion of the total Fe and Mn demonstrating the amorphous character of these metal oxides. Many of the trace elements were enriched in this component of the suspended matter. An average of 85% and 76% of the total Ni and Cu, respectively, were present in this phase, while half of the Zn and Cr were also present. The residual material, which is comprised of highly crystalline material, contained 90% of the Al and Pb, and a lesser fraction of the other metals. As a consequence of vertical mixing in this region, the elemental compositions and phase associations of the surface and near-bottom suspended matter samples were not significantly different ($p<0.05$). The time-series data at CB-10, east of Kalgin Island in September-August, showed the same constancy in elemental compositions and phase associations (fig. 30). There were no significant differences ($p<0.05$) between surface and near bottom samples in the fall time series. Comparison of the two time-series data in the Kalgin Island region showed no differences in elemental compositions nor phase associations. In summary, the Kalgin Island region is characterized by a highly fluctuating amount of suspended matter of a constant composition. This suspended matter is composed primarily of structured aluminosilicates coated with Fe-Mn oxyhydroxides. With the exception of Pb and Zn, these coatings contain the largest fraction of trace elements in the particulate matter. The small amount of organic matter present is of terrestrial origin and contains less than 2% of the total amount of trace metals present in suspension.

Water originating from the Kalgin Island region flows along the western side of lower Cook Inlet where a major portion is diverted into Kamishak Bay (Muench et al., 1978). Consistent with this observation, the major element composition of Kamishak Bay suspended material reflects the dominance of illite material similar to that found in upper Cook Inlet. (Feely and Massoth, in press). However, analysis of a single large volume surface sample from Kameshak Bay shows enrichments of Cr, Cu, Ni, Zn, and Pb relative to that of Kalgin Island (table 12). Although organic matter comprises 6% of the suspended material, the increased amount of metals in the peroxide extractable phase cannot account for the enrichments of the whole sample. Examination of the weak-acid extractable phase suggests that the additional Zn, Cu, and Pb were associated with a weakly structured phase while the additional Cr and Ni were present in a highly crystalline phase. These enrichments are probably due to either resuspension of bottom material or a source of trace metal-enriched illite material transported by local rivers flowing into Kamishak Bay.

Unlike the upper Cook Inlet region, the suspended matter concentration in Kachemak showed smaller fluctuations with time and little difference with depth (fig. 31). However, the fluctuation in elemental composition and phase associations was greater than in upper Cook Inlet and there was significant difference between the composition of surface and bottom material (fig. 31 and table 12). The surface suspended material consisted of 35% organic matter and had a C/N ratio of 7.6, characteristic of a marine origin (Loder and Hood 1972). The remaining material consisted of 40% biogenic SiO_2 and 20% aluminosilicates. The marine origin of this material can also be seen in the trace element composition and phase association data (table 12). The surface suspended matter was depleted in all elements relative to terrestrial aluminosilicates. The Mn concentration of this material was 540 ppm while that of CB-9 was 1300 ppm. The greater organic matter content of the surface material resulted in increase in the amount of trace metal present in the peroxide extractable phase. In the

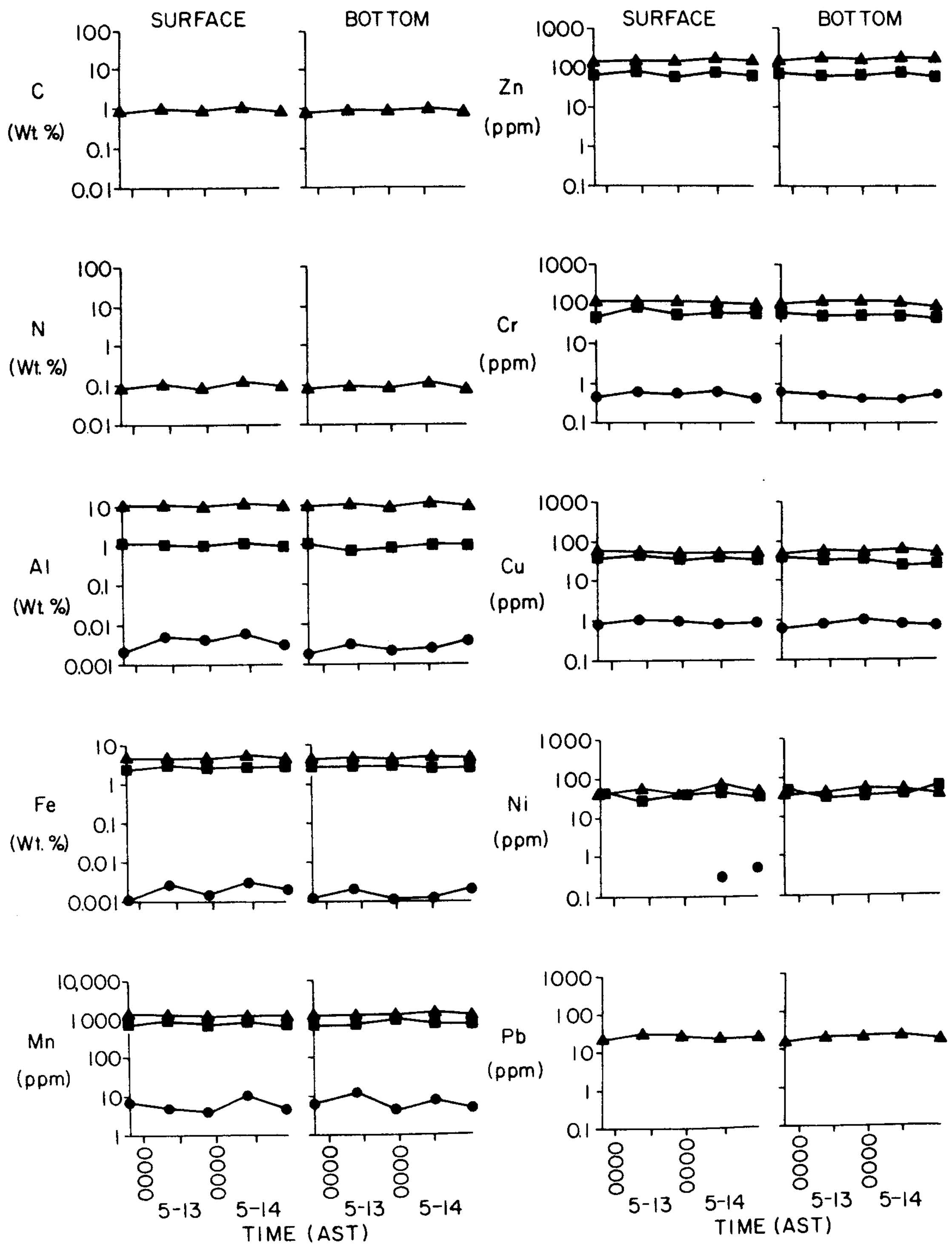

Figure 29. Temporal variations of major and trace elements in suspended matter (total concentration [▲], weak acid extractable [■], and peroxide extractable [●] from station CB-9 in lower Cook Inlet.) Samples were collected 13-14 May 1978.

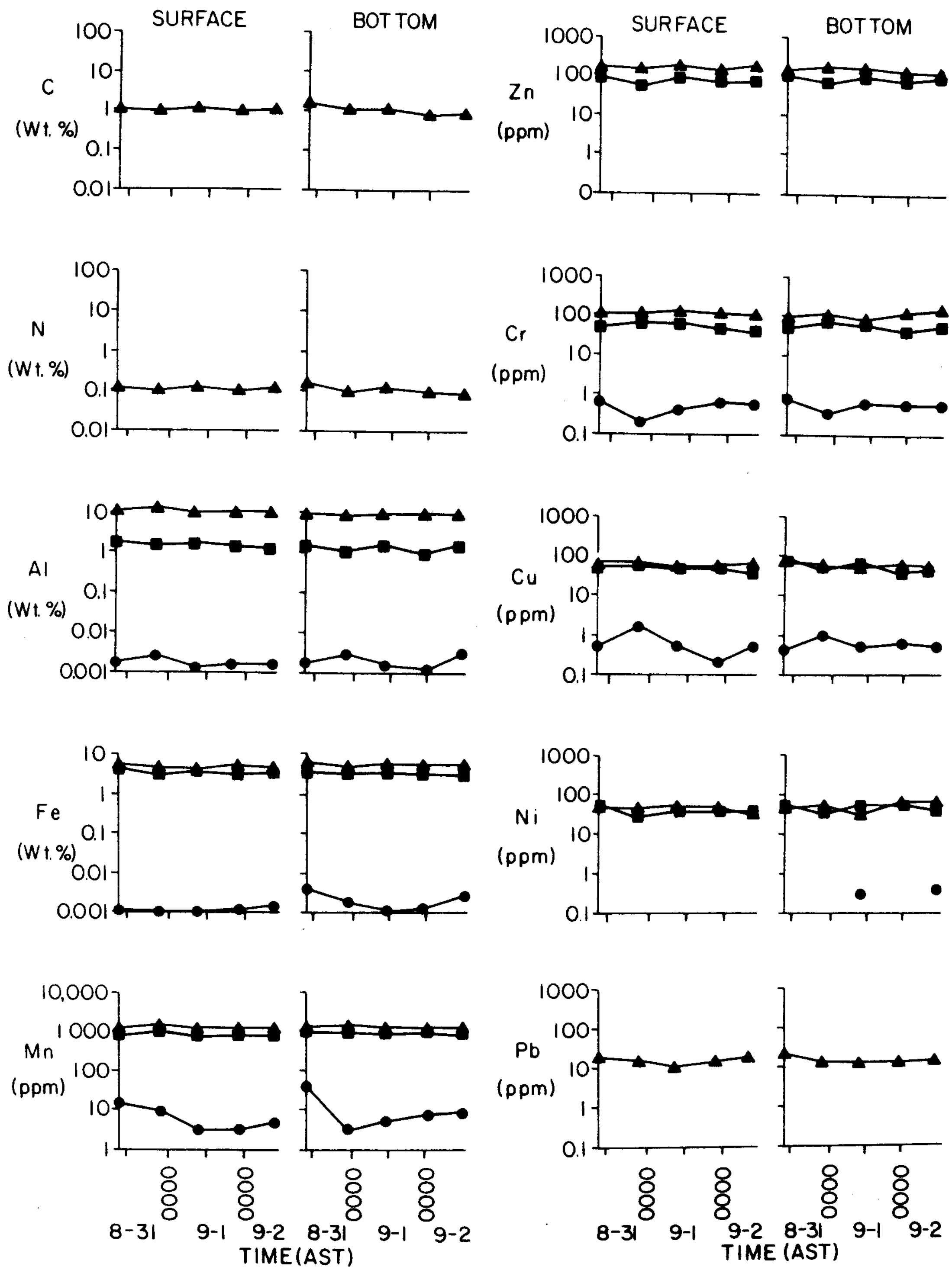

Figure 30. Temporal variations of major and trace elements in suspended matter (total concentration [▲], weak acid extractable [■], and peroxide extractable [●] from station CB-10 in lower Cook Inlet.) Samples were collected 31 August and 1-2 September 1978).

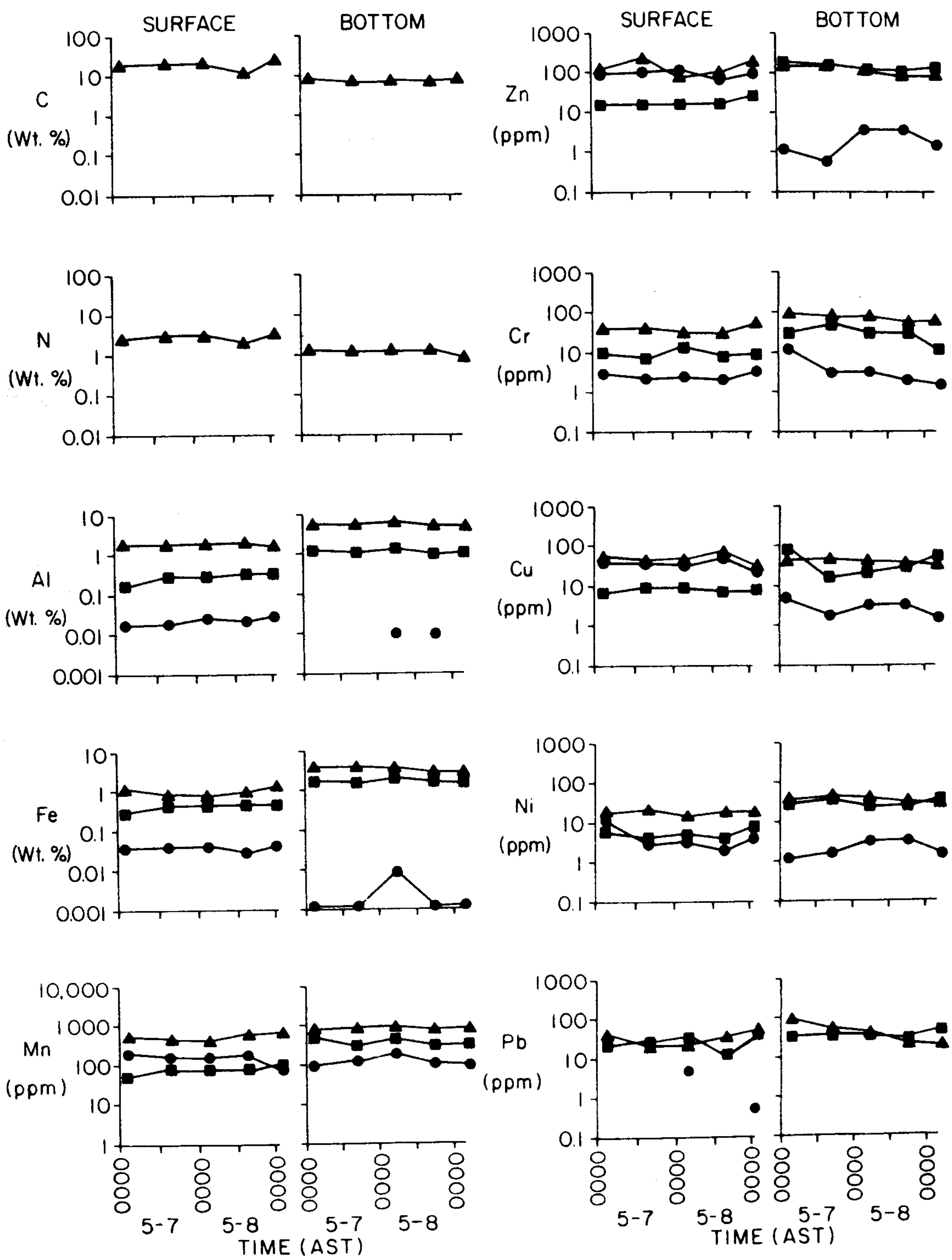

Figure 31. Temporal variations of major and trace elements in suspended matter (total concentration [▲], weak acid extractable [■], and peroxide extractable [●] from station CB-7 in lower Cook Inlet.) Samples were collected 7-9 May 1978.

TABLE 11. Elemental composition and phase association of trace metals in suspended particulate matter from the Kalgin Island Region. Values are the average of samples throughout the time series. Errors are ±1 σ.

	KALGIN ISLAND REGION											
	Surface (CB-9)			Bottom (CB-9)			Surface (CB-10)			Bottom (CB-10)		
	Elemental Composition	Peroxide Extractable	Weak Acid Extractable	Elemental Composition	Peroxide Extractable	Weak Acid Extractable	Elemental Composition	Peroxide Extractable	Weak Acid Extractable	Elemental Composition	Peroxide Extractable	Weak Acid Extractable
C(wt%)	0.95 ± 0.09			0.89 ± 0.09			1.1 ± 0.1			1.1 ± 0.3		
N(wt%)	0.098 ± 0.014			0.090 ± 0.014			0.11 ± 0.01			0.11 ± 0.03		
Si(wt%)	25.8 ± 1.5			24.7 ± 1.6			25.2 ± 1.0			25.5 ± 2.4		
Al(wt%)	10.4 ± 0.7	0.0038 ± 0.0014	1.04 ± 0.08	10.1 ± 1.5	0.0026 ± 0.0008	0.95 ± 0.15	9.9 ± 1.0	0.0015 ± 0.0002	1.32 ± 0.38	9.0 ± 0.7	0.0021 ± 0.0008	1.26 ± 0.28
Fe(wt%)	5.1 ± 0.5	0.0020 ± 0.0010	3.2 ± 0.5	4.8 ± 0.2	0.0020 ± 0.0012	3.2 ± 0.2	5.3 ± 0.5	0.0010 ± 0.0002	3.3 ± 0.1	5.4 ± 0.8	0.0017 ± 0.0013	3.3 ± 0.6
Mn(ppm)	1310 ± 20	6.3 ± 2.8	1000 ± 180	1300 ± 80	7.3 ± 3.2	940 ± 90	1280 ± 100	8.3 ± 5.9	1060 ± 100	1260 ± 70	6.0 ± 2.2	1030 ± 30
Zn(ppm)	158 ± 9	ND	72 ± 11	151 ± 12	ND	67 ± 7	158 ± 18	ND	86 ± 16	146 ± 18	ND	83 ± 13
Cr(ppm)	108 ± 7	0.5 ± 0.1	55 ± 12	112 ± 12	0.5 ± 0.1	51 ± 5	113 ± 7	0.5 ± 0.2	48 ± 20	110 ± 27	0.6 ± 0.2	47 ± 17
Cu(ppm)	58 ± 3	1.00 ± 0.13	43 ± 4	55 ± 6	0.80 ± 0.14	36 ± 7	60 ± 6	0.67 ± 0.50	49 ± 15	60 ± 11	0.61 ± 0.24	47 ± 7
Ni(ppm)	46 ± 10	0.25* ± 0.05	38 ± 6	48 ± 6	ND	46 ± 10	45 ± 7	ND	44 ± 9	49 ± 15	0.35* ± 0.05	49 ± 6
Pb(ppm)	23 ± 4	ND	ND	20 ± 2	ND	ND	16 ± 4	ND	ND	14 ± 4	ND	ND

ND - Not Detected (< 0.2 ppm for Ni, 0.5 ppm Zn and 1.0 ppm Pb)

* - Three of five samples had nondetectable values. The mean and error are for the two samples with detectable values.

TABLE 12. Elemental composition and phase association of trace metals in suspended matter from Kamishak and Kachemak Bays. Elemental composition values for Kamishak are the averages of duplicate analysis of a single sample. Values for Kachemak Bay are the average of samples throughout the time series. Errors are ±1 σ.

	KAMISHAK BAY			KACHEMAK BAY					
	Surface (CB-1)			Surface (CB-7)			Bottom (CB-7)		
	Elemental Composition	Peroxide Extractable	Weak Acid Extractable	Elemental Composition	Peroxide Extractable	Weak Acid Extractable	Elemental Composition	Peroxide Extractable	Weak Acid Extractable
C(wt%)	3.93			19.3 ± 5.6			7.65 ± 0.5		
N(wt%)	0.50			2.9 ± 0.6			1.29 ±0.03		
Si(wt%)	18.9 ± 0.2			18.7 ± 3.7			24.6 ± 2.9		
AL(wt%)	9.3 ± 1.1	0.0035	2.1	2.2 ± 0.4	0.022 ±0.004	0.29 ± 0.26	5.2 ± 0.5	0.0009 ±0.0005	1.12 ± 0.13
Fe(wt%)	4.5 ± 0.1	0.022	3.5	1.0 ± 0.3	0.038 ±0.004	0.44 ± 0.08	3.4 ± 0.4	0.0027 ±0.0033	1.78 ± 0.19
Mn(ppm)	1110 ± 30	21	882	539 ± 86	264 ± 77	81 ± 15	887 ± 81	124 ± 39	338 ± 89
Zn(ppm)	210 ± 20	0.8	140	159 ± 72	106 ± 20	28 ± 7	162 ± 62	2.6 ± 2.0	155 ± 38
Cr(ppm)	158 ± 4	2.1	55	39 ± 12	2.5 ± 0.6	10 ± 2	83 ± 13	2.9 ± 0.6	33 ± 14
Cu(ppm)	146 ± 6	14	134	43 ± 12	35 ± 13	8 ± 1	39 ± 6	3.3 ± 1.5	42 ± 27
Ni(ppm)	60 ± 2	2.5	37	17 ± 2	5 ± 4	17 ± 2	37 ± 5	2.2 ± 1.0	34 ± 7
Pb(ppm)	66 ± 3	ND	63	32 ± 17	ND	26 ± 6	45 ± 29	ND	38 ± 8

ND - Not Detected (< 1.0 ppm for Pb)

case of Cu, Zn and Mn, a major fraction of these elements were present in the organic phase (81%, 66%, and 49%, respectively). The near bottom suspended samples contained 50% aluminosilicates and only 14% organic matter. This influx of inorganic material was probably a result of resuspension of bottom sediments. As expected, the trace metal content in the weak-acid extractable phase increased relative to the surface, consistent with the increased amount of oxyhydroxides associated with the aluminosilicates. The decrease in organic matter content of the near-bottom sample resulted in a smaller portion of the trace metals being present in the peroxide extractable phase.

6.2.5 Elemental Composition of Particulate Matter Collected from Sediment Traps

After the sediment trap particulates were collected and dried for gravimetric measurement, the samples collected at ST-1, ST-2, and CB-7 were analyzed for total elemental composition and phase associations according to section 5. The results of these analyses are listed in table 13.

There are significant regional differences in the major elemental composition of the sediment trap particulates which can be related to the source suspended particulate matter. The Al content of the sediment trap particulates at ST-1 in Kamishak Bay was higher than that at CB-7 in Kachemak Bay. The Al content of the suspended particulate material also follows this relationship (Feely and Massoth, in press), indicating the dominance of aluminosilicates on the western side of lower Cook Inlet. Several trace metals (Fe, Cr, and Ni) which are associated with aluminosilicates in the suspended particulate matter also had significantly greater concentrations in the sediment trap particulates of Kamishak Bay relative to those of Kachemak Bay.

In contrast, Kachemak Bay sediment trap samples contained three times as much organic C as those of Kamishak Bay, indicating a similar relationship in the organic C flux (0.95 g m^{-2} d^{-1} at CB-7 as compared to 0.32 g m^{-2} d^{-1} at ST-1). As a result of high primary productivity in Kachemak Bay (Larrance et al., 1977), the suspended particulate matter contained about 20% organic C and had a C/N ratio of 6.7 characteristic of a marine origin. The sediment trap particulates also had a C/N characteristic of a marine origin, indicating that the surface suspended matter was a major source of organic C to the sediment trap. The lower primary productivity in Kamishak Bay resulted in a significant portion of the organic C flux being terrestrial in origin as indicated by a C/N ratio midway between marine and terrestrial organic matter. Therefore, it appears that there is a definite relationship between production of organic matter in the water column and the amount and type of organic matter settling to the bottom, thus providing a food source for filter-feeding benthic organisms.

The trace metal data for the sediment trap particulates showed similar associations with the oxyhydroxide phase in all three sediment trap stations. For instance, the portion of Cr present in the weak-acid extractable phase ranged from 49% - 56% of total Cr for the samples from the three stations, while 100% of the Ni was present in this phase. These trace metal associations were similar to those found in the suspended matter, emphasizing the importance of the oxyhydroxide phase in transporting metals through the water column.

The trace metal data in the peroxide extractable phase show regional differences consistent with the organic fluxes. With the exception of Cr, the trace metals present in the peroxide extractable phase follow the order: CB-7 > ST-1 > ST-2. The organic fraction of Kachemak Bay sediment trap particulates contained 5.3% and 10.9% of the total Mn and Cu, respectively, present in the whole sample. The coupling between biological accumulation of trace metals in the water column and the flux of organically bound trace metals is demonstrated by the fact that a major portion of both Cu and Mn were also present in the organic fraction of the surface suspended matter (see section 6.2.3). This coupling may be a major mechanism for transporting these trace metals to the benthic community.

The significance of these results is evident when one considers recent studies of the availability of sediment bound trace elements to organisms. Luoma and Bryan (1978) studied the distribution of Pb and Fe in the soft tissues of the deposit feeding bivalve Scorbicularia plana and in the underlying sediments from 20 estuaries in southern and western England and northwest France. It was found that the Pb concentrations in the bivalves directly correlated with the Pb/Fe ratio in the sediment. The authors concluded that the Fe concentration in the sediments was influencing the availability of Pb to the bivalves. To be more specific, they suggested that the availability of Pb to the bivalves may be a function of the partitioning of Pb between organically bound Pb and Fe oxide-bound Pb in the sediments, with the organically bound Pb being more biologically available. Similarly, Eaganhouse and others (1976; 1978) found enrichments of Hg in tissues of the intertidal mussel Mytilus californianus in sediments that contained high concentrations of organically bound Hg. Here again, the implication is that organically bound trace elements are more available to organisms than trace elements that are bound to some other less available phase in the sediments. In lower Cook Inlet organically bound trace elements predominate only in Kachemak Bay where primary production is higher than any other region in the inlet. It is also the region

TABLE 13. Elemental composition and phase association of trace metals in sediment trap particulates at ST-1, ST-2 and CB-7. Values for ST-1 and ST-2 are the average of triplicate analysis of a single sample from a long-term deployment. Values for CB-7 are the average of four samples from short-term deployment. Errors are ±1 σ.

	ST-1 (32m)			ST-2 (75m)			CB-7 (60m)		
	Elemental Composition	Peroxide Extractable	Weak Acid Extractable	Elemental Composition	Peroxide Extractable	Weak Acid Extractable	Elemental Composition	Peroxide Extractable	Weak Acid Extractable
C(wt%)	0.87 ± 0.02			0.84 ± 0.40			2.8 ± 0.4		
N(wt%)	0.09 ± 0.01			0.09 ± 0.05			0.35 ± 0.05		
Si(wt%)	21.8 ± 1.0			26.5 ± 1.0			22.5 ± 3.2		
Al(wt%)	9.4 ± 0.9	0.0011 ±0.0004	3.0 ± 0.3	7.8 ± 1.0	0.0004 ±0.0004	1.2 ± 0.6	6.5 ± 0.5	0.0035 ±0.0017	1.16 ± 0.10
Fe(wt%)	4.6 ± 0.2	0.0010 ±0.0004	3.22 ±0.05	3.4 ± 0.1	0.0004 ±0.0002	2.1 ± 0.3	3.8 ± 0.9	0.0022 ±0.0007	1.2 ± 0.2
Mn(ppm)	880 ± 80	3 ± 3	426 ± 27	660 ± 35	0.6 ± 0.1	265 ± 45	915 ± 170	48 ± 29	570 ± 140
Zn(ppm)	142 ± 6	ND	118 ± 5	106 ± 20	ND	74 ± 2	215 ± 120	0.6 ± 0.3	160 ± 86
Cr(ppm)	82 ± 2	0.3 ± 0.1	40 ± 2	55 ± 6	1.5 ± 0.5	31 ± 2	63 ± 8	2.4 ± 0.3	35 ± 3
Cu(ppm)	29 ± 2	0.12 ± 0.01	23 ± 2	18 ± 2	0.04 ± 0.01	13 ± 3	43 ± 3	4.7 ± 0.8	36 ± 7
Ni(ppm)	51 ± 14	ND	51 ± 1	30 ± 7	ND	30 ± 6	34 ± 2	1.3 ± 0.1	37 ± 6
Pb(ppm)	15 ± 2	ND	ND	10 ± 2	ND	ND	13 ± 6	ND	1.1 ± 0.5

ND - Not Detected (< 0.2 ppm for Ni and Zn and 1.0 ppm for Pb) where water circulation is the least dynamic. Therefore, it is possible to speculate that anthropogenic inputs of dissolved trace metals resulting from development activities would have a more profound impact on biological communities in Kachemak Bay than other regions in lower Cook Inlet because of their apparent incorporation into biologically available organic matter.

6.3 Southeastern Bering Shelf

6.3.1 Particulate Matter Distribution

Figures 32 thru 35 show the distribution of suspended matter at the surface and 5 meters above the bottom for the fall and summer cruises in the southeastern Bering Sea Shelf (RP-4-Di-76B-III, 12 September - 5 October 1975 and RP-4-MW-76B-VIII, 24 June - 9 July 1976). As shown in figures 32 and 34, the surface particulate matter distributions are dominated by the discharge of suspended material from the northern rivers. Large plumes of suspended matter extend to the southwest from Kuskokwim Bay and the region east of Cape Newenham. Similar suspended matter distributions were found by Sharma et al. (1974) from samples collected during June-July 1973. The authors suggested that suspended material originating from the Kvichak and Nushagak Rivers moves generally to the west until it reaches Cape Newenham where it combines with a portion of the material discharged from the Kuskokwim River and is deflected to the southwest. Chemical analysis of the particulate matter suggests that the material is essentially of terrestrial origin (> 76% inorganic).

Along the Alaska Peninsula surface suspended matter concentrations decrease rapidly away from the coast. This is due to rapid mixing of the highly turbid Shelf water with the relatively clear Pacific Ocean water which originates from the passes west of the Alaska Peninsula and is deflected to the northeast along the coast of the Alaska Peninsula.

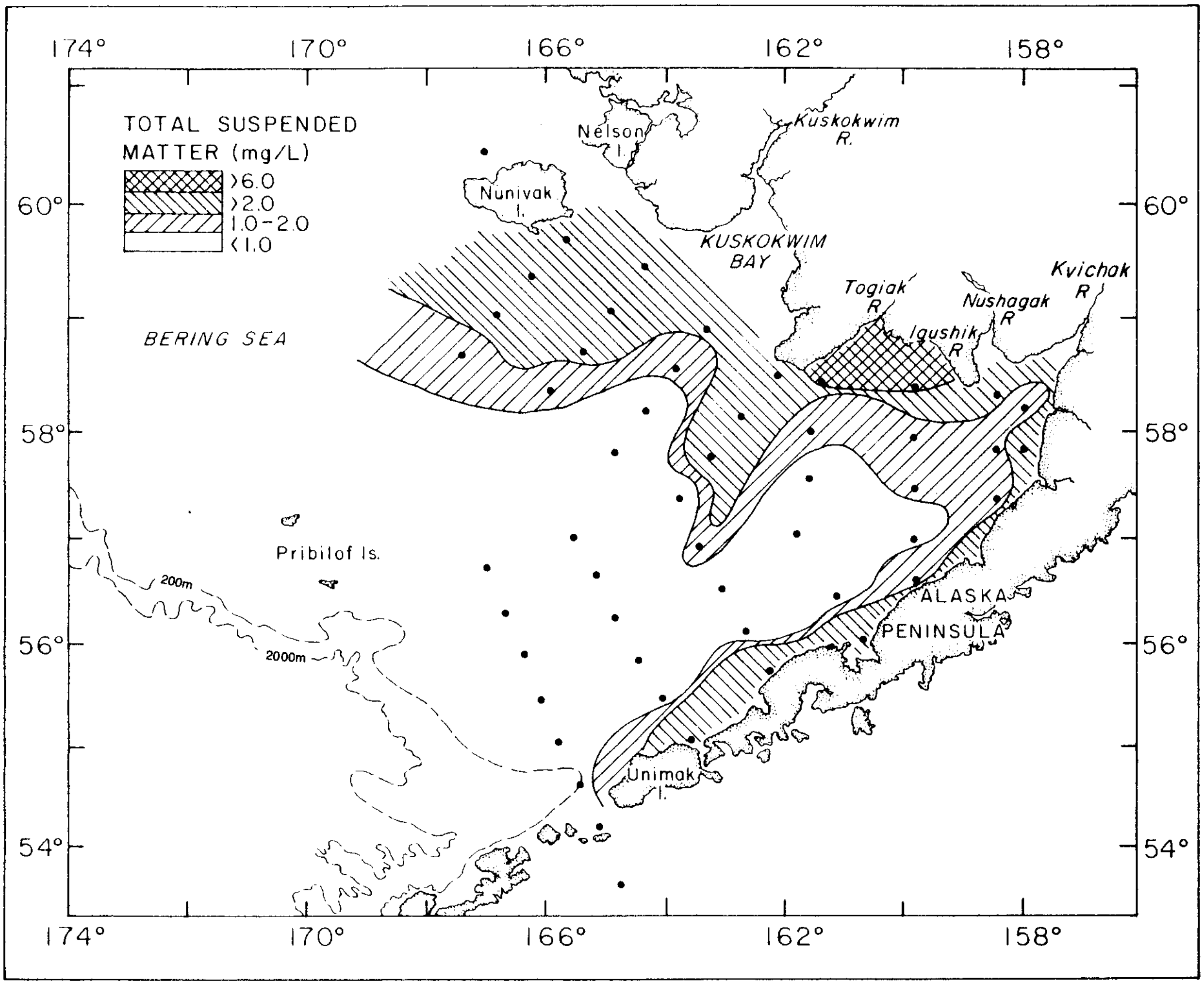

Figure 32. Distribution of total suspended matter at the surface in the southeastern Bering Shelf (Cruise RP-4-Di-75B-III, 12 September - 5 October 1975).

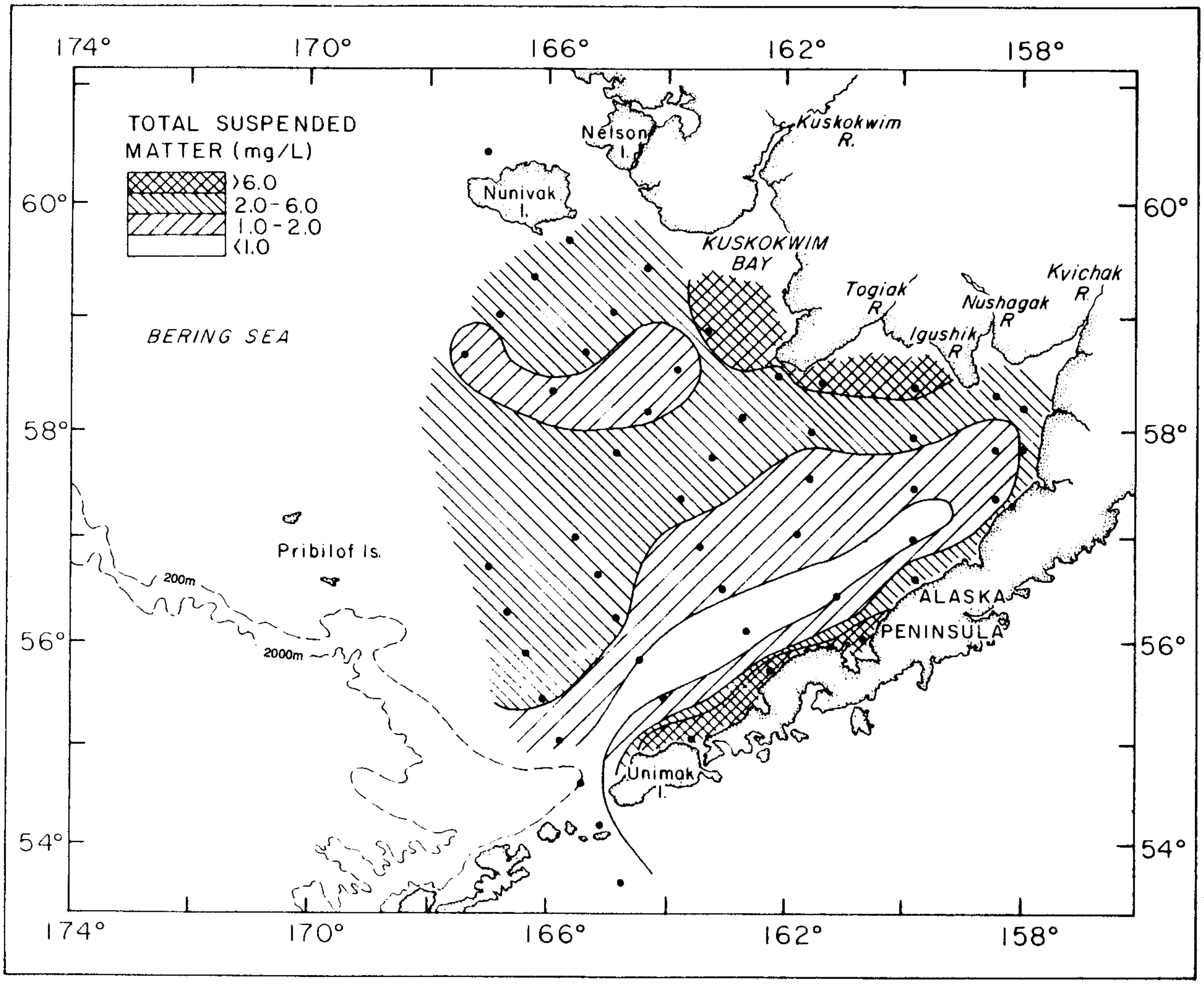

Figure 33. Distribution of total suspended matter 5 meters above the bottom in the southeastern Bering Shelf (Cruise RP-4-Di-75B-III, 12 September - 5 October 1975).

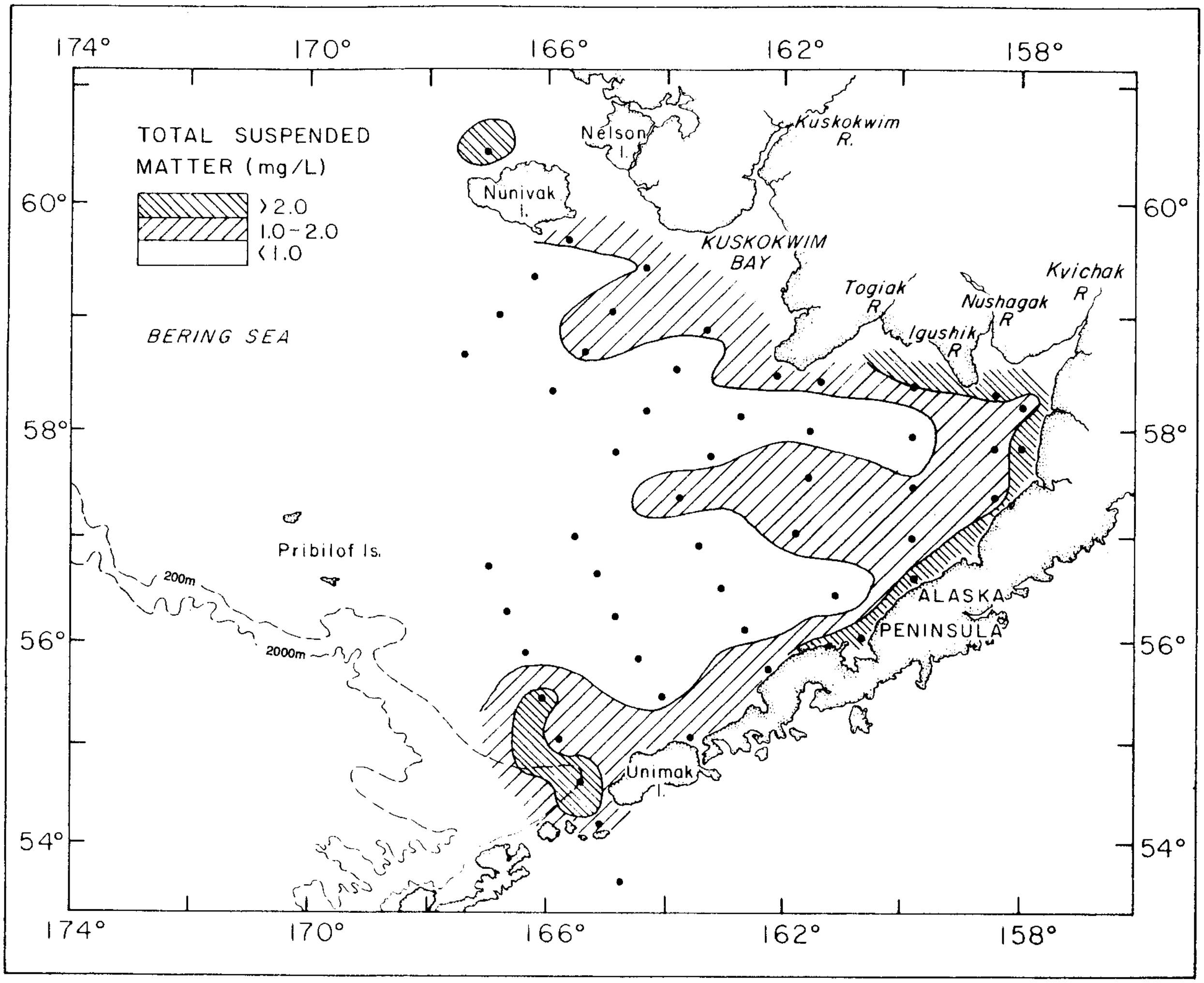

Figure 34. Distribution of total suspended matter at the surface in the southeastern Bering Shelf (Cruise RP-4-MW-76B-VII, 24 June - 9 July 1976).

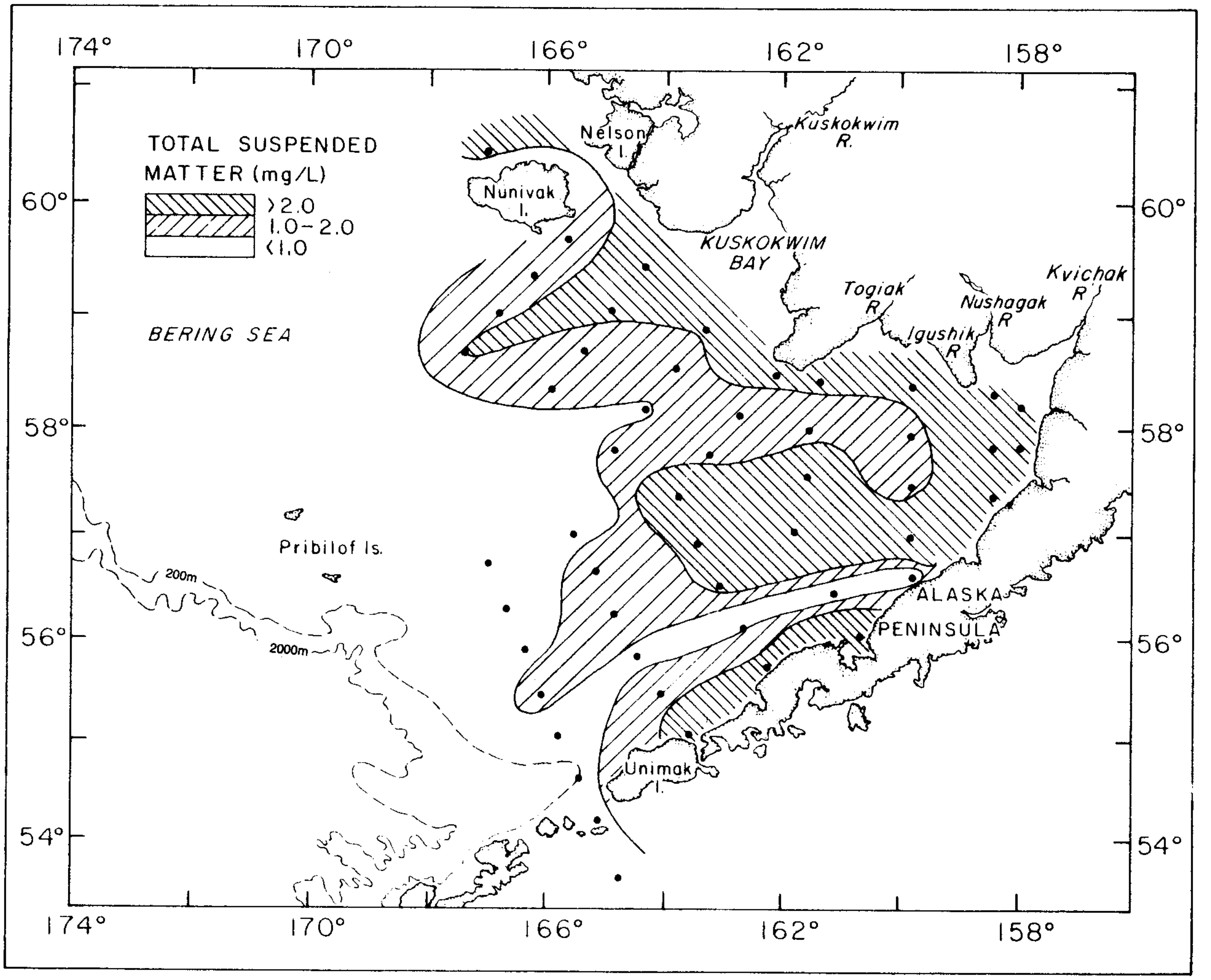

Figure 35. Distribution of total suspended matter 5 meters above the bottom in the southeastern Bering Shelf (Cruise RP-4-MW-76B-VII, 24 June - 9 July 1976).

At the time of the summer cruise, plumes of turbid water were observed north of Unimak Island and in the region west of the northern end of the Alaska Peninsula which were not observed during the fall cruise (figure 34). These plumes might be attributed to the large seasonal variations in primary productivity which are characteristic of this region. Sharma et al. (1974) observed turbid plumes in the region northwest of Unimak Pass which they attributed to similar processes.

Near the bottom, suspended matter concentrations are high (> 1.0 mg/L) throughout most of the study region, indicating possible resuspension of bottom sediments. Figures 36 and 37 show vertical cross-sections of the distribution of particulate matter from Kuskokwim Bay to Unimak Island for both cruises. The figures show increasing suspended matter gradients near the bottom which are attributed to resuspension and redistribution of bottom sediments. Since Bristol Bay is a relatively shallow embayment, it is possible that waves and tides play a major role in the redistribution of sediments. The suspended matter concentrations near the bottom were 2-3 times higher in the fall. This may be due to the increased effect of storms which occur more regularly during the fall months.

6.3.2 Elemental Chemistry of the Particulate Matter

Tables 14 and 15, respectively, summarize the data on the elemental composition of the particulate matter from the major rivers discharging into Bristol Bay and from 42 stations on the Shelf. For convenience, the surface data in table 15 have been arranged into three groups. Group I contains all the northern stations in which the sum of the major inorganic element concentrations (expressed as oxides) is greater than 60 percent of the total weight of material on the filter. Group II contains all the southern stations

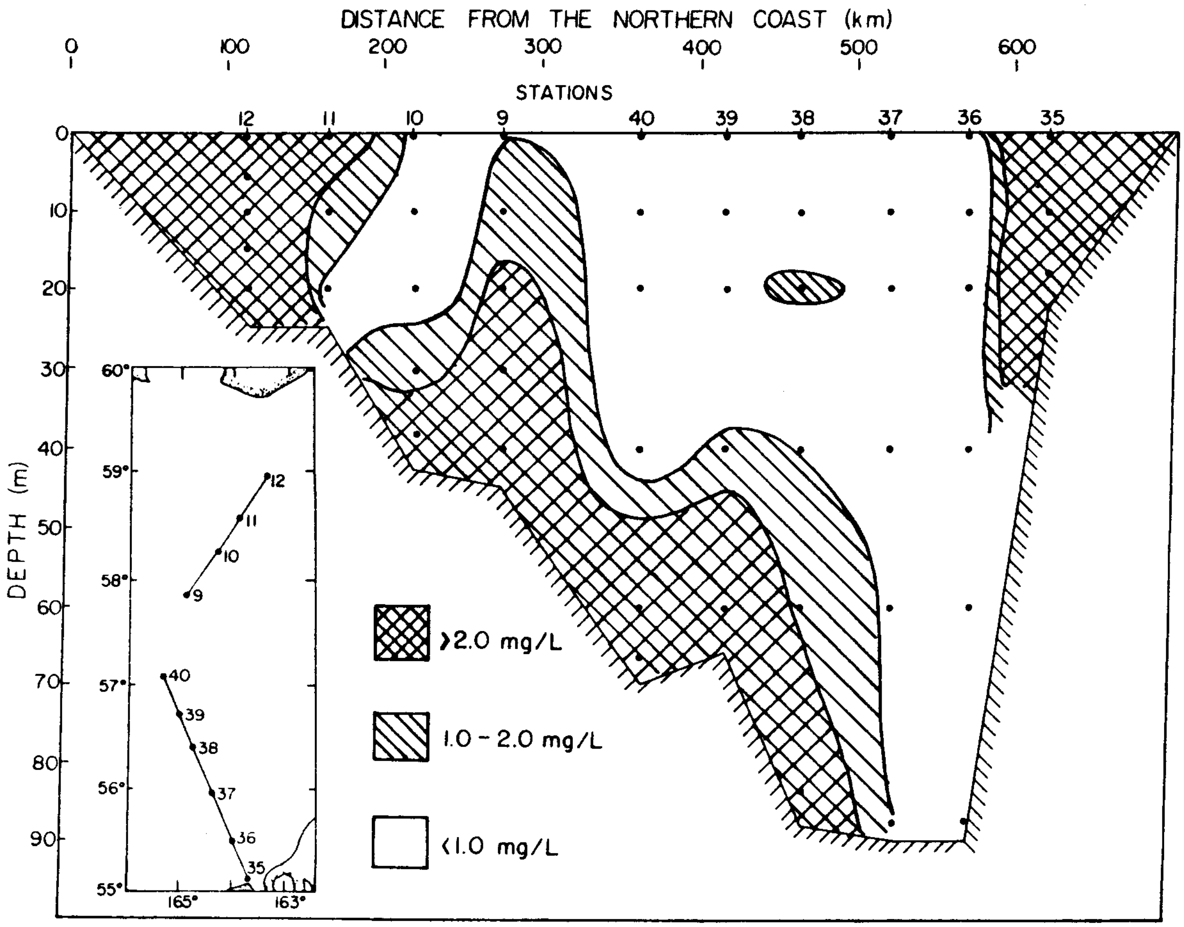

Figure 36. Vertical cross-section of the distribution of total suspended matter for stations 9 thru 12 and 35 thru 40 in the southeastern Bering Shelf (Cruise RP-4-Di-75B-III, 12 September - 5 October 1975).

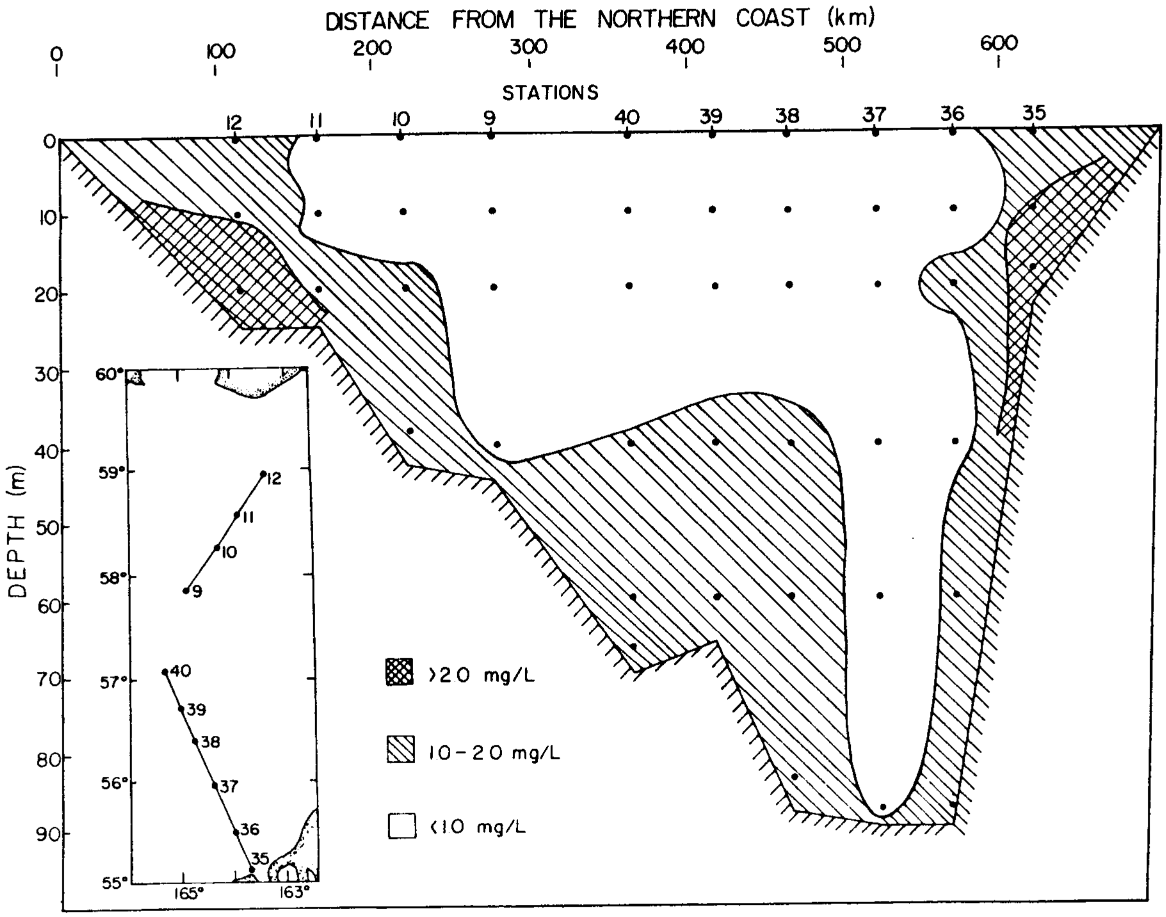

Figure 37. Vertical cross-section of the distribution of total suspended matter for stations 9 thru 12 and 35 thru 40 in the southeastern Bering Shelf (Cruise RP-4-MW-76B-VIII, 24 June - 9 July 1976).

in which the sum of the major inorganic element concentrations is also greater than 60 percent of the total weight. Group III contains all the stations in between in which the sum is less than 60 percent of the total suspended load.

As shown in table 15, Groups I and II are very similar and appear to be dominated by the supply of terrigeneous material from the Kuskokwim, Nushagak, and Kvichak Rivers to the north (for Group I) and the coastal streams and lagoons to the south (for Group II). Several authors have suggested that since Mg, Al, K, and Ti are almost exclusively associated with aluminosilicate minerals, the presence of these elements in particulate matter is indicative of terrestrial input (Spencer and Sachs, 1970; Price and Calvert, 1973; and Feely, 1975). The high concentrations of these elements in the samples from Groups I and II indicate that aluminosilicate minerals are the most dominant solid phase in the particulate matter. The data from table 15 show that for Groups I and II approximately 35-60 percent of the particulate matter is aluminosilicate material. In contrast, the particulate matter samples from Group III only contain about 20 percent aluminosilicate material.

The Group III samples are significantly depleted in particulate Mg, Al, Si, K, Ca, Ti, Mn, and Fe and are enriched in Ni, Cu, and Zn. The trace element enrichments are 134, 53, 21 percent, respectively, for Ni, Cu, and Zn. However, considering the large sample variability associated with the low sample loadings, these enrichments may not be significant.

Since the early work of Menzel and Vaccaro (1964), many investigators have used particulate C as a tracer of particulate organic matter in the oceans. Gordon (1970) suggested that a factor of 1.8 be used to estimate concentrations of particulate organic matter from particulate C. Recent investigators have used the C/N ratios in particulate matter to distinguish

TABLE 14

Summary of the elemental composition of particulate matter from the major rivers that discharge into the southeastern Bering Shelf. (Surface samples were obtained with a precleaned 4-L polyethylene bottle extended from a helicopter, 12-21 September 1976.)

Sample Location	No. of Samples	C wt. %	N wt. %	Mg wt. %	Al wt. %	Si wt. %	K wt. %	Ca wt. %	Ti wt. %	Cr ppm	Mn ppm	Fe wt. %	Ni ppm	Cu ppm	Zn ppm
Kuskokwim River	9	2.96 ±2.63	0.38 ±0.42	2.13 ±0.39	7.77 ±0.98	32.13 ±2.86	1.68 ±0.16	1.59 ±0.07	0.56 ±0.04	105.3 ±14.9	1498 ±105	6.57 ±0.45	69.8 ±4.8	77.6 ±7.3	281.4 ±34.2
Kvichak	6	2.66 ±0.15	0.23 ±0.15	1.24 ±0.44	4.26 ±1.07	26.78 ±10.30	0.81 ±0.16	0.48 ±0.13	0.42 ±0.11	62.2 ±18.3	941 ±53	4.36 ±1.32	36.3 ±10.9	63.3 ±8.7	232.1 ±108.8

TABLE 15

Summary of the elemental composition of the particulate matter samples from the southeastern Bering Shelf (Cruise RP-4-Di-75B-III, 12 September - 6 October 1975)

Sample Description	No. of Samples	C wt. %	N wt. %	Mg wt. %	Al wt. %	Si wt. %	K wt. %	Ca wt. %	Ti wt. %	Cr ppm	Mn ppm	Fe wt. %	Ni ppm	Cu ppm	Zn ppm
Surface (Group I)	24	17.7 ±10.3	2.1 ±1.3	0.86 ±0.14	3.52 ±2.22	25.85 ±5.28	0.51 ±0.17	1.32 ±0.28	0.24 ±0.06	41.2 ±19.3	893 ±285	2.68 ±0.63	24.1	41.9 ±13.9	210.7 ±88.0
Surface (Group II)	4	22.9		1.75 ±0.08	6.11 ±1.32	31.74 ±6.40	0.37 ±0.14	2.66 ±0.89	0.28 ±0.07		1377 ±519	3.15 ±0.35		42.4 ±21.8	353.0 ±127.0
Surface (Group III)	11	35.3 ±19.3	4.8 ±2.7			10.89 ±6.73	0.26 ±0.20	1.14 ±0.50	0.18 ±0.07	60.4 ±32.2	355 ±233	1.92 ±0.66	56.5 ±11.7	64.0 ±31.4	256.0 ±215.0
5 m above the bottom	42	12.2 ±7.6	1.8 ±1.1	1.45 ±0.66	3.92 ±1.27	29.45 ±6.12	0.53 ±0.17	1.64 ±0.65	0.28 ±0.07	50.0 ±20.9	581 ±304	3.16 ±0.82	30.7 ±17.9	54.2 ±47.7	219.6 ±107.6

between terrestrial and marine sources of organic matter (Loder and Hood, 1972). The authors found that riverborne organic matter has C/N ratios which range between 15-22. In contrast, ratios for marine organic matter range between 5-15.

The distribution of particulate C and N at the surface in the southeastern Bering Shelf are presented in figures 38 and 39. Generally speaking, the surface distributions follow the same pattern as total suspended matter. High concentrations of particulate C and N are found along the coast with concentration gradients decreasing slowly in a seaward direction from the northern coast and rapidly from the coast of the Alaska Peninsula. A plume of turbid water containing high concentrations of particulate C and N extends to the southwest from Kuskokwim Bay. Apparently, the semipermanent counterclockwise currents which appear to be controlling the distributions of total particulate matter at the surface also control the distribution of particulate C and N.

The C/N ratios in the particulate matter at the surface indicate that the organic matter is primarily of marine origin. Ratios range from 0.7 to 29.4 with a mean 7.2. Although the ratios increase slightly from south to north, studies of the variability of C/N ratios in marine phytoplankton indicate that these small increases are probably not significant (Banse, 1974).

6.4 Norton Sound

6.4.1 Particulate Matter Distribution and Transport

Figures 40 and 41 show the distributions of total suspended matter at the surface and 5 m above the bottom for the July 1979 cruise in Norton Sound. As shown in figure 40, surface particulate matter distributions were dominated by

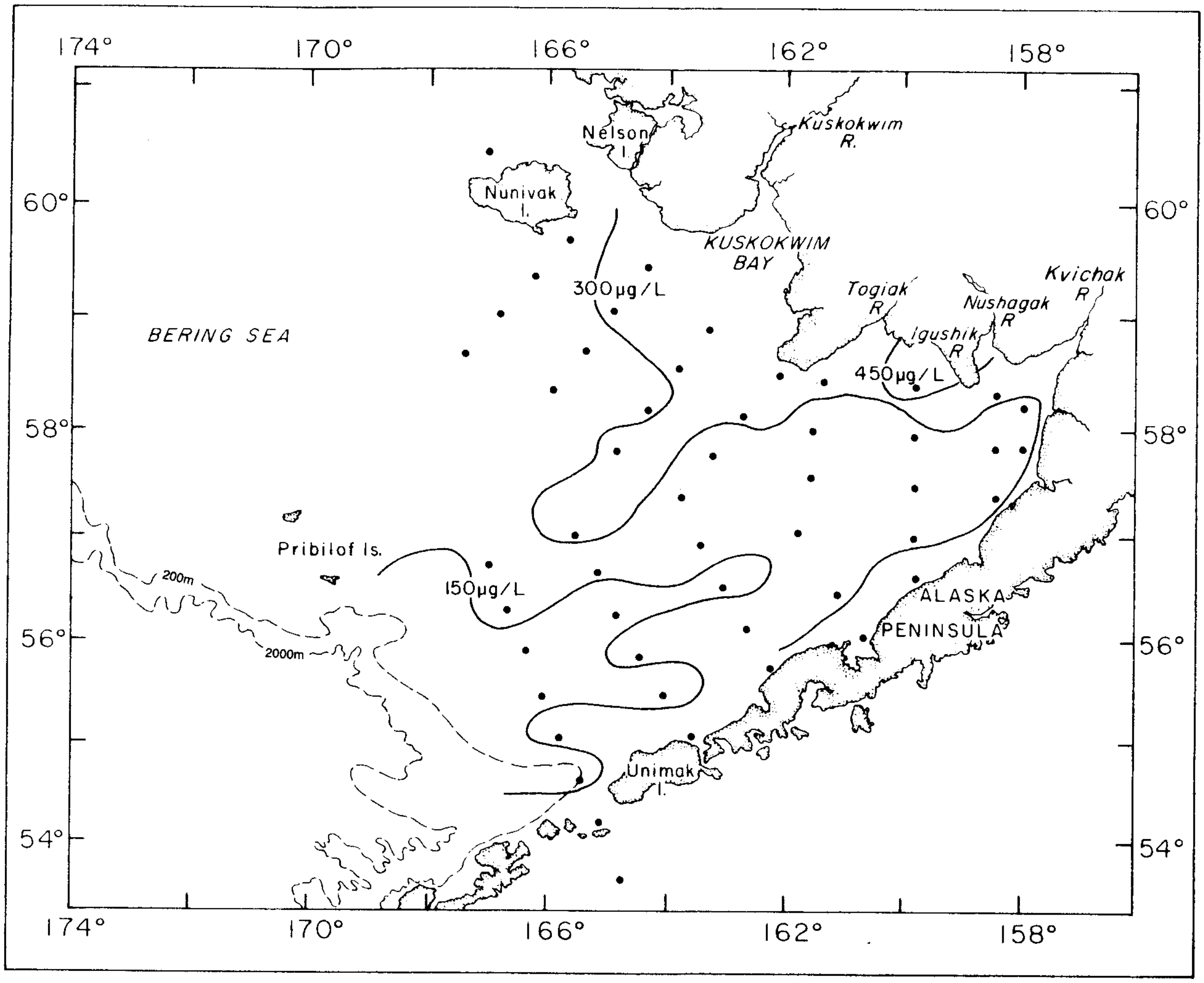

Figure 38. Distribution of total particulate carbon at the surface in the southeastern Bering Shelf (Cruise RP-4-Di-75B-III, 12 September - 5 October 1975).

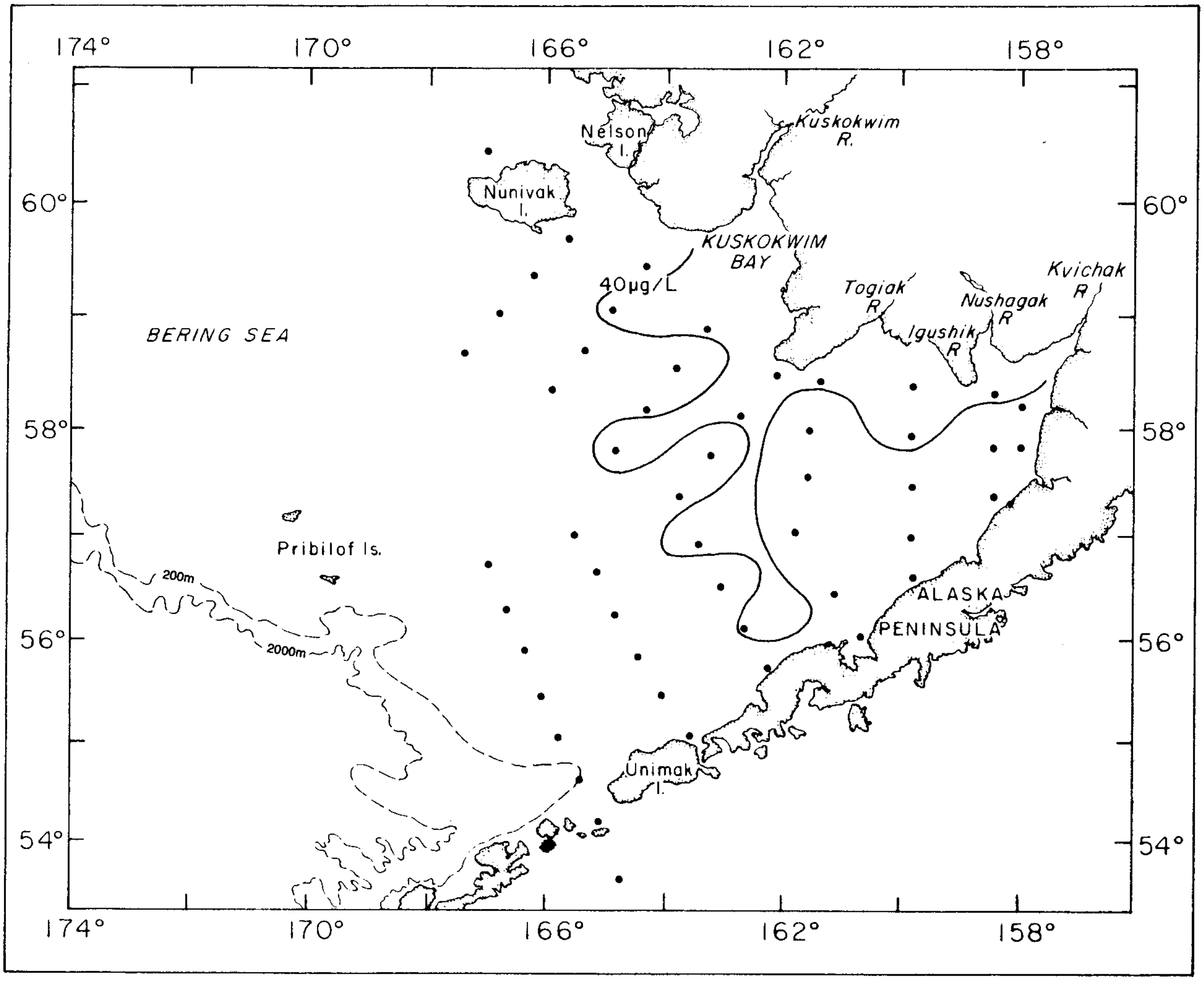

Figure 39. Distribution of total particulate nitrogen at the surface in the southeastern Bering Shelf (Cruise RP-4-Di-75B-III, 12 September - 5 October 1975).

the discharge of sedimentary material from the Yukon River. Surface suspended matter concentrations were highest near the mouth of the Yukon River, where values ranging between 100 and 154 mg/L were observed. The Yukon River plume (as indicated by the 5.0 mg/L isopleth) extended to the north and northeast across the length of the Sound. Another portion of the plume with lesser suspended matter concentrations (1.0-2.7 mg/L) extended north and northwest to a point about 20 km southwest of Cape Rodney. Both portions appear to have originated from the Yukon River and their trajectories tend to follow the general pattern of cyclonic circulation in the Sound (i.e., Yukon River material enters the Sound from the southwest, is transported north and northeast around the inside perimeter of the Sound, and exits the Sound from the northwest). These data are supported by the salinity and temperature measurements which indicated movements of low-salinity ($12-24^{o}/oo$), relatively warm ($10-11^{\circ}C$) water to the northeast along the coast (Feely et al., 1981). These results are consistent with the general conclusions of Sharma et al. (1974) for suspended matter data obtained in August 1973. They are also consistent with dispersal patterns of the Yukon River plume inferred from LANDSAT satellite photographs (Nelson et al., 1975). For example, figure 42 shows a LANDSAT photograph of the Yukon River plume taken on July 20, 1979, a few days following Cruise RP-4-Di-79A-VI. The plume, which appears lighter in the grey tones than the less turbid water, can be traced as far north as approximately 70 km from the Yukon River Delta and as far east as 50 km from Stuart Island. These features are also consistent with the data of Cacchione and Drake (1979) for surveys made during quiescent periods in September 1976 and July 1977. Thus, it would appear that the transport processes described above predominate throughout the region, at least during periods of calm weather in the summer.

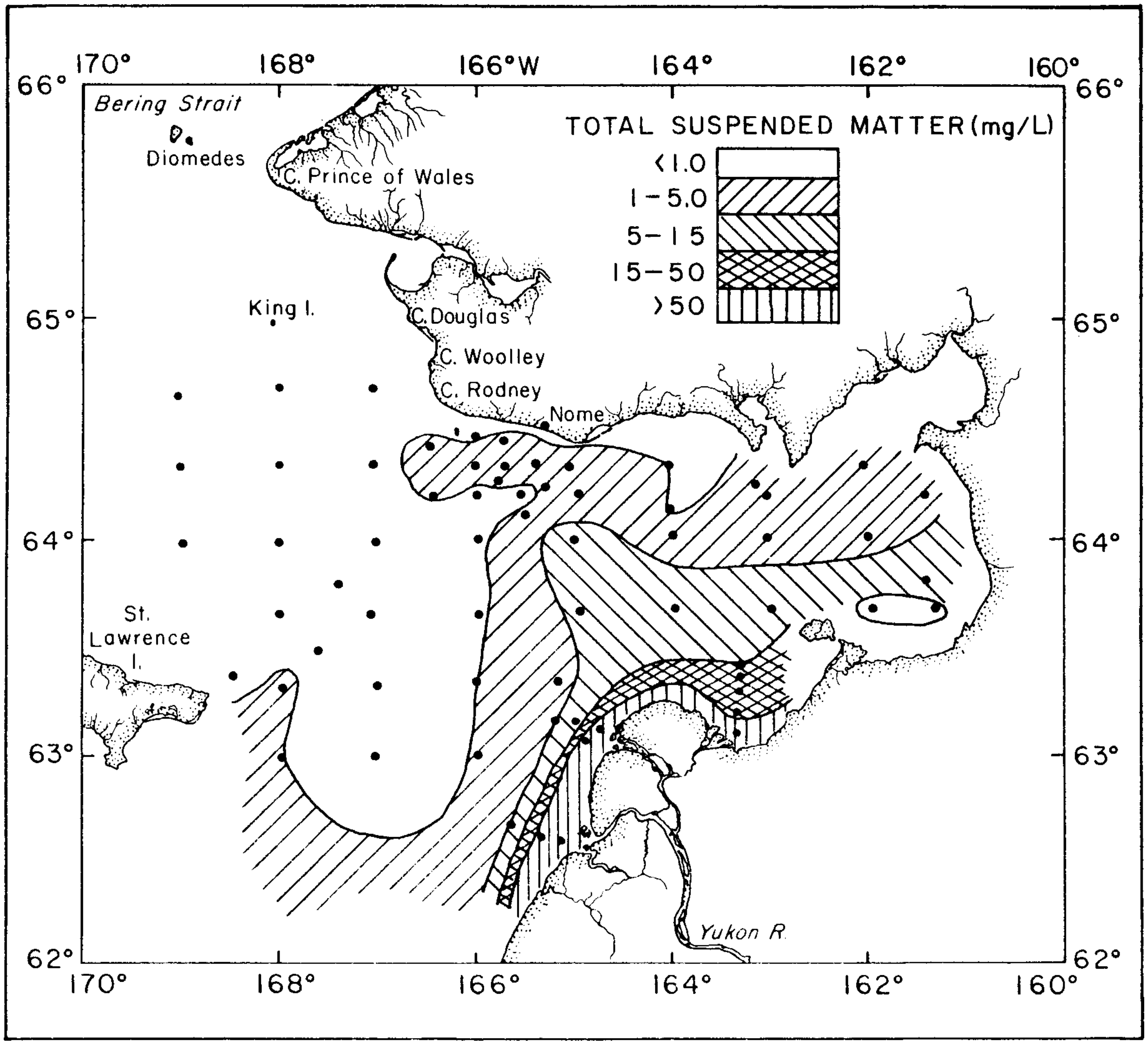

Figure 40. Distribution of total suspended matter at the surface in Norton Sound (Cruise RP-4-Di-79A-VI, 7-18 July 1979).

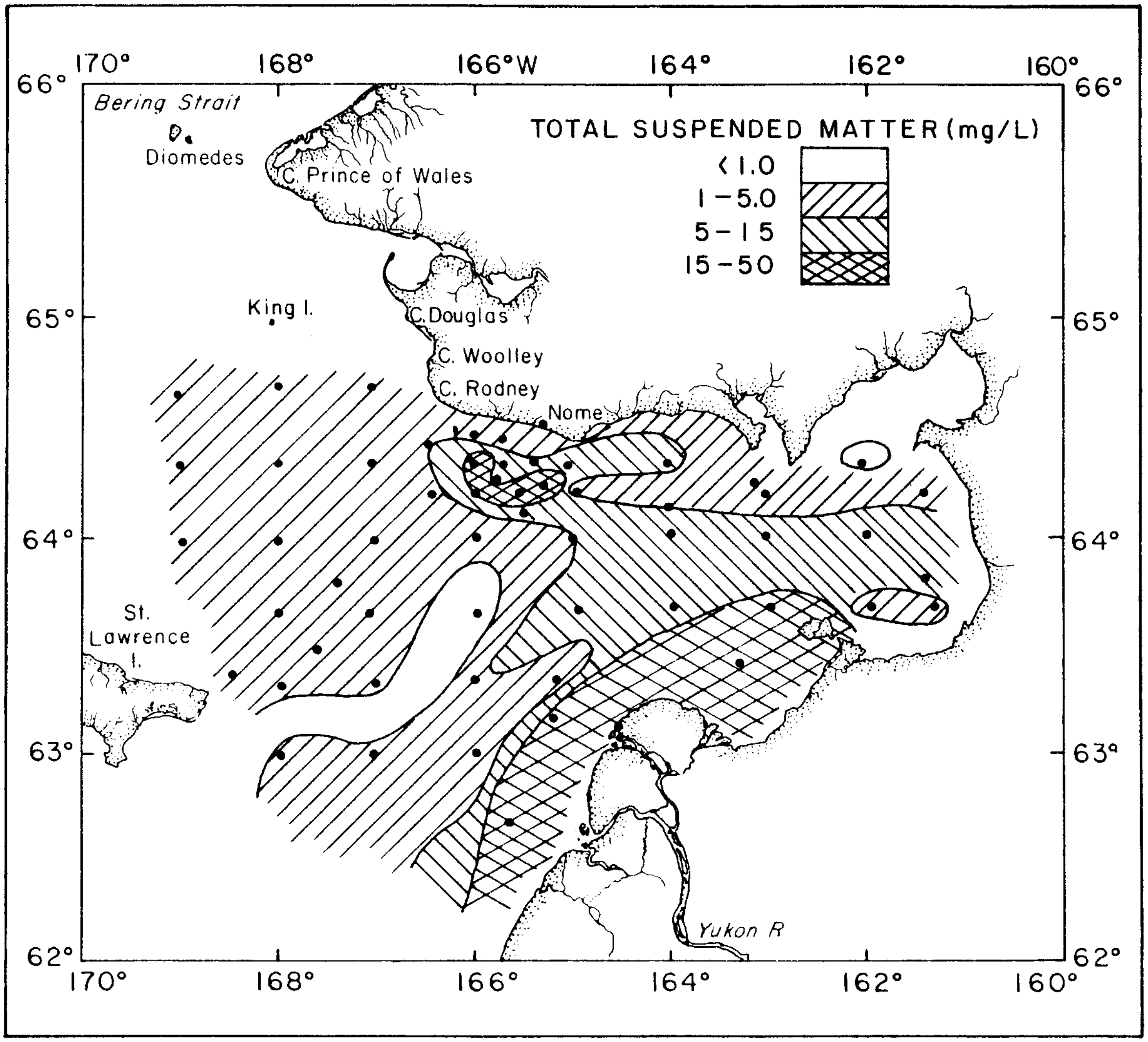

Figure 41. Distribution of total suspended matter at 5 m above the bottom in Norton Sound (Cruise RP-4-Di-79A-VI, 7-18 July 1979).

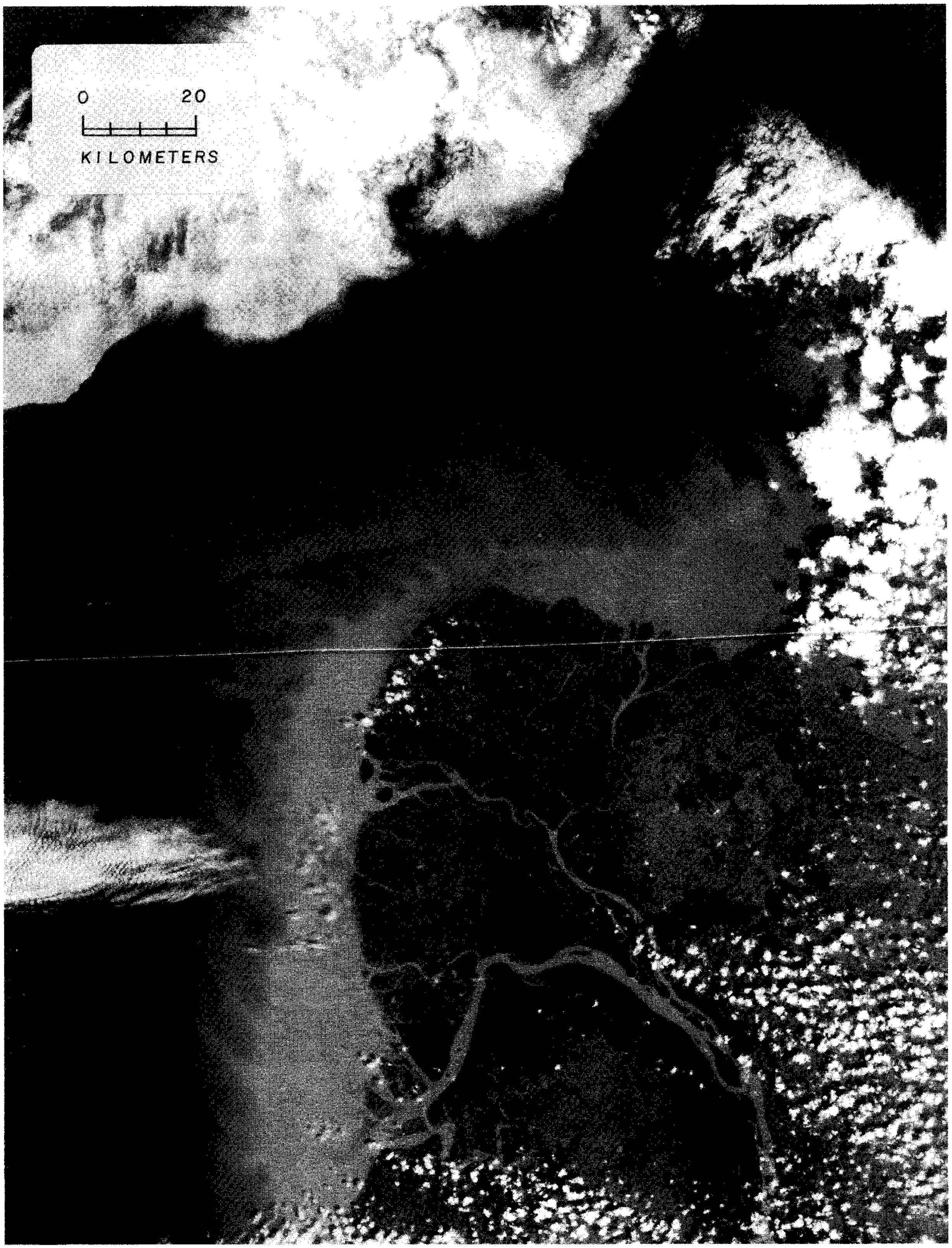

Figure 42. MSS Band 5 of LANDSAT images E-21640-21360-5 and and E-21640-21363-5 taken on 20 July 1979, showing inferred transport of suspended matter (appearing lighter in tone than the less turbid water) into Norton Sound.

The near-bottom distribution of total suspended matter (fig. 41) also indicated evidence for cyclonic movement of turbid water to the northeast along the coast. Near-bottom suspended matter concentrations were highest near the mouth of the Yukon River and in the region about 20-30 km south-southwest of Nome. The near-bottom plume just seaward of the Yukon River extended to the northeast along the coast in a manner very similar to the surface plume. The near-bottom concentrations were generally higher than surface concentrations, indicating that: (1) some fraction of the Yukon River material had settled to the near-bottom region during transit, and/or (2) a portion of the bottom sediments had been resuspended and remained in suspension.

6.4.2 Particulate Elemental Composition

In order to determine regional variations of the chemical composition of suspended material in Norton Sound, the particulate samples from the July 1979 cruise were analyzed for their major and trace element content by the methods described previously. The resulting data have been separated into five regions: Yukon River estuary with salinities less than 15 parts per thousand; Yukon River estuary with salinities between 15 and 25 parts per thousand; eastern Norton Sound; central Norton Sound; and western Norton Sound-northeastern Bering Sea Shelf. The averaged chemical data, along with published data for the Yukon River, are given in Tables 16 and 17. Table 18 shows C/N and element/Al ratios for the averaged data.

The elemental concentrations and elemental ratios illustrate some compositional differences between the suspended material discharging from the Yukon River and suspended matter in the Sound. These differences can be viewed in terms of relative aluminosilicate and organic matter percentages. Since most of the Al in marine particulate matter is located in aluminosilicate material (Sackett and Archenius 1962), the Al concentrations in the suspended matter when multiplied by 10 can be used to estimate aluminosilicate percentages in the particulate matter. Based on the particulate Al and particulate C concentrations, the suspended matter from the Yukon River estuary was composed of approximately 88% aluminosilicate material and 6% organic matter. In like manner, samples from eastern and central Norton Sound contain about the same percentage of aluminosilicate material (88-92%). These results illustrate the predominance of the detrital material from the Yukon River in the central and eastern regions of the Sound. This finding is additionally supported by the chemical data for Si, K, Ca, Ti, Fe, Ni, and Cu which are at about the same concentration levels in eastern and central Norton Sound and the Yukon River estuary. Only C, N, Mn, and Zn show enrichments offshore. For C and N these enrichments are attributed to a relative increase in the concentration of marine organic matter in offshore waters, which is probably due to increased light penetration away from the zone of high turbidity. This conclusion is supported by the C/N ratios (table 17) which show a general decrease seaward, indicating a transition from organic matter dominated by terrestrial material of marine origin with C/N ratios ranging between 6 and 9 (Loder and Hood, 1972). Mn and Zn enrichments can be attributed to a number of processes which are discussed in detail later.

In the western Norton Sound-northeastern Bering Sea Shelf region, the suspended matter was depleted in particulate Mg, Al, K, Ti, Fe and Ni and enriched in particulate C and N relative to the Yukon River estuarine samples. These depletions are attributed to a drop in the relative amount of aluminosilicate material in the suspended matter (< 52% by weight) and an increase in the proportion of marine organic matter (> 40% by weight), which is depleted in Mg, Al, K, Ti, Mn, Fe, Ni and Zn relative to aluminosilicate material (Martin and Knauer, 1973). It is important to note, however, that Mn and Zn concentrations do not decrease appreciably in the samples from this region. These findings indicate that Mn and Zn concentrations in the suspended matter are controlled by distinctly different chemical processes.

In an attempt to determine the chemical nature and source of the enriched Mn and Zn in the offshore suspended matter, selected surface and near-bottom samples were treated with 25% (v/v) acetic acid to separate poorly structured oxyhydroxides from the more crystalline phases. This procedure has been shown to selectively dissolve trace elements precipitated in acid-soluble metal oxides and those adsorbed onto mineral surfaces without affecting highly oxidized ferromanganese minerals or the lattice structure of clays (Hirst and Nicholls, 1958, Chester and Hughes, 1967; and Bolger et al., 1978). The results of these experiments are given in table 18. The data show increased amounts of weak-acid-soluble Mn in the offshore samples relative to the estuarine samples, which are significant at the $p < 0.05$ level. These increases, which are computed by taking the differences between the offshore samples and estuarine samples as a ratio to the estuarine samples, range between 134% and 351% and account for all of the excess Mn in the suspended matter. Similarly, the data for Zn in the weak-acid-soluble fraction show enrichments ranging between 61% and 83% in the offshore samples which are significant at the $p < 0.20$ level. These results indicate that in the offshore waters Mn and Zn are being concentrated in the weak-acid-soluble fraction of the particulate matter, which in these samples probably consists of poorly structured oxhydroxides of Mn.

There are several possible sources for the excess Mn in the suspended matter of Norton Sound. These include: (1) differential settling of particles of various sizes; (2) resuspension of Mn-enriched sediments; and (3) reductive dissolution of Mn within recent sediments followed by oxidative precipitation of Mn onto particulate phases in the water column. The first mechanism is unlikely in view of Gibbs' (1977) data for the chemical variations in the various size fractions of Yukon River suspended material. The mean particle size distribution of suspended material in the Sound would have to decrease by about an order of magnitude (i.e., a decrease from an average size of about 20 μm to about 2 μm) before the two- to threefold increases in total Mn would be observed. Unless some unusual chemical interactions were occurring in the estuary, this would necessarily be accompanied by a similar enrichment of total Fe and Cu in the suspended matter. No enrichments of that magnitude were observed in the Fe and Cu data. Furthermore, the particle size data of Cacchione and Drake (1979) indicate that suspended matter in Norton Sound is primarily composed of fine-to-medium silt in the range between 4 and 32 μm. These data indicate that if differential settling occurs in Norton Sound, it is definitely not of the magnitude required to produce the observed Mn enrichments in the suspended matter.

The resuspension mechanism can also be refuted using a similar argument. While the suspended matter distributions indicated that bottom sediments were being resuspended, the Mn content of the bulk sediments have been reported to be only in the range between 600 and 1650 ppm (Larsen et al., in press). This means that the Mn content of the resuspended material would have to exceed the concentration observed within the sediments by a factor of about 2-4 to account for the observed Mn concentrations in the suspended matter. This would occur only if the clay size fraction of the sediments were being preferentially resuspended. Since the particle size data of Cacchione and Drake (1979) do not show any evidence for a decrease of this kind, this mechanism does not seem likely.

Reduction of Mn after burial in recent sediments with accompanying upward transport of dissolved Mn into the overlying water, followed by precipitation onto suspended matter best explains the observed data. Efflux of Mn from rapidly accumulating sediments have been reported for several estuarine and coastal environments (Elderfield, 1976; Graham et al., 1976; Aller, 1977; Trefry, 1977; Yeats et al., 1979; and Massoth et al., 1979). From studies of the sediments extending seaward of the Mississippi River, Trefry (1977) found that Mn fluxes from recent sediments varied directly with sedimentation rate. High Mn fluxes (i.e., ≅ 2.7 g Mn $cm^{-2}d^{-1}$) were observed in sediments that accumulate at a rate of about 2.0 g cm^{-2} y^{-1}, whereas low Mn fluxes (0.71 g Mn $cm^{-2}d^{-1}$) were observed in sediments that accumulate at a rate of 0.08 g $cm^{-2}y^{-1}$. In Norton Sound modern sediments with accumulation rates ranging from 0.05 to 0.17 g $cm^{-2}y^{-1}$ cover an area of approximately 22,000 km^2 (Nelson and Creager, 1977). Assuming an average sedimentation rate of 0.1g $cm^{-2}y^{-1}$ for these sediments and using linear interpolation of Trefry's (1977) Mn flux data (i.e., 0.68 g Mn $cm^{-2}d^{-1}$), approximately 1.5 x 10^8g Mn would be released daily into Norton Sound from this source. At this rate it would require approximately 21 days to account for all of the estimated excess Mn in the particulate matter (approximately 3.1 x 10^9g Mn, assuming a total area of 45,000 km^2, an average depth of 16 m, an average suspended matter concentration of 4.0 mg/L, and an average concentration of excess Mn at 1079 ppm). If it is assumed that the rate of Mn oxidation is fast relative to an accumulation time of 21 days, then contact periods approximately equal to this time would be required for the chemical interactions to occur. While circulation in the Sound is not completely understood, studies conducted during summer indicate relatively sluggish circulation (Muench et al). Net currents, with speeds varying between 10 and 15 km d^{-1} in surface waters and between 1 and 4 km d^{-1} in deep water, have been measured for short periods of time. Using a mean current of 8 km d^{-1} and a mean travel distance of 400 km, it is estimated that about 50 days are required for water to pass through the Sound. This is a little more than twice the time required for the Mn from the sediment to accumulate onto the suspended matter. Thus, if the underlying assumption that the kinetic rate of Mn oxidation in coastal waters is relatively rapid is correct, then the sediments could easily be the major source of the excess Mn in the suspended matter. The assumption of a rapid rate for Mn oxidation is supported by the recent findings of Wollast et al. (1979), who found that in the Rhine and Scheldt estuaries, Mn oxidation is essentially complete within 10 days and the process is mediated by several strains of marine bacteria indigenous to coastal environments.

The preceding discussion about the geochemical behavior of Mn in the Sound is also important for understanding the chemical behavior of Zn in the suspended matter. As noted earlier, both Zn and Mn are enriched in the weak-acid-soluble fraction of the particulate matter. This is probably due to adsorption and/or coprecipitation of Zn on or in the newly formed Mn oxyhydroxides. Figure 43 shows a plot of the relationship between total Zn and total Mn and for both surface and near-bottom samples. The plot of total Zn versus total Mn is roughly linear (r = 0.60) indicating an association between these two metals in the particulate matter. These results suggest that as the Mn oxyhydroxides form on the particulate matter, Zn is scavenged from solution. In similar fashion, the relationship between weak-acid-soluble Zn and weak-acid-soluble Mn is also roughly linear (r = 0.39). This process effectively concentrates Zn and Mn in the suspended matter, which eventually either settles to the bottom of the Sound or is transported to the northwest into northeastern Bering Sea Shelf and beyond.

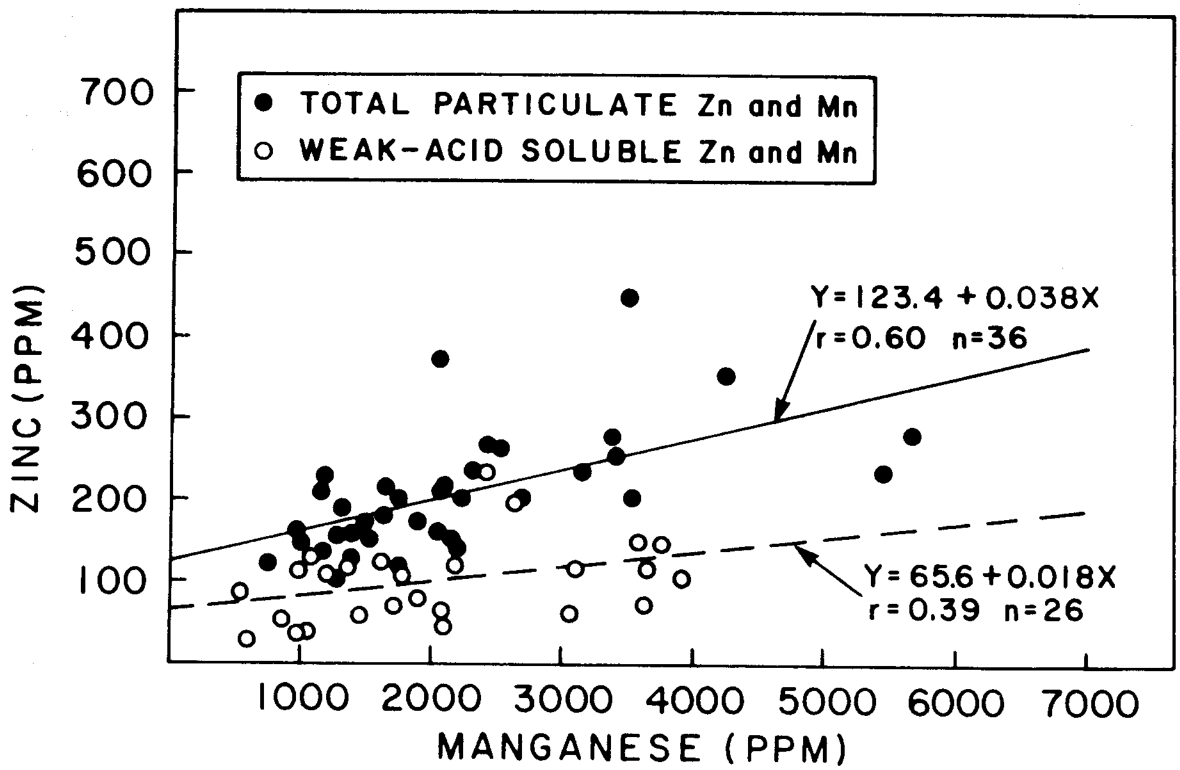

Figure 43. Scatter plot of the relationships between total particulate Zn and Mn (●) and weak-acid soluble Zn and Mn (○) in suspended matter from Norton Sound.

TABLE 16. Comparison of the elemental composition of suspended material from the Yukon River with the composition of suspended material collected from the near-shore regions seaward of the mouths of Yukon River distributaries (surface samples collected with precleaned polyethylene bottles, 11-12 July 1979). Standard deviations are given only for data obtained during a single sampling event wherever applicable.

Sample Description	No. of Samples	C†† Wt. % ± 1σ	N†† Wt. % ± 1σ	Mg Wt. % ± 1σ	Al Wt. % ± 1σ	Si Wt. % ± 1σ	K Wt. % ± 1σ	Ca Wt. % ± 1σ	Ti Wt. % ± 1σ	Cr ppm ±1σ	Mn ppm ±1σ	Fe Wt. % ± 1σ	Ni ppm ±1σ	Cu ppm ±1σ	Zn ppm ±1σ
<u>Yukon River Suspended Material</u>															
Yukon River at Klakanak*										147	1079	5.4	109	320	
Yukon River at Pilot Station**		0.24-3.8								48	788-1308	3.1-4.3		24-148	49-142
<u>Yukon River Estuary</u>															
Surface Samples ($0-15^{\circ}/_{oo}$)	6	2.9 ±0.6	0.2 ±0.04	2.3 ±0.7	8.3 ±1.3	30.6 ±1.9	2.2 ±0.3	1.5 ±0.2	0.50 ±0.06	110 ±15	992 ±131	5.5 ±0.8	59 ±8	59 ±8	171 ±49
<u>Yukon River Estuary</u>															
Surface Samples ($15-25^{\circ}/_{oo}$)	6	4.2 ±1.2	0.4 ±0.8	3.1 ±0.8	9.3 ±1.8	31.5 ±3.7	2.1 ±0.2	1.6 ±0.2	0.52 ±0.03	129 ±15	1299 ±192	5.8 ±0.4	60 ±5	61 ±10	193 ±30

*Data from Gibbs (1977)

**Water Resources Data (1976-1977) U.S. Geological Survey

††Weight percentages of C and N were determined using two different filter types (Selas® silver filters and Nuclepore® filters) and, therefore, are subject to a greater number of errors than the data obtained for the inorganic elements, which were obtained from a single filter type.

TABLE 17. Summary of the elemental composition of suspended material collected from selected locations in Norton Sound and northeastern Bering Sea Shelf (samples were collected with 10-L Niskin bottles, 7-18 July 1979).

Sample Description	No. of Samples	C†† Wt. % ± 1σ	N†† Wt. % ± 1σ	Mg Wt. % ± 1σ	Al Wt. % ± 1σ	Si Wt. % ± 1σ	K Wt. % ± 1σ	Ca Wt. % ± 1σ	Ti Wt. % ± 1σ	Cr ppm ±1σ	Mn ppm ±1σ	Fe Wt. % ± 1σ	Ni ppm ±1σ	Cu ppm ±1σ	Zn ppm ±1σ
Eastern Norton Sound															
Surface	7	15.4 ±4.8	2.4 ±0.9	3.1 ±0.5	9.2 ±1.4	30.1 ±3.7	1.7 ±0.3	1.4 ±0.3	0.44 ±0.06	199 ±59	2346 ±845	5.3 ±0.6	52 ±8	60 ±9	201 ±41
5 m Above Bottom	7	10.1 ±6.2	1.1 ±0.8	2.9 ±0.5	9.1 ±1.3	31.0 ±2.7	2.0 ±0.2	1.4 ±0.2	0.53 ±0.08	144 ±38	2182 ±682	5.7 ±0.4	57 ±5	62 ±10	276 ±289
Central Norton Sound															
Surface	18	14.6 ±8.6	1.9 ±1.1	3.3 ±0.7	9.0 ±1.7	30.8 ±4.8	1.7 ±0.4	1.7 ±0.2	0.48 ±0.08	148 ±36	2672 ±1104	5.4 ±0.8	59 ±21	61 ±12	246 ±90
5 m Above Bottom	18	5.6 ±3.6	0.7 ±0.5	3.0 ±0.6	8.8 ±1.2	32.4 ±2.5	2.0 ±0.2	1.6 ±0.6	0.54 ±0.06	138 ±27	1797 ±287	5.8 ±0.6	57 ±7	58 ±6	196 ±65
Western Norton Sound-northeastern-Bering Sea Shelf															
Surface	18	25.6 ±6.8	4.0 ±0.9	0.9 ±0.7	3.2 ±1.4	20.0 ±7.9	0.5 ±0.2	1.4 ±0.4	0.23 ±0.10	100 ±93	2160 ±1392	2.3 ±0.9	29 ±17	50 ±39	194 ±111
5 m Above Bottom	18	12.3 ±6.9	1.3 ±0.4	1.9 ±0.5	5.1 ±1.2	31.8 ±3.5	0.9 ±0.3	1.2 ±0.2	0.31 ±0.07	81 ±17	1506 ±761	3.4 ±0.7	30 ±13	36 ±11	137 ±60

†† Weight percentages of C and N were determined using two different filter types (Selas® silver filters and Nuclepore® filters) and, therefore, are subject to a greater number of errors than the data obtained for the inorganic elements, which were obtained from a single filter type.

TABLE 18. Average C/N and Element/Al ratios for suspended materials from the Yukon River Estuary, Norton Sound and northeastern Bering Sea Shelf.

Sample Description	C/N	C/Al	N/Al	Mg/Al	Si/Al	K/Al	Ca/Al	Ti/Al	Cr/Al $\times 10^{-3}$	Mn/Al $\times 10^{-3}$	Fe/Al	Ni/Al $\times 10^{-3}$	Cu/Al $\times 10^{-3}$	Zn/Al $\times 10^{-3}$
Yukon River Estuary (0-15°/oo)	14.5	0.35	0.02	0.28	3.73	0.27	0.18	0.06	1.34	12.1	0.66	0.72	0.72	2.08
Yukon River Estuary (15-25°/oo)	10.5	0.45	0.04	0.33	3.39	0.23	0.17	0.06	1.38	14.0	0.62	0.64	0.66	2.07
Eastern Norton Sound														
Surface	6.4	1.71	0.27	0.34	3.34	0.19	0.16	0.05	2.21	26.1	0.59	0.58	0.66	2.23
5 m Above Bottom	9.2	1.11	0.12	0.32	3.41	0.22	0.15	0.06	1.58	24.0	0.63	0.63	0.68	3.03
Central Norton Sound														
Surface	7.7	1.62	0.21	0.37	3.42	0.19	0.19	0.05	1.64	29.7	0.60	0.65	0.67	2.73
5 m Above Bottom	8.0	0.63	0.08	0.34	3.68	0.23	0.18	0.06	1.57	20.4	0.66	0.65	0.66	2.23
Western Norton Sound-Northeastern Bering See Shelf														
Surface	6.4	8.0	1.30	0.28	6.35	0.16	0.44	0.07	3.12	67.5	0.72	0.91	1.56	6.06
5 m Above Bottom	9.5	2.4	0.25	0.37	6.23	0.17	0.24	0.06	1.59	29.5	0.66	0.59	0.67	2.68

TABLE 19. Partitioning of Mn and Zn between weak-acid-soluble (WAS) and weak-acid-insoluble (WAI) fractions of suspended material from Norton Sound and northeastern Bering Sea (data presented as a percentage of total suspended matter).

Sample Location	No. of Samples	WAS Mn $\pm 1\sigma$	WAI Mn $\pm 1\sigma$	WAS Zn $\pm 1\sigma$	WAI Zn $\pm 1\sigma$
Yukon River Estuary	3	0.066 ±0.017	0.052 ±0.006	0.0059 ±0.0028	0.0140 ±0.0031
Eastern Norton Sound	5	0.155 ±0.038	0.040 ±0.011	0.0095 ±0.0031	0.0099 ±0.0021
Central Norton Sound	9	0.184 ±0.085	0.054 ±0.017	0.0108 ±0.0056	0.0114 ±0.0026
Western Norton Sound	9	0.298 ±0.092	0.074 ±0.041	0.0107 ±0.0053	0.0125 ±0.0070

7. CONCLUSIONS

7.1 Northeast Gulf of Alaska

The most significant conclusions of the particulate matter studies in the northeastern Gulf of Alaska are listed below:

1. The distribution of suspended matter at the surface appear to follow the general pattern of water circulation in the Gulf. East of Kayak Island sedimentary material, which is discharged along the coast, is quickly deflected to the west by coastal currents. This material is deflected to the southwest near Kayak Island and is trapped by a clockwise gyre.

2. Sedimentary material from the Copper River is carried to the northwest along the coast until it reaches Hinchinbrook Island where a portion of the material passes into Prince William Sound and the remaining material is carried to the southwest along the southeastern coast of Montague Island.

3. Comparisons of surface suspended matter distribution maps for the three cruises in the Gulf show significant variations which can be related to seasonal variations in the discharge of terrestrially derived suspended matter, seasonal variations in primary productivity, and occasional offshore transport of suspended matter by wind-generated eddies.

4. A bottom nepheloid layer is present throughout most of the Gulf. The height of the nepheloid layer appears to be dependent upon the bottom topography and local currents. Studies of the temporal variability of suspended matter near the bottom show evidence for resuspension and redistribution of bottom sediments. These processes occur as a result of interactions between tidal and storm-induced bottom currents and the surficial sediments.

5. Studies of the chemical composition of the suspended matter show significant spatial and seasonal variations. These variations have been

correlated with: (1) seasonal variations in primary production; (2) seasonal variations in the supply and transport of terrestrially derived suspended matter from coastal rivers; and (3) resuspension of bottom sediments.

7.2 Lower Cook Inlet and Shelikof Strait

The most significant findings of the suspended matter program in lower Cook Inlet are listed below.

1. The suspended matter distributions appear to follow the general pattern of circulation in lower Cook Inlet and Shelikof Strait. The inflowing relatively clear Gulf of Alaska water, which contains significant amounts of biogenic particles as well as aluminosilicate material from the Copper River, flows northward along the eastern coast until it reaches Cape Ninilchik, where it mixes with the outflowing turbid brackish water. The outflowing turbid water moves along the western side of the inlet past Augustine Island and Cape Douglas into Shelikof Strait where it mixes with the oceanic water and is dispersed. Comparison of suspended matter and sediment characteristics as well as regional sedimentation rates indicates that net sedimentation of suspended matter in the central basin of lower Cook Inlet is minimal. However, net sedimentation is occurring in the embayments along the coast and in Shelikof Strait.

2. Chemical analysis of the suspended material from lower Cook Inlet reveals that aluminosilicate minerals from the coastal rivers comprise about 80-95% of the suspended matter, with biogenic matter making up the rest. Analysis of seasonal and regional variations of C/N ratios indicates that organic matter of marine origin predominates the eastern part of lower Cook Inlet throughout the year, whereas organic matter of terrestrial origin predominates the western part of the inlet during winter and early spring when primary production is at a minimum.

3. Comparisons of regional average concentrations of major and trace elements in the particulate matter indicate regional differences which can be related to differences in the average composition of source material and the relative amounts of biogenic and terrigenous components.

4. Studies of trace metal associations with particulate matter reveal that: (1) Mn, Cu, and Zn are enriched in the organic phase of suspended matter in surface waters of Kachemak Bay; and (2) the weak acid soluble phase contains about 46-99% of the total Cu, Ni, and Zn in the samples from the Kalgin Island region. These differences are attributed to differences in the sources for the particles, with primary production of biogenic particles predominant in Kachemak Bay and river discharge of terrestrial rock debris predominant in the Kalgin Island region.

5. Studies of sediment accumulation rates in lower Cook Inlet indicate that most of the suspended material discharged from the local rivers is deposited in Shelikof Strait, not in Cook Inlet. This finding is important for understanding and predicting the long-term fates of contaminants associated with suspended matter.

7.3 Southeastern Bering Sea Shelf

The most significant conclusions of the suspended matter program in the southeastern Bering Shelf are listed below.

1. The surface suspended matter distributions appear to follow the general pattern of circulation in Bristol Bay. Terrestrial suspended matter from the northern rivers is generally carried to the west and southwest by the counterclockwise currents.

2. Large plumes of suspended matter can be seen extending to the southwest from Cape Newenham and to the west from Kuskokwim Bay. Apparently these plumes represent sedimentary material derived from the Kvichak, Nushagak, and Kuskokwim Rivers.

3. Suspended material of marine origin is carried into Bristol Bay along the northern coast of the Alaska Peninsula. In the region north of Unimak Pass large suspended matter plumes have been observed in the early summer and are apparently the result of seasonal productivity.

4. Sharp increases in suspended matter concentrations near the bottom indicate that resuspension of bottom sediments is occurring.

7.4 Norton Sound

The most significant findings of the suspended matter program in Norton Sound are listed below.

1. The suspended matter distribution appears to follow the general pattern of cyclonic circulation in the Sound. The inflowing water picks up terrigenous aluminosilicate material from the Yukon River and transports it to the north and northeast around the inside periphery of the Sound, with one-half to two-thirds of the material being deposited as a band of sediments extending from the Yukon River Delta northward and eastward and the remaining material being transported to the northwest through the Bering Strait and deposited in the Chukchi Sea.

2. Chemical analysis of the suspended material from Norton Sound reveals that aluminosilicate material from the Yukon River comprises about 88-92% of the suspended matter, with biogenic matter making up the rest. Analysis of regional variations of C/N ratios indicates that organic matter of marine

origin predominates in Norton Sound basin, whereas organic matter of terrestrial origin predominates in the Yukon River Estuary.

3. Comparisons of regional average concentrations of major and trace elements in the particulate matter indicate regional differences which can be attributed to differences in the average composition of source material and the relative amounts of biogenic and terrigenous components.

4. Studies of trace metal associations with particulate matter reveal that Mn and Zn are enriched in an oxyhydroxide phase of the surface and near-bottom suspended matter in Norton Sound.

8. Publications and Presentations

Following is a list of publications and presentations that have resulted from this research unit:

Feely, R. A. and G. J. Massoth (in press). Sources, composition, and transport of suspended particulate matter in lower Cook Inlet and northwestern Shelikof Strait, Alaska, U. S. Geological Survey Professional Paper.

Feely, R. A., G. J. Massoth, and A. J. Paulson (1981). The distribution and elemental composition of suspended particulate matter in Norton Sound and the northeastern Bering Sea Shelf: implication for Mn and Zn recycling in coastal waters. In: The Eastern Bering Sea Shelf: Oceanography and Resources, D. W. Hood and J. A. Calder (eds.), Vol I pp. 321-338. U.S. Dept. of Commerce, Washington, D.C.

Feely, R. A., A. J. Chester, A. J. Paulson, and J. D. Larrance (in press). Relationships between organically bound Cu and Mn in settling particulate matter and biological processes in a subarctic estuary, Estuaries.

Landing, W. M., and R. A. Feely (1981). Major and trace element distributions among vertically settling particles and underlying sediments from the northeast Gulf of Alaska, Deep-Sea Res. 28A: 19-37.

Feely, R. A., G. J. Massoth and W. M. Landing. Major and trace element composition of suspended matter in the northeast Gulf of Alaska: Relationships with major sources, submitted to Marine Chem.

Feely, R. A., E. T. Baker, J. D. Schumacher, G. J. Massoth, and W. M. Landing (1979). "Processes affecting the distribution and transport of suspended matter in the northeast Gulf of Alaska," Deep-Sea Res. 26(4A):445-464.

Feely, R. A., E. T. Baker, J. D. Schumacher, G. J. Massoth, and W. M. Landing (1979). "Seasonal variations of the distribution and transport of suspended matter in the northeast Gulf of Alaska," Trans. Amer. Geophys. Union, 60(7):89.

Chester, A. J., R. A. Feely, A. J. Paulson, and J. D. Larrance (1979). "Vertical transport of organically bound trace metals in a subarctic estuary. EDS Trans. Amer. Geophys. Union, 60(46):853.

Massoth, G. J., R. A. Feely, Pierre Y. Appriou, and S. J. Ludwig (1979). "Anomalous concentrations of particulate manganese in Shelikof Strait, Alaska: An indicator of sediment-seawater exchange processes," Trans. Amer. Geophys. Union, 60(46):852.

Landing, W. M., R. A. Feely, and G. J. Massoth (1977). "The distribution and vertical transport of copper and other trace metals in two size fractions of marine particulate matter," Trans. Amer. Geophys. Union, 58(12):1157.

Fisher, J. S., R. A. Feely, and A. W. Young (1977). "A study of particulate matter fluxes on the continental shelf of the Northeast Gulf of Alaska using self-closing sediment traps," Trans. Amer. Geophys. Union, 58(12): 1160.

Landing, W. M., and R. A. Feely (1978). "Major and trace element distributions among suspended particulate matter, vertically settling particles, and underlying sediments from the northeast Gulf of Alaska," Amer. Soc. Limnol. Oceanogr. (abstract).

Feely, R. A., G. J. Massoth, and W. M. Landing (1976). "Factors controlling the trace element composition of suspended matter from the Northeast Gulf of Alaska, Trans. Amer. Geophys. Union, 57(12):931.

References

Aller, R. C. (1977): The influences of macroenthos on chemical diagenesis of marine sediments. Ph.D. dissertation. Yale University, New Haven, CT.

Baier, R. E. (1970): Surface quality assessment of natural bodies of water. Proc. Conf. Great Lakes Res., 13:114-227.

Baker, E. T., and D. Z. Piper (1976): Suspended particulate matter: Collection by pressure filtration and elemental analysis by thin-film x-ray fluorescence. Deep-Sea Res., 23:181-186.

Baker, E. T., J. D. Cline, R. A. Feely, and J. Quan (1978): Seasonal distribution, trajectory studies, and sorption characteristics of suspended particulate matter in the northern Puget Sound region. MESA Rept., EPA-600/7-78-126, 140 pp.

Banse, K. (1974): On the interpretation of data for the carbon to nitrogen ratio of phytoplankton. Limnol. and Oceanogr., 19(4):695-699.

Biscaye, P. E. and Olsen, C. R. (1976): Suspended particulate concentrations and compositions in the New York Bight. In: Middle Atlantic Continental Shelf and the New York Bight, M. G. Gross (Editor), Am. Soc. Limnol Oceanogr., Lawrence, Kansas, pp. 124-137.

Bogdanov, Y. A. (1955): Suspended organic matter in the Pacific, Oceanol., 5(2):77-85.

Bolger, G. W., P. R. Betzer, and V. V. Gordeev (1978): Hydrothermally-derived manganese suspended over the Galapagos Spreading Center, Deep-Sea Res., 25:721-733.

Bouma, A. H., and M. A. Hampton (1976): Preliminary report on the surface and shallow subsurface geology of lower Cook Inlet and Kodiak Shelf, Alaska. U. S. Geological Survey Open File Report. 76-695, 36 pp.

Burbank, D. C. (1974): Suspended sediment transport and deposition in Alaskan coastal waters. M.S. Thesis, University of Alaska, Fairbanks, Alaska, 222 pp.

Burbank, D. C. (1977): Circulation studies in Kachemak Bay and lower Cook Inlet, Alaska, Dept. of Fish and Game, Anchorage, Alaska, 207 pp.

Burrell, D. C. (1977): Natural distribution of trace heavy metals and environmental background in Alaskan Shelf and estuarine areas. In: Environmental Assessment of Alaskan Continental Shelf, Annual Report to Outer Continental Shelf Environmental Assessment Program, Environmental Research Laboratories, National Oceanographic and Atmospheric Administration, Boulder, Colorado, 13:290-481.

Cacchione, D. H. and D. E. Drake (1979): Sediment Transport in Norton Sound, Alaska. U. S. Geological Survey Open File Report 79-1555.

Carlson, P. R., T. J. Conomos, and D. H. Peterson (1975): Principal sources and dispersal patterns of suspended particulate matter in nearshore surface water of the northeast Pacific Ocean. U.S.G.S. 139 pp.

Carlson, P. R., B. F. Molnia, S. C. Kittelson, and J. C. Hampson (1977): Map of the distribution of bottom sediments on the Continental Shelf, Northern Gulf of Alaska. U.S.G.S. Miscellaneous Field Studies Map MF-876.

Charnell, R. L., J. D. Schumacher, and C. A. Pearson (1976): Extreme value analysis applied to current meter data. Submitted for publication.

Chester, R. and M. J. Hughes (1967): A chemical technique for the separation of ferro-manganese minerals, carbonate minerals and adsorbed trace elements from pelagic sediments. Chem. Geol., 2:249-262.

Coachman, L. K., K. Aagaard, and R. B. Tripp (1975): Bering Strait: The regional physical oceanography. Univ. of Washington Press, Seattle, WA., 172 pp.

Crecelius, E. A., M. H. Bothner, and R. Carpenter (1974): Geochemistries of arsenic, antimony, mercury, and related elements in sediments of Puget Sound. Env. Sci Tech., 9:325-333.

Drake, D. E. (1971): Suspended sediment and thermal stratification in Santa Barbara Channel, California. Deep Sea Res., 18:763-769.

Eganhouse, R. P. and D. R. Young (1976): Mercury in tissues of mussels off southern California. Mar. Pol. Bul., 7(8):145-147.

Eganhouse, R. P., D. R. Young, and J. N. Johnson (1979): Geochemistry of mercury in Palos Verdes sediments. Environ. Sci. and Tech., 12(10): 1151-1157.

Eggimann, D. W., and P. R. Betzer (1976): Decomposition and analysis of refractory oceanic suspended materials. Anal. Chem., 48(6):866-890.

El Wardani, S. A. (1960): Total and organic phosphorus in waters of the Bering Sea, Aleutian Trench and Gulf of Alaska. Deep Sea Res., 7: 201-207.

Elderfield, H. (1976): Manganese fluxes to the oceans. Mar. Chem., 4:103-132.

Feely, R. A. (1975): Major element composition of the particulate matter in the near-bottom nepheloid layer of the Gulf of Mexico. Mar. Chem., 3: 121-1256.

Feely, R. A., E. T. Baker, J. D. Schmacher, G. J. Massoth, and W. M. Landing (1979): Processes affecting the distribution and transport of suspended matter in the northeast Gulf of Alaska. Deep-Sea Res., 26(4A): 445-464.

Feely, R. A., J. D. Cline, and G. J. Massoth (1978): Transport in mechanisms and hydrocarbon adsorption properties of suspended matter in lower Cook Inlet. In: Environmental Assessment of the Alaskan Continental Shelf. Annual Report to Outer Continental Shelf Environmental Assessment Program, Environmental Research Laboratories, National Oceanographic and Atmospheric Administration, Boulder, Colorado, 8:11-72.

Feely, R. A. and G. J. Massoth (in press): Sources, composition and transport of suspended particulate matter in lower Cook Inlet and northwestern Shelikof Strait, Alaska. In: Geology of lower Cook Inlet, Alaska, U.S.G.S. Professional Paper, A. H. Bouma, Editor.

Feely, R. A., G. J. Massoth, and A. J. Paulson (1981): The distribution and elemental composition of suspended particulate matter in Norton Sound and the northeastern Bering Sea Shelf: implication for Mn and Zn recycling in coastal waters. In: The Eastern Bering Sea Shelf: Oceanography and Resources, D. W. Hood and J. A. Calder, (eds.), Vol I pp. 321-338. U.S. Dept. of Commerce, Washington, D.C.

Forrester, W. D. (1971): Distribution of suspended-oil particles following the wreck of the tanker ARROW. J. Mar. Res., 29:151-170.

Galt, J. A., and T. C. Royer (1975): Physical oceanography and dynamics of the northeast Gulf of Alaska. Paper presented at Arctic Institute Symposium on the Gulf of Alaska, Anchorage, Alaska, October 1975, 14 p.

Gatto, L. W. (1976a): Circulation and sediment distribution in Cook Inlet, Alaska. In: Assessment of Arctic Marine Environment Selected Types. D. W. Hood and D. C. Burrell (eds.). Occasional Pub. No. 4, Univ. of Alaska, Fairbanks, Alaska, pp. 205-227.

Gatto, L. W. (1976b): Baseline data on the oceanography of Cook Inlet, Alaska. Rep. 76-25, U. S. Army Cold Regions Research and Engineering Laboratory, Hanover, N.H., 84 pp.

Gibbs, R. J. (1973): Mechanisms of trace metal transport in rivers. Science, 18:71-73.

Gibbs, R. J. (1977): Transport phases of transition metals in the Amazon and Yukon Rivers. Geol. Soc. Amer. Bull., 88:829-843.

Gordon, D. C. (1970): Some studies of the distribution and composition of particulate organic carbon in the North Atlantic Ocean. Deep Sea Res., 17:233-244.

Graham, W. F., M. L. Bender, and G. P. Klinkhammer (1976): Manganese in Nargansett Bay. Limnol. Oceanogr., 21(5):665-673.

Hayes, S. P., and J. D. Schumacher (1976): Description of wind current and bottom pressure variations on the Continental Shelf in the N.E. Gulf of Alaska: February-May 1975, Jour. of Geophysical Res., 81:6411-6419.

Hayes, S. P., and J. D. Schumacher (1977): Gulf of Alaska study of mesoscale oceanographic processes. In: Environmental Assessment of Alaskan Continental Shelf, Annual Report of Outer Continental Shelf Environmental Assessment Program, Environmental Research Laboratories, National Oceanic and Atmospheric Administration, Boulder, Colorado, 14:251-328.

Hebard, J. F. (1959): Currents in southeastern Bering Sea and possible effects upon king crab larvae. U. S. Fish and Wildlife Service Special Scientific Report--Fisheries No. 293. 11 pp.

Hein, J. R., A. H. Bouma, M. A. Hampton, and C. S. Ross (1979): Clay minerology, suspended sediment dispersal, and inferred current patterns, lower Cook Inlet and Kodiak Shelf, Alaska. Sedimentary Geology, 24:291-306.

Hirst, D. M., and G. D. Nicholls (1958): Techniques in sedimentary geochemistry. I. Separation of the detrital and non-detrital fractions of limestones. J. Sediment. Petrol., 28:461-468.

Inman, D. L., and C. E. Nordstrom (1971): On the tectonic and morphologic classification of coasts. Jour. Geology, 79:1-21.

Kharkar, D. P., K. K. Turekian, and K. K. Bertine (1968): Stream supply of dissolved silver, molybdenum, antimony, selenium, chromium, cobalt, rubidium, and cesium to the oceans. Geochim. et Cosmochim. Acta., 32: 285-298.

Kinney, P. J., D. K. Button, D. M. Schell, B. R. Robertson, and J. Groves (1970): Quantitative assessment of oil pollution problems in Alaska's Cook Inlet. Rep. R-169. Institute of Marine Science, Univ. of Alaska, Fairbanks.

Klemas, V., and D. F. Polis (1977): A study of density fronts and their effects on coastal pollutants. Remote Sensing of Environment, 6:95-126.

Knauer, G. A., and J. H. Martin (1973): Seasonal variations of cadmium, copper, manganese, lead, and zinc in water and phytoplankton in Monterey Bay, California. Limnol. and Oceanogr., 4:597-604.

Kolpack, R. L. (1971): Biological and oceanographic survey of the Santa Barbara channel oil spill, 1969-1970. Vol. II. Physical, Chemical, Geological Studies, Allen Handcock Foundation, University of Southern California, Los Angeles, 477 pp.

Kreider, R. E. (1971): Identification of oil leaks and spills. In: Proceedings, Joint Conference on Prevention and Control of Oil Spills. American Petroleum Institute, Washington, D.C., pp. 119-124.

Landing, W. M. (1978): The chemistry and vertical flux of particulate materials in the northeast Gulf of Alaska. M.S. Thesis, Univ. of Washington, Seattle, WA., 102 pp.

Larrance, J. D., D. A. Tennant, A. J. Chester, and P. A. Ruffio (1977): Phytoplankton and primary productivity in the northeast Gulf of Alaska. In: Environmental Assessment of the Alaskan Continental Shelf, Annual Report to the Outer Continental Shelf Environmental Assessment Program, Environmental Research Laboratories, National Oceanic and Atmospheric Administration, Boulder, CO., 10:1-136.

Larrance, J. D. and A. J. Chester (1978): Organic detritus and primary productivity in lower Cook Inlet. In: Environmental Assessment of the Alaskan Continental Shelf, Annual Report to the Outer Continental Shelf Environmental Assessment Program, Environmental Research Laboratories, National Oceanic and Atmospheric Administration, Boulder, CO., 15 pp. ch

Larrance, J. D., and A. J. Chester (1979): Primary productivity and sedimentation of organic detritus in lower Cook Inlet. In: Environmental Assessment of the Alaskan Continental Shelf, Final Report to the Outer Continental Shelf Environmental Assessment Program, Environmental Research Laboratories, National Oceanic and Atmospheric Administration, Boulder, CO., 50 pp.

Larrance, J. D., and D. A. Tennant (March 1977): Phytoplankton studies in the northeast Gulf of Alaska, Cook Inlet and Prince William Sound. In: Environmental Assessment of the Alaskan Continental Shelf, Final Report to the Outer Continental Shelf Environmental Assessment Program, ERL, NOAA, Boulder, CO., 10:1-136.

Larsen, B. R., C. H. Nelson, C. Heropoulos, and S. S. Patry (in press): Distribution of trace elements in bottom sediments of northern Bering Sea. U. S. Geological Survey Open File Report.

Loder, T. C., III (1971): Distribution of dissolved and particulate organic carbon in Alaskan polar, subpolar and estuarine waters. Ph.D. Thesis, Institute of Marine Science, University of Alaska, Fairbanks, Alaska.

Loder, T. C., and D. W. Hood (1972): Distribution of organic carbon in a glacial estuary in Alaska. Limnol. and Oceanogr., 17(3):349-355.

Luoma, S. N., and G. W. Bryan (1978): Factors controlling the availability of sediment-bound lead to the estuarine bivalve Scorbicularia plana. J. Mar. Biol. Ass. U.K., 58:793-802.

Malo, B. A. (1977): Partial extraction of metals from aquatic sediments. Env. Sci. Tech., 11:277-282.

Martin, J. H., and G. A. Knauer (1973): The elemental composition of plankton. Geochim. et Cosmochim Acta., 37:1639-1653.

Massoth, G. J., R. A. Feely, Pierre Y. Appriou, and S. J. Ludwig (1979): Anomalous concentrations of particulate manganese in Shelikof Strait, Alaska: An indicator of sediment-seawater exchange processes. EOS Transactions Amer. Geophys. Union, 60(46):852.

McAuliffe, C. (1966): Solubility in water of paraffin, cycloparaffin, olefin, acetylene, eycloulefin, and aromatic hydrocarbons. J. Phy. Chem., 70:1267-1273.

McAuliffe, C. (1969): Solubility in water of normal C_9 and C_{10} alkane hydrocarbons. Science, 158:478-479.

McManus, D. A., V. Kolla, D. M. Hopkins, and C. H. Nelson (1974): Yukon River sediment of the northernmost Bering Sea Shelf. J. Sediment Petrol., 44:1052-1060.

McManus, D. A., V. Kolla, D. M. Hopkins, and C. H. Nelson (1977): Distribution of bottom sediments on the Continental Shelf, Northern Bering Sea. U.S. Geological Survey Prof. Pub. 759-C, pp. C1-C31.

Meade, R. H., P. L. Sachs, R. T. Manheim, J. C. Hathaway, and D. W. Spencer (1975): Sources of suspended matter in waters of the Middle Atlantic Bight. J. Sedimentary Petrol., 45:171-188.

Menzel, D. W., and R. F. Vaccaro (1964): The measurement of dissolved organic and particulate carbon in seawater. Limnol and Oceanogr., 9:138-142.

Morris, A. W. (1971): Trace metal variations in sea water of the Menai Straits caused by a bloom of Phaeocystis. Nature, 233:427-428.

Muench, R. D. and K. Ahlnäs (1976): Ice movement and distribution in the Bering Sea from March to June 1974. J. Geophys. Res., 81:4467-4476.

Muench, R. D., H. O. Mofjeld, and R. L. Charnell (1978): Oceanographic conditions in lower Cook Inlet: spring and summer 1973. J. Geophys Res., 83:5090-5098.

Muench, R. D., R. B. Tripp, and J. D. Cline (1981): Circulation and hydrography of Norton Sound. In: The Eastern Bering Sea Shelf: Oceanography and Resources, D. W. Hood and J. A. Calder (eds.), Vol. I. pp. 77-94, U.S. Dept. of Commerce, Washington, D.C.

Nelson, C. H. (1974): Late holocene sediment dispersal in northeastern Bering Sea. In: U.S. Geological Survey Alaska Program, 1974 (circ. 700) (C. Carter, ed.), U.S. Geol. Survey, Reston, Virginia.

Nelson, C. H., and J. S. Creager (1977): Displacement of Yukon-derived sediment from Bering Sea to Chukchi Sea during Holocene Time. Geology, 5:141-146.

Nelson, C. H., D. M. Hopkins, and D. W. Scholl (1974): Cenzole sedimentary and tectonic history of the Bering Sea. In: D. W. Hood and E. J. Kelley (eds.), Oceanography of the Bering Sea, Institute of Marine Science Occasional Pub. No. 2, Univ. of Alaska, Fairbanks, Alaska, 485-510.

Nelson, C. H., B. R. Larsen, and R. W. Rowland (1975): ERTS Imagery and dispersal of the Yukon and Kuskokwim River Plumes. In: Curlson, P. R. (ed.), Principal sources of dispersal patterns of suspended particulate matter in nearshore surface waters of the northeast Pacific Ocean. U.S. Dept. of Commerce, Natl. Tech. Inf. Serv., E75-10266, pp. 26-40.

NOAA Special Report (1977): The ARGO MERCHANT oil spill - a preliminary scientific report. National Oceanic and Atmospheric Administration, Boulder, CO.

Price, N. B., and S. E. Calvert (1973): A study of the geochemistry of suspended particulate matter in coastal waters. Mar. Chem., 1:169-189.

Reimnitz, E. (1966): Late quartenary history and sedimentation of the Copper River Delta and vicinity, Alaska. Unpublished Ph.D. dissertation, Univ. of California, La Jolla, 255 pp.

Rosenberg, D. H., and D. W. Hood (1967): Descriptive oceanography of Cook Inlet, Alaska. Am. Geophys. Union Trans., 048, No. 1, p. 132.

Sackett, W. M., and G. Arrhenius (1962): Distribution of aluminum species in the hydrosphere. I. Aluminum in the oceans. Geochim et Cosmochim. Acta,: 26:955-968.

Sharma, G. D., and D. C. Burrell (1970): Sedimentary environment and sediments of Cook Inlet, Alaska. Amer. Assoc. Pet. Geol. Bull., 54(4): 647-654.

Sharma, G. D., F. F. Wright, J. J. Burns, and O. C. Burbank (1974): Sea surface circulation, sediment transport and marine mammal distribution, Alaska Continental Shelf: ERTS Final Report. Natl. Tech. Serv. Report E74-10711.

Sharma, G. D. (1974): Contemporary depositional environment of the eastern Bering Sea. In: D. W. Hood and E. J. Kelley (eds.) Oceanography of the Bering Sea. Institute of Marine Science Occasional Pub. No. 2, Univ. of Alaska, Fairbanks, Alaska, pp. 517-552.

Sharma, G. D. (1979): The Alaskan Shelf: Hydrographic, Sedimentary and Geochemical Environment. Springer Verlag, New York.

Sharp, J. H. (1974): Improved analysis for particulate organic carbon and nitrogen from seawater. Limnol. and Oceanogr., 6(19):984-989.

Sholkovitz, E. R. (1976): Flocculation of dissolved organic and inorganic matter during the mixing of river water and seawater. Geochim. et Cosmochim. Acta., 40:831-845.

Spencer, D. W., and P. L. Sachs (1970): Some aspects of the distribution, chemistry and mineralogy of suspended matter in the Gulf of Maine. Mar. Geol., 9:117-136.

Sternberg, R. W., E. T. Baker, D. A. McManus, S. Smith, and D. R. Morrison (1974): An integrating nephelometer for measuring particle concentrations in the deep sea. Deep Sea Res., 21:887-892.

Trefry, J. H. (1977): The transport of heavy metals by the Mississippi River and their fate in the Gulf of Mexico. Ph.D. dissertation, Texas A & M Univ., College Station, Texas 77843.

Tsunogai, S. M., M. Nozaki, M. Minagawa, and S. Yamamoto (1974): Dynamics of particulate material in the ocean. In: Oceanography of the Bering Sea. D. W. Hood and E. J. Kelley (eds.). Institute of Marine Science, Univ. of Alaska, Fairbanks, Alaska.

Turekian, K. K. (1971): Transport processes and reservoirs. Part II. Rivers, tributaries and estuaries. In: Impingement of Man on the Oceans. D. W. Hood (ed.). Wiley-Interscience, New York, pp. 9-75.

Wright, F. F., G. D. Sharma, and D. C. Burbank (1973): ERTS-1 observations of sea surface circulation and sediment transport, Cook Inlet, Alaska. In: Proceedings of the Symposium on Significant Results Obtained from the Earth Resources Technology Satellite-1. National Aeronautics and Space Administration, Washington, D.C., pp. 1315-1322.

Wollast, R., G. Billen, and J. C. Duninker (1979): Behavior of manganese in the Rhine and Scheldt Estuaries. Estuarine and Coastal Marine Science, 9:161-169.

Yeats, P. A., B. Sunby, and J. M. Bewers (1979): Manganese recycling in coastal waters. Mar. Chem., 8:43-55.

TIDAL DATA FROM THE

BERING, CHUKCHI, AND BEAUFORT SEAS

by

Ronald W. Pitman

Brown and Caldwell
Marine Sciences Division

Final Report
Outer Continental Shelf Environmental Assessment Program
Research Unit 642

May 1984

TABLE OF CONTENTS

LIST OF FIGURES

LIST OF TABLES

INTRODUCTION

This report relates Brown and Caldwell's activities for the Outer Continental Shelf Environmental Assessment Program (OCSEAP) project entitled Oceanographic Data for the Bering, Chukchi and Beaufort Seas (WASC 8300114). The purpose of the project was to obtain and process measurements of tide along the Alaskan coast from Norton Sound north to Pt. Barrow and east of Pt. Barrow to the United States/Canada Border. Desired information from these measurements were amplitude and phase of astronomical tidal constituents at locations throughout the study area, which covers thousands of miles of the Alaskan coast. Tidal measurements are necessary to adapt a numerical model of deep-water tidal circulation to the relatively shallow continental shelf areas of potential petroleum exploration and development. The tidal circulation model is a sub-model of an oil-spill risk analysis, and knowledge of the tidal circulation is required in order to estimate oil spill transport. Since the study area is in the harsh Arctic environment, historical data is very limited, and simultaneous tidal measurements did not exist for this area prior to this study.

Scope of Work

This project involved collection and analyses of pressure data from bottom mounted sensors in order to determine amplitude and phase of major tidal constituents. Most of the study area is north of the Arctic Circle, and is covered by ice most of the year. Therefore, deployment and retrieval of in-situ recording pressure gauges was scheduled for the short period of ice breakup during the summer. A minimum of 29 days of measurement were required at each location in order to obtain the amplitude and phase of the tidal constituents by harmonic analysis. Additionally, a minimum overlap of 20 days of simultaneous measurements at all locations was required to allow estimation of tidal constituents at locations between measurement sites.

Brown and Caldwell (BC) was responsible for collection and analysis of data for determination of amplitude and phase of tidal constituents. OCSEAP supplied most of the instrumentation and logistical support for the project. The scope of work was separated into four major tasks: prefield work, field effort, data processing and analyses, and reporting and deliverables.

Prefield effort included: (1) final planning and coordination with NOAA agencies such as OCSEAP, Pacific Marine Center (PMC), Pacific Marine Environmental Laboratories (PMEL), and others, (2) check out of pressure gauges and acoustic releases supplied by PMEL and other equipment supplied by Brown and Caldwell (BC), (3) construction of moorings for instrumentation, and (4) initial data processing.

Field effort involved mobilization and demobilization of equipment and personnel to or from Prudhoe Bay, Dutch Harbor, Nome, and Barrow, Alaska, and deployment and retrieval of instrumentation. NOAA supplied logistical support for deployments in Norton Sound and Chukchi Sea from the R/V Discoverer. The R/V Surveyor was used for recoveries from these areas. Logistical support for Beaufort Sea deployments was provided by OCSEAP personnel and NOAA's helicopter group. Personnel from BC supervised deployment and retrieval of instrumentation.

Data processing and analysis tasks included: (1) preliminary processing to scale data to engineering units, (2) correcting absolute pressure data for the effects of barometric pressure, (3) conversion of pressure data to elevation of water over the pressure sensor, and (4) harmonic analysis of data to determine amplitude and phase of tidal constituents.

Reporting involved preparing work products for the study which included: (1) a field work report, (2) this final report, (3) a magnetic tape of all data, and (4) presentation of preliminary results at the Chukchi Sea Synthesis meeting, held in Aleyska in November 1983.

Station Locations and Measurement Periods

The eight measurement sites used in this project were selected by OCSEAP and the contractor responsible for modeling. Two of the sites were located in Norton Sound, two in the Chukchi Sea and four along the Beaufort Coast of the North Slope. Near shore measurements were required to adapt the deep water tidal circulation models to the shallow nearshore area. Station locations are shown on Figures 1 and 2.

The deployment and retrieval of pressure gauges along the northern Alaskan coast were accomplished during a severe year for ice. The late ice breakup along the Beaufort coast and the short ice free season did not allow the instruments to be deployed at the originally selected sites. Ice along most the Beaufort coast was against the outer edge of the barrier island or up against the shore, with the only areas of open water being inside the barrier islands. After discussions with Dr. Liu of the Rand Corporation and Dr.Hameedi of OCSEAP, alternative sites were chosen for Stations 5 through 8. Most of these alternative sites were located along the inner edge of a barrier island at locations relatively protected from ice floes and close to major inlets in the barrier island chain. The original locations for pressure gauges are shown by the circled station numbers on Figure 2. Actual deployment locations are shown by the point of the arrow and on Figures 2-a through 2-d.

Deployments of instrumentation in the Beaufort and Chukchi Seas were carried out simultaneously between August 5 and August 8, 1983, as presented in Table 1. Instruments were recovered from the

Beaufort coast between September 8 and 10, 1983. Instruments in the Chukchi Sea and Norton Sound were recovered between September 15 and 19, 1983.

METHODS

This section relates instrumentation and methods used in the study. Pertinent information on predeployment planning and testing, the type of mooring used, deployment and retrieval of instrumentation, and data processing and analyses is presented.

Instrumentation

Most of the instrumentation for this project was provided by the National Oceanographic and Atmospheric Administration (NOAA) through an agreement between OCSEAP and Pacific Marine Environmental Laboratories (PMEL). Eight Aanderaa pressure gauges and eight AMF acoustic releases were provided by PMEL. The Aanderaa pressure gauges included one model TG3, two model TG4A, and five model WLR-5. All of these models use a Paroscientific pressure sensor to sense absolute pressure by the variation in frequency of oscillations of a quartz crystal. A temperature sensor was included in all but one of the pressure instruments. The different models of pressure gauges were similar, but differed in the sample integration time, sampling interval, range of pressure measurement, and recording scheme.

The AMF acoustic releases supplied by PMEL included four squib fired releases (Model 242) and four solenoid actuated releases (Model 395). The acoustic releases were used to retrieve the pressure gauges from the ocean bottom at sampling locations in Norton Sound and the Chukchi Sea. PMEL also provided the deck unit for the AMF releases. Model 395 acoustic releases were not used at Stations 5 through 8, since these stations had to be moved to ice-free, shallow-water sites near the barrier islands.

Calibration and Testing Procedures

Prior to deployment, instrumentation was shipped from PMEL to Brown and Caldwell's Costa Mesa test facility. Proper operation of instrumentation was verified in a relatively short period of time, between July 8 and 12, 1983. Proper operation of pressure gauges was tested by creating test tapes of barometric pressure and processing these data tapes. Pressure gauges had previously been calibrated at NOAA's Northwest Regional Calibration Center, and calibration reports were supplied to BC by PMEL. Barometric pressure data recorded by the Aanderaa instruments was compared to that of a precision mecury laboratory barometer. Upon receiving the deck unit for the acoustic releases, proper operation of the releases was verified by the system air acoustic check recommended by the manufacturer.

Mooring Design

The mooring design was a taut-leg, near-bottom mooring shown in

Figure 3. The height of this taut-leg mooring was kept to a minimum so that the mooring would not be destroyed by ice. The mooring design included a polypropylene tag line which could be used for recovery should the acoustic release fail.

Ice conditions on the Beaufort Coast during the summer of 1983 were quite severe and prevented deployment of pressure gauges at the water depth desired. Mooring design for Stations 5 through 8 had to be modified to allow the mooring to be placed in ice free areas inside of the barrier islands along the Beaufort coast. This mooring design consisted of the Aanderaa pressure gauge encased inside a PVC pipe, a small flotation ball, a chain anchor, and a tag line which was anchored on the beach of the barrier island using a Danforth anchor. This type of mooring is illustrated in Figure 4.

Deployment and Retrieval

Methods of deployment and retrieval differed for the Chukchi and Beaufort Sea deployment areas. Deployments in Norton Sound and Chukchi Sea were made from the NOAA Ship R/V Discoverer, and retrieval of instruments was accomplished from the R/V Surveyor. Beaufort Sea deployments and retrievals of pressure gauges was accomplished from a chartered sea plane and/or a NOAA helicopter.

Aboard the Discoverer, the taut leg moorings were assembled on deck. The AMF acoustic release was connected to the 28-inch diameter submerged float and anchor chain clump by a seized shackle. The 100-meter tag line was attached to the anchor chain clump. The pressure gauge, mounted inside a protective PVC tube, was attached to the stainless steel mooring rod of the AMF release. After the ship had been positioned on station by Loran C and/or satellite navigation equipment, the mooring was deployed. A crane was used to lift the mooring off the deck and lower it to the ocean floor. A gravity hook detached the mooring from the crane when the anchor reached the ocean floor. As the mooring was lowered over the side, the tag line was let out slowly to keep slight tension on the mooring. Once the mooring was on the bottom, the tag line was stretched out from the mooring on a known bearing and then deployed. After deployment of the instrumentation, a CTD cast was made to determine the density of the water column at the site.

Retrieval of instrumentation was accomplished from the NOAA ship R/V Surveyor. Upon arrival at the station, a CTD cast was obtained. An EG&G acoustic release deck unit and hydrophone were used to confirm that the acoustic release was operational and nearby. The release command was sent after receiving confirmation that the release was in the general vicinity and that the whale boat used for recovery was ready. The AMF acoustic release disconnected itself from the clump of anchor chain and the submerged flotation ball brought the release and pressure gauge to the surface. The whale boat retrieved the instrumentation and brought it alongside the R/V Surveyor. A crane was used to lift the instrumentation aboard.

Beaufort Sea deployments were made from a charted sea plane and/or NOAA helicopter. Ice conditions prevented deployment by vessel. Moorings were deployed along barrier islands in ice protected areas near major inlets in the barrier island chain. These moorings consisted of the Aanderaa pressure gauges in a PVC tube,

The pressure gauge and tube were supported by an 8-in submerged float attached to the top of the tube, and anchored by a 50-lb piece of chain attached to the bottom of the tube. A tag line was tied to this chain and led to a Danforth anchor which was buried on the beach of the barrier island. Pressure gauges along the coast were retrieved using a chartered helicopter.

Preliminary Data Processing

Preliminary data processing consisted of the steps necessary to get raw data ready for harmonic analysis. Raw data were transcribed from the internally-recorded, 1/4-inch, reel-to-reel tape to Brown and Caldwell's computer system via the RS232C output port of an Aanderaa 2650 tape reader. Instruments recorded raw data as counts. Data were scaled to engineering units of degrees Celsius and pounds per square inch absolute (psia) using calibration coefficents determined by NOAA's Northwest Regional Calibration Center. Time history plots of the absolute pressure fluctuations about the mean were prepared for quality assurance checks of the data.

Barometric pressure data were subtracted from the absolute pressure records. Hourly records of barometric pressure from the following locations were obtained from the National Weather Service (NWS) for the deployment period: Unalakleet, Nome, Kotzebue, Cape Lisburne, Barrow, Deadhorse, and Barter Island. Measurements at Deadhorse and Unalakleet were available for approximately half the day. Barometric pressure data for periods of data gaps were determined from weather charts produced by the NWS Anchorage Forecast Center for the Alaskan region. These weather charts are produced at six-hour intervals. Since no barometric pressure records were readily available for locations close to Thetis Island, Flaxman Island, and Demarcation Bay, barometric pressure data for these stations were also determined from weather charts. Data were interpolated between the six-hour synoptic times of the weather charts.

Time history plots of barometric pressure and gauge pressures corrected for barometric pressure were created to allow quick quality assurance checks of the data. Pressure measurements were converted to the height of water above the pressure sensor by dividing the pressure by the product of a constant density times the accleration of gravity. Density for the deployment period was estimated from density profile measurements during deployment and retrieval of instruments.

Harmonic Analyses

Harmonic analyses of these pressure records were performed on BC's computer system using a program developed by Dennis and Long

(1971) and adapted to a Digital Equipment Corporation computer system. This program performs harmonic analyses base on work by Schureman (1958). As originally presented in our proposal,Brown and Caldwell intended to perform the harmonic analyses with the aid of the Rapid Retrieval Data Display (R2D2) software on the Environmental Research Laboratories computer in Boulder Colorado. Since access to this computer system was not available to BC in a timely and cost-efficient manner, the analyses were performed on BC's computer with software very similar to that of the R2D2 system.

RESULTS

This section presents results of the project and discusses data recovery and quality. Data presented in graphical and tabular form in the report are contained on a magnetic tape transmitted with the final report.

Data Recovery and Quality

Each Aanderaa pressure gauge operated correctly during the entire deployment period and recorded accurate pressure data. Since simultaneous records of more than 29 days duration were obtained at each station, harmonic analyses were performed on the same 29-day period for each sampling location.

The instrument at Station 7, offshore of Flaxman Island, was deployed on August 5. The instrument was pulled ashore by someone on August 12. The instrument was returned to the shallow water intertidal area on August 20 and recorded tidal fluctuations through August 26. The data then became erratic and was not representative of tidal fluctuations after that date. Approximately 13 days of actual tidal data were recorded by this instrument.

Data from all other stations were valid and had durations of 32 to 35 days at Beaufort stations and 39 to 42 days at Chukchi and Norton stations. The interference with the instrument deployed offshore of Flaxman Island reduced valid data return from 100 to 93 percent.

Time history plots of corrected pressure measurements at Stations 1 through 4 in the Chukchi Sea and Norton Sound are presented on Figures 5 and 6, and similar plots for Stations 5 through 8 in the Beaufort Sea are presented on Figures 7 and 8. Time history plots of near bottom temperatures at these same locations are presented in Figures 9 through 12.

Time history plots show the fluctuations of temperature or pressure around the monthly mean of the data. Pressure plots for the various stations are offset by 2 psi from one another, and temperature plots are offset by 6 degrees C from one another.

Barometric Pressure Data

Measurements of absolute pressure near the ocean bottom were adjusted for barometric pressure. Time history plots of barometric pressure used to correct pressure records are presented in Figures 13 through 16. Actual barometric pressure records from Unalakleet, Nome, Kotzebue, Cape Lisburne, and Barrow were obtained from NWS. Since no weather stations were located near the other measurement sites on the Beaufort coast, barometric pressure data were determined from synoptic weather charts at six hour intervals.

Density Profiles

Density profiles were measured just after deployment and prior to recovery of pressure gauges at Stations 1 through 4. These density profiles were used to determine an average density for the deployment period. This density data were required to convert pressure measurements to a water depth. The average densities used for these conversions were as follows:

Station No.	Location	Density (Sigma-t)
1	Cape Denbigh	1.01750
2	Nome	1.02230
3	Kotzebue	1.02400
4	Ledyard Bay	1.02400
5	Cooper Is.	1.02486
6	Thetis Is.	1.02486
7	Flaxman Is.	1.02486
8	Demarcation Bay	1.02453

Actual density data measured at Stations 1 through 4 during deployment and retrieval cruises are presented in Tables 2 through 9. No density profile measurements were obtained for Stations 5 through 8 because water depths at these stations were very shallow. Density at Stations 5 through 8 were estimated from temperature measurements recorded by the instruments and an assumed salinity.

Harmonic Analysis

Results of harmonic analysis of pressure records are summarized in Table 10. Amplitudes and phases are presented for the primary, harmonic, and secondary tidal constituents. The amplitudes are in centimeters and Greenwich phases are in degrees.

DISCUSSION

The amplitude of tides in the study area were fairly small compared to that previously measured in the eastern Bering Sea, to the South of the present study area. In the eastern Bering Sea, the amplitude of tidal constituents generally ranged from tens of centimeters to approximately a meter (Pearson et al. 1981). The amplitude of the primary tidal constituents for the present study area ranged from a few centimeters to tens of centimeters.

Tidal conditions were significantly different at the eight sampling stations. Tidal fluctuations were largest at Cape Denbigh and smallest at Ledyard Bay.

Tides at Cape Denbign were predominately diurnal with the Luni-solar (K1), principal lunar (O1), and solar diurnal (P1) having the larger amplitudes, as shown in Table 10. The principal semi-diurnal lunar component (M2) had a amplitude similar to that of the solar diurnal component. At Nome, tides were mixed. The principle semi-diurnal lunar component was approximately 10 cm in amplitude, but the three principal diurnal components were predominant, with amplitudes of 5 to 15 cm. In Kotzebue Sound tidal fluctuations were predominately semi-diurnal, with M2 having an average amplitude of 9.7 cm. The largest diurnal component was K1 and it's amplitude was only 2.9 cm.

In Ledyard Bay, tidal fluctuations were almost nil. The principal semi-diurnal lunar component had an amplitude of 3.0 cm, and the other constituents had even smaller amplitudes. As previously predicted by the tidal circulation model, an amphdromic point for M2 and other constituents are located in Ledyard Bay.

Tides along the entire Beaufort coast were also fairly small and predominantely semi-diurnal. The principal semi-diurnal lunar component (M2) was the largest tidal constituent at all stations on the Beaufort Coast. The amplitude of M2 ranged from 5.1 cm at Cooper Island to 7.2 cm at Demarcation Bay. The amplitude of the diurnal components O1 and K1 were also small at stations on the Beaufort Coast, ranging from 1.2 to 4.3 cm.

Significant nontidal fluctuations were observed in the pressure records. Many of the larger fluctuations with durations of 1 to 2 days were related to storm surge. The barometric pressure plots presented on Figures 13 through 16 illustrate the passage of low pressure systems on August 8 and 18, and September 7, 1983. Significant storm surges with magnitudes up to a meter in height were observed in the pressure records. Most of these storm surges were observed throughout the Chukchi and Beaufort Seas, but not in Norton Sound, especially during storms on August 18 and September 7, 1983. These storm surges were associated with the passage of arctic low pressure systems from west to east a couple of hundred miles offshore of the Beaufort coast. These summer storms were not as intense as many of the fall and winter storms which would probably cause larger storm surges.

The pressure records also exhibit longer period fluctuations, such as the general decrease in pressure from August 8 to 18 and the general increase in pressure on the Beaufort coasts and Chukchi Sea in late August. Temperature records also show significant changes during these general changes in pressure, suggesting changes in water characteristics. A cursory inspection of weather charts suggest that these long term pressure fluctuations are related to large scale meteorological events throughout the Bering Sea and Chukchi Sea.

REFERENCES

Dennis, R.E., and E. E. Long. A Users Guide to a Computer Program for Harmonic Analysis of Data at Tidal Frequencies. NOAA Technical Report NOS 41 July 1971

Pearson, Carl A., Harold O. Mofjeld, and Richard B. Tripp. Tides of the Eastern Bering Sea Shelf The Eastern Bering Sea Shelf Oceanography and Resources. Volume 1, editied by Donald W. Hood and John A. Calder 1980

Schureman, Paul Manual of Harmonic Analysis and Prediction of Tides. Special Publication No. 98 Department of Commerce, October, 1971

Table 1. Tide Sampling Locations and Times (GMT)

STA	LOCATION	LAT (N) DEG	MIN	LONG (W) DEG	MIN	DEPLOYMENT DATE	TIME	RECOVERY DATE	TIME
1	CAPE DENBIGH	64	20.2	161	30.7	AUG 6	1718	SEP 16	0434
2	NOME	64	19.9	165	00.8	AUG 7	0218	SEP 15	0253
3	KOTZEBUE SOUND	67	30.2	165	00.3	AUG 8	0301	SEP 19	0130
4	LEDYARD BAY	69	28.8	165	03.2	AUG 8	1838	SEP 19	1901
5	COOPER ISLAND	71	14.0	155	44.5	AUG 7	2103	SEP 9	1925
6	THETIS ISLAND	70	33.0	150	11.0	AUG 6	0057	SEP 10	0150
7	FLAXMAN ISLAND	70	11.0	145	57.7	AUG 5	2236	SEP 9	0140
8	DEMARCATION BAY	69	41.2	141	17.6	AUG 5	2032	SEP 8	2335

Table 2. Density Profile Data After Deployment of Instruments at Station 1

SDS-IIA Lister Program 8006.3

08-AUG-83 08:31:33 Data Base: CTD001.DBS

First Line Absolute Time= 218/ 17:59:10.1 Time Relative to: 218/ 17:59:10

Time	CTD-TEMP DEG-C	CTD-DEPT METERS	CTD-COND MS-CM	SALINITY PPT	SIGMA-T G/CC-1
17:59:10.1	14.062	1.885	29.922	24.027	17.844
17:59:12.1	14.092	2.114	29.927	24.012	17.827
17:59:14.1	14.099	2.343	29.924	24.006	17.821
17:59:16.1	14.085	2.874	29.969	24.054	17.861
17:59:18.1	14.120	3.432	30.006	24.065	17.863
17:59:20.1	14.123	3.771	30.002	24.059	17.858
17:59:22.1	14.126	4.439	29.986	24.043	17.845
17:59:24.1	14.125	4.943	29.995	24.052	17.852
17:59:26.1	14.127	5.337	30.004	24.058	17.857
17:59:28.1	14.125	5.877	30.036	24.087	17.879
17:59:30.1	14.127	6.472	30.033	24.083	17.876
17:59:32.1	14.124	6.939	30.001	24.057	17.856
17:59:34.1	14.128	7.433	30.002	24.055	17.854
17:59:36.1	14.129	7.900	30.018	24.068	17.864
17:59:38.1	14.125	8.459	30.020	24.073	17.868
17:59:40.1	14.125	9.081	30.025	24.077	17.872
17:59:42.1	14.124	9.392	30.021	24.073	17.869
17:59:44.1	14.130	10.097	30.065	24.109	17.896
17:59:46.1	14.144	10.509	30.079	24.112	17.895
17:59:48.1	14.147	11.004	30.076	24.108	17.891
17:59:50.1	14.150	11.489	30.073	24.103	17.887
17:59:52.1	14.148	12.093	30.062	24.095	17.881
17:59:54.1	14.147	12.532	30.059	24.092	17.879
17:59:56.1	14.147	12.908	30.062	24.095	17.881
17:59:58.1	14.148	13.476	30.074	24.104	17.889
18:00:00.1	14.148	13.604	30.075	24.105	17.889

Table 3. Density Profile Data Before Retrieval of Instruments at Station 1

DIGITAL DATA LOGGER DUMP PAGE NO.

PROGRAM: DDL2 8006.20 SHIP: S132 READ FROM MT0: FILE NO. 2 PFREQ: 16 00—00 00:01:5

RECORD	SI	DEPTH METERS	CONDUCTVTY M-MHO	TEMPERATURE DEG-C	SOUND VEL M/SECOND	SALINITY PER-MILLE	DENSITY SIGMA-T	SOUND VEL. METERS/SEC
1	11	2.45	24.89	9.444	14.811	22.202	17.096	1472.0
2	11	2.60	24.87	9.444	14.812	22.182	17.081	1472.0
3	11	2.60	24.86	9.444	14.812	22.173	17.073	1471.9
4	11	2.60	24.86	9.444	14.812	22.173	17.073	1471.9
5	11	2.75	24.87	9.444	14.812	22.182	17.081	1472.0
6	11	2.90	24.87	9.444	14.812	22.182	17.081	1472.0
7	11	2.75	24.87	9.444	14.812	22.182	17.081	1472.0
8	11	2.90	24.88	9.444	14.913	22.192	17.089	1472.0
9	11	2.75	24.86	9.444	14.812	22.173	17.073	1471.9
10	11	2.75	24.85	9.444	14.912	22.173	17.073	1471.9
11	11	2.75	24.85	9.444	14.813	22.163	17.065	1471.9
12	11	3.04	24.87	9.434	14.813	22.189	17.087	1471.9
13	11	2.90	24.86	9.444	14.813	22.173	17.073	1471.9
14	11	3.19	24.86	9.444	14.813	22.172	17.073	1471.9
15	11	3.94	24.89	9.444	14.914	22.202	17.095	1472.0
16	11	4.98	24.90	9.434	14.813	22.217	17.109	1472.0
17	11	6.22	24.90	9.424	14.814	22.223	17.115	1472.0
18	11	7.80	24.95	9.404	14.314	22.284	17.165	1472.0
19	11	9.14	26.03	9.474	14.813	23.302	17.945	1473.6
20	11	10.63	26.05	9.604	14.913	23.237	17.876	1474.0
21	11	10.93	26.06	9.654	14.814	23.215	17.851	1474.2
22	11	12.27	26.06	9.664	14.814	23.208	17.845	1474.2
23	11	12.12	26.07	9.664	14.814	23.218	17.952	1474.2
24	11	12.42	26.07	9.664	14.914	23.218	17.952	1474.2
25	11	12.42	26.08	9.654	14.914	23.227	17.860	1474.3
26	11	12.27	26.08	9.664	14.314	23.227	17.860	1474.2
27	11	12.57	26.08	9.664	14.814	23.227	17.860	1474.3
28	11	12.42	26.07	9.664	14.814	23.218	17.852	1474.2
29	11	12.42	26.06	9.664	14.814	23.208	17.845	1474.2
30	11	12.42	26.07	9.664	14.914	23.218	17.852	1474.2
31	11	12.42	26.06	9.664	14.914	23.208	17.845	1474.2
32	11	12.57	26.07	9.664	14.914	23.217	17.852	1474.2

TAPE MARK

TAPE MARK

Table 4. Density Profile Data After Deployment of Instruments at Station 2

SDS-IIA Lister Program 8006.3

00--00 00:34:27 Data Base: CTD002.DBS

First Line Absolute Time= 219/ 2:40:42.0 Time Relative to: 219/ 2:40:42

Time	CTD-TEMP DEG-C	CTD-DEPT METERS	CTD-COND MS-CM	SALINITY PPT	SIGMA-T G/CC-1
02:40:42.0	11.648	1.702	33.751	29.259	22.321
02:40:44.0	11.588	2.004	33.765	29.319	22.378
02:40:46.0	11.639	1.501	33.668	29.186	22.266
02:40:48.0	11.720	1.180	33.633	29.089	22.177
02:40:50.0	11.674	1.739	33.724	29.212	22.280
02:40:52.0	11.626	1.849	33.688	29.215	22.291
02:40:54.0	11.710	1.382	33.615	29.079	22.171
02:40:56.0	11.754	1.400	33.552	28.985	22.090
02:40:58.0	11.817	1.839	33.616	28.997	22.090
02:41:00.0	11.739	1.592	33.655	29.095	22.179
02:41:02.0	11.724	1.482	33.572	29.027	22.128
02:41:04.0	11.738	1.519	33.580	29.025	22.124
02:41:06.0	11.721	1.775	33.618	29.074	22.166
02:41:08.0	11.720	1.546	33.542	29.002	22.109
02:41:10.0	11.729	1.491	33.569	29.021	22.122
02:41:12.0	11.756	1.574	33.565	28.995	22.098
02:41:14.0	11.768	2.196	33.649	29.067	22.152
02:41:16.0	11.651	2.434	33.839	29.341	22.385
02:41:18.0	11.516	2.993	33.865	29.473	22.510
02:41:20.0	11.504	3.661	33.898	29.514	22.543
02:41:22.0	11.453	4.210	33.937	29.592	22.613
02:41:24.0	11.435	4.577	33.944	29.613	22.632
02:41:26.0	11.457	5.740	33.954	29.604	22.621
02:41:28.0	11.455	6.921	34.008	29.658	22.664
02:41:30.0	11.445	7.534	34.049	29.706	22.703
02:41:32.0	11.486	8.724	34.270	29.886	22.836
02:41:34.0	11.554	10.024	34.447	30.002	22.916
02:41:36.0	11.582	10.802	34.471	30.002	22.912
02:41:38.0	11.597	11.644	34.486	30.004	22.911
02:41:40.0	11.604	12.835	34.546	30.056	22.951
02:41:42.0	11.575	13.677	34.561	30.094	22.985
02:41:44.0	11.565	14.885	34.545	30.086	22.980
02:41:46.0	11.540	15.700	34.513	30.075	22.975
02:41:48.0	11.498	16.414	34.504	30.101	23.002
02:41:50.0	11.497	17.650	34.489	30.086	22.991
02:41:52.0	11.479	18.914	34.488	30.099	23.004
02:41:54.0	11.474	19.362	34.489	30.104	23.009
02:41:56.0	11.447	20.214	34.494	30.130	23.034
02:41:58.0	11.427	21.687	34.513	30.164	23.063
02:42:00.0	11.452	22.685	34.545	30.174	23.067

Table 5. Density Profile Data Before Retrieval of Instruments at Station 2

DIGITAL DATA LOGGER DUMP — PAGE NO.

PROGRAM: DDL2 8006.20 SHIP: S132 READ FROM MT0: FILE NO. 1 PFRED: 16 00--00 00:01:36

RECORD	SI	DEPTH METERS	CONDUCTVTY M-MHO	TEMPERATURE DEG-C	SOUND VEL M/SECOND	SALINITY PER-MILLE	DENSITY SIGMA-T	SOUND VEL. METERS/SEC
1	11	2.45	30.82	9.904	14.810	27.747	21.327	1480.7
2	11	2.90	30.85	9.954	14.810	27.738	21.313	1480.9
3	11	2.75	30.85	9.944	14.811	27.746	21.320	1480.8
4	11	2.75	30.82	9.914	14.811	27.739	21.320	1480.7
5	11	2.90	30.82	9.904	14.811	27.747	21.327	1480.7
6	11	2.75	30.88	9.964	14.811	27.761	21.328	1480.9
7	11	2.90	30.82	9.904	14.811	27.747	21.327	1480.7
8	11	2.75	30.82	9.904	14.811	27.747	21.327	1480.7
9	11	3.04	30.81	9.914	14.811	27.729	21.312	1480.7
10	11	2.60	30.82	9.894	14.812	27.755	21.335	1480.6
11	11	2.90	30.83	9.944	14.812	27.726	21.305	1480.8
12	11	2.90	30.82	9.894	14.811	27.754	21.335	1480.7
13	11	2.60	30.82	9.894	14.811	27.755	21.335	1480.6
14	11	2.90	30.81	9.884	14.812	27.752	21.335	1480.6
15	11	3.04	30.82	9.884	14.812	27.762	21.342	1480.6
16	11	4.53	30.83	9.914	14.812	27.748	21.327	1480.7
17	11	5.42	30.83	9.934	14.811	27.733	21.311	1480.9
18	11	6.76	30.79	9.864	14.812	27.746	21.333	1480.6
19	11	7.80	30.82	9.854	14.812	27.783	21.363	1480.6
20	11	8.85	30.85	9.864	14.812	27.805	21.379	1480.7
21	11	10.04	30.91	9.884	14.812	27.849	21.410	1480.8
22	11	11.37	30.95	9.904	14.812	27.873	21.425	1481.0
23	11	12.86	30.97	9.904	14.812	27.892	21.440	1481.0
24	11	13.76	31.07	9.914	14.813	27.984	21.509	1481.2
25	11	15.24	31.10	9.934	14.812	27.998	21.517	1481.3
26	11	16.28	31.12	9.934	14.813	28.017	21.532	1481.3
27	11	17.77	31.33	9.984	14.812	28.187	21.656	1481.8
28	11	18.81	31.39	10.034	14.812	28.207	21.663	1482.0
29	11	20.45	31.50	10.034	14.812	28.316	21.748	1482.2
30	11	21.79	31.53	10.034	14.813	28.346	21.770	1482.2
31	11	23.13	31.54	10.034	14.813	28.355	21.778	1482.3
32	11	24.76	31.55	10.024	14.813	28.372	21.793	1482.3
33	11	25.66	31.56	10.034	14.813	28.374	21.792	1482.3
34	11	27.59	31.56	10.034	14.813	28.373	21.792	1482.3
35	11	28.63	31.57	10.034	14.812	28.383	21.799	1482.4
36	11	29.52	31.57	10.034	14.813	28.382	21.799	1482.4
37	11	31.46	31.62	10.044	14.813	28.423	21.829	1482.5
38	11	32.35	31.66	10.064	14.813	28.447	21.844	1482.6
39	11	33.84	31.67	10.064	14.814	28.457	21.852	1482.7
40	11	34.58	31.68	10.064	14.813	28.466	21.859	1482.7
41	11	34.88	31.68	10.064	14.813	28.466	21.859	1482.7
42	11	34.43	31.67	10.064	14.813	28.456	21.851	1482.7
43	11	34.58	31.67	10.064	14.813	28.456	21.851	1482.7

Table 6. Density Profile Data After Deployment of Instruments at Station 3

SDS-IIA Lister Program 8006.3

08-AUG-83 08:22:56 Data Base: CTD003.DBS

First Line Absolute Time= 220/ 3:18:12.0 Time Relative to: 220/ 3:18:12

Time	CTD-TEMP DEG-C	CTD-DEPT METERS	CTD-COND MS-CM	SALINITY PPT	SIGMA-T G/CC-1
03:19:02.0	11.109	1.592	35.019	30.929	23.712
03:19:04.0	11.110	1.931	35.018	30.927	23.710
03:19:06.0	11.110	2.370	35.023	30.932	23.714
03:19:08.0	11.110	2.599	35.022	30.931	23.713
03:19:10.0	11.110	3.222	35.021	30.930	23.712
03:19:12.0	11.110	3.835	35.022	30.931	23.713
03:19:14.0	11.110	3.835	35.022	30.930	23.712
03:19:16.0	11.110	4.751	35.023	30.931	23.713
03:19:18.0	11.110	5.373	35.025	30.934	23.715
03:19:20.0	11.110	5.758	35.023	30.931	23.713
03:19:22.0	11.110	6.518	35.025	30.933	23.715
03:19:24.0	11.111	7.360	35.023	30.930	23.713
03:19:26.0	11.111	7.781	35.026	30.933	23.714
03:19:28.0	11.109	8.568	35.031	30.938	23.719
03:19:30.0	11.109	9.466	35.032	30.940	23.720
03:19:32.0	11.102	9.758	35.043	30.956	23.734
03:19:34.0	11.106	10.637	35.086	30.995	23.764
03:19:36.0	11.109	11.599	35.115	31.020	23.783
03:19:38.0	11.109	11.846	35.115	31.020	23.783
03:19:40.0	11.107	13.009	35.123	31.029	23.790
03:19:42.0	11.106	13.750	35.127	31.033	23.794

Table 7. Density Profile Data Before Retrieval of Instruments at Station 3

DIGITAL DATA LOGGER DUMP PAGE NO.

PROGRAM: DDL2 8006.20 SHIP: S132 READ FROM MT0: FILE NO. 3 PFREQ: 16 00--00 00:02:10

RECORD	SI	DEPTH METERS	CONDUCTVTY M-MHO	TEMPERATURE DEG-C	SOUND VEL M/SECOND	SALINITY PER-MILLE	DENSITY SIGMA-T	SOUND VEL. METERS/SEC
1	11	2.30	30.55	6.653	14.810	30.139	23.658	1471.2
2	11	2.45	30.54	6.653	14.810	30.128	23.649	1471.2
3	11	2.30	30.53	6.643	14.811	30.126	23.649	1471.1
4	11	2.30	30.52	6.643	14.810	30.115	23.641	1471.1
5	11	2.15	30.52	6.643	14.811	30.115	23.641	1471.1
6	11	2.30	30.52	6.633	14.810	30.124	23.649	1471.1
7	11	2.30	30.52	6.633	14.811	30.124	23.649	1471.1
8	11	2.30	30.52	6.643	14.811	30.115	23.641	1471.1
9	11	2.30	30.52	6.643	14.811	30.115	23.641	1471.1
10	11	2.15	30.52	6.633	14.811	30.124	23.649	1471.1
11	11	2.30	30.52	6.633	14.811	30.124	23.649	1471.1
12	11	2.30	30.52	6.643	14.811	30.115	23.641	1471.1
13	11	2.45	30.52	6.633	14.812	30.124	23.649	1471.1
14	11	2.75	30.53	6.633	14.811	30.135	23.657	1471.1
15	11	4.38	30.53	6.643	14.812	30.125	23.648	1471.1
16	11	5.72	30.53	6.643	14.811	30.124	23.648	1471.2
17	11	6.91	30.53	6.643	14.811	30.124	23.647	1471.2
18	11	8.10	30.53	6.643	14.811	30.123	23.647	1471.2
19	11	9.74	30.53	6.593	14.812	30.167	23.687	1471.1
20	11	11.09	30.49	6.503	14.812	30.202	23.726	1470.8
21	11	12.42	30.49	6.433	14.811	30.263	23.783	1470.6
22	11	13.76	30.46	6.363	14.812	30.292	23.814	1470.4
23	11	15.09	30.44	6.303	14.812	30.323	23.846	1470.2
24	11	16.58	30.36	6.233	14.812	30.296	23.833	1469.9
25	11	17.77	30.14	5.622	14.812	30.600	24.145	1467.8
26	11	19.26	30.28	5.242	14.812	31.107	24.528	1467.0
27	11	20.45	30.32	5.322	14.812	31.079	24.556	1467.3
28	11	21.79	30.26	5.282	14.812	31.046	24.535	1467.1
29	11	23.13	30.26	5.252	14.812	31.073	24.560	1467.0
30	11	24.47	30.25	5.242	14.813	31.071	24.559	1467.0
31	11	25.95	30.24	5.192	14.812	31.105	24.592	1466.9
32	11	27.29	30.01	5.082	14.812	30.945	24.477	1466.2
33	11	28.63	30.00	4.852	14.812	31.147	24.662	1465.6
34	11	29.52	30.00	4.822	14.813	31.175	24.687	1465.5
35	11	30.57	30.00	4.812	14.813	31.184	24.695	1465.5
36	11	31.16	30.00	4.812	14.813	31.184	24.695	1465.5
37	11	32.20	29.99	4.812	14.813	31.172	24.685	1465.5
38	11	32.35	29.99	4.802	14.812	31.181	24.694	1465.5

Table 8. Density Profile Data After Deployment of Instruments at Station 4

SDS-IIA Lister Program 8006.3

08-AUG-83 00:02:09

Data Base: CTD004.DBS

First Line Absolute Time= 220/ 20:18:38.0 Time Relative to: 220/ 20:18:38

Time	CTD-TEMP DEG-C	CTD-DEPT METERS	CTD-COND MS-CM	SALINITY PPT	SIGMA-T G/CC-1
20:18:38.0	7.507	2.343	30.686	29.546	23.135
20:18:40.0	7.508	2.554	30.689	29.549	23.137
20:18:42.0	7.506	2.819	30.685	29.546	23.135
20:18:44.0	7.506	3.084	30.689	29.550	23.138
20:18:46.0	7.507	3.487	30.689	29.549	23.137
20:18:48.0	7.511	3.579	30.687	29.544	23.133
20:18:50.0	7.509	3.991	30.685	29.543	23.133
20:18:52.0	7.505	4.229	30.682	29.544	23.133
20:18:54.0	7.504	4.467	30.684	29.546	23.135
20:18:56.0	7.503	4.842	30.683	29.545	23.135
20:18:58.0	7.503	5.108	30.679	29.542	23.132
20:19:00.0	7.487	5.346	30.677	29.553	23.143
20:19:02.0	7.486	5.602	30.676	29.552	23.142
20:19:04.0	7.485	5.932	30.679	29.556	23.145
20:19:06.0	7.487	6.206	30.678	29.553	23.143
20:19:08.0	7.486	6.573	30.680	29.556	23.145
20:19:10.0	7.490	6.655	30.682	29.554	23.143
20:19:12.0	7.488	7.150	30.680	29.554	23.144
20:19:14.0	7.488	7.396	30.680	29.554	23.144
20:19:16.0	7.489	7.662	30.681	29.554	23.143
20:19:18.0	7.488	7.882	30.680	29.554	23.143
20:19:20.0	7.487	8.275	30.677	29.552	23.142
20:19:22.0	7.483	8.605	30.671	29.547	23.139
20:19:24.0	7.432	8.770	30.669	29.590	23.178
20:19:26.0	7.427	9.145	30.666	29.590	23.179
20:19:28.0	7.407	9.328	30.657	29.598	23.188
20:19:30.0	7.423	9.621	30.650	29.576	23.169
20:19:32.0	7.403	9.978	30.642	29.585	23.178
20:19:34.0	7.371	10.226	30.633	29.603	23.196
20:19:36.0	7.336	10.436	30.618	29.617	23.211
20:19:38.0	7.237	10.931	30.598	29.679	23.272
20:19:40.0	7.172	11.068	30.581	29.717	23.310
20:19:42.0	7.123	11.470	30.649	29.832	23.405
20:19:44.0	7.087	11.608	30.721	29.941	23.496
20:19:46.0	7.099	11.983	31.022	30.255	23.742
20:19:48.0	7.393	12.258	31.934	30.978	24.275
20:19:50.0	7.826	12.478	32.180	30.856	24.125
20:19:52.0	8.002	12.743	32.044	30.557	23.867
20:19:54.0	7.431	13.063	31.321	30.285	23.725
20:19:56.0	6.366	13.347	30.370	30.190	23.774
20:19:58.0	5.654	13.567	30.323	30.780	24.316
20:20:00.0	5.242	14.034	29.457	30.175	23.880
20:20:02.0	4.450	14.180	29.087	30.476	24.193
20:20:04.0	4.188	14.491	29.316	30.986	24.622
20:20:06.0	4.363	14.638	29.485	31.019	24.632
20:20:08.0	4.446	15.096	29.561	31.030	24.633

Table 8. Density Profile Data After Deployment of Instruments at Station 4 (cont'd)

SDS-IIA Lister Program 8006.3
08-AUG-83 00:02:34
Data Base: CTD004.DBS

First Line Absolute Time= 220/ 20:20:10.0 Time Relative to: 220/ 20:18:38

Time	CTD-TEMP DEG-C	CTD-DEPT METERS	CTD-COND MS-CM	SALINITY PPT	SIGMA-T G/CC-1
20:20:10.0	4.450	15.324	29.586	31.054	24.651
20:20:12.0	4.403	15.599	29.508	31.007	24.619
20:20:14.0	4.324	15.901	29.461	31.027	24.642
20:20:16.0	4.205	16.148	29.332	30.989	24.622
20:20:18.0	4.146	16.368	29.322	31.033	24.662
20:20:20.0	4.076	16.771	29.278	31.047	24.680
20:20:22.0	4.077	16.945	29.293	31.064	24.693
20:20:24.0	4.071	17.211	29.277	31.051	24.683
20:20:26.0	4.066	17.677	29.288	31.067	24.697
20:20:28.0	4.066	17.696	29.307	31.090	24.714
20:20:30.0	4.050	18.172	29.286	31.080	24.708
20:20:32.0	4.067	18.337	29.292	31.071	24.700
20:20:34.0	4.059	18.712	29.328	31.121	24.739
20:20:36.0	4.066	18.978	29.331	31.118	24.737
20:20:38.0	4.066	19.216	29.387	31.183	24.789
20:20:40.0	4.048	19.527	29.381	31.194	24.799
20:20:42.0	4.010	19.737	29.296	31.129	24.751
20:20:44.0	3.807	20.094	28.957	30.923	24.605
20:20:46.0	3.614	20.333	28.853	30.983	24.668
20:20:48.0	3.286	20.781	28.571	30.960	24.677
20:20:50.0	3.130	20.992	28.474	30.993	24.715
20:20:52.0	2.834	21.284	28.299	31.067	24.796
20:20:54.0	2.649	21.468	28.167	31.087	24.826
20:20:56.0	2.550	21.413	28.156	31.170	24.899
20:20:58.0	2.253	22.045	27.714	30.918	24.718
20:21:00.0	2.027	22.374	27.519	30.897	24.717
20:21:02.0	1.784	22.603	27.360	30.938	24.765
20:21:04.0	1.358	22.859	26.988	30.890	24.752
20:21:06.0	1.153	23.106	26.906	30.990	24.844
20:21:08.0	1.005	23.518	26.782	30.980	24.843
20:21:10.0	0.863	23.747	26.745	31.076	24.928
20:21:12.0	0.785	23.994	26.704	31.102	24.952
20:21:14.0	0.768	24.315	26.694	31.105	24.956
20:21:16.0	0.764	24.626	26.672	31.081	24.937
20:21:18.0	0.717	24.956	26.674	31.130	24.978
20:21:20.0	0.699	25.056	26.654	31.124	24.974
20:21:22.0	0.687	25.322	26.611	31.080	24.940
20:21:24.0	0.686	25.624	26.614	31.085	24.944
20:21:26.0	0.687	25.826	26.622	31.094	24.951
20:21:28.0	0.683	26.027	26.614	31.088	24.946
20:21:30.0	0.627	26.448	26.607	31.134	24.986
20:21:32.0	0.628	26.530	26.631	31.165	25.010
20:21:34.0	0.626	26.832	26.611	31.142	24.992

Table 9. Density Profile Data Before Retrieval of Instruments at Station 4

DIGITAL DATA LOGGER DUMP PAGE NO.

PROGRAM: DDL2 8006.20 SHIP: S132 READ FROM MT0: FILE NO. 4 PFREQ: 16 00—00 00:02:32

RECORD	SI	DEPTH METERS	CONDUCTVTY M-MHO	TEMPERATURE DEG-C	SOUND VEL M/SECOND	SALINITY PER-MILLE	DENSITY SIGMA-T	SOUND VEL. METERS/SEC
1	11	2.45	29.57	5.602	14.807	29.995	23.663	1466.7
2	11	2.60	29.59	5.602	14.807	30.008	23.680	1466.7
3	11	2.75	29.59	5.612	14.807	29.999	23.672	1466.8
4	11	2.45	29.57	5.602	14.807	29.985	23.663	1466.7
5	11	2.45	29.57	5.602	14.807	29.995	23.663	1466.7
6	11	2.45	29.57	5.602	14.807	29.995	23.663	1466.7
7	11	2.60	29.60	5.632	14.808	29.992	23.665	1466.8
8	11	2.60	29.59	5.632	14.807	29.981	23.655	1466.9
9	11	2.75	29.57	5.622	14.807	29.967	23.646	1466.8
10	11	2.75	29.59	5.612	14.808	29.999	23.672	1466.8
11	11	3.64	29.77	5.682	14.808	30.137	23.773	1467.3
12	11	5.13	29.76	5.742	14.807	30.072	23.715	1467.4
13	11	6.61	29.79	5.762	14.808	30.087	23.724	1467.6
14	11	8.10	29.81	5.792	14.808	30.091	23.725	1467.7
15	11	9.74	29.83	5.802	14.808	30.094	23.726	1467.8
16	11	11.23	29.84	5.812	14.808	30.096	23.726	1467.9
17	11	12.71	29.84	5.812	14.808	30.095	23.725	1467.9
18	11	14.50	29.89	5.822	14.808	30.141	23.760	1468.0
19	11	16.59	29.91	5.832	14.809	30.154	23.769	1468.1
20	11	18.96	30.01	5.812	14.809	30.282	23.872	1468.2
21	11	20.90	30.12	5.882	14.808	30.341	23.911	1468.6
22	11	22.99	30.63	5.972	14.808	30.827	24.283	1469.7
23	11	25.21	30.81	6.273	14.809	30.753	24.189	1470.8
24	11	27.29	30.72	6.313	14.809	30.617	24.076	1470.8
25	11	28.93	30.66	6.193	14.808	30.658	24.123	1470.4
26	11	30.57	30.67	6.133	14.808	30.723	24.181	1470.3
27	11	31.61	30.65	6.123	14.809	30.720	24.180	1470.3
28	11	31.61	30.66	6.123	14.809	30.720	24.180	1470.3
29	11	31.76	30.65	6.113	14.808	30.718	24.180	1470.2
30	11	31.76	30.65	6.123	14.809	30.709	24.171	1470.2
31	11	31.76	30.65	6.123	14.809	30.709	24.171	1470.2
32	11	31.61	30.65	6.123	14.809	30.709	24.171	1470.2
33	11	31.61	30.66	6.123	14.808	30.720	24.180	1470.3
34	11	31.76	30.64	6.123	14.809	30.698	24.163	1470.2
35	11	31.61	30.65	6.123	14.809	30.709	24.171	1470.2
36	11	31.61	30.65	6.113	14.809	30.718	24.180	1470.2
37	11	31.61	30.65	6.123	14.809	30.709	24.171	1470.2

Table 10. Summary of harmonic analysis of pressure records. (Amplitude (H) in Centimeters and Greenwich Epoch (G) in Degrees for Harmonic Constants)

STATION	1		2		3		4		5		6		8	
LOCATION	CAPE DENBIGH		NOME		KOTZEBUE SOUND		LEDYARD BAY		COOPER ISLAND		THETIS ISLAND		DEMARCATION BAY	
	DEG	MIN	DEG	MIN	DEG	MIN	DEG	MIN	DEG	MIN	DEG	MIN	DEG	MIN
LATITUDE (N)	64	20.2	64	19.9	67	30.2	69	28.8	71	14.0	70	33.0	69	41.2
LONGITUDE (W)	161	30.7	165	00.8	165	00.3	165	03.2	155	44.5	150	11.0	141	17.6
HARMONIC CONSTANTS	H	G	H	G	H	G	H	G	H	G	H	G	H	G
PRIMARY CONSTITUENTS														
M2	16.4	264	10.2	029	9.7	274	3.0	268	5.1	264	6.5	272	7.2	266
N2	5.0	212	3.3	346	2.1	207	1.9	246	0.5	232	0.1	250	0.9	278
S2	3.6	004	2.2	118	2.5	348	1.3	192	2.6	325	3.3	316	3.1	306
O1	25.4	077	10.0	073	1.8	149	0.4	167	1.2	182	4.3	180	2.5	162
K1	43.9	127	15.5	130	2.9	058	1.3	085	2.8	210	2.2	148	3.0	126
HARMONICS														
M4	0.3	279	0.4	170	0.2	009	0.4	203	0.3	339	0.2	182	0.1	180
M6	0.3	029	0.5	075	0.2	316	0.0	085	0.1	162	0.0	284	0.0	259
M8	0.0	030	0.1	209	0.1	207	0.0	168	0.1	308	0.1	128	0.1	327
S4	0.2	352	0.3	267	0.1	058	0.2	147	0.3	080	0.3	195	0.1	050
S6	0.1	213	0.1	246	0.0	118	0.0	135	0.1	102	0.1	205	0.1	037
SECONDARY CONSTITUENTS														
J1	2.0	152	0.8	157	0.1	013	0.0	044	0.1	225	0.3	132	0.2	108
K2	1.0	004	0.6	118	0.7	348	0.3	192	0.7	325	0.9	316	0.9	309
L2	0.5	315	0.3	072	0.3	342	0.1	290	0.1	295	0.2	293	0.2	274
M1	1.8	102	0.7	101	0.1	103	0.0	126	0.1	196	0.3	164	0.2	144
2N	0.7	161	0.4	304	0.3	140	0.3	225	0.1	201	0.1	228	0.1	250
OO	1.0	177	0.4	186	0.1	328	0.0	003	0.1	239	0.2	116	0.1	089
P1	14.5	127	5.1	130	0.9	058	0.4	085	0.9	210	0.7	148	1.0	126
Q1	4.9	053	1.9	045	0.3	194	0.1	208	0.2	167	0.8	196	0.5	180
2Q	0.7	028	0.3	017	0.0	239	0.0	250	0.0	308	0.1	212	0.1	196
R2	0.0	004	0.0	118	0.0	348	0.0	192	0.0	325	0.0	316	0.0	309
T2	0.2	004	0.1	118	0.1	348	0.1	192	0.2	325	0.2	316	0.2	309
LAMBDA	0.1	310	0.1	070	0.1	309	0.0	233	0.0	292	0.0	292	0.1	286
NU2	1.0	219	0.6	352	0.4	216	0.4	249	0.1	237	0.2	253	0.2	259
RHO1	1.0	217	0.4	049	0.1	187	0.0	203	0.0	169	0.2	194	0.1	319

NOTE: ALL RECORDS BEGIN ON AUGUST 9, 1983 AT 1100 GMT AND ARE 29 DAYS IN DURATION

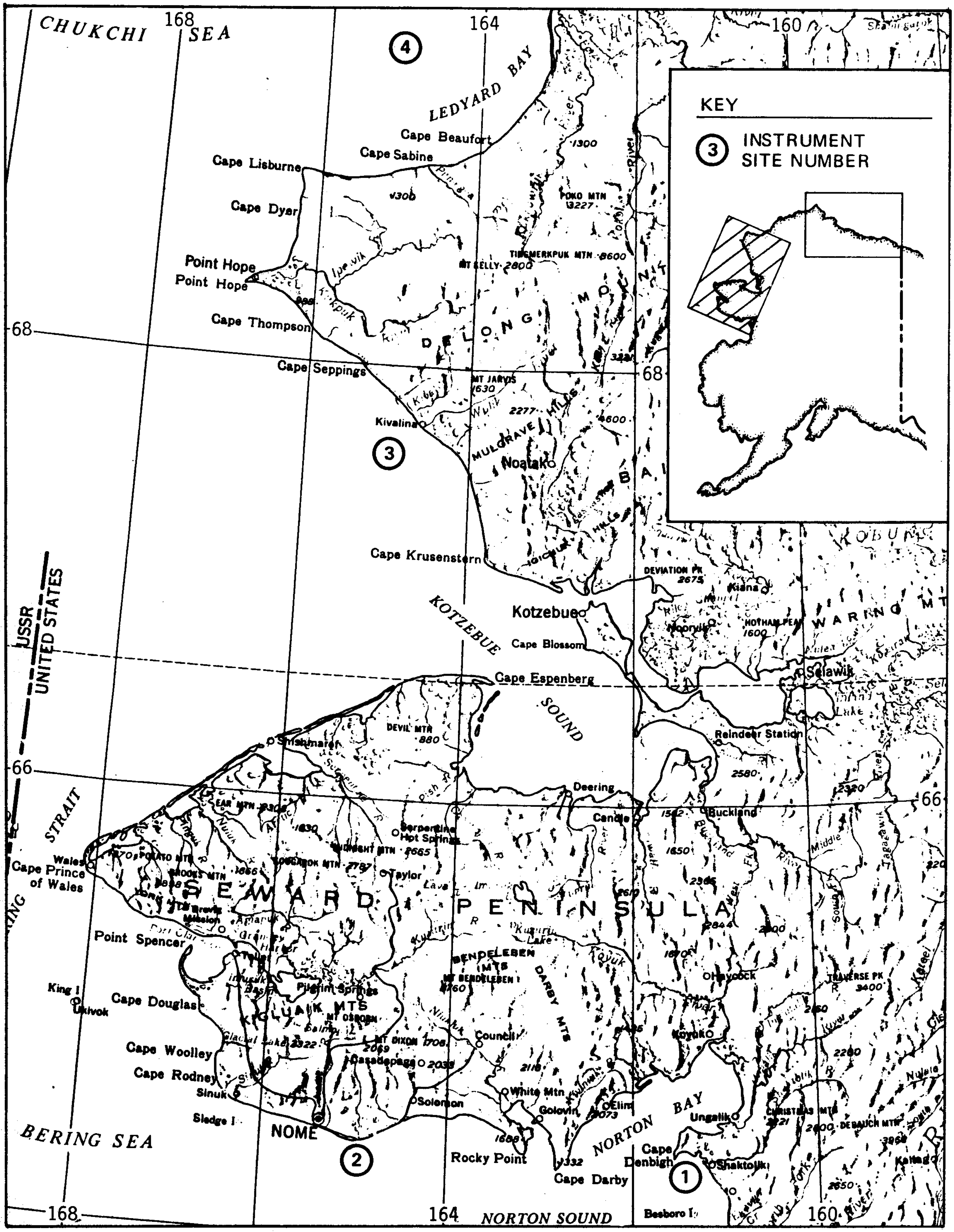

Figure 1 Norton Sound and Chukchi Sea Instrument Sites

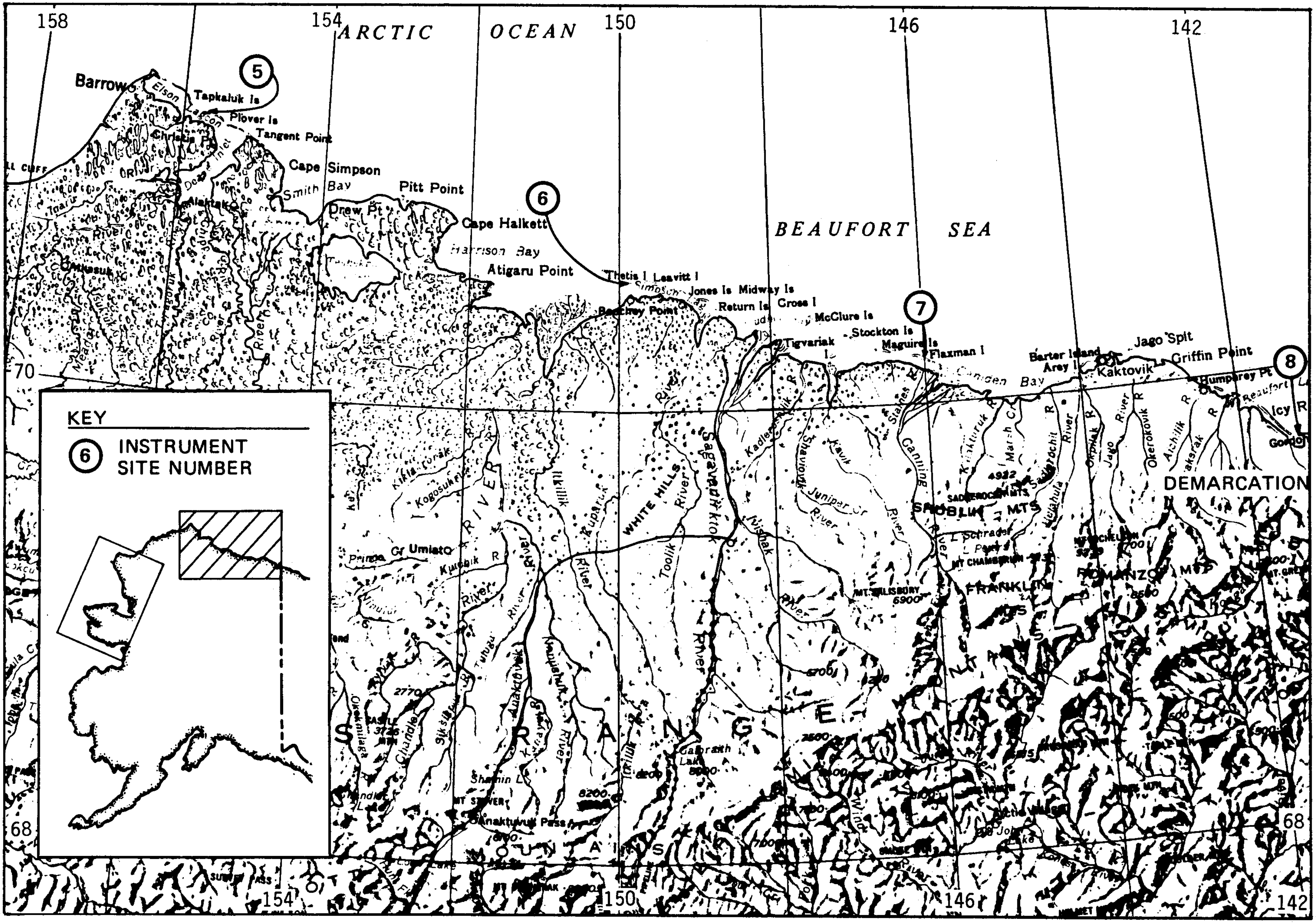

Figure 2 Beaufort Sea Instrument Sites

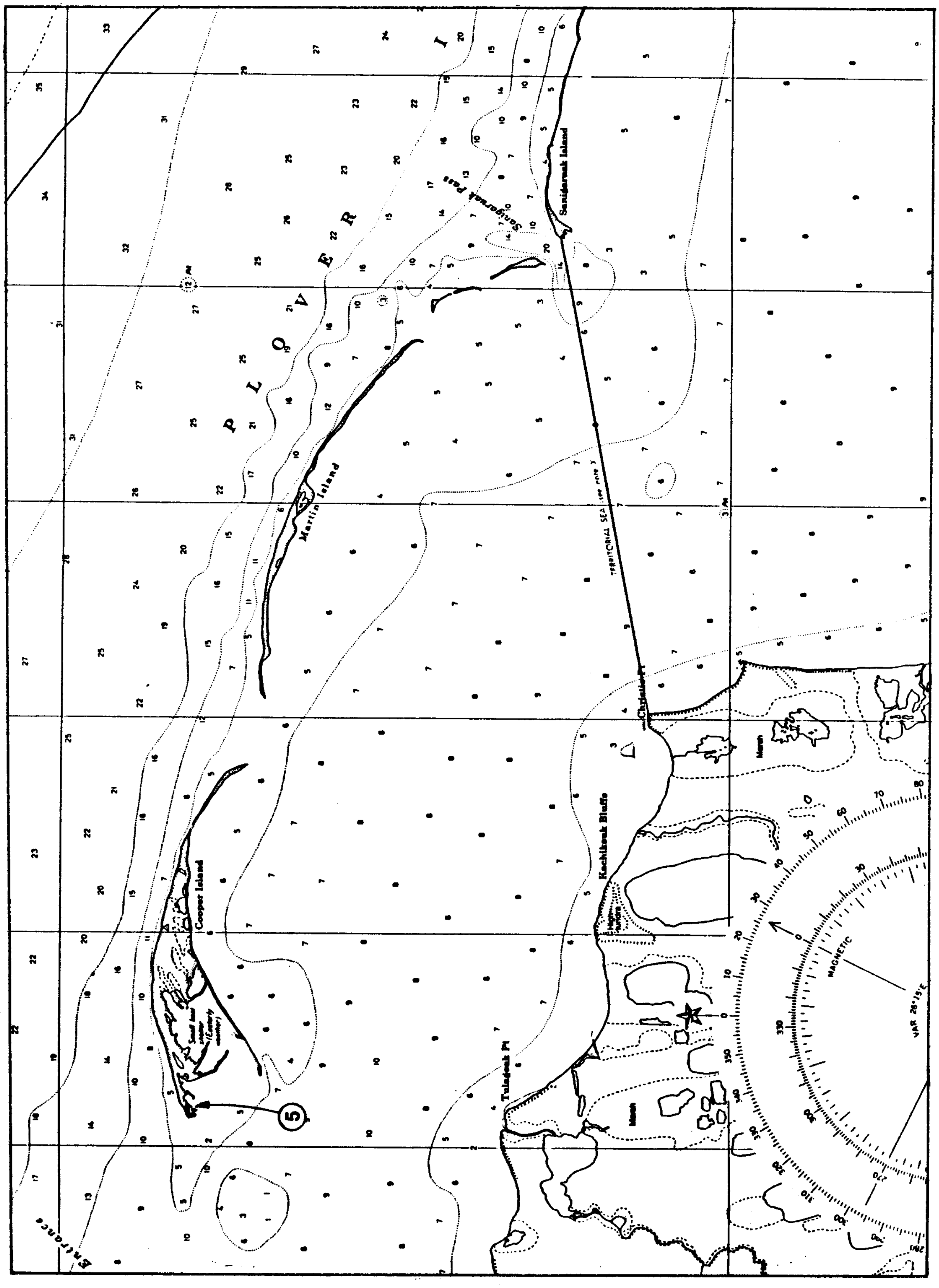

Fig. 2-a. Location of Station 5

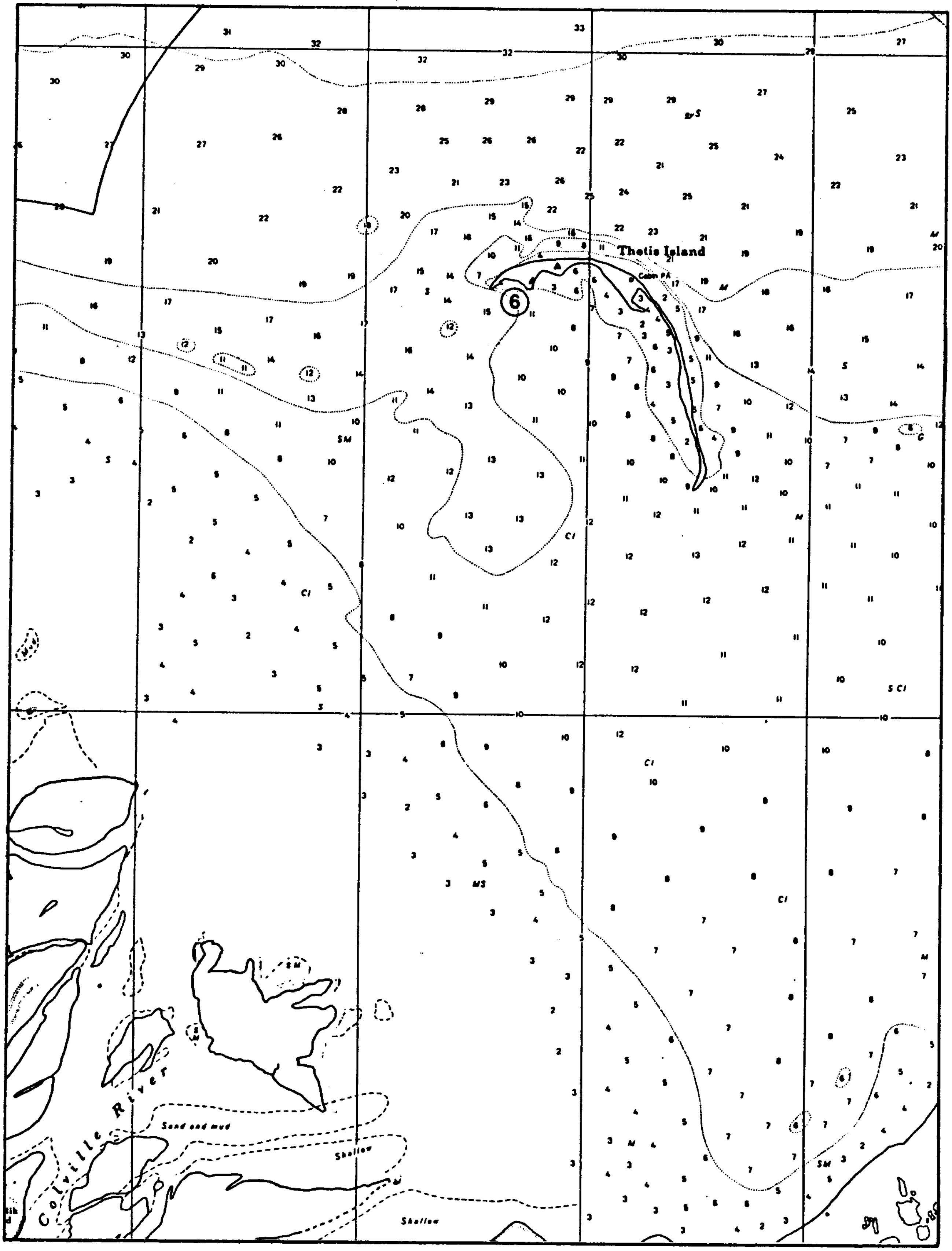

Fig. 2-b. Location of Station 6

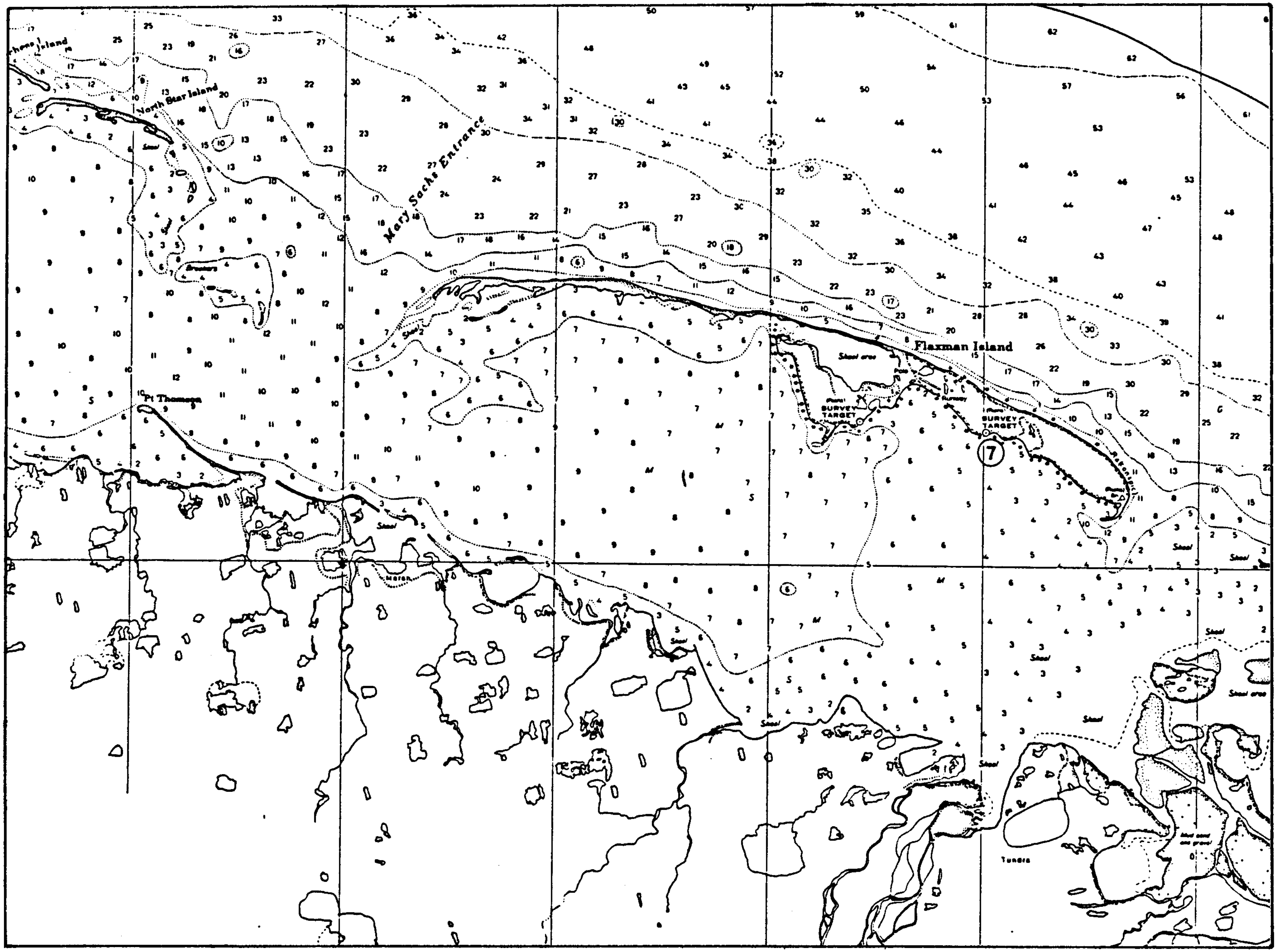

Fig. 2-c. Location of Station 7

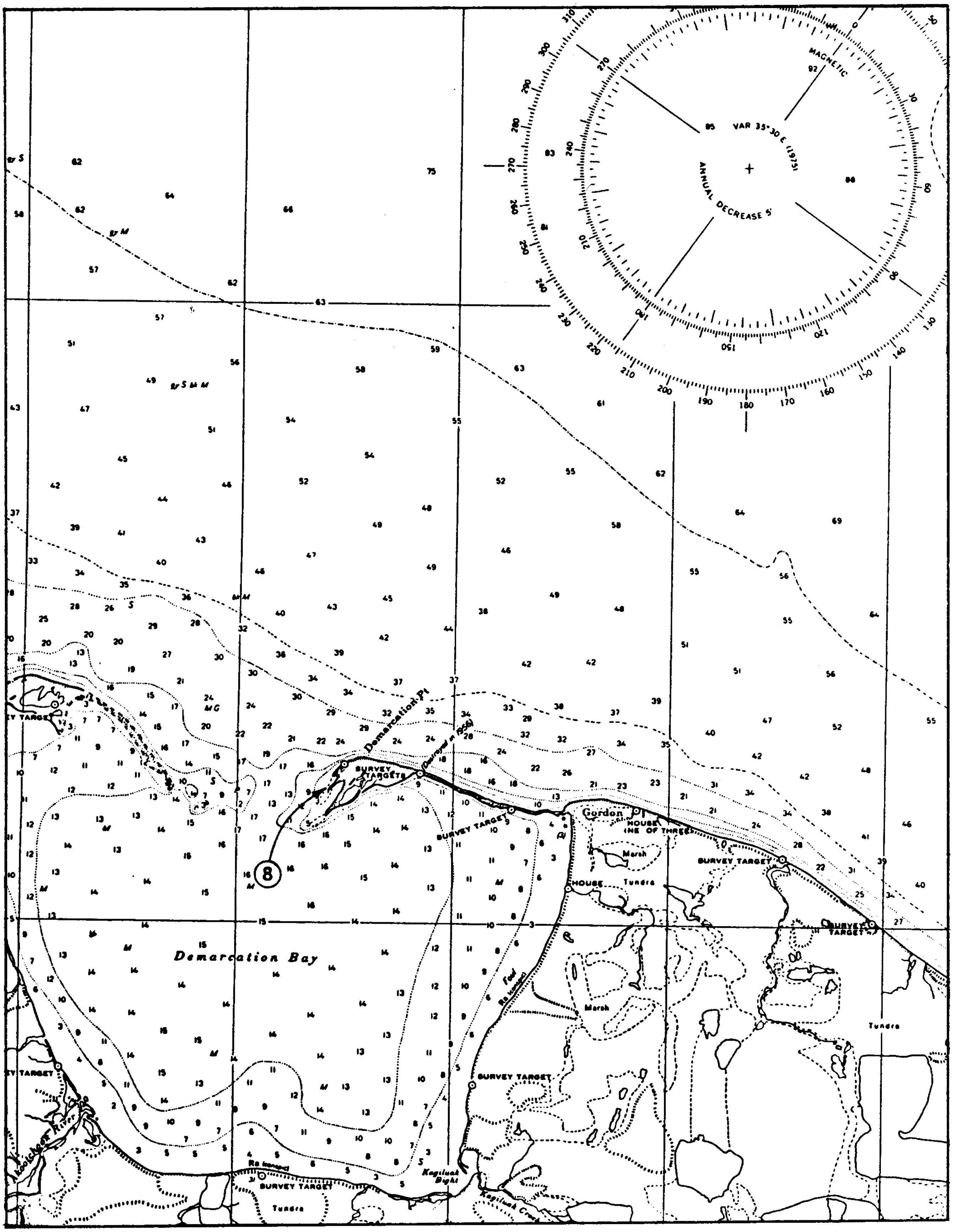

Fig. 2-d. Location of Station 8

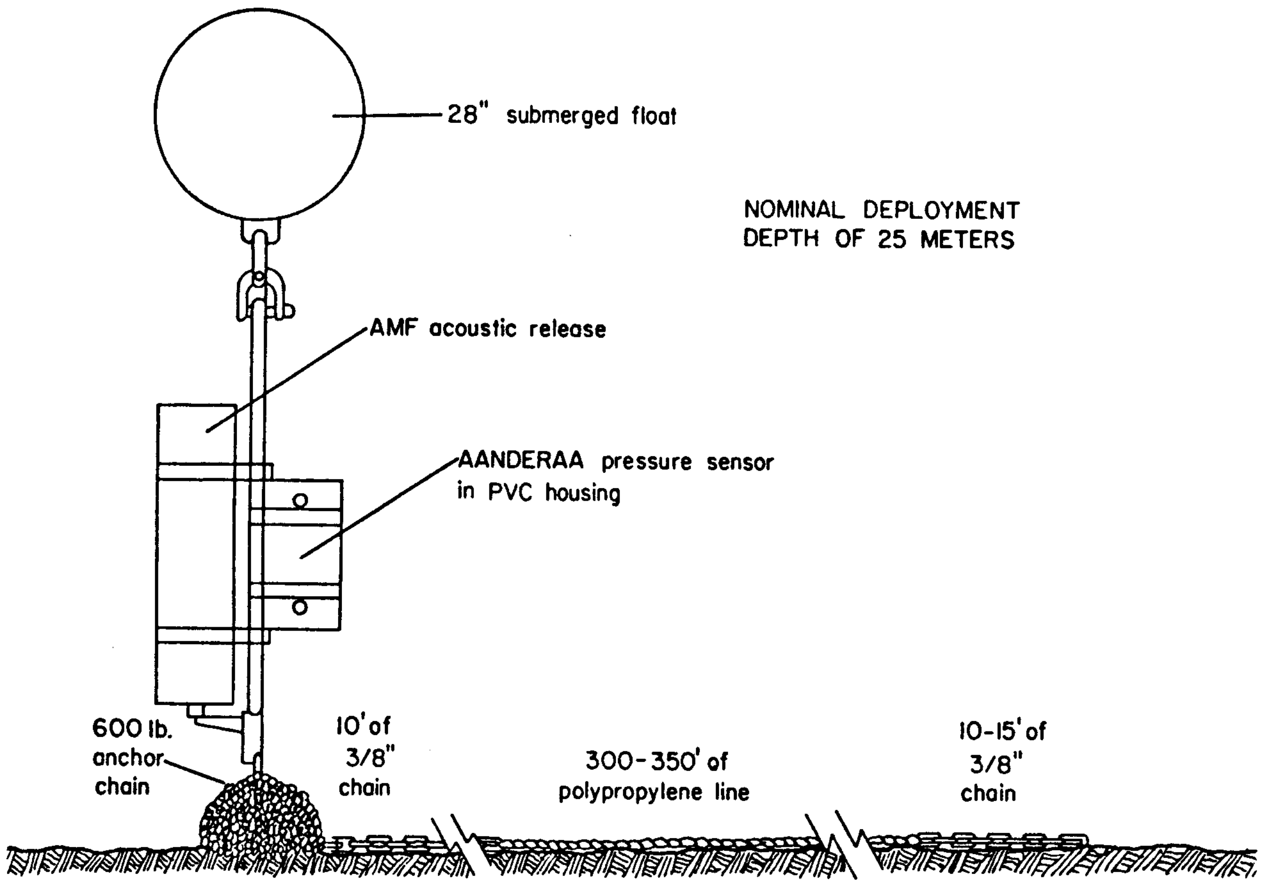

Figure 3 Mooring Design for Norton Sound and Chukchi Sea Deployments

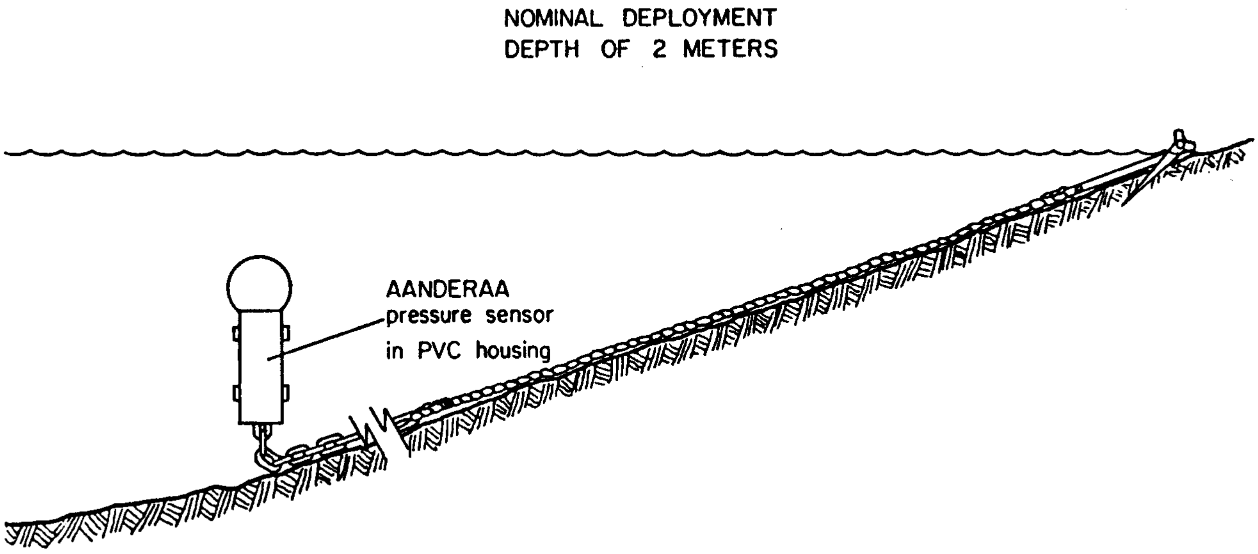

Figure 4 Mooring Design for Beaufort Sea Deployments

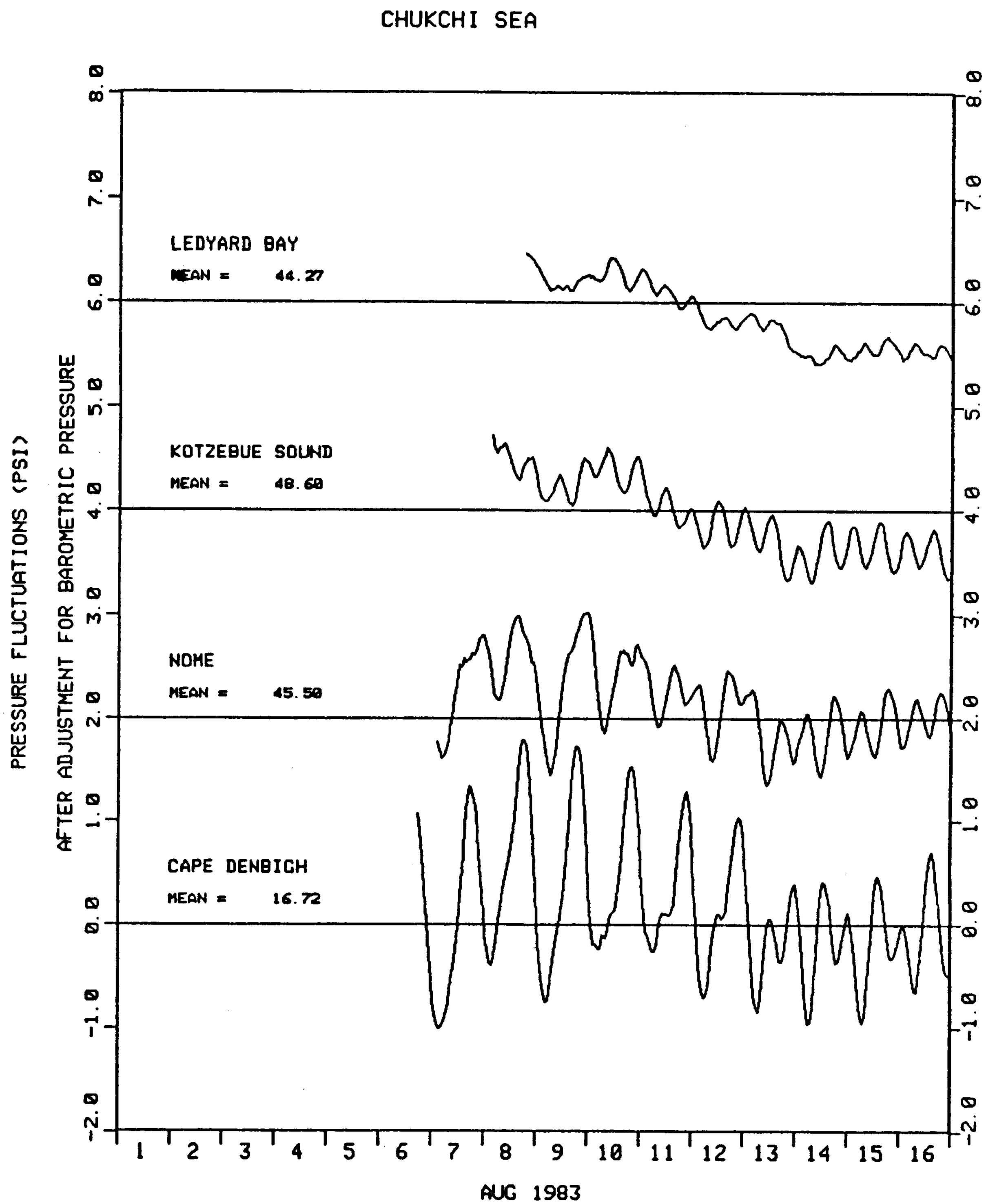

Fig. 5. Pressure Fluctuations About the Monthly Mean at Stations 1 through 4 in August 1983

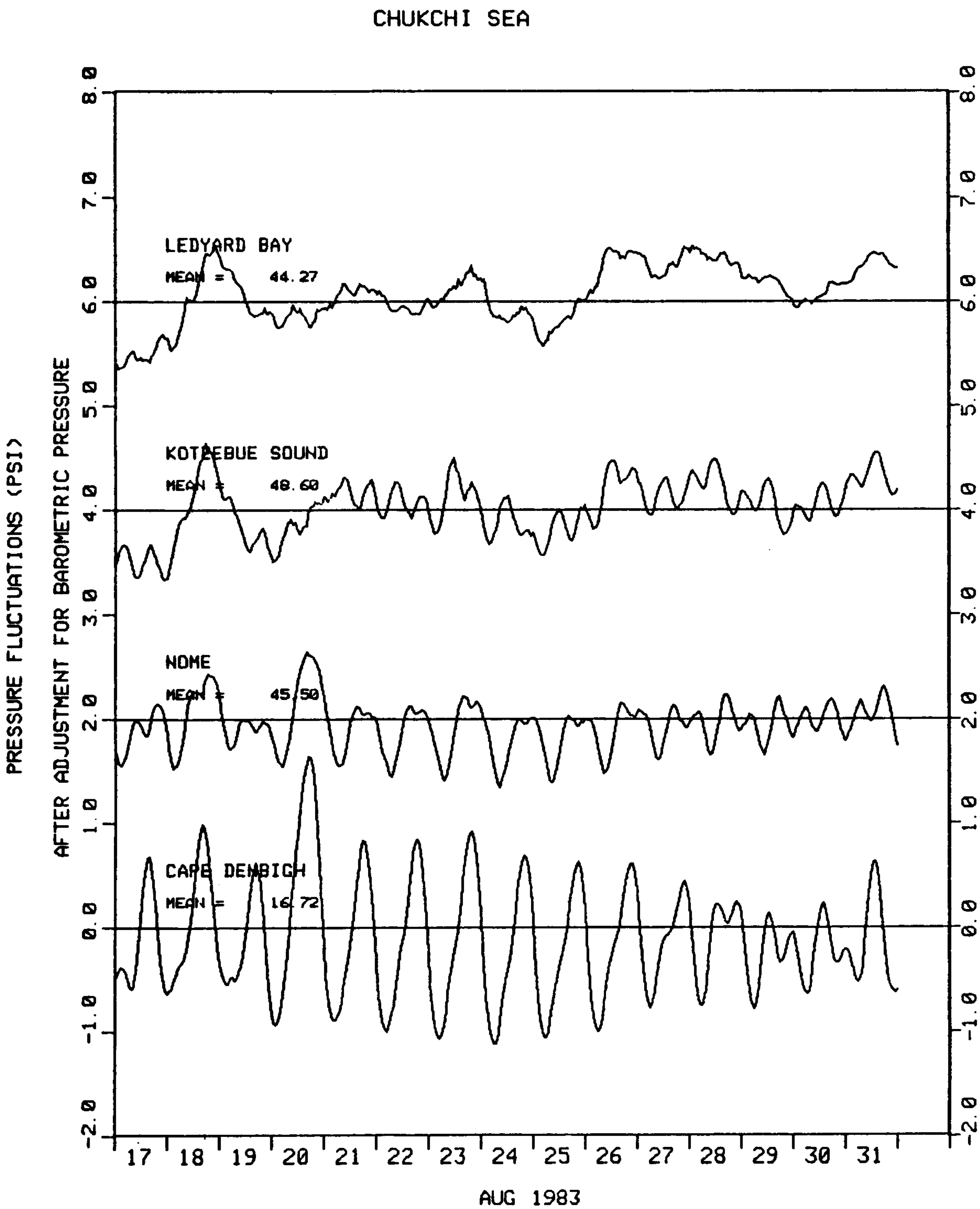

Fig. 5. Pressure Fluctuations About the Monthly Mean at Stations 1 through 4 in August 1983 (contd)

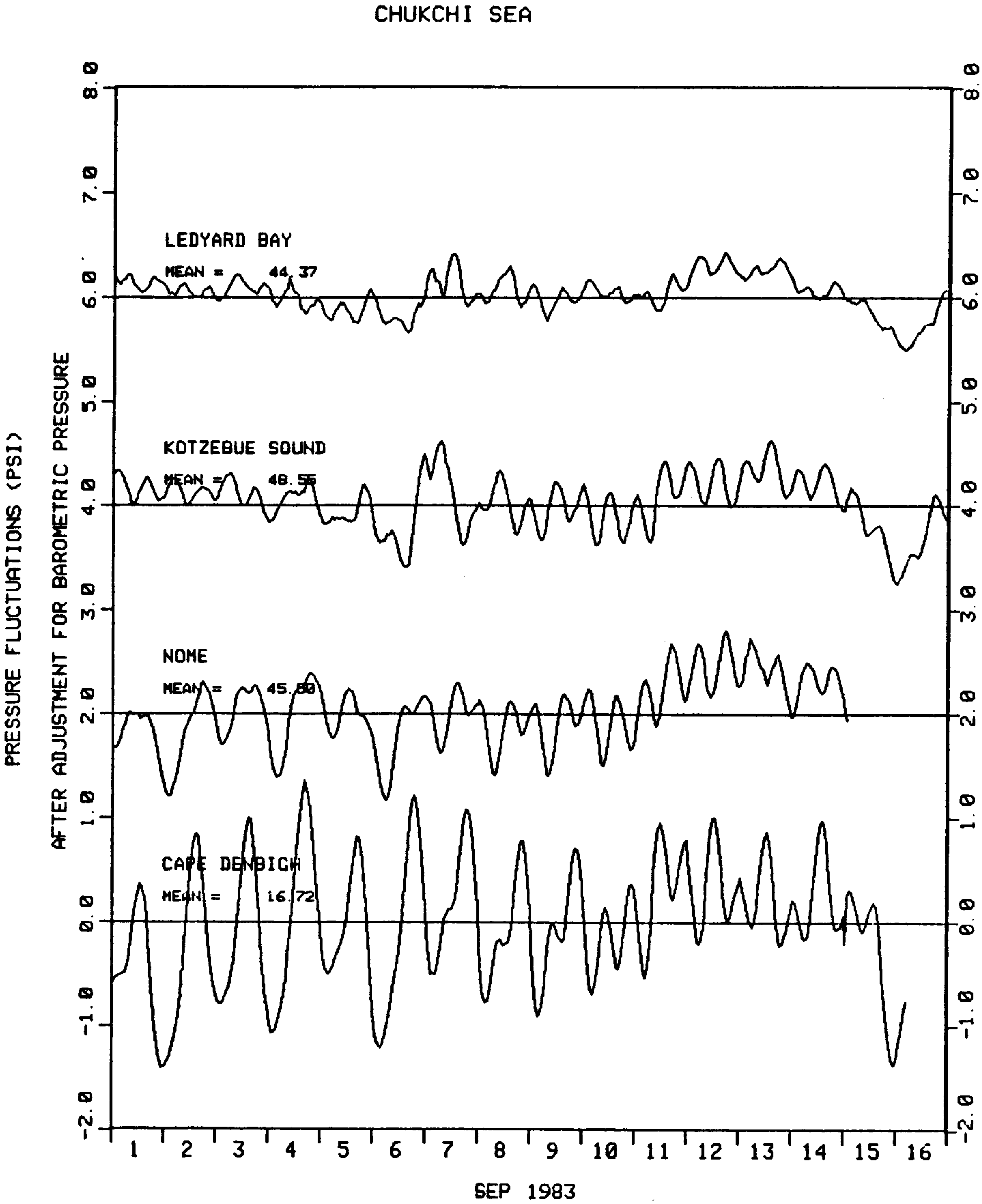

Fig. 6. Pressure Fluctuations About the Monthly Mean at Stations 1 through 4 in September 1983

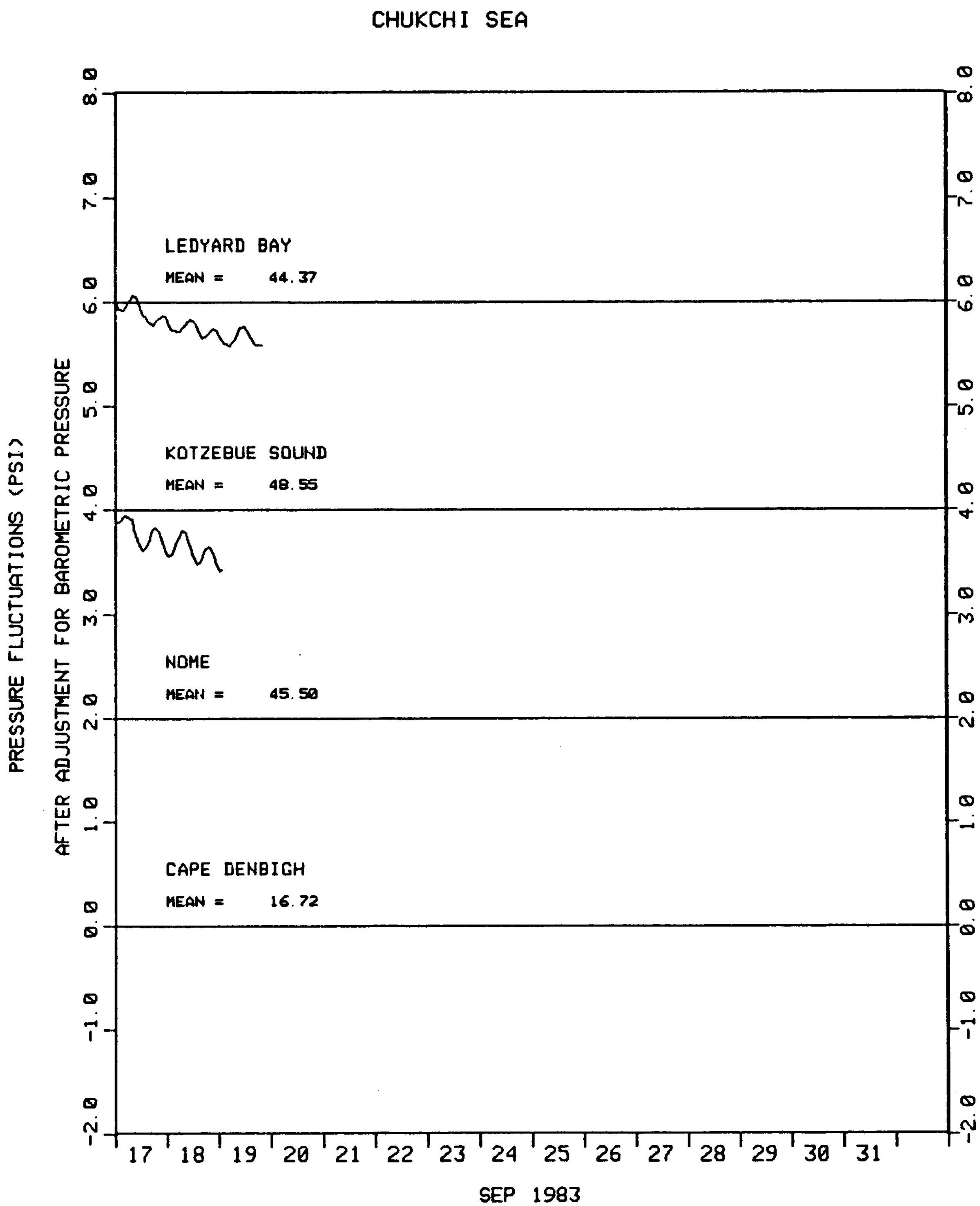

Fig. 6. Pressure Fluctuations About the Monthly Mean at Stations 1 through 4 in September 1983 (contd)

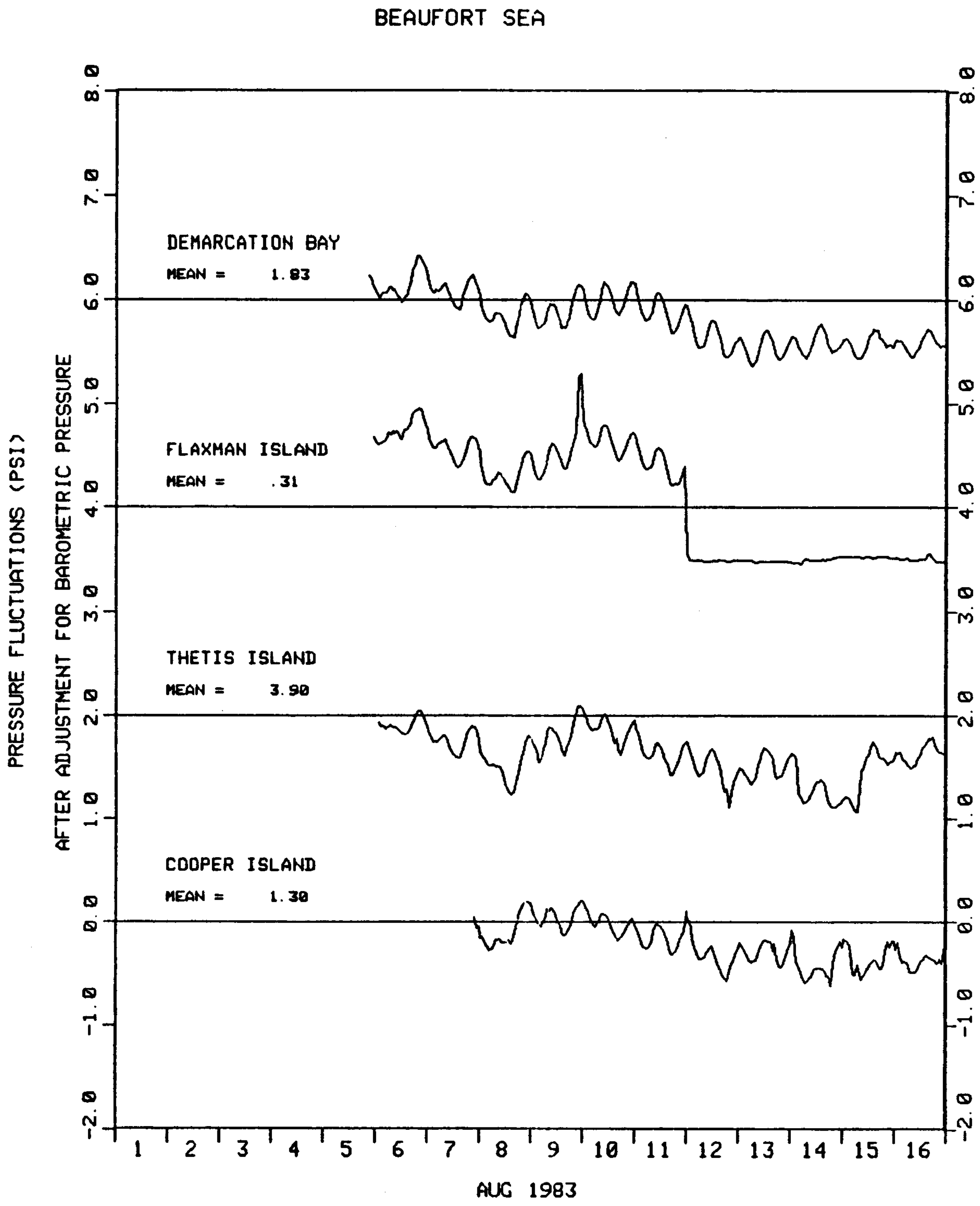

Fig. 7. Pressure Fluctuations About the Monthly Mean at Stations 5 through 8 in August 1983

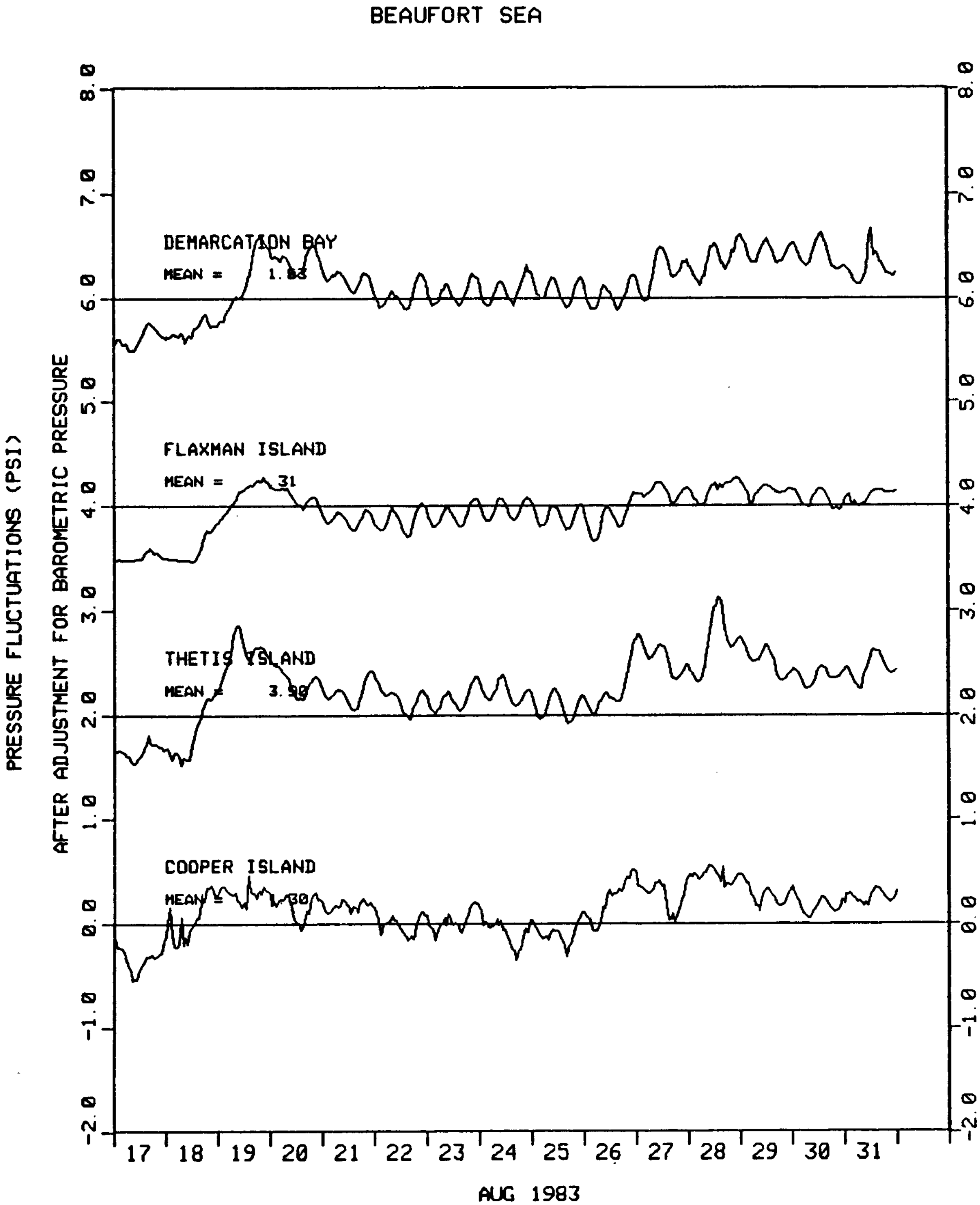

Fig. 7. Pressure Fluctuations About the Monthly Mean at Stations 5 through 8 in August 1983 (contd)

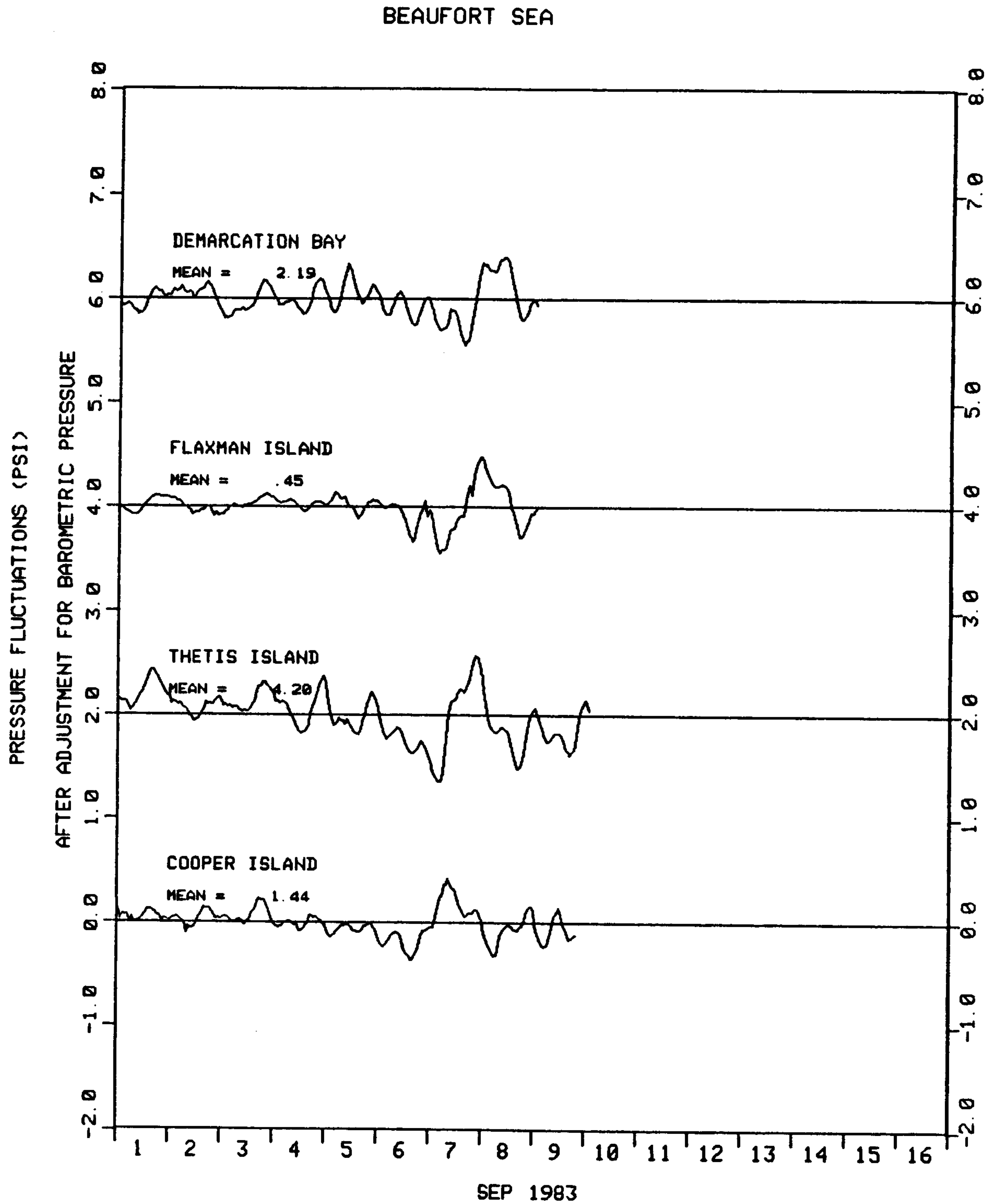

Fig. 8. Pressure Fluctuations About the Monthly Mean at Stations 5 through 8 in September 1983

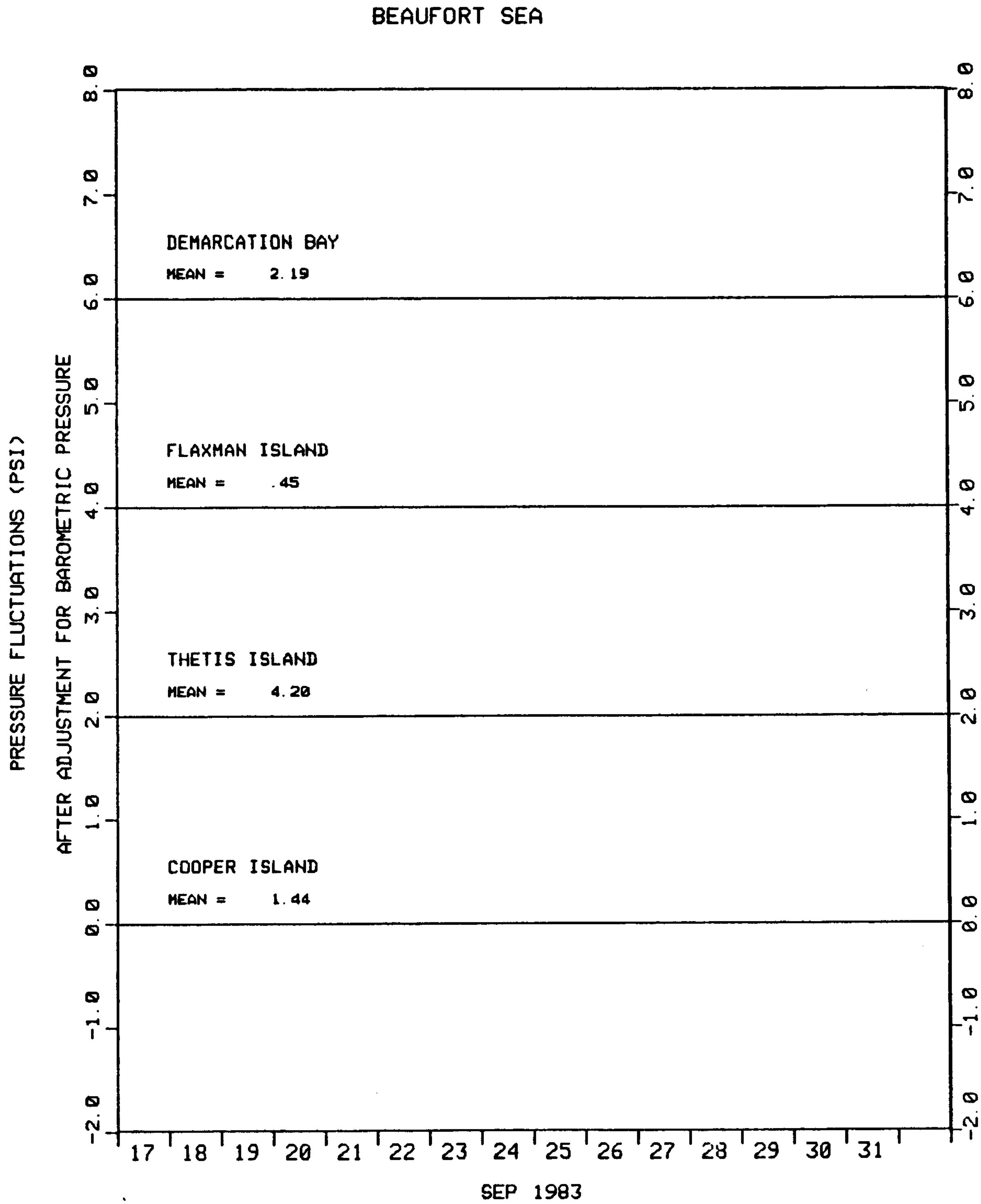

Fig. 8. Pressure Fluctuations About the Monthly Mean at Stations 5 through 8 in September 1983 (contd)

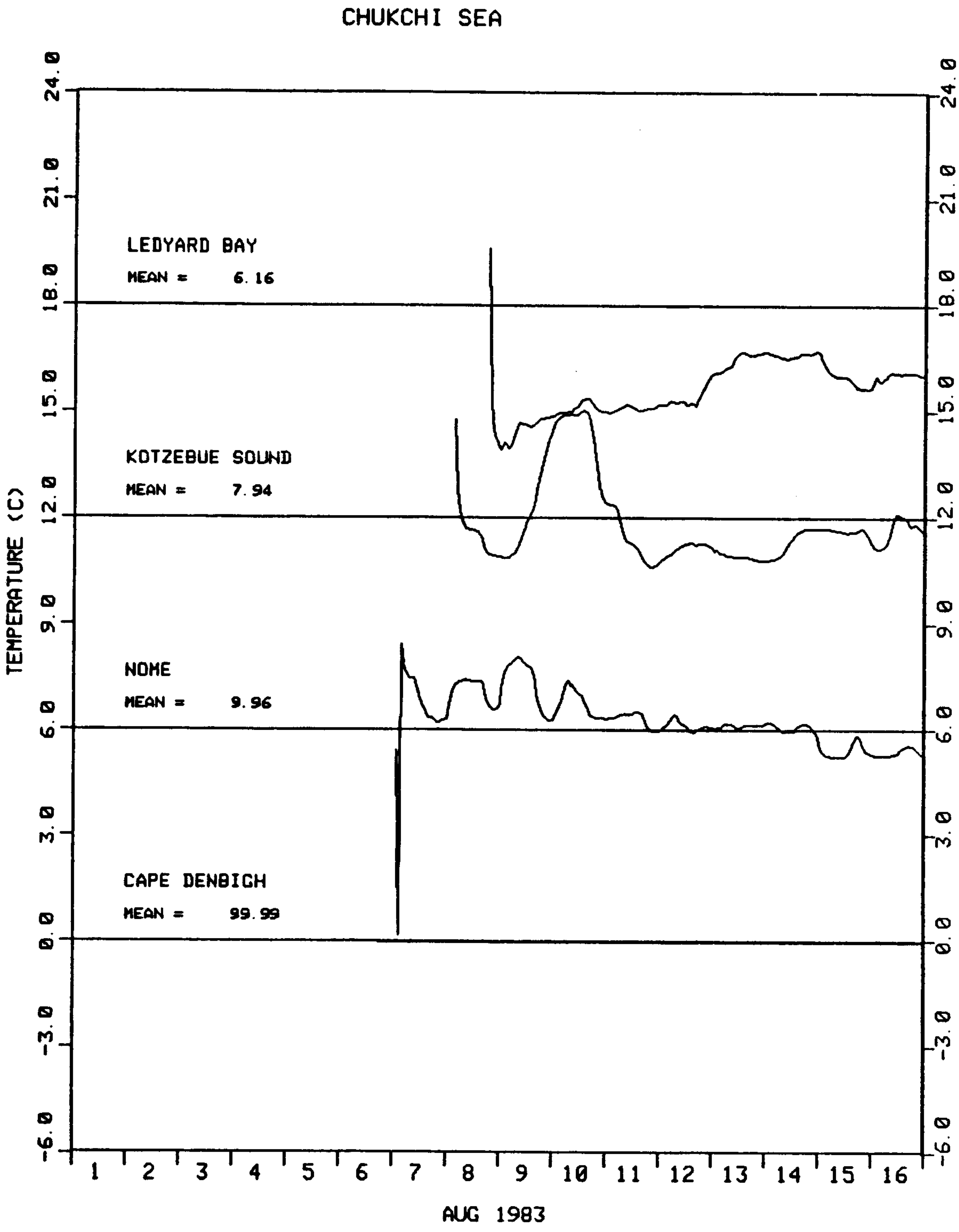

Fig. 9. Temperature Fluctuations About the Monthly Mean at Stations 1 through 4 in August 1983

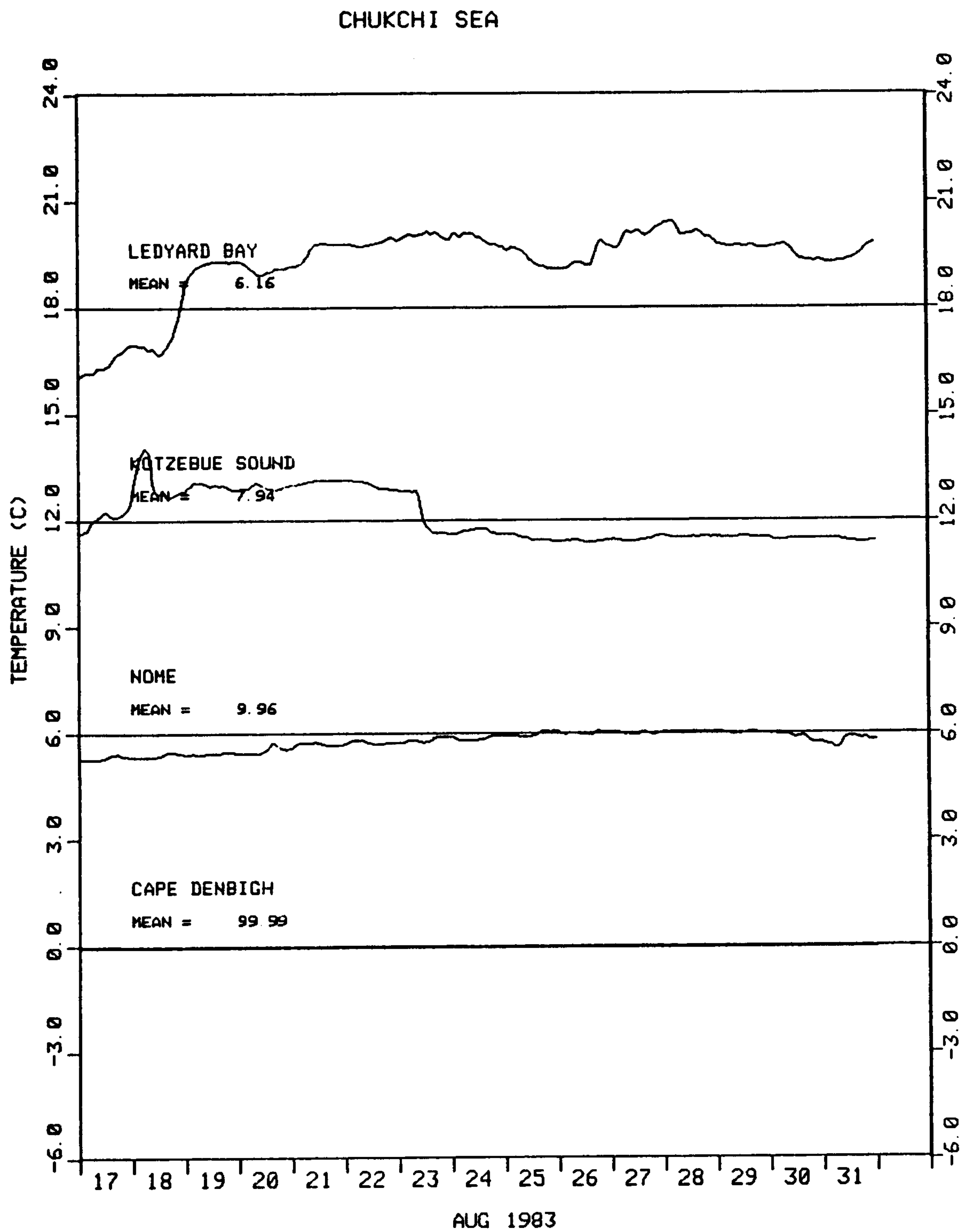

Fig. 9. Temperature Fluctuations About the Monthly Mean at Stations 1 through 4 in August 1983 (contd)

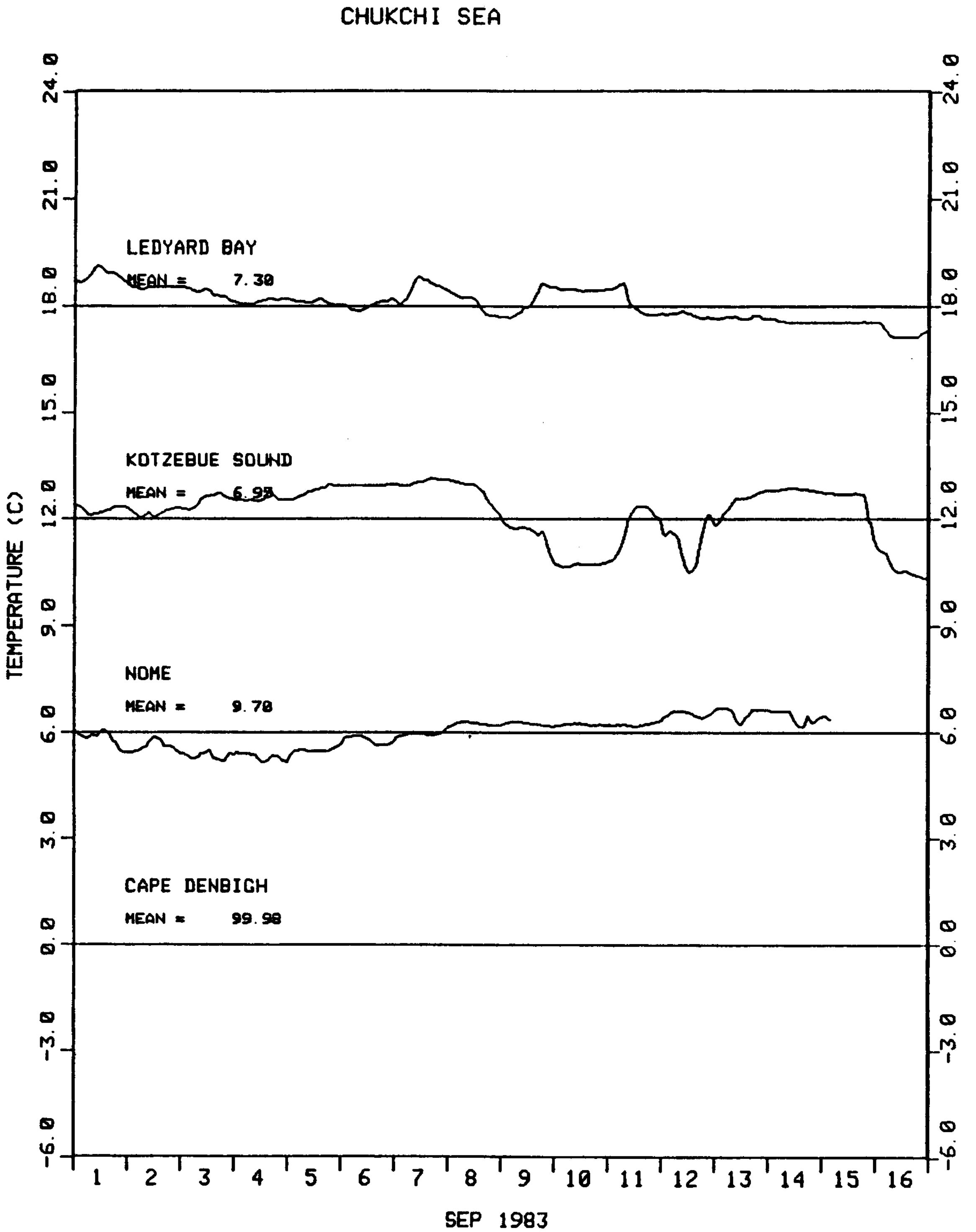

Fig. 10. Temperature Fluctuations About the Monthly Mean at Stations 1 through 4 in September 1983

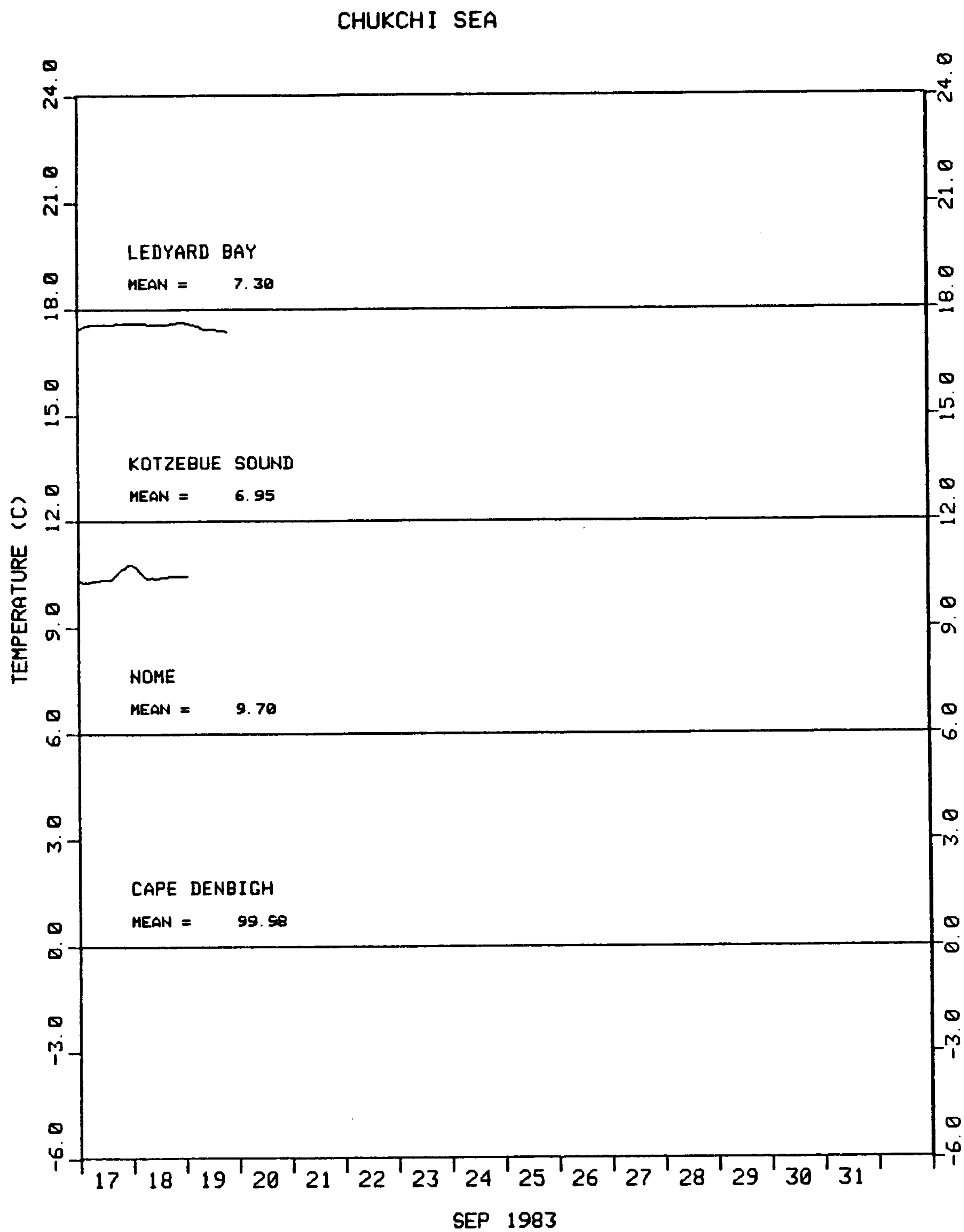

Fig. 10. Temperature Fluctuations About the Monthly Mean at Stations 1 through 4 in September 1983 (contd)

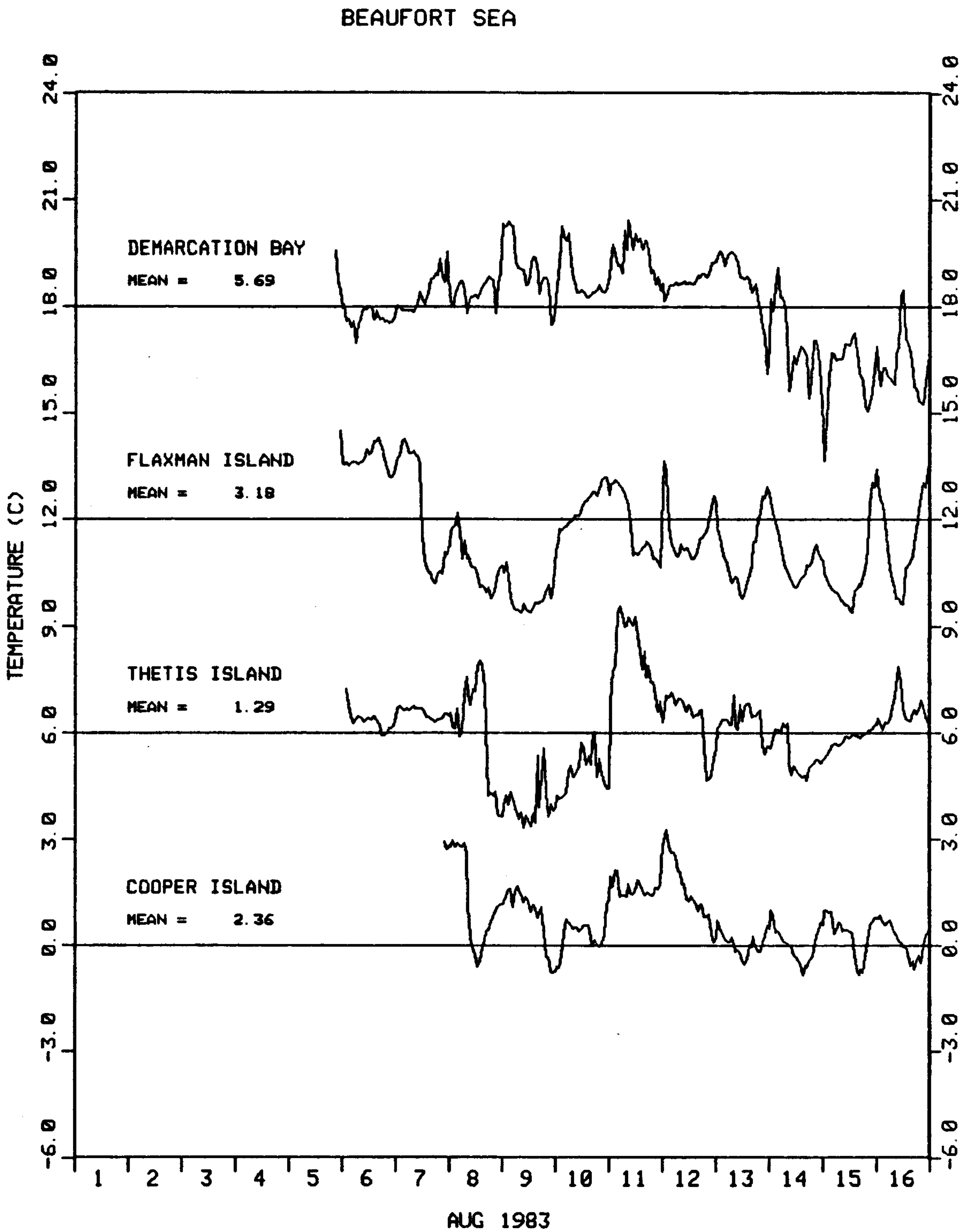

Fig. 11. Temperature Fluctuations About the Monthly Mean at Stations 5 through 8 in August 1983

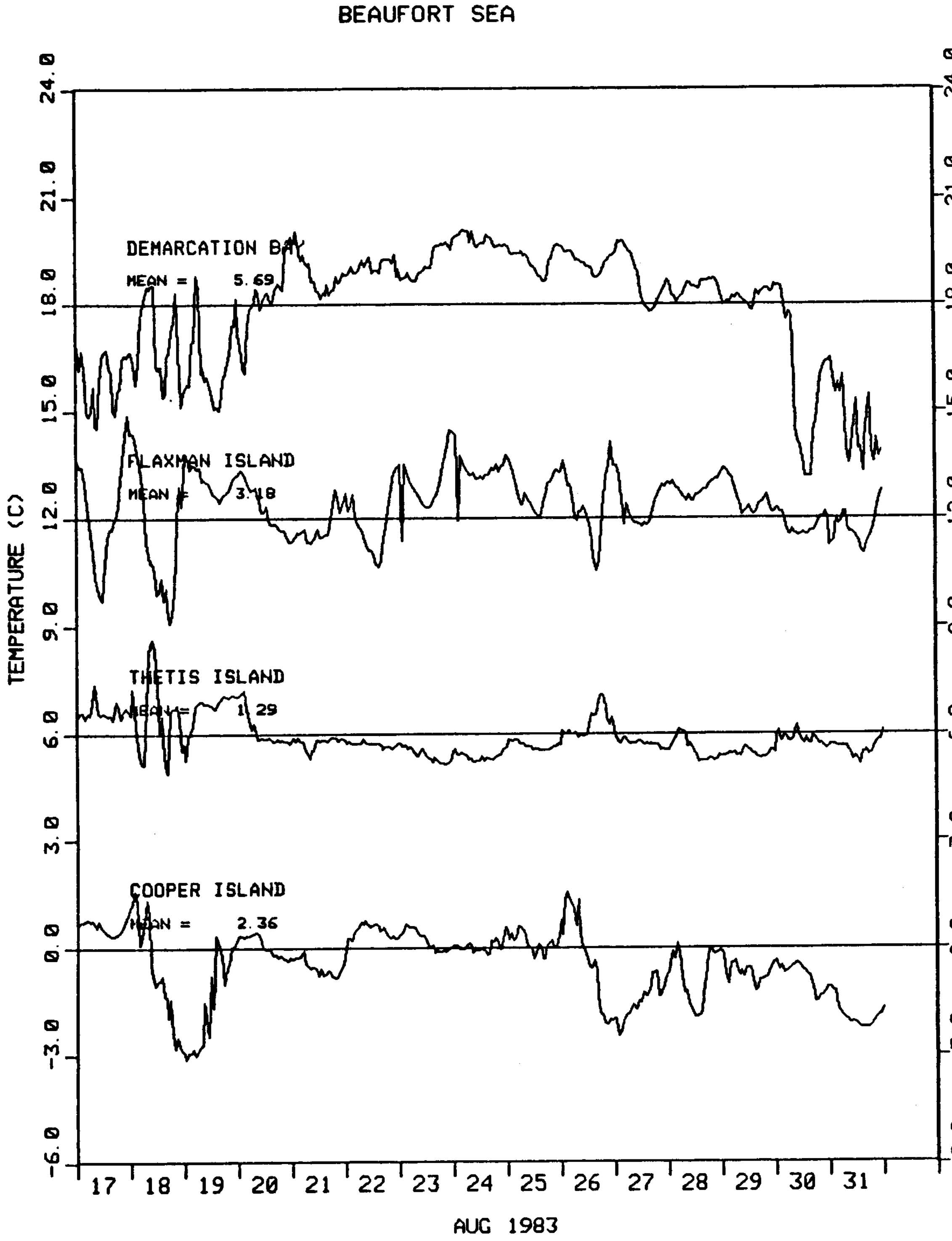

Fig. 11. Temperature Fluctuations About the Monthly Mean at Stations 5 through 8 in August 1983 (contd)

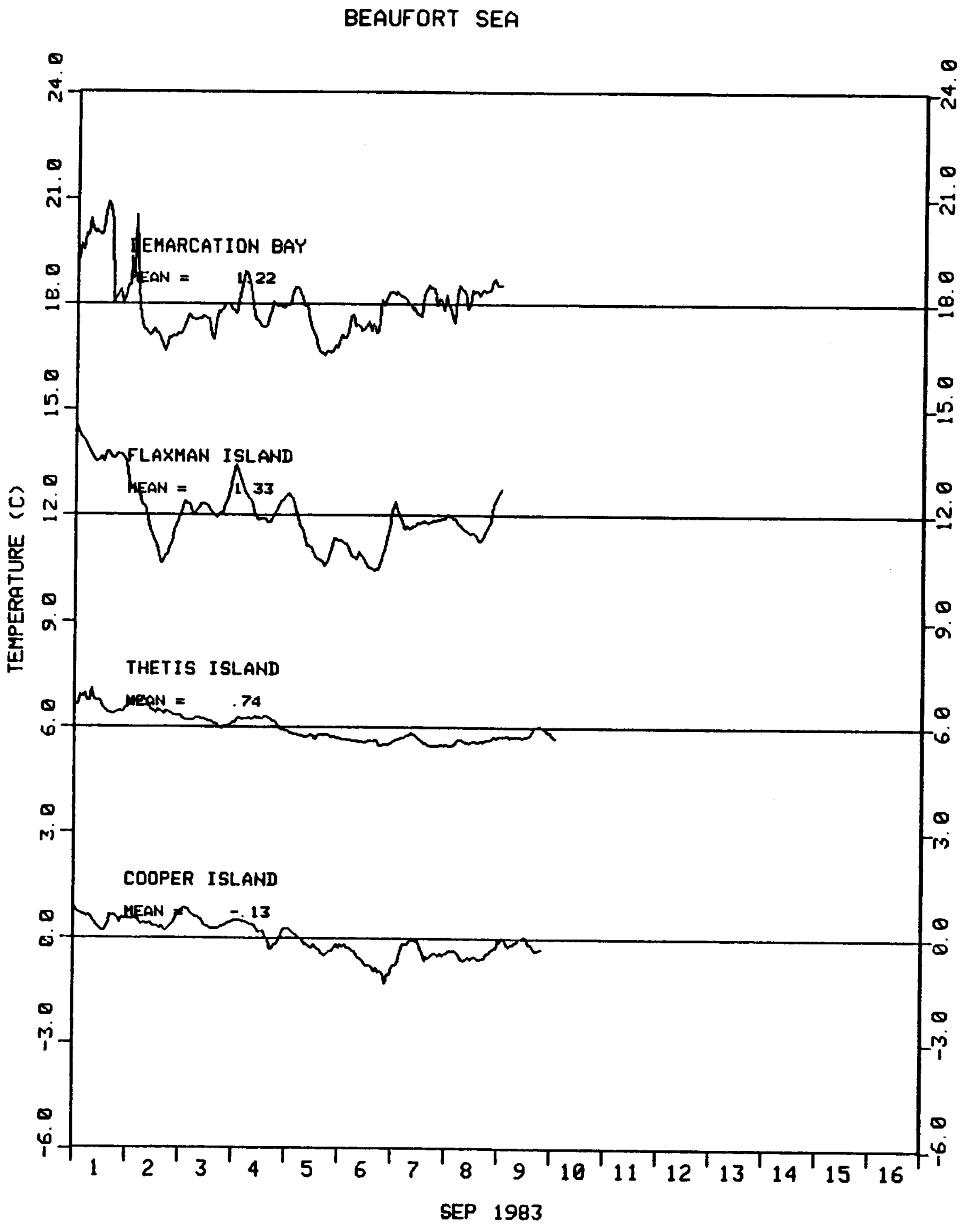

Fig. 12. Temperature Fluctuations About the Monthly Mean at Stations 5 through 8 in September 1983

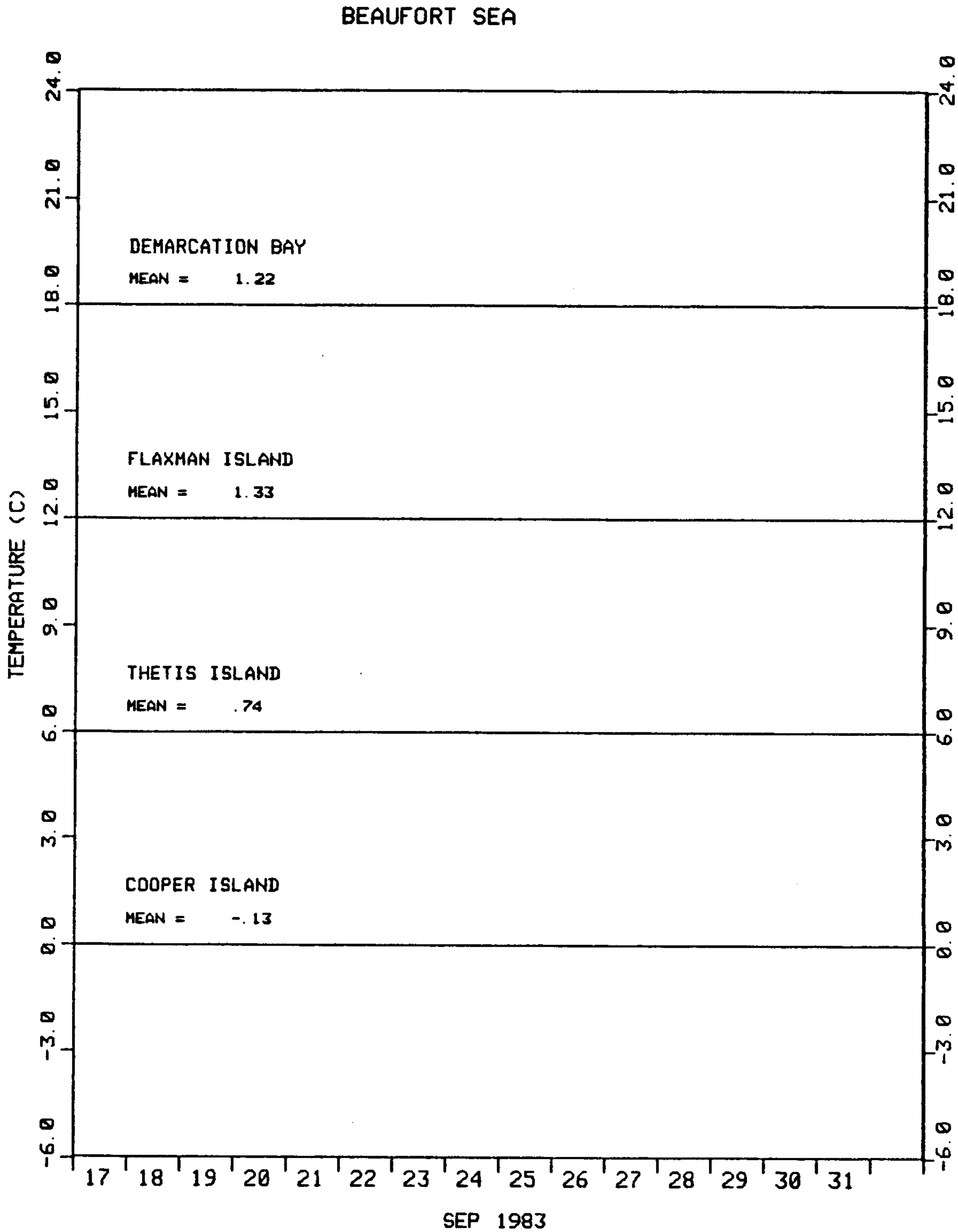

Fig. 12. Temperature Fluctuations About the Monthly Mean at Stations 5 through 8 in September 1983 (contd)

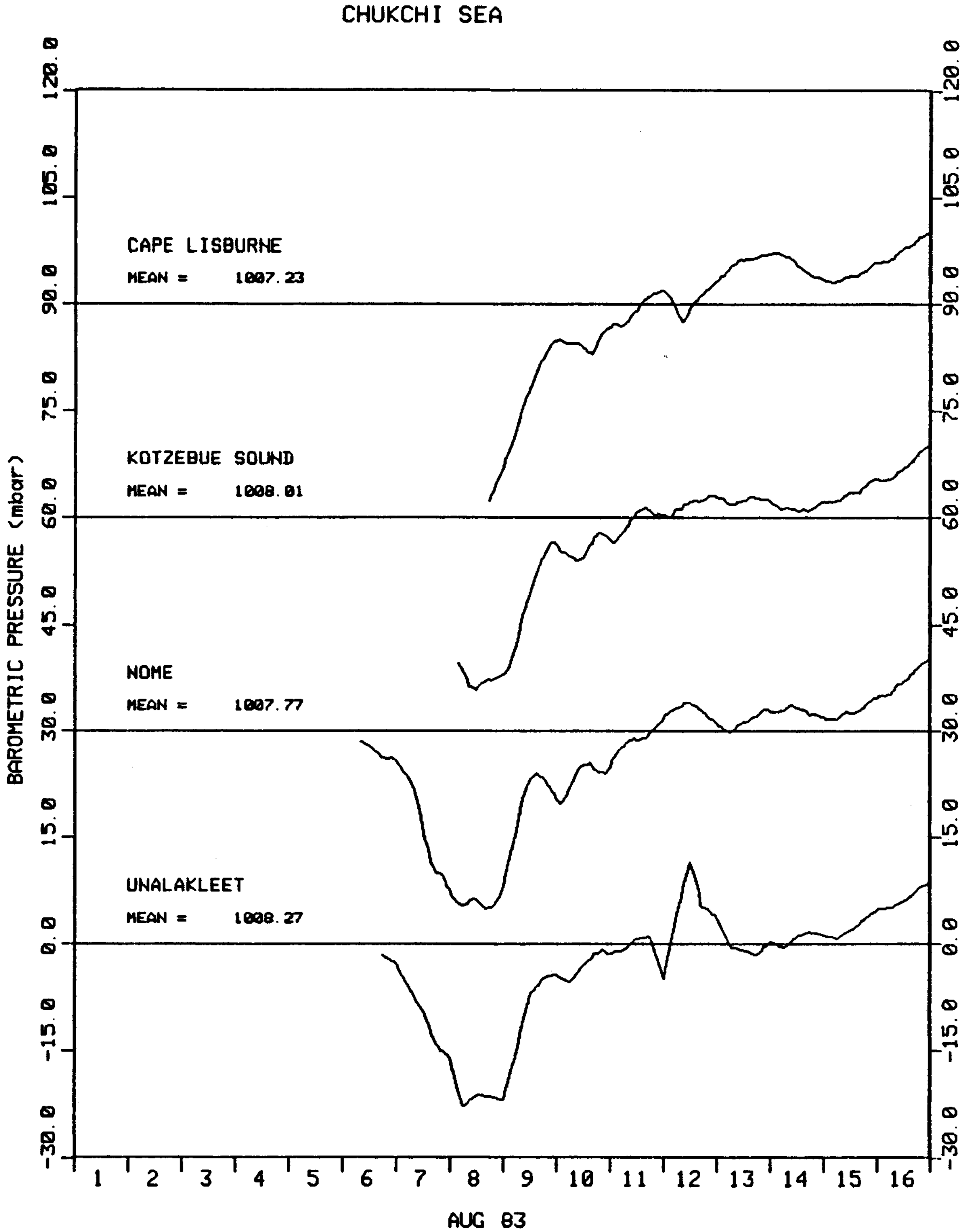

Fig. 13. Barometric Pressure Fluctuations Used to Correct Absolute Pressure Data from Stations 1 through 4 in August 1983

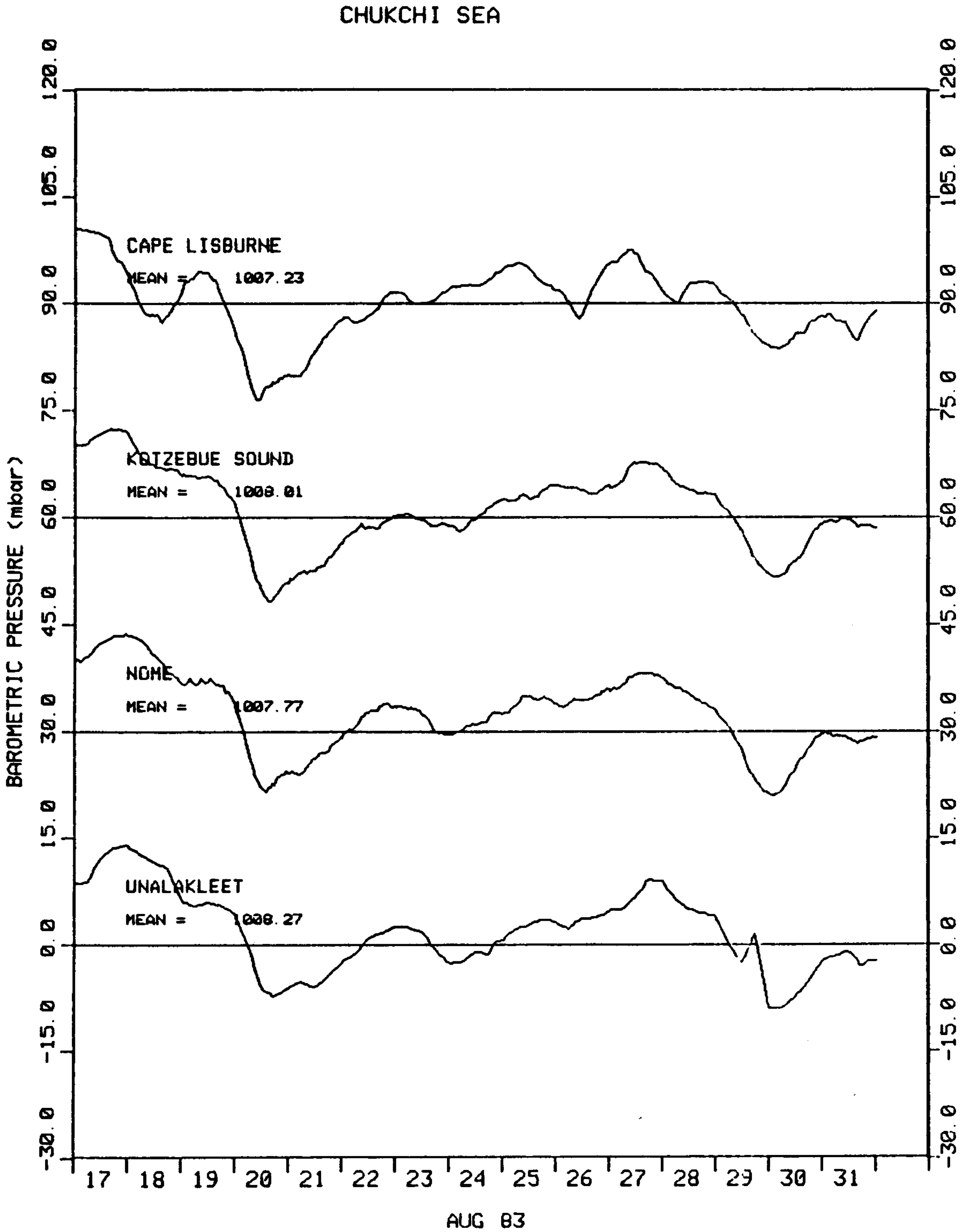

Fig. 13. Barometric Pressure Fluctuations Used to Correct Absolute Pressure Data from Stations 1 through 4 in August 1983 (contd)

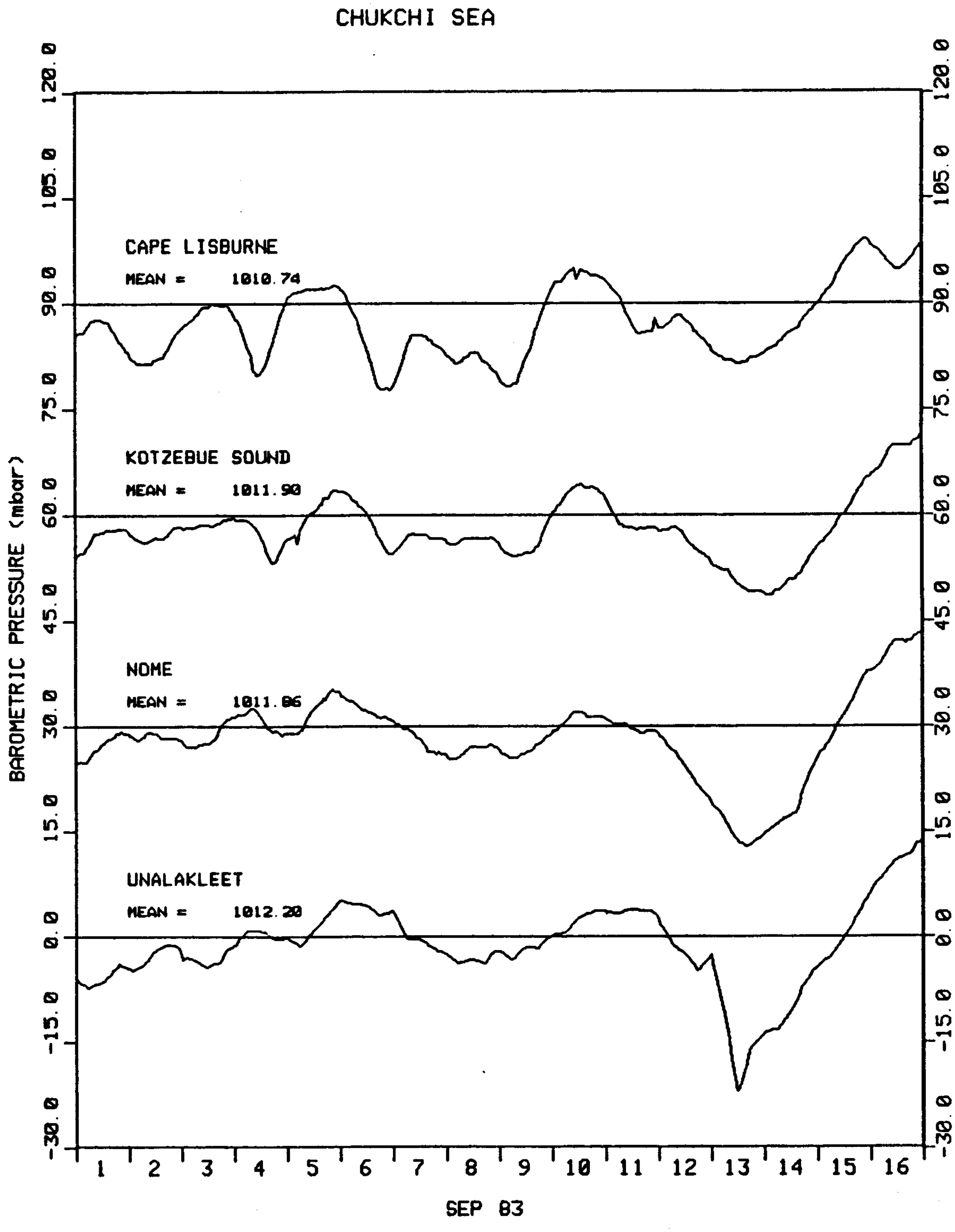

Fig. 14. Barometric Pressure Fluctuations Used to Correct Absolute Pressure Data from Stations 1 through 4 in September 1983

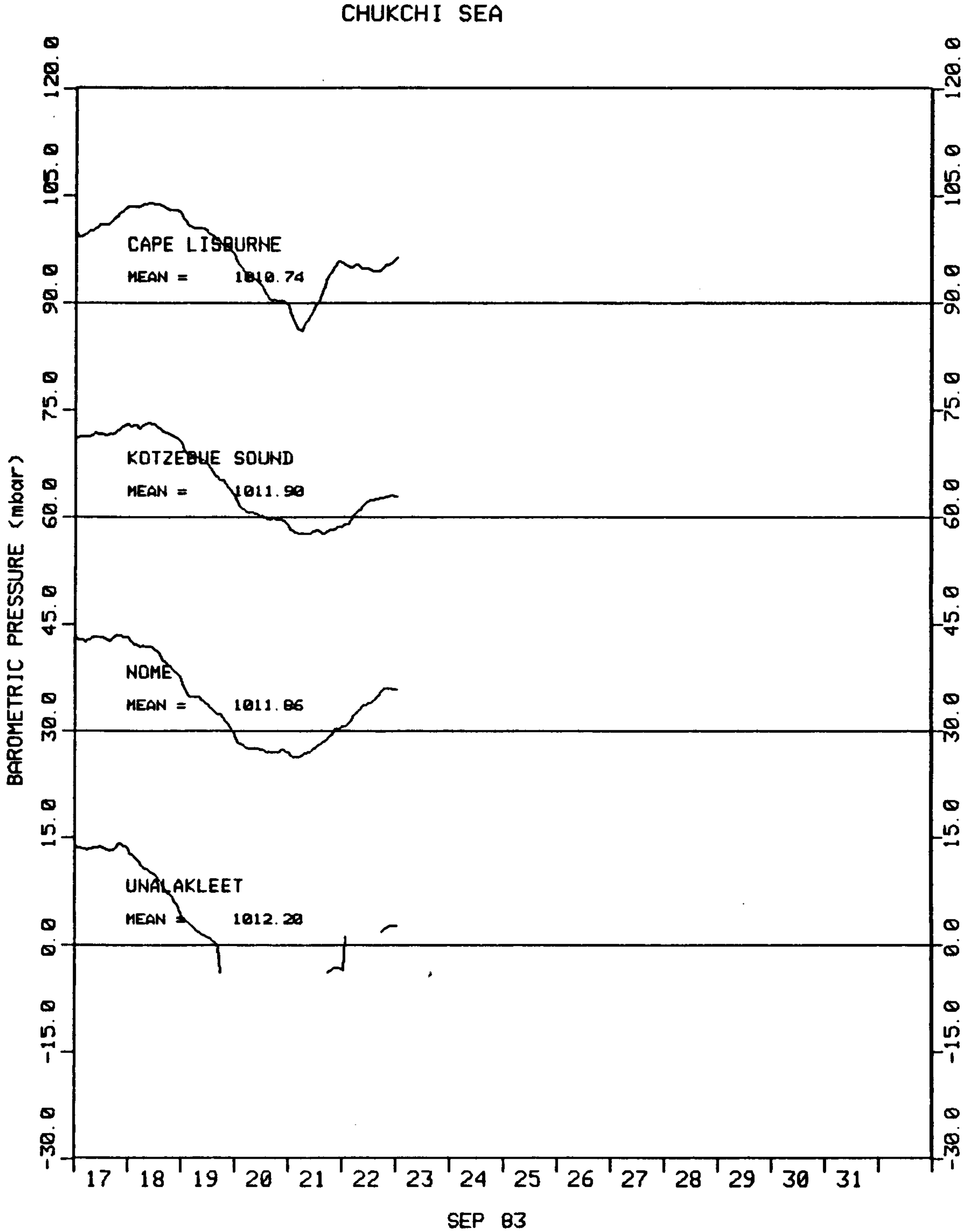

Fig. 14. Barometric Pressure Fluctuations Used to Correct Absolute Pressure Data from Stations 1 through 4 in September 1983 (contd)

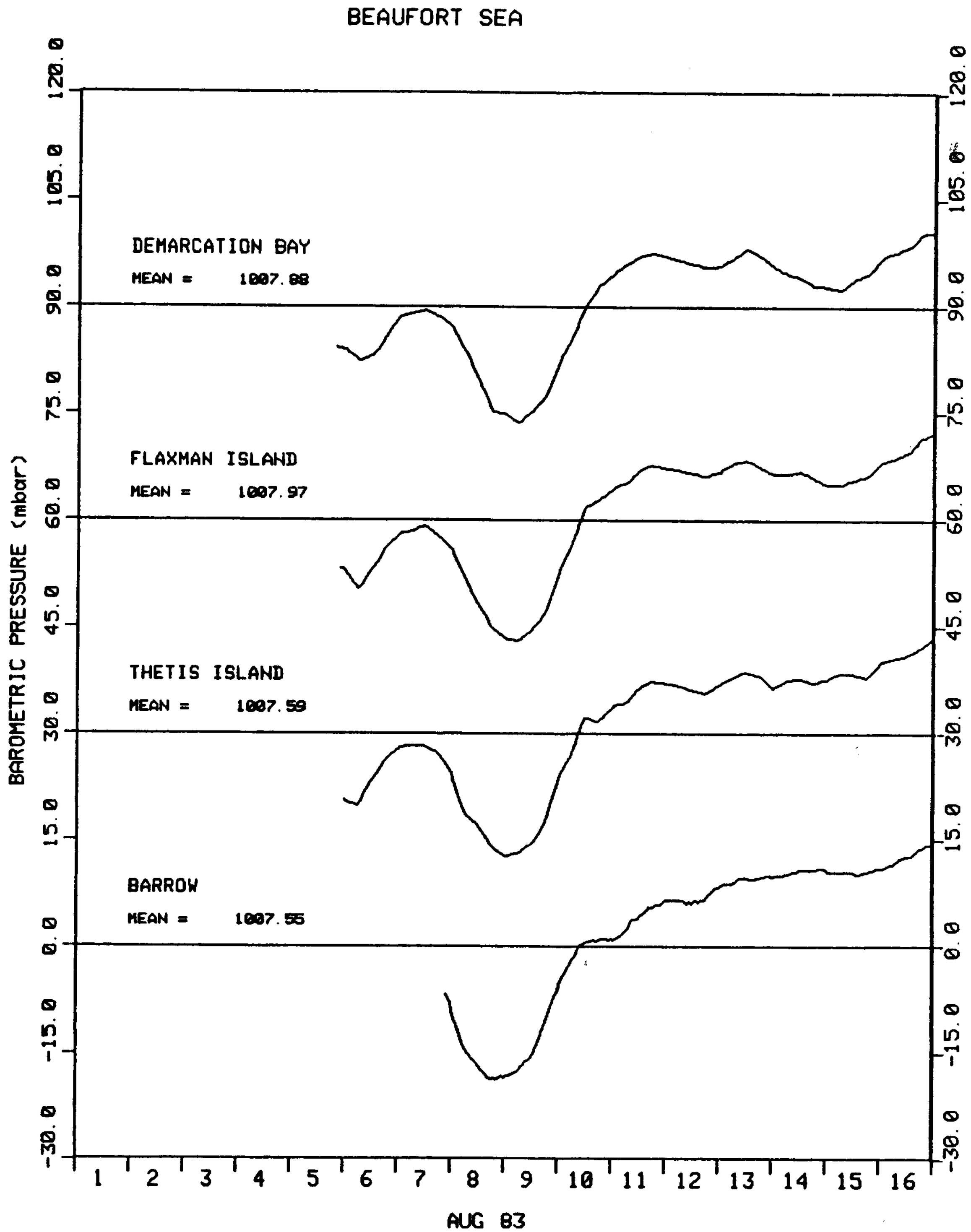

Fig. 15. Barometric Pressure Fluctuations Used to Correct Absolute Pressure Data from Stations 5 through 8 in August 1983

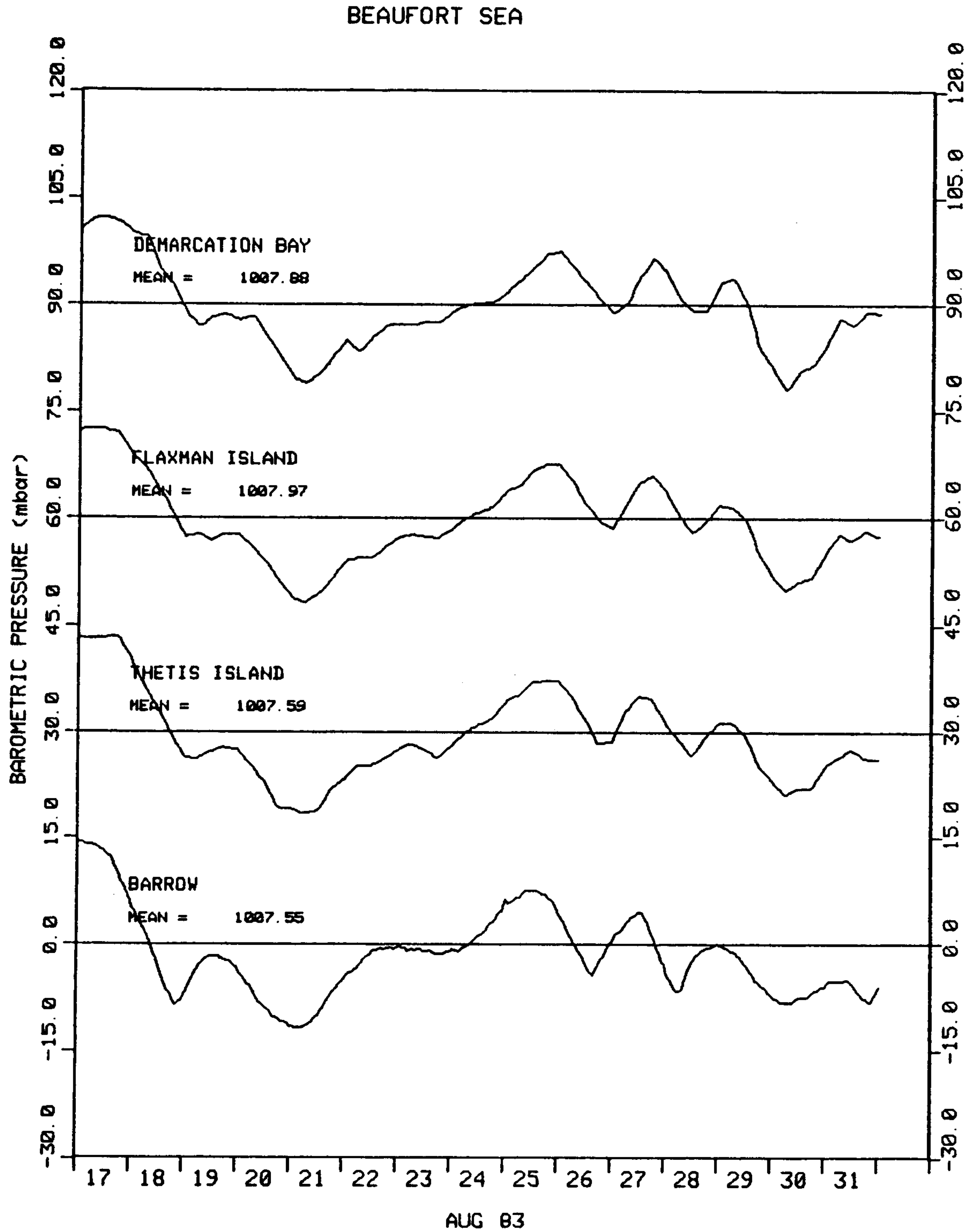

Fig. 15. Barometric Pressure Fluctuations Used to Correct Absolute Pressure Data from Stations 5 through 8 in August 1983 (contd)

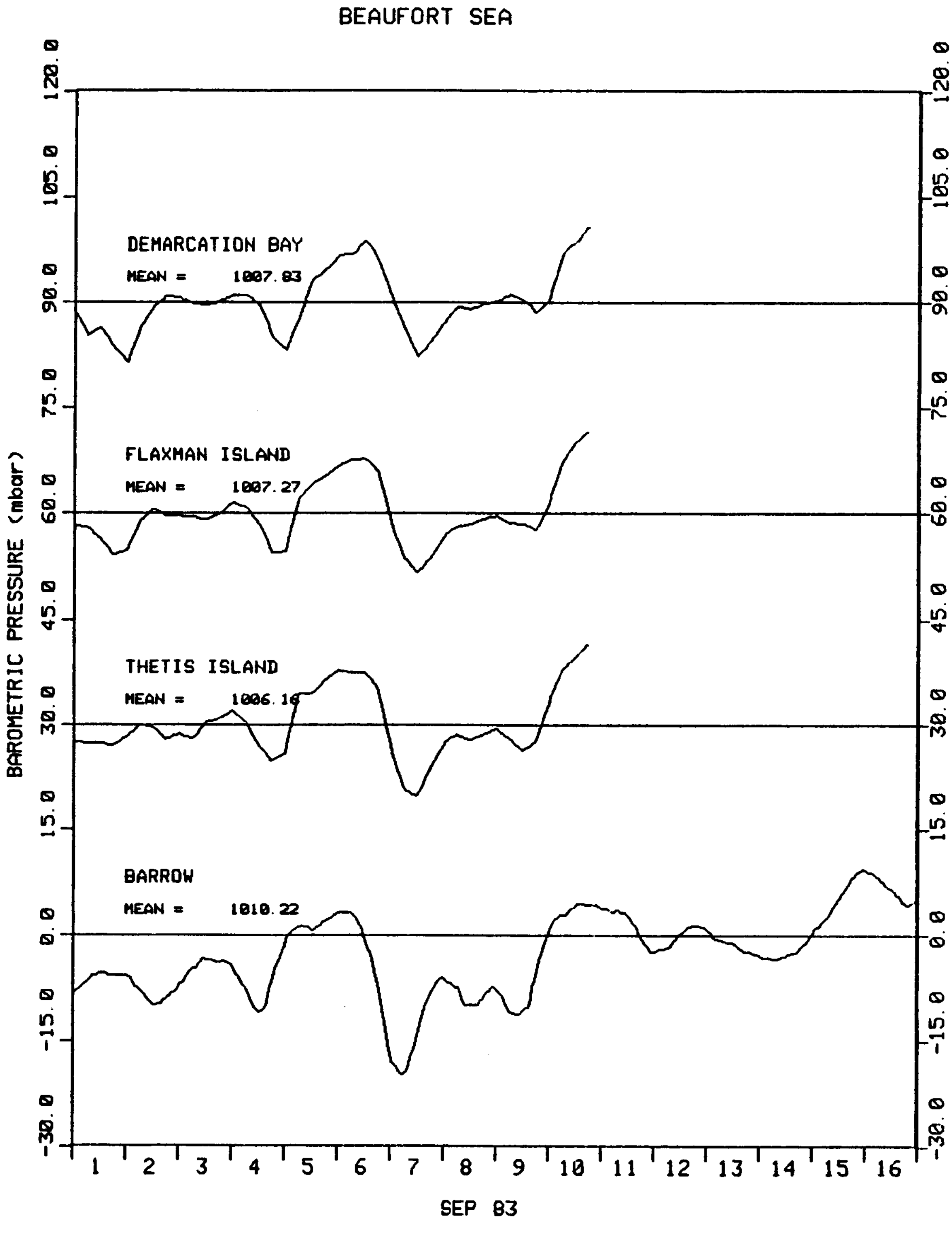

Fig. 16. Barometric Pressure Fluctuations Used to Correct Absolute Pressure Data from Stations 5 through 8 in September 1983

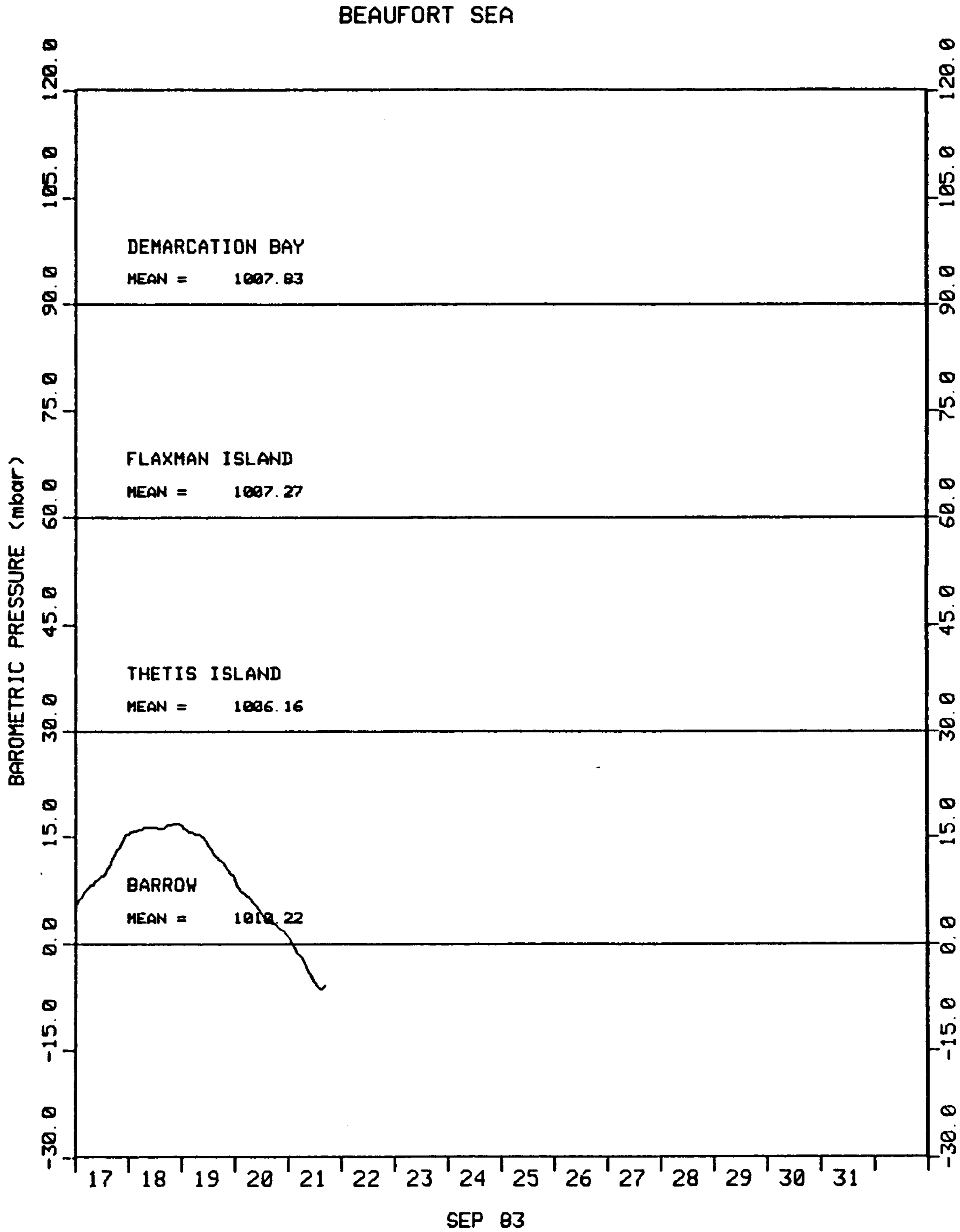

Fig. 16. Barometric Pressure Fluctuations Used to Correct Absolute Pressure Data from Stations 5 through 8 in September 1983 (contd)

NEARSHORE COASTAL CURRENTS--

CHUKCHI SEA, SUMMER 1981

by

Donald E. Wilson, Stephen D. Pace,
Philip D. Carpenter, Howard Teas,
Toby Goddard, Peter Wilde, and Patrick Kinney

Kinnetic Laboratories, Inc.

Final Report
Outer Continental Shelf Environmental Assessment Program
Research Unit 531

June 1982

TABLE OF CONTENTS

LIST OF FIGURES

36. Cross correlations: Point Barrow-Lisburn barometric pressure differences vs. lagged inshore Wainwright (bottom) drift current, 12 August - 1 September 1981.

37. Spectral density: Wainwright wind, 12 August - 1 September 1981.

38. Spectral density: inshore Wainwright (bottom) drift current, 12 August - 1 September 1981.

39. Cross correlation: Wainwright wind vs. lagged inshore Wainwright (bottom) drift current, 12 August - 1 September 1981.

40. Squared coherence spectrum: Wainwright wind vs. inshore Wainwright (bottom) drift current, 12 August - 1 September 1981.

41. Phase spectrum: Wainwright wind vs. inshore Wainwright (bottom) drift current, 12 August - 1 September 1981.

42. Squared coherence spectrum: Wainwright wind vs. inshore Wainwright (bottom) drift current, 12 August - 1 September 1981.

43. Phase spectrum: Wainwright wind vs. inshore Wainwright (bottom) drift current, 12 August - 1 September 1981.

44. Cross correlations: Point Barrow wind vs. lagged inshore Barrow (bottom) drift current, 8 August - 6 September 1981.

45. Cross correlations: Point Barrow-Cape Lisburne barometric pressure differences vs. lagged wainwright winds, 3 August - 4 September 1981.

46. Cross correlations: Point Barrow-Cape Lisburne barometric pressure differences vs. lagged Point Barrow wind, 1 August - 4 September 1981.

47. Comparison of temperature/salinity time series and current records.

LIST OF TABLES

ACKNOWLEDGEMENTS

This study would not have been completed over the course of the 1981 season without the support of several individuals within the Arctic community. Within this vein, we thank the crew of the USGS's research vessel, KARLUK, and the crew of the Crowley Corp. tug, GUARDSMAN, for their invaluable assistance and companionship. We thank Jim and Elaine Childs of Childs Equipment Services for their extensive logistical support. Similarly, we thank Ray Dronenberg and the Native Whaling Association for their local assistance in Barrow, and Sam Stoker for his stalwart logistical support.

This work was funded as part of the Outer Continental Shelf Environmental Assessment Program (OCSEAP) of the National Oceanic and Atmospheric Administration (NOAA), U.S. Department of Commerce, and primarily funded by the Minerals Management Service (MMS), U.S. Department of the Interior, through an interagency agreement.

SUMMARY

Nearshore currents measured along the Chukchi Sea coast from Point Barrow to Wainwright during the period 7 August to 7 September 1981 flowed predominantly upcoast. However, downcoast flow was measured between 33 and 47 percent of the time in these records. Speeds were up to 50 cm/sec, except offshore Point Barrow in the vicinity of Barrow Canyon, where speeds up to 100 cm/sec were recorded.

All currents from the different moorings, depths, and from both Wainwright and Point Barrow locations were closely correlated (correlation coefficients of about 0.90). These currents were also strongly correlated with atmospheric pressure differences between Point Barrow and Cape Lisburne (correlation coefficients about -0.81 to -0.85, zero lag). These currents were not as strongly correlated with the respective local winds (correlation coefficients about 0.65 to 0.72).

Hydrographic transects taken perpendicular to the coast at seven locations between Point Barrow and Akunik Pass (south of Icy Cape) were supplemented by continuous records of temperature and salinity from the moored meters off Point Barrow. Highly variable temperature and salinity regimes are indicated by this nearshore data. Pycnoclines at 5-10 meters depth inshore and 10-15 meters depth offshore were found. Cooler, more saline water nearshore may indicate upwelling but was not consistent with upcoast or downcoast flow regimes. Features of sharp temperature/salinity fronts are evident in the time series data.

A group of twelve drogues tracked off Wainwright by a MiniRanger III positioning system drifted downcoast, consistent with measured coastal currents. A diffusivity value of up to 9 x 10^3 cm^2/sec was indicated from spreading of the twelve drogues about their centroid.

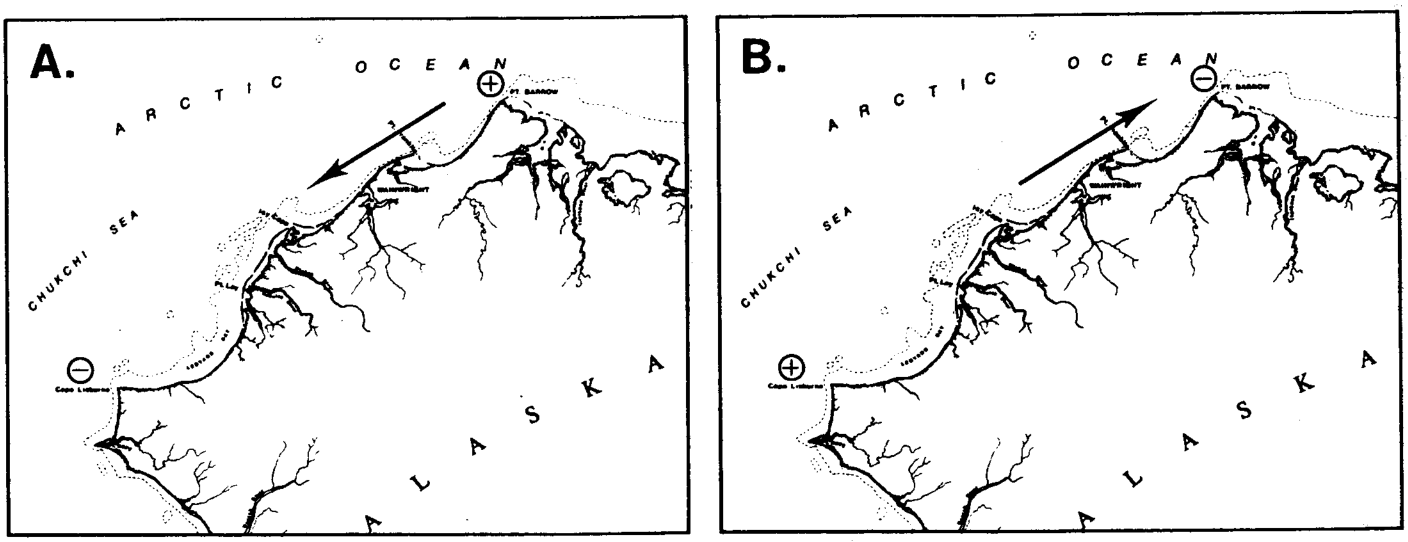

Schematic of Coastal Current Direction vs. Atmospheric Pressure Difference (Pt. Barrow - Cape Lisburne). A: ΔP Positive. B: ΔP Negative.

INTRODUCTION

The Outer Continental Shelf Environmental Asessment Program (OCSEAP) was established by a basic agreement between the National Oceanic and Atmospheric Administration (NOAA) and the Bureau of Land Management (BLM). Its purpose is to conduct environmental research along the Alaskan shelf areas identified for potential oil and gas development. The present work was conducted by Kinnetic Laboratories, Inc. as Research Unit 531 of OCSEAP. The purpose of RU 531 has been to provide data and numerical modeling results on nearshore currents and on possible pollutant trajectory analyses.

Considerable delay was experienced during this year by RU 531 due to a reassessment of priorities between Beaufort Sea and Chukchi Sea tasks by NOAA (Arctic Project Office, Fairbanks; Alaska Office of the Office of Marine Pollution Assessment, Juneau) and BLM, Anchorage and by the unavailability of the usual NOAA-provided ship, plane, and other logistics.

Kinnetic Laboratories, Inc. (KLI) was not authorized until July 1981 to conduct this 1981 summer program along the Chukchi Sea coast. KLI was requested to supply all logistics, including the 32-foot survey vessel, D.W. HOOD. Notwithstanding the resulting time and material constraints, the data acquired on summer coastal currents along the Chukchi Sea coast are reported herein.

Objectives

Specific objectives of the present study were the following:

1. Obtain measurements of nearshore coastal currents by moored instrumentation along the Chukchi Sea coast from Point Barrow as far south as Cape Lisburne, if possible;

2. Obtain auxiliary water-level measurements, hydrographic section data, and meteorological observations;

3. Collect synoptic wind and barometric pressure data from reporting stations along this coast from Nome to Pt. Barrow;

4. Conduct current-drogue tracking studies as time permits and as a lower priority item;

5. Present and interpret the data obtained. Pay particular attention to episodes of wind and

pressure patterns, and their resulting effects on measured coastal currents. Perform analyses of co-variance, if appropriate;

6. Furnish raw data, in card image format, conforming to NODC/OCSEAP formats, on nine-track digital tape.

Previous Work

Although there are many previous oceanographic studies in the Chukchi Sea, there have been relatively few measurements of nearshore currents along the Chukchi Sea coast. Earlier work in the Chukchi Sea, generally confined to the deeper offshore waters, was reviewed by Coachman in 1963. A later review, including most of the available inshore data, was also given by Coachman et al. in 1975.

A warm current, originating in the Bering Strait flows northeastward approximately 100 km offshore (Coachman et al. 1975; Ingham and Rutland 1972; Fleming and Heggarty 1966; Paquette and Bourke 1974). To the north, the current approaches the coast and flows through Barrow Canyon into the Beaufort Sea (Mountain et al. 1976). South of Icy Cape, there is evidence of an anticyclonic eddy separating the coast and the warm current (Fleming and Heggarty 1966; Ingham and Rutland 1972). Offshore, a pycnocline occurs between ten and fifteen meters depth because of ice melt (Ingham and Rutland 1972), but shoals occur five to ten meters inshore, and are more intense due to freshwater runoff (Wiseman et al. 1974).

Two previous investigations are particularly relevant to the present data. Mountain et al. (1976) obtained 120-day records of currents and temperatures from two moored Aanderaa meters at 96 and 126 meter depths in 150 meters of water offshore in Barrow Canyon. These records showed mean currents of 25 cm/sec toward the northeast (along the axis of the canyon which approximately parallels the shoreline). However, the records were characterized by higher speeds (commonly greater than 50 cm/sec) and large variations, including periods of reversed upcanyon motion. A close relationship was shown to exist between the measured currents and the north-south pressure gradient, such that when the pressure rose to the north, the northward flow of water through the canyon decreased.

Wiseman and Rouse (1980) obtained current-drogue tracks, wind measurements, and inshore hydrographic measurements near the Point Lay - Icy Cape area in 1972. They conclude that these data support the thesis of a well-developed baroclinic coastal jet.

Present Study

The present work was meant to supplement the sparse data on Chukchi Sea coastal currents, chiefly the deeper moored data of Mountain et al. (1976) off Barrow, the brief observations of

Wiseman and Rouse (1980) off Pt. Lay, and sporadic ship observations as summarized by Coachman et al. (1975). An objective was to obtain coastal field data prior to anticipated NOAA numerical modeling efforts. Such data will aid numerical modeling efforts by guiding the selection of the appropriate physics for incorporation into coastal models, as well as providing data for hindcast verifications.

The work described herein was carried out between 7 August 1981 and 8 September 1981 in the open-water/floating ice regime of the Chukchi Sea summer season.

MATERIALS AND METHODS

Current Metering

Current data were obtained by deploying and retrieving current meters along the Chukchi Sea coast during the initial and final stages of the study. Stations were located at Barrow, Wainwright, and Akunik Pass (Figure 1). Each location was moored with both an onshore and offshore string of meters. Relative depths of meters are shown in Figure 2.

Meter strings were composed of the two instrument packages and bridles attached with an appropriate length of 1/4-inch stainless steel cable, subsurface floats, acoustic pinger, primary anchor (250-300 lbs.), 600-foot tag line, and secondary anchor (40 lbs.), as shown in Figure 3. The instrument packages varied between stations. Both Barrow stations were equipped with Aanderaa model RCM-4 (magnetic recording) current meters, while the Wainwright stations were composed of General Oceanic model 2010 (film recording) current meters. The Akunik stations were moored in the inshore area with Aanderaa model RCM-4 meters. The offshore Akunik station was comprised of an Aanderaa model RCM-4 meter at the bottom position and a Marsh-McBirney model ARC-585 (electromagnetic) current meter at the subsurface position. All stations were equipped with collapsible and noncollapsible subsurface floats to and with acoustic pingers (Helle model 2215) providing verification of meter location.

Deployment procedures were carried out after establishing shore transponder sites for the Motorola Miniranger III locating system. After the instrument packages were deployed and their positions recorded, a tag line was stretched between the primary and secondary anchors along a recorded magnetic heading.

Current meter recovery depended on relocating the position of deployment, checking for the presence and actual location of the meter string with the acoustic pinger detector, marking the exact location with a buoy and weighted line and snagging the tag line with a grapnel hook.

Raw current meter data retrieved from the field is processed, analyzed and correlated with meterological data products by a series of computer programs in the laboratory. The initial production in the process varies between types of meters used (Aanderaa and General Oceanics), but the screening, presentation, production and correlation processes are identical.

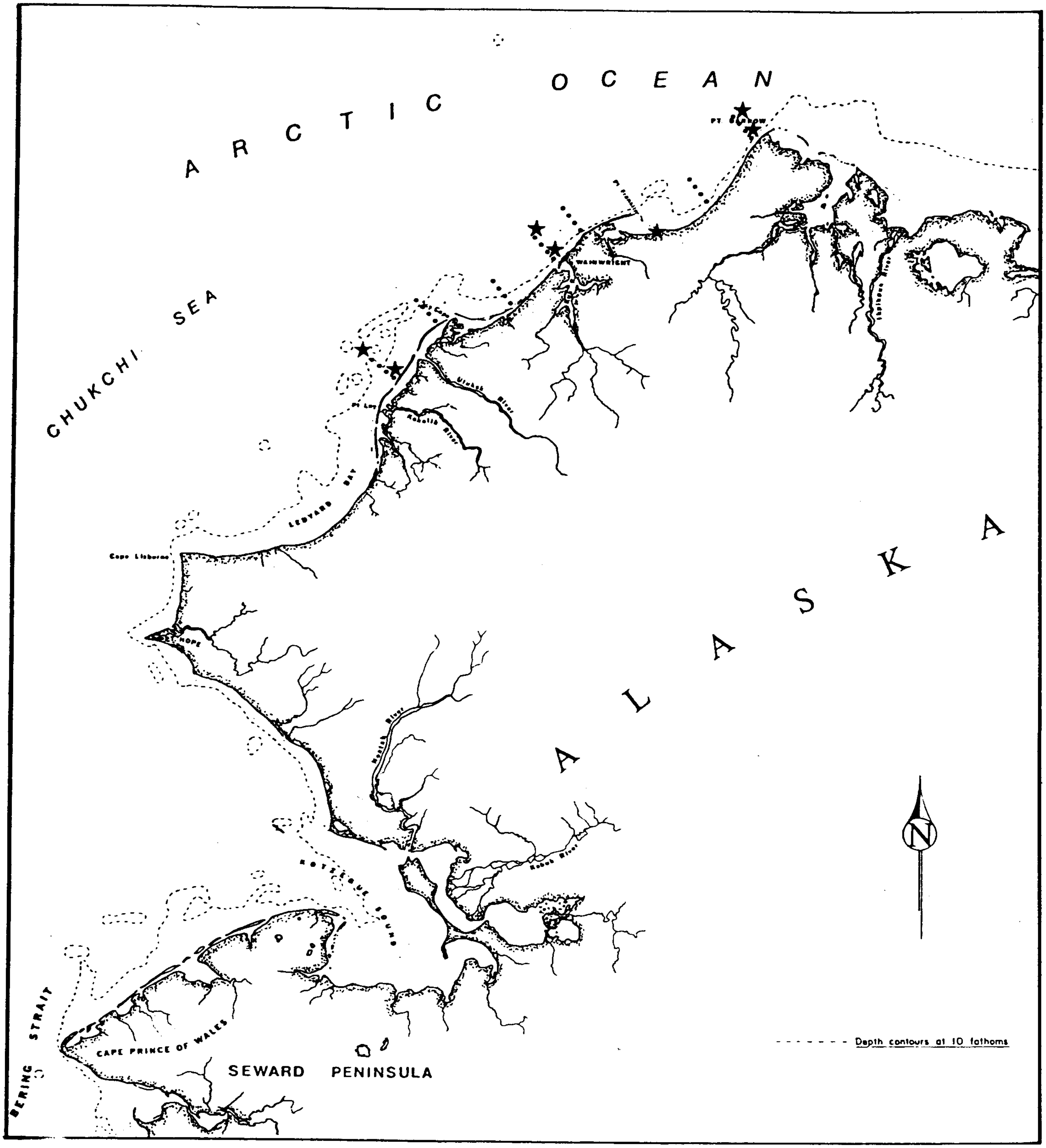

★ Instrument Mooring Locations
···· C/STD Transects

Figure 1. Chukchi Sea Coast Study Sites (August - September 1981)

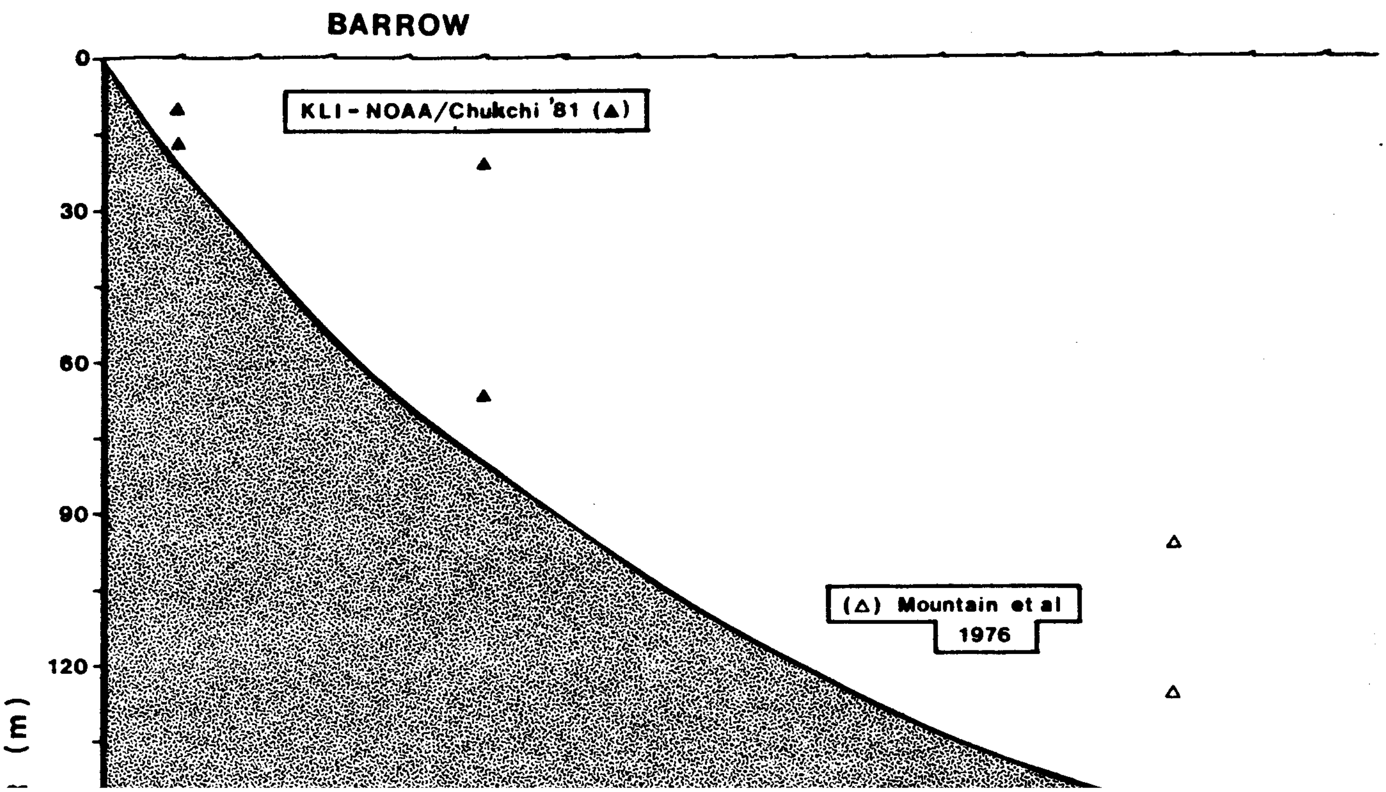

BARROW
0
30
60
90
120
(m)
KLI-NOAA/Chukchi '81 (▲)
(△) Mountain et al
1976

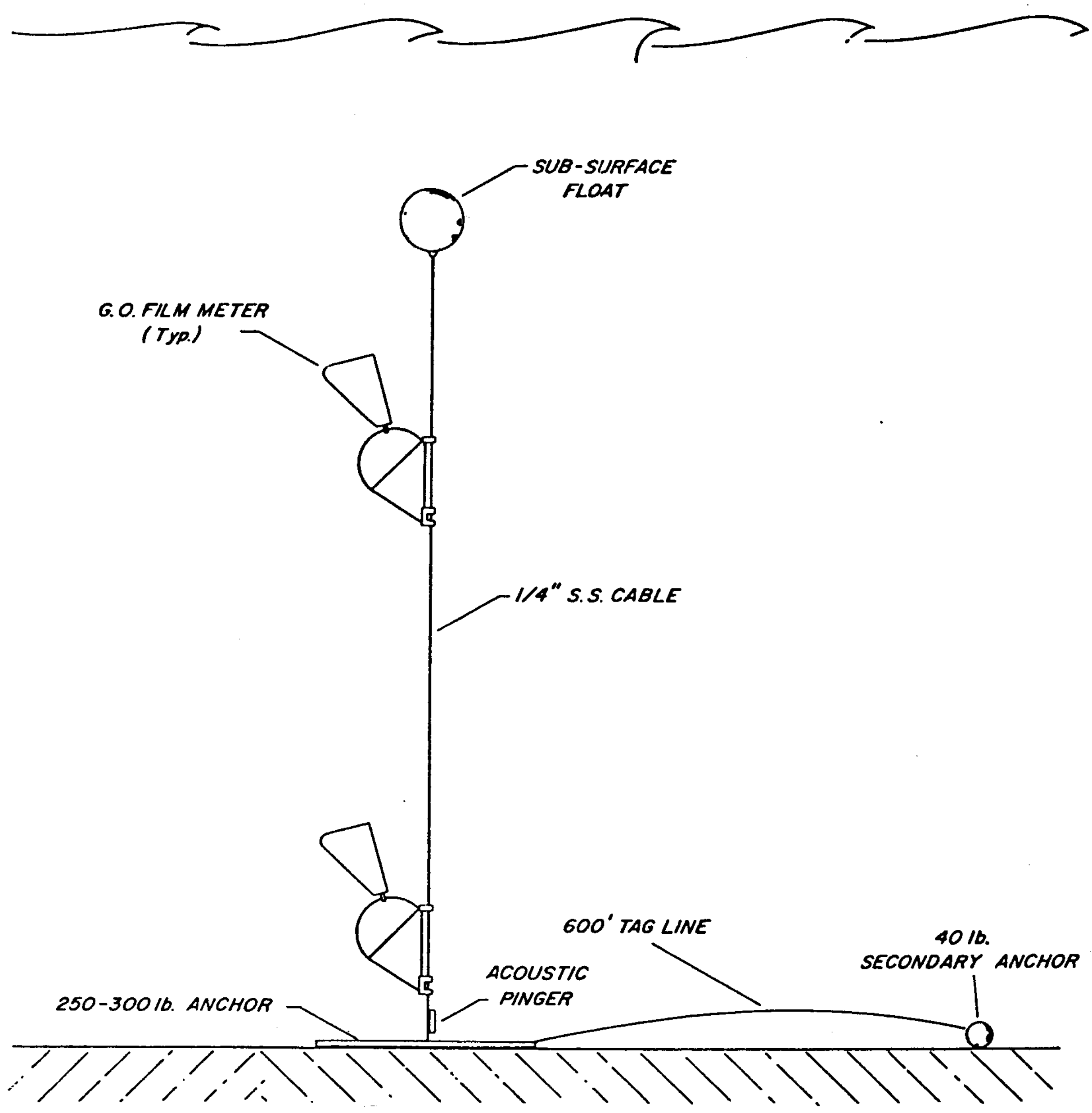

Figure 3. Schematic of Current Meter Mooring, General Oceanic Film Meters (not to scale)

Meteorology

Weather observations of wind speed and direction were taken from the Air Force and NOAA weather service records at weather stations and DEW-line sites at Cape Lisburne, Point Lay, Wainwright and Barrow from August to September 1981.

Atmospheric pressure differences were calculated from values extracted from National Weather Service maps for Nome, Cape Lisburne and Barrow for the month of August 1981. Differences in pressure were correlated with current data to describe forcing functions.

Hydrography

Nearshore density profiles of the water column were acquired with an InterOceans C/STD system model 513D. Data was recorded with a Datel model DPP-7 printer and later screened and analyzed for content. Surface water samples were taken during each transect to check temperature and salinity values.

Stations were located 1.0, 1.5, and 2.0 nautical miles apart along transects surveyed at Barrow, Skull Cliffs, Point Belcher, Wainwright, Pingorarok Pass, Icy Cape, and Akunik Pass (Figures 4 - 6). Cast depths were limited by the length of C/STD cable to 90 meters or less, depending on wire angle and bottom depth.

Most of the profiles were taken within a period of a week at depth intervals of one meter. Values were recorded for the parameters of temperature, conductivity, depth, and transparency.

Drogue Studies

Twelve drogues were weighted to present a minimum of float area to the wind. Sails were of the windowshade design, seven square feet in area, and set within a meter of the water surface. Small flags attached to the drogues permitted identification at a distance.

Deployment procedure involved setting all twelve drogues in the form of a cross at 12:00 hours on 20 August 1981 five nautical miles offshore of Wainwright in 72 feet of water. Deployment and drift position were recorded with a Motorola Miniranger III locating system. Positions were taken every hour from the research vessel D.W. HOOD, as were local wind and weather observations for the twelve-hour duration of the experiment.

The analyses were carried out using the methods of Okubo et al (8) and Ichiye et al (9). The range-range data recorded from the miniranger system were converted to latitude and

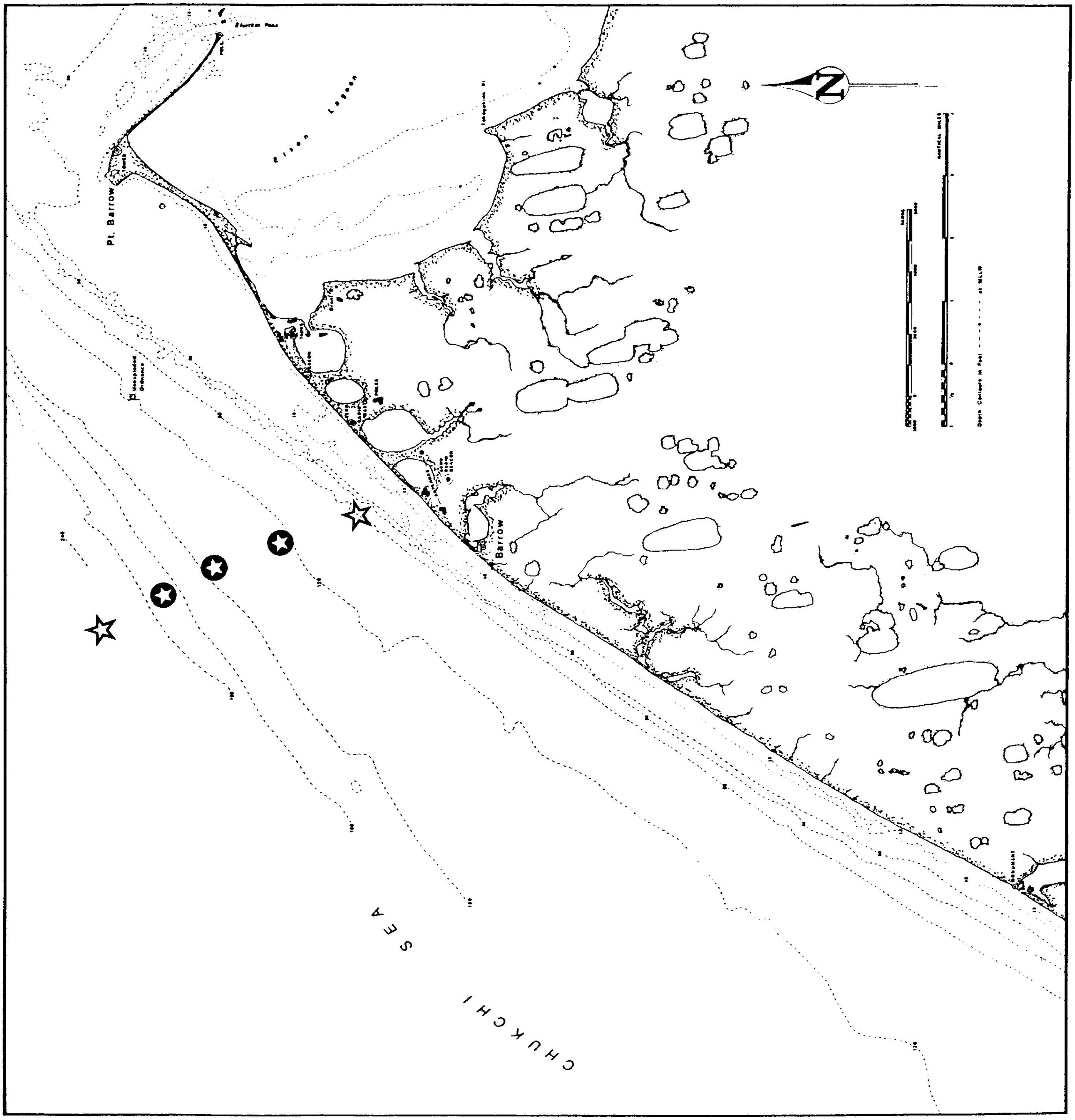

CTD Cast

Current Meter & CTD Cast

Figure 4. Locations of Current Meter Stations and C/STD Casts off Point Barrow.

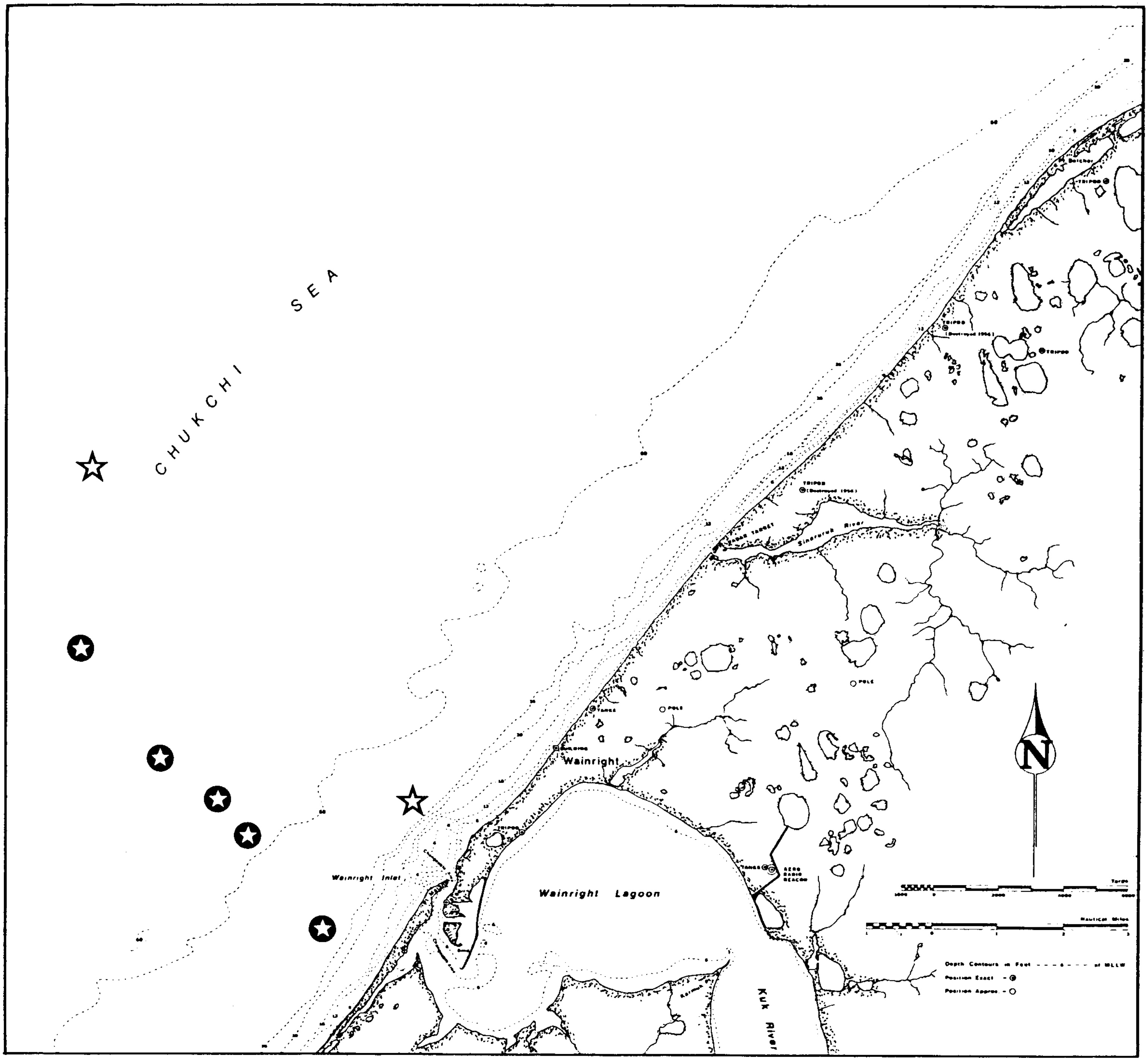

- CTD Cast

- Current Meter &CTD Cast

Figure 5. Locations of Current Meter Stations and C/STD Casts off Wainwright.

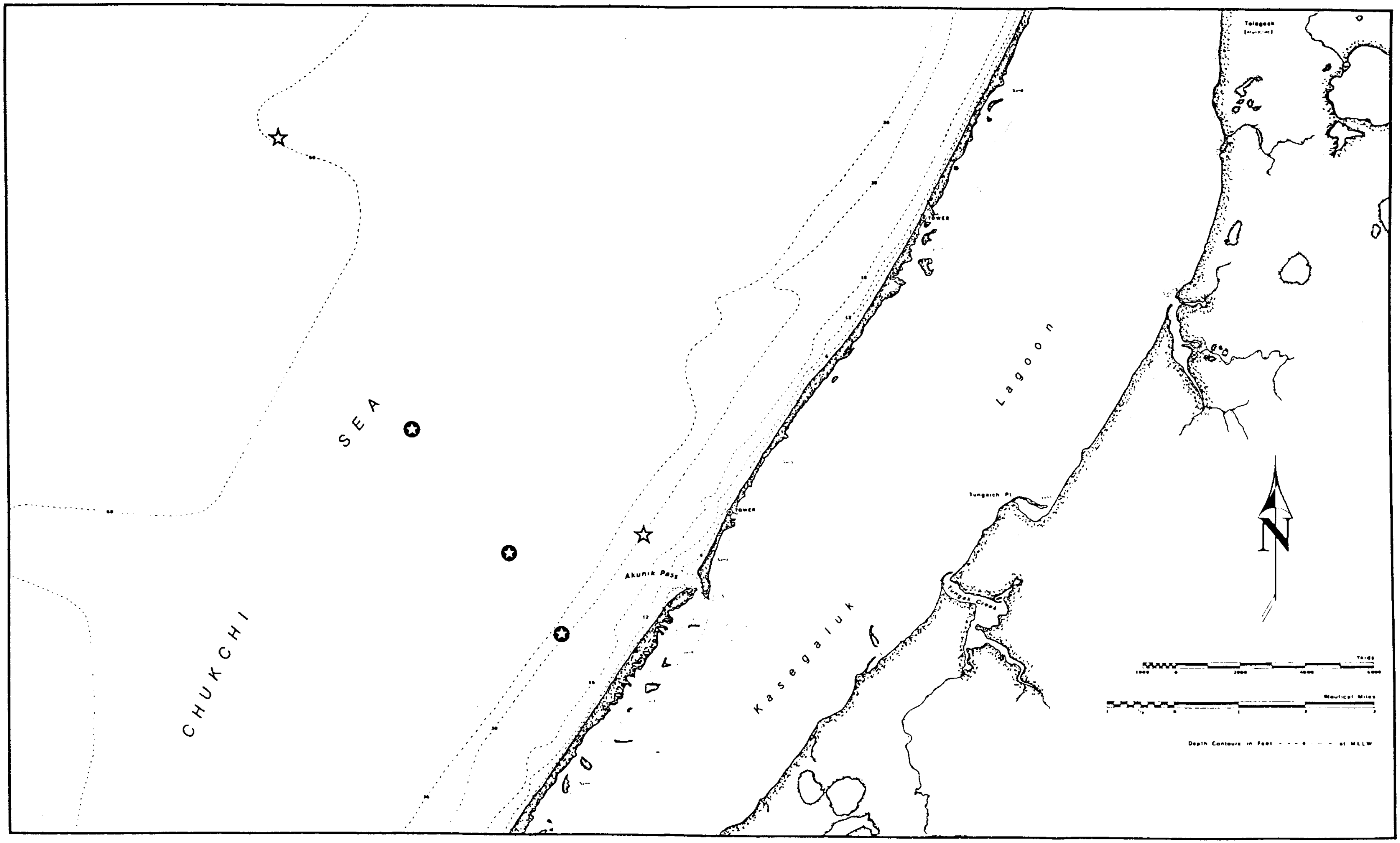

- CTD Cast

- Current Meter & CTD Cast

Figure 6. Locations of Current Meter Stations and C/STD Casts off Akunik Pass.

longitude, and then to localized cartesian coordinates. Variances of σX^2 and σY^2 and covariance σXY were then computed. The lengths and orientations of major and minor axes of ellipses describing the characteristics of the dispersion were then calculated and plotted.

Correlation Methods for Time Series

The current meter records were averaged to one-hour increments, then usually digitally filtered using a 35-hour low-pass (Doodson) filter. After filtering, the principal axis of the remaining drift currents were determined for use in correlation and spectral analyses.

These principal component series from the drift current records were compared with two other time series using methodology of Jenkins and Watts (1968). These other time series were the components of the local wind along the appropriate axis, and the difference in barometric pressure between Point Barrow and Cape Lisburne, both for the intervals of 6 and 18 hours.

First, lagged correlations were calculated for paired series. The extent to which the lags were carried depended on the point at which the cross-correlation function seemed to damp out. This point was usually 250 to 350 hours out, or 40-60 lags for the 6 hour series, and 14-19 lags for the 18-hour series.

Spectral analysis was conducted using a Tukey lag window. Window sizes ranged from 20 to 60 weights for the 6-hour series and 10-18 weights for the 18-hour series. In general, stable results for coherence spectra were obtained only for the smaller window sizes, which did not give a great amount of detail in most of the spectra. Features in the spectra much narrower than the bandwidth of the window size are very likely spurious, resulting from the spectral smoothing calculations.

The features of interest in the wind and current time series data are low frequency events, usually of orders of days to weeks. Because the total record lengths are short (of the order of one month), complete resolution of low frequency features by spectral analysis techniques cannot be expected.

RESULTS

The current, hydrographic, meteorologic, and drogue dispersion data are presented in graphical forms, with additional presentations, including tabular forms contained in the Appendices. In addition, all data have been digitally recorded on nine-track tape in NOAA/OCSEAP format and have been submitted separately.

Current and Water Level Metering

Of the twelve current meters deployed, seven were recovered successfully with long term data records. Current meter stations are summarized in Table 1, which indicates the degree of difficulty experienced in retrieving the meter strings. Of the moorings, the inshore mooring north of Pt. Lay was not given back to us by Pt. Lay villagers who recovered it. The corresponding offshore mooring was lost to unkown causes. Of the records retrieved, three are of 22 day lengths from Wainwright and three are of 31 day lengths from Barrow. The Aanderaa meters at Barrow were installed on 7 August and retrieved on 2 September. The fourth meter from Wainwright (inshore, surface) malfunctioned, giving intermittent data for the time of installation. The fourth meter from Barrow (inshore, surface) was lost due to ice damage, and the water level meter recovered from Peard Bay malfunctioned during the study, eliminating water level data from the report.

Similar patterns of current speed and direction were recorded at all Barrow and Wainwright stations (Figures 7 and 8). Though unalike in detail, the three complete records at Barrow indicate four major current reversals, while the records at Wainwright show three major reversals. Common to both sites are the reversals occurring during the period of 25 - 27 August, during which time currents reversed directions from the northeast to the southwest. Somewhat less common are the double reversals occurring during 19 - 21 and on 22 August when currents switched from northeast to southwest to northeast. The double reversal is more evident in the Wainwright data than in the Barrow data, where it appears as a pause in the currents rather than as a complete reversal. The fourth reversal in the Barrow data occurred at the beginning of the records before the placement of the Wainwright meters.

Overall current velocities were more consistent at the Wainwright station than at the Barrow station. Maximum velocities for the study were noted at the offshore surface station at Barrow where peak current velocities of two knots were recorded on the 8, 19, 20, 25, 26, 28 and 29 of August and during the 3 and 5 of September. The records at the other Barrow

Table 1 . Equipment Deployment and Retrieval Log, Chukchi Sea, 1981

Date		Instrument*	Location		Meter Depth (feet)	Bottom Depth (feet)	Comments
Deployed	Retrieved		Latitude	Longitude			
7 Aug 81	7 Sep 81	Aanderaa CM	71°19'31"N	156°45'19"W	57 (17m)	63 (19m)	[Barrow onshore] Station located by by pinger after moved (by ice?) 2,000 meters.
7 Aug 81	Missing	Aanderaa CM	71°19'31"N	156°45'19"W	37 (11m)	63 (19m)	Top meter barrel missing and damage to mooring. Possibly broken free by iceberg.
7 Aug 81	8 Sep 81	Aanderaa CM	71°23'27"N	156°50'52"W	220 (67m)	270 (82m)	[Barrow offshore] Difficult recovery, rough seas and currents.
7 Aug 81	8 Sep 81	Aanderaa CM	71°23'27"N	156°50'52"W	70 (21m)	270 (82m)	Difficult recovery, rough seas and currents.
9 Aug 81	3 Sep 81	Aanderaa tide gauge	70°48'39"N	158°22'12"W	6 (1.8m)	6 (1.8m)	[Peard Bay] Easily found by Zodiac crew.
11 Aug 81	2 Sep 81	G.O. CM (film)	70°37'36"N	160°08'12"W	43 (13m)	50 (15m)	[Wainwright onshore] Easily recovered.
11 Aug 81	2 Sep 81	G.O. CM (film)	70°37'36"N	160°08'12"W	17 (5.2m)	50 (15m)	Easily recovered.

* Abbreviations: CM = current meter; G.O. = General Oceanics.

Table 1. (continued)

Date		Instrument	Location		Meter Depth (feet)	Bottom Depth (feet)	Comments
Deployed	Retrieved		Latitude	Longitude			
11 Aug 81	2 Sep 81	G.O. CM (film)	70°42'46"N	160°22'48"W	97 (24.9m)	120 (36m)	[Wainwright offshore] Snagged meter string w/dragline between Hood & Zodiac drifting in 2 knot current & 2-3 ft. seas. Grapnel hook didn't work on cobble bottom.
11 Aug 81	2 Sep 81	G.O. CM (film)	70°42'46"N	160°22'48"W	32 (9.7m)	120 (36m)	
14 Aug 81	Lost	Aanderaa CM	69°54'33"N	162°52'30"W	27 (8.2m)	30 (9m)	[Akunik Pass onshore] Station missing or floats damaged. No clear pinger signal.
14 Aug 81	Lost	Aanderaa CM	69°54'33"N	162°52'30"W	8 (2.4m)	30 (9m)	Station missing or floats damaged. No clear pinger signal.
14 Aug 81	Lost	Aanderaa CM	70°00'30"N	163°07'42"W	37 (11.2m)	63 (19m)	[Akunik Pass offshore] Mini-Ranger batteries discharged. No pinger signal in area reached by dead reckoning. No pinger signal rec'd by R.V. _Oceanographer_ in correct area. Station assumed missing or pinger and float malfunctioning.
14 Aug 81	Lost	Marsh-McBirney CM	70°00'30"N	163°07'42"W	16 (4.8m)	63 (19m)	

* Abbreviations: CM = current meter; G.O. = General Oceanics.

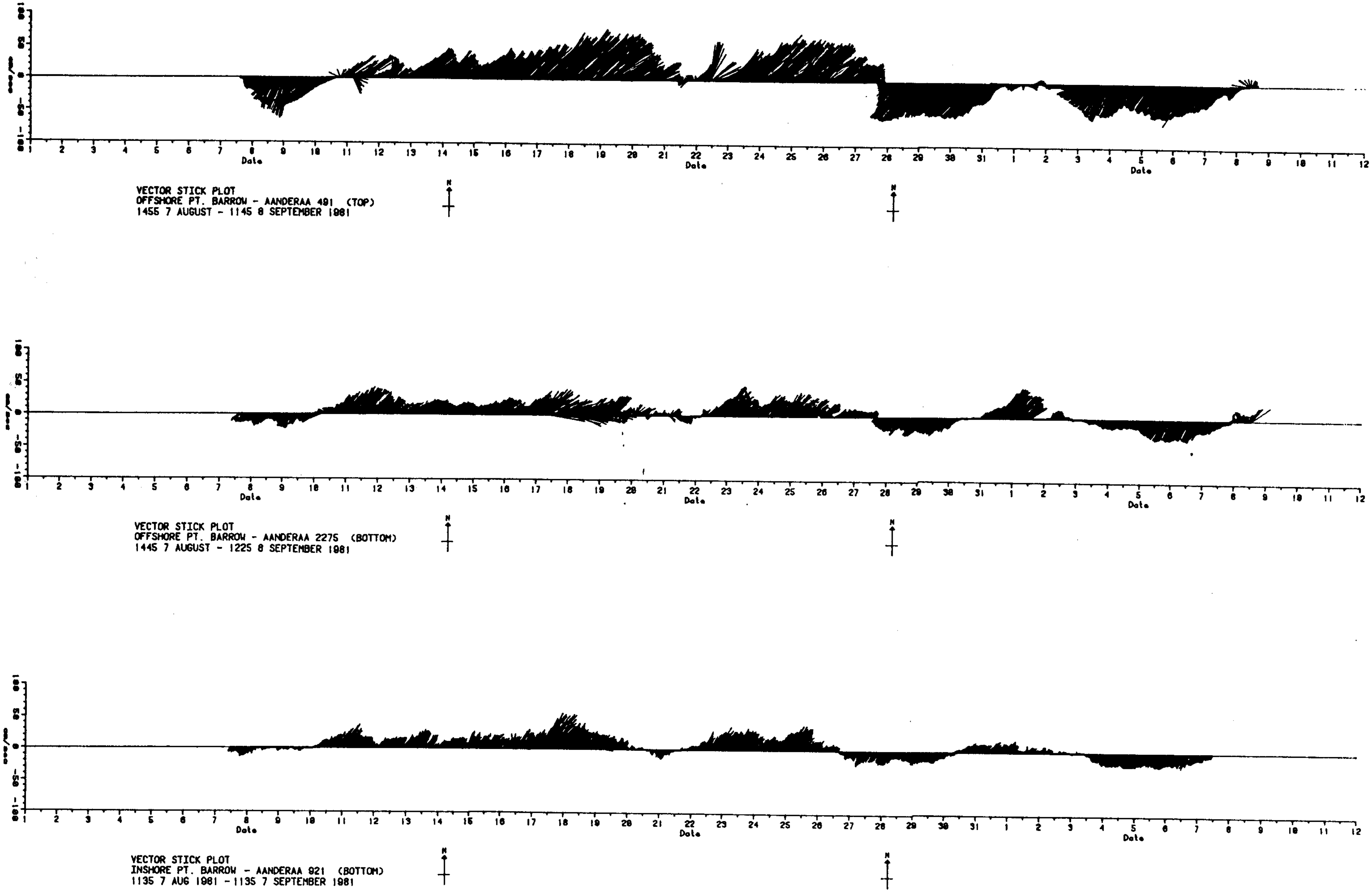

Figure 7. Current Direction and Velocity as a Function of Time at Point Barrow, 7 August to 7 September 1981.

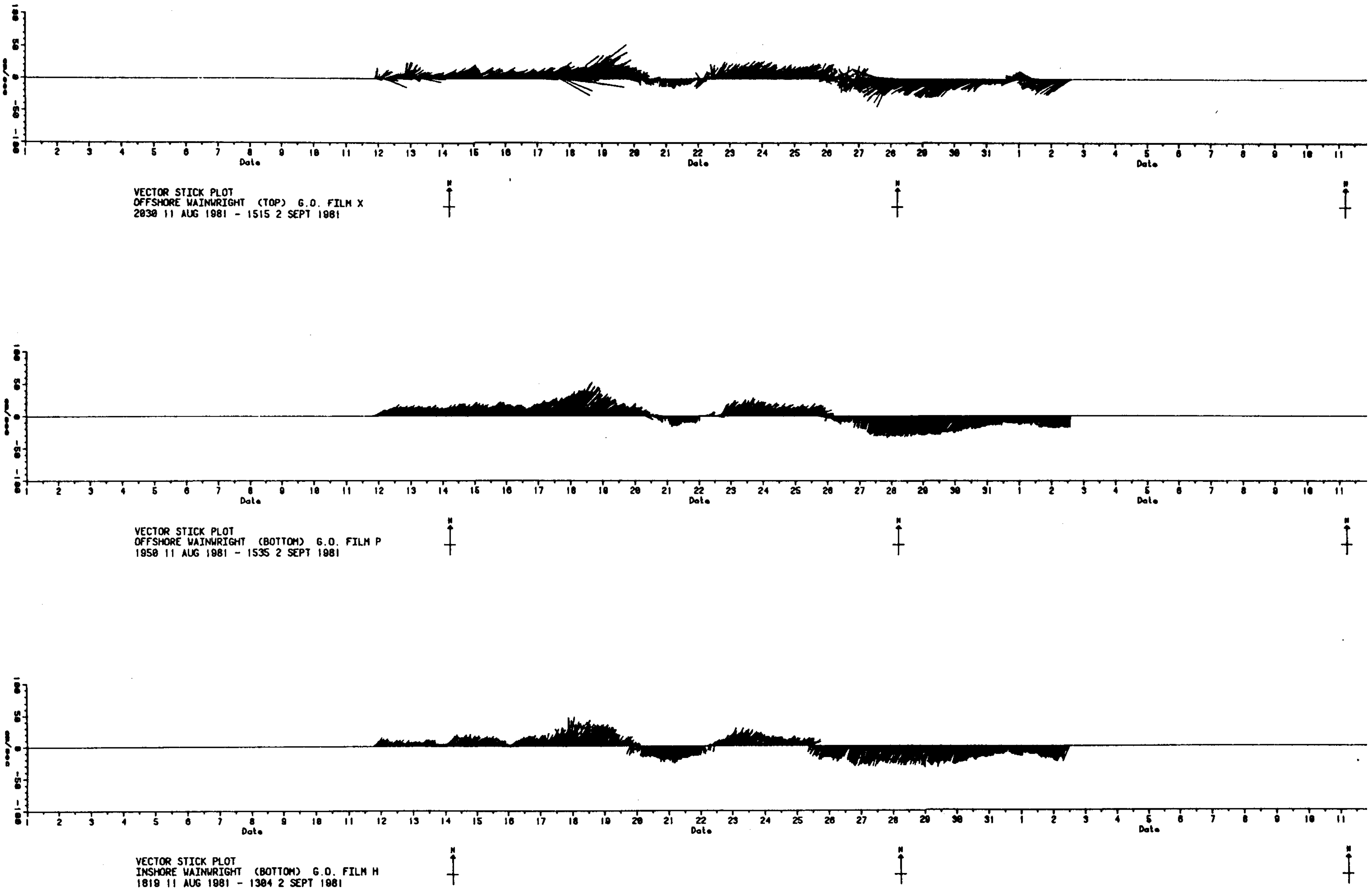

Figure 8. Current Direction and Velocity as a Function of Time at Wainwright, 11 August to 2 September 1981.

station show a similar pattern of current direction, but emphasize a difference in local current velocities. The initial peak in velocity of 8 August is not evident at either bottom station of offshore or inshore Barrow, while the reversal evident in the records of Barrow during 31 August and 1 and 2 September registers as a cessation of current velocity at Wainwright (Figure 8).

Continuous temperature and salinity records taken at the Barrow current meter stations illustrate differences in water properties at each of the stations. The offshore records at Barrow are most similar to one another. The dominant peak in the temperature record occurs through 17 to 26/27 August, when temperatures change by three degrees (Figure 9). Additional temperature changes of four degrees occurred during the periods of 10 August through 16 August and during 31 August to 5 September only at the offshore surface station at Barrow. The temperature and salinity changes at the inshore bottom station at Barrow are more cyclic and of shorter duration. Major peaks in temperatures occur during 12 - 16 August, 20 - 22 August, and 24 - 28 August at the inshore Barrow station, demonstrating differences in hydrographic properties between nearshore and offshore sites at Barrow.

Meteorological Data

Meteorological data were obtained through a variety of sources. Barometric pressure values were recorded from weather maps provided by NOAA weather service. Pressure differences were calculated from values at Barrow, Cape Lisburne and Nome on a 24-hour basis (Figure 10). Positive differences represent higher pressures present at Barrow than at Lisburne or at Barrow than at Nome. Conversely, negative values represent lower atmospheric pressures present at Barrow than at Lisburne or at Barrow than at Nome. Wind data was obtained from the NOAA National Weather Service for Barrow and from the DEW-line station at Wainwright. The frequency of the recorded observations varied with the source of information. Barrow wind data was recorded hourly, while Wainwright wind data was recorded once every three hours (Figure 10).

Though the frequencies of recorded wind observations are different at Barrow and Wainwright, changes in wind direction generally coincide in both areas. Dominant reversals in direction occur during 5, 16, 19, 21 and 23/24 August (Figure 10).

Winds blew predominantly from the north-northeast or from the south-southwest along the coast, coinciding with changes in atmospheric pressure between Barrow and Cape Lisburne and between Barrow and Nome.

The plots of atmospheric pressure differences at Barrow and Lisburne, and Barrow and Nome follow similar gross changes

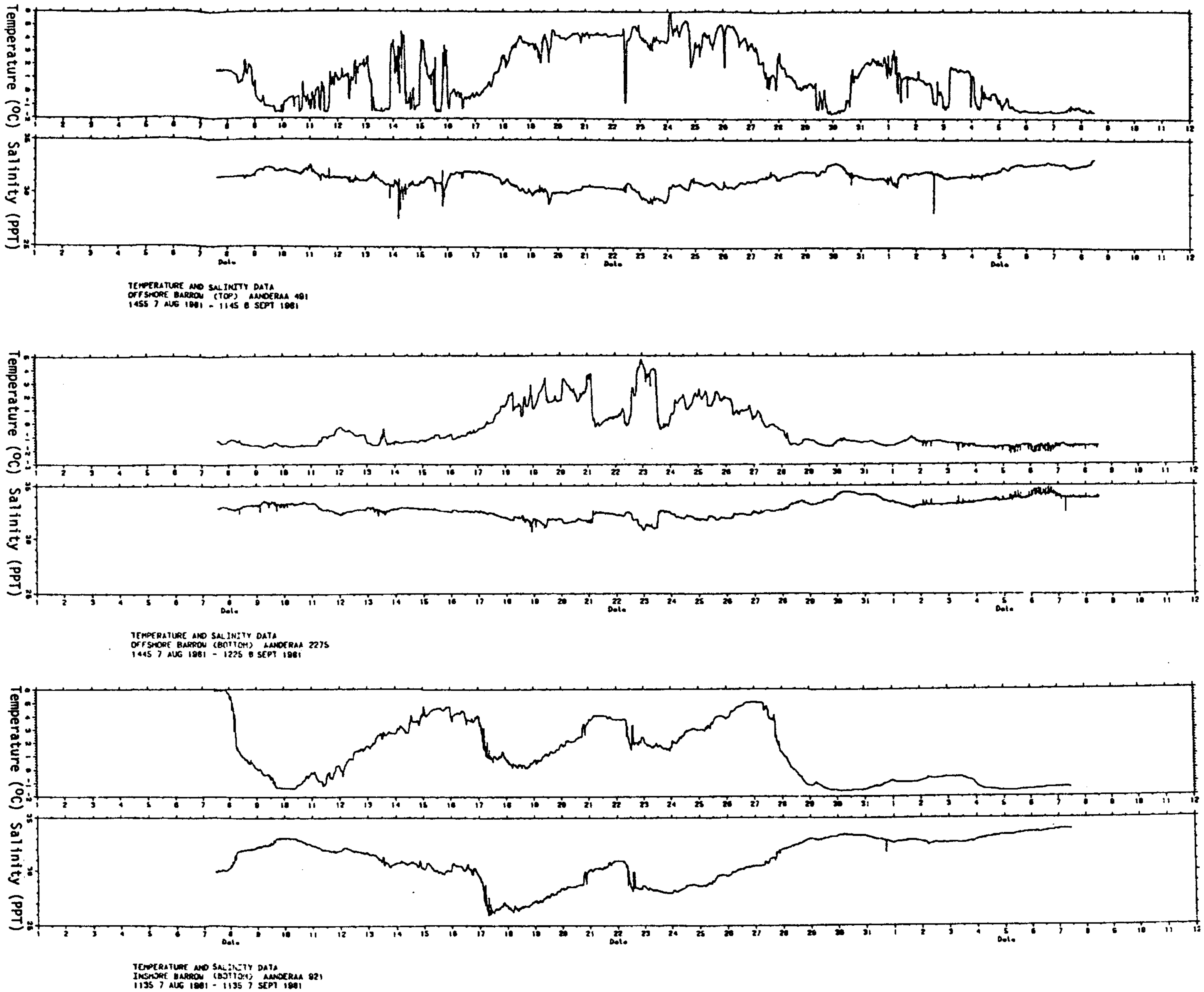

Figure 9. Temperature and Salinity Data Recorded with Aanderaa RMC-4 Current Meters at Point Barrow Stations, 7 August to 8 September 1981.

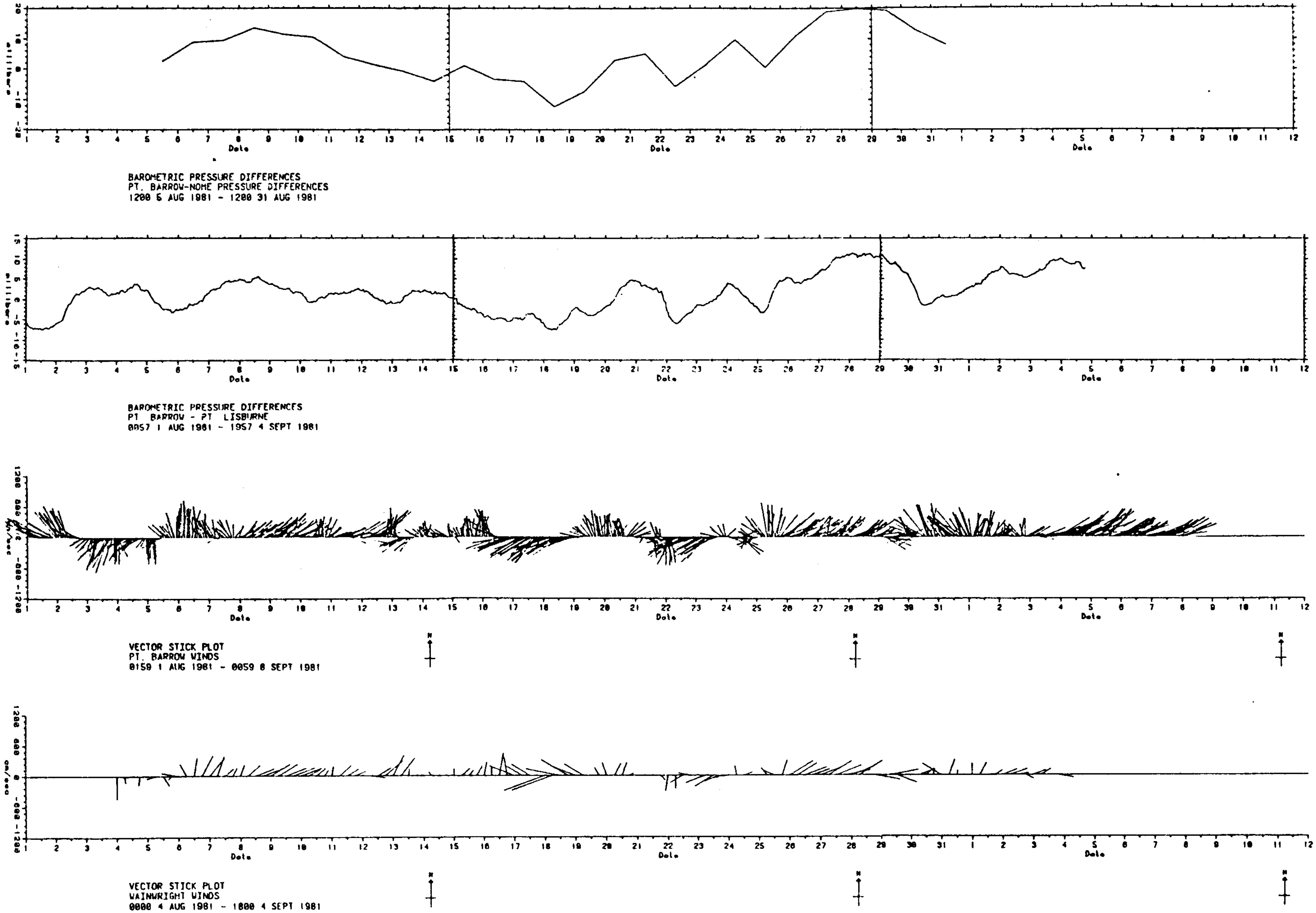

Figure 10. Meteorological Parameters of Atmospheric Pressure Differences (Barrow-Cape Lisburne and Barrow-Nome) and Local Winds (Barrow and Wainwright), 1 August to

through August 1981 (Figure 10). Noticeable divergence in the trend occurs during 6 - 10 August, when greater differences were recorded between Barrow and Nome than between Barrow and Lisburne. The divergence occurs when westward moving high pressure areas create large differences between Nome and Lisburne leaving a series of isobars between the two areas (Figure 11).

Hydrographic Transects

Transects perpendicular to shore were made for hydrographic measurements at seven locations between Pt. Barrow and Akunik Pass as opportunities arose during the cruise and are tabulated in Table 2. These data are presented graphically in Figures 12 through 18 as two-dimensional sections of the water column. Hydrographic profiles of individual stations are graphed in Appendix C along with the tabulated data.

The majority of the profiles taken during the second week in August show colder, more saline, and denser waters intruding from the depths of the offshore regions into the shallows of the nearshore coastal areas (Figures 12 through 18). Though not as evident at the Barrow site near the submarine canyon, the other sites with less bottom relief show varying degrees of upwelling conditions. Acute sigma-t differences are illustrated for Skull Cliffs, Point Belcher and Wainwright, where several isopleths occupy the nearshore areas in increasing values from the offshore direction (Figures 14 and 15). Similar patterns of a gentler degree are evident in the distributions of water densities at Pingorarok Pass, Icy Cape and Akunik Pass transects, where the distributions of sigma-t isopleths are spread over a greater nearshore area than in the three previous cases (Figures 16 - 18).

Patterns in water transparency also are similar between stations. Generally, clearer conditions are associated with offshore surface waters as turbidity is associated with deeper upwelled shelf waters (Figures 12 through 18).

Drogue Dispersion Data

The drogues tended to move parallel to the bathymetry, drifting in concordance with wind speed and direction (Figures 19 and 20 and Table 3). Plots of the trajectories of the centroids of the group of twelve drogues are shown in Figure 19 along with the mean spreading about these centroids. A similar plot of trajectories corrected for wind drag of the surface above the waterline is given in Figure 20. Statistics associated with the spreading of this patch of twelve drogues are tabulated in Table 3.

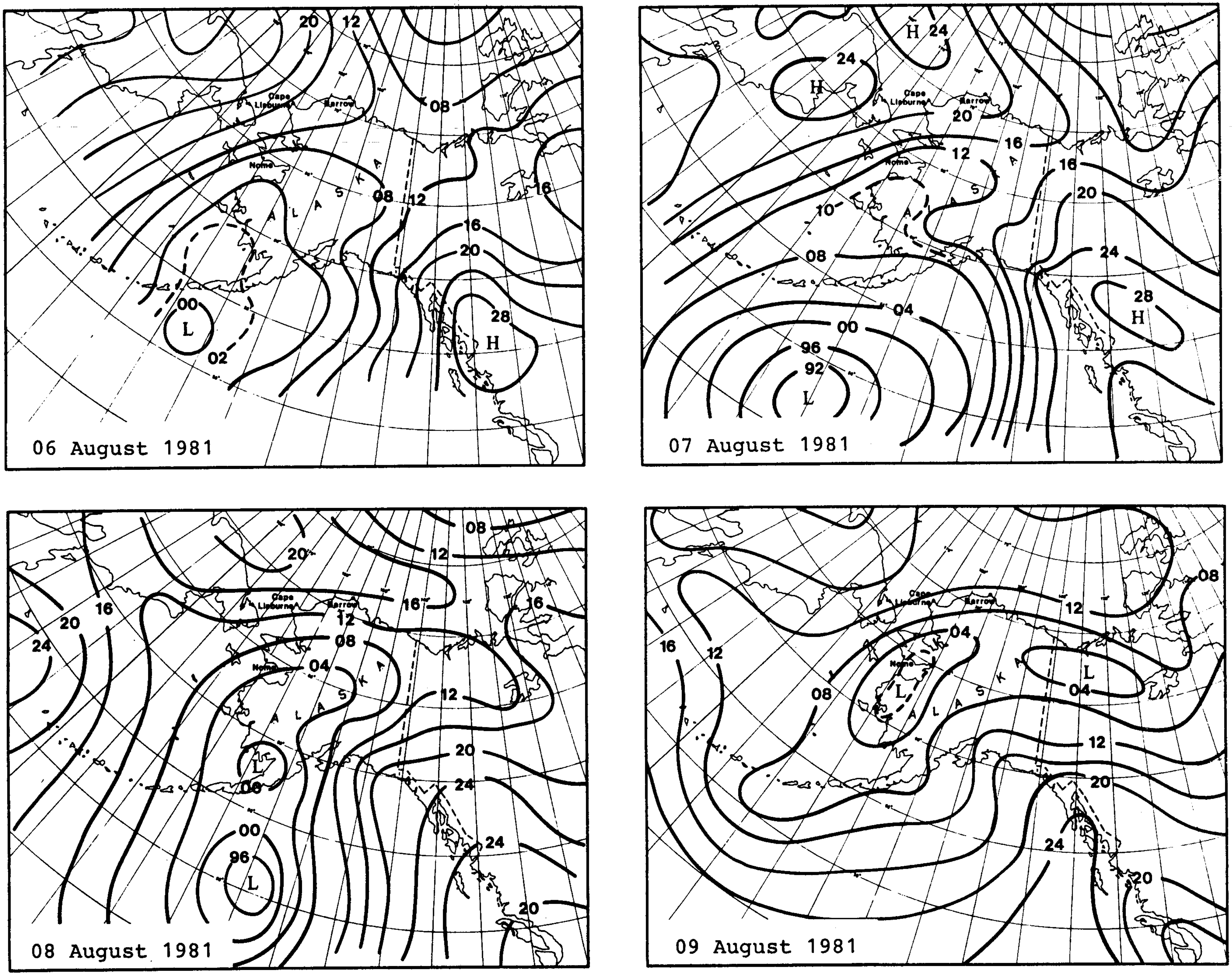

Figure 11. Weather Maps for Chukchi Sea Coast for 6 to 10 August 1981.

Table 2. C/STD TRANSECT LOG

Date	Area	Cast Depths (feet)	Station Distances from Land in Nautical Miles	Weather Observations
7 Aug 81	Barrow	57	1	
		90	2	Wind: 4-6 knots, 300° mag.
		90	3	
		90	4	Air temperature: 37°F
		90	5	
8 Aug 81	Skull Cliffs	35	1	
		54	2	Wind: 10 knots, 020° mag.
		60	3	
		65	4	Air temperature: 44°F
		67	5	
		75	7	
		90	9	
10 Aug 81	Pt. Belcher	65	1	
		90	2	Wind: 5-6 knots, 020° mag.
		90	3	
		90	5	Air temperature: 49°F
		90	7	
		90	9	
13 Aug 81	Pingorarok Pass	24	1	
		37	2	Wind: 0-2 knots, 0° mag.
		47	3	
		55	5	Air temperature: 47°F
		67	7	
		75	9	
14 Aug 81	Akunik Pass	24	1	
		45	3	Wind: 16-20 knots, 300° mag.
		52	5	
		60	7	Air temperature: 44°F
		60	9	
14 Aug 81	Icy Cape	36	1	
		44	2	Wind: 10 knots, 010° mag.
		47	4	
		54	6	Air temperature: 46°F
		70	8	
		87	10	
2 Sep 81	Wainwright	45	1	
		60	2.5	Wind: 10-12 knots, 020° mag.
		70	3.5	
		75	4.5	Air temperature: 45°F
		90	6.5	
		90	8.5	

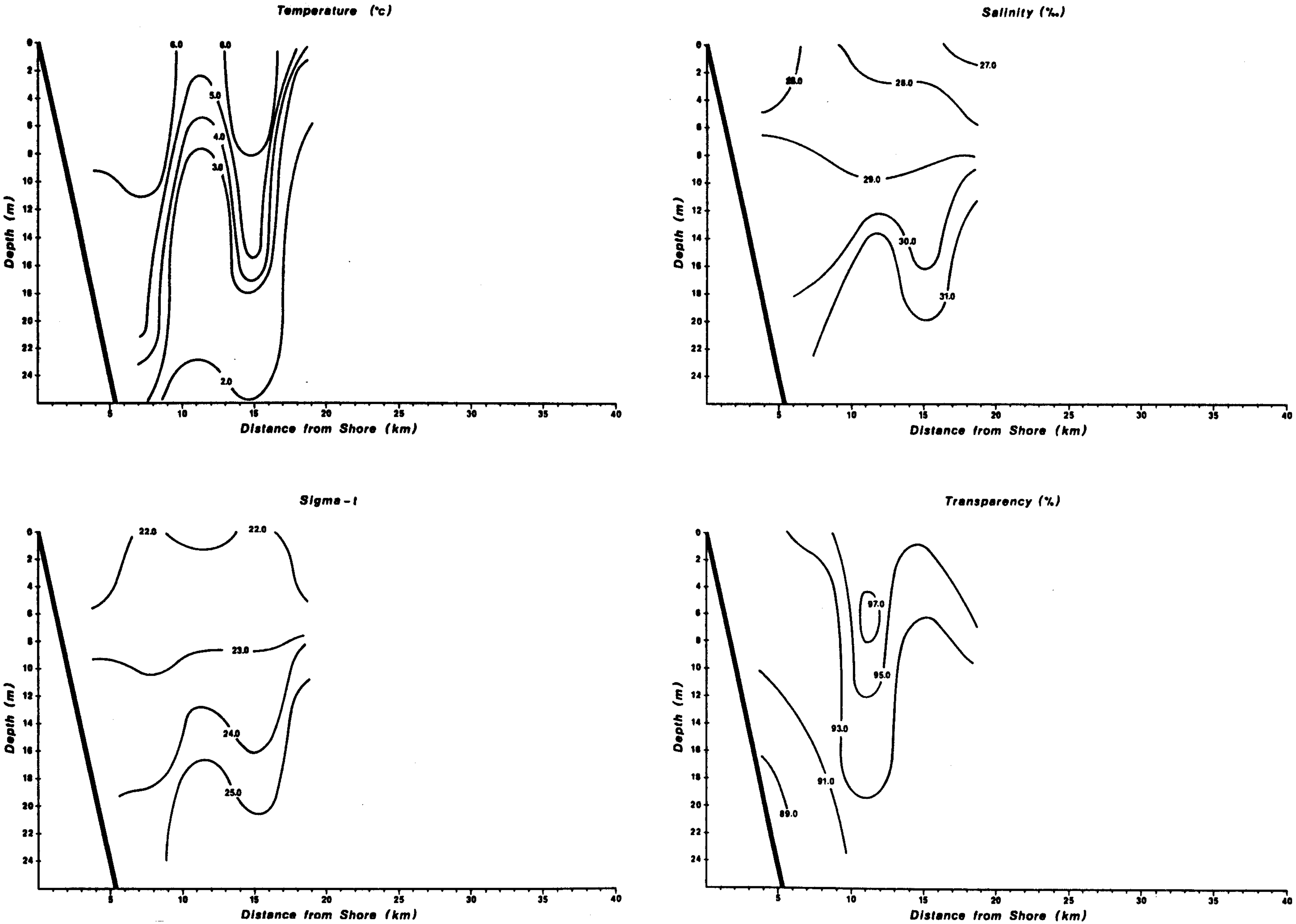

Figure 12. C/STD Transects Taken at Point Barrow on 7 August 1981.

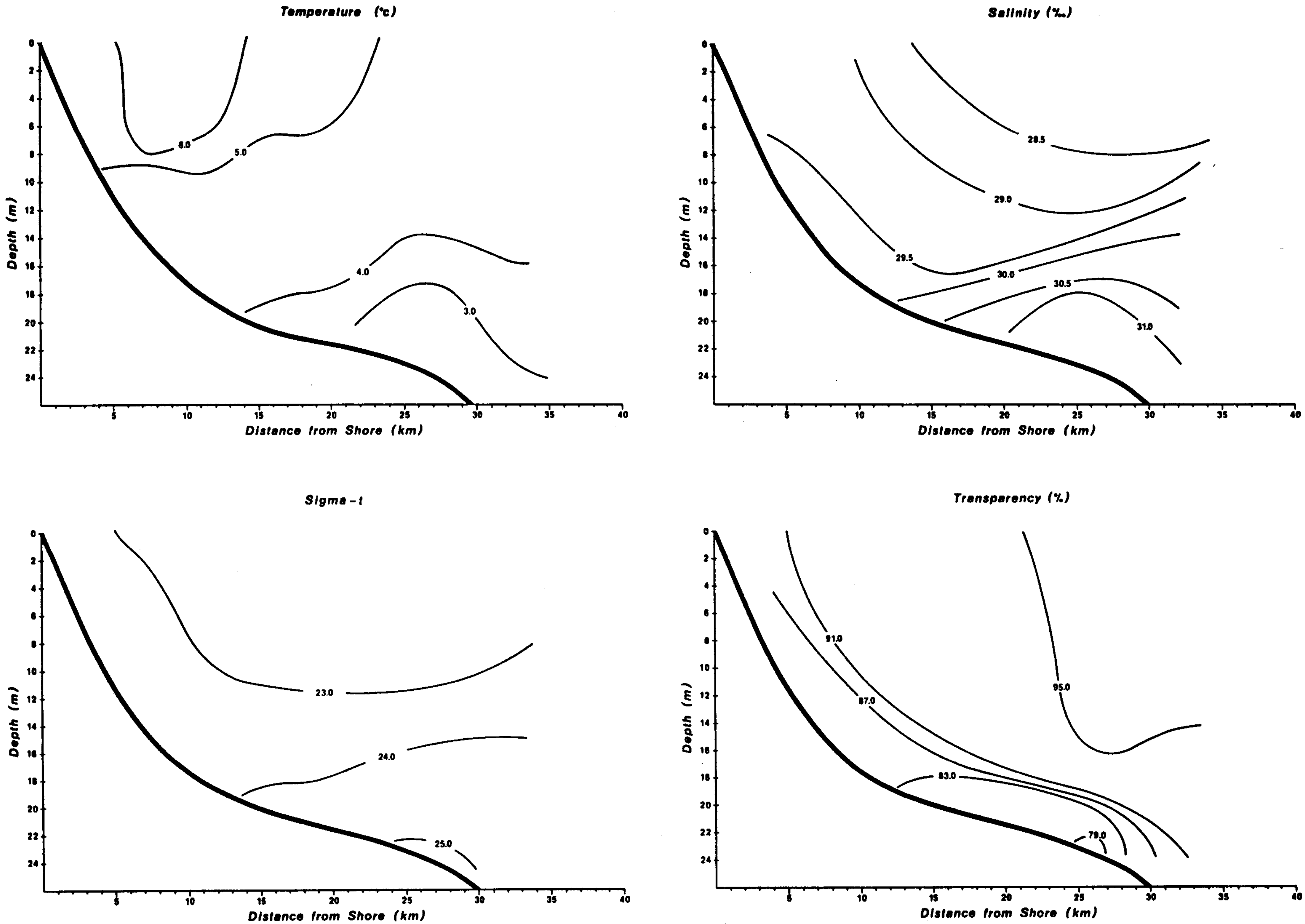

Figure 13. C/STD Transects Taken at Skull Cliffs on 8 August 1981.

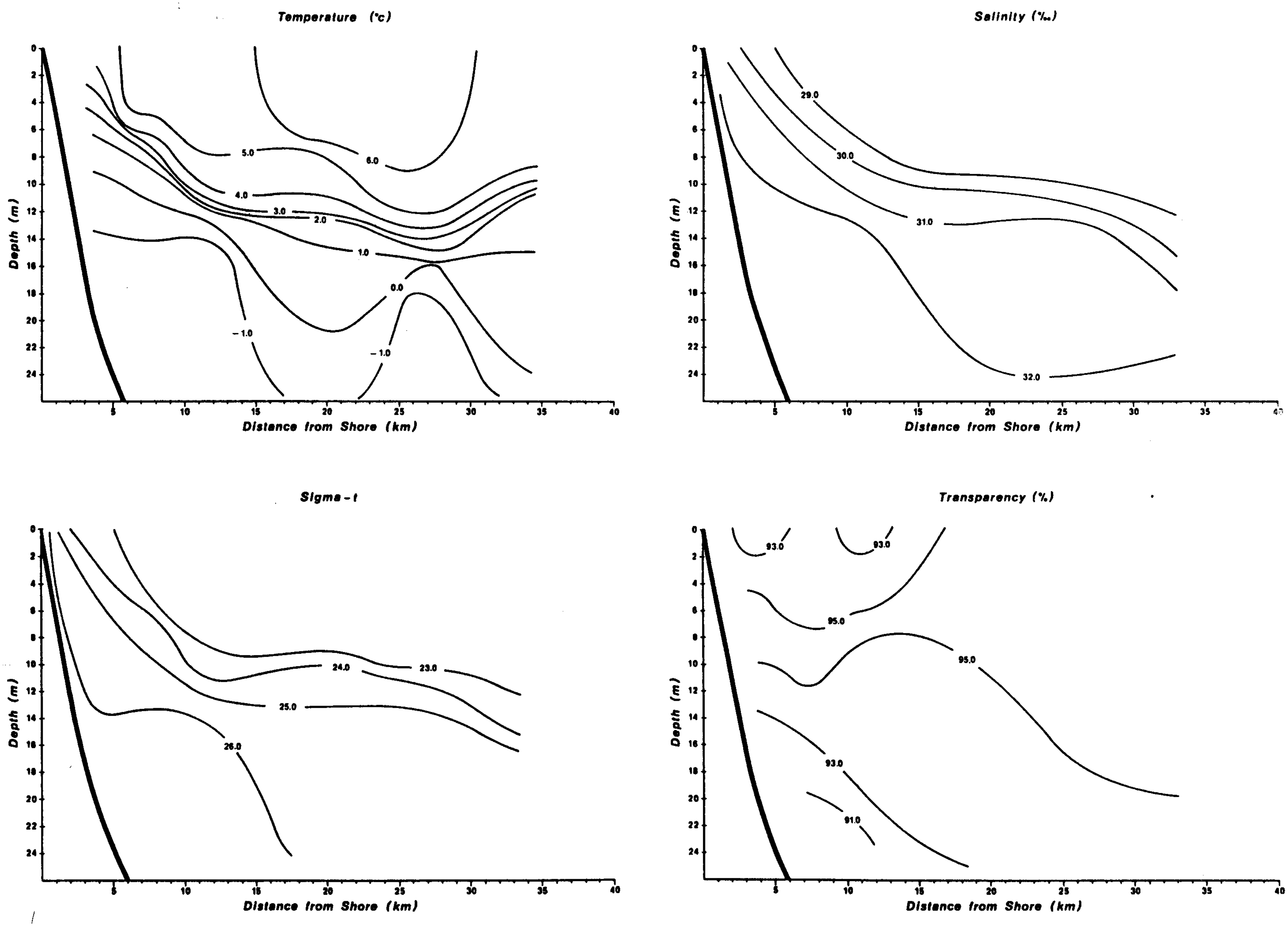

Figure 14. C/STD Transects Taken at Point Belcher on 10 August 1981.

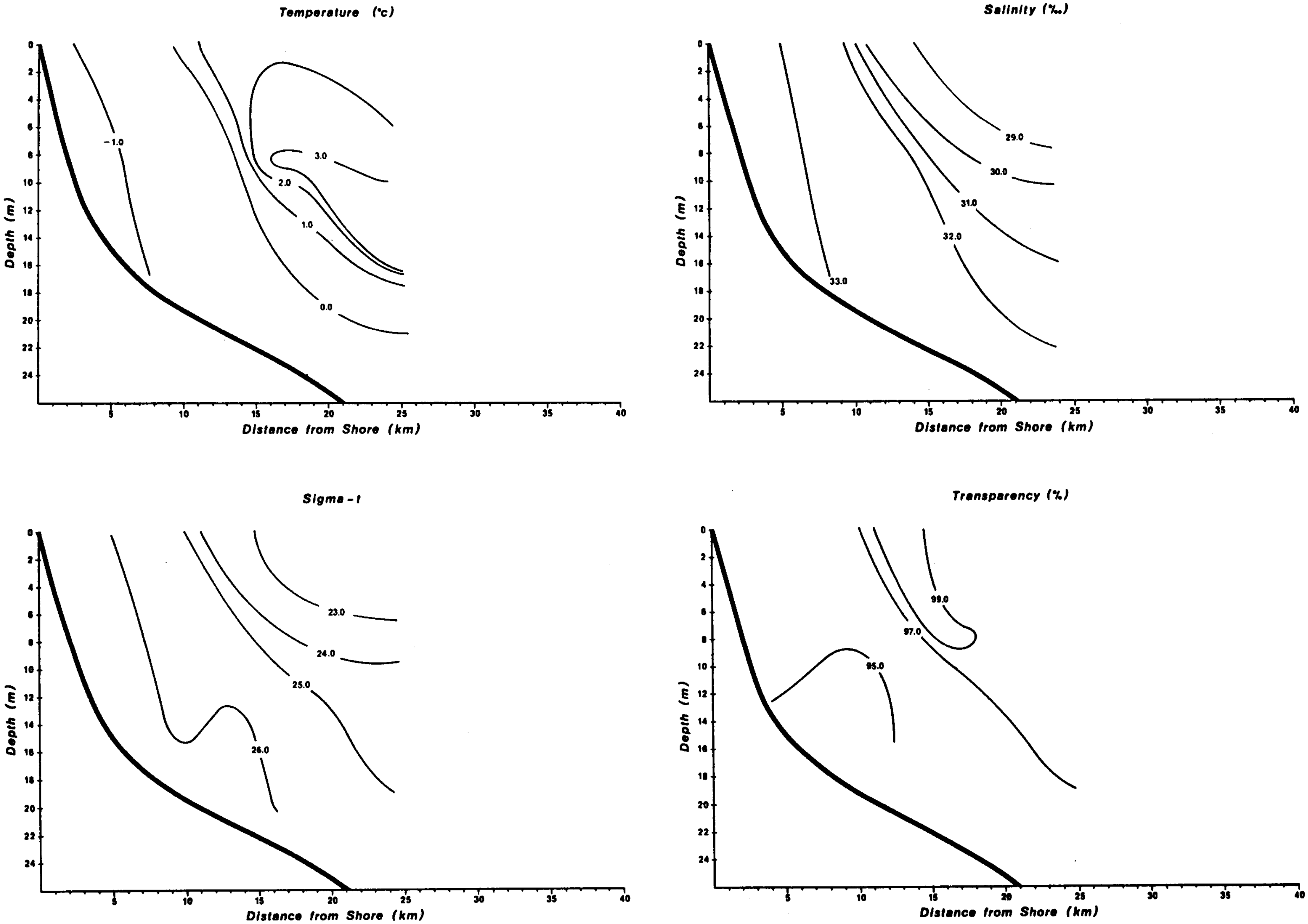

Figure 15. C/STD Transects Taken at Pingorarok Pass on 13 August 1981.

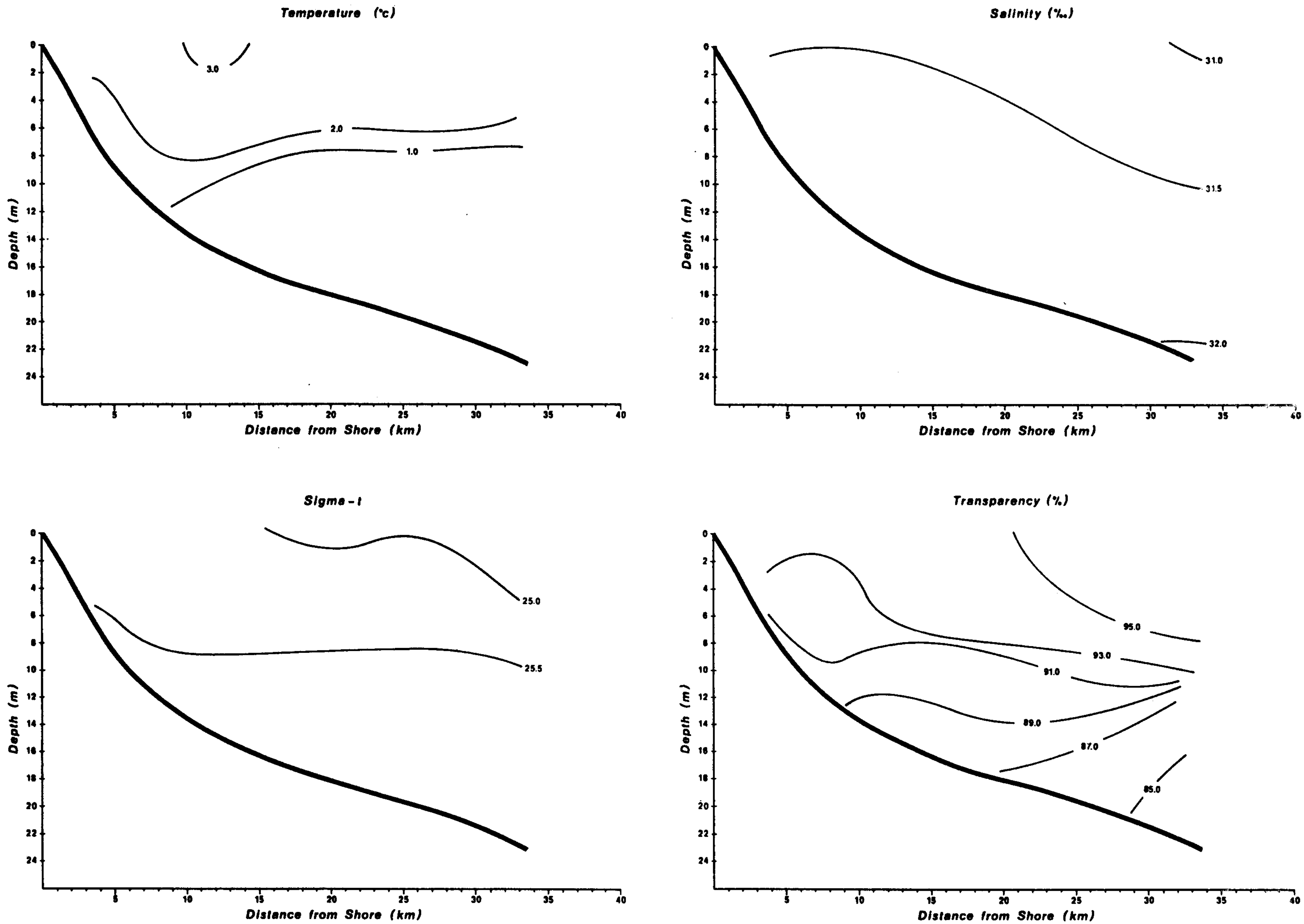

Figure 16. C/STD Transects Taken at Akunik Pass on 14 August 1981.

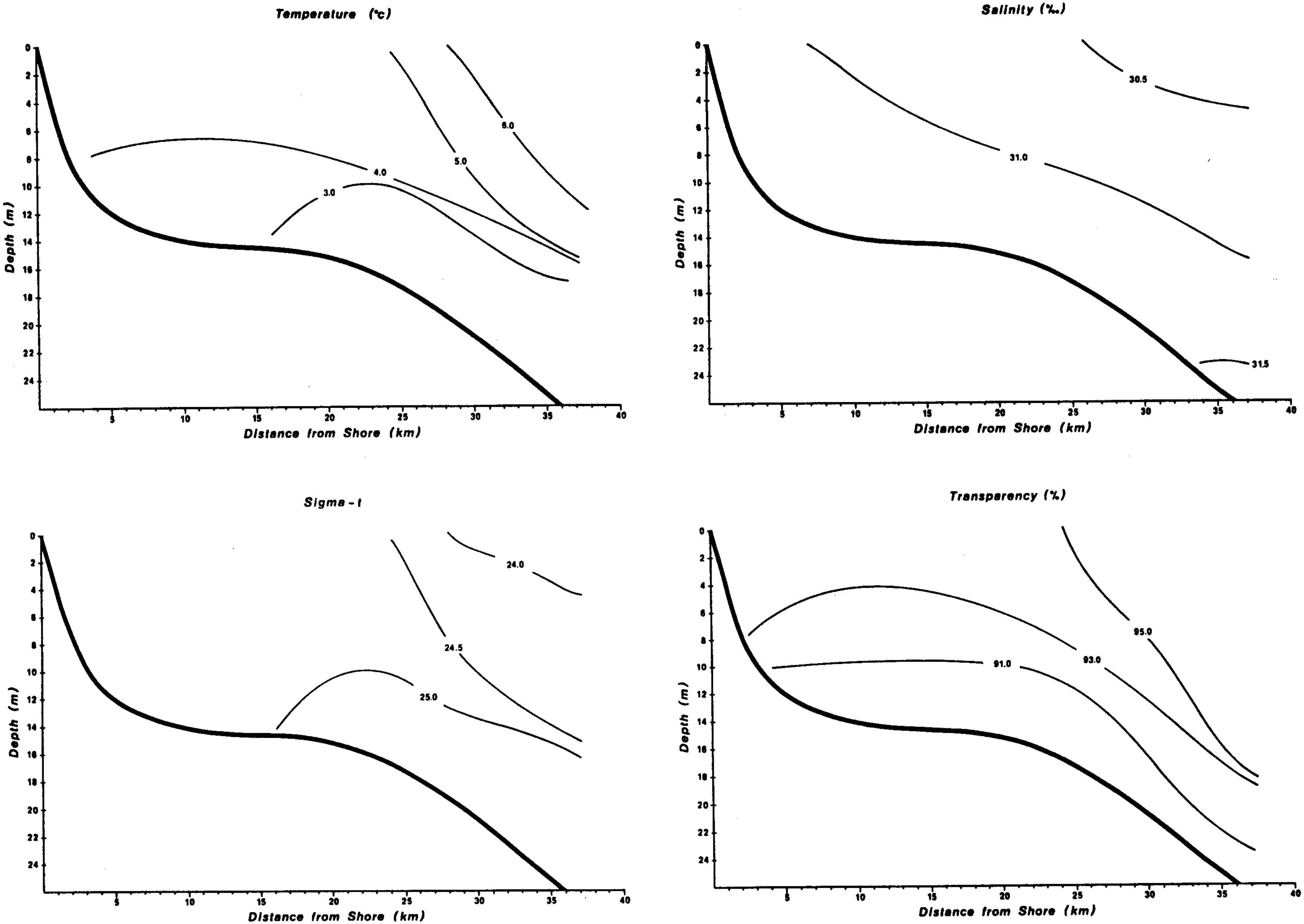

Figure 17. C/STD Transects Taken at Icy Cape on 14 August 1981.

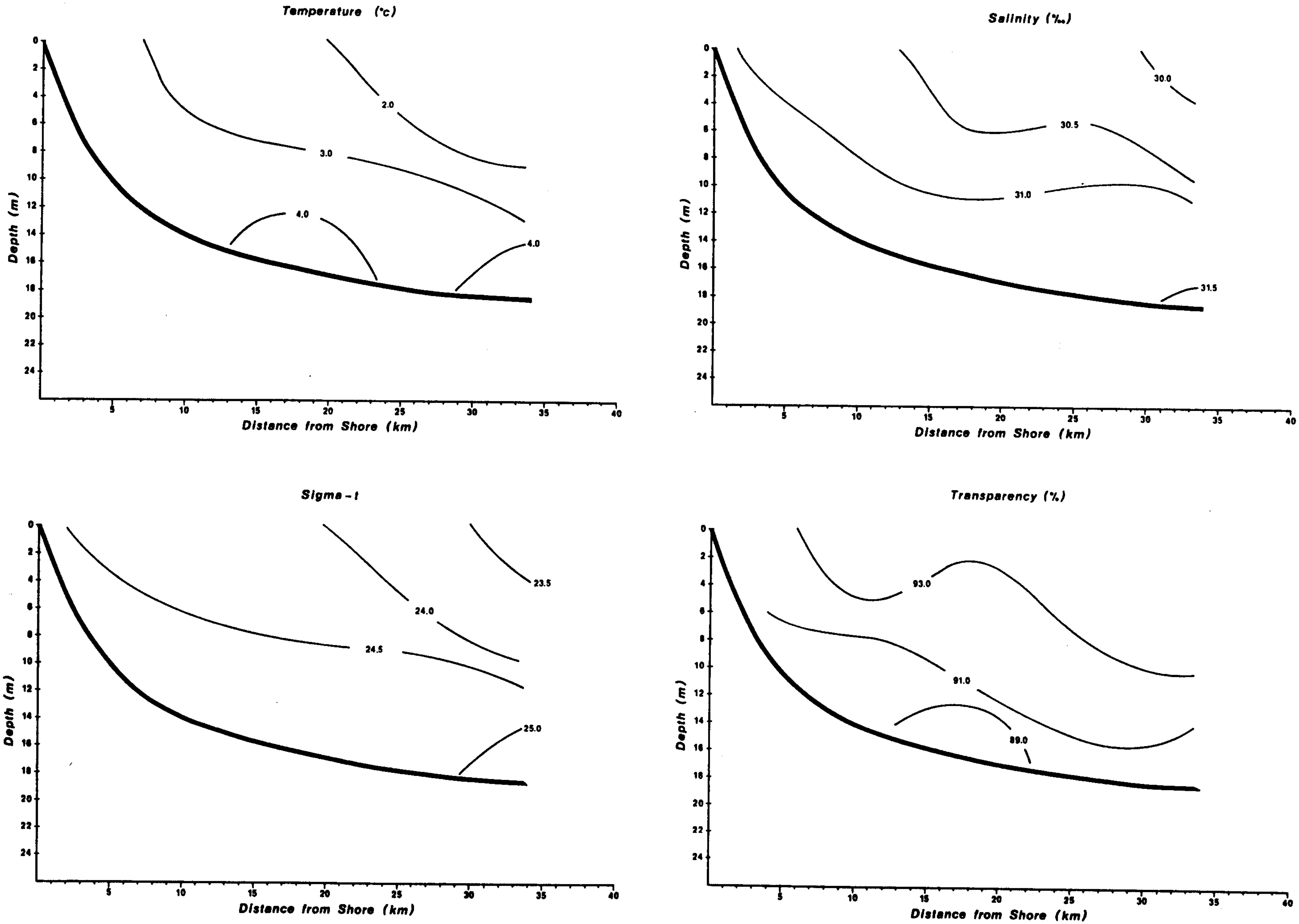

Figure 18. C/STD Transects Taken at Wainwright on 2 September 1981.

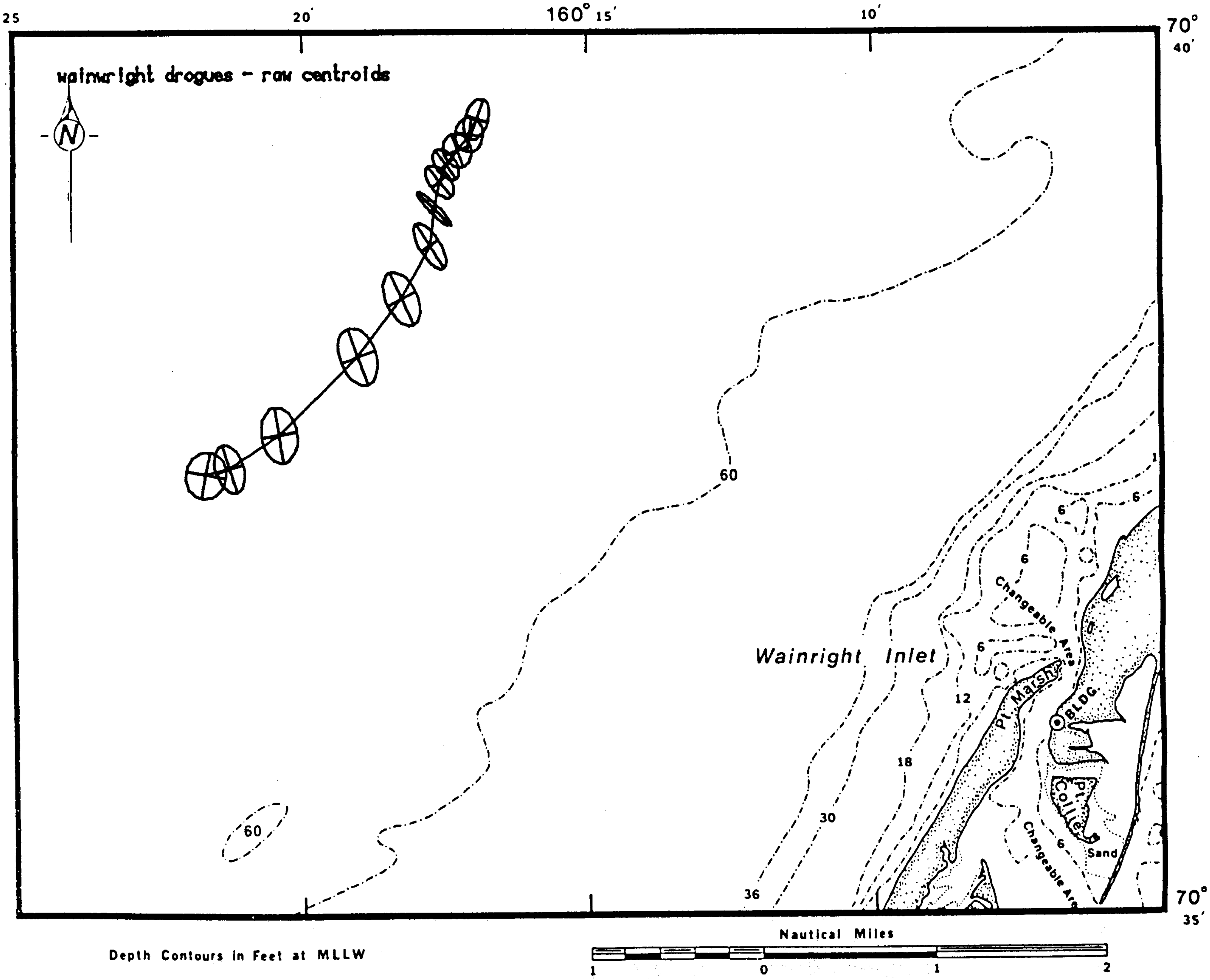

Figure 19. Trajectories of Centroids and Mean Spreading of Twelve Current Drogues, 1200 - 2400 Hours, 20 August 1981.

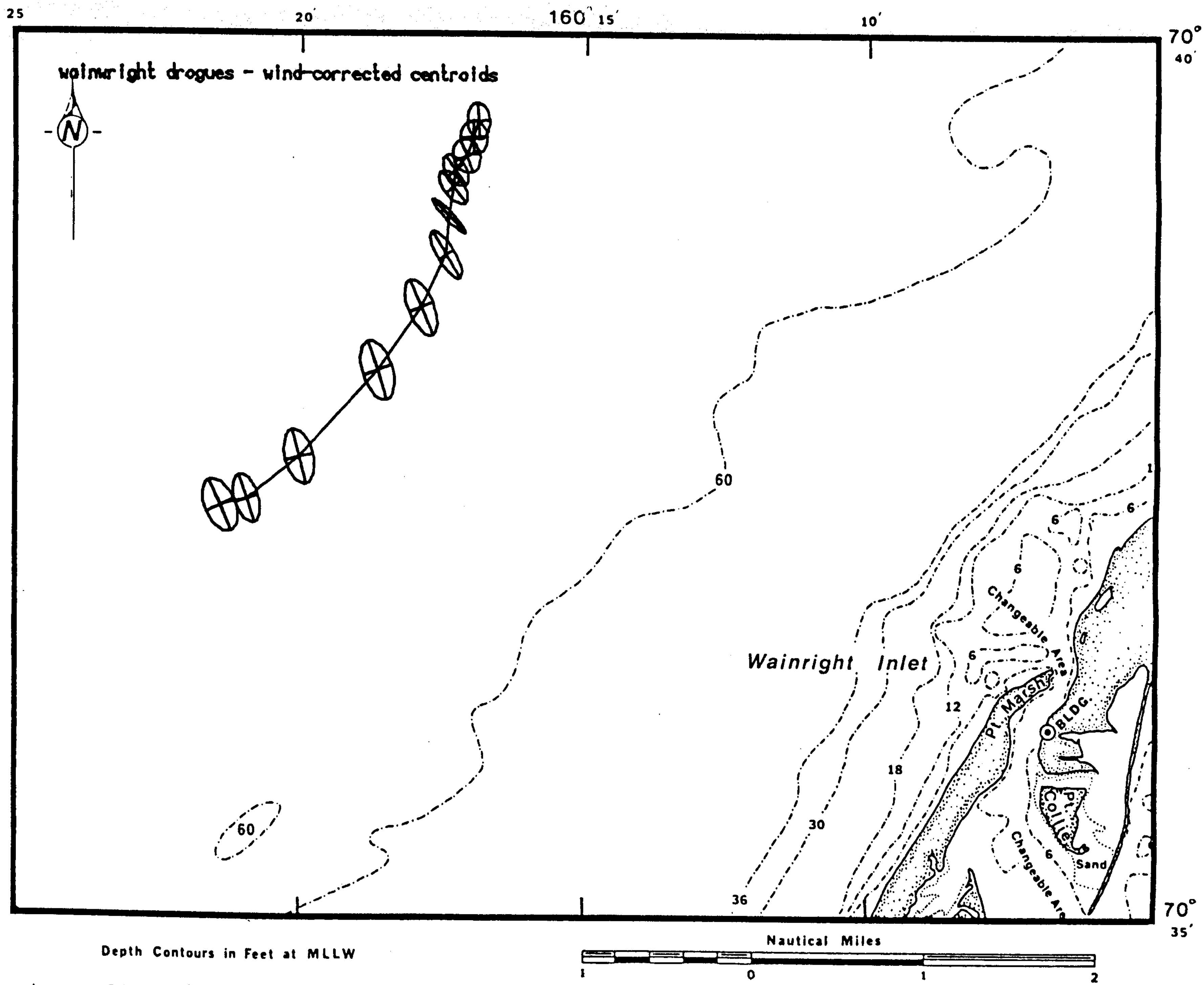

Figure 20. Wind Corrected Trajectories and Mean Spreading of Twelve Current Drogues, 1200 - 2400 Hours, 20 August 1981.

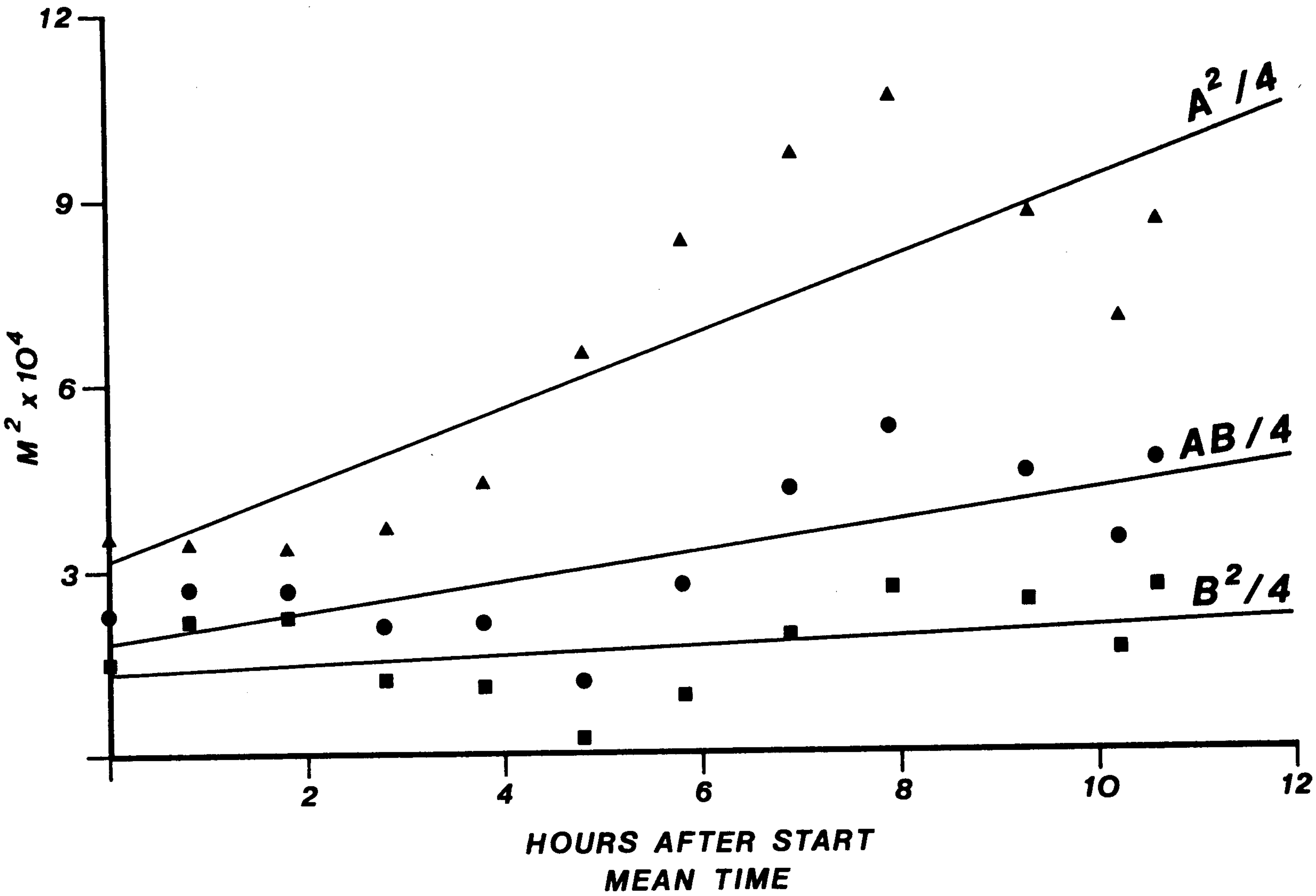

Figure 21. Variances Calculated From The Spreading of Twelve Drogues

Table 3. Dispersion Statistics for Wind-Corrected Drogue Data, Chukchi Sea, 1981.

Time (hours)	Major Axis a (meters)	Minor Axis b (meters)	$a^2/4$ (m^2)	$b^2/4$ (m^2)	$ab/4$ (m^2)	Wind Speed (m/s)	Wind Direction °T
0.0	376	245	35344	15006	23030	-	-
0.8	369	294	34040	21609	27122	2.6	95
1.8	365	295	33306	21756	26919	0.8	90
2.8	384	216	36864	11664	20736	0.0	-
3.8	420	206	44100	10609	21630	2.1	65
4.8	510	90	65025	2025	11475	1.0	110
5.8	577	189	83232	8930	27263	2.1	98
6.9	624	276	97344	19044	43056	-	-
7.9	653	323	106602	26082	52730	2.6	150
9.3	592	308	87616	23716	45584	-	-
10.2	531	258	70490	16641	34250	-	-
10.6	586	324	85849	26244	47466	4.6	185
		Correlation:	0.83	0.33	0.70		
		Slope:	0.43	0.05	0.17		

$a^2/4 = 31684 + 1.716t$ (t in seconds)

$b^2/4 = 13245 + 0.190t$

$ab/4 = 18606 + 0.677t$

Slopes: $^1/_2(^d/dt)(\sigma x^2) = 8580.6\ cm^2/sec$

$^1/_2(^d/dt)(\sigma y^2) = 948.5\ cm^2/sec$

$^1/_2(^d/dt)(\sigma x \sigma y) = 3386.8\ cm^2/sec$

DISCUSSION

For purposes of visual comparisons the current, wind, and atmospheric pressure difference records are displayed in time series plots to the same scales for the Point Barrow site and for the Wainwright site in Figures 22 and 23. Seven time intervals have been identified for special consideration, based upon the oceanographic and meteorologic events contained in these records. The respective depths of these moored meters, and those of Mountain et al. (1976) have been shown schematically in Figure 2.

Coastal Currents

Magnitudes and Directions. The coastal currents, as measured by the moored meters at Barrow, show both northeast and southwest flows, paralleling the local bathymethry, but at different time intervals. The offshore meter at 21m depth showed intervals of northeast currents approaching two knots, while those of the inshore meter at 17m depth showed simultaneous currents also to the northeast, of a reduced magnitude of less than one knot maximums. Meters at Wainwright yielded similar records, also with maximums of less than one knot.

Principal axis analyses and progressive vector diagrams were done in order to determine the directions of the predominant drift currents. The results are summarized in Table 4. Examples of these analyses are shown in Figures 24 and 25 for the Pt. Barrow offshore (top) meter, with the rest contained in Appendix A. Statistical (speed and direction) tables for the current data are also given in Appendix A.

The principal axis directions of the predominant drift currents are compared to the principal directions of the coastline or bathymetry in Table 4. As expected for inshore data, good agreement is indicated. Only the top meter of the offshore Wainwright mooring deviates from the coastline/bathymetry data. The reason for this one deviation, whether real or an artifact, is not clear at present.

Results of statistical analyses of the current records show that reversed flow (southwestern currents) occurred frequently in this August-September time period. Although upcoast flow was predominant, downcoast flow ranged from 33 to 47 percent of the time in the different current records. Table 5 summarizes these frequencies of upcoast and downcoast flow. In contrast, records taken at deeper depths of 96m and 126m in Barrow Canyon in 1976 (Mountain et al. 1976) showed less frequent flow reversals in April through June and practically none in July into August. These more frequent current reversals in our August-September records may reflect more frequent storm activity in the fall.

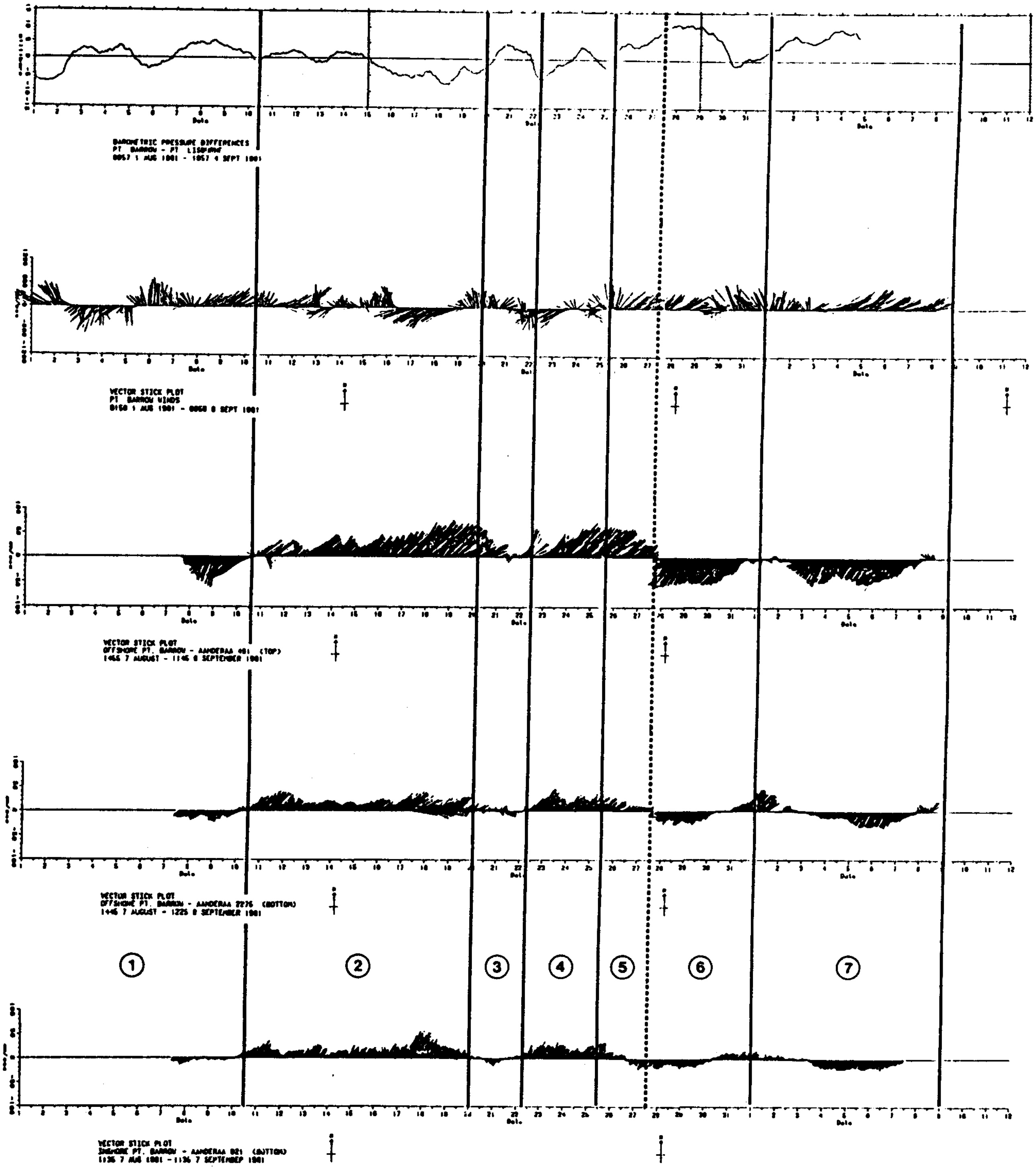

Figure 22. Seven Physical Events in the Meteorological and Current Meter Data of Pt. Barrow, August-September 1981.

37

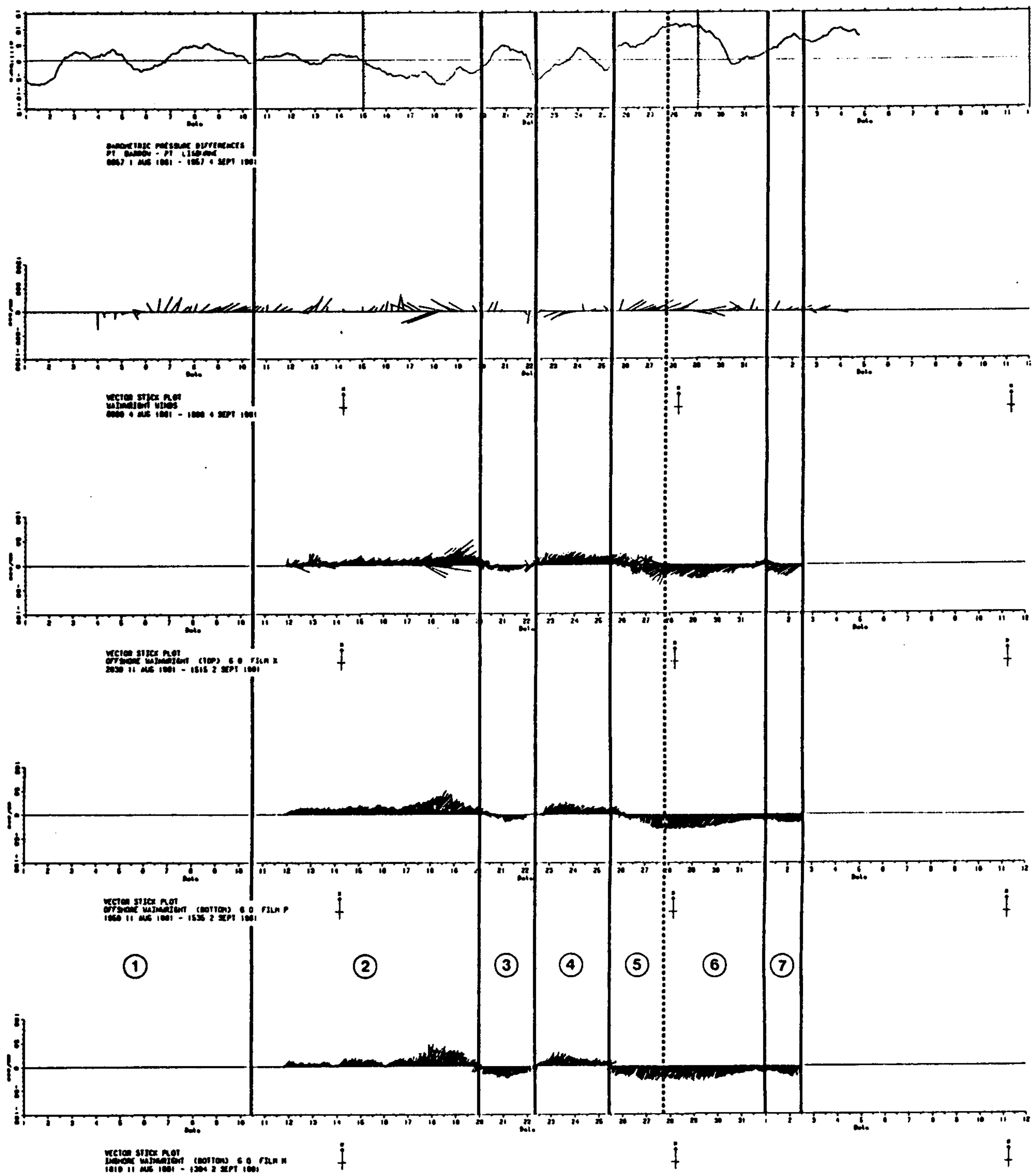

Figure 23 . Seven Physical Events in the Meteorological and Current Meter Data of Wainwright, August-September 1981.

Table 4. Summary of Results . Principal Axis Analysis of Pt. Barrow and Wainwright Moored Current Meters, 7 August - 8 September 1981.

Meter Location	Principal Axis of Current Flow (°T)	Principal Axis Shoreline/Bathymetry (°T)
Barrow		
offshore top	46 - 55	56
offshore bottom	30 - 50	56
inshore bottom	36 - 40	40
Wainwright		
offshore top	68 - 70	40
offshore bottom	40 - 55	40
inshore bottom	33 - 40	40

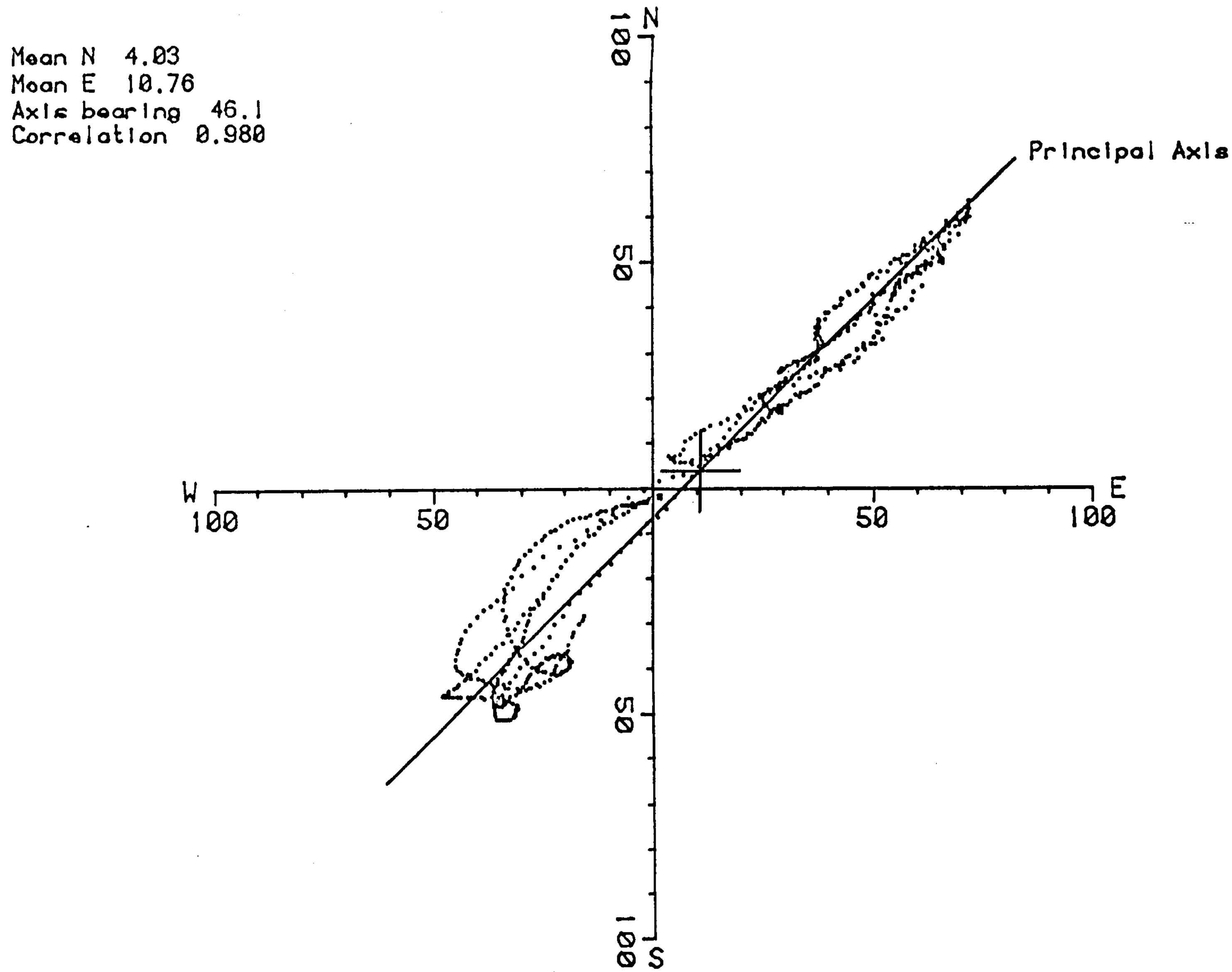

(Speeds in cm/sec)

FIGURE 24. POLAR PLOT - SPEED AND DIRECTION DATA
OFFSHORE BARROW (TOP) DRIFT CURRENT
1020 8 AUG 1981 - 1620 7 SEPT 1981

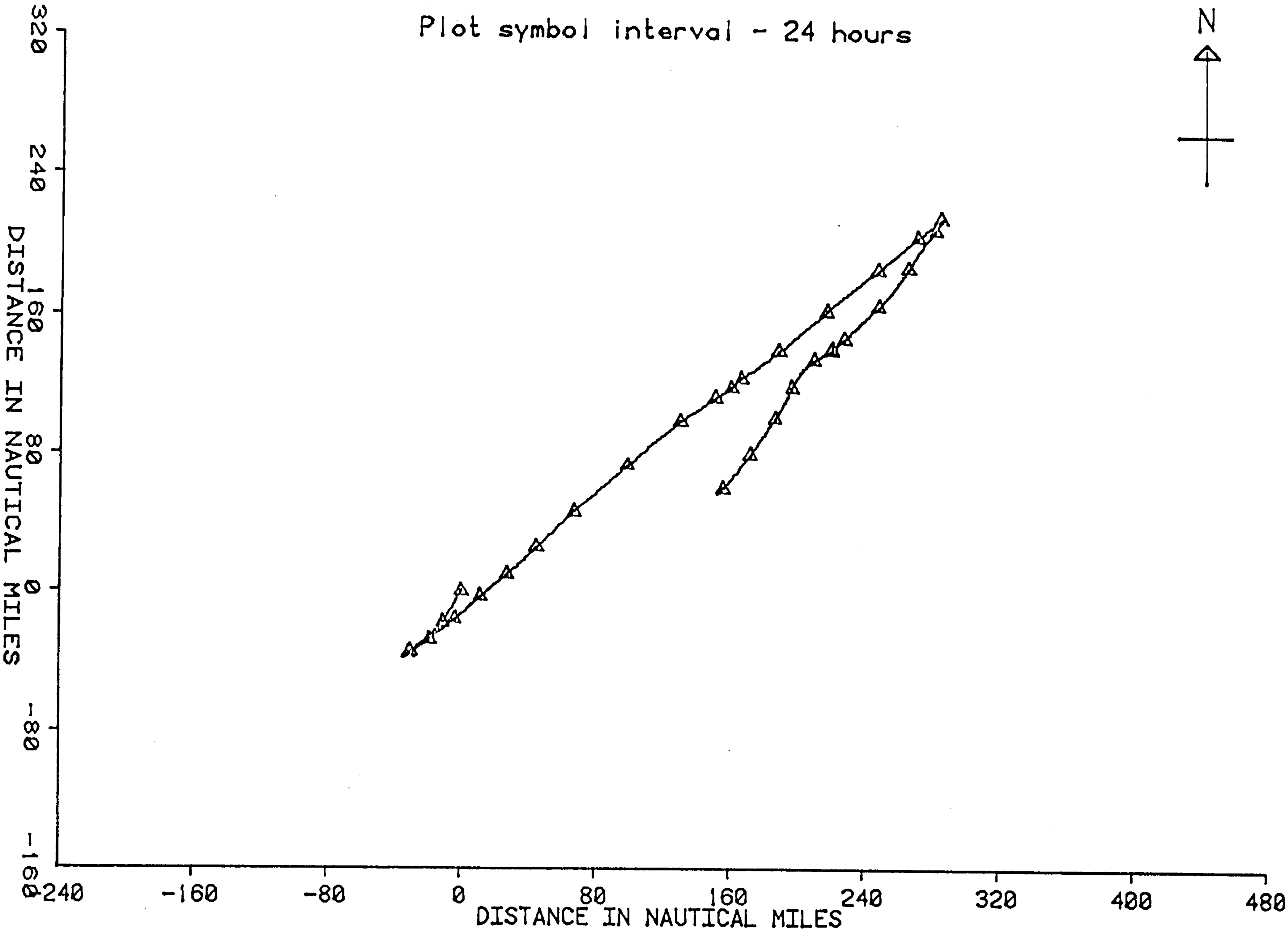

FIGURE 25. PROGRESSIVE VECTOR DIAGRAM
OFFSHORE BARROW (TOP) DRIFT CURRENT
1020 8 AUG 1981 - 1620 7 SEPT 1981

Table 5. Frequencies of Upcoast and Downcoast Flow in the August-September 1981 Chukchi Sea Current Records.

Meter Location	Percent of Readings	
	Upcoast	Downcoast
Barrow		
offshore top	55.7	44.3
offshore bottom	68.1	31.9
inshore bottom	67.0	33.0
Wainwright		
offshore top	63.3	36.7
offshore bottom	61.4	38.6
inshore bottom	52.7	47.3

Correlations Between Current Records (Depths and Stations). A simple visual comparison of the six current meter records from Wainwright to Pt. Barrow, which are displayed in Figures 22 and 23, clearly show a high degree of coherence between all meters,both between onshore and offshore moorings as well as between the Wainwright and Barrow coastal areas.

Seven time periods are delineated on both the Pt. Barrow and Wainwright records. Before 10 August, flows were downcoast as shown by the Barrow meters (Wainwright moorings were not yet emplaced). On the 10th, all three meters reversed, starting an approximately ten-day period (Period 2) of consistent upcoast flow. Wainwright records also recorded this upcoast flow during Period 2. On the 20th, a pause or reversal occurred, lasting until about the 22nd (Period 3). Period 3 seemed to start on the 21st on the Barrow offshore top meter, but otherwise was consistent on all records.

Period 4, starting on 22 August, again was a time of upcoast flow consistent on all records. Period 5, lasting about two and a half days, was a period of changing or reversed flow on all records, except for the two offshore Barrow meters where persistent (though weakening) upcoast flow prevailed.

Both Periods 6 and 7 were times of predominant downcoast flow, separated by a weakening or reversal of flow centered about 1 September.

Thus, as one steps through all records, very close similarities are apparent. These similarities are in directions and magnitudes, and also appear in other features such as times of change and shapes of the current vector plots. The similarities are also very consistent throughout the records.

Statistical correlation analyses were performed from a few selected current records in order to illustrate these similiarities between currents measured at different locations. Results of such a correlation are illustrated in Figure 26 for the inshore Point Barrow and Wainwright longshore current drift components. A correlation coefficient at zero lag of about 0.90 is indicated. This high correlation coefficient, between currents measured by these widely separated stations using different instrument types confirms the similarities observed visually in Figures 22 and 23.

Corresponding spectral density plots of a typical raw current record and of the same record filtered by use of a low-pass (Doodson) filter for drift components (Jenkins and Watts 1968) are shown in Figure 27. The lack of tidal components and the high relative power at low frequencies are noted as expected. The cross-correlation of the filtered and unfiltered records is shown in Figure 28 just for illustration.

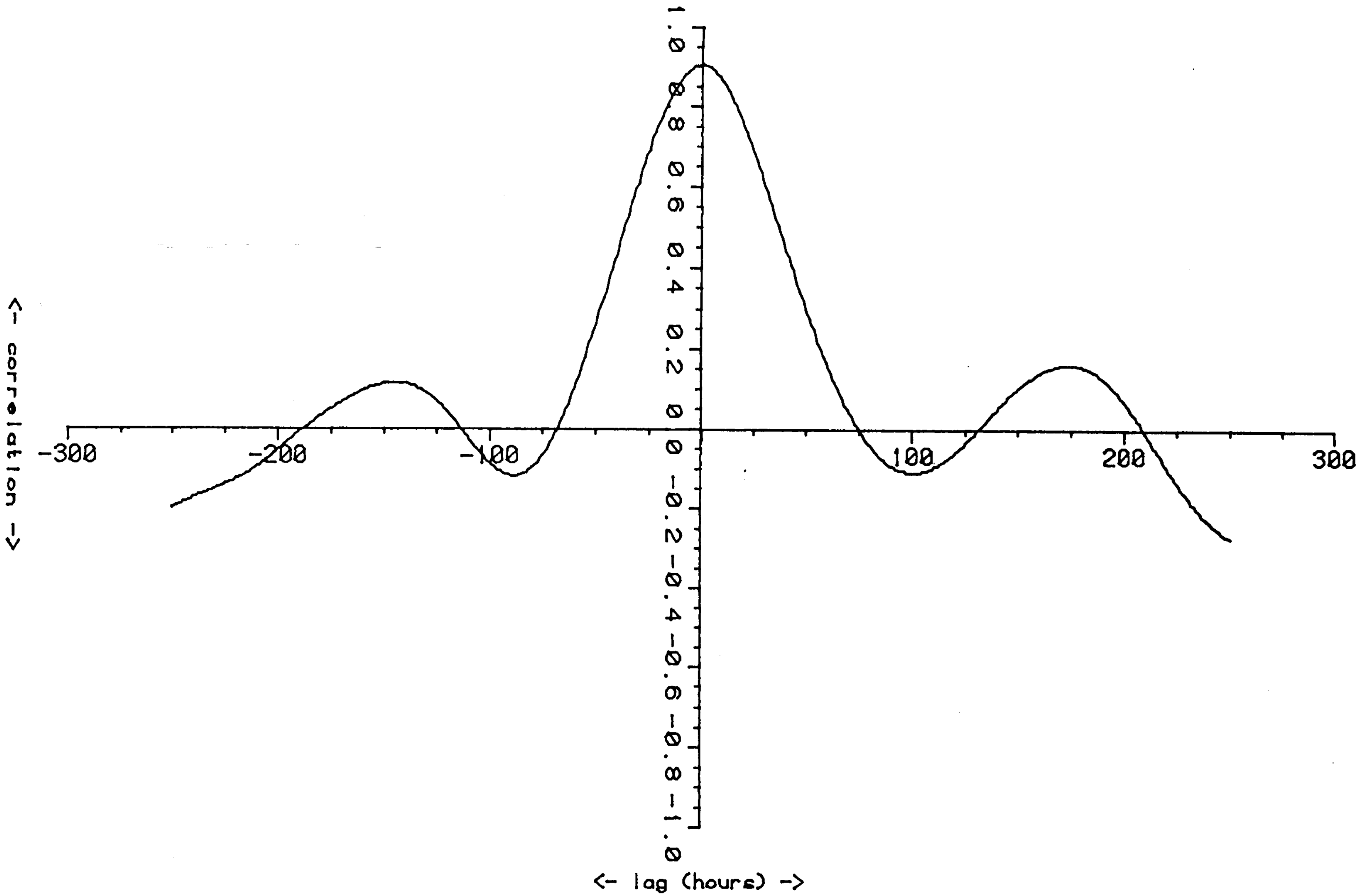

FIGURE 26. CROSS CORRELATIONS
INSHORE BARROW DRIFT CURRENT (35.9 DEGREE COMPONENT) VS.
LAGGED INSHORE WAINWRIGHT DRIFT CURRENT (33.7 DEG. COMP.)
1251 12 AUG 1981 - 1751 1 SEPT 1981

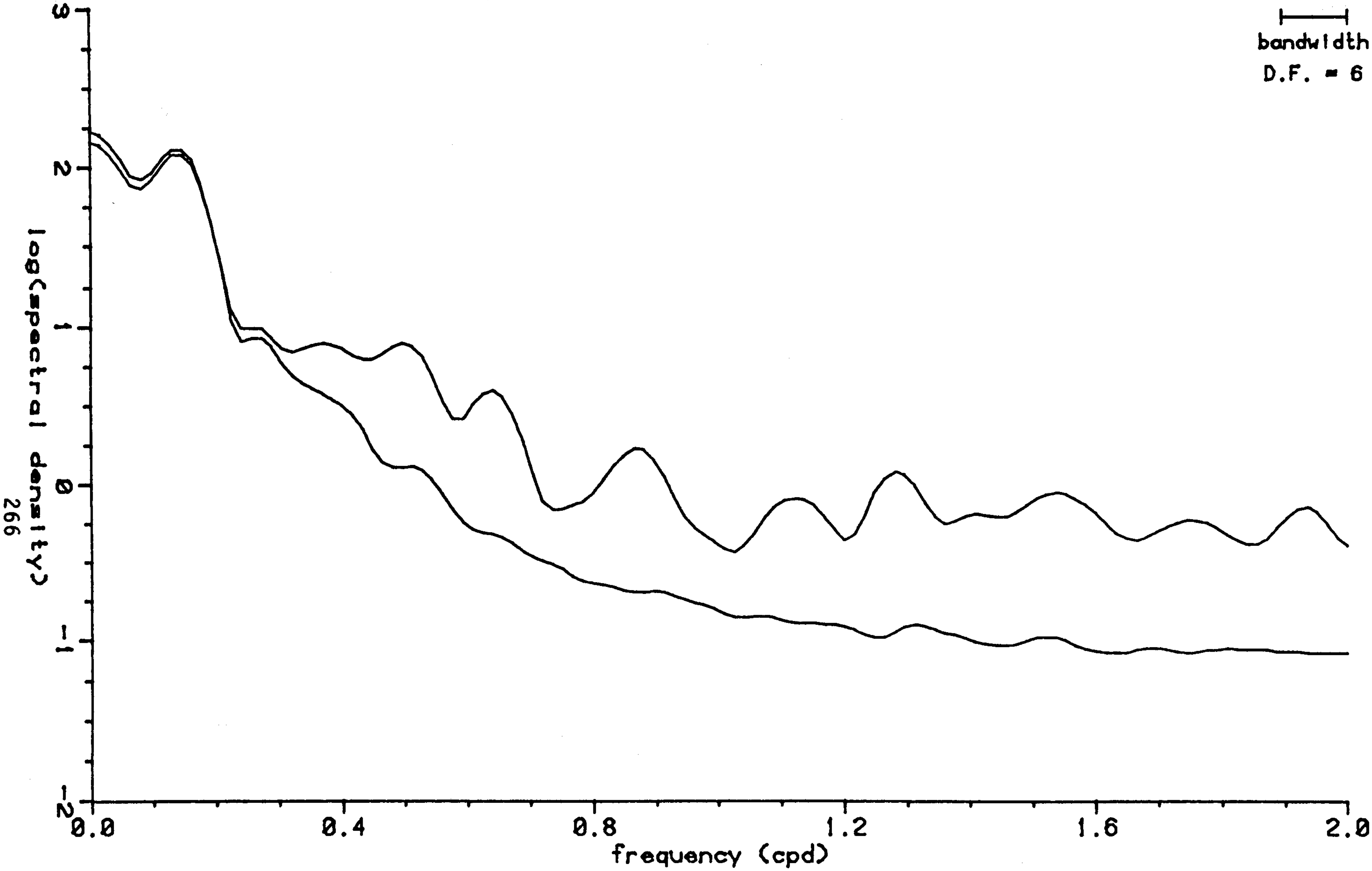

FIGURE 27. SPECTRAL DENSITY
A) INSHORE BARROW (BOTTOM) DRIFT CURRENT - 35.9 DEGREE COMP.
B) INSHORE BARROW (BOTTOM) CURRENT - 35.9 DEGREE COMP.
0703 8 AUG 1981 - 1303 6 SEPT 1981

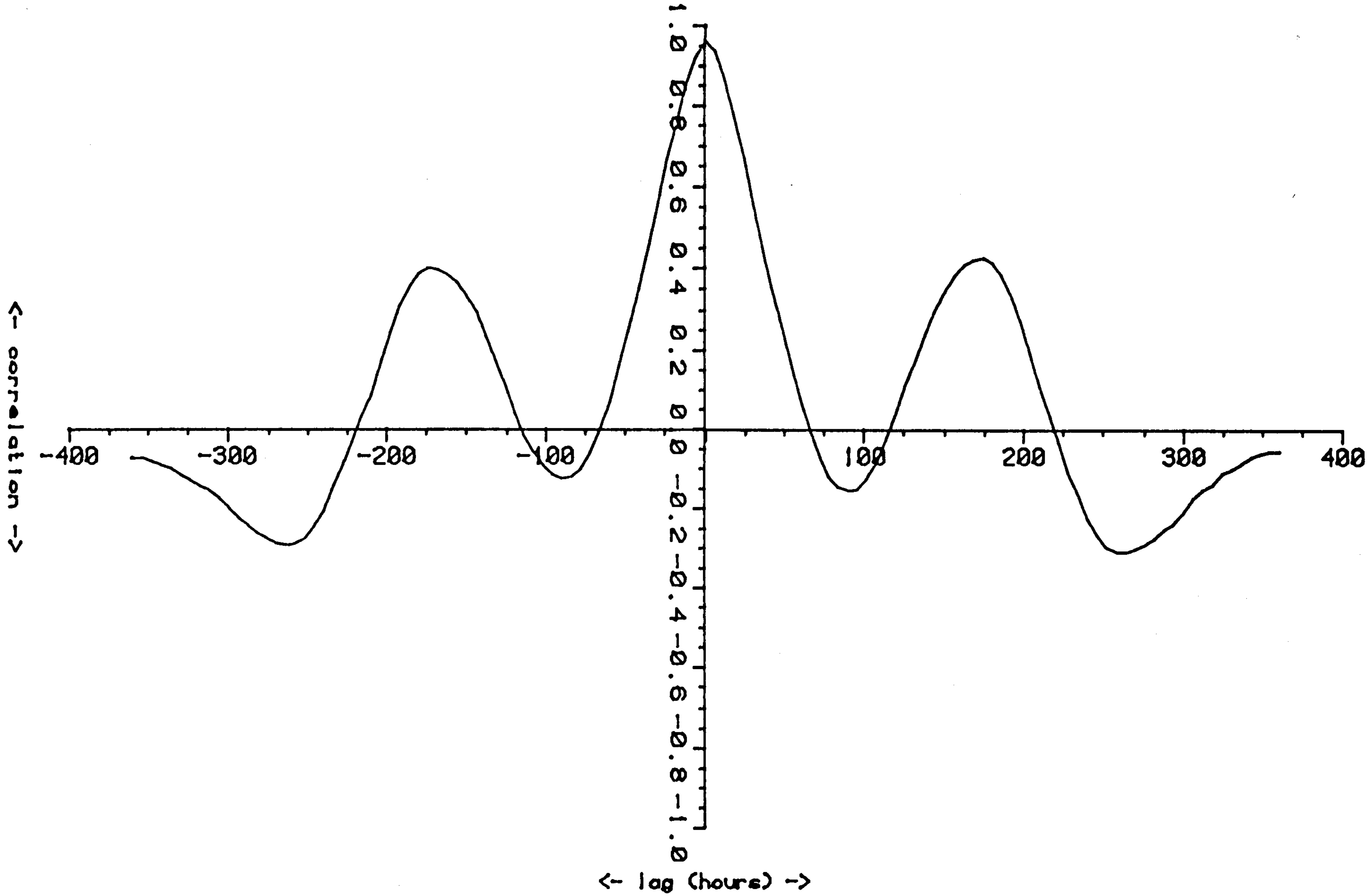

FIGURE 28. CROSS CORRELATIONS
INSHORE BARROW (BOTTOM) DRIFT CURRENT VS. LAGGED INSHORE BARROW (BOTTOM) CURRENT (35.9 DEGREE COMPONENTS)
0703 8 AUG 1981 - 1303 6 SEPT 1981

Meteorological Forcing

Of prime interest to later modeling efforts is the relationship of the coastal currents to the meteorological parameters of atmospheric pressure and local winds. Therefore, graphical comparisons of these two meteorological time-series parameters with those of the coastal current records are also included in Figures 22 and 23. In addition, computerized cross-correlations of these time-series spectra have been done to further determine these cause and effect relationships.

Correlations with Pressure Differences. With reference to Figures 22 and 23 (which also display the current and meteorological time series data), a comparison of current data with the pressure data can be made, utilizing the same seven time periods as used above when comparing different current meter data. The pressure data are plotted as the difference between atmospheric pressure at Pt. Barrow and Cape Lisburne where the frequency of recorded data was higher than at Nome. Pt. Barrow - Nome pressure difference plots are very similar (Figure 10).

In going through the seven time periods for both Pt. Barrow and Wainwright areas, high pressure at Pt. Barrow relative to the southern stations is strongly associated with downcoast flow. Conversely, low or negative pressure differences are strongly associated with upcoast flow. By taking each of the seven delineated time periods in turn for comparisons of coastal currents and pressure differences, the reader can visually demonstrate how strong this pressure difference - coastal current linkage shows up in the data.

Cross correlations of these time series current data with pressure difference series (Pt. Barrow - Cape Lisburne) were also carried out. A series of plots of the results are shown in Figures 29 through 35 for the case of the pressure difference and inshore Barrow current data correlations.

The spectral density plots for both the pressure difference and current data again illustrate that the major variations occur in the low frequency end, below 0.8 cpd (cycles per day). The cross-correlations (Figure 31) show a correlation coefficient of about -0.85 at zero lag, again confirming the visual relationship evident between the records in Figures 22 and 23. A high pressure at Barrow relative to Cape Lisburne (or Nome) drives downcoast (southwestern) currents and vice-versa.

The accompanying squared coherence spectra (Figures 32 and 34) show peaks at about 0.45 and 1.3 cpd (53 hours and 18 hours). Though the former has significant power, it is not clear from these fairly short records if these low frequency peaks are indeed physically real. Corresponding phase spectra are shown in Figures 33 and 35.

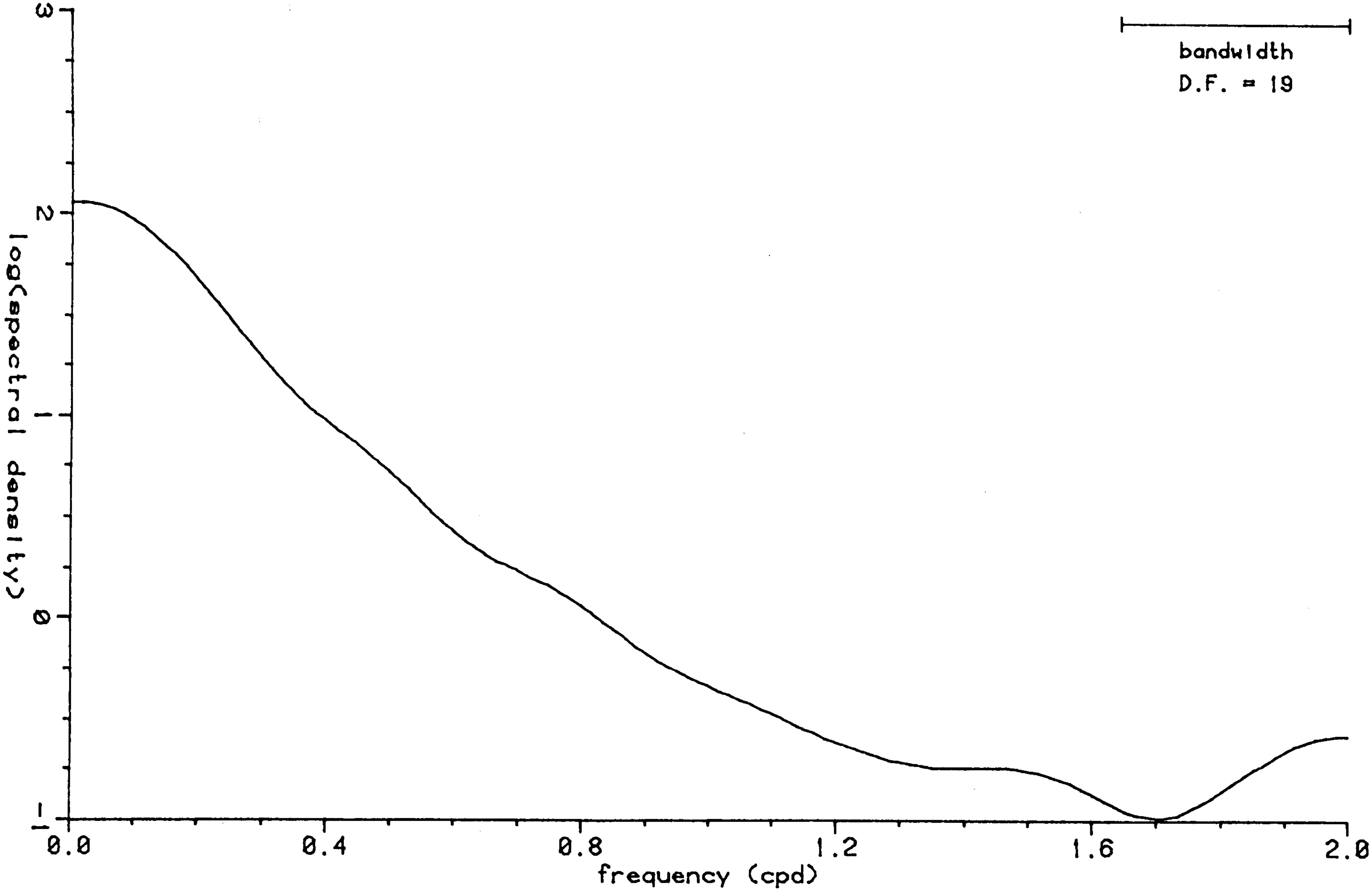

FIGURE 29. SPECTRAL DENSITY
PT. BARROW - CAPE LISBURNE BAROMETRIC PRESSURE DIFFERENCES
0659 8 AUG 1981 - 1859 4 SEPT 1981

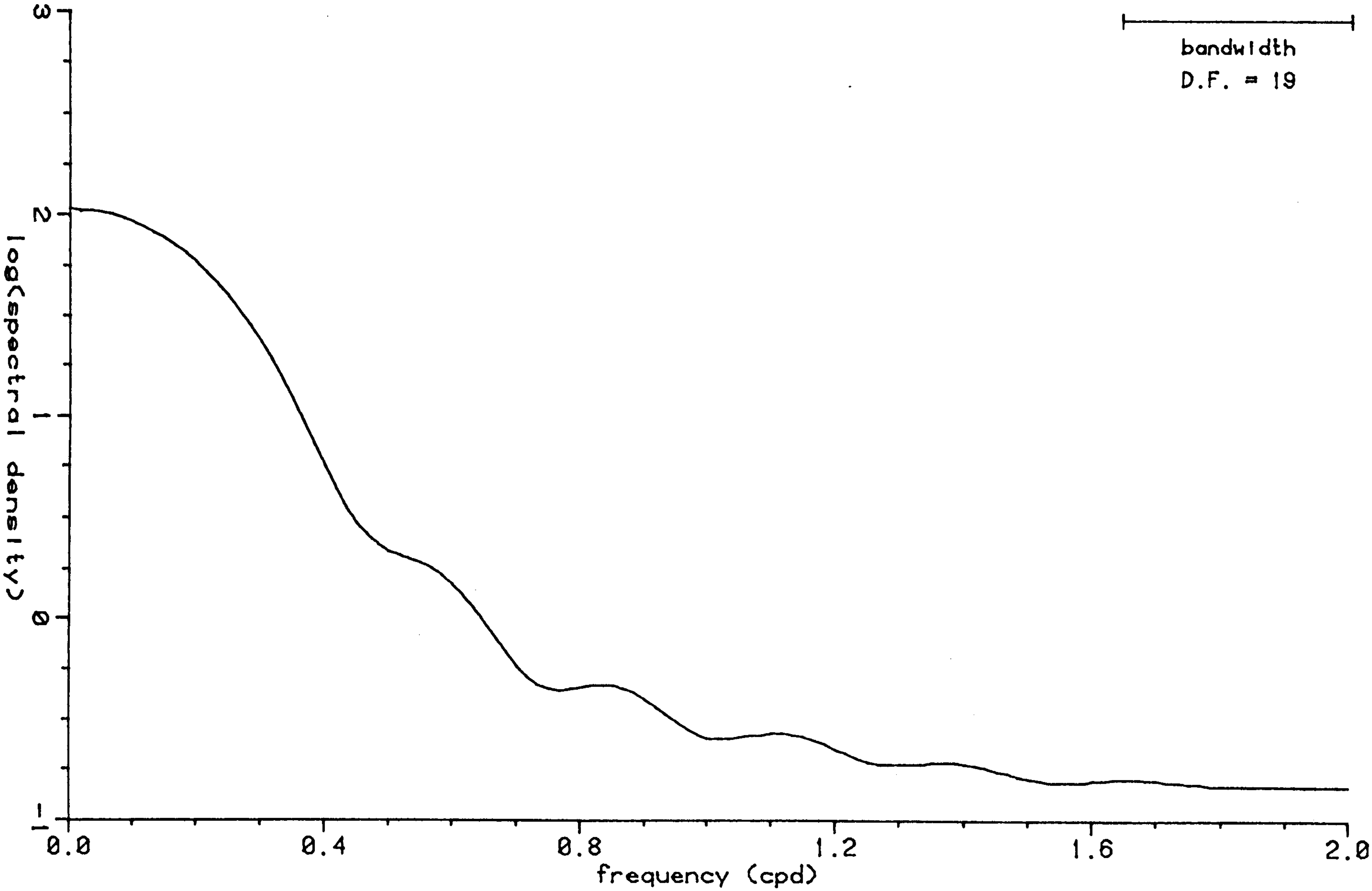

FIGURE 30. SPECTRAL DENSITY
INSHORE BARROW (BOTTOM) DRIFT CURRENT (35.9 DEGREE COMPONENT)
0659 8 AUG 1981 - 1859 4 SEPT 1981

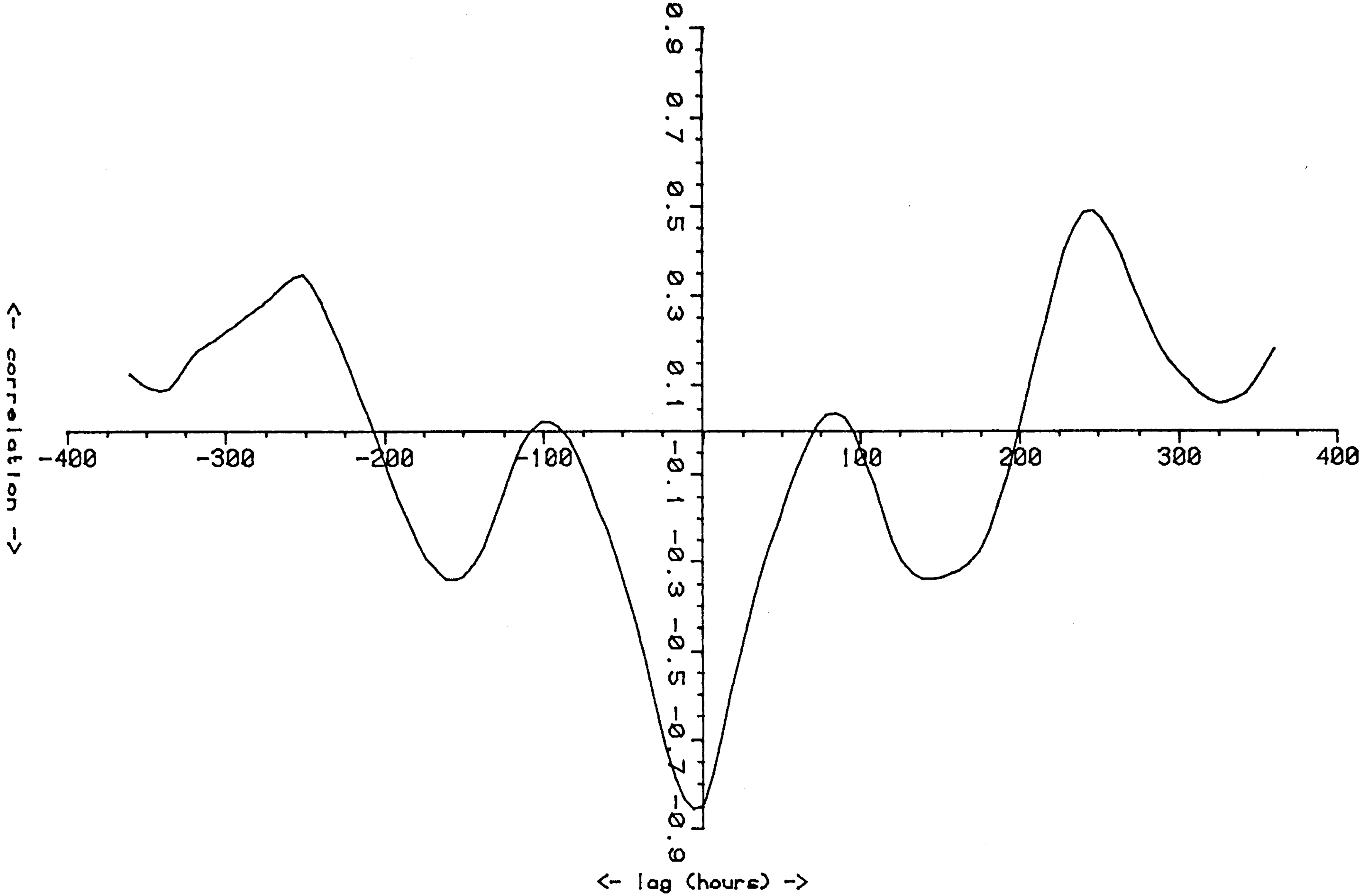

FIGURE 31. CROSS CORRELATIONS
PT. BARROW - CAPE LISBURNE BAROMETRIC PRESSURE DIFFERENCES
VS. LAGGED INSHORE BARROW DRIFT CURRENT (35.9 DEGREE COMP.)
0659 8 AUG 1981 - 1859 4 SEPT 1981

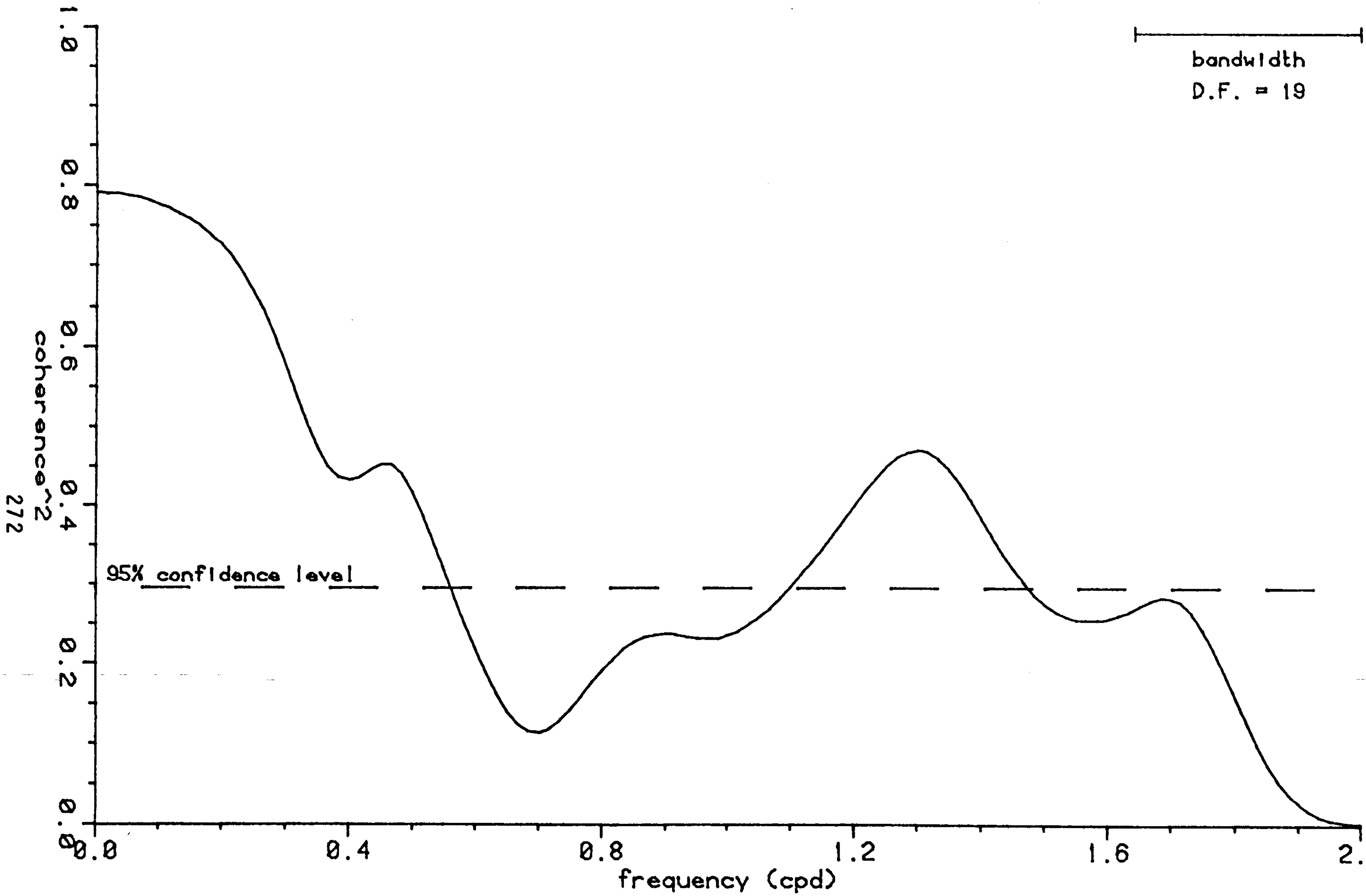

FIGURE 32. SQUARED COHERENCE SPECTRUM
PT. BARROW-CAPE LISBURNE BAROMETRIC PRESSURE DIFFERENCES VS.
INSHORE BARROW (BOTTOM) DRIFT CURRENT (35.9 DEGREE COMPONENT)
0659 8 AUG 1981 - 1859 4 SEPT 1981

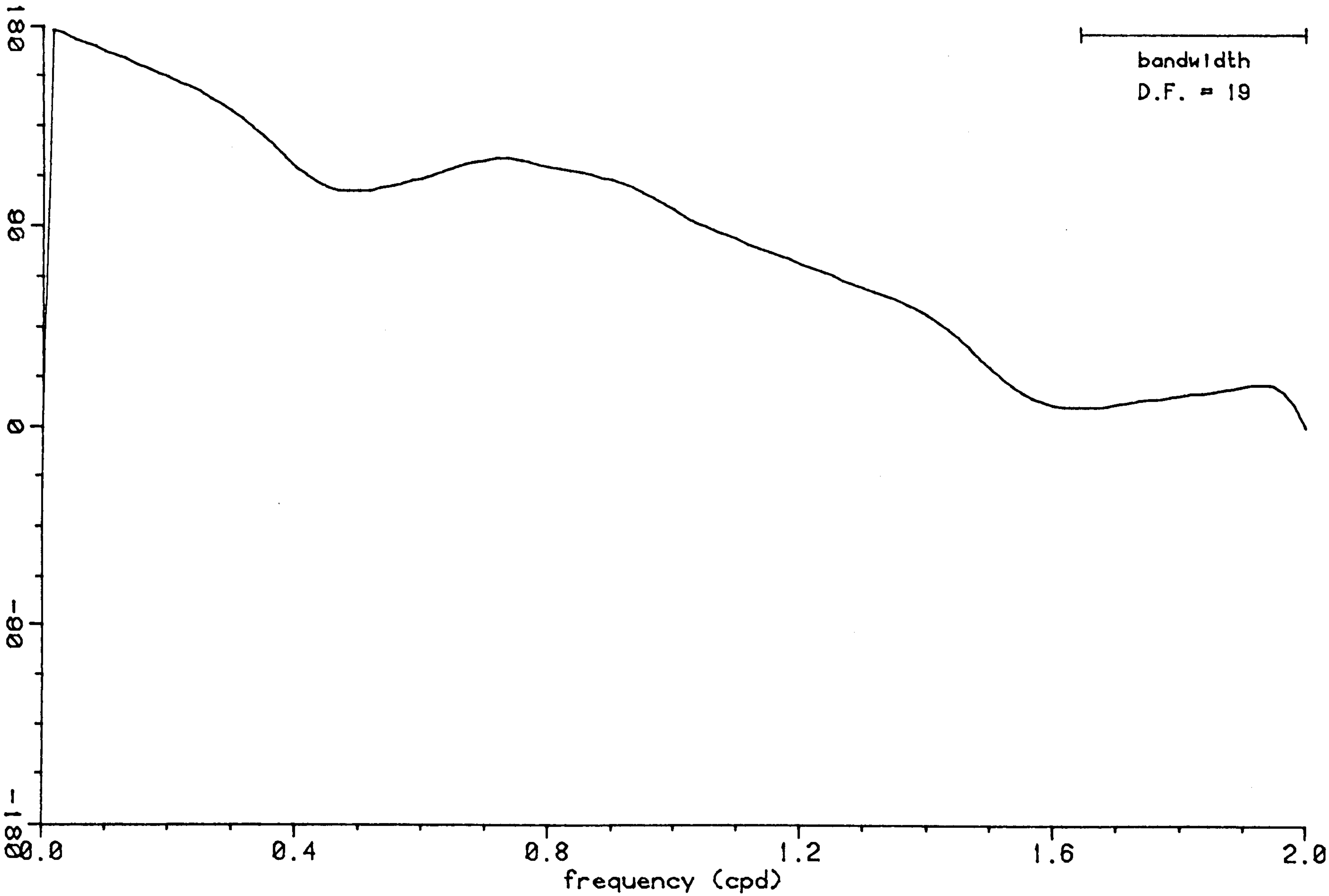

FIGURE 33

PHASE SPECTRUM
PT. BARROW-CAPE LISBURNE BAROMETRIC PRESSURE DIFFERENCES VS.
INSHORE BARROW (BOTTOM) DRIFT CURRENT (35.9 DEGREE COMPONENT)
0659 8 AUG 1981 - 1859 4 SEPT 1981

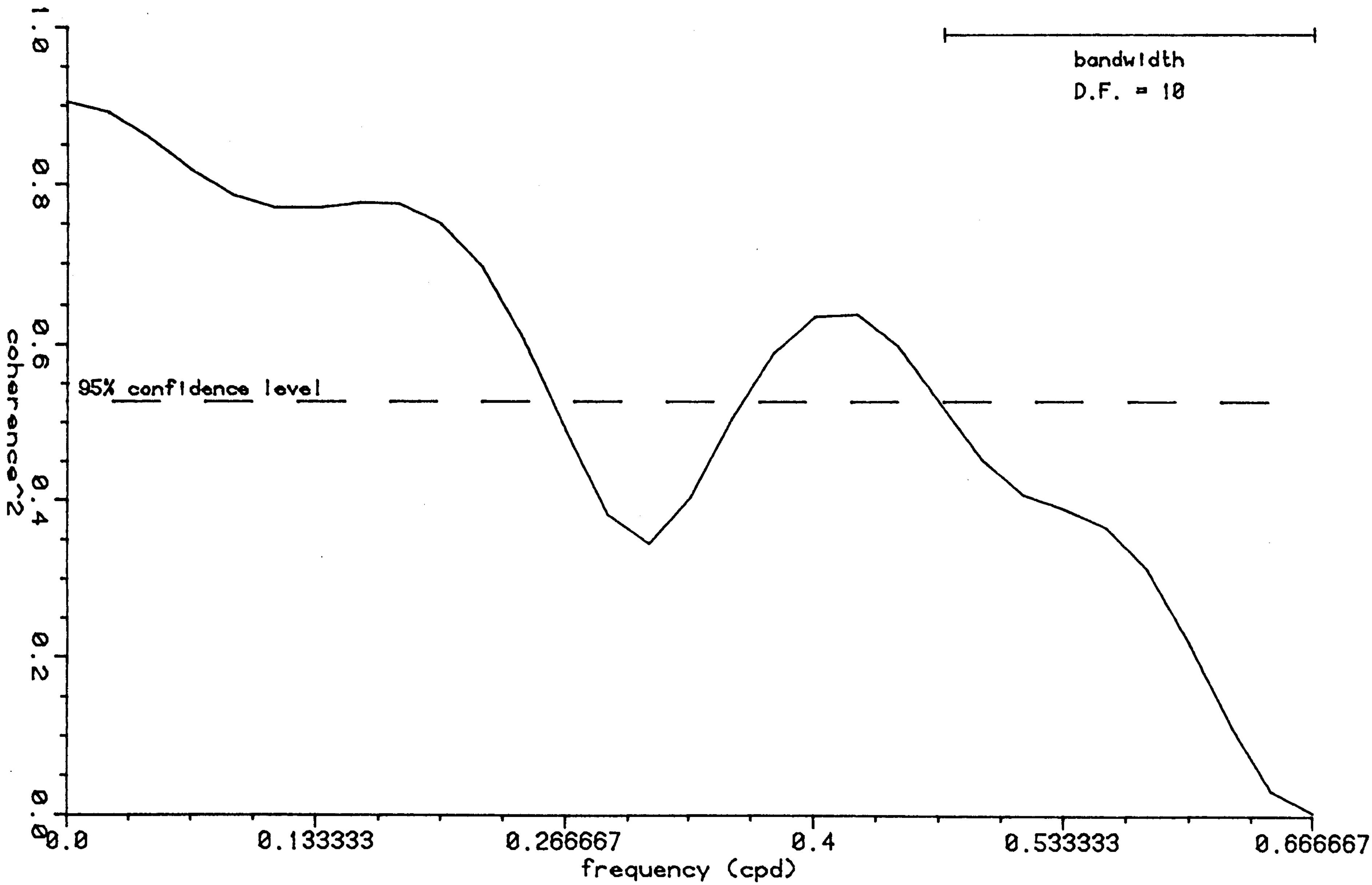

FIGURE 34. SQUARED COHERENCE SPECTRUM
PT. BARROW-CAPE LISBURNE BAROMETRIC PRESSURE DIFFERENCES VS.
INSHORE BARROW (BOTTOM) DRIFT CURRENT (35.9 DEGREE COMPONENT)
0659 8 AUG 1981 - 0659 4 SEPT 1981

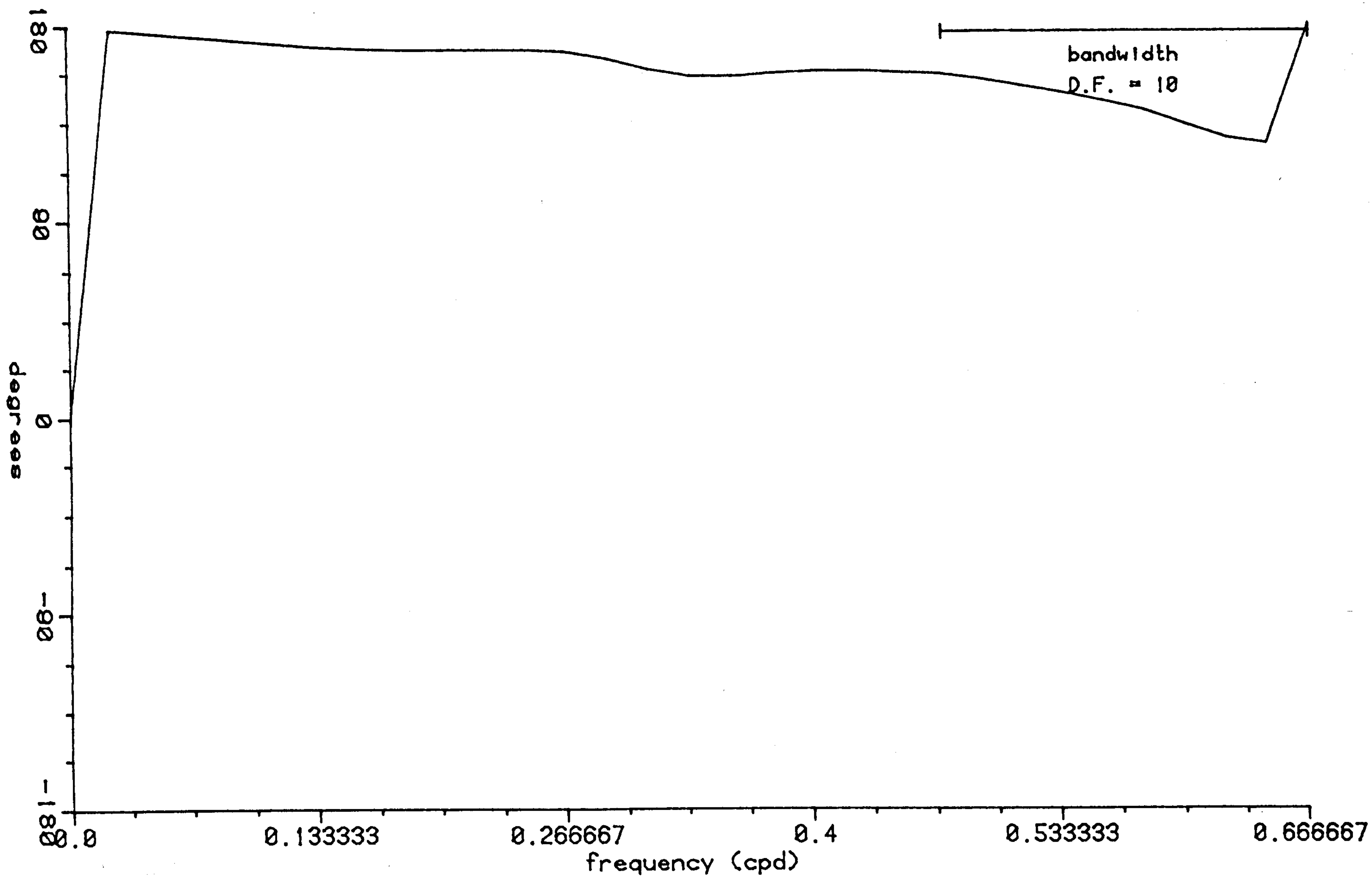

FIGURE 35. PHASE SPECTRUM
PT. BARROW-CAPE LISBURNE BAROMETRIC PRESSURE DIFFERENCES VS.
INSHORE BARROW (BOTTOM) DRIFT CURRENT (35.9 DEGREE COMPONENT)
0659 8 AUG 1981 - 0659 4 SEPT 1981

The cross correlation of the same Barrow - Lisburne pressure difference with the inshore Wainwright current meter is shown in Figure 36, for comparison with Figure 31 for the Barrow case. Again, a high negative correlation coefficient of 0.81 is obtained at zero lag.

Thus we have found a high correlation between coastal currents at all stations, including both the Point Barrow and Wainwright areas. We have also found a high correlation of these currents with Pt. Barrow - Lisburne atmospheric pressure differences. Therefore, the evidence indicates that these shallow, near-coast currents are driven by the same atmospheric pressure forcing function along this stretch of coast. Mountain et al. (1976) found the same atmospheric pressure forcing for the currents measured much deeper in Barrow Canyon as we did for the shallow coastal currents.

Correlations with Local Winds. A similar examination of the wind and current plots of Figures 22 and 23 shows a relationship of northeast winds with southwest (downcoast) currents, but not quite to the same high degree as the pressure difference - current relationship.

Spectral and cross correlations of winds with currents were also done. Results of the Wainwright local wind and the inshore Wainwright drift current data are shown in Figures 37 through 43. The cross correlation results for the local wind and the inshore meter for Point Barrow are illustrated in Figure 44. The correlation coefficients are about 0.65 and 0.72 for the Wainwright and Barrow cases respectively, thus somewhat lower than found above for the pressure difference - current data correlations.

Pressure Difference - Local Wind Correlations. Cross correlations of the Point Barrow - Cape Lisburne pressure differences with the Wainwright and the Point Barrow local winds are shown in Figures 45 and 46. Correlation coefficients of about 0.52 and 0.56 are obtained. Again, these coefficients are significantly lower than those obtained in the case of the pressure difference - current correlations.

Hydrographic Transects

Data from the hydrographic transects taken during the cruise, perpendicular to the coastline, and extending up to 35 km offshore are shown in two formats. Individual station profiles with depth are plotted in Figures C-1 through C-43 profiles with depth are plotted in Figures C-1 through C-42 sigma-t, and transparency were plotted as vertical sections perpendicular to the coast in Figures 12 through 18 above. Time series of temperature and salinity were also obtained from the moored meters at Point Barrow.

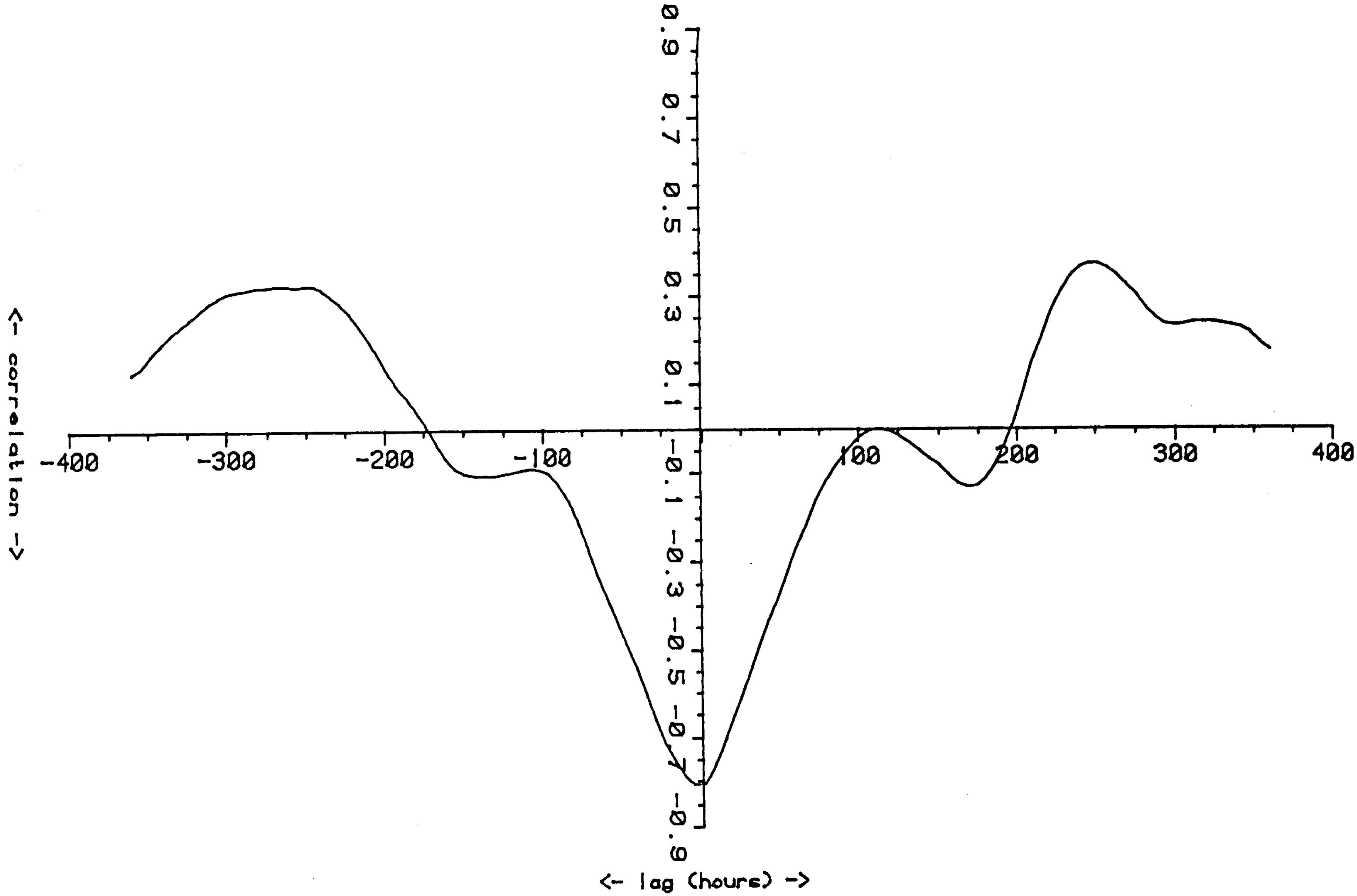

FIGURE 36. CROSS CORRELATIONS
BARROW-LISBURNE BAROMETRIC PRESSURE DIFFERENCES VS. LAGGED
INSHORE WAINWRIGHT (BOTTOM) DRIFT CURRENT (33.7 DEG. COMP.)
1350 12 AUG 1981 - 1350 1 SEPT 1981

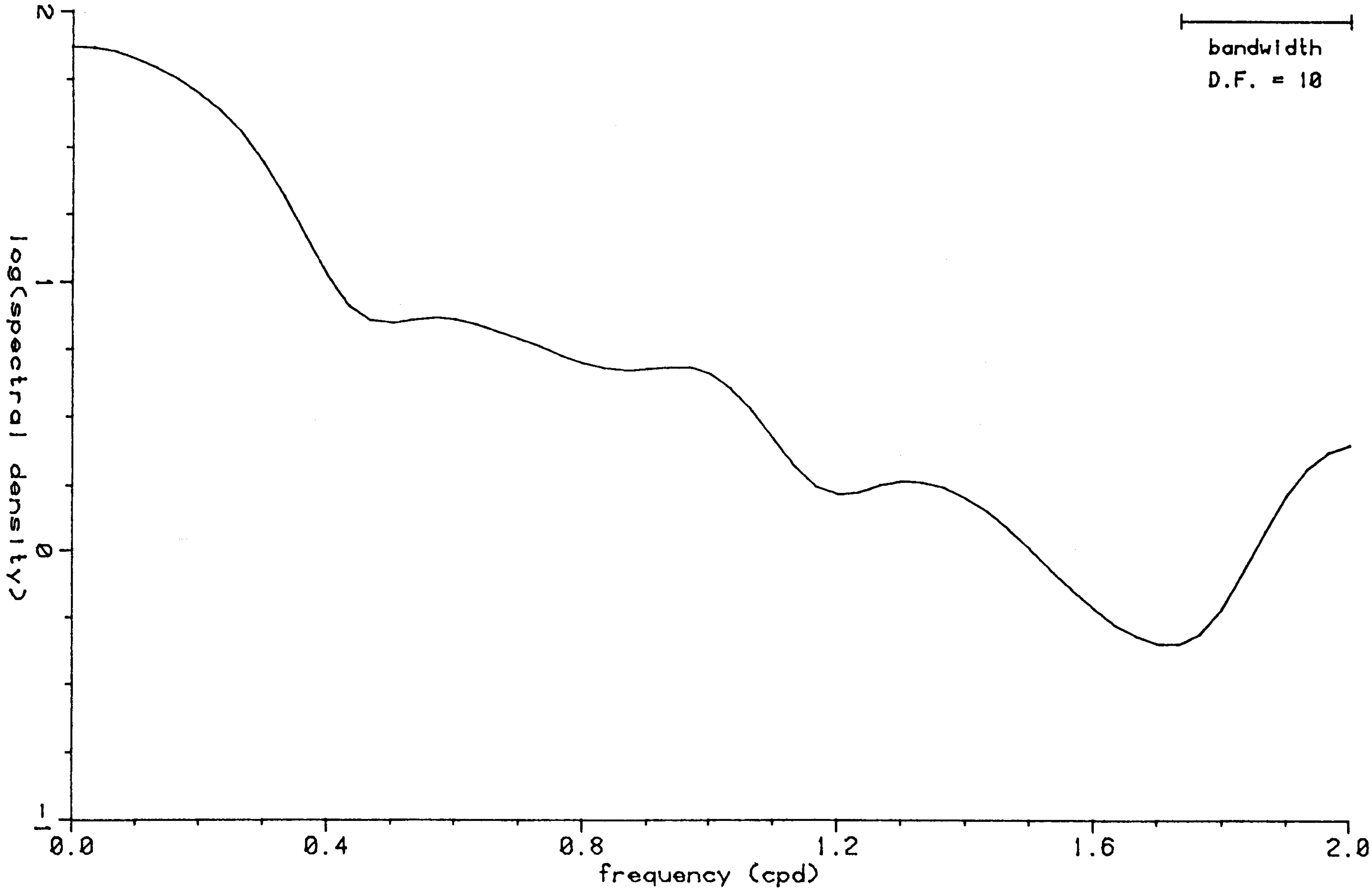

FIGURE 37. SPECTRAL DENSITY
WAINWRIGHT WIND (33.7 DEGREE COMPONENT)
1751 12 AUG 1981 - 1751 1 SEPT 1981

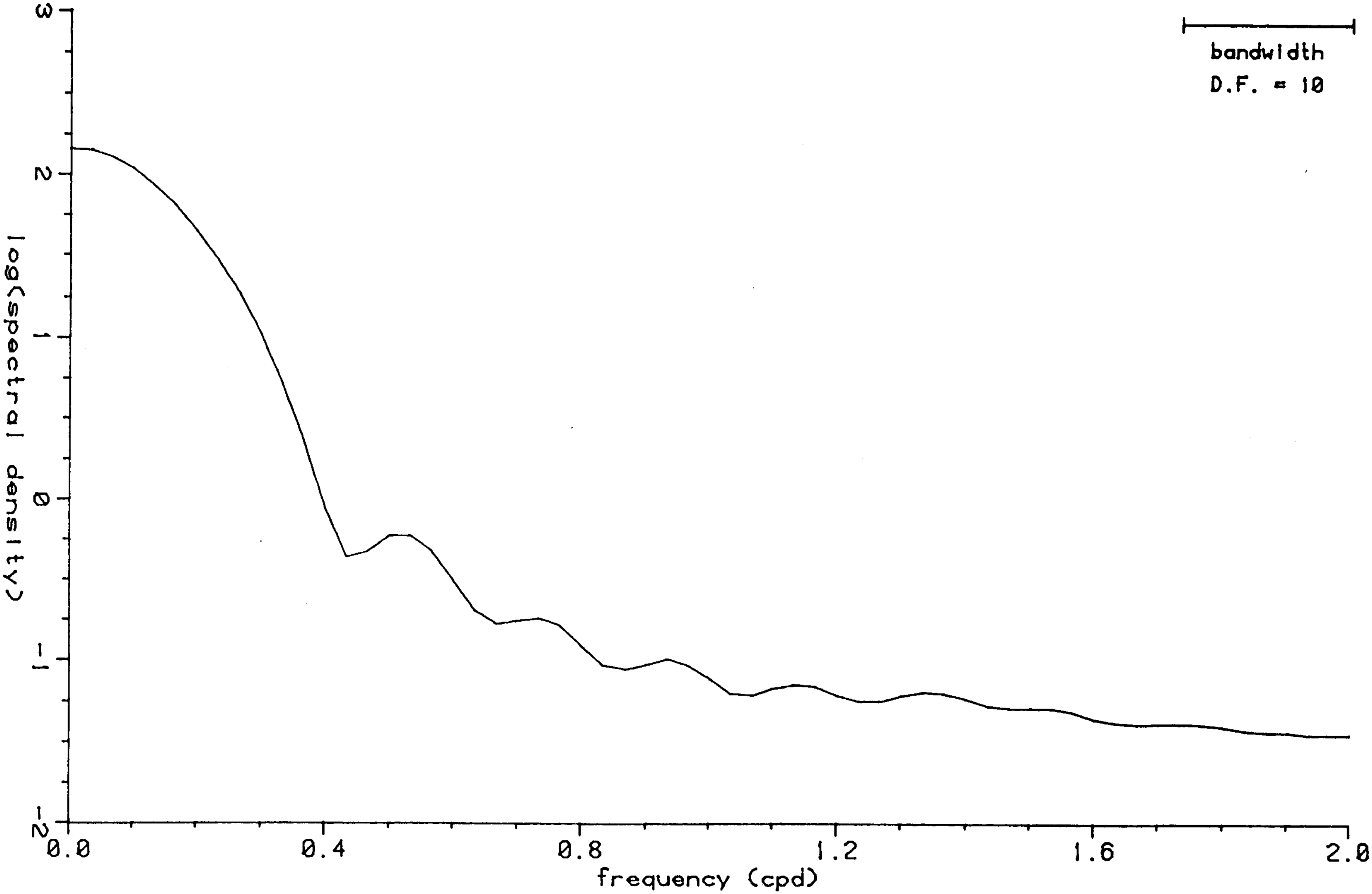

FIGURE 38. SPECTRAL DENSITY
INSHORE WAINWRIGHT (BOTTOM) DRIFT CURRENT
(33.7 DEGREE COMPONENT)
1751 12 AUG 1981 - 1751 1 SEPT 1981

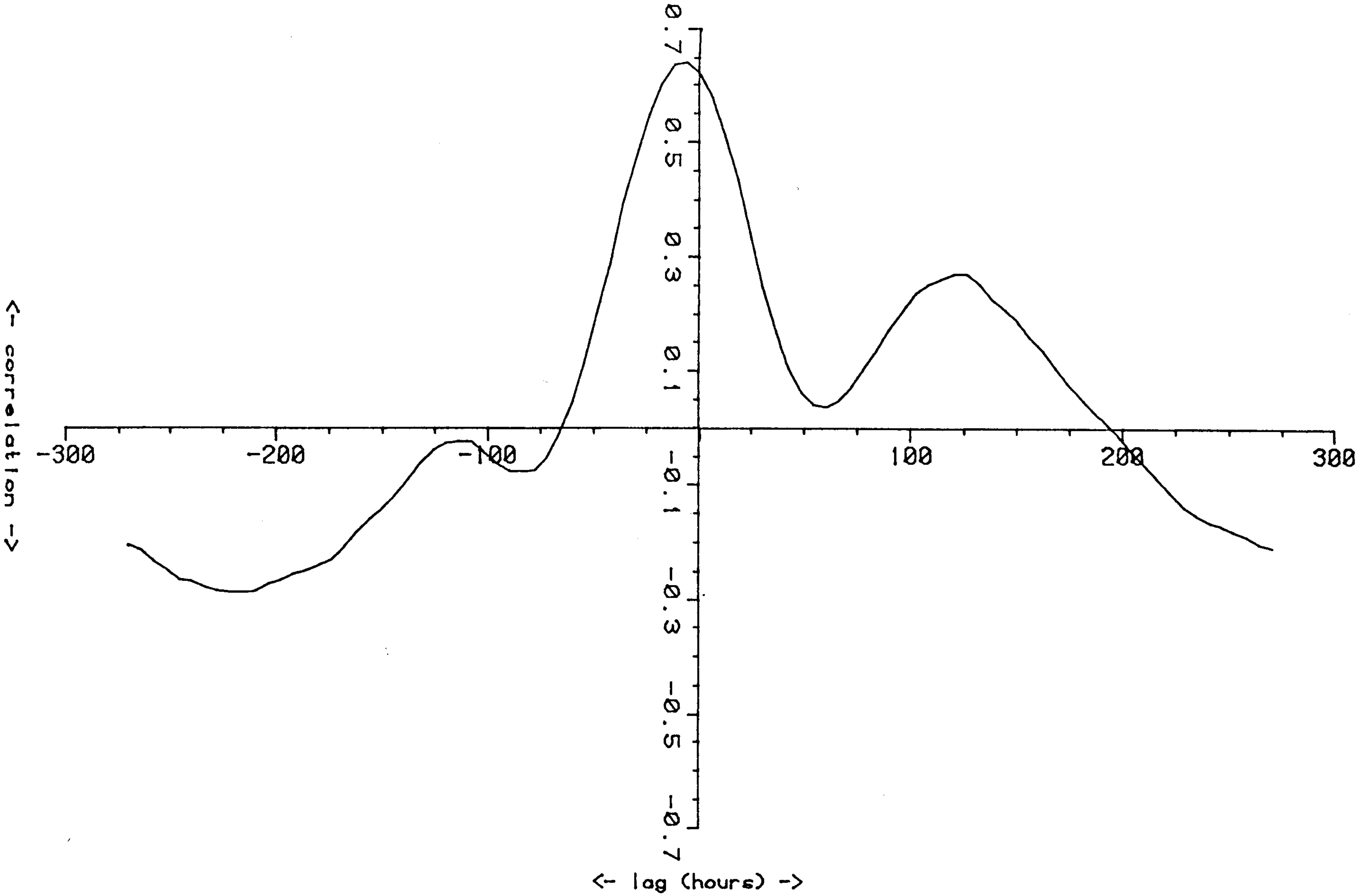

FIGURE 39 CROSS CORRELATIONS
WAINWRIGHT WIND (33.7 DEGREE COMPONENT) VS. LAGGED INSHORE
WAINWRIGHT (BOTTOM) DRIFT CURRENT (33.7 D.)
1751 12 AUG 1981 - 1751 1 SEPT 1981

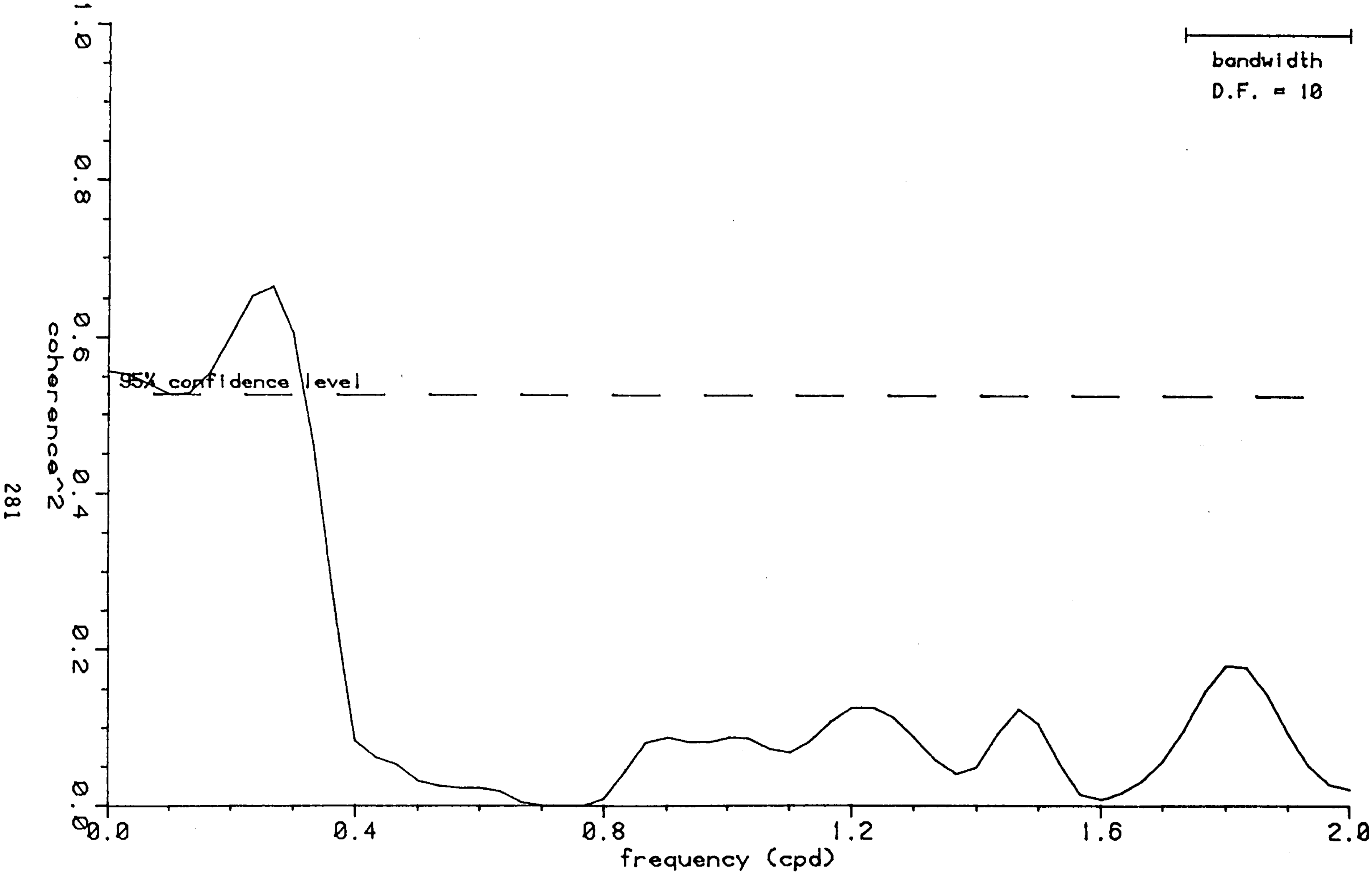

FIGURE 40. SQUARED COHERENCE SPECTRUM
WAINWRIGHT WIND (33.7 DEGREE COMPONENT) VS. INSHORE
WAINWRIGHT (BOTTOM) DRIFT CURRENT (33.7 DEGREE COMP.)
1751 12 AUG 1981 - 1751 1 SEPT 1981

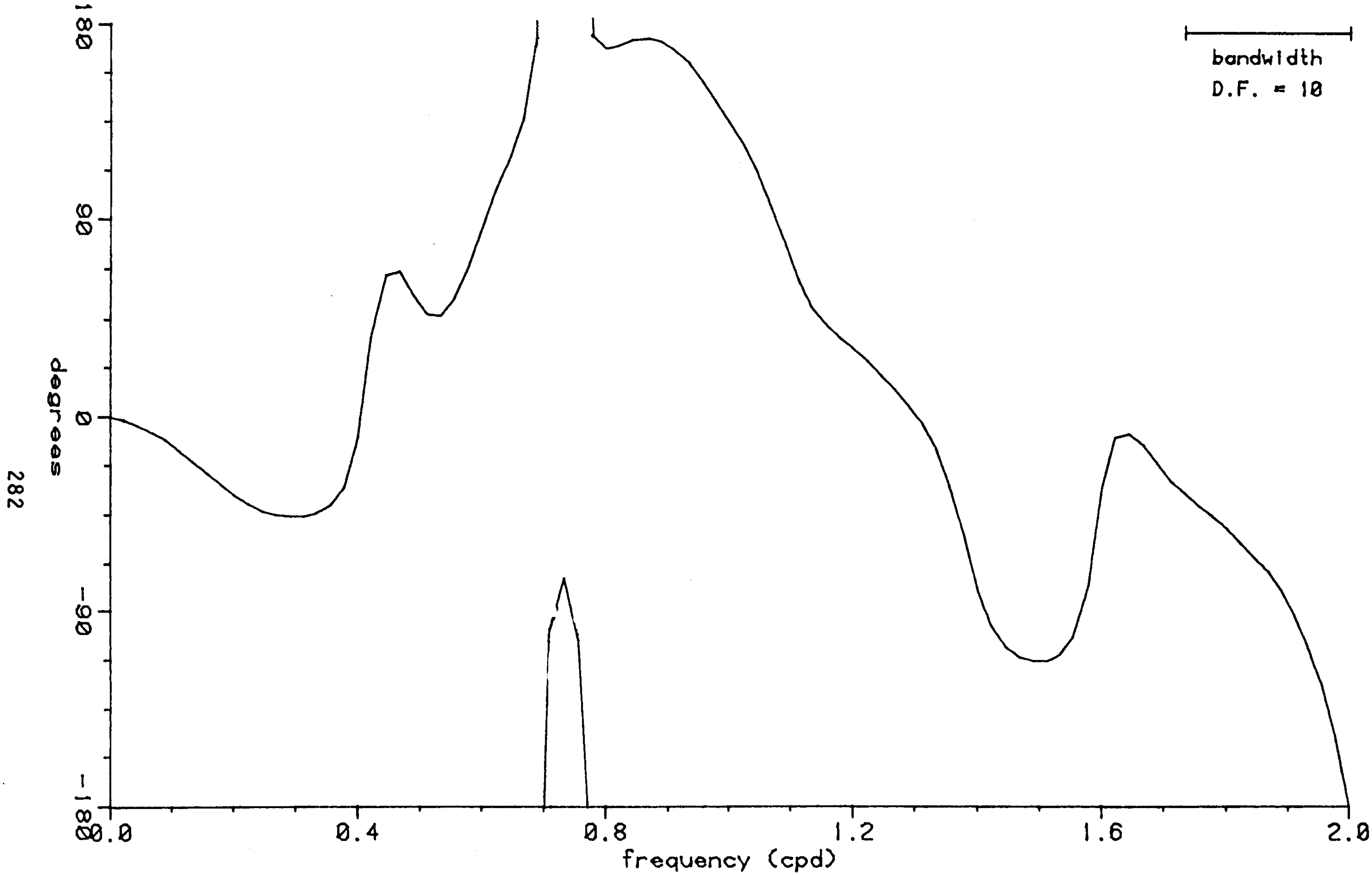

FIGURE 41. PHASE SPECTRUM
WAINWRIGHT WIND (33.7 DEGREE COMPONENT) VS. INSHORE
WAINWRIGHT (BOTTOM) DRIFT CURRENT (33.7 DEGREE COMP.)
1751 12 AUG 1981 - 1751 1 SEPT 1981

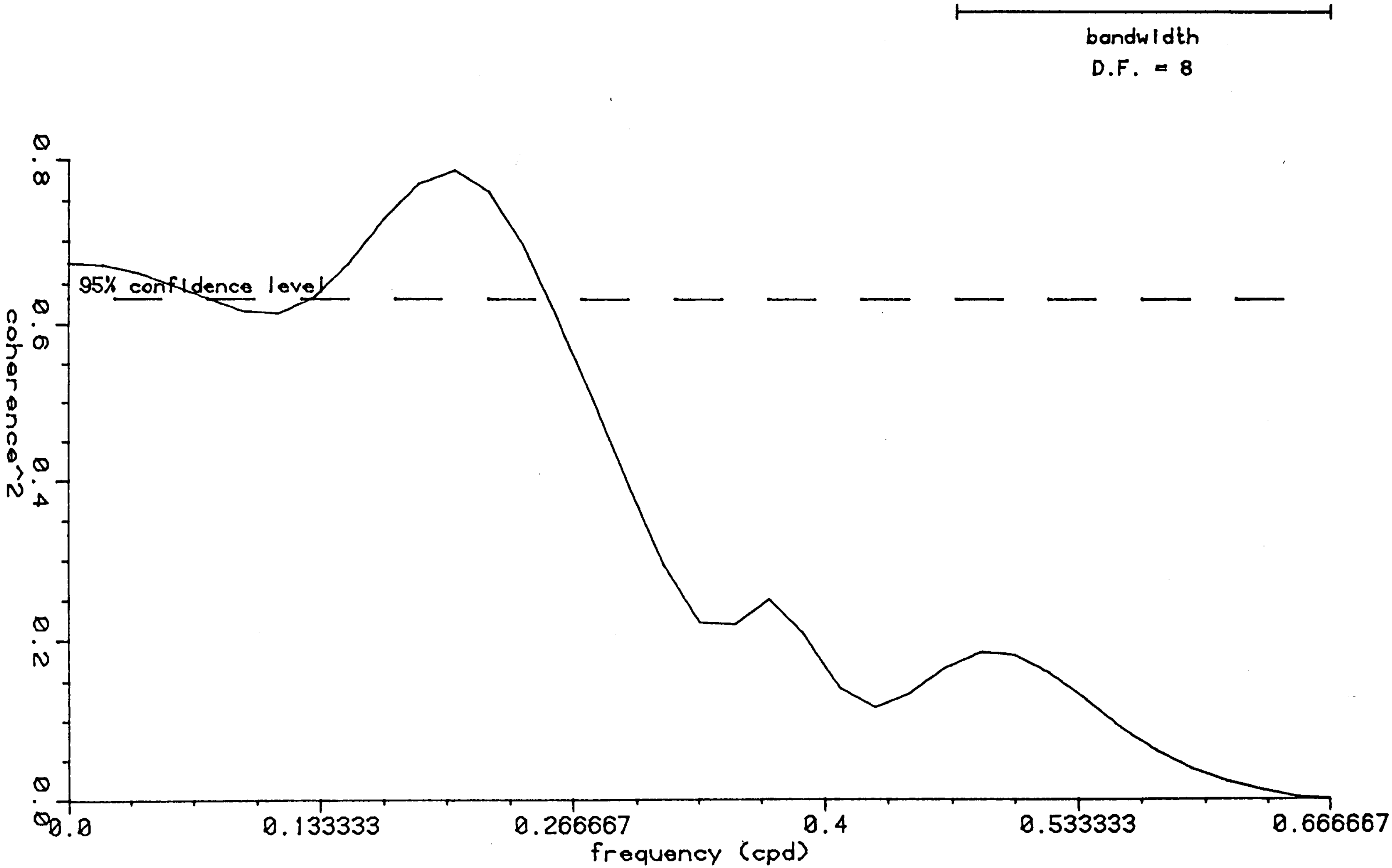

FIGURE 42. SQUARED COHERENCE SPECTRUM
WAINWRIGHT WIND (33.7 DEGREE COMPONENT) VS. INSHORE
WAINWRIGHT (BOTTOM) DRIFT CURRENT (33.7 DEGREE COMP.)
1751 12 AUG 1981 - 1751 1 SEPT 1981

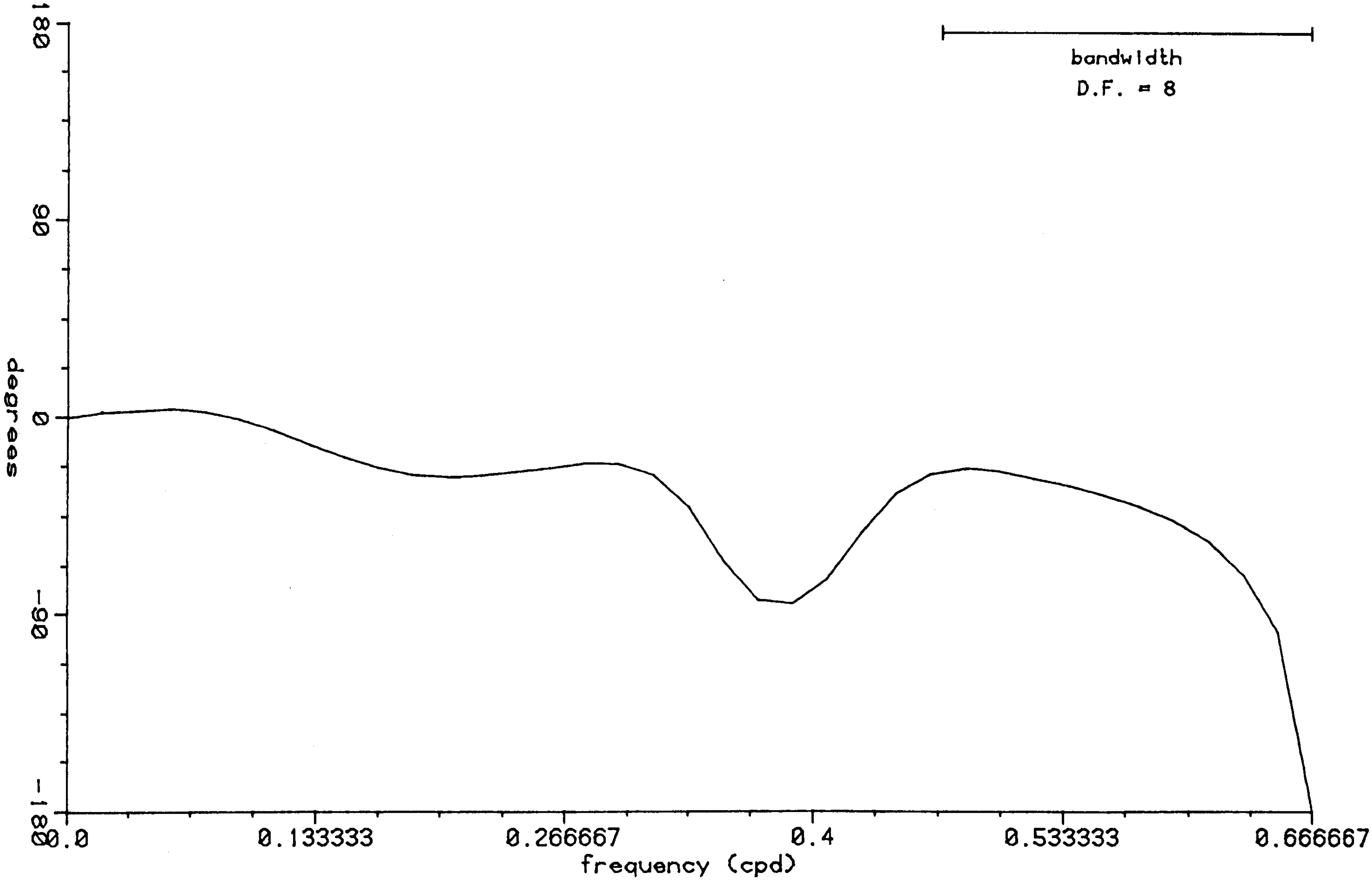

FIGURE 43. PHASE SPECTRUM
WAINWRIGHT WIND (33.7 DEGREE COMPONENT) VS. INSHORE
WAINWRIGHT (BOTTOM) DRIFT CURRENT (33.7 DEGREE COMP.)
1751 12 AUG 1981 - 1751 1 SEPT 1981

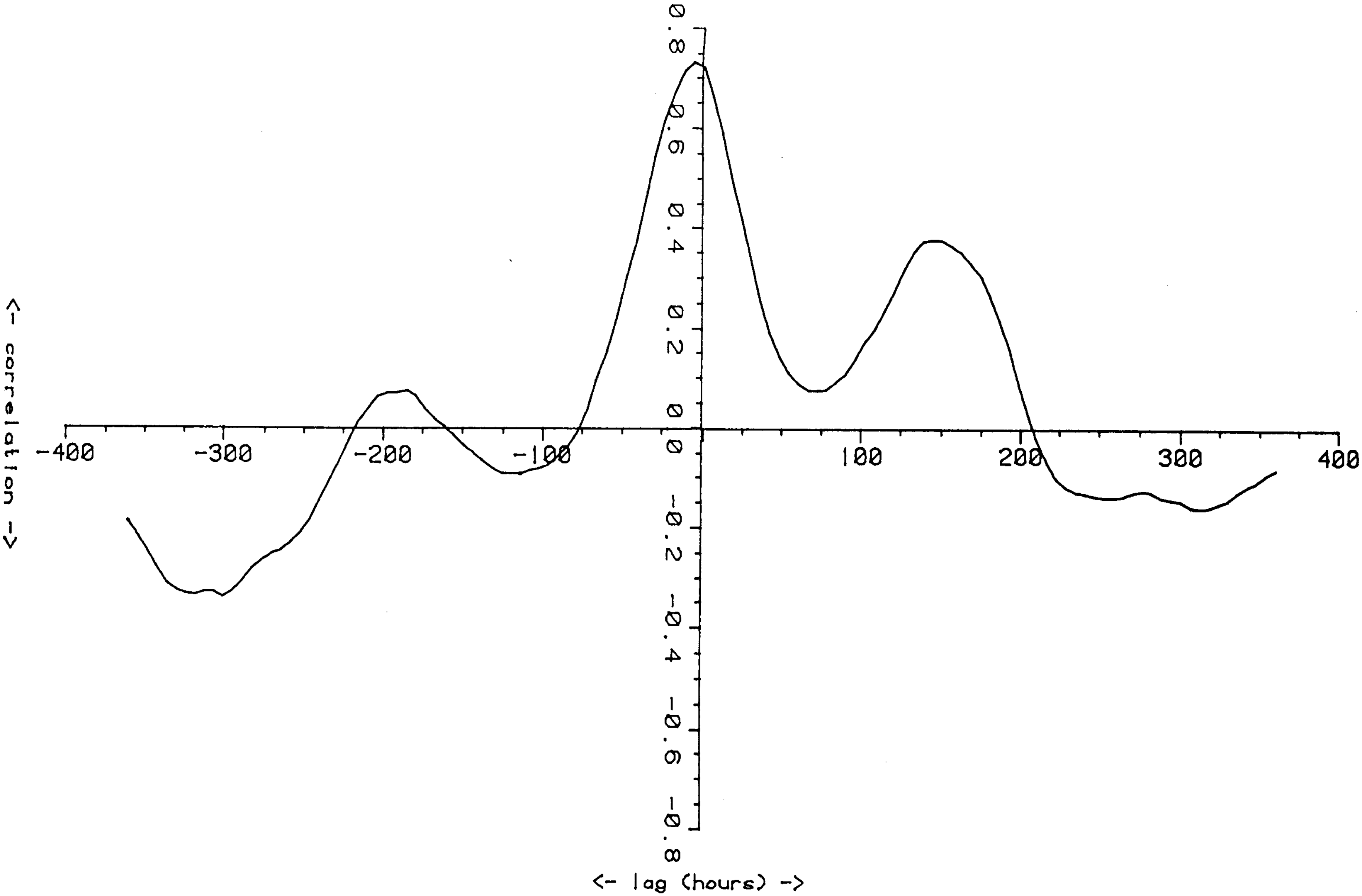

FIGURE 44. CROSS CORRELATIONS
PT. BARROW WIND (35.9 DEGREE COMPONENT) VS. LAGGED INSHORE BARROW (BOTTOM) DRIFT CURRENT (35.9 DEGREE COMPONENT)
0700 8 AUG 1981 - 1300 6 SEPT 1981

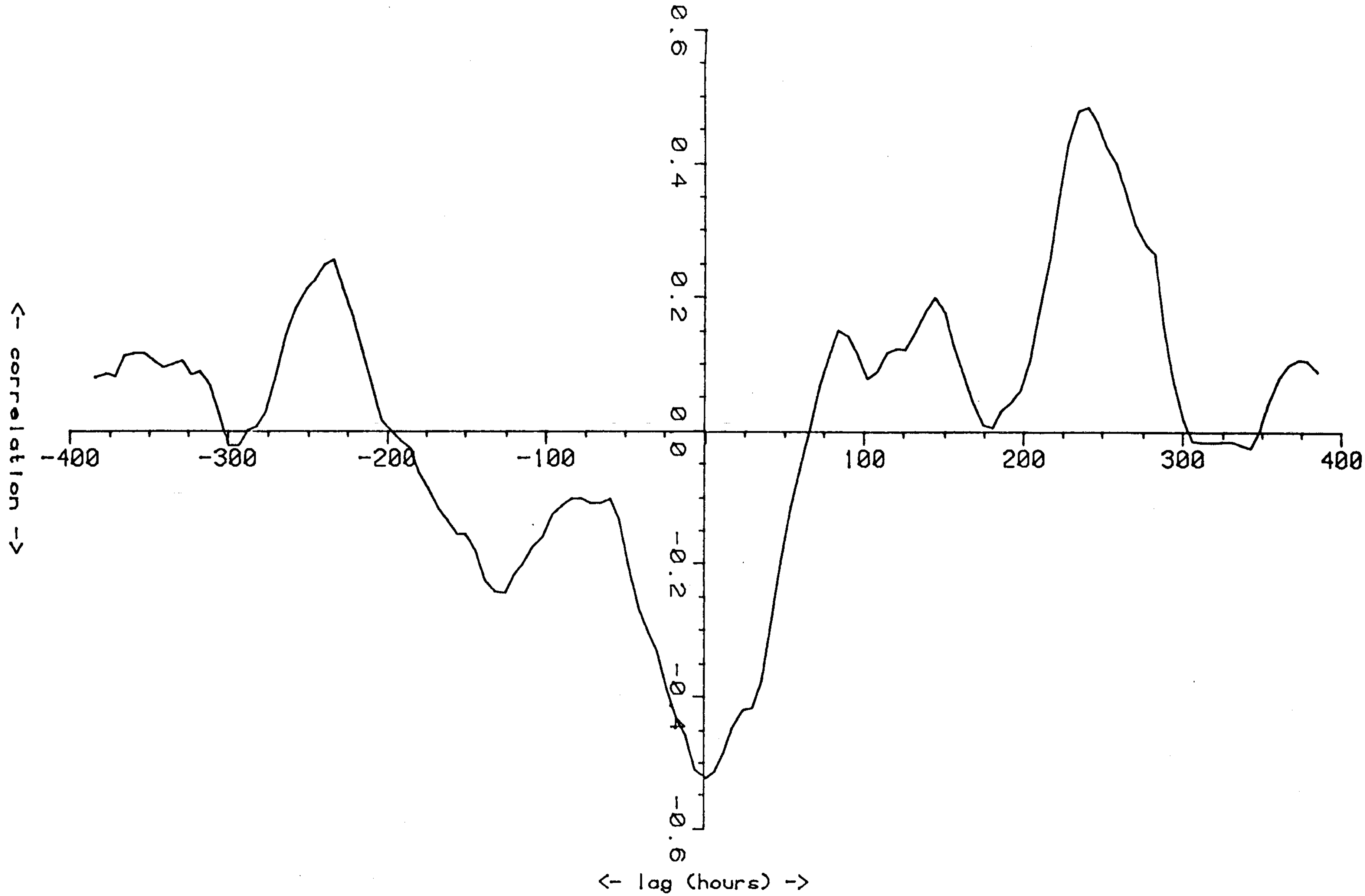

FIGURE 45. CROSS CORRELATIONS
PT. BARROW - CAPE LISBURNE BAROMETRIC PRESSURE DIFFERENCES
VS. LAGGED WAINWRIGHT WINDS
2359 3 AUG 1981 - 1759 4 SEPT 1981

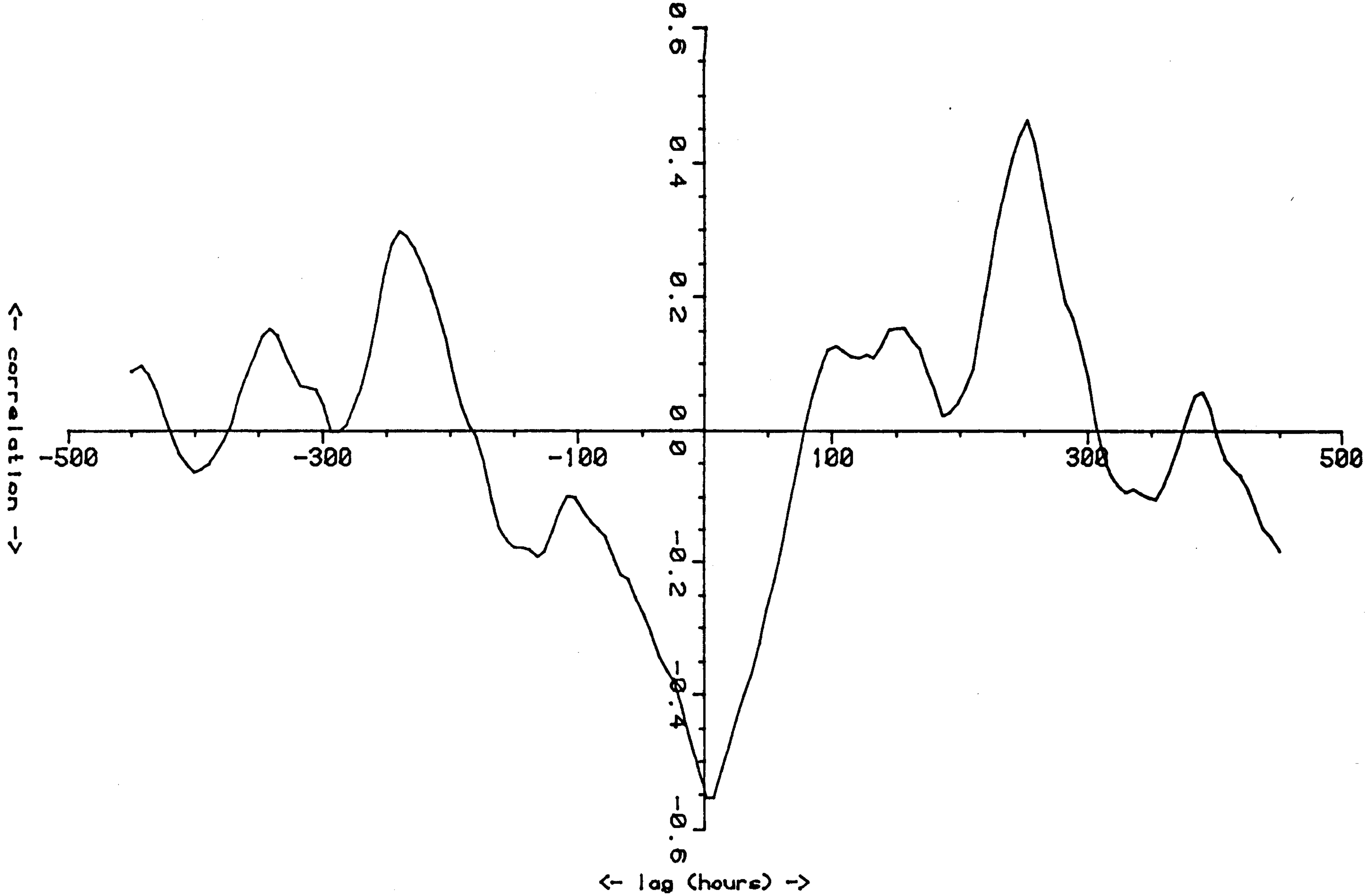

FIGURE 46. CROSS CORRELATIONS
PT. BARROW-CAPE LISBURNE BAROMETRIC PRESSURE DIFFERENCES VS.
LAGGED PT. BARROW WIND (35.9 DEGREE COMPONENT)
0158 1 AUG 1981 - 1358 4 SEPT 1981

The vertical profiles included in the appendix generally show pycnoclines varying between 5 to 10 meters depth inshore and deepening to about 15 meters depth further offshore. The hydrographic section plots (Figures 12 through 18) generally indicate cooler, more saline water upwelling close to shore, though not all transects are consistent. No apparent correlation exists in these limited number of transects with the simultaneous upcoast or downcoast flow regimes during which sampling took place. With reference to Figures 12 through 18, downcoast flow regimes were prevalent during the Pt. Barrow and Skull Cliffs transects; transitory flow during the Pt. Belcher transect; upcoast flow during the Pingorarok Pass, Akunik Pass, and Icy Cape transects; and downcoast flow again during the Wainwright transect.

Comparisons of the salinity/temperature time series obtained for the Pt. Barrow moorings are shown in Figure 47 along with the respective current records. Temperatures and salinities obtained from individual meters are clearly related; however, the records from the different meters at other depths and locations are not closely similar. Also consistent variations of the temperature/salinity with respective current regimes are not present in these records.

The inshore record indicates that wide variations of temperature and salinity occur in this shallow water. Temperatures during this month of record vary from about +6°C to -1.5°C. Corresponding salinities varied from 26 to 34 $^{o}/oo$ (parts per thousand). The existence of sharp fronts are also indicated, not correlating in time however, with variations in measured currents. The offshore records indicate similar temporal variations, though of somewhat lesser amplitudes (particularly for salinity) in the deeper locations.

Thus the available temperature/salinity data for this Chukchi Sea coastal area indicate temporal and spatial patchiness in water masses, probably due to variable contributions of ice melt, upwelling, wind mixing, solar heating, and freshwater inputs, moved by atmospherically forced current events.

Drogue Dispersion Data

The twelve current drogues tracked by means of the MiniRanger III system on 20 August off Wainwright moved downcoast to the southwest and spread as shown in Figure 20 above. A comparison of the movement of the centroid of these drogues with the currents measured by means of the moored meters at Wainwright is included in Table 6.

The overall movement of the drogues was downcoast parellel to the bathymetry, though the weather and coastal currents were in the process of changing. The current meter

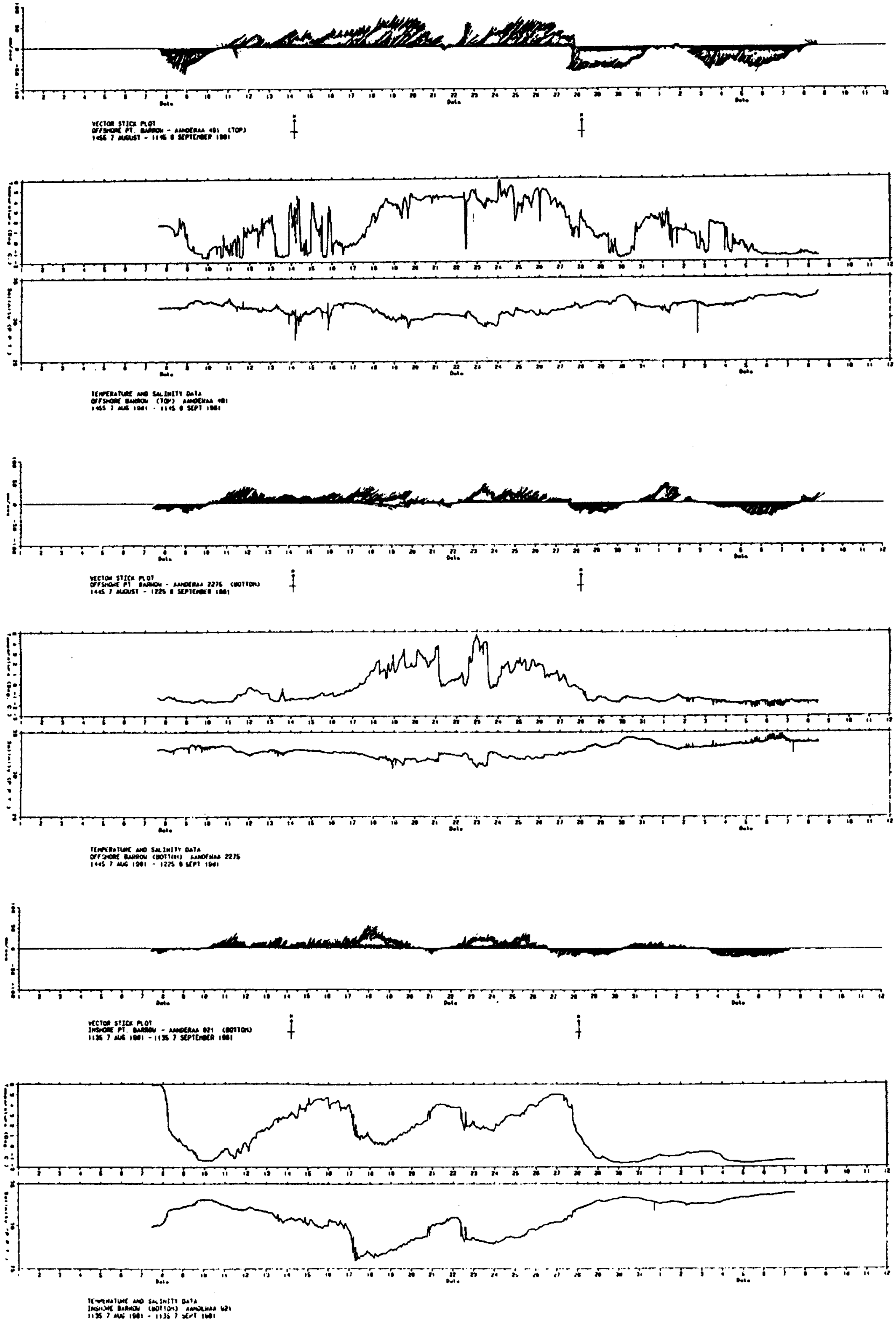

Figure 47. Comparisons of Temperature/Salinity Time Series and Current Records

Table 6. Analysis of Wainwright Current Drogue Trajectories.

Time	Mean Wind		Mean Drogue Movement		Mean Current Movements					
					Inshore (13m)		Offshore (9.7m)		Offshore (29m)	
	Speed cm/sec	Direction °True	Speed cm/sec	Direction True	Speed cm/sec	Direction °True	Speed cm/sec	Direction °True	Speed cm/sec	Direction °True
1336-1438	257	120	4.9	S	17	200	12.5	90	18	100
1438-1536	77	115	6.4	SW	17	200	10.0	90	18	120
1536-1636	0	-	5.1	S	17	195	12.5	90	17	140
1636-1735	206	90	9.4	S	15	195	12.5	100	15	140
1735-1835	103	135	11.6	S	17	190	12.5	110	13	150
1835-1938	206	100	16.2	SWS	18	190	12.5	120	8	140
1938-2038	230	136	22.7	SW	19	195	10.0	150	7	160
2038-2205	257	175	77.8	SW	20	195	12.5	180	5	180
2205-2255	No data		23.5	SW	21	190	12.5	200	6	180
2255-2323	No data		18.2	W	23	195	12.5	210	6	180

records (Table 6) illustrate that the downcoast flow still predominated during the time of the drogue tracking experiment. Overall mean drogue speeds of approximately 13 cm/sec were close to the speeds indicated by the top offshore current meter.

Dispersion statistics for the spread of the drogues about the centroid have been presented above in Table 3. Variances about the centroid for both the minor and major axis are graphed in Figure 21. Associated diffusivities of about $9 \times 10^4 cm^2/sec$ are about one half those measured in Prudhoe Bay previously, but about an order of magnitude higher than those measured in Harrison Bay in one experiment in 1979 (Wilson et al. 1981).

CONCLUSIONS

Coastal Currents

Coastal currents measured at Point Barrow and at Wainwright along the Chukchi Sea coast show both northeast (upcoast) and southwest (downcoast) flows. Speeds ranged up to 50 cm/sec (1 knot), but with up to 100 cm/sec being measured offshore Point Barrow in the vicinity of the Barrow submarine canyon. Although upcoast flow was predominant, downcoast flows occurred from 33 to 47 percent of the time in these different current records.

All current records taken inshore and offshore, at both Point Barrow and Wainwright, showed close similarities in directions, magnitudes, and other features such as in the times of change and in the shapes of the current vector plots. These similarities were very consistent throughout the records. Statistical cross correlations of these current meter time series yielded a correlation coefficient at zero lag of 0.90 for inshore records taken at Point Barrow and at Wainwright.

Meteorological Forcing

Visual comparisons of the current meter time series data with similar plots of atmospheric pressure differences between Point Barrow - Cape Lisburne (also Pt. Barrow - Nome) show strong correlations. High pressure at Point Barrow relative to the southern stations is strongly correlated with downcoast flow. Conversely, low or negative pressure differences are strongly associated with upcoast flow.

Cross correlations of these time series current data with the pressure difference series (Pt. Barrow - Cape Lisburne) indicate high negative correlation coefficients of -0.81 and -0.85 for the Wainwright and Pt. Barrow current data respectively, confirming the similarities observed visually.

Visual cross correlations of the local winds with the currents were not quite as evident as with the atmospheric pressures. Cross correlation coefficients of 0.65 and 0.72 were obtained for the Wainwright and Point Barrow cases respectively. Correlation coefficients of the local winds with the pressure differences were only 0.52 and 0.56 for Wainwright and Point Barrow.

Thus the high correlations between the individual current records, plus the high correlations of these currents with the atmospheric pressure difference along the coast, indicates that these shallow, nearcoast currents are driven by the same atmospheric pressure forcing function all along this stretch of coast.

Hydrographic Transects

The hydrographic transect data, along with temperature/salinity time series data show highly variable temperature and salinity conditions in this nearshore area. Pycnoclines are evident between 5 and 10 meters depth inshore, deepening offshore to 10-15 meters. Hydrographic section plots generally indicate cooler, more saline water upwelling close to shore, though not always consistent or correlated with upcoast or downcoast flow regimes. Temperatures varied from below -1.5°C up to +6°C, salinities from 34^o/oo down to 26^o/oo. Features of sharp fronts are also evident in the time series data. The temporal and spacial patchiness in water masses is probably due to variable contributions of ice melt, upwelling, wind mixing, solar heating, and freshwater inputs modifying the source waters of the Chukchi Sea, and transported by currents driven by atmospheric pressure forcing.

Drogue Dispersions

Twelve current drogues released off Wainwright drifted downcoast parallel to the shoreline and in general agreement with measured coastal currents. Diffusivity values, derived from spreading of the drogues about the centroid, ranged up to 9×10^3 cm^2/sec.

REFERENCES

1. Coachman, L.K. 1963. Water masses of the Arctic. Proc. Arctic Basin Symposium, October 1962, Hershey, PA. Arctic Institute of North America. Tidewater Publishing Co., Centreville, MD. pp143-167.

2. Coachman, L.K., K. Aagaard, and R.B. Tripp. 1975. Bering Strait, the Regional Physical oceanography. University of Washington Press, Seattle, WA. 172pp.

3. Fleming, R.H. and D. Heggarty. 1966. Oceanography of the southern Chukchi Sea In: Wilimovsky, N.J. and J.N. Wolfe (eds), Environments of the Cape Thompson Region, Alaska. Atomic Energy Commission, Oak Ridge, TN. pp697-754.

4. Ichiye, T., C. Mungall, M. Inoue, D. Horne. 1978. Gulf of Mexico Dispersion Calculations. Texas A&M University, Department of Oceanography, Report 78-10-T.

5. Ingham, M.C. and B.A. Rutland. 1972. Physical oceanography of the eastern Chukchi Sea off Cape Lisburne-Icy Cape In: Ingham, M.C. et al. (eds.), WEBSEC-70, An Ecological Survey of the Eastern Chukchi Sea, September-October 1970. U.S. Coast Guard Oceanographic Report 50, C6373-50. pp1-86.

6. Jenkins, G.M. and D.G. Watts. 1968. Spectral Analysis Applications. Holden-Day Publishing, San Francisco.

7. Mountain, D.G., L.K. Coachman and K. Aagaard. 1976. On the flow through Barrow Canyon. J. Phys. Oceanogr. 6:461-470.

8. Okubo, A., C.C. Effesmeyer, and J.M. Helseth. 1976. Determination of lagrangian deformations from analysis of current followers. J. Phys. Oceanogr. 6:524-527.

9. Paquette, R.G. and R.H. Bourke. 1974. Observations of the coastal current of arctic Alaska. J. Mar. Res. 32:195-207.

10. Wilson, D.E. et al. 1981. Numerical Trajectory Modeling and Associated Field Measurements in The Beaufort Sea and Chukchi Sea Nearshore Areas. Kinnetic Laboratories Inc. Annual Report Research Unit 531, Contract NA79RAC00086, NOAA/OCSEAP Report No. KLI-81-9.

11. Wiseman, W.M.J. and L.J. Rouse. 1980. A coastal jet in the Chukchi Sea. Arctic 33:21-29.

APPENDIX A

Current Meter Data

Principal Axis and

Progressive Vector Plots

Barrow

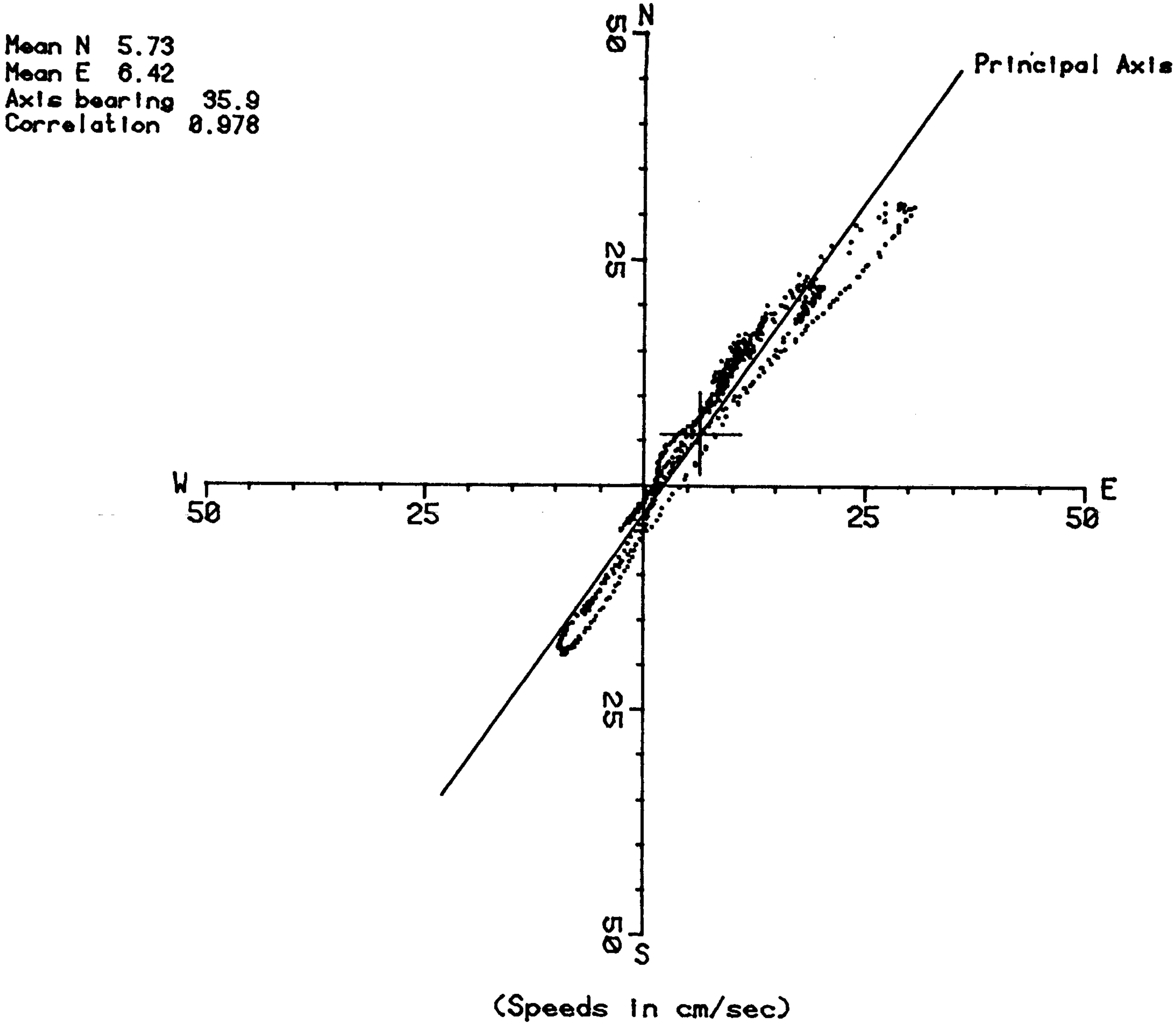

FIGURE A-1 POLAR PLOT - SPEED AND DIRECTION DATA
INSHORE BARROW (BOTTOM) DRIFT CURRENT
0700 8 AUG 1981 - 1600 6 SEPT 1981

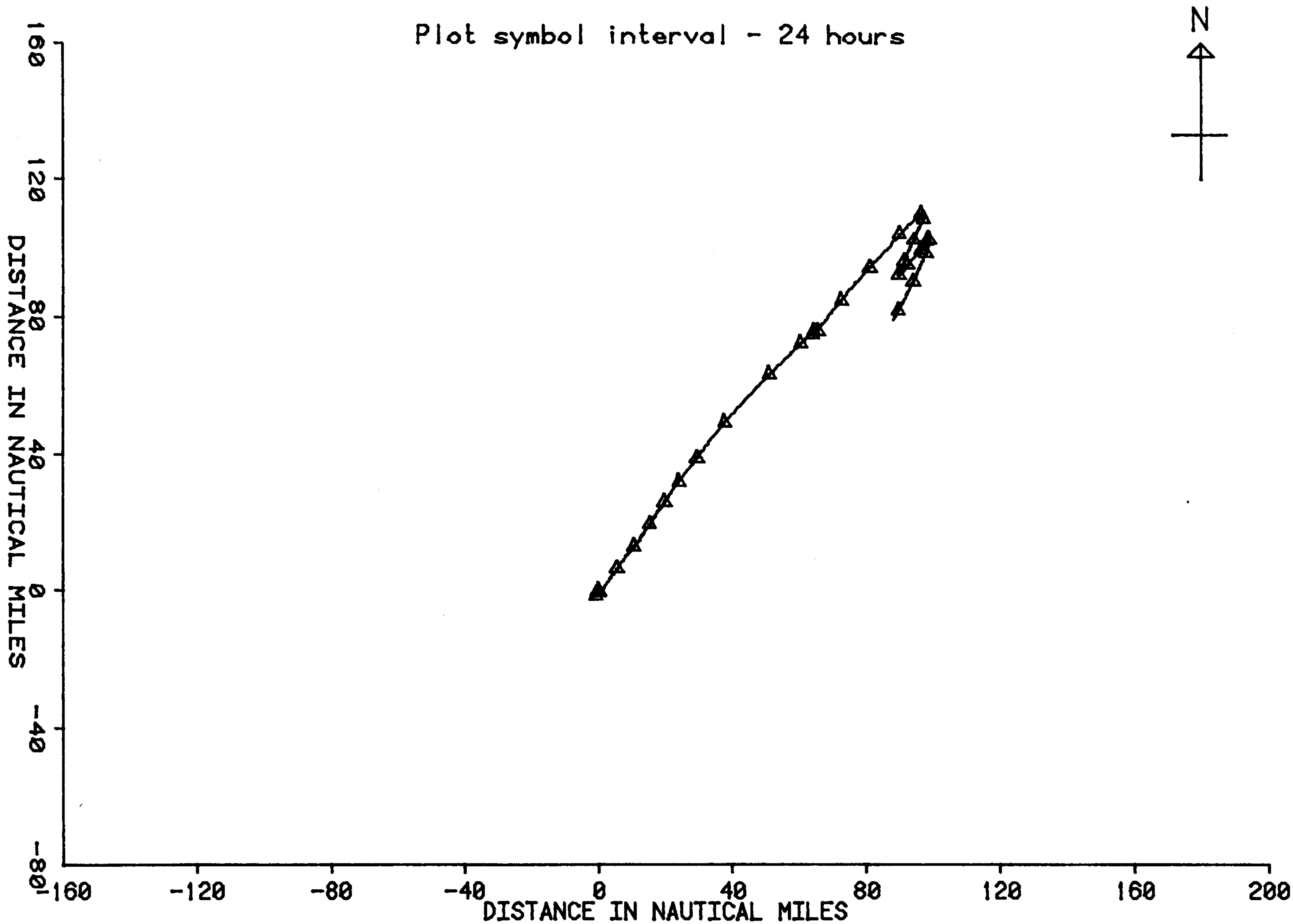

300

FIGURE A-2 PROGRESSIVE VECTOR DIAGRAM
INSHORE BARROW (BOTTOM) DRIFT CURRENT
0700 8 AUG 1981 - 1600 6 SEPT 1981

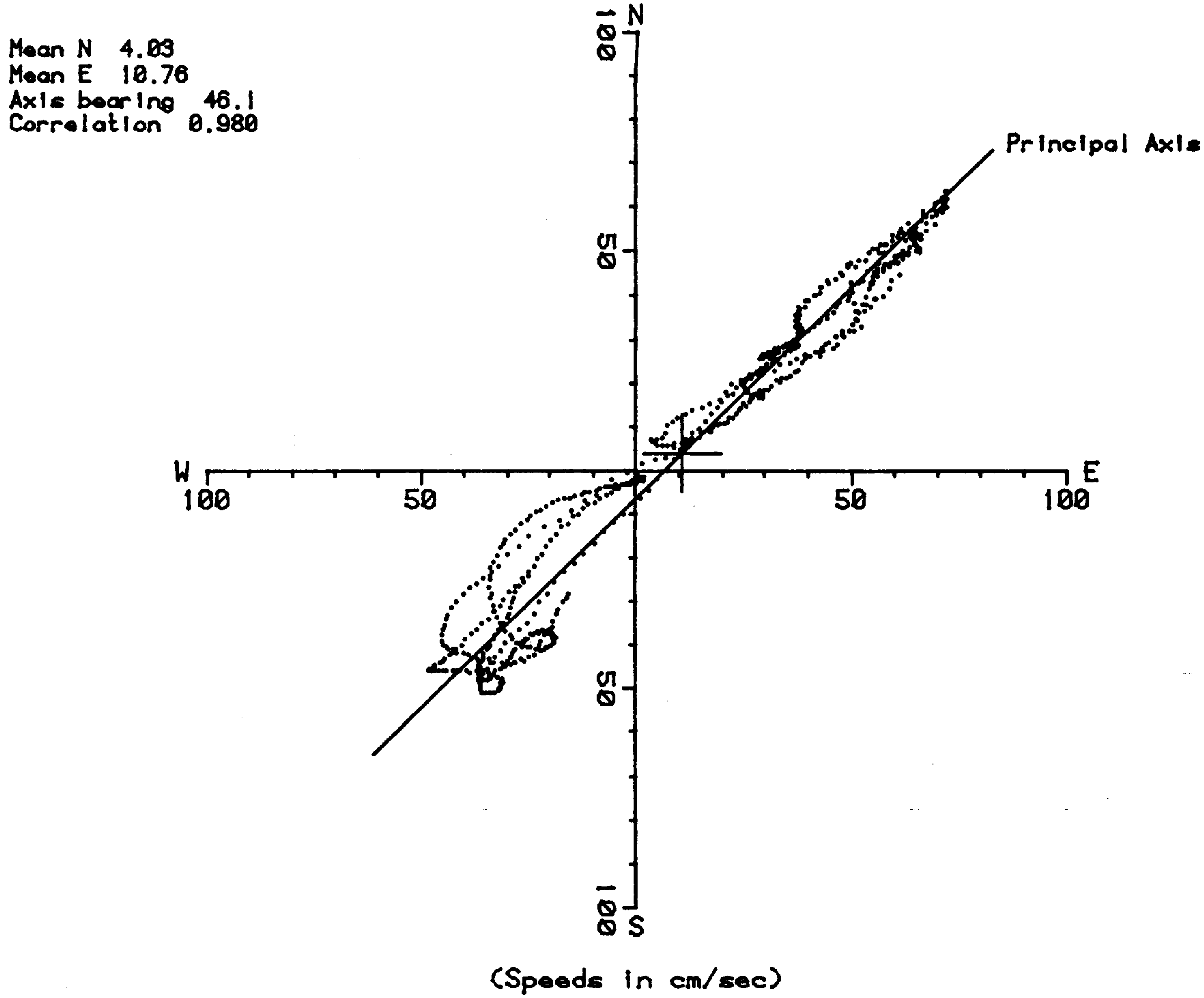

FIGURE A-3 POLAR PLOT - SPEED AND DIRECTION DATA
OFFSHORE BARROW (TOP) DRIFT CURRENT
1020 8 AUG 1981 - 1620 7 SEPT 1981

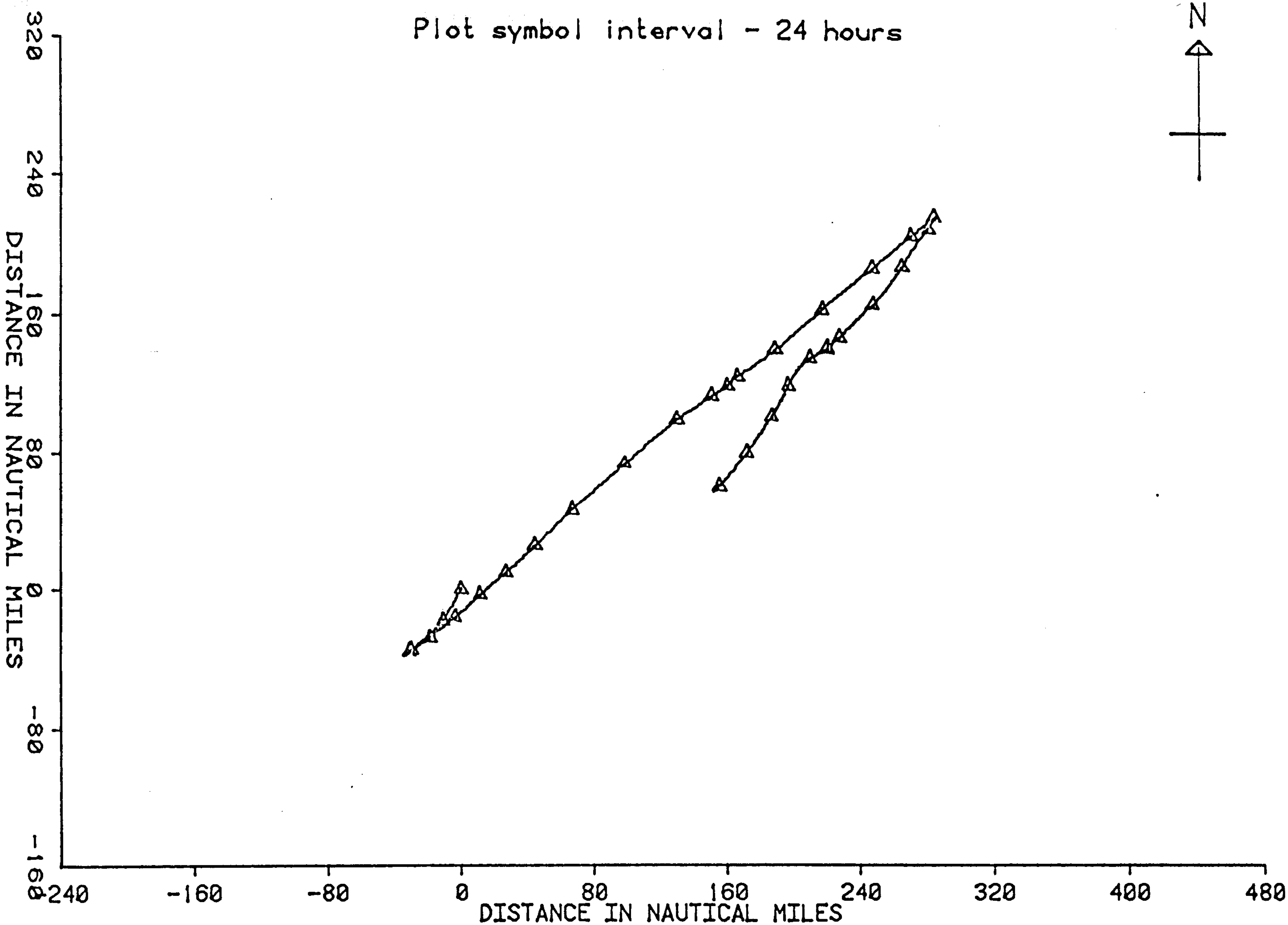

FIGURE A-4 PROGRESSIVE VECTOR DIAGRAM
OFFSHORE BARROW (TOP) DRIFT CURRENT
1020 8 AUG 1981 - 1620 7 SEPT 1981

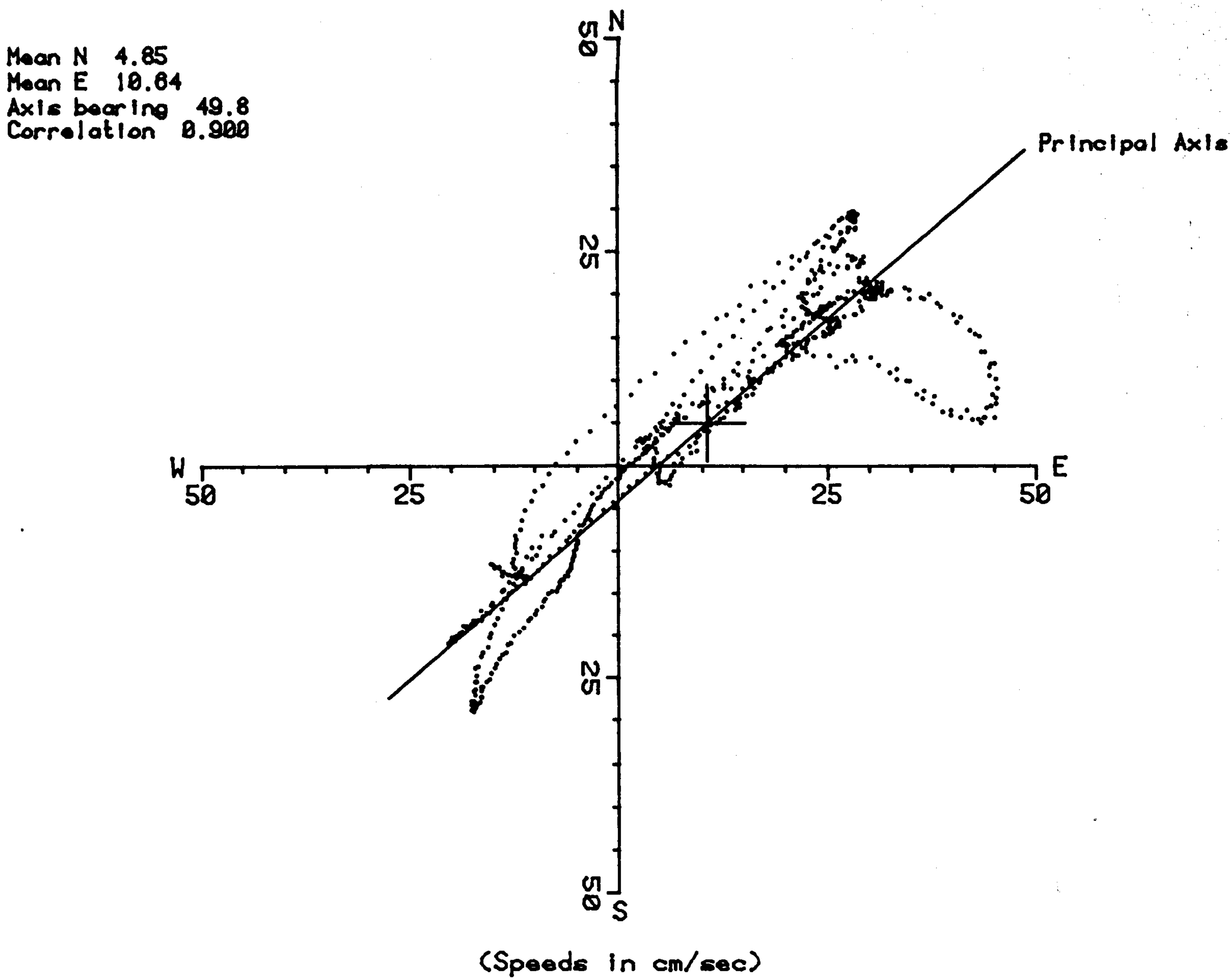

FIGURE A-5 POLAR PLOT - SPEED AND DIRECTION DATA
OFFSHORE BARROW (BOTTOM) DRIFT CURRENT
1010 8 AUG 1981 - 1610 7 SEPT 1981

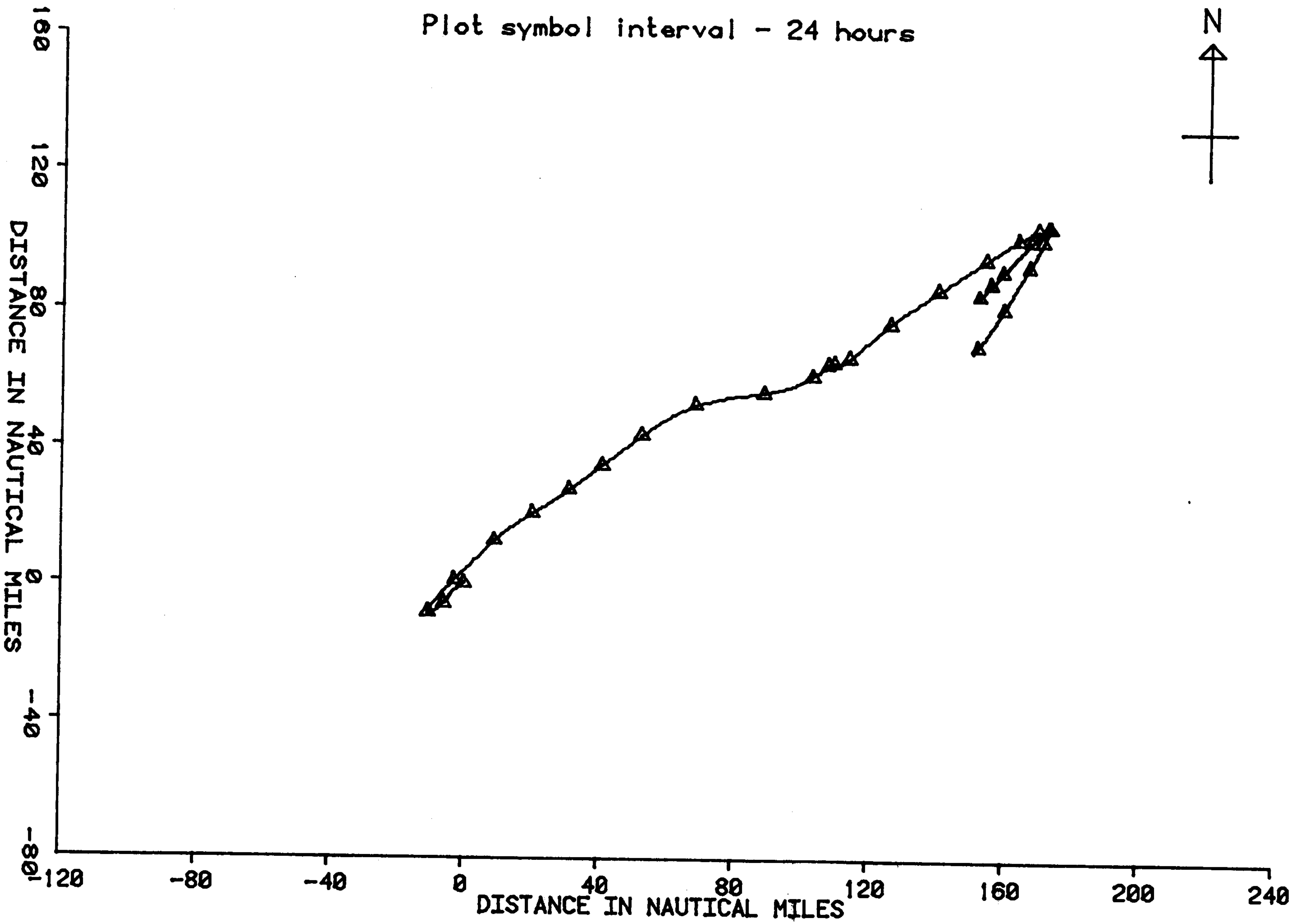

FIGURE A-6 PROGRESSIVE VECTOR DIAGRAM
OFFSHORE BARROW (BOTTOM) DRIFT CURRENT
1010 8 AUG 1981 - 1610 7 SEPT 1981

Principal Axis and Progressive

Vector Plot. Wainwright

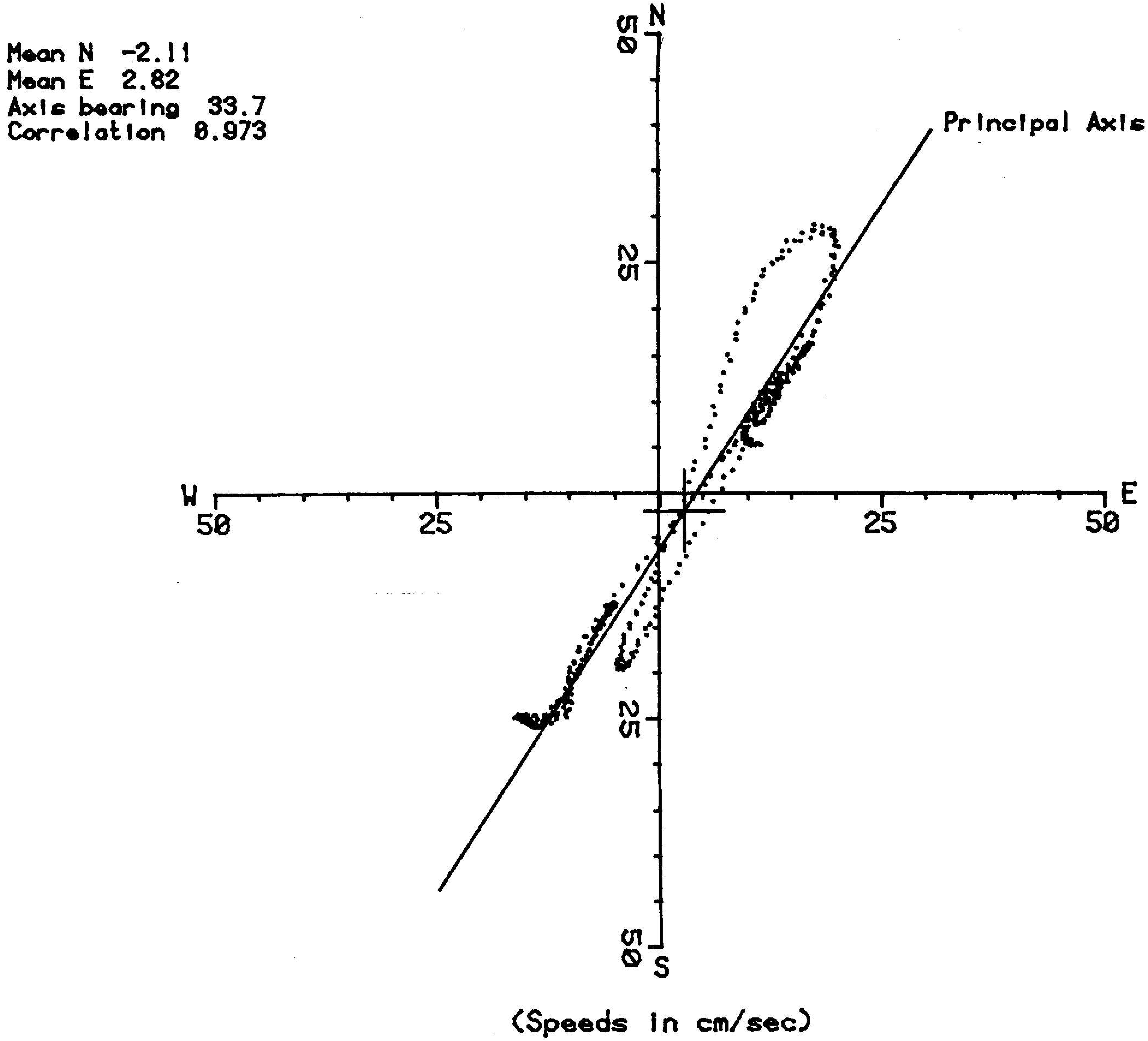

FIGURE A-7 POLAR PLOT - SPEED AND DIRECTION DATA
INSHORE WAINWRIGHT (BOTTOM) DRIFT CURRENT
1342 12 AUG 1981 - 1742 1 SEPT 1981

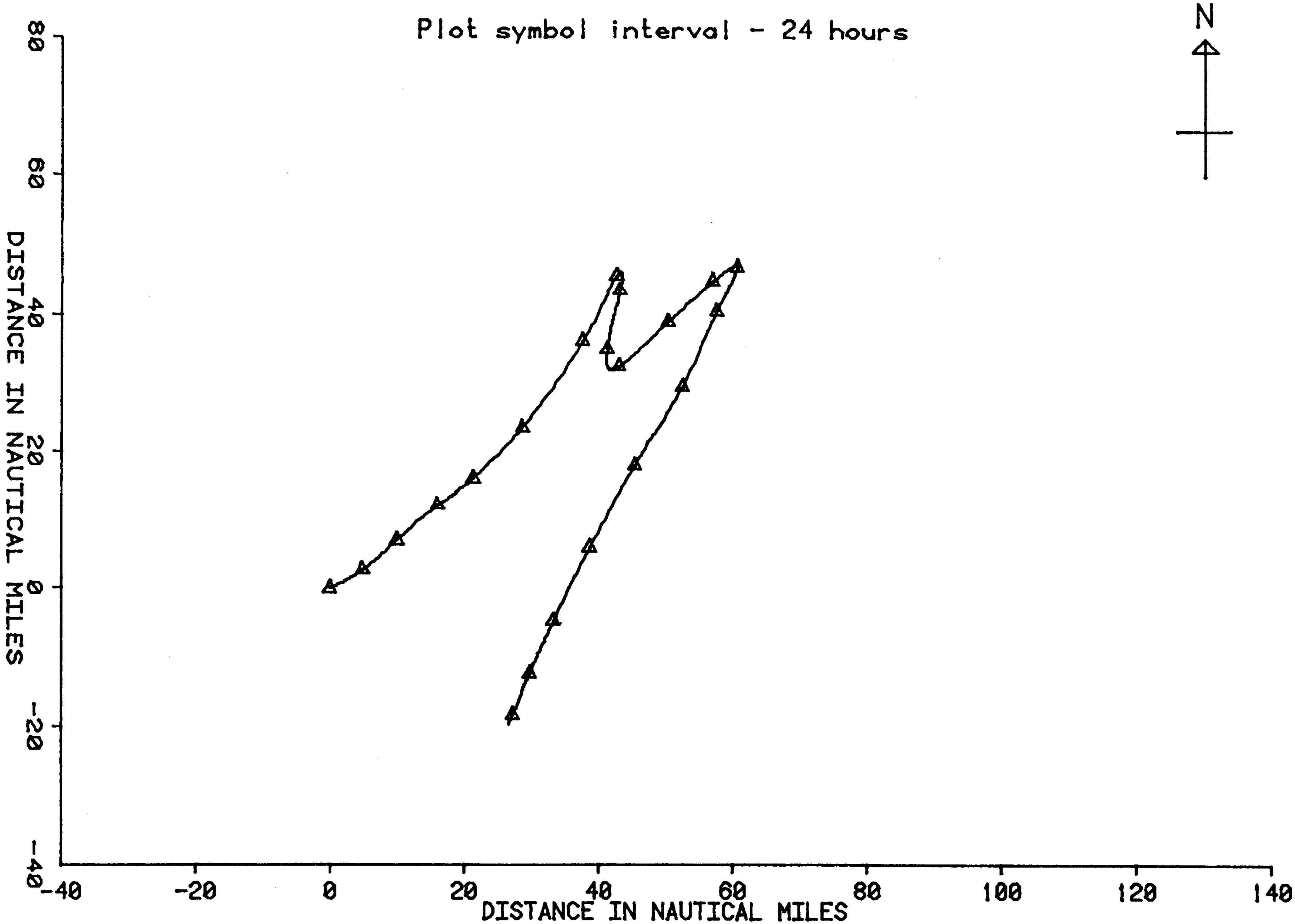

FIGURE A-8 PROGRESSIVE VECTOR DIAGRAM
INSHORE WAINWRIGHT (BOTTOM) DRIFT CURRENT
1342 12 AUG 1981 - 1742 1 SEPT 1981

Mean N 1.77
Mean E 8.85
Axis bearing 68.0
Correlation 0.935

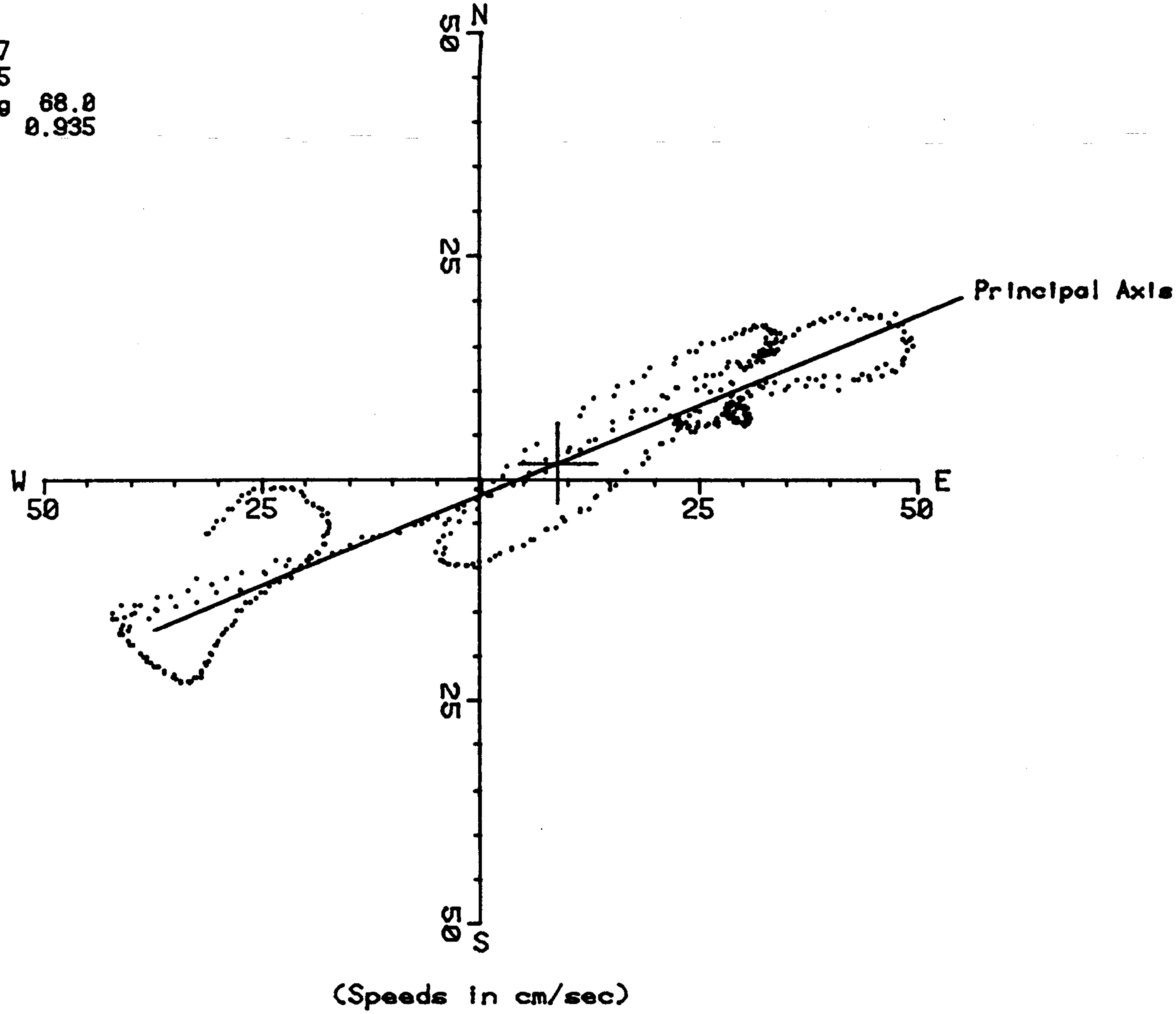

FIGURE A-9 POLAR PLOT - SPEED AND DIRECTION DATA
OFFSHORE WAINWRIGHT (TOP) DRIFT CURRENT
1553 12 AUG 1981 - 1953 1 SEPT 1981

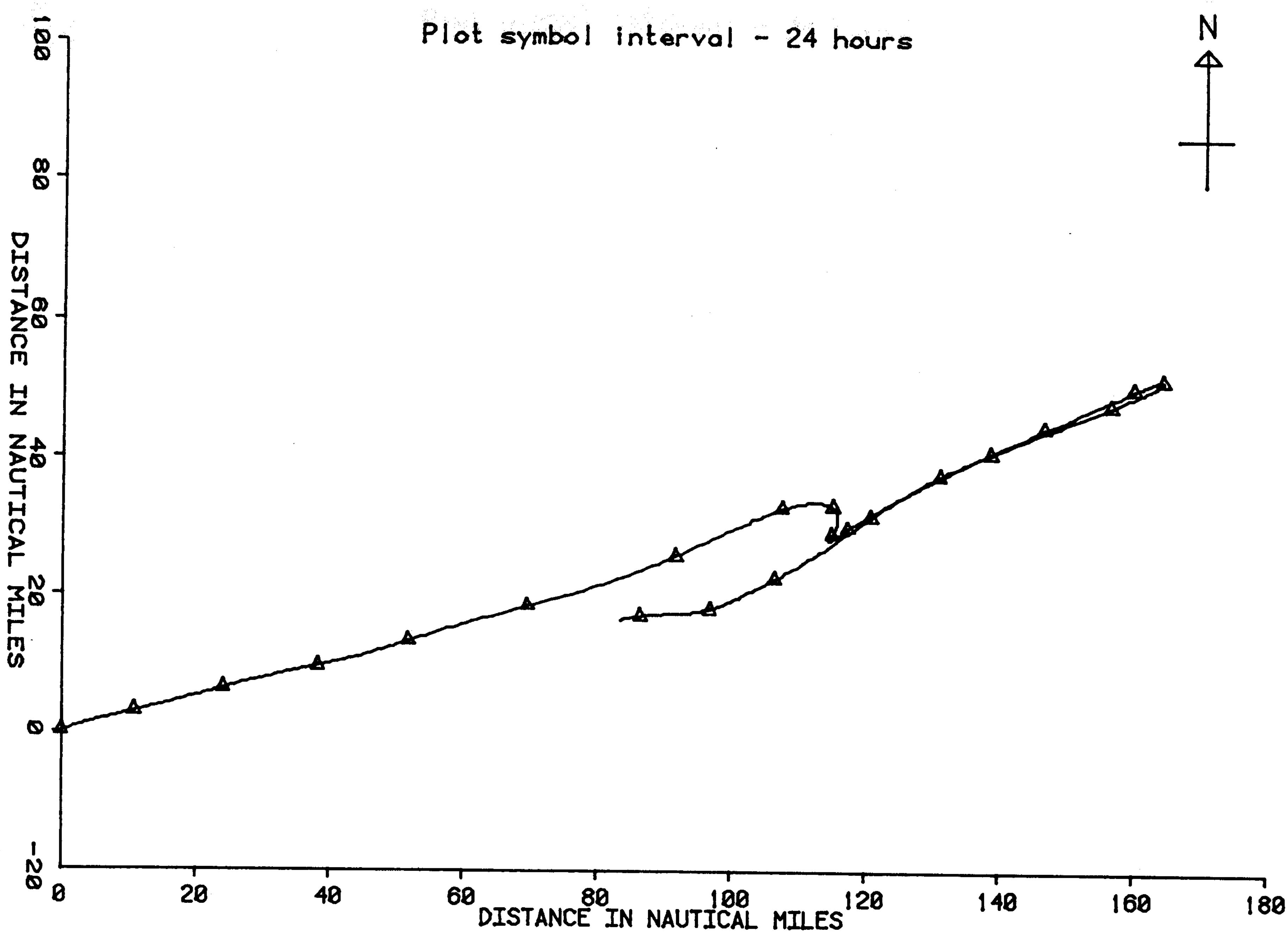

310

FIGURE A-10 PROGRESSIVE VECTOR DIAGRAM
OFFSHORE WAINWRIGHT (TOP) DRIFT CURRENT
1553 12 AUG 1981 - 1953 1 SEPT 1981

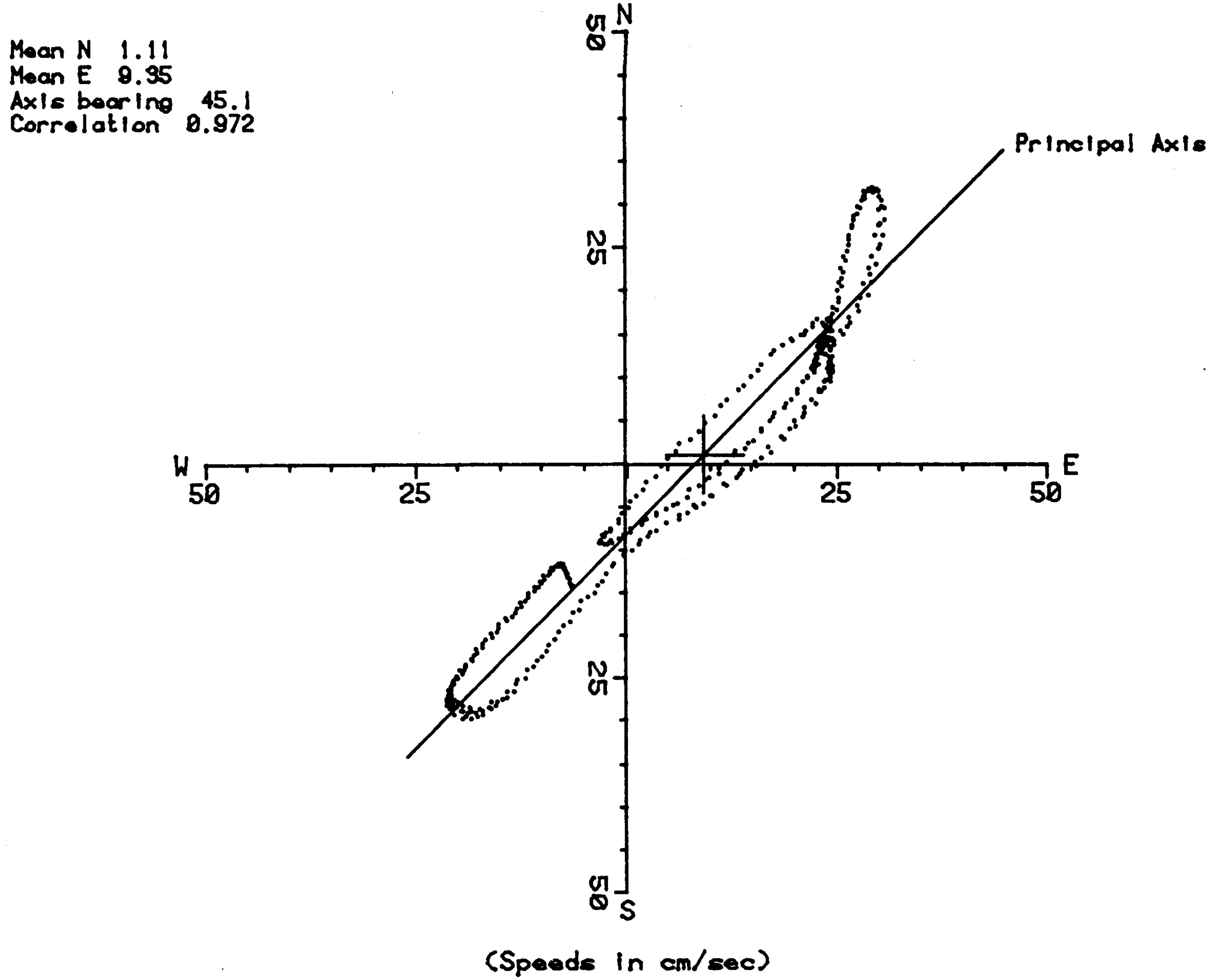

FIGURE A-11 POLAR PLOT - SPEED AND DIRECTION DATA
OFFSHORE WAINWRIGHT (BOTTOM) DRIFT CURRENT
1513 12 AUG 1981 - 2013 1 SEPT 1981

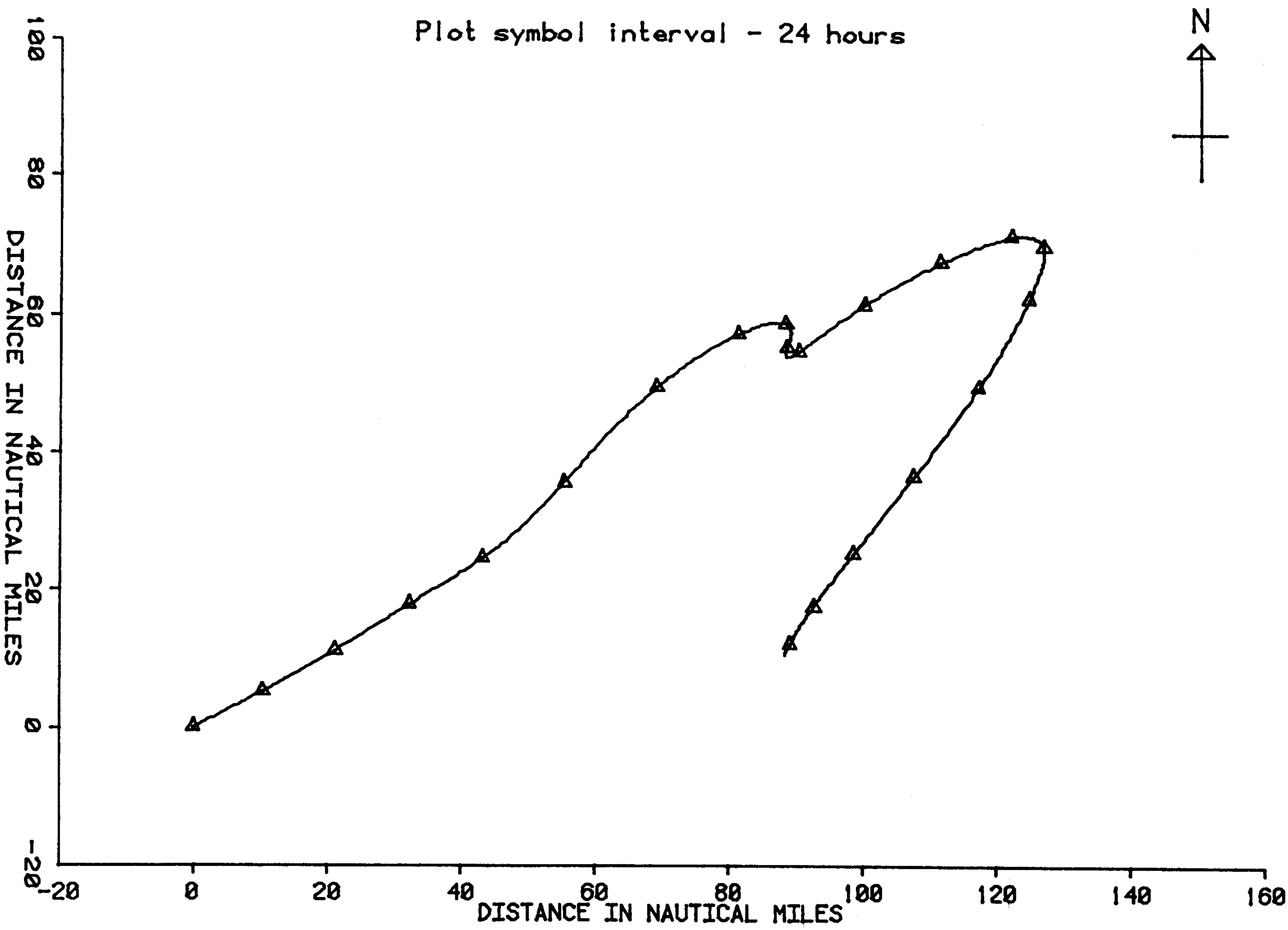

FIGURE A-12 PROGRESSIVE VECTOR DIAGRAM
OFFSHORE WAINWRIGHT (BOTTOM) DRIFT CURRENT
1513 12 AUG 1981 - 2013 1 SEPT 1981

Current Correlations

Barrow/Wainwright

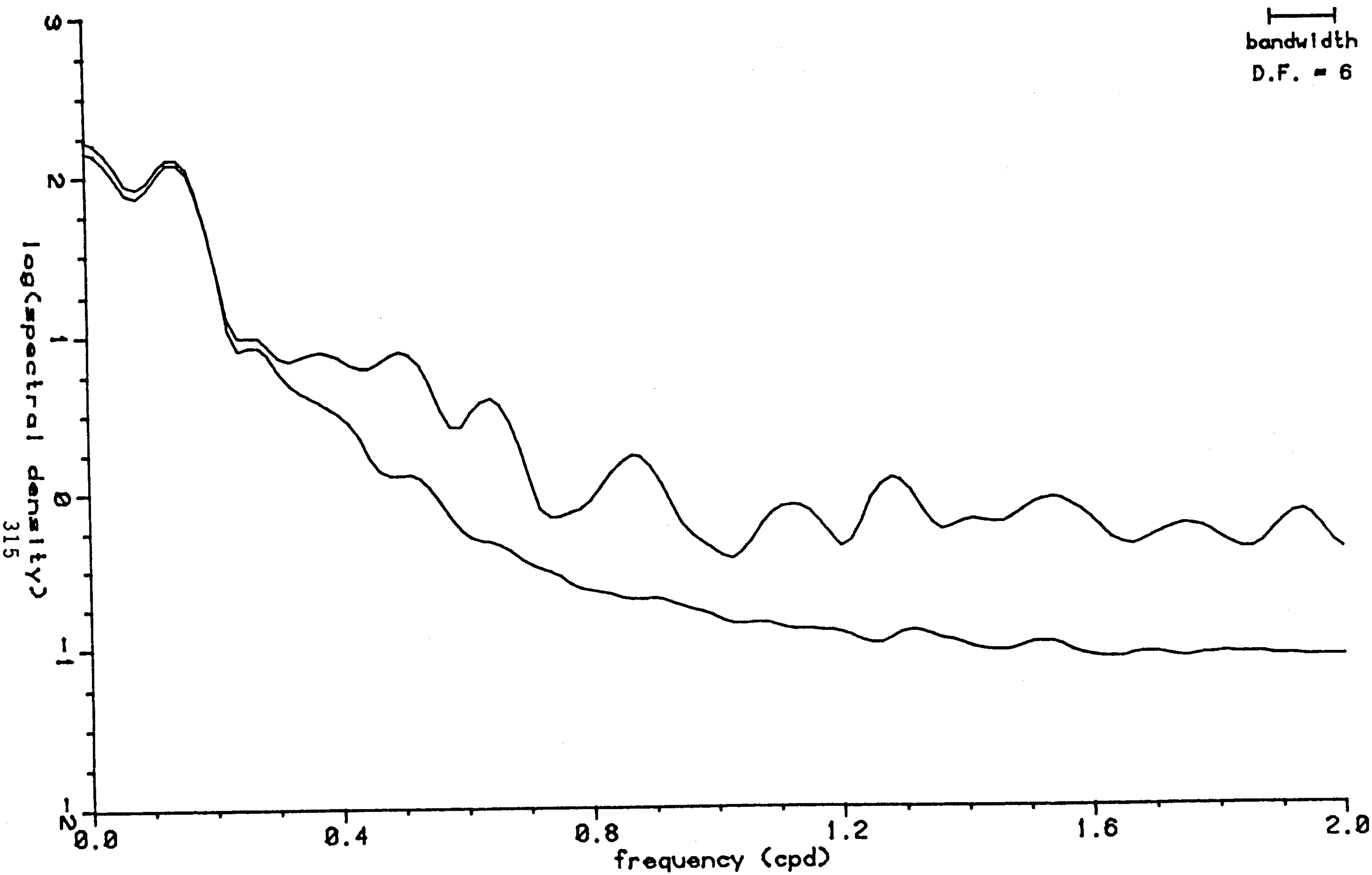

FIGURE A-13 SPECTRAL DENSITY
A) INSHORE BARROW (BOTTOM) DRIFT CURRENT - 35.9 DEGREE COMP.
B) INSHORE BARROW (BOTTOM) CURRENT - 35.9 DEGREE COMP.
0703 8 AUG 1981 - 1303 6 SEPT 1981

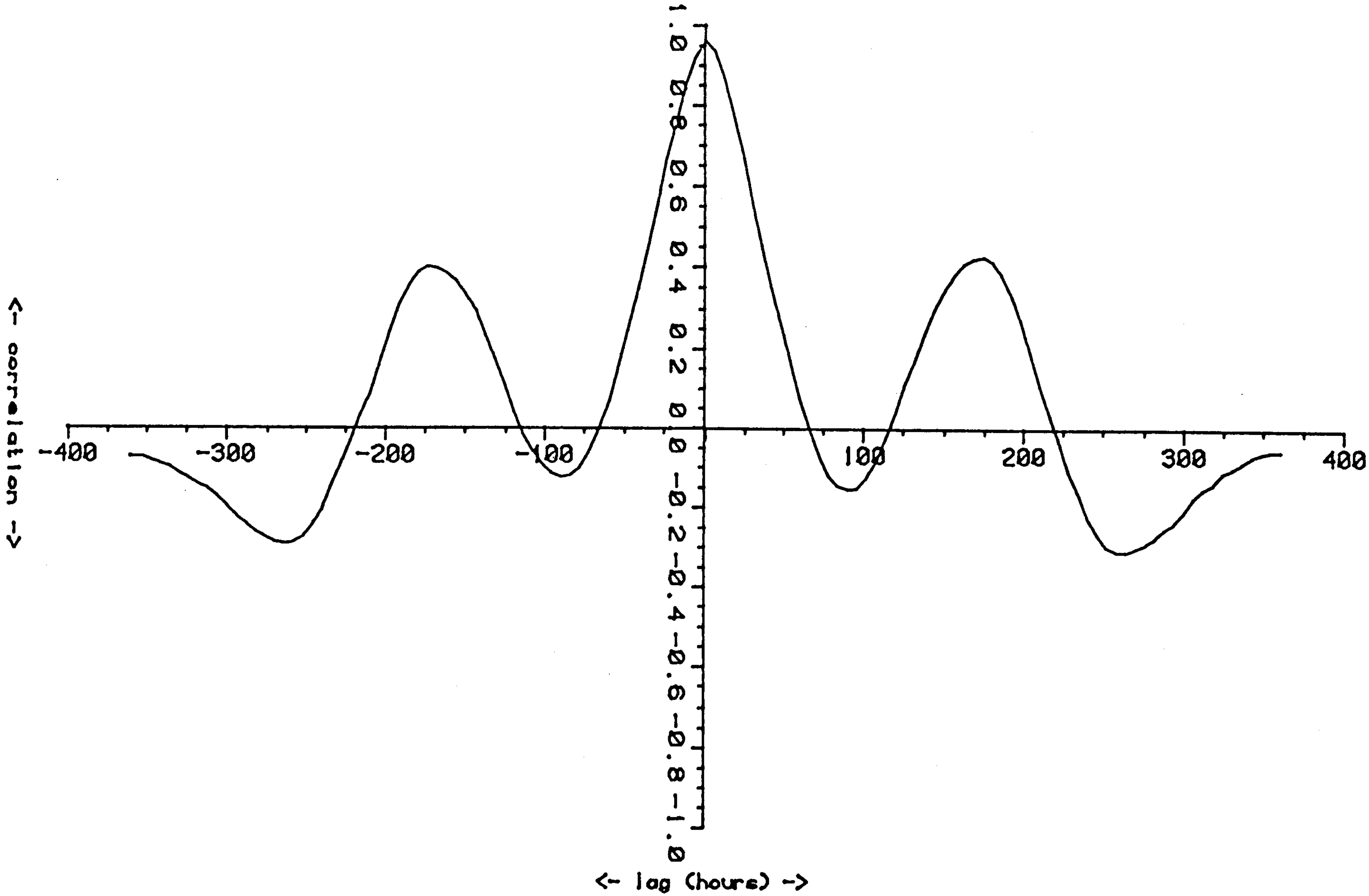

FIGURE A-14 CROSS CORRELATIONS
INSHORE BARROW (BOTTOM) DRIFT CURRENT VS. LAGGED INSHORE
BARROW (BOTTOM) CURRENT (35.9 DEGREE COMPONENTS)
0703 8 AUG 1981 - 1303 6 SEPT 1981

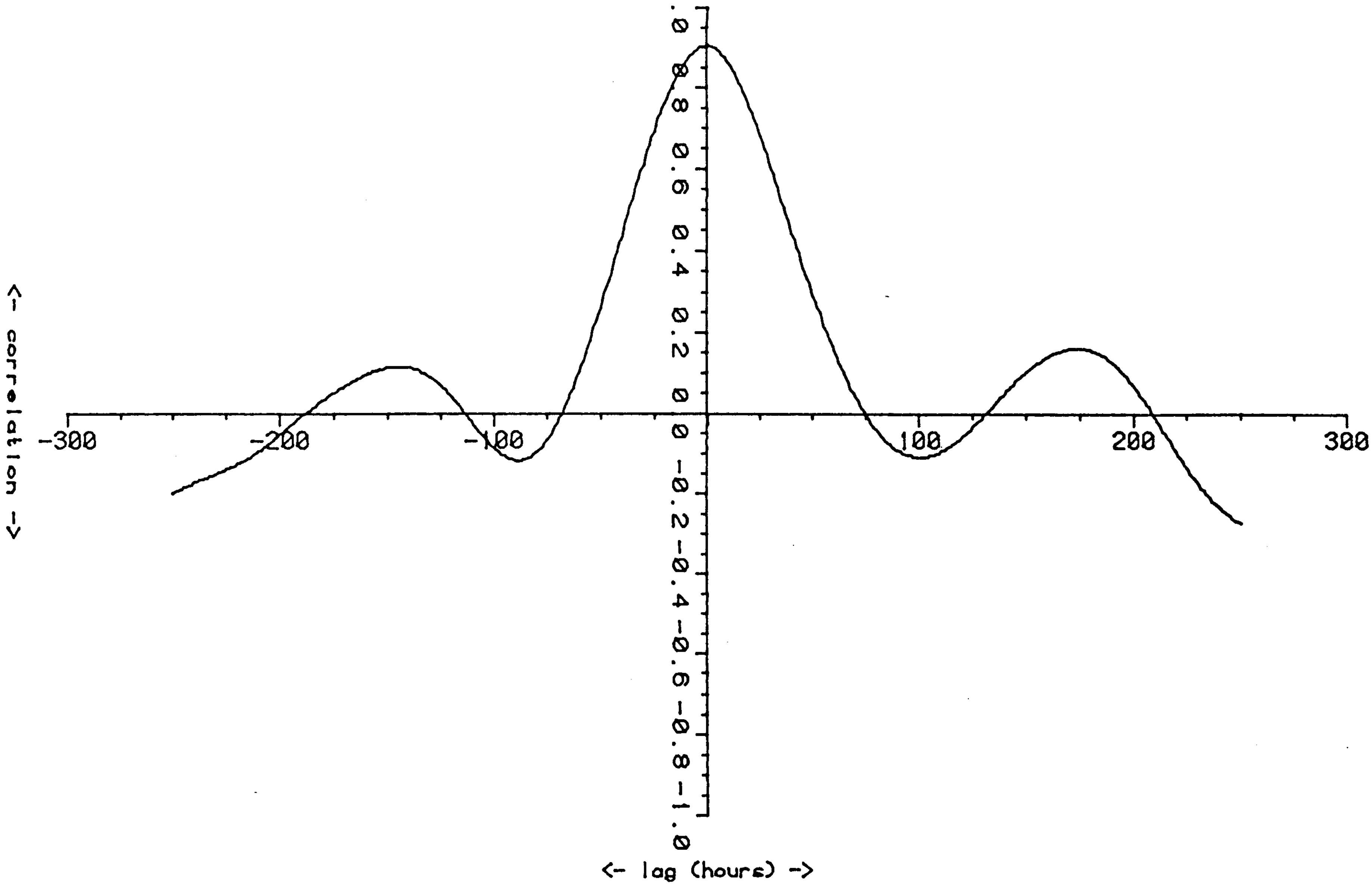

FIGURE A-15 CROSS CORRELATIONS
INSHORE BARROW DRIFT CURRENT (35.9 DEGREE COMPONENT) VS.
LAGGED INSHORE WAINWRIGHT DRIFT CURRENT (33.7 DEG. COMP.)
1251 12 AUG 1981 - 1751 1 SEPT 1981

Pressure vs. Current

Inshore Barrow

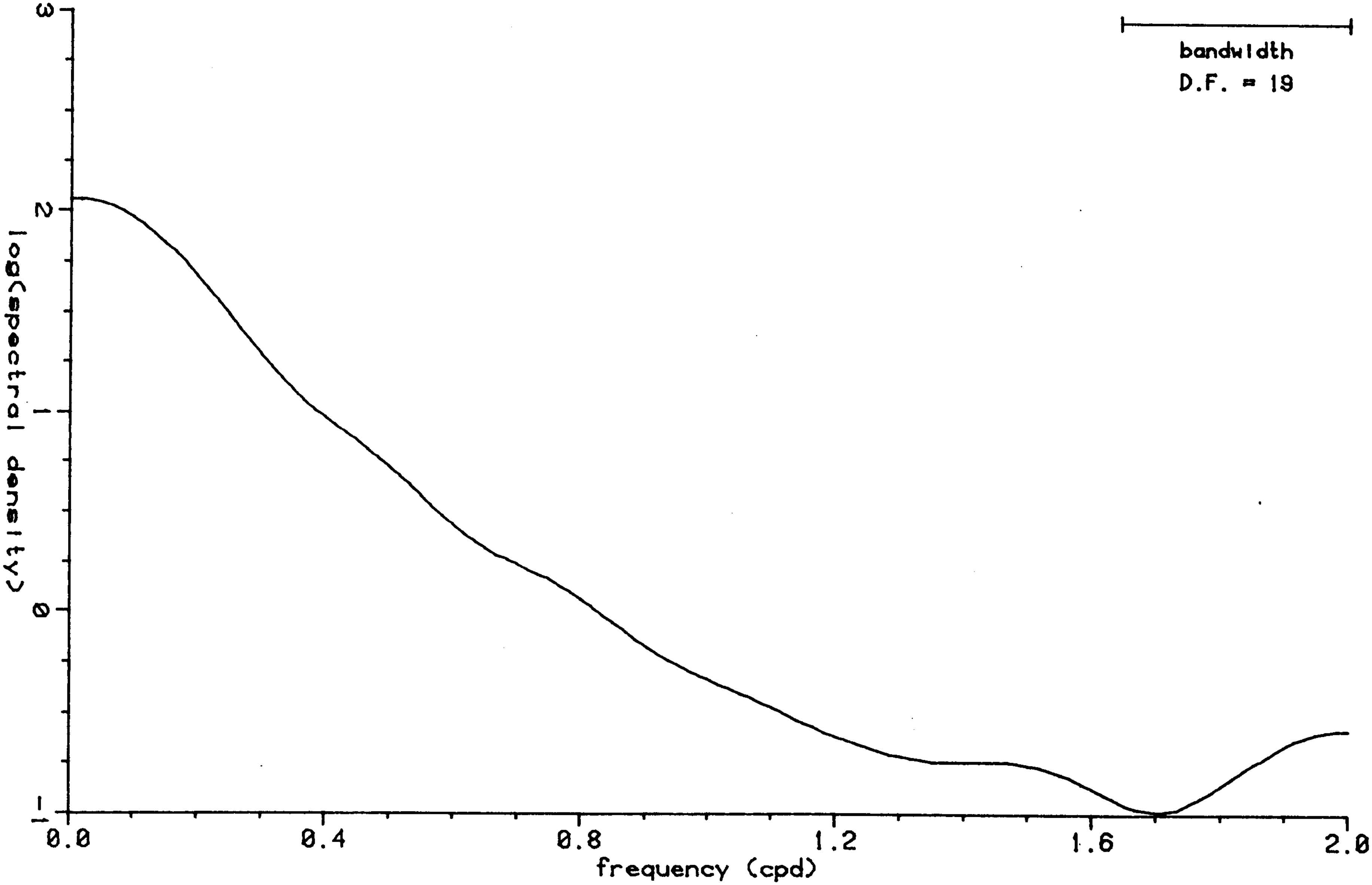

FIGURE A-16 SPECTRAL DENSITY
PT. BARROW - CAPE LISBURNE BAROMETRIC PRESSURE DIFFERENCES
0659 8 AUG 1981 - 1859 4 SEPT 1981

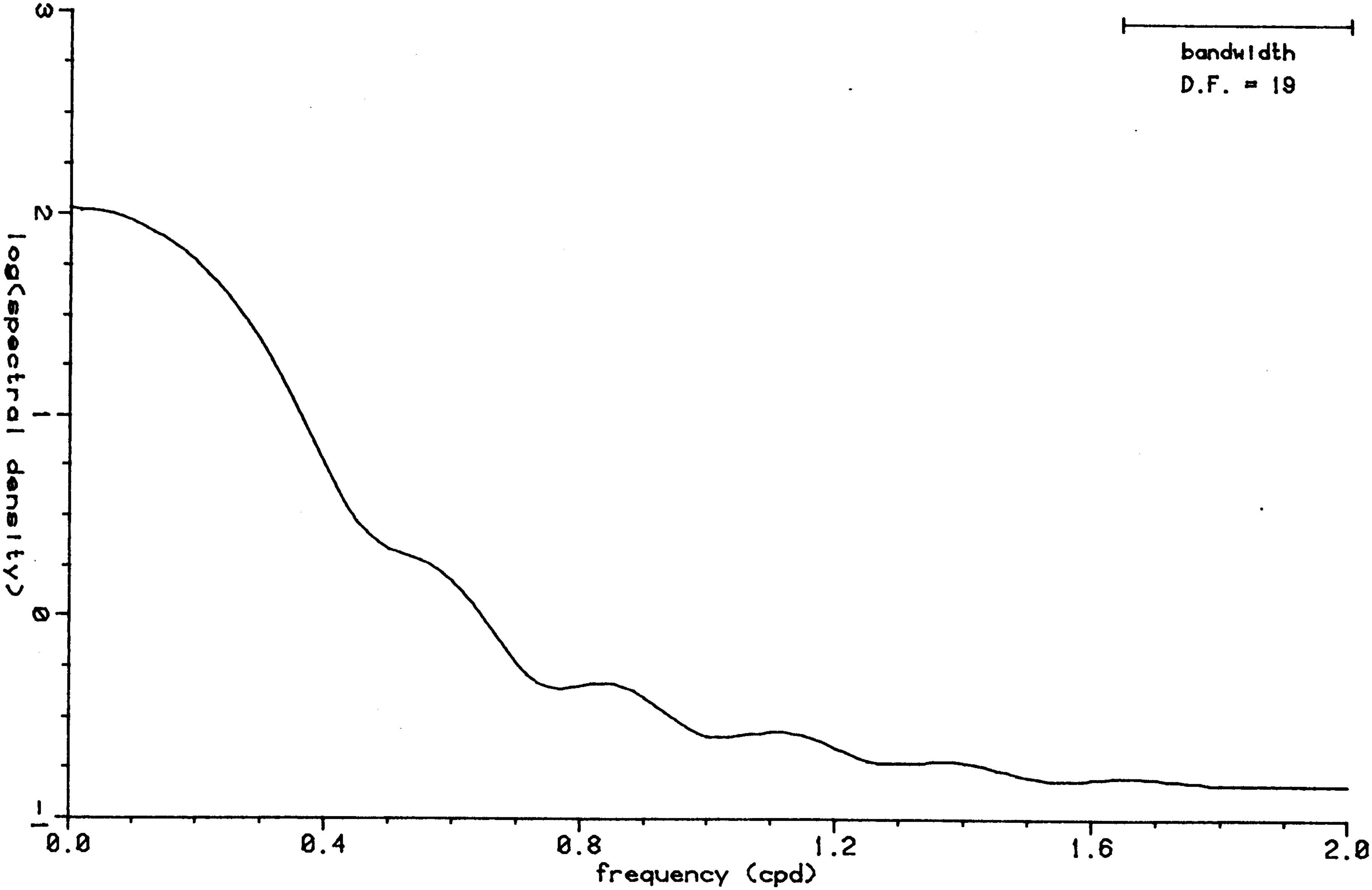

FIGURE A-17 SPECTRAL DENSITY
INSHORE BARROW (BOTTOM) DRIFT CURRENT (35.9 DEGREE COMPONENT)
0659 8 AUG 1981 - 1859 4 SEPT 1981

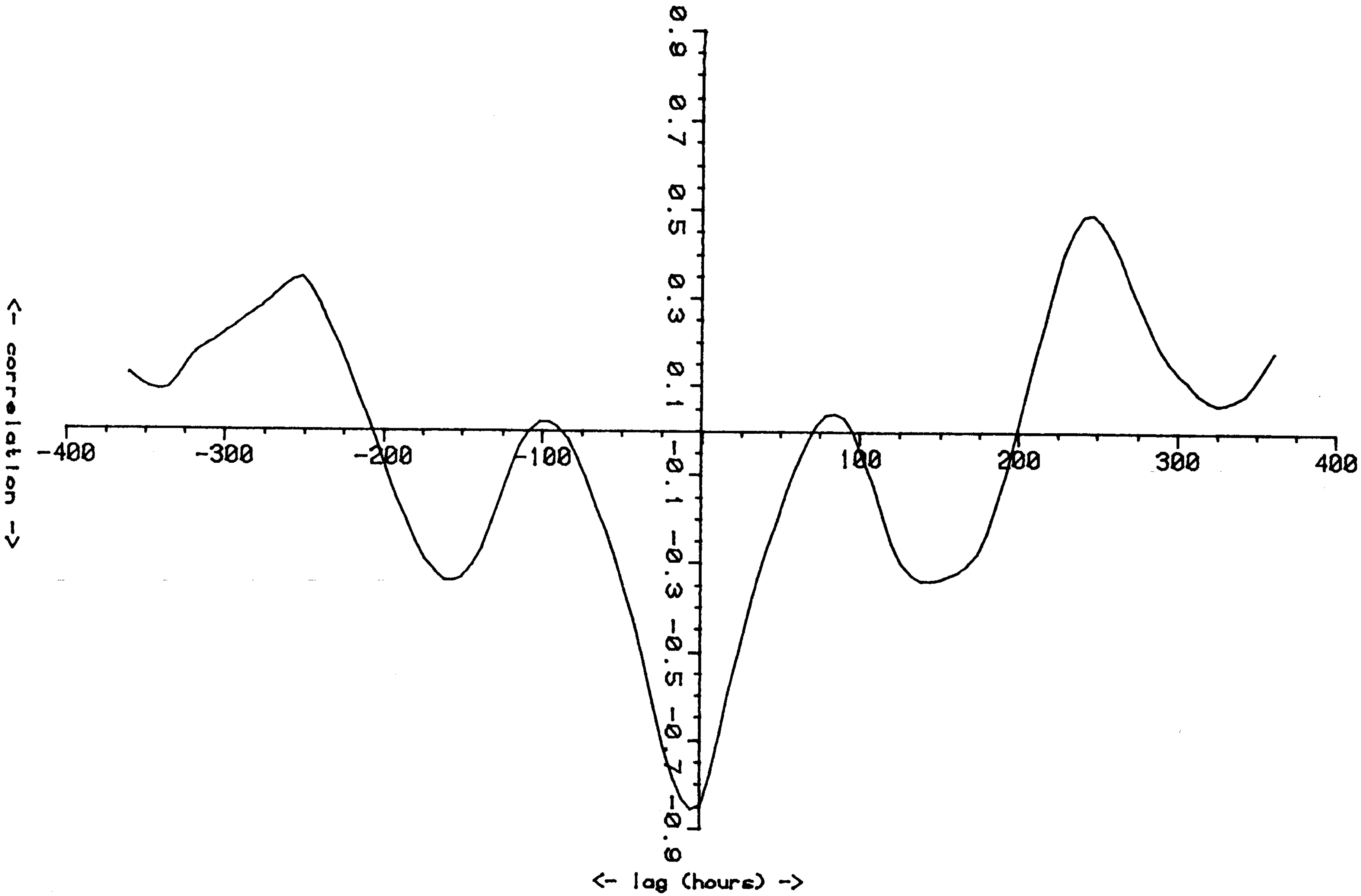

FIGURE A-18 CROSS CORRELATIONS
PT. BARROW - CAPE LISBURNE BAROMETRIC PRESSURE DIFFERENCES
VS. LAGGED INSHORE BARROW DRIFT CURRENT (35.9 DEGREE COMP.)
0659 8 AUG 1981 - 1859 4 SEPT 1981

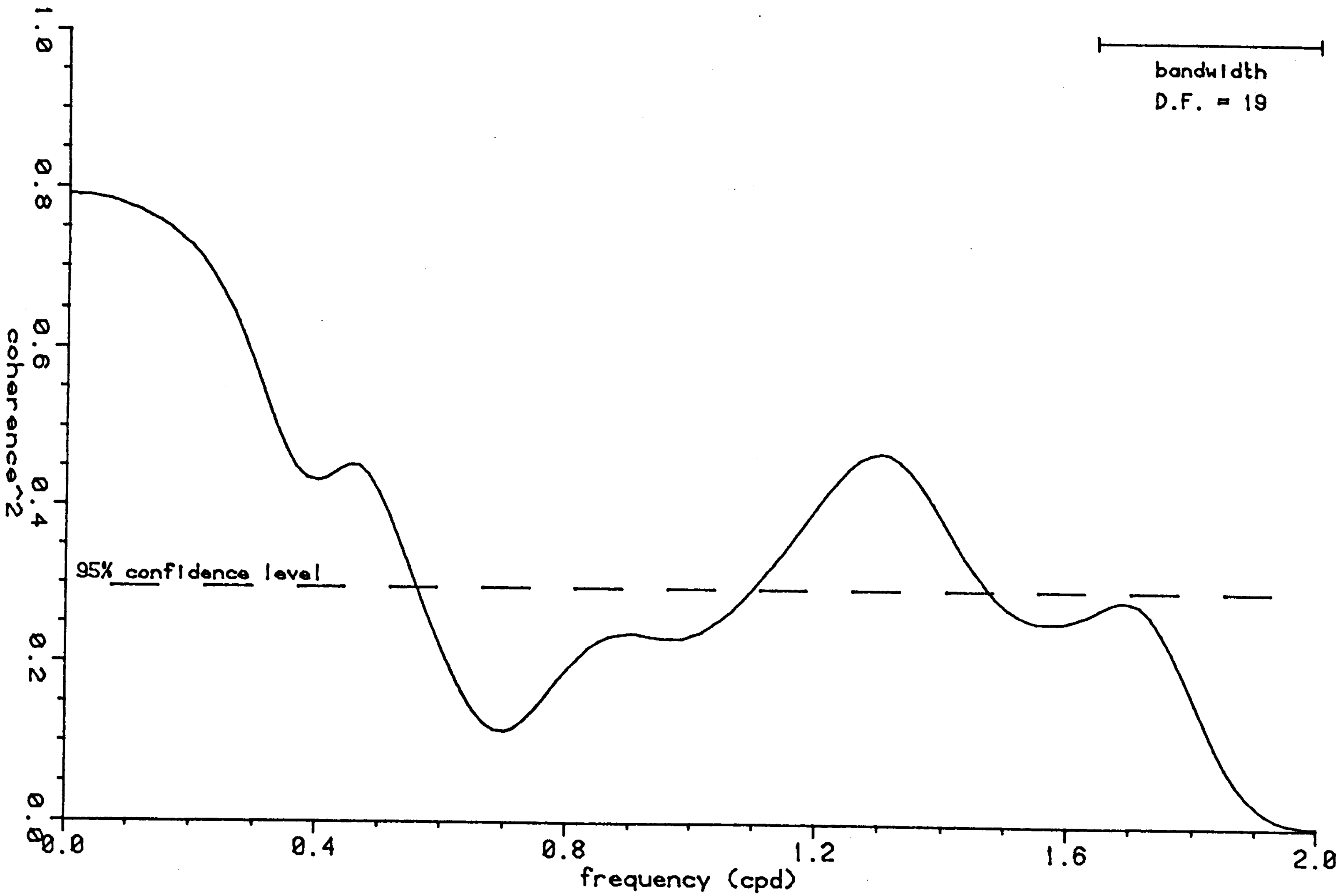

FIGURE A-19 SQUARED COHERENCE SPECTRUM
PT. BARROW-CAPE LISBURNE BAROMETRIC PRESSURE DIFFERENCES VS.
INSHORE BARROW (BOTTOM) DRIFT CURRENT (35.9 DEGREE COMPONENT)
0659 8 AUG 1981 - 1859 4 SEPT 1981

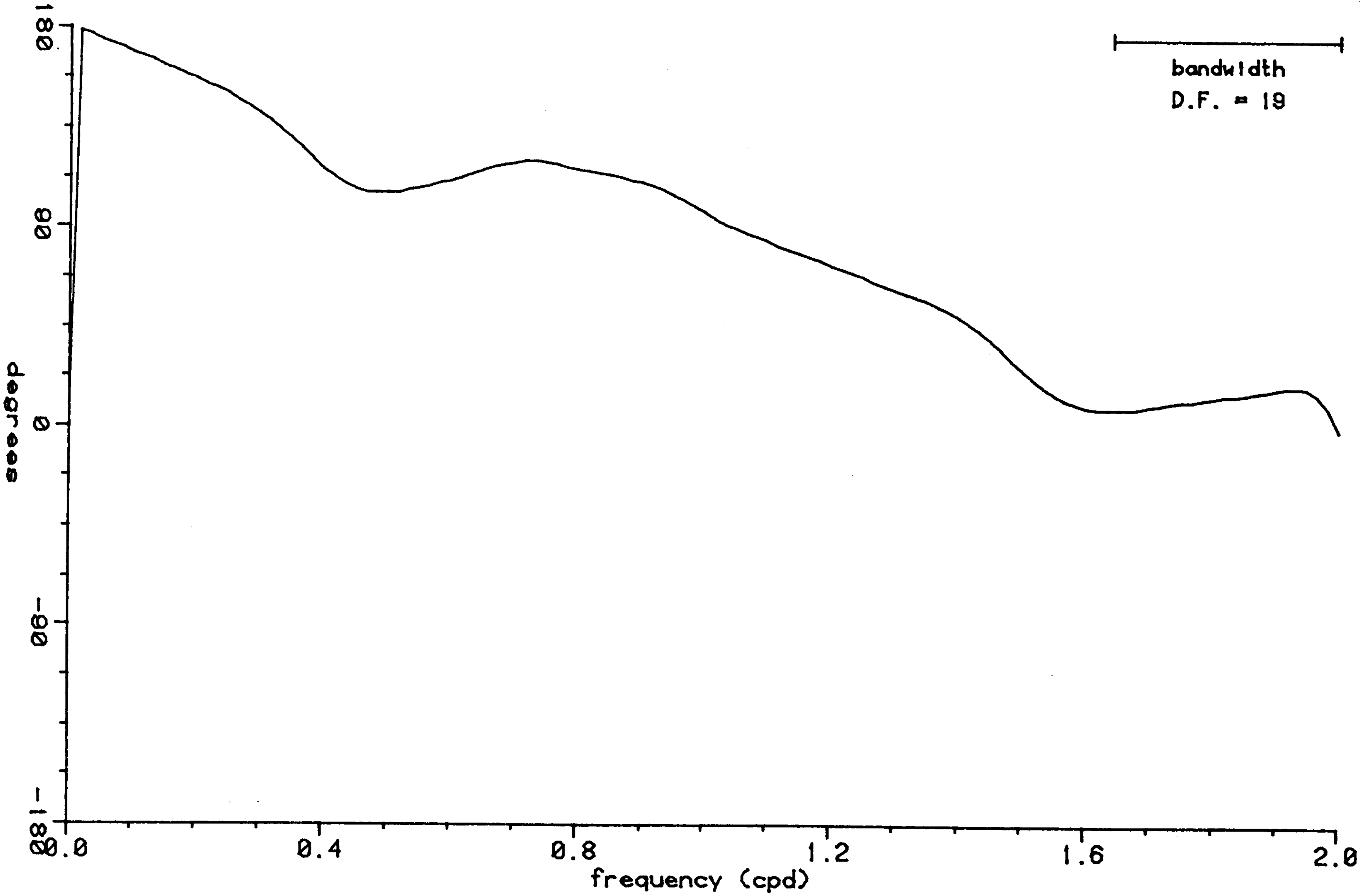

FIGURE A-20 PHASE SPECTRUM
PT. BARROW-CAPE LISBURNE BAROMETRIC PRESSURE DIFFERENCES VS.
INSHORE BARROW (BOTTOM) DRIFT CURRENT (35.9 DEGREE COMPONENT)
0659 8 AUG 1981 - 1859 4 SEPT 1981

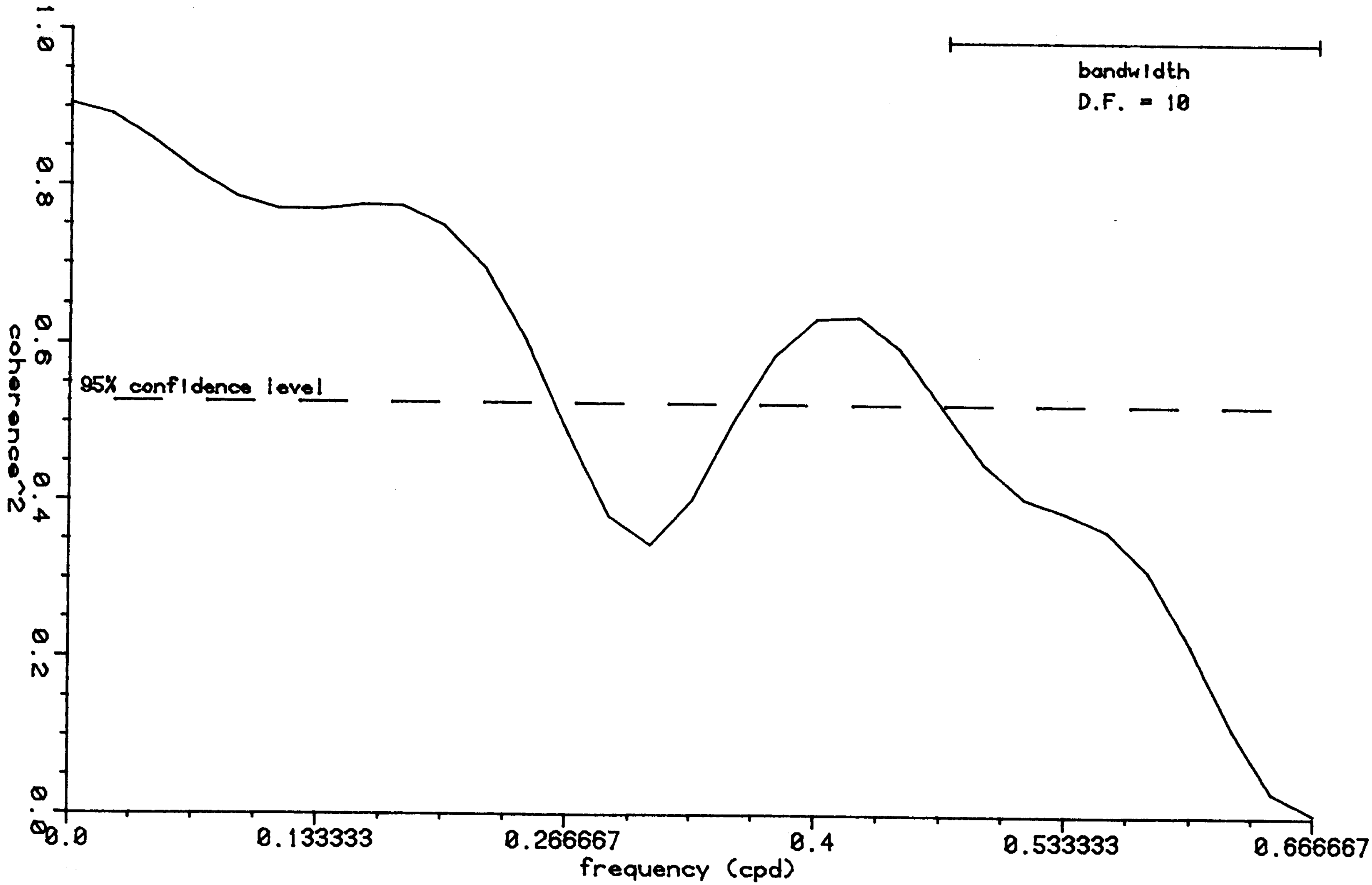

FIGURE A-21 SQUARED COHERENCE SPECTRUM
PT. BARROW-CAPE LISBURNE BAROMETRIC PRESSURE DIFFERENCES VS.
INSHORE BARROW (BOTTOM) DRIFT CURRENT (35.9 DEGREE COMPONENT)
0659 8 AUG 1981 - 0659 4 SEPT 1981

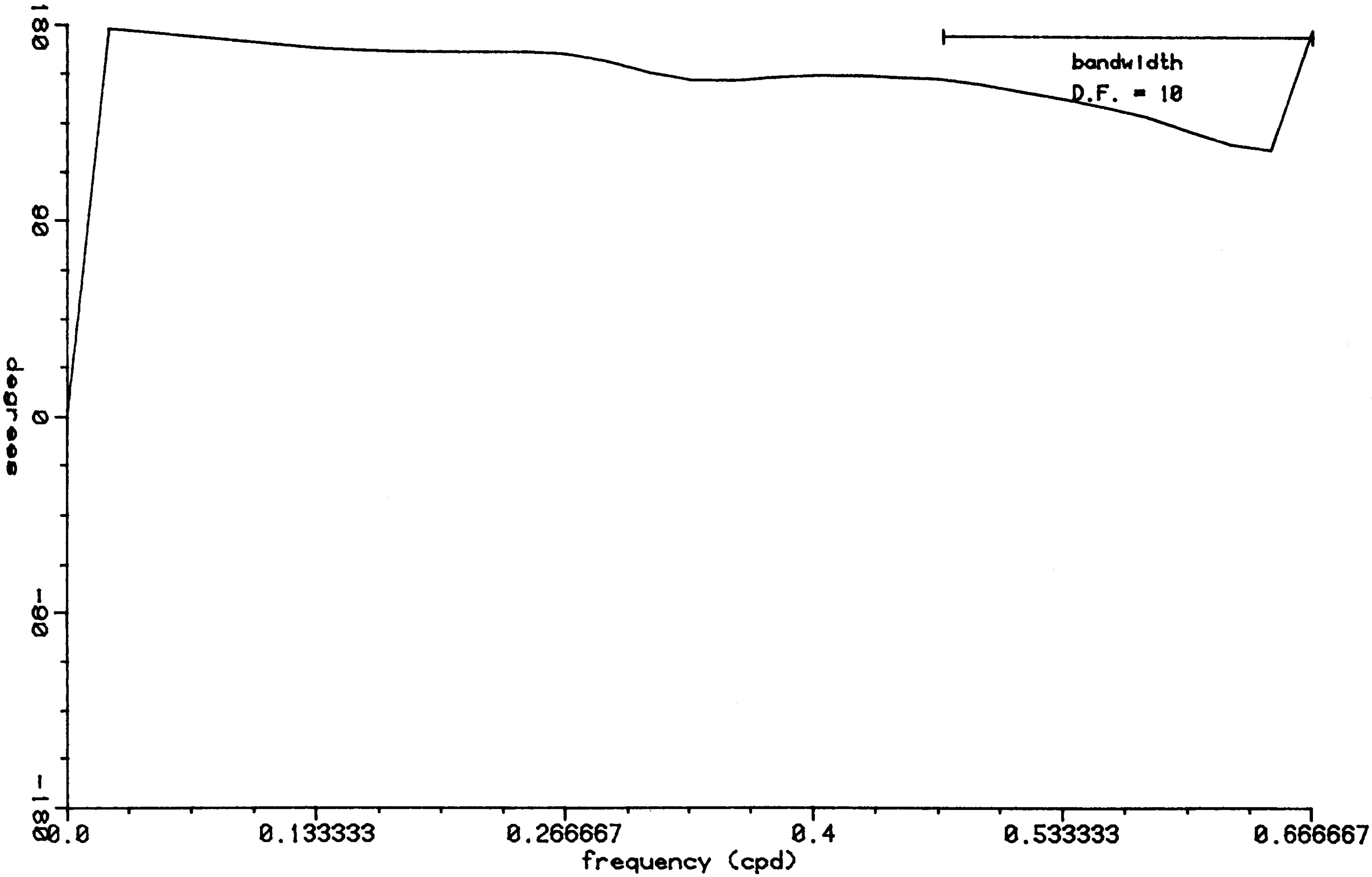

<u>FIGURE</u> A-22 PHASE SPECTRUM
PT. BARROW-CAPE LISBURNE BAROMETRIC PRESSURE DIFFERENCES VS.
INSHORE BARROW (BOTTOM) DRIFT CURRENT (35.9 DEGREE COMPONENT)
0659 8 AUG 1981 - 0659 4 SEPT 1981

Pressure vs. Current

Inshore Wainwright

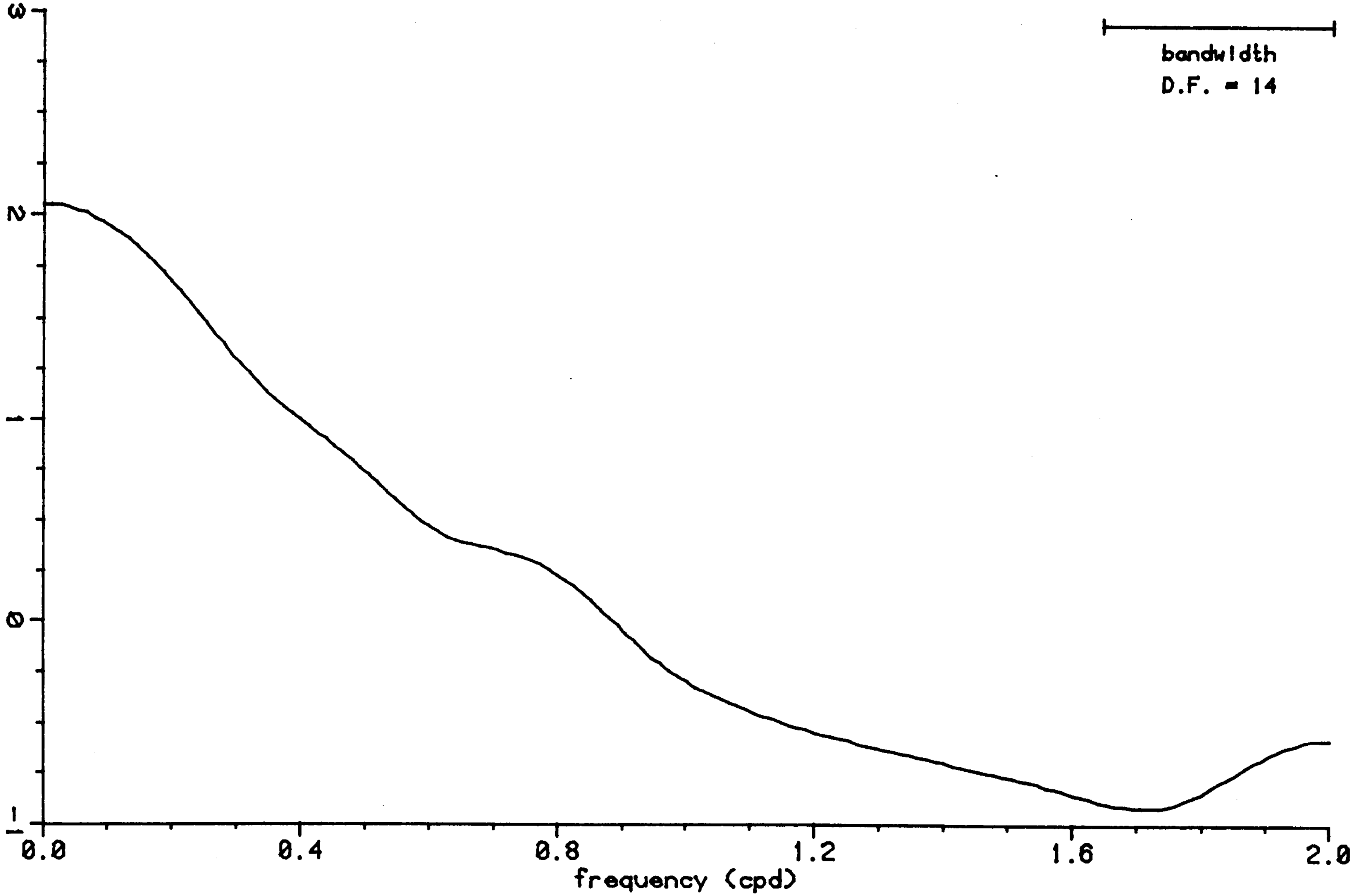

FIGURE A-23 SPECTRAL DENSITY
PT. BARROW-CAPE LISBURNE BAROMETRIC PRESSURE DIFFERENCES
1350 12 AUG 1981 - 1350 1 SEPT 1981

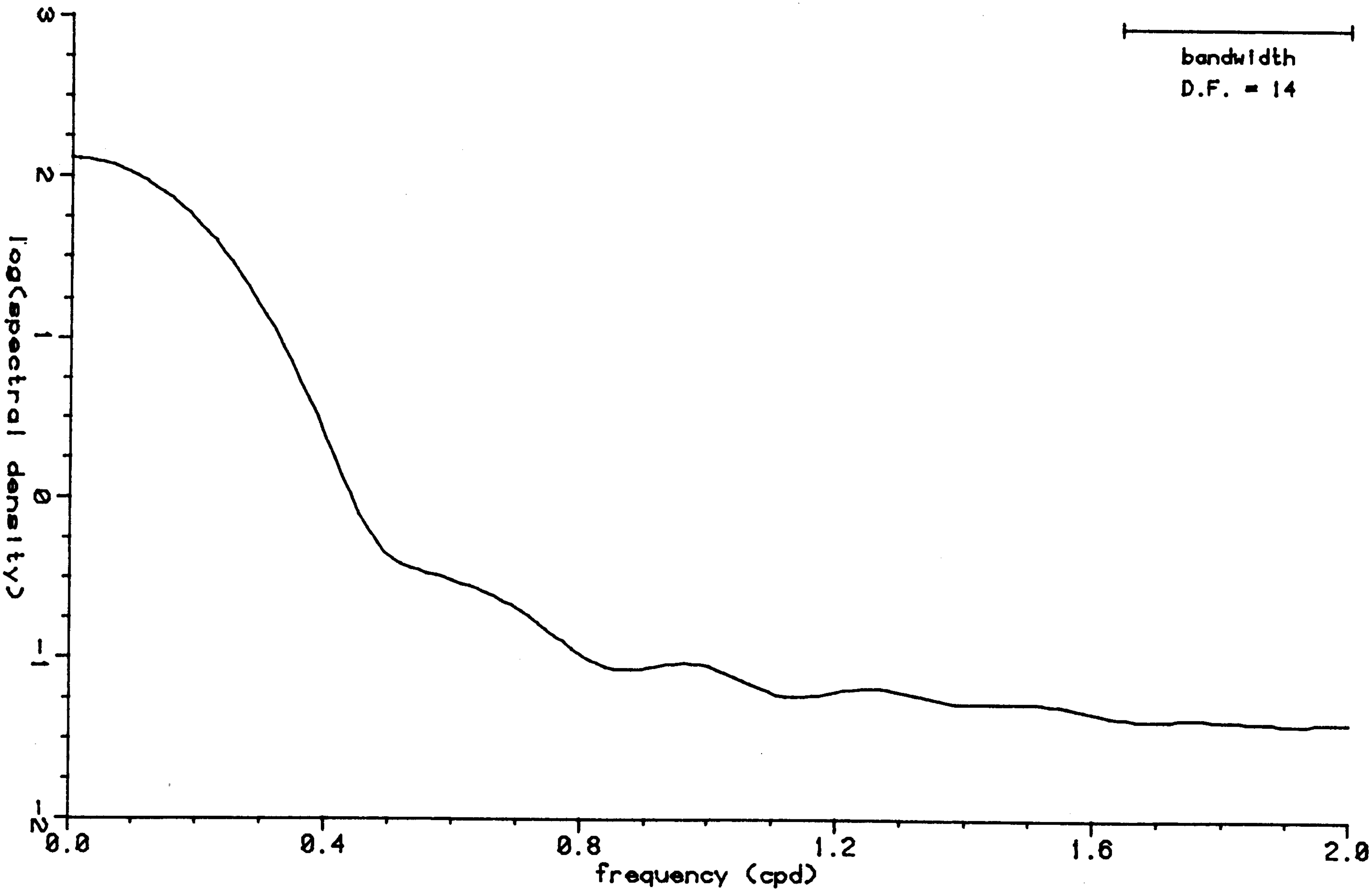

FIGURE A-24 SPECTRAL DENSITY
INSHORE WAINWRIGHT (BOTTOM) DRIFT CURRENT (33.7 DEGREE COMPONENT
1350 12 AUG 1981 - 1350 1 SEPT 1981

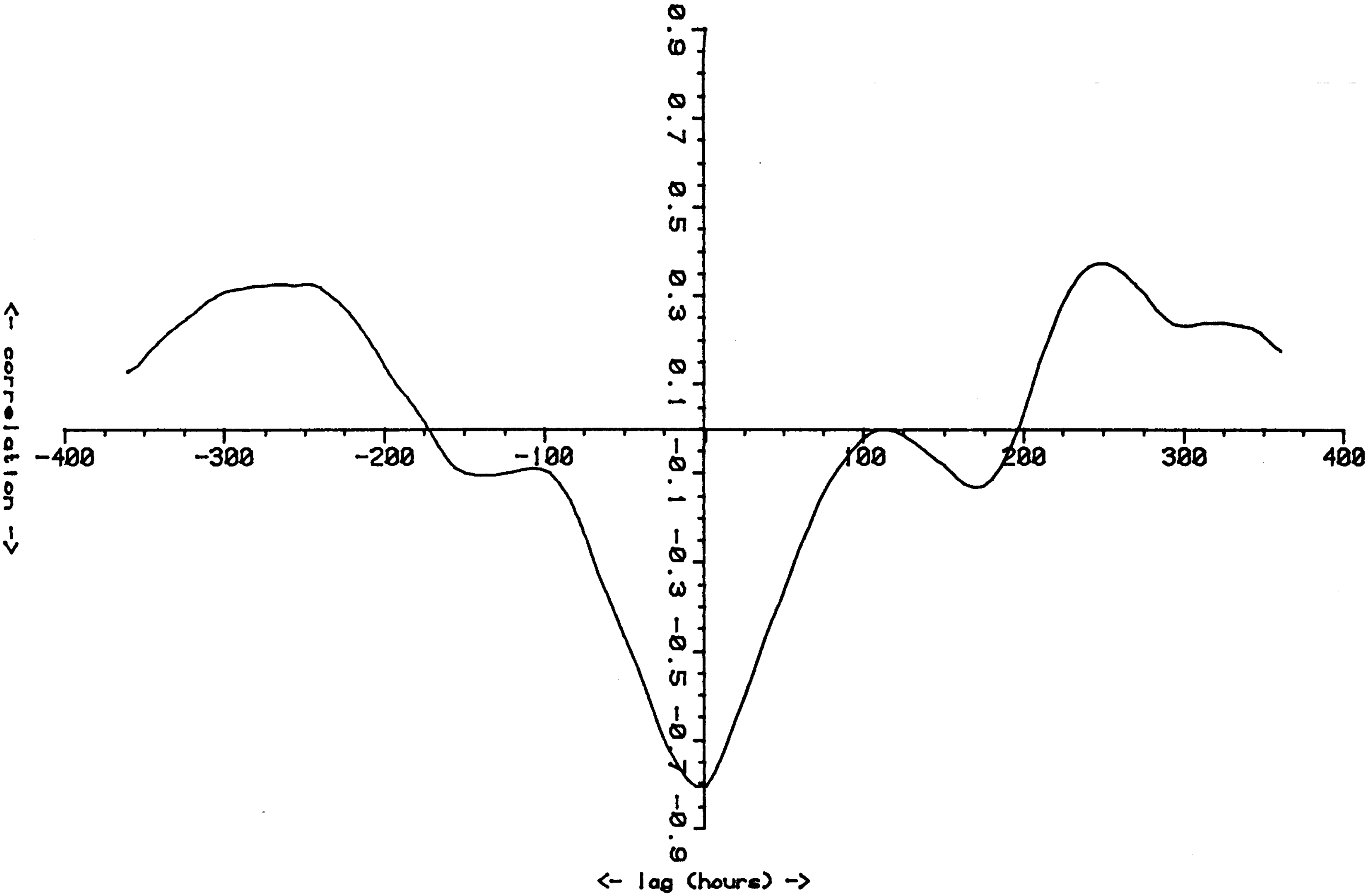

FIGURE A-25 CROSS CORRELATIONS
BARROW-LISBURNE BAROMETRIC PRESSURE DIFFERENCES VS. LAGGED
INSHORE WAINWRIGHT (BOTTOM) DRIFT CURRENT (33.7 DEG. COMP.)
1350 12 AUG 1981 - 1350 1 SEPT 1981

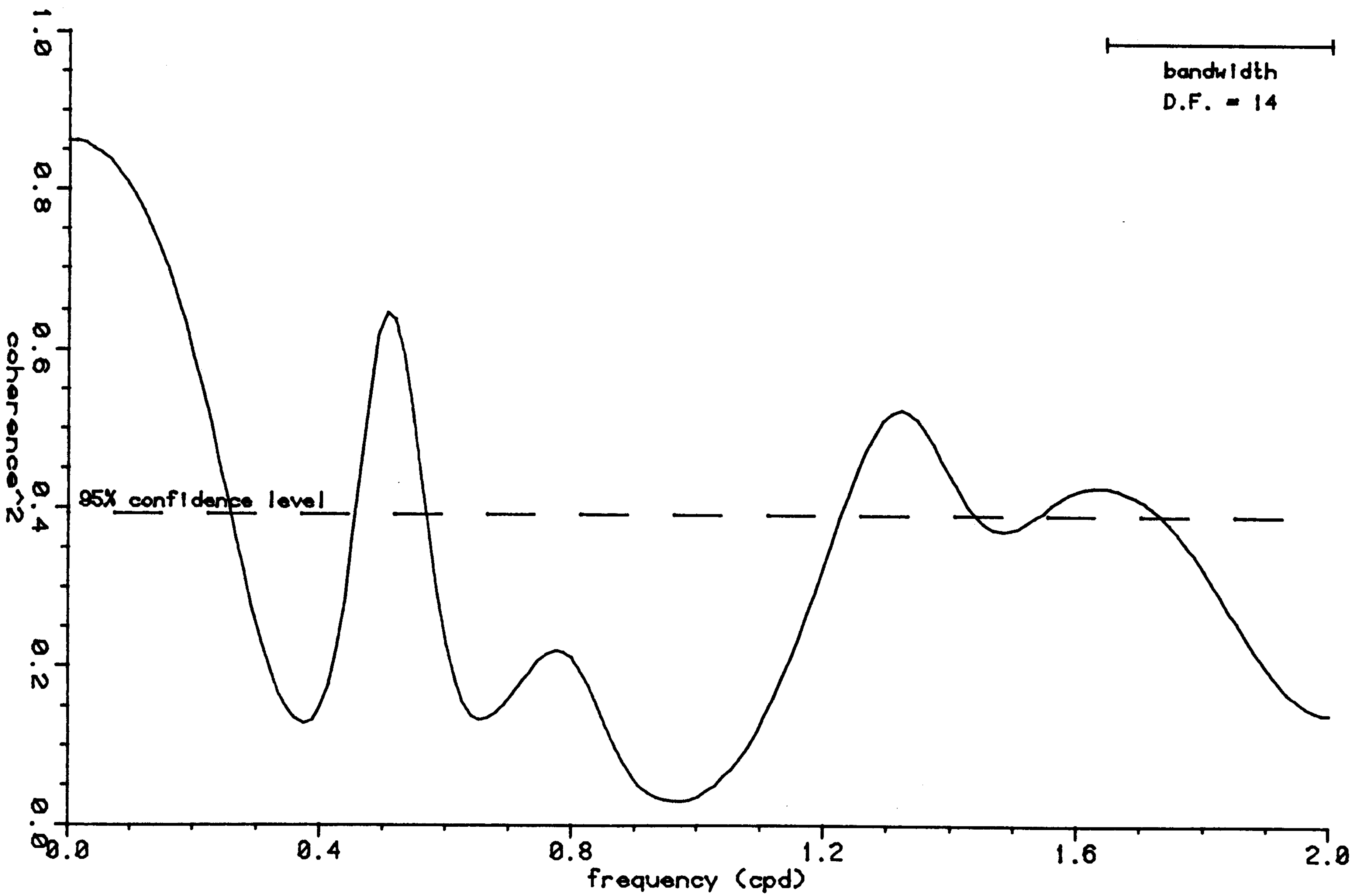

FIGURE A-26 SQUARED COHERENCE SPECTRUM
BARROW-LISBURNE PRESSURE DIFFERENCES VS. INSHORE WAINWRIGHT
(BOTTOM) DRIFT CURRENT (33.7 DEGREE COMPONENT)
1350 12 AUG 1981 - 1350 1 SEPT 1981

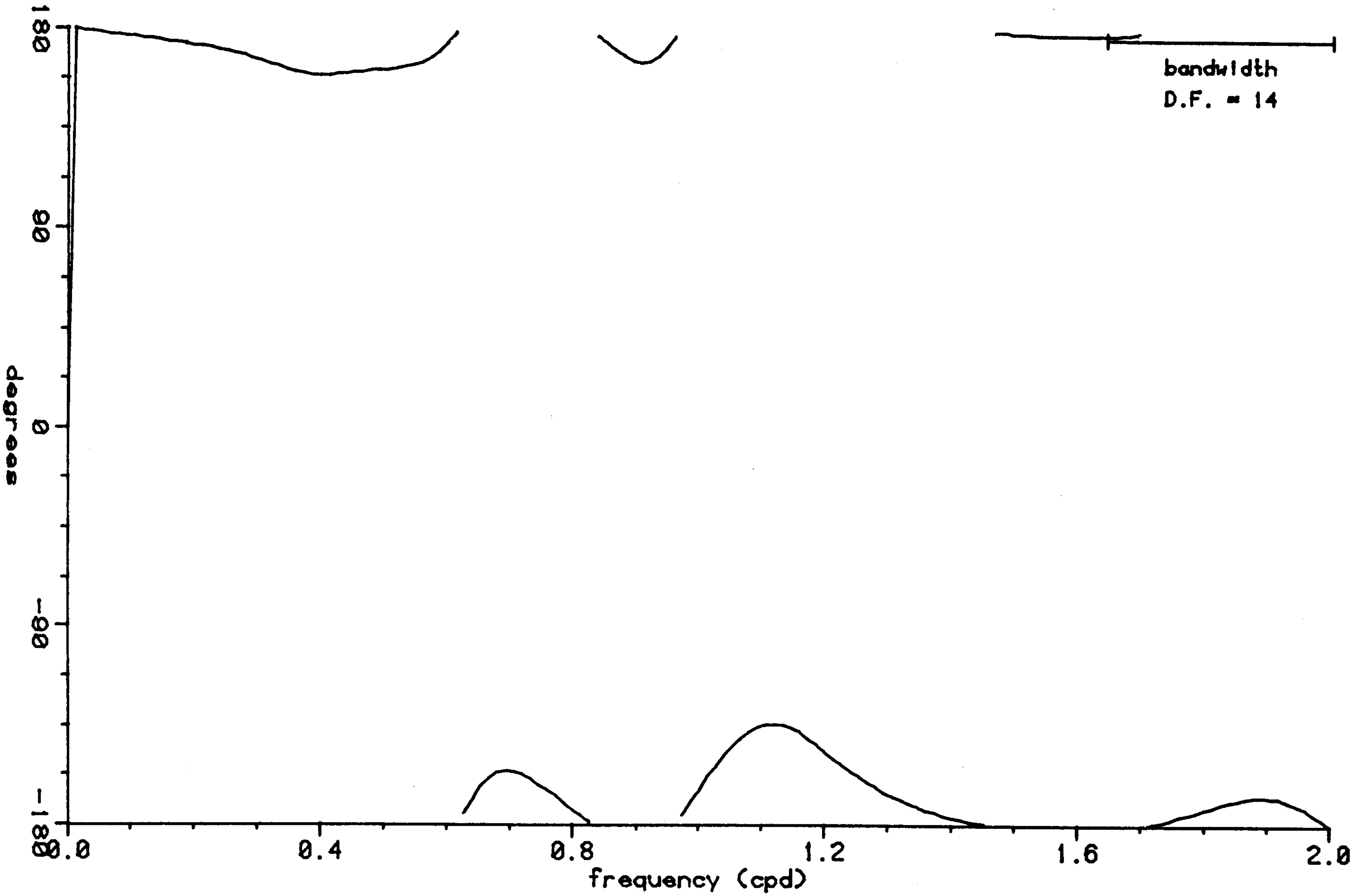

FIGURE A-27 PHASE SPECTRUM
BARROW-LISBURNE PRESSURE DIFFERENCES VS. INSHORE WAINWRIGHT
(BOTTOM) DRIFT CURRENT (33.7 DEGREE COMPONENT)
1350 12 AUG 1981 - 1350 1 SEPT 1981

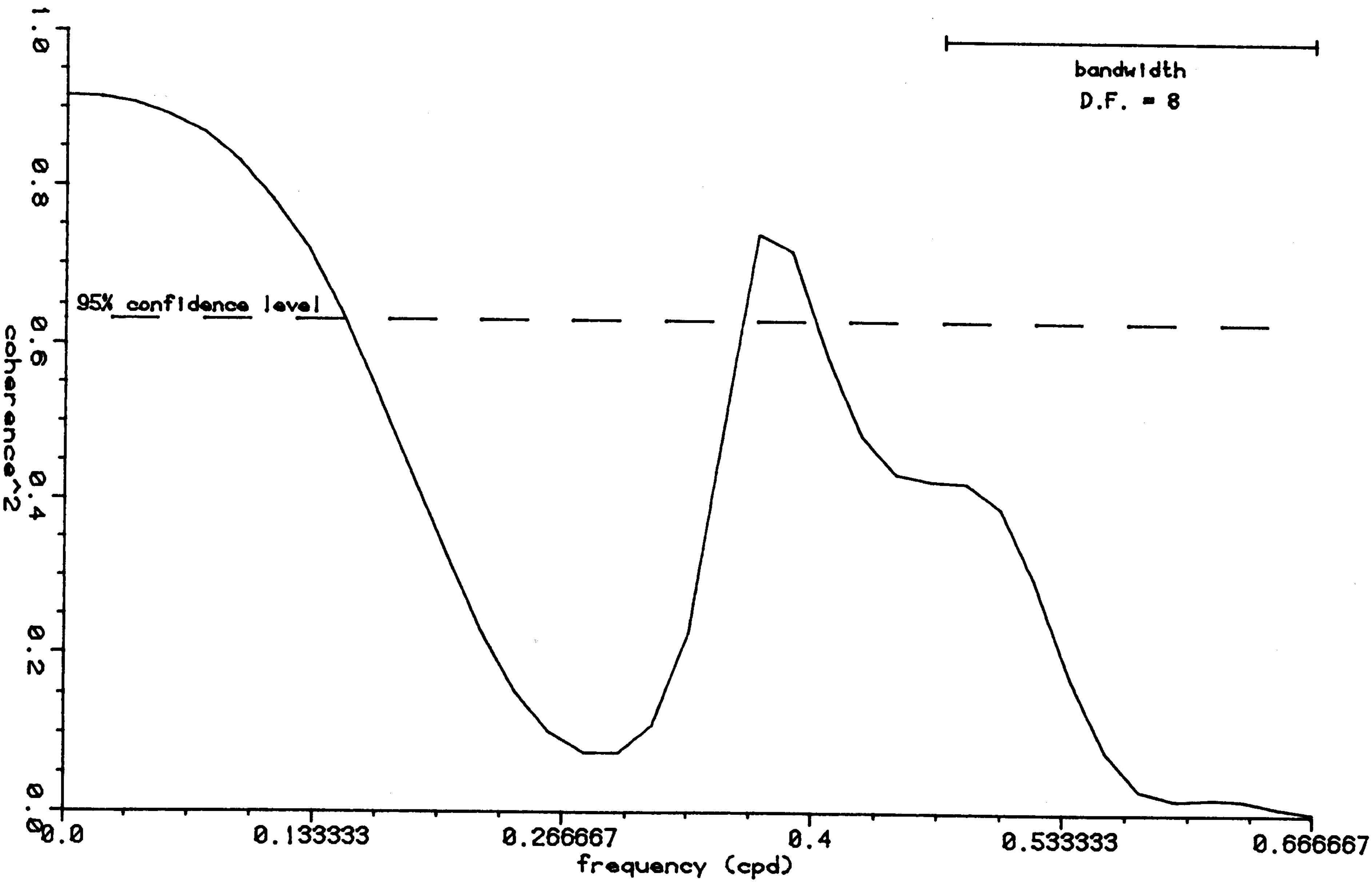

FIGURE A-28 SQUARED COHERENCE SPECTRUM
BARROW-LISBURNE BAROMETRIC PRESSURE DIFFERENCES VS.
INSHORE WAINWRIGHT (BOTTOM) DRIFT CURRENT (33.7 DEGREE COMP.)
1350 12 AUG 1981 - 0150 1 SEPT 1981

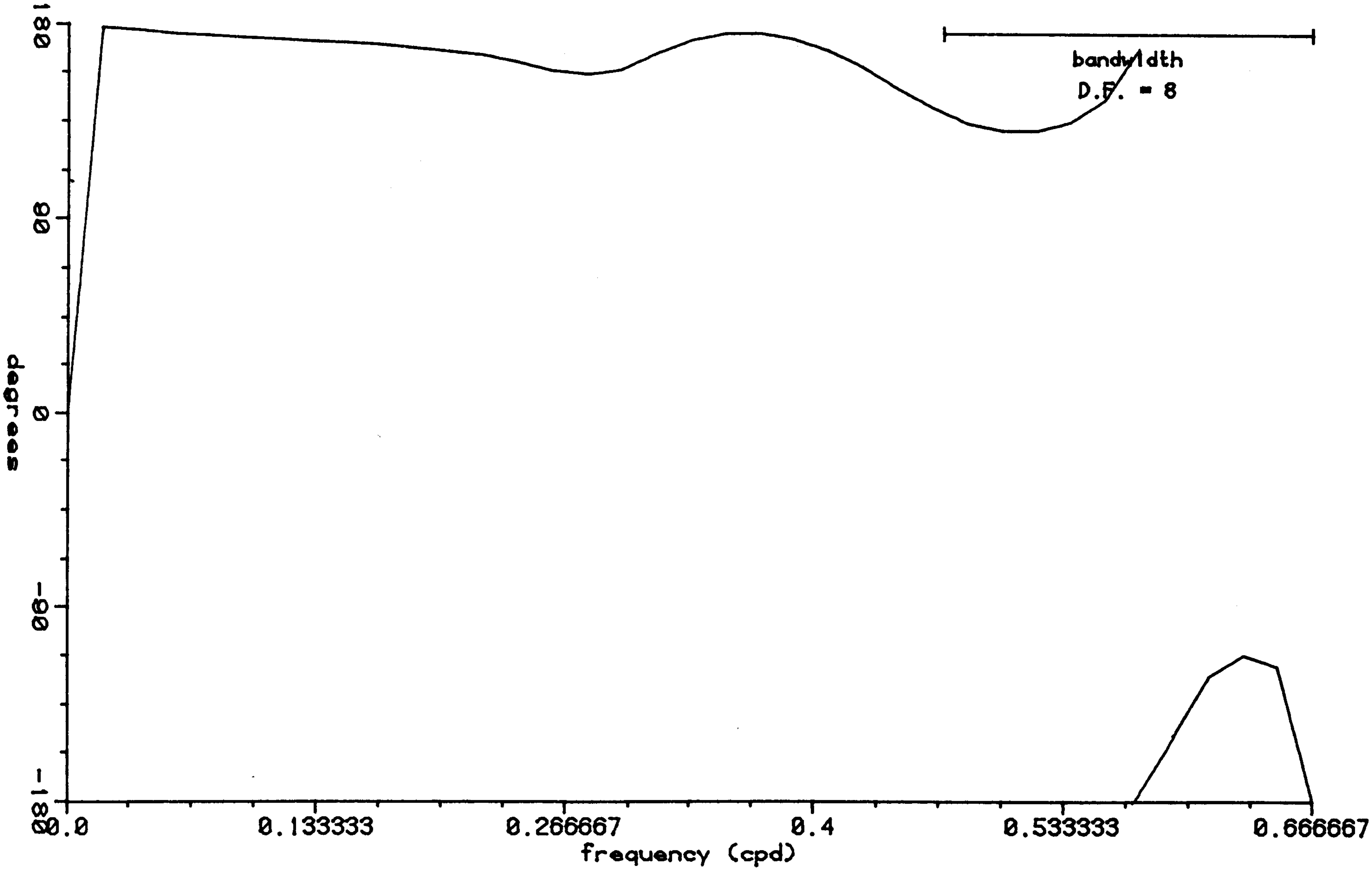

FIGURE A-29 PHASE SPECTRUM
BARROW-LISBURNE BAROMETRIC PRESSURE DIFFERENCES VS.
INSHORE WAINWRIGHT (BOTTOM) DRIFT CURRENT (33.7 DEGREE COMP.)
1350 12 AUG 1981 - 0150 1 SEPT 1981

Wind versus Current

Inshore Barrow

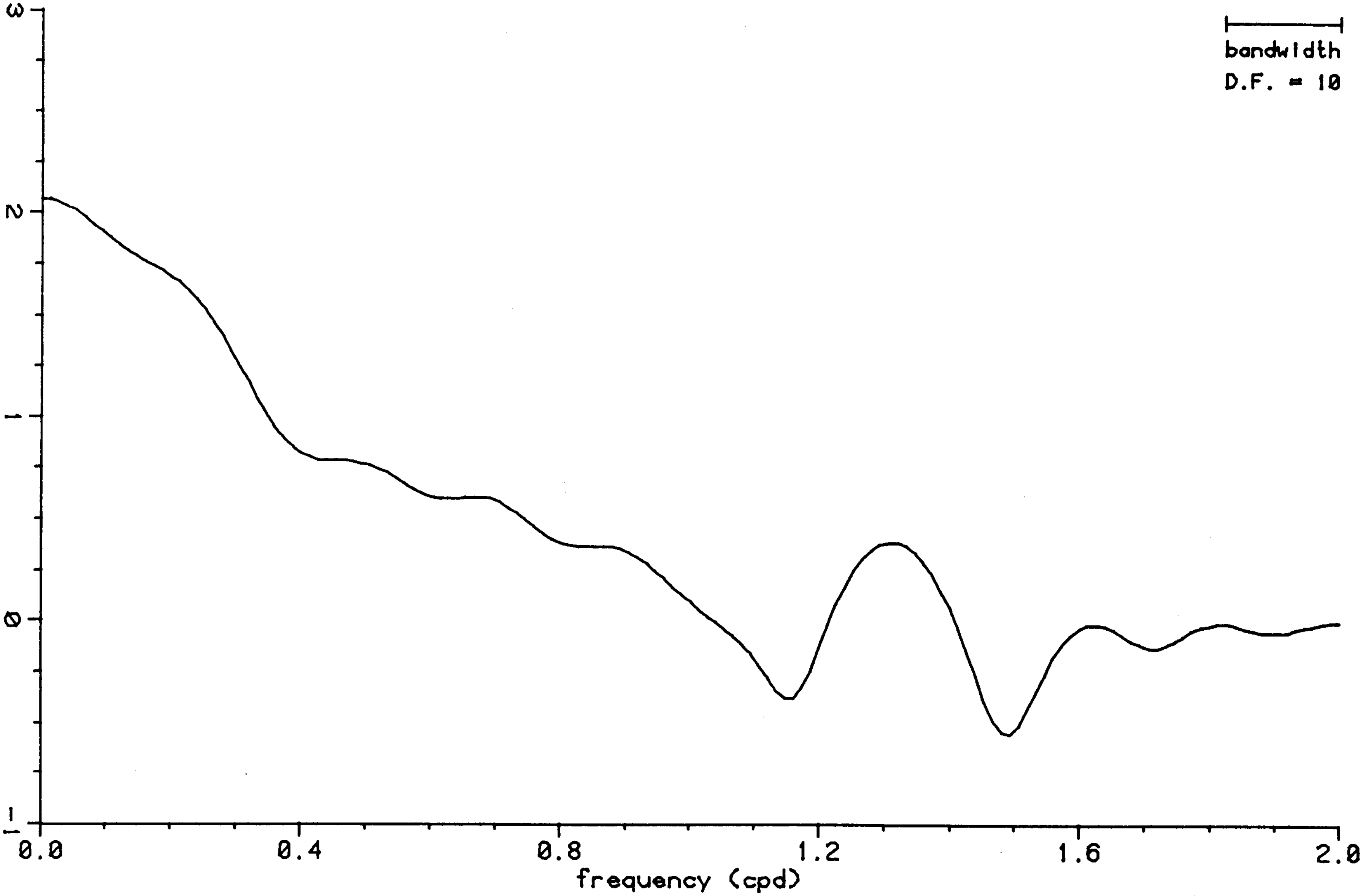

FIGURE A-30 SPECTRAL DENSITY
PT. BARROW WIND (35.9 DEGREE COMPONENT)
0700 8 AUG 1981 - 1300 6 SEPT 1981

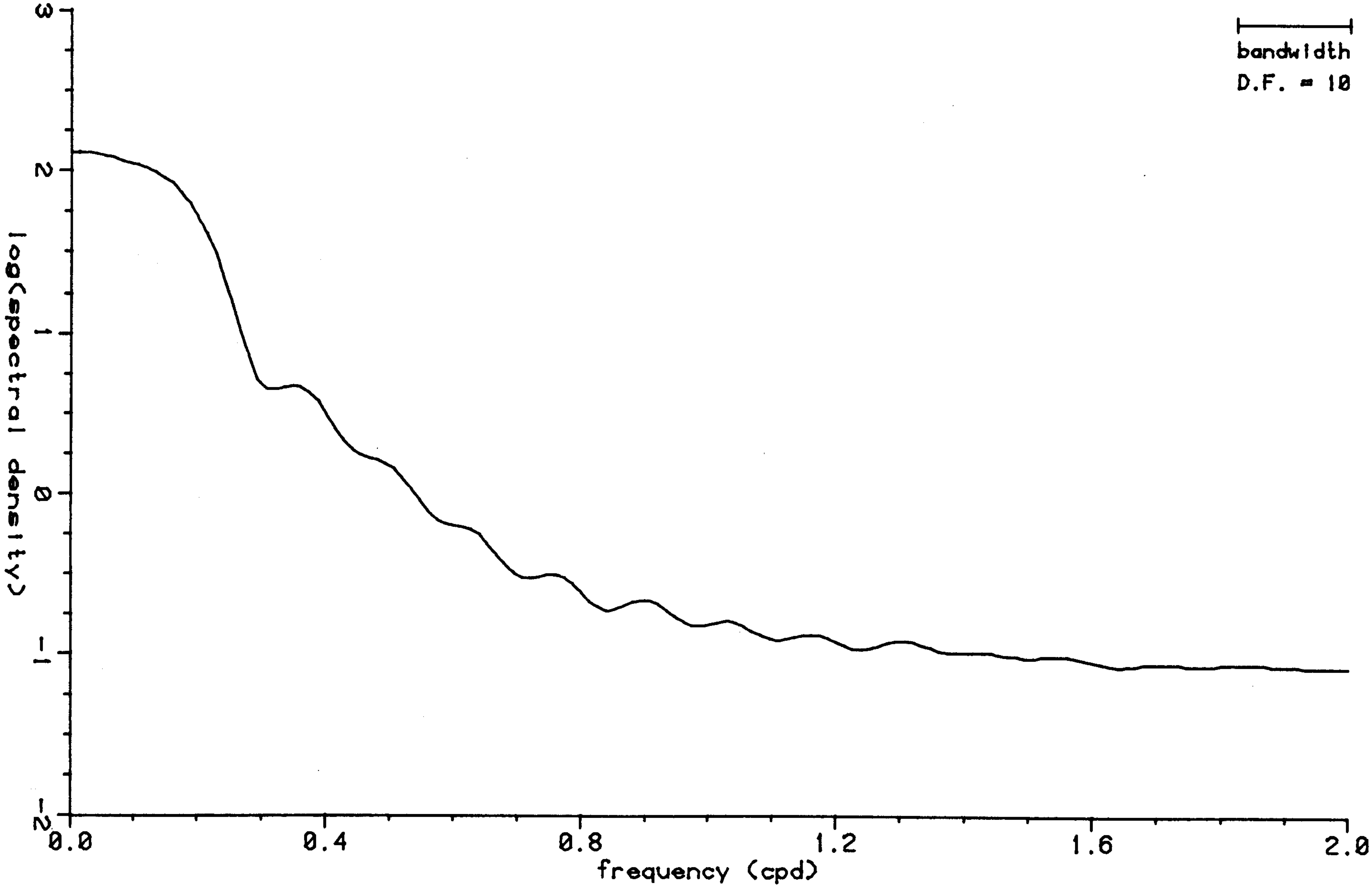

FIGURE A-31 SPECTRAL DENSITY
INSHORE BARROW (BOTTOM) DRIFT CURRENT (35.9 DEGREE COMPONENT)
0700 8 AUG 1981 - 1300 6 SEPT 1981

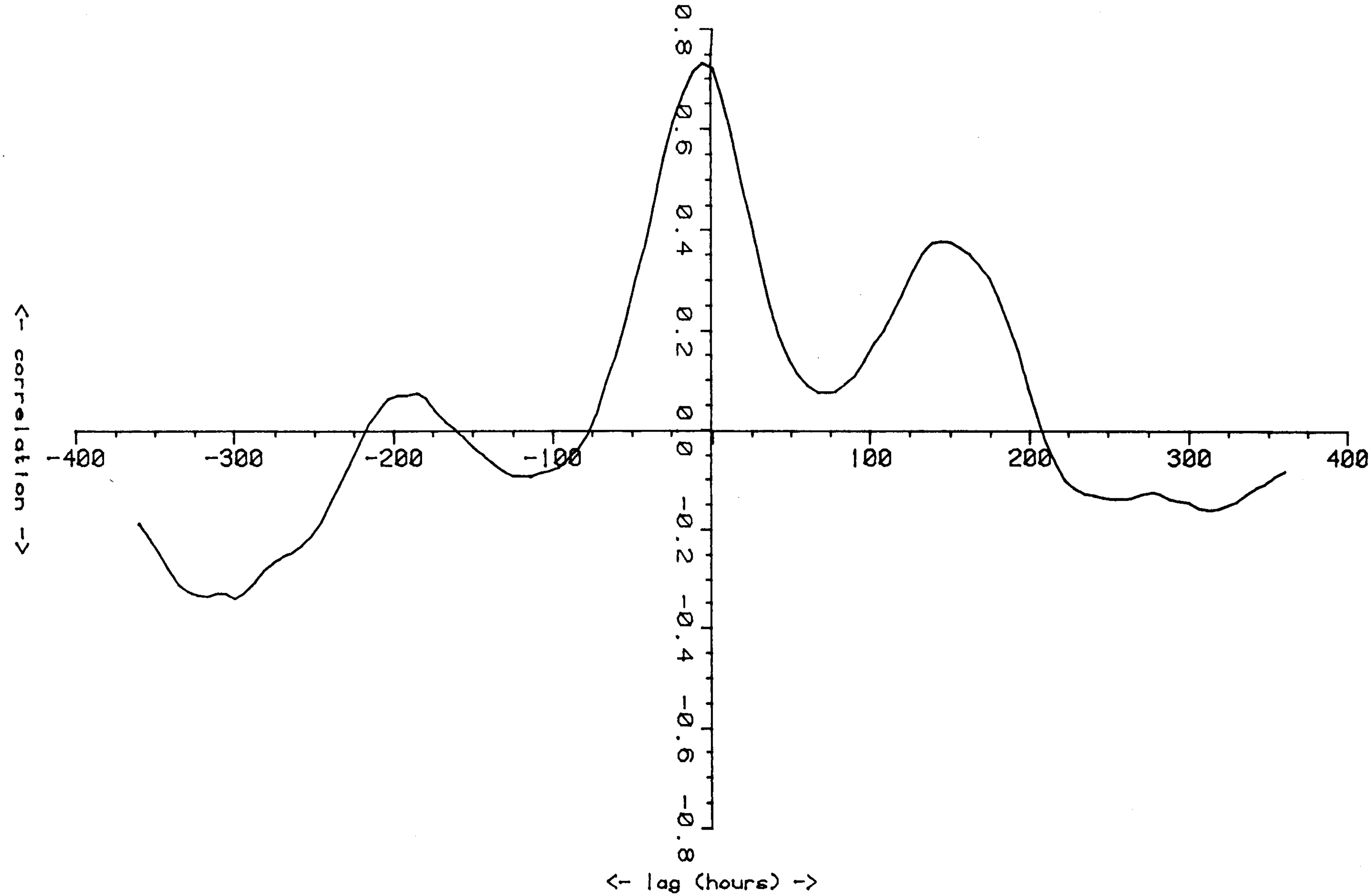

FIGURE A-32 CROSS CORRELATIONS
PT. BARROW WIND (35.9 DEGREE COMPONENT) VS. LAGGED INSHORE BARROW (BOTTOM) DRIFT CURRENT (35.9 DEGREE COMPONENT)
0700 8 AUG 1981 - 1300 6 SEPT 1981

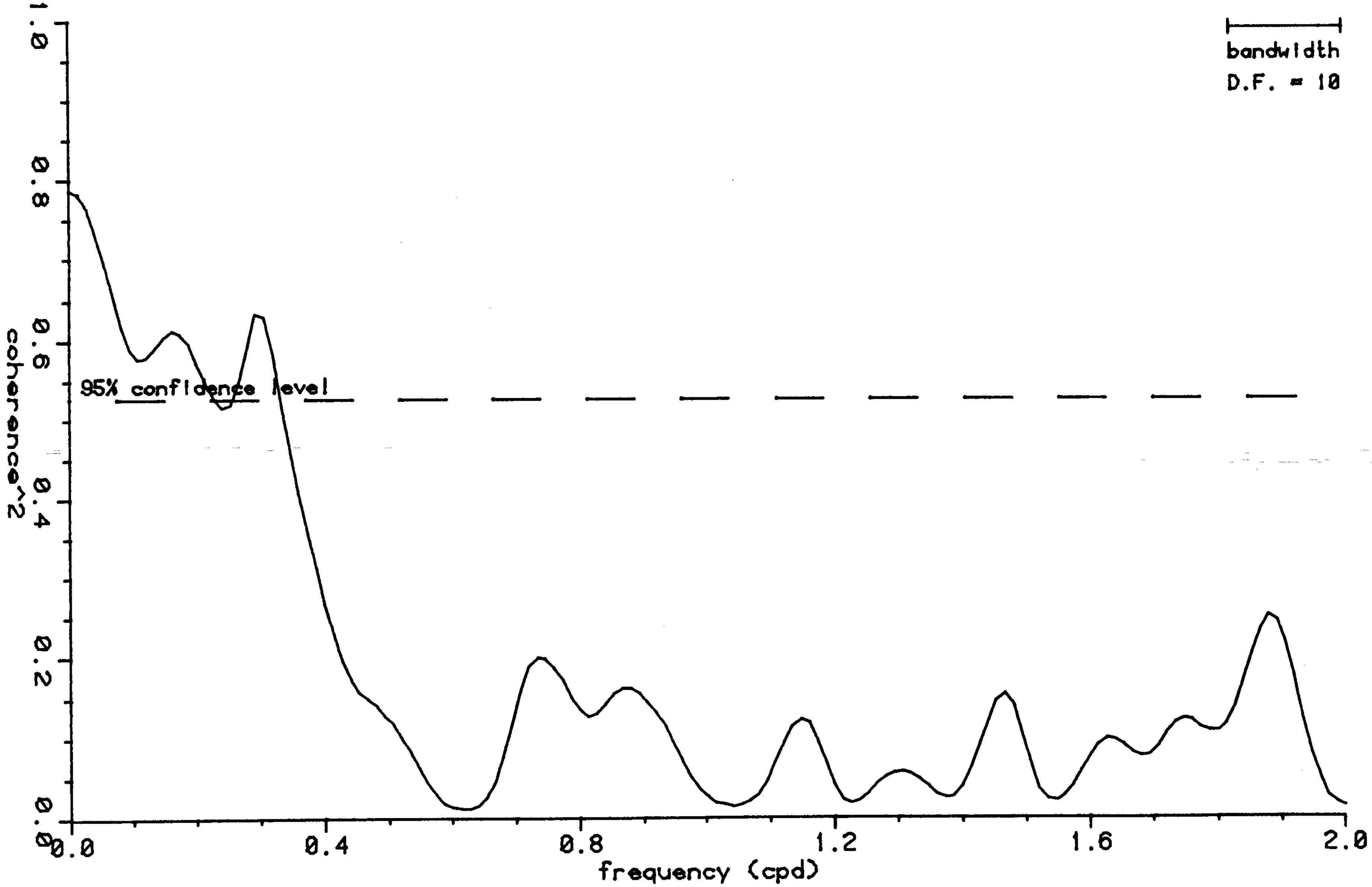

FIGURE A-33 SQUARED COHERENCE SPECTRUM
PT. BARROW WIND (35.9 DEGREE COMPONENT) VS. INSHORE BARROW (BOTTOM) DRIFT CURRENT (35.9 DEGREE COMPONENT)
0700 8 AUG 1981 - 1300 6 SEPT 1981

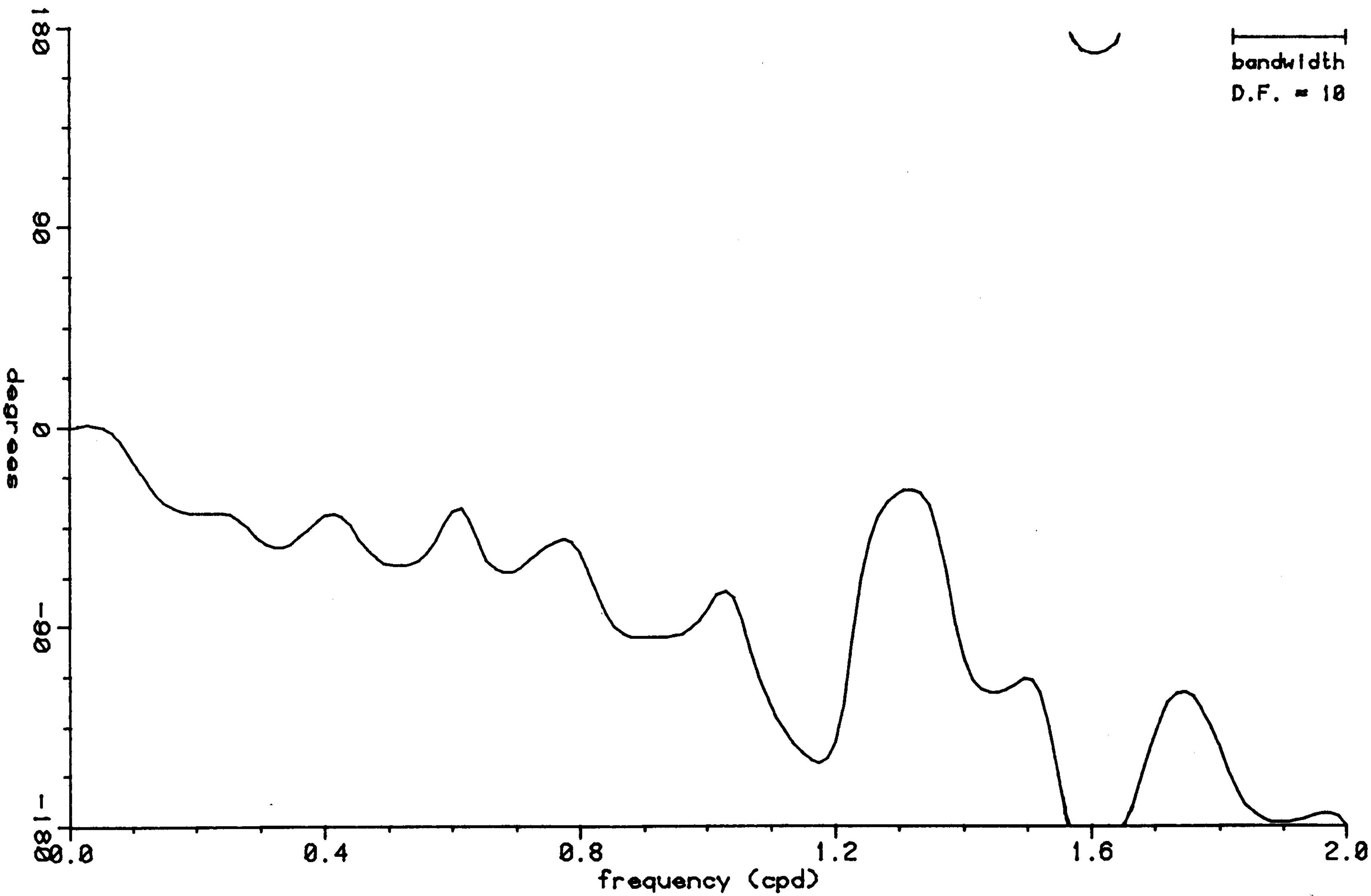

345

FIGURE A-34 PHASE SPECTRUM
PT. BARROW WIND (35.9 DEGREE COMPONENT) VS. INSHORE BARROW (BOTTOM) DRIFT CURRENT (35.9 DEGREE COMPONENT)
0700 8 AUG 1981 - 1300 6 SEPT 1981

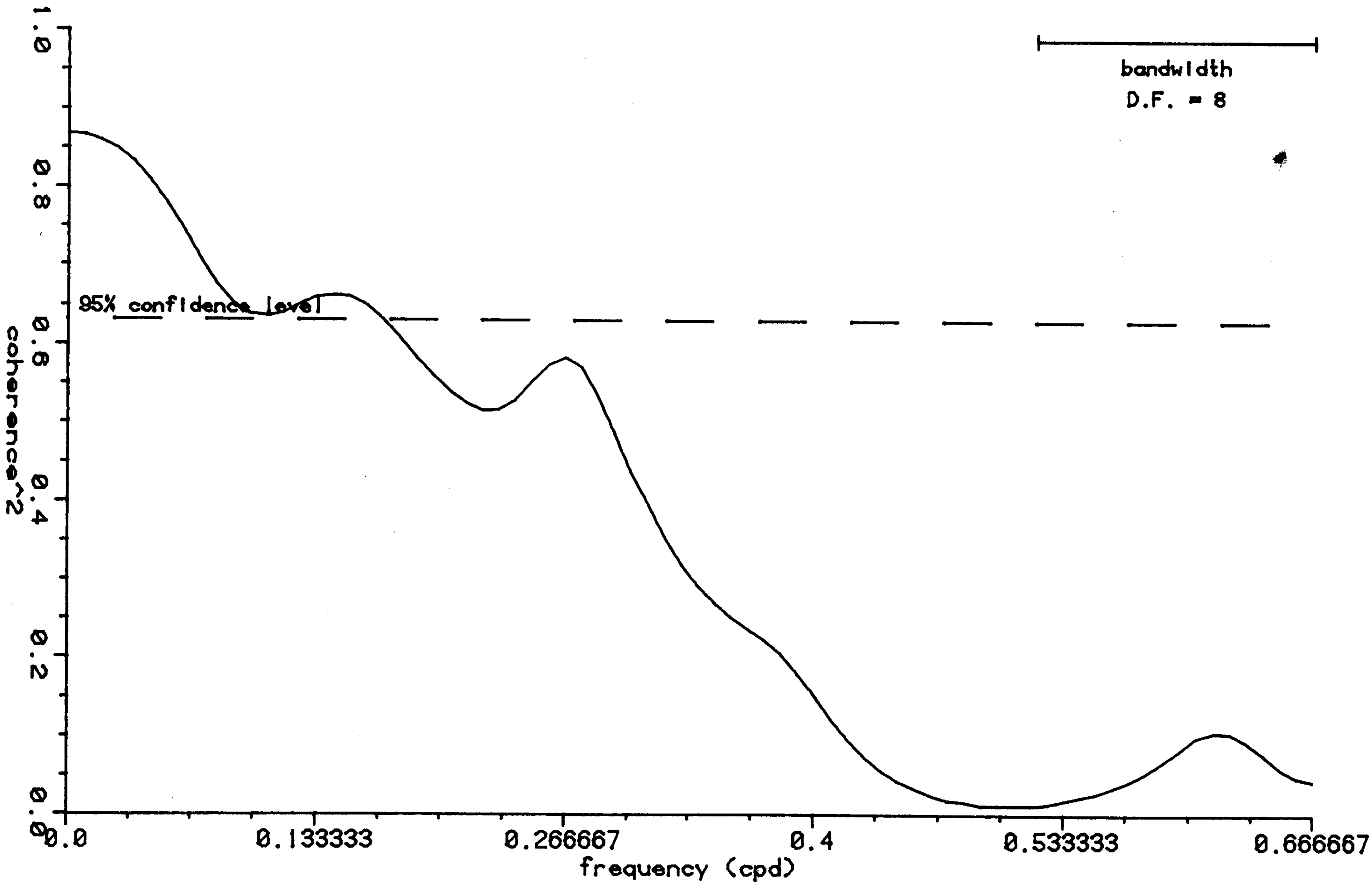

FIGURE A-35 SQUARED COHERENCE SPECTRUM
PT. BARROW WIND (35.9 DEGREE COMPONENT) VS. INSHORE BARROW (BOTTOM) DRIFT CURRENT (35.9 DEGREE COMPONENT)
0700 8 AUG 1981 - 1300 6 SEPT 1981

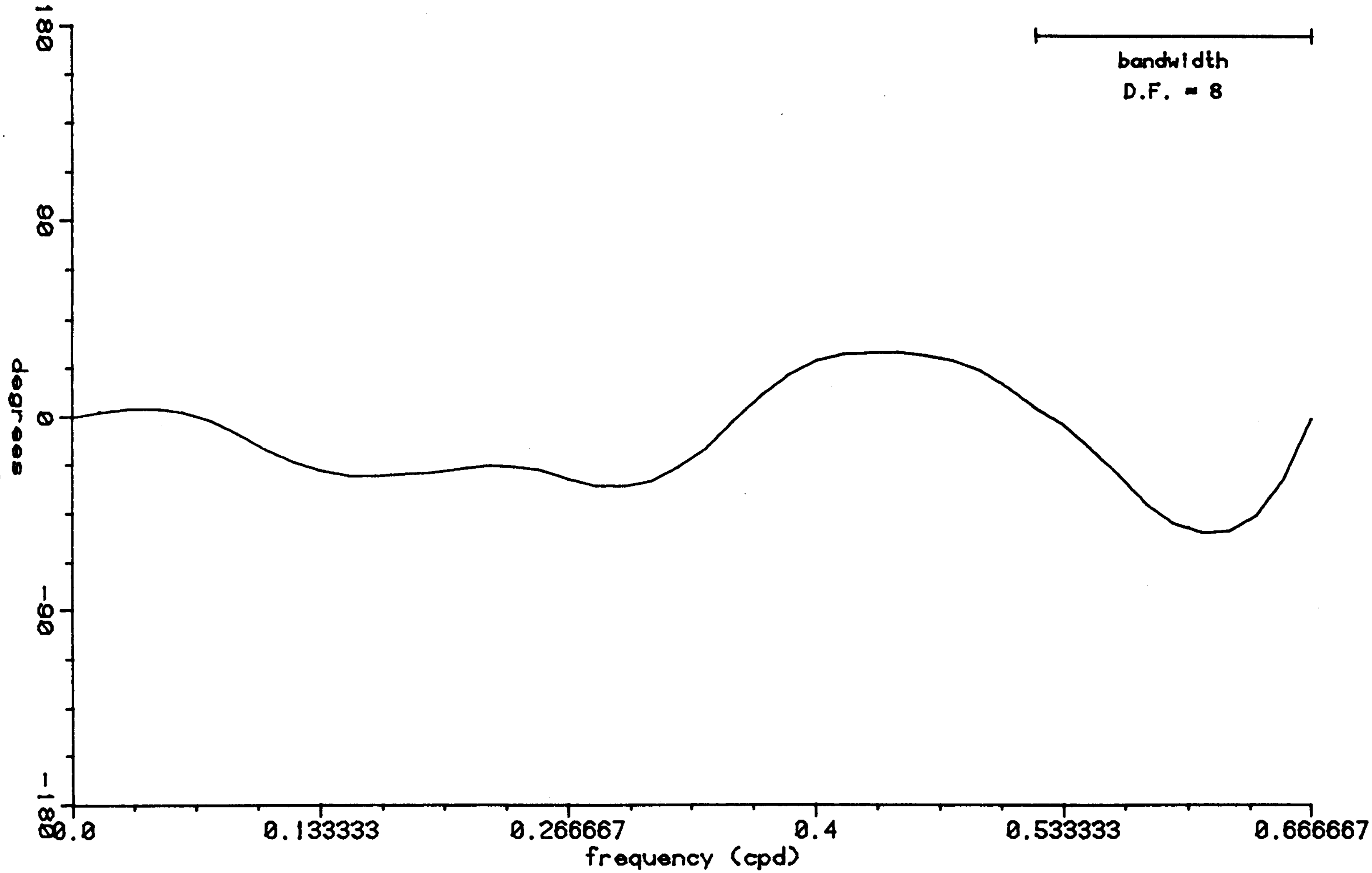

FIGURE A-36 PHASE SPECTRUM
PT. BARROW WIND (35.9 DEGREE COMPONENT) VS. INSHORE BARROW (BOTTOM) DRIFT CURRENT (35.9 DEGREE COMPONENT)
0700 8 AUG 1981 - 1300 6 SEPT 1981

Wind vs. Current

Inshore Wainwright

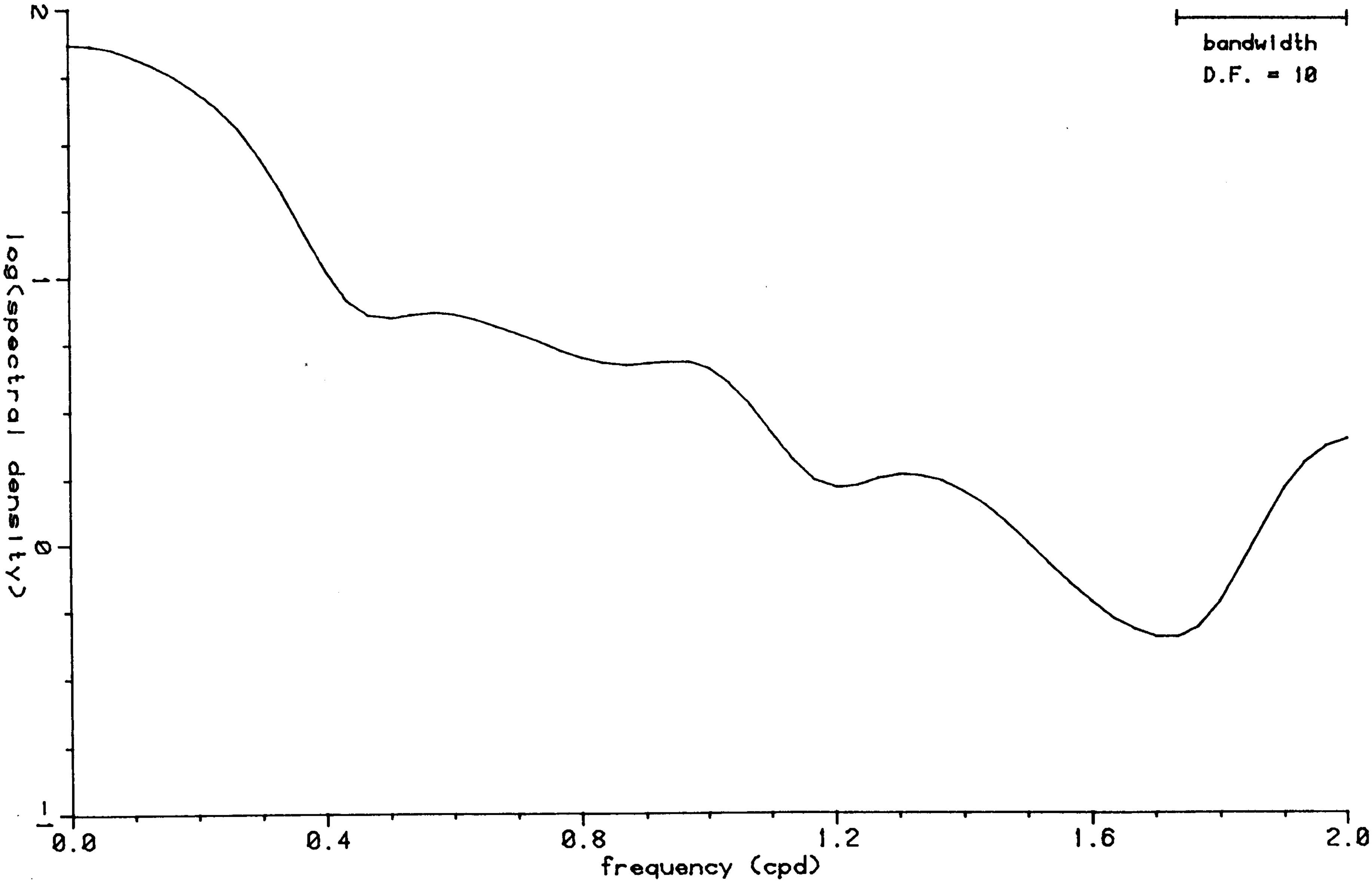

FIGURE A-37 SPECTRAL DENSITY
WAINWRIGHT WIND (33.7 DEGREE COMPONENT)
1751 12 AUG 1981 - 1751 1 SEPT 1981

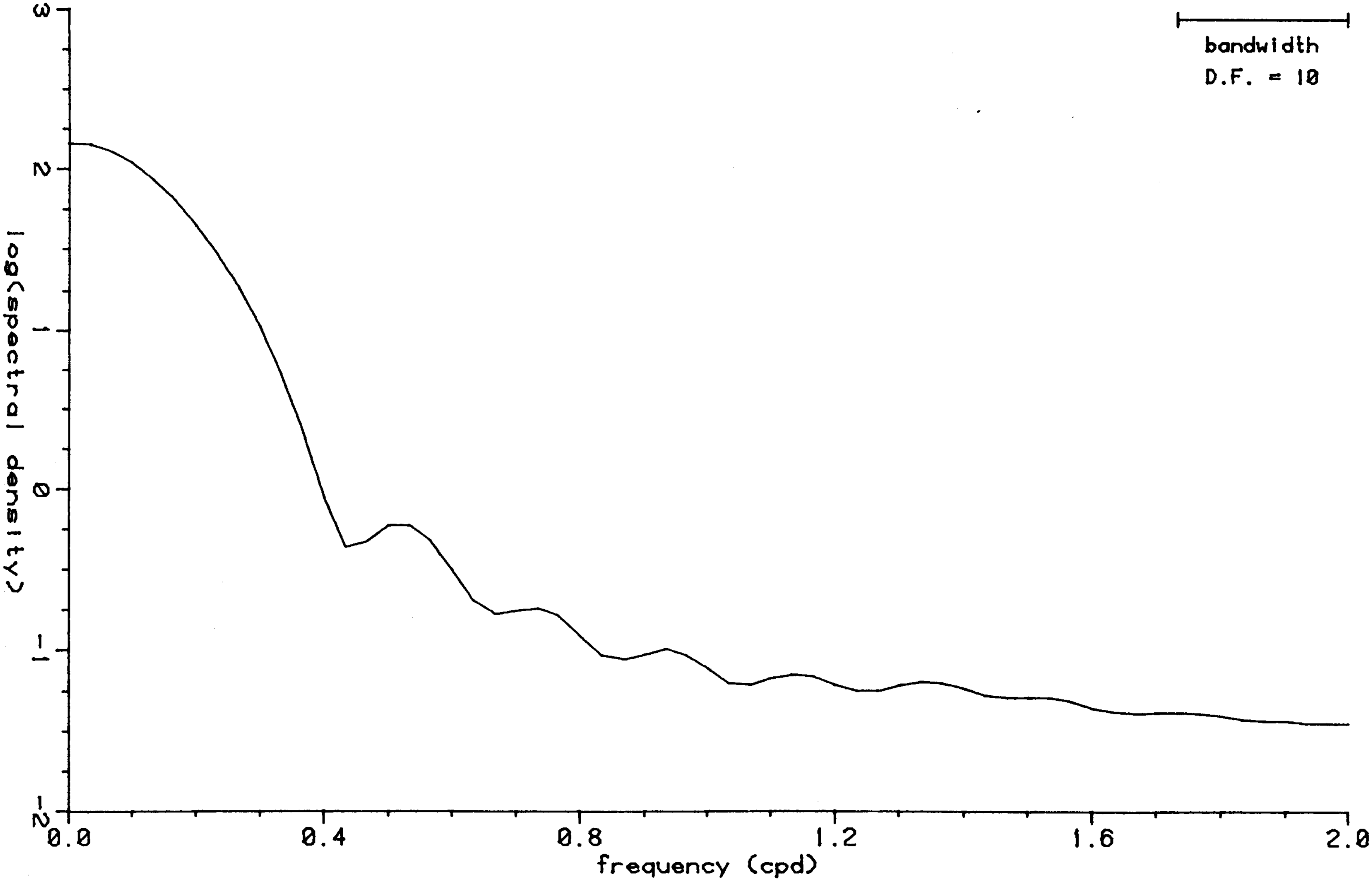

FIGURE A-38 SPECTRAL DENSITY
INSHORE WAINWRIGHT (BOTTOM) DRIFT CURRENT
(33.7 DEGREE COMPONENT)
1751 12 AUG 1981 - 1751 1 SEPT 1981

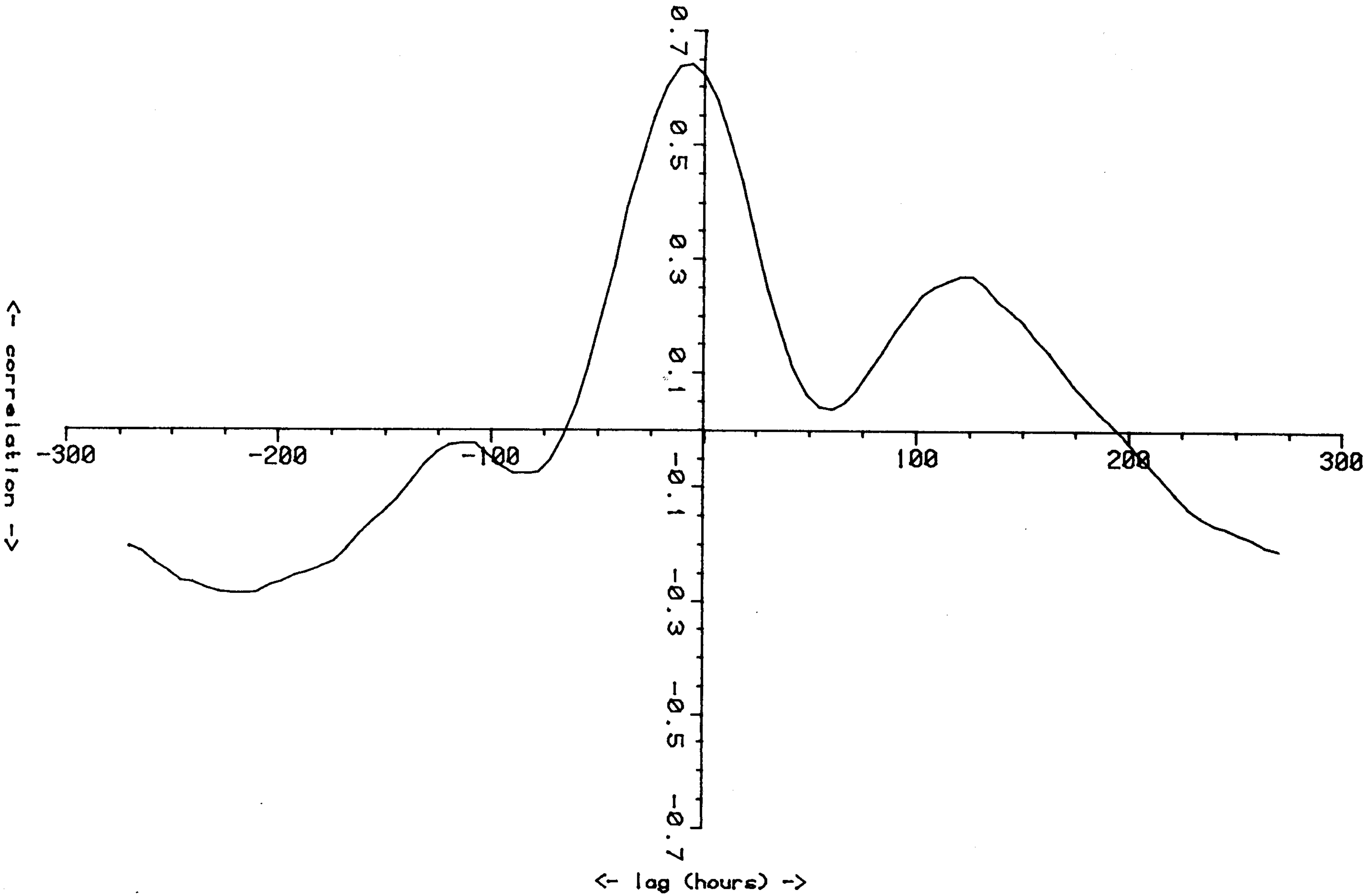

FIGURE A-39 CROSS CORRELATIONS
WAINWRIGHT WIND (33.7 DEGREE COMPONENT) VS. LAGGED INSHORE
WAINWRIGHT (BOTTOM) DRIFT CURRENT (33.7 D.)
1751 12 AUG 1981 - 1751 1 SEPT 1981

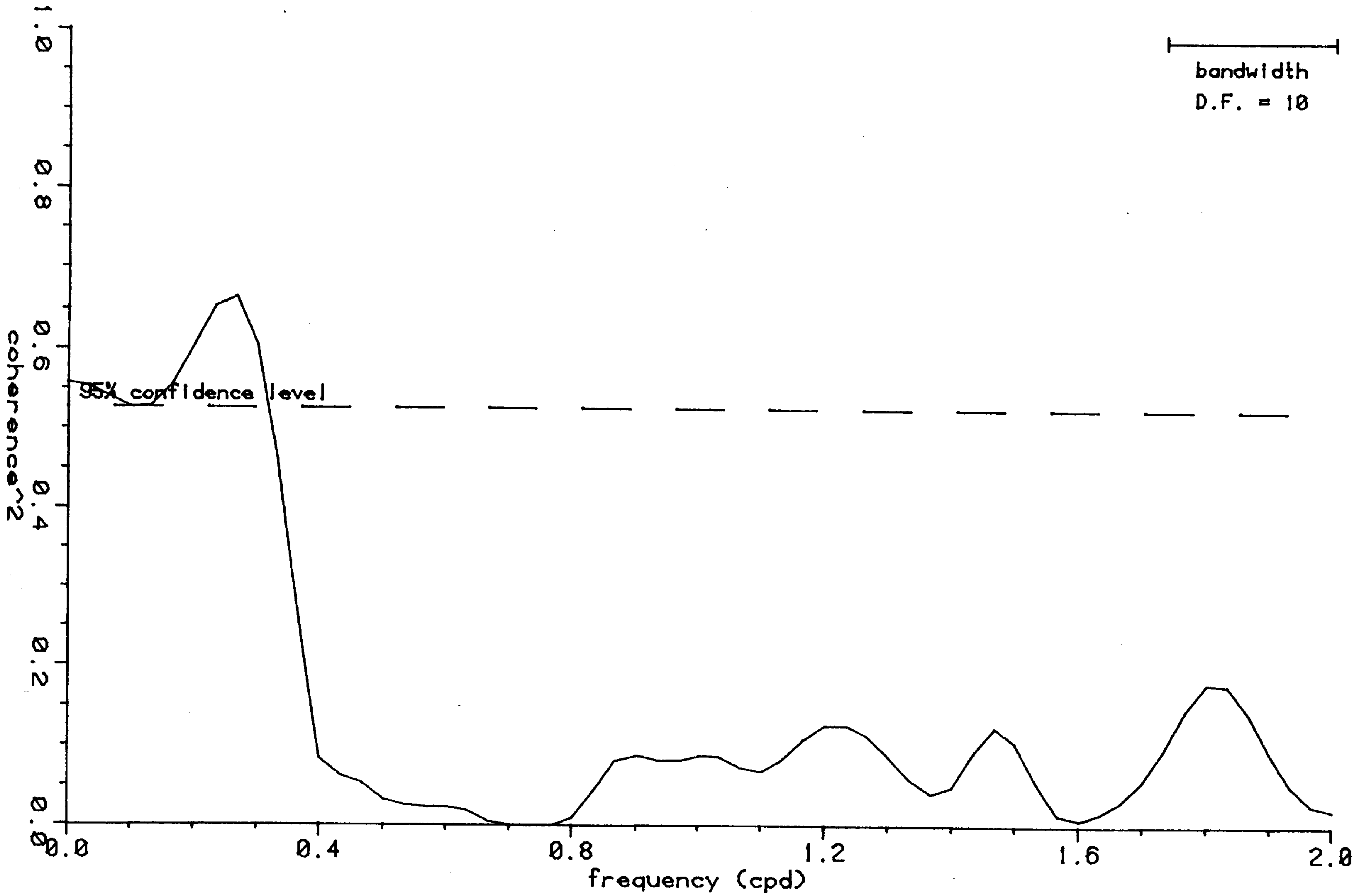

FIGURE A-40 SQUARED COHERENCE SPECTRUM
WAINWRIGHT WIND (33.7 DEGREE COMPONENT) VS. INSHORE
WAINWRIGHT (BOTTOM) DRIFT CURRENT (33.7 DEGREE COMP.)
1751 12 AUG 1981 - 1751 1 SEPT 1981

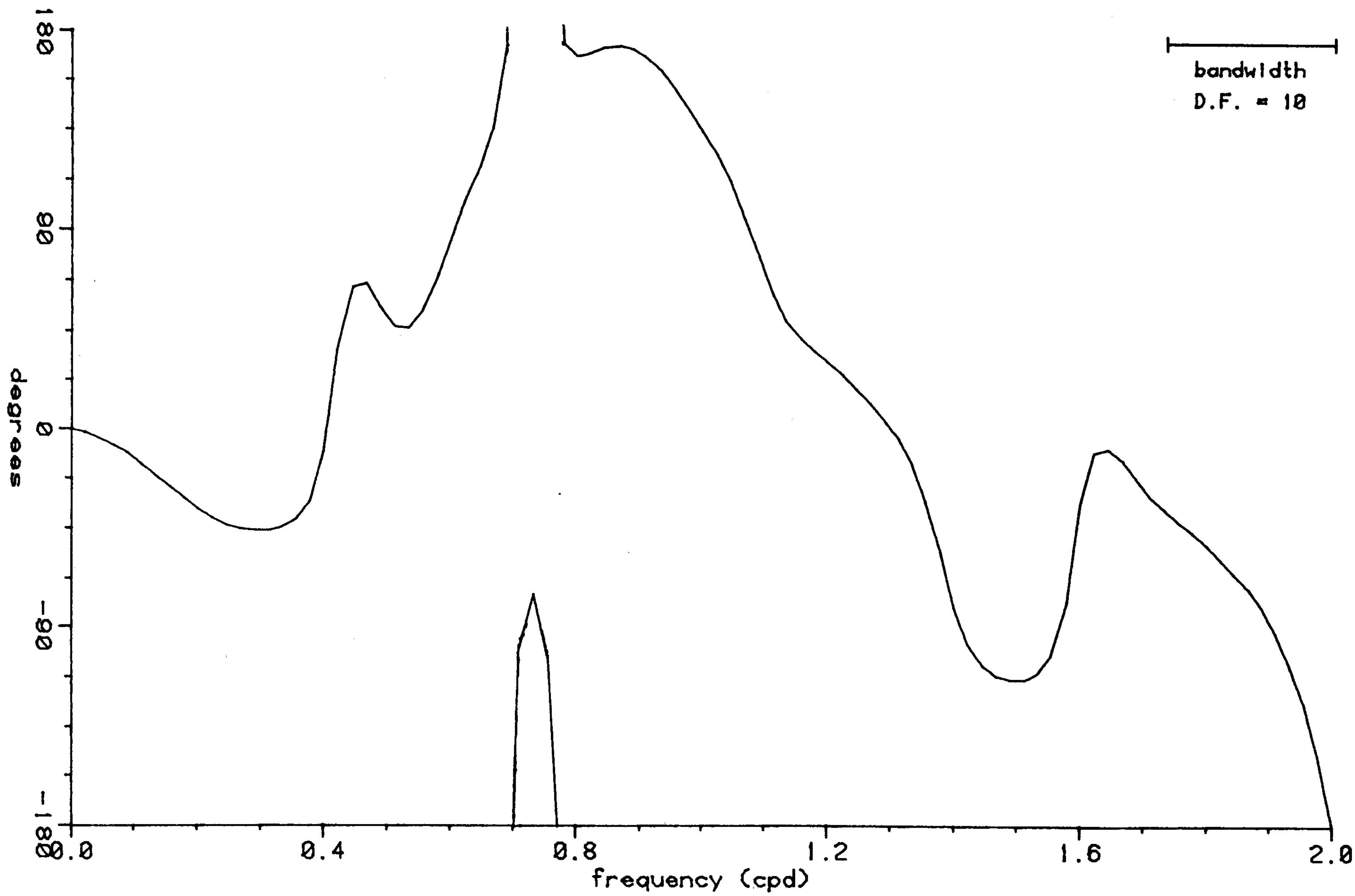

355

FIGURE A-41 PHASE SPECTRUM
WAINWRIGHT WIND (33.7 DEGREE COMPONENT) VS. INSHORE
WAINWRIGHT (BOTTOM) DRIFT CURRENT (33.7 DEGREE COMP.)
1751 12 AUG 1981 - 1751 1 SEPT 1981

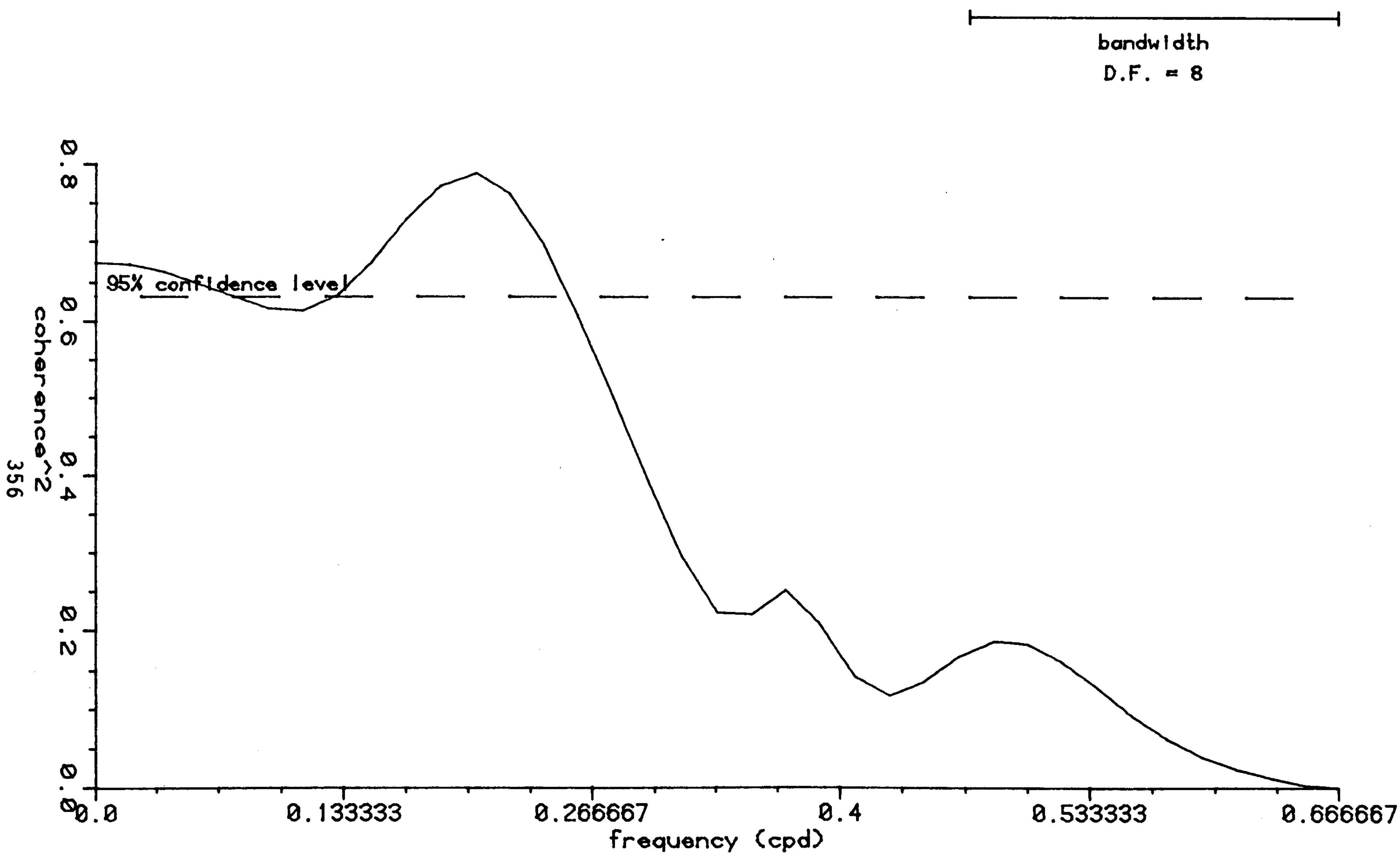

FIGURE A-42 SQUARED COHERENCE SPECTRUM
WAINWRIGHT WIND (33.7 DEGREE COMPONENT) VS. INSHORE
WAINWRIGHT (BOTTOM) DRIFT CURRENT (33.7 DEGREE COMP.)
1751 12 AUG 1981 - 1751 1 SEPT 1981

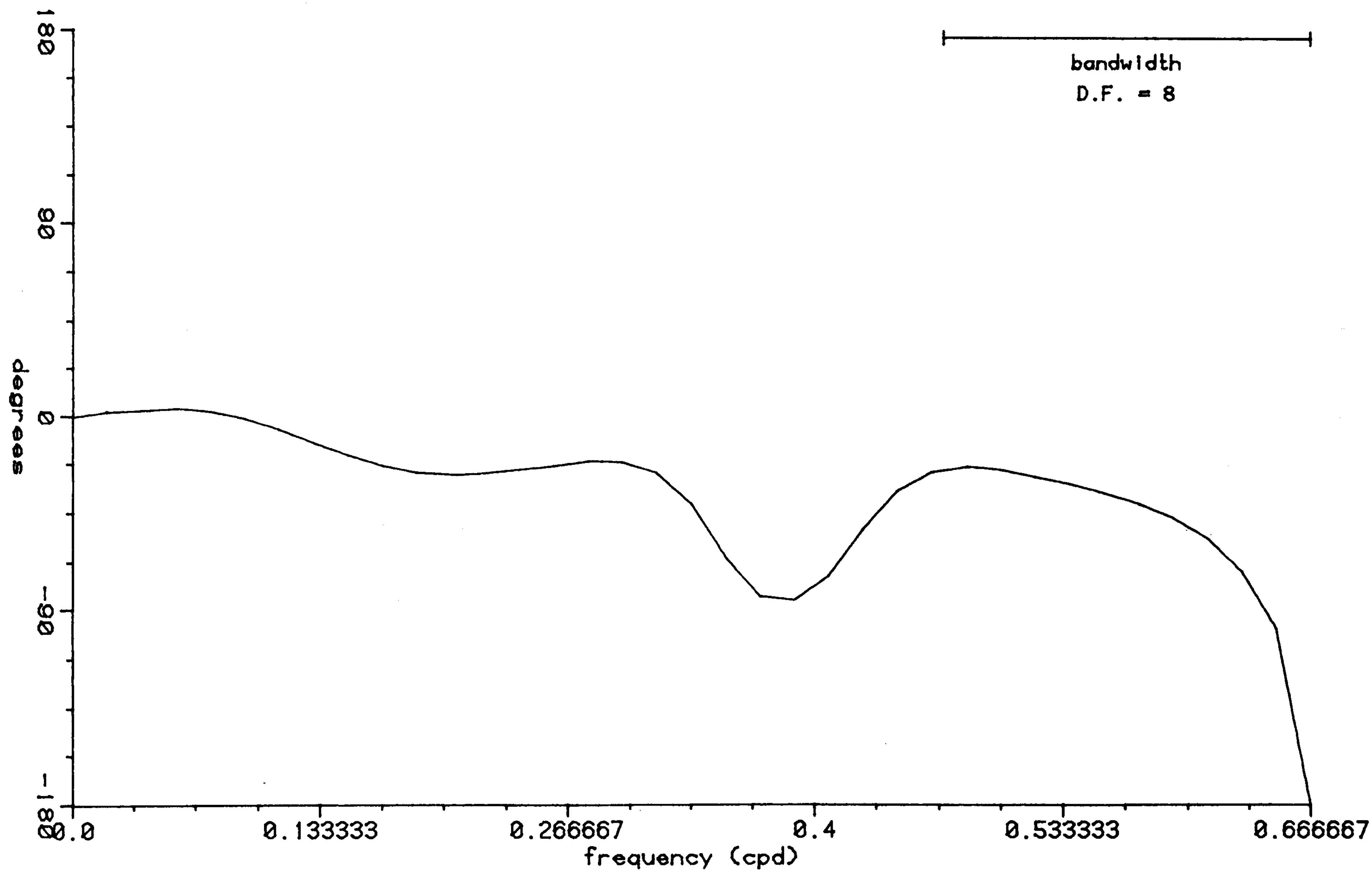

FIGURE A-43 PHASE SPECTRUM
WAINWRIGHT WIND (33.7 DEGREE COMPONENT) VS. INSHORE
WAINWRIGHT (BOTTOM) DRIFT CURRENT (33.7 DEGREE COMP.)
1751 12 AUG 1981 - 1751 1 SEPT 1981

Pressure versus Wind

Pt. Barrow and Wainwright

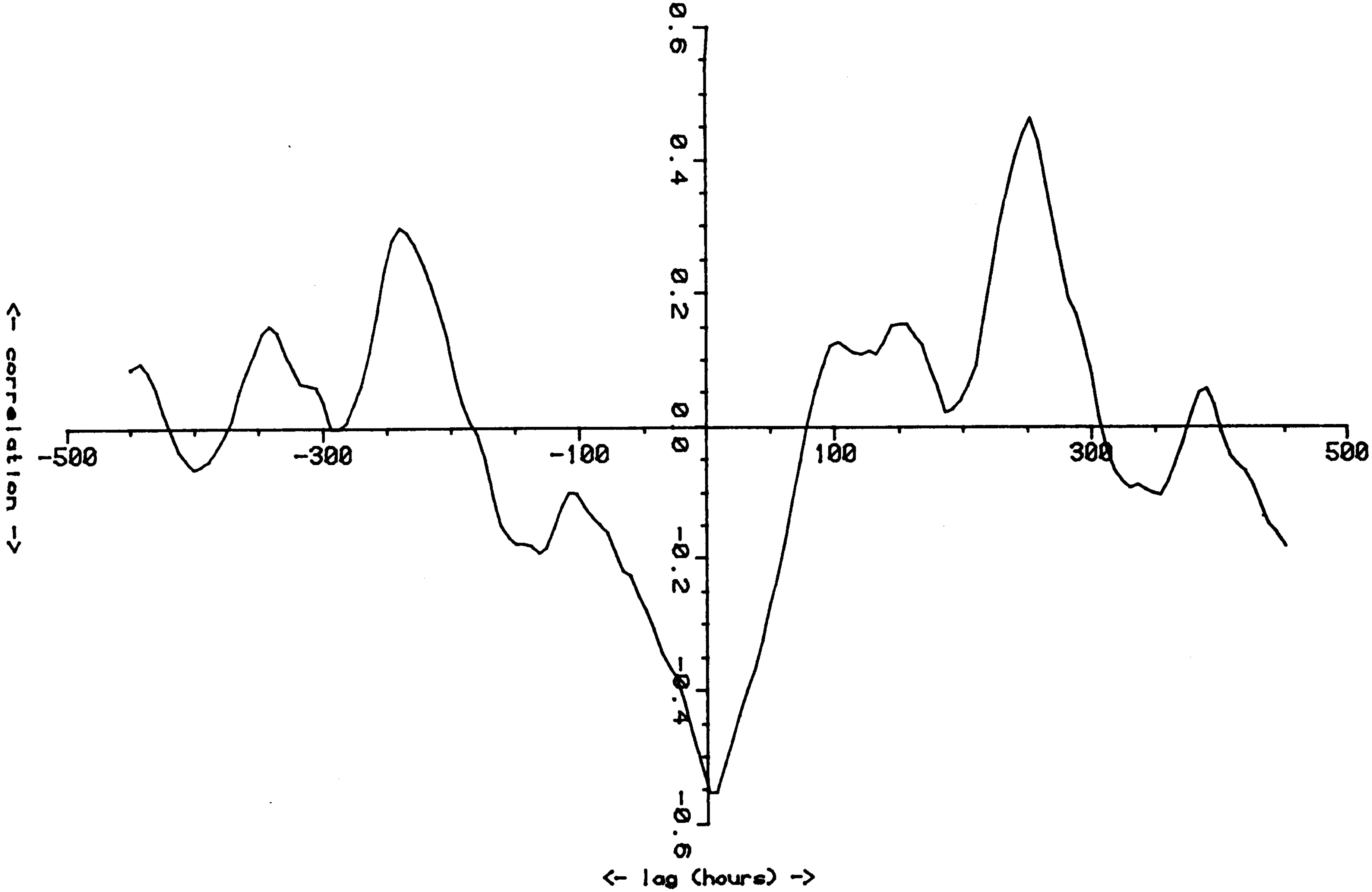

FIGURE A-44 CROSS CORRELATIONS
PT. BARROW-CAPE LISBURNE BAROMETRIC PRESSURE DIFFERENCES VS.
LAGGED PT. BARROW WIND (35.9 DEGREE COMPONENT)
0158 1 AUG 1981 - 1358 4 SEPT 1981

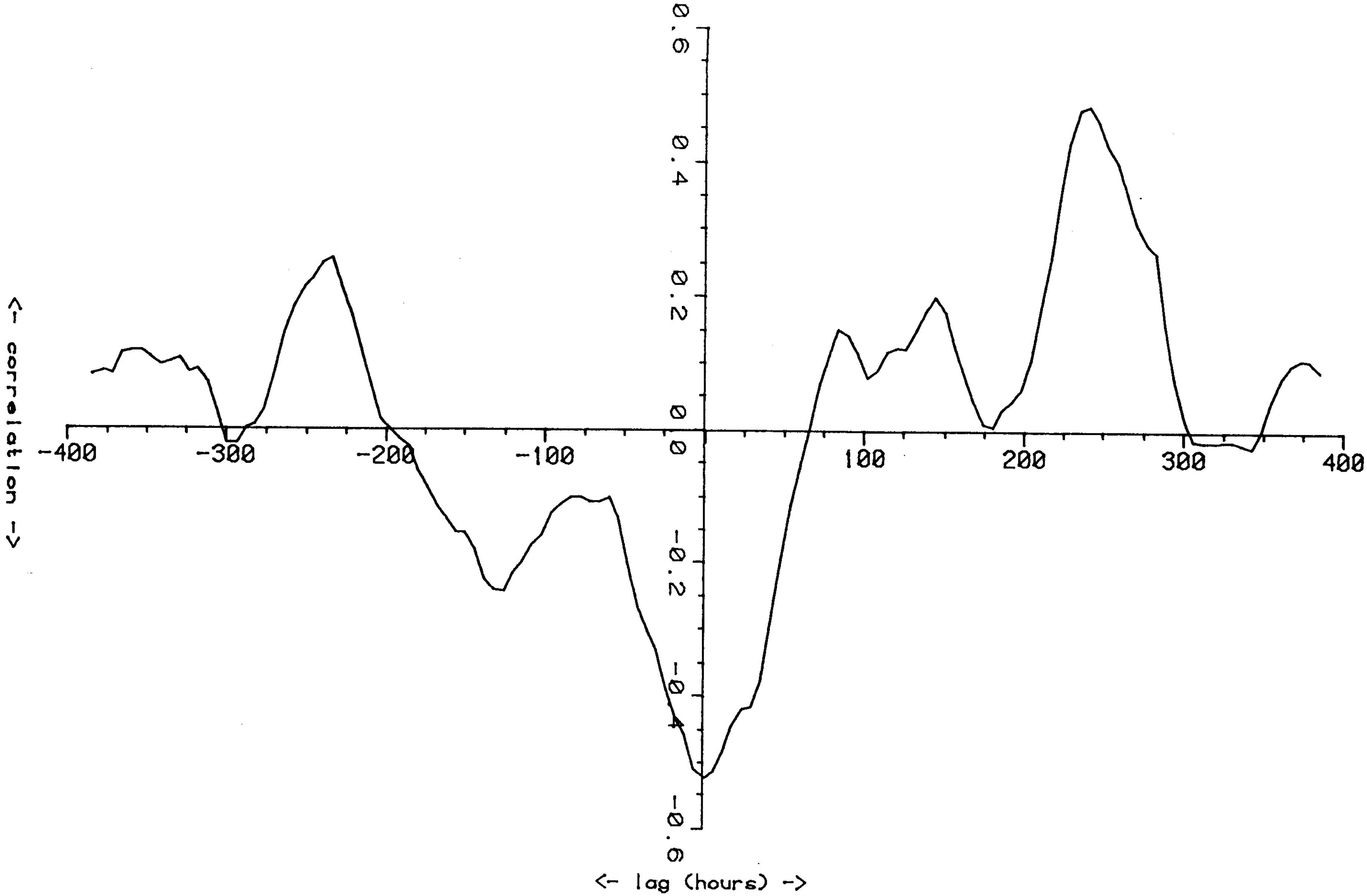

FIGURE A-45 CROSS CORRELATIONS
PT. BARROW - CAPE LISBURNE BAROMETRIC PRESSURE DIFFERENCES
VS. LAGGED WAINWRIGHT WINDS
2359 3 AUG 1981 - 1759 4 SEPT 1981

Statistical

Cross Tabulations

of Current Data

Table A-1
INSHORE BARROW (BOTTOM) DRIFT CURRENT
0700 8 AUG 1981 - 1600 6 SEPT 1981

Frequencies:

Bearing Range	Speed Range (cm/sec) 0.00 15.00	15.00 30.00	30.00 45.00	45.00 60.00	60.00 75.00	> 75.00	total
0 15	0	0	0	0	0	0	0
15- 30	6	0	0	0	0	0	6
30- 45	112	212	24	0	0	0	348
45- 60	41	28	20	0	0	0	89
60- 75	13	0	0	0	0	0	13
75- 90	6	0	0	0	0	0	6
90-105	5	0	0	0	0	0	5
105-120	4	0	0	0	0	0	4
120-135	3	0	0	0	0	0	3
135-150	7	0	0	0	0	0	7
150-165	6	0	0	0	0	0	6
165-180	15	0	0	0	0	0	15
180-195	32	0	0	0	0	0	32
195-210	96	76	0	0	0	0	172
210-225	0	0	0	0	0	0	0
225-240	0	0	0	0	0	0	0
240-255	0	0	0	0	0	0	0
255-270	0	0	0	0	0	0	0
270-285	0	0	0	0	0	0	0
285-300	0	0	0	0	0	0	0
300-315	0	0	0	0	0	0	0
315-330	0	0	0	0	0	0	0
330-345	0	0	0	0	0	0	0
345-360	0	0	0	0	0	0	0
total	346	316	44	0	0	0	706

Table A-2

INSHORE BARROW (BOTTOM) DRIFT CURRENT
0700 8 AUG 1981 - 1600 6 SEPT 1981

Percentages:

Bearing Range	Speed Range (cm/sec) 0.00 15.00	15.00 30.00	30.00 45.00	45.00 60.00	60.00 75.00	> 75.00	total
0 15	0.0	0.0	0.0	0.0	0.0	0.0	0.0
15- 30	0.8	0.0	0.0	0.0	0.0	0.0	0.8
30- 45	15.9	30.0	3.4	0.0	0.0	0.0	49.3
45- 60	5.8	4.0	2.8	0.0	0.0	0.0	12.6
60- 75	1.8	0.0	0.0	0.0	0.0	0.0	1.8
75- 90	0.8	0.0	0.0	0.0	0.0	0.0	0.8
90-105	0.7	0.0	0.0	0.0	0.0	0.0	0.7
105-120	0.6	0.0	0.0	0.0	0.0	0.0	0.6
120-135	0.4	0.0	0.0	0.0	0.0	0.0	0.4
135-150	1.0	0.0	0.0	0.0	0.0	0.0	1.0
150-165	0.8	0.0	0.0	0.0	0.0	0.0	0.8
165-180	2.1	0.0	0.0	0.0	0.0	0.0	2.1
180-195	4.5	0.0	0.0	0.0	0.0	0.0	4.5
195-210	13.6	10.8	0.0	0.0	0.0	0.0	24.4
210-225	0.0	0.0	0.0	0.0	0.0	0.0	0.0
225-240	0.0	0.0	0.0	0.0	0.0	0.0	0.0
240-255	0.0	0.0	0.0	0.0	0.0	0.0	0.0
255-270	0.0	0.0	0.0	0.0	0.0	0.0	0.0
270-285	0.0	0.0	0.0	0.0	0.0	0.0	0.0
285-300	0.0	0.0	0.0	0.0	0.0	0.0	0.0
300-315	0.0	0.0	0.0	0.0	0.0	0.0	0.0
315-330	0.0	0.0	0.0	0.0	0.0	0.0	0.0
330-345	0.0	0.0	0.0	0.0	0.0	0.0	0.0
345-360	0.0	0.0	0.0	0.0	0.0	0.0	0.0
total	49.0	44.8	6.2	0.0	0.0	0.0	100.0

largest screened speed = 43.45 cm/sec
total time period spanned (hours) = 705
sample interval (hours) = 1
total possible observations = 706
actual observations = 706

Table A-3
INSHORE BARROW (BOTTOM) DRIFT CURRENT
0700 8 AUG 1981 - 1600 6 SEPT 1981

Row Percents:

Bearing Range	Speed Range (cm/sec) 0.00 15.00	15.00 30.00	30.00 45.00	45.00 60.00	60.00 75.00	> 75.00	total
0 15	0.0	0.0	0.0	0.0	0.0	0.0	0.0
15- 30	100.0	0.0	0.0	0.0	0.0	0.0	100.0
30- 45	32.2	60.9	6.9	0.0	0.0	0.0	100.0
45- 60	46.1	31.5	22.5	0.0	0.0	0.0	100.0
60- 75	100.0	0.0	0.0	0.0	0.0	0.0	100.0
75- 90	100.0	0.0	0.0	0.0	0.0	0.0	100.0
90-105	100.0	0.0	0.0	0.0	0.0	0.0	100.0
105-120	100.0	0.0	0.0	0.0	0.0	0.0	100.0
120-135	100.0	0.0	0.0	0.0	0.0	0.0	100.0
135-150	100.0	0.0	0.0	0.0	0.0	0.0	100.0
150-165	100.0	0.0	0.0	0.0	0.0	0.0	100.0
165-180	100.0	0.0	0.0	0.0	0.0	0.0	100.0
180-195	100.0	0.0	0.0	0.0	0.0	0.0	100.0
195-210	55.8	44.2	0.0	0.0	0.0	0.0	100.0
210-225	0.0	0.0	0.0	0.0	0.0	0.0	0.0
225-240	0.0	0.0	0.0	0.0	0.0	0.0	0.0
240-255	0.0	0.0	0.0	0.0	0.0	0.0	0.0
255-270	0.0	0.0	0.0	0.0	0.0	0.0	0.0
270-285	0.0	0.0	0.0	0.0	0.0	0.0	0.0
285-300	0.0	0.0	0.0	0.0	0.0	0.0	0.0
300-315	0.0	0.0	0.0	0.0	0.0	0.0	0.0
315-330	0.0	0.0	0.0	0.0	0.0	0.0	0.0
330-345	0.0	0.0	0.0	0.0	0.0	0.0	0.0
345-360	0.0	0.0	0.0	0.0	0.0	0.0	0.0
total	49.0	44.8	6.2	0.0	0.0	0.0	100.0

Table A-4

INSHORE BARROW (BOTTOM) DRIFT CURRENT
0700 8 AUG 1981 - 1600 6 SEPT 1981

Column Percents:

Bearing Range	Speed Range (cm/sec) 0.00 15.00	15.00 30.00	30.00 45.00	45.00 60.00	60.00 75.00	> 75.00	total
0 15	0.0	0.0	0.0	0.0	0.0	0.0	0.0
15- 30	1.7	0.0	0.0	0.0	0.0	0.0	0.8
30- 45	32.4	67.1	54.5	0.0	0.0	0.0	49.3
45- 60	11.8	8.9	45.5	0.0	0.0	0.0	12.6
60- 75	3.8	0.0	0.0	0.0	0.0	0.0	1.8
75- 90	1.7	0.0	0.0	0.0	0.0	0.0	0.8
90-105	1.4	0.0	0.0	0.0	0.0	0.0	0.7
105-120	1.2	0.0	0.0	0.0	0.0	0.0	0.6
120-135	0.9	0.0	0.0	0.0	0.0	0.0	0.4
135-150	2.0	0.0	0.0	0.0	0.0	0.0	1.0
150-165	1.7	0.0	0.0	0.0	0.0	0.0	0.8
165-180	4.3	0.0	0.0	0.0	0.0	0.0	2.1
180-195	9.2	0.0	0.0	0.0	0.0	0.0	4.5
195-210	27.7	24.1	0.0	0.0	0.0	0.0	24.4
210-225	0.0	0.0	0.0	0.0	0.0	0.0	0.0
225-240	0.0	0.0	0.0	0.0	0.0	0.0	0.0
240-255	0.0	0.0	0.0	0.0	0.0	0.0	0.0
255-270	0.0	0.0	0.0	0.0	0.0	0.0	0.0
270-285	0.0	0.0	0.0	0.0	0.0	0.0	0.0
285-300	0.0	0.0	0.0	0.0	0.0	0.0	0.0
300-315	0.0	0.0	0.0	0.0	0.0	0.0	0.0
315-330	0.0	0.0	0.0	0.0	0.0	0.0	0.0
330-345	0.0	0.0	0.0	0.0	0.0	0.0	0.0
345-360	0.0	0.0	0.0	0.0	0.0	0.0	0.0
total	100.0	100.0	100.0	0.0	0.0	0.0	100.0

largest screened speed = 43.45 cm/sec
total time period spanned (hours) = 705
sample interval (hours) = 1
total possible observations = 706
actual observations = 706

Table A-5

OFFSHORE BARROW (TOP) DRIFT CURRENT

1020 8 AUG 1981 - 1620 7 SEPT 1981

Frequencies:

Bearing Range	Speed Range (cm/sec) 0.00 15.00	15.00 30.00	30.00 45.00	45.00 60.00	60.00 75.00	> 75.00	total
0 15	0	0	0	0	0	0	0
15- 30	2	0	0	0	0	0	2
30- 45	9	3	0	0	0	0	12
45- 60	8	18	99	90	59	91	365
60- 75	7	14	1	0	0	0	22
75- 90	1	0	0	0	0	0	1
90-105	0	0	0	0	0	0	0
105-120	1	0	0	0	0	0	1
120-135	2	0	0	0	0	0	2
135-150	5	0	0	0	0	0	5
150-165	2	0	0	0	0	0	2
165-180	4	0	0	0	0	0	4
180-195	4	0	0	0	0	0	4
195-210	6	2	25	10	0	0	43
210-225	4	3	17	104	19	0	147
225-240	12	13	26	25	16	0	92
240-255	8	11	5	0	0	0	24
255-270	1	0	0	0	0	0	1
270-285	0	0	0	0	0	0	0
285-300	0	0	0	0	0	0	0
300-315	0	0	0	0	0	0	0
315-330	0	0	0	0	0	0	0
330-345	0	0	0	0	0	0	0
345-360	0	0	0	0	0	0	0
total	76	64	173	229	94	91	727

Table A-6
OFFSHORE BARROW (TOP) DRIFT CURRENT
1020 8 AUG 1981 - 1620 7 SEPT 1981

Percentages:

Bearing Range	Speed Range (cm/sec) 0.00 15.00	15.00 30.00	30.00 45.00	45.00 60.00	60.00 75.00	> 75.00	total
0 15	0.0	0.0	0.0	0.0	0.0	0.0	0.0
15- 30	0.3	0.0	0.0	0.0	0.0	0.0	0.3
30- 45	1.2	0.4	0.0	0.0	0.0	0.0	1.7
45- 60	1.1	2.5	13.6	12.4	8.1	12.5	50.2
60- 75	1.0	1.9	0.1	0.0	0.0	0.0	3.0
75- 90	0.1	0.0	0.0	0.0	0.0	0.0	0.1
90-105	0.0	0.0	0.0	0.0	0.0	0.0	0.0
105-120	0.1	0.0	0.0	0.0	0.0	0.0	0.1
120-135	0.3	0.0	0.0	0.0	0.0	0.0	0.3
135-150	0.7	0.0	0.0	0.0	0.0	0.0	0.7
150-165	0.3	0.0	0.0	0.0	0.0	0.0	0.3
165-180	0.6	0.0	0.0	0.0	0.0	0.0	0.6
180-195	0.6	0.0	0.0	0.0	0.0	0.0	0.6
195-210	0.8	0.3	3.4	1.4	0.0	0.0	5.9
210-225	0.6	0.4	2.3	14.3	2.6	0.0	20.2
225-240	1.7	1.8	3.6	3.4	2.2	0.0	12.7
240-255	1.1	1.5	0.7	0.0	0.0	0.0	3.3
255-270	0.1	0.0	0.0	0.0	0.0	0.0	0.1
270-285	0.0	0.0	0.0	0.0	0.0	0.0	0.0
285-300	0.0	0.0	0.0	0.0	0.0	0.0	0.0
300-315	0.0	0.0	0.0	0.0	0.0	0.0	0.0
315-330	0.0	0.0	0.0	0.0	0.0	0.0	0.0
330-345	0.0	0.0	0.0	0.0	0.0	0.0	0.0
345-360	0.0	0.0	0.0	0.0	0.0	0.0	0.0
total	10.5	8.8	23.8	31.5	12.9	12.5	100.0

largest screened speed = 96.2 cm/sec
total time period spanned (hours) = 726
sample interval (hours) = 1
total possible observations = 727
actual observations = 727

Table A-7
OFFSHORE BARROW (TOP) DRIFT CURRENT
1020 8 AUG 1981 - 1620 7 SEPT 1981

Row Percents:

Bearing Range	Speed Range (cm/sec) 0.00 15.00	15.00 30.00	30.00 45.00	45.00 60.00	60.00 75.00	> 75.00	total
0 15	0.0	0.0	0.0	0.0	0.0	0.0	0.0
15- 30	100.0	0.0	0.0	0.0	0.0	0.0	100.0
30- 45	75.0	25.0	0.0	0.0	0.0	0.0	100.0
45- 60	2.2	4.9	27.1	24.7	16.2	24.9	100.0
60- 75	31.8	63.6	4.5	0.0	0.0	0.0	100.0
75- 90	100.0	0.0	0.0	0.0	0.0	0.0	100.0
90-105	0.0	0.0	0.0	0.0	0.0	0.0	0.0
105-120	100.0	0.0	0.0	0.0	0.0	0.0	100.0
120-135	100.0	0.0	0.0	0.0	0.0	0.0	100.0
135-150	100.0	0.0	0.0	0.0	0.0	0.0	100.0
150-165	100.0	0.0	0.0	0.0	0.0	0.0	100.0
165-180	100.0	0.0	0.0	0.0	0.0	0.0	100.0
180-195	100.0	0.0	0.0	0.0	0.0	0.0	100.0
195-210	14.0	4.7	58.1	23.3	0.0	0.0	100.0
210-225	2.7	2.0	11.6	70.7	12.9	0.0	100.0
225-240	13.0	14.1	28.3	27.2	17.4	0.0	100.0
240-255	33.3	45.8	20.8	0.0	0.0	0.0	100.0
255-270	100.0	0.0	0.0	0.0	0.0	0.0	100.0
270-285	0.0	0.0	0.0	0.0	0.0	0.0	0.0
285-300	0.0	0.0	0.0	0.0	0.0	0.0	0.0
300-315	0.0	0.0	0.0	0.0	0.0	0.0	0.0
315-330	0.0	0.0	0.0	0.0	0.0	0.0	0.0
330-345	0.0	0.0	0.0	0.0	0.0	0.0	0.0
345-360	0.0	0.0	0.0	0.0	0.0	0.0	0.0
total	10.5	8.8	23.8	31.5	12.9	12.5	100.0

Table A-8
OFFSHORE BARROW (TOP) DRIFT CURRENT
1020 8 AUG 1981 - 1620 7 SEPT 1981

Column Percents:

Bearing Range	Speed Range (cm/sec) 0.00 15.00	15.00 30.00	30.00 45.00	45.00 60.00	60.00 75.00	> 75.00	total
0 15	0.0	0.0	0.0	0.0	0.0	0.0	0.0
15- 30	2.6	0.0	0.0	0.0	0.0	0.0	0.3
30- 45	11.8	4.7	0.0	0.0	0.0	0.0	1.7
45- 60	10.5	28.1	57.2	39.3	62.8	100.0	50.2
60- 75	9.2	21.9	0.6	0.0	0.0	0.0	3.0
75- 90	1.3	0.0	0.0	0.0	0.0	0.0	0.1
90-105	0.0	0.0	0.0	0.0	0.0	0.0	0.0
105-120	1.3	0.0	0.0	0.0	0.0	0.0	0.1
120-135	2.6	0.0	0.0	0.0	0.0	0.0	0.3
135-150	6.6	0.0	0.0	0.0	0.0	0.0	0.7
150-165	2.6	0.0	0.0	0.0	0.0	0.0	0.3
165-180	5.3	0.0	0.0	0.0	0.0	0.0	0.6
180-195	5.3	0.0	0.0	0.0	0.0	0.0	0.6
195-210	7.9	3.1	14.5	4.4	0.0	0.0	5.9
210-225	5.3	4.7	9.8	45.4	20.2	0.0	20.2
225-240	15.8	20.3	15.0	10.9	17.0	0.0	12.7
240-255	10.5	17.2	2.9	0.0	0.0	0.0	3.3
255-270	1.3	0.0	0.0	0.0	0.0	0.0	0.1
270-285	0.0	0.0	0.0	0.0	0.0	0.0	0.0
285-300	0.0	0.0	0.0	0.0	0.0	0.0	0.0
300-315	0.0	0.0	0.0	0.0	0.0	0.0	0.0
315-330	0.0	0.0	0.0	0.0	0.0	0.0	0.0
330-345	0.0	0.0	0.0	0.0	0.0	0.0	0.0
345-360	0.0	0.0	0.0	0.0	0.0	0.0	0.0
total	100.0	100.0	100.0	100.0	100.0	100.0	100.0

largest screened speed = 96.2 cm/sec
total time period spanned (hours) = 726
sample interval (hours) = 1
total possible observations = 727
actual observations = 727

Table A-9
OFFSHORE BARROW (BOTTOM) DRIFT CURRENTS
1010 8 AUG 1981 - 1610 7 SEPT 1981

Frequencies:

Bearing Range	Speed Range (cm/sec) 0.00 15.00	15.00 30.00	30.00 45.00	45.00 60.00	60.00 75.00	> 75.00	total
0 15	1	0	0	0	0	0	1
15- 30	3	1	0	0	0	0	4
30- 45	14	14	35	0	0	0	63
45- 60	43	112	143	0	0	0	298
60- 75	23	17	19	4	0	0	63
75- 90	15	0	16	12	0	0	43
90-105	9	0	0	0	0	0	9
105-120	11	0	0	0	0	0	11
120-135	1	0	0	0	0	0	1
135-150	1	0	0	0	0	0	1
150-165	1	0	0	0	0	0	1
165-180	2	0	0	0	0	0	2
180-195	2	0	0	0	0	0	2
195-210	23	10	0	0	0	0	33
210-225	30	99	27	0	0	0	156
225-240	7	20	0	0	0	0	27
240-255	4	0	0	0	0	0	4
255-270	2	0	0	0	0	0	2
270-285	2	0	0	0	0	0	2
285-300	0	0	0	0	0	0	0
300-315	1	0	0	0	0	0	1
315-330	1	0	0	0	0	0	1
330-345	1	0	0	0	0	0	1
345-360	1	0	0	0	0	0	1
total	198	273	240	16	0	0	727

Table A-10
OFFSHORE BARROW (BOTTOM) DRIFT CURRENTS
1010 8 AUG 1981 - 1610 7 SEPT 1981

Percentages:

Bearing Range	Speed Range (cm/sec) 0.00 15.00	15.00 30.00	30.00 45.00	45.00 60.00	60.00 75.00	> 75.00	total
0 15	0.1	0.0	0.0	0.0	0.0	0.0	0.1
15- 30	0.4	0.1	0.0	0.0	0.0	0.0	0.6
30- 45	1.9	1.9	4.8	0.0	0.0	0.0	8.7
45- 60	5.9	15.4	19.7	0.0	0.0	0.0	41.0
60- 75	3.2	2.3	2.6	0.6	0.0	0.0	8.7
75- 90	2.1	0.0	2.2	1.7	0.0	0.0	5.9
90-105	1.2	0.0	0.0	0.0	0.0	0.0	1.2
105-120	1.5	0.0	0.0	0.0	0.0	0.0	1.5
120-135	0.1	0.0	0.0	0.0	0.0	0.0	0.1
135-150	0.1	0.0	0.0	0.0	0.0	0.0	0.1
150-165	0.1	0.0	0.0	0.0	0.0	0.0	0.1
165-180	0.3	0.0	0.0	0.0	0.0	0.0	0.3
180-195	0.3	0.0	0.0	0.0	0.0	0.0	0.3
195-210	3.2	1.4	0.0	0.0	0.0	0.0	4.5
210-225	4.1	13.6	3.7	0.0	0.0	0.0	21.5
225-240	1.0	2.8	0.0	0.0	0.0	0.0	3.7
240-255	0.6	0.0	0.0	0.0	0.0	0.0	0.6
255-270	0.3	0.0	0.0	0.0	0.0	0.0	0.3
270-285	0.3	0.0	0.0	0.0	0.0	0.0	0.3
285-300	0.0	0.0	0.0	0.0	0.0	0.0	0.0
300-315	0.1	0.0	0.0	0.0	0.0	0.0	0.1
315-330	0.1	0.0	0.0	0.0	0.0	0.0	0.1
330-345	0.1	0.0	0.0	0.0	0.0	0.0	0.1
345-360	0.1	0.0	0.0	0.0	0.0	0.0	0.1
total	27.2	37.6	33.0	2.2	0.0	0.0	100.0

largest screened speed = 46.55 cm/sec
total time period spanned (hours) = 726
sample interval (hours) = 1
total possible observations = 727
actual observations = 727

Table A-11
OFFSHORE BARROW (BOTTOM) DRIFT CURRENTS
1010 8 AUG 1981 - 1610 7 SEPT 1981

Row Percents:

Bearing Range	Speed Range (cm/sec) 0.00 15.00	15.00 30.00	30.00 45.00	45.00 60.00	60.00 75.00	> 75.00	total
0 15	100.0	0.0	0.0	0.0	0.0	0.0	100.0
15- 30	75.0	25.0	0.0	0.0	0.0	0.0	100.0
30- 45	22.2	22.2	55.6	0.0	0.0	0.0	100.0
45- 60	14.4	37.6	48.0	0.0	0.0	0.0	100.0
60- 75	36.5	27.0	30.2	6.3	0.0	0.0	100.0
75- 90	34.9	0.0	37.2	27.9	0.0	0.0	100.0
90-105	100.0	0.0	0.0	0.0	0.0	0.0	100.0
105-120	100.0	0.0	0.0	0.0	0.0	0.0	100.0
120-135	100.0	0.0	0.0	0.0	0.0	0.0	100.0
135-150	100.0	0.0	0.0	0.0	0.0	0.0	100.0
150-165	100.0	0.0	0.0	0.0	0.0	0.0	100.0
165-180	100.0	0.0	0.0	0.0	0.0	0.0	100.0
180-195	100.0	0.0	0.0	0.0	0.0	0.0	100.0
195-210	69.7	30.3	0.0	0.0	0.0	0.0	100.0
210-225	19.2	63.5	17.3	0.0	0.0	0.0	100.0
225-240	25.9	74.1	0.0	0.0	0.0	0.0	100.0
240-255	100.0	0.0	0.0	0.0	0.0	0.0	100.0
255-270	100.0	0.0	0.0	0.0	0.0	0.0	100.0
270-285	100.0	0.0	0.0	0.0	0.0	0.0	100.0
285-300	0.0	0.0	0.0	0.0	0.0	0.0	0.0
300-315	100.0	0.0	0.0	0.0	0.0	0.0	100.0
315-330	100.0	0.0	0.0	0.0	0.0	0.0	100.0
330-345	100.0	0.0	0.0	0.0	0.0	0.0	100.0
345-360	100.0	0.0	0.0	0.0	0.0	0.0	100.0
total	27.2	37.6	33.0	2.2	0.0	0.0	100.0

Table A-12
OFFSHORE BARROW (BOTTOM) DRIFT CURRENTS
1010 8 AUG 1981 - 1610 7 SEPT 1981

Column Percents:

Bearing Range	Speed Range (cm/sec) 0.00 15.00	15.00 30.00	30.00 45.00	45.00 60.00	60.00 75.00	> 75.00	total
0 15	0.5	0.0	0.0	0.0	0.0	0.0	0.1
15- 30	1.5	0.4	0.0	0.0	0.0	0.0	0.6
30- 45	7.1	5.1	14.6	0.0	0.0	0.0	8.7
45- 60	21.7	41.0	59.6	0.0	0.0	0.0	41.0
60- 75	11.6	6.2	7.9	25.0	0.0	0.0	8.7
75- 90	7.6	0.0	6.7	75.0	0.0	0.0	5.9
90-105	4.5	0.0	0.0	0.0	0.0	0.0	1.2
105-120	5.6	0.0	0.0	0.0	0.0	0.0	1.5
120-135	0.5	0.0	0.0	0.0	0.0	0.0	0.1
135-150	0.5	0.0	0.0	0.0	0.0	0.0	0.1
150-165	0.5	0.0	0.0	0.0	0.0	0.0	0.1
165-180	1.0	0.0	0.0	0.0	0.0	0.0	0.3
180-195	1.0	0.0	0.0	0.0	0.0	0.0	0.3
195-210	11.6	3.7	0.0	0.0	0.0	0.0	4.5
210-225	15.2	36.3	11.3	0.0	0.0	0.0	21.5
225-240	3.5	7.3	0.0	0.0	0.0	0.0	3.7
240-255	2.0	0.0	0.0	0.0	0.0	0.0	0.6
255-270	1.0	0.0	0.0	0.0	0.0	0.0	0.3
270-285	1.0	0.0	0.0	0.0	0.0	0.0	0.3
285-300	0.0	0.0	0.0	0.0	0.0	0.0	0.0
300-315	0.5	0.0	0.0	0.0	0.0	0.0	0.1
315-330	0.5	0.0	0.0	0.0	0.0	0.0	0.1
330-345	0.5	0.0	0.0	0.0	0.0	0.0	0.1
345-360	0.5	0.0	0.0	0.0	0.0	0.0	0.1
total	100.0	100.0	100.0	100.0	0.0	0.0	100.0

largest screened speed = 46.55 cm/sec
total time period spanned (hours) = 726
sample interval (hours) = 1
total possible observations = 727
actual observations = 727

Table A-13
INSHORE WAINWRIGHT (BOTTOM) DRIFT CURRENT
1342 12 AUG 1981 - 1742 1 SEPT 1981

Frequencies:

Bearing Range	Speed Range (cm/sec) 0.00 15.00	15.00 30.00	30.00 45.00	45.00 60.00	60.00 75.00	> 75.00	total
0 15	0	0	0	0	0	0	0
15- 30	1	16	4	0	0	0	21
30- 45	6	10	23	0	0	0	39
45- 60	59	101	0	0	0	0	160
60- 75	26	0	0	0	0	0	26
75- 90	3	0	0	0	0	0	3
90-105	4	0	0	0	0	0	4
105-120	2	0	0	0	0	0	2
120-135	1	0	0	0	0	0	1
135-150	4	0	0	0	0	0	4
150-165	6	0	0	0	0	0	6
165-180	6	0	0	0	0	0	6
180-195	15	28	0	0	0	0	43
195-210	31	112	0	0	0	0	143
210-225	0	27	0	0	0	0	27
225-240	0	0	0	0	0	0	0
240-255	0	0	0	0	0	0	0
255-270	0	0	0	0	0	0	0
270-285	0	0	0	0	0	0	0
285-300	0	0	0	0	0	0	0
300-315	0	0	0	0	0	0	0
315-330	0	0	0	0	0	0	0
330-345	0	0	0	0	0	0	0
345-360	0	0	0	0	0	0	0
total	164	294	27	0	0	0	485

Table A-14
INSHORE WAINWRIGHT (BOTTOM) DRIFT CURRENT
1342 12 AUG 1981 - 1742 1 SEPT 1981

Percentages:

Bearing Range	Speed Range (cm/sec) 0.00 15.00	15.00 30.00	30.00 45.00	45.00 60.00	60.00 75.00	> 75.00	total
0 15	0.0	0.0	0.0	0.0	0.0	0.0	0.0
15- 30	0.2	3.3	0.8	0.0	0.0	0.0	4.3
30- 45	1.2	2.1	4.7	0.0	0.0	0.0	8.0
45- 60	12.2	20.8	0.0	0.0	0.0	0.0	33.0
60- 75	5.4	0.0	0.0	0.0	0.0	0.0	5.4
75- 90	0.6	0.0	0.0	0.0	0.0	0.0	0.6
90-105	0.8	0.0	0.0	0.0	0.0	0.0	0.8
105-120	0.4	0.0	0.0	0.0	0.0	0.0	0.4
120-135	0.2	0.0	0.0	0.0	0.0	0.0	0.2
135-150	0.8	0.0	0.0	0.0	0.0	0.0	0.8
150-165	1.2	0.0	0.0	0.0	0.0	0.0	1.2
165-180	1.2	0.0	0.0	0.0	0.0	0.0	1.2
180-195	3.1	5.8	0.0	0.0	0.0	0.0	8.9
195-210	6.4	23.1	0.0	0.0	0.0	0.0	29.5
210-225	0.0	5.6	0.0	0.0	0.0	0.0	5.6
225-240	0.0	0.0	0.0	0.0	0.0	0.0	0.0
240-255	0.0	0.0	0.0	0.0	0.0	0.0	0.0
255-270	0.0	0.0	0.0	0.0	0.0	0.0	0.0
270-285	0.0	0.0	0.0	0.0	0.0	0.0	0.0
285-300	0.0	0.0	0.0	0.0	0.0	0.0	0.0
300-315	0.0	0.0	0.0	0.0	0.0	0.0	0.0
315-330	0.0	0.0	0.0	0.0	0.0	0.0	0.0
330-345	0.0	0.0	0.0	0.0	0.0	0.0	0.0
345-360	0.0	0.0	0.0	0.0	0.0	0.0	0.0
total	33.8	60.6	5.6	0.0	0.0	0.0	100.0

largest screened speed = 34.66 cm/sec
total time period spanned (hours) = 484
sample interval (hours) = 1
total possible observations = 485
actual observations = 485

Table A-15
INSHORE WAINWRIGHT (BOTTOM) DRIFT CURRENT
1342 12 AUG 1981 - 1742 1 SEPT 1981

Row Percents:

Bearing Range	Speed Range (cm/sec) 0.00 15.00	15.00 30.00	30.00 45.00	45.00 60.00	60.00 75.00	> 75.00	total
0 15	0.0	0.0	0.0	0.0	0.0	0.0	0.0
15- 30	4.8	76.2	19.0	0.0	0.0	0.0	100.0
30- 45	15.4	25.6	59.0	0.0	0.0	0.0	100.0
45- 60	36.9	63.1	0.0	0.0	0.0	0.0	100.0
60- 75	100.0	0.0	0.0	0.0	0.0	0.0	100.0
75- 90	100.0	0.0	0.0	0.0	0.0	0.0	100.0
90-105	100.0	0.0	0.0	0.0	0.0	0.0	100.0
105-120	100.0	0.0	0.0	0.0	0.0	0.0	100.0
120-135	100.0	0.0	0.0	0.0	0.0	0.0	100.0
135-150	100.0	0.0	0.0	0.0	0.0	0.0	100.0
150-165	100.0	0.0	0.0	0.0	0.0	0.0	100.0
165-180	100.0	0.0	0.0	0.0	0.0	0.0	100.0
180-195	34.9	65.1	0.0	0.0	0.0	0.0	100.0
195-210	21.7	78.3	0.0	0.0	0.0	0.0	100.0
210-225	0.0	100.0	0.0	0.0	0.0	0.0	100.0
225-240	0.0	0.0	0.0	0.0	0.0	0.0	0.0
240-255	0.0	0.0	0.0	0.0	0.0	0.0	0.0
255-270	0.0	0.0	0.0	0.0	0.0	0.0	0.0
270-285	0.0	0.0	0.0	0.0	0.0	0.0	0.0
285-300	0.0	0.0	0.0	0.0	0.0	0.0	0.0
300-315	0.0	0.0	0.0	0.0	0.0	0.0	0.0
315-330	0.0	0.0	0.0	0.0	0.0	0.0	0.0
330-345	0.0	0.0	0.0	0.0	0.0	0.0	0.0
345-360	0.0	0.0	0.0	0.0	0.0	0.0	0.0
total	33.8	60.6	5.6	0.0	0.0	0.0	100.0

Table A-16
INSHORE WAINWRIGHT (BOTTOM) DRIFT CURRENT
1342 12 AUG 1981 - 1742 1 SEPT 1981

Column Percents:

Bearing Range	Speed Range (cm/sec) 0.00 15.00	15.00 30.00	30.00 45.00	45.00 60.00	60.00 75.00	> 75.00	total
0 15	0.0	0.0	0.0	0.0	0.0	0.0	0.0
15- 30	0.6	5.4	14.8	0.0	0.0	0.0	4.3
30- 45	3.7	3.4	85.2	0.0	0.0	0.0	8.0
45- 60	36.0	34.4	0.0	0.0	0.0	0.0	33.0
60- 75	15.9	0.0	0.0	0.0	0.0	0.0	5.4
75- 90	1.8	0.0	0.0	0.0	0.0	0.0	0.6
90-105	2.4	0.0	0.0	0.0	0.0	0.0	0.8
105-120	1.2	0.0	0.0	0.0	0.0	0.0	0.4
120-135	0.6	0.0	0.0	0.0	0.0	0.0	0.2
135-150	2.4	0.0	0.0	0.0	0.0	0.0	0.8
150-165	3.7	0.0	0.0	0.0	0.0	0.0	1.2
165-180	3.7	0.0	0.0	0.0	0.0	0.0	1.2
180-195	9.1	9.5	0.0	0.0	0.0	0.0	8.9
195-210	18.9	38.1	0.0	0.0	0.0	0.0	29.5
210-225	0.0	9.2	0.0	0.0	0.0	0.0	5.6
225-240	0.0	0.0	0.0	0.0	0.0	0.0	0.0
240-255	0.0	0.0	0.0	0.0	0.0	0.0	0.0
255-270	0.0	0.0	0.0	0.0	0.0	0.0	0.0
270-285	0.0	0.0	0.0	0.0	0.0	0.0	0.0
285-300	0.0	0.0	0.0	0.0	0.0	0.0	0.0
300-315	0.0	0.0	0.0	0.0	0.0	0.0	0.0
315-330	0.0	0.0	0.0	0.0	0.0	0.0	0.0
330-345	0.0	0.0	0.0	0.0	0.0	0.0	0.0
345-360	0.0	0.0	0.0	0.0	0.0	0.0	0.0
total	100.0	100.0	100.0	0.0	0.0	0.0	100.0

largest screened speed = 34.66 cm/sec
total time period spanned (hours) = 484
sample interval (hours) = 1
total possible observations = 485
actual observations = 485

Table A-17
OFFSHORE WAINWRIGHT (TOP) DRIFT CURRENT
1553 12 AUG 1981 - 1953 1 SEPT 1981

Frequencies:

Bearing Range	Speed Range (cm/sec) 0.00 15.00	15.00 30.00	30.00 45.00	45.00 60.00	60.00 75.00	> 75.00	total
0 15	0	0	0	0	0	0	0
15- 30	0	0	0	0	0	0	0
30- 45	0	0	0	0	0	0	0
45- 60	6	11	1	0	0	0	18
60- 75	9	44	109	26	0	0	188
75- 90	3	38	30	5	0	0	76
90-105	7	1	0	0	0	0	8
105-120	6	0	0	0	0	0	6
120-135	3	0	0	0	0	0	3
135-150	4	0	0	0	0	0	4
150-165	4	0	0	0	0	0	4
165-180	2	0	0	0	0	0	2
180-195	8	0	0	0	0	0	8
195-210	12	0	0	0	0	0	12
210-225	8	0	0	0	0	0	8
225-240	6	0	25	0	0	0	31
240-255	2	37	50	0	0	0	89
255-270	0	24	3	0	0	0	27
270-285	0	0	0	0	0	0	0
285-300	0	0	0	0	0	0	0
300-315	0	0	0	0	0	0	0
315-330	0	0	0	0	0	0	0
330-345	0	0	0	0	0	0	0
345-360	0	0	0	0	0	0	0
total	80	155	218	31	0	0	484

Table A-18
OFFSHORE WAINWRIGHT (TOP) DRIFT CURRENT
1553 12 AUG 1981 - 1953 1 SEPT 1981

Percentages:

Bearing Range	Speed Range (cm/sec) 0.00 15.00	15.00 30.00	30.00 45.00	45.00 60.00	60.00 75.00	> 75.00	total
0 15	0.0	0.0	0.0	0.0	0.0	0.0	0.0
15- 30	0.0	0.0	0.0	0.0	0.0	0.0	0.0
30- 45	0.0	0.0	0.0	0.0	0.0	0.0	0.0
45- 60	1.2	2.3	0.2	0.0	0.0	0.0	3.7
60- 75	1.9	9.1	22.5	5.4	0.0	0.0	38.8
75- 90	0.6	7.9	6.2	1.0	0.0	0.0	15.7
90-105	1.4	0.2	0.0	0.0	0.0	0.0	1.7
105-120	1.2	0.0	0.0	0.0	0.0	0.0	1.2
120-135	0.6	0.0	0.0	0.0	0.0	0.0	0.6
135-150	0.8	0.0	0.0	0.0	0.0	0.0	0.8
150-165	0.8	0.0	0.0	0.0	0.0	0.0	0.8
165-180	0.4	0.0	0.0	0.0	0.0	0.0	0.4
180-195	1.7	0.0	0.0	0.0	0.0	0.0	1.7
195-210	2.5	0.0	0.0	0.0	0.0	0.0	2.5
210-225	1.7	0.0	0.0	0.0	0.0	0.0	1.7
225-240	1.2	0.0	5.2	0.0	0.0	0.0	6.4
240-255	0.4	7.6	10.3	0.0	0.0	0.0	18.4
255-270	0.0	5.0	0.6	0.0	0.0	0.0	5.6
270-285	0.0	0.0	0.0	0.0	0.0	0.0	0.0
285-300	0.0	0.0	0.0	0.0	0.0	0.0	0.0
300-315	0.0	0.0	0.0	0.0	0.0	0.0	0.0
315-330	0.0	0.0	0.0	0.0	0.0	0.0	0.0
330-345	0.0	0.0	0.0	0.0	0.0	0.0	0.0
345-360	0.0	0.0	0.0	0.0	0.0	0.0	0.0
total	16.5	32.0	45.0	6.4	0.0	0.0	100.0

largest screened speed = 51.81 cm/sec
total time period spanned (hours) = 483
sample interval (hours) = 1
total possible observations = 484
actual observations = 484

Table A-19
OFFSHORE WAINWRIGHT (TOP) DRIFT CURRENT
1553 12 AUG 1981 - 1953 1 SEPT 1981

Row Percents:

Bearing Range	Speed Range (cm/sec) 0.00 15.00	15.00 30.00	30.00 45.00	45.00 60.00	60.00 75.00	> 75.00	total
0 15	0.0	0.0	0.0	0.0	0.0	0.0	0.0
15- 30	0.0	0.0	0.0	0.0	0.0	0.0	0.0
30- 45	0.0	0.0	0.0	0.0	0.0	0.0	0.0
45- 60	33.3	61.1	5.6	0.0	0.0	0.0	100.0
60- 75	4.8	23.4	58.0	13.8	0.0	0.0	100.0
75- 90	3.9	50.0	39.5	6.6	0.0	0.0	100.0
90-105	87.5	12.5	0.0	0.0	0.0	0.0	100.0
105-120	100.0	0.0	0.0	0.0	0.0	0.0	100.0
120-135	100.0	0.0	0.0	0.0	0.0	0.0	100.0
135-150	100.0	0.0	0.0	0.0	0.0	0.0	100.0
150-165	100.0	0.0	0.0	0.0	0.0	0.0	100.0
165-180	100.0	0.0	0.0	0.0	0.0	0.0	100.0
180-195	100.0	0.0	0.0	0.0	0.0	0.0	100.0
195-210	100.0	0.0	0.0	0.0	0.0	0.0	100.0
210-225	100.0	0.0	0.0	0.0	0.0	0.0	100.0
225-240	19.4	0.0	80.6	0.0	0.0	0.0	100.0
240-255	2.2	41.6	56.2	0.0	0.0	0.0	100.0
255-270	0.0	88.9	11.1	0.0	0.0	0.0	100.0
270-285	0.0	0.0	0.0	0.0	0.0	0.0	0.0
285-300	0.0	0.0	0.0	0.0	0.0	0.0	0.0
300-315	0.0	0.0	0.0	0.0	0.0	0.0	0.0
315-330	0.0	0.0	0.0	0.0	0.0	0.0	0.0
330-345	0.0	0.0	0.0	0.0	0.0	0.0	0.0
345-360	0.0	0.0	0.0	0.0	0.0	0.0	0.0
total	16.5	32.0	45.0	6.4	0.0	0.0	100.0

Table A-20
OFFSHORE WAINWRIGHT (TOP) DRIFT CURRENT
1553 12 AUG 1981 - 1953 1 SEPT 1981

Column Percents:

Bearing Range	Speed Range (cm/sec) 0.00 15.00	15.00 30.00	30.00 45.00	45.00 60.00	60.00 75.00	> 75.00	total
0 15	0.0	0.0	0.0	0.0	0.0	0.0	0.0
15- 30	0.0	0.0	0.0	0.0	0.0	0.0	0.0
30- 45	0.0	0.0	0.0	0.0	0.0	0.0	0.0
45- 60	7.5	7.1	0.5	0.0	0.0	0.0	3.7
60- 75	11.3	28.4	50.0	83.9	0.0	0.0	38.8
75- 90	3.8	24.5	13.8	16.1	0.0	0.0	15.7
90-105	8.8	0.6	0.0	0.0	0.0	0.0	1.7
105-120	7.5	0.0	0.0	0.0	0.0	0.0	1.2
120-135	3.8	0.0	0.0	0.0	0.0	0.0	0.6
135-150	5.0	0.0	0.0	0.0	0.0	0.0	0.8
150-165	5.0	0.0	0.0	0.0	0.0	0.0	0.8
165-180	2.5	0.0	0.0	0.0	0.0	0.0	0.4
180-195	10.0	0.0	0.0	0.0	0.0	0.0	1.7
195-210	15.0	0.0	0.0	0.0	0.0	0.0	2.5
210-225	10.0	0.0	0.0	0.0	0.0	0.0	1.7
225-240	7.5	0.0	11.5	0.0	0.0	0.0	6.4
240-255	2.5	23.9	22.9	0.0	0.0	0.0	18.4
255-270	0.0	15.5	1.4	0.0	0.0	0.0	5.6
270-285	0.0	0.0	0.0	0.0	0.0	0.0	0.0
285-300	0.0	0.0	0.0	0.0	0.0	0.0	0.0
300-315	0.0	0.0	0.0	0.0	0.0	0.0	0.0
315-330	0.0	0.0	0.0	0.0	0.0	0.0	0.0
330-345	0.0	0.0	0.0	0.0	0.0	0.0	0.0
345-360	0.0	0.0	0.0	0.0	0.0	0.0	0.0
total	100.0	100.0	100.0	100.0	0.0	0.0	100.0

largest screened speed = 51.81 cm/sec
total time period spanned (hours) = 483
sample interval (hours) = 1
total possible observations = 484
actual observations = 484

Table A-21
OFFSHORE WAINWRIGHT (BOTTOM) DRIFT CURRENT
1513 12 AUG 1981 - 2013 1 SEPT 1981

Frequencies:

Bearing Range	Speed Range (cm/sec) 0.00 15.00	15.00 30.00	30.00 45.00	45.00 60.00	60.00 75.00	> 75.00	total
0 15	0	0	0	0	0	0	0
15- 30	0	0	0	0	0	0	0
30- 45	0	0	21	0	0	0	21
45- 60	2	87	39	0	0	0	128
60- 75	5	99	0	0	0	0	104
75- 90	7	13	0	0	0	0	20
90-105	10	1	0	0	0	0	11
105-120	8	0	0	0	0	0	8
120-135	7	0	0	0	0	0	7
135-150	6	0	0	0	0	0	6
150-165	6	0	0	0	0	0	6
165-180	8	0	0	0	0	0	8
180-195	19	1	0	0	0	0	20
195-210	13	24	7	0	0	0	44
210-225	17	34	52	0	0	0	103
225-240	0	0	0	0	0	0	0
240-255	0	0	0	0	0	0	0
255-270	0	0	0	0	0	0	0
270-285	0	0	0	0	0	0	0
285-300	0	0	0	0	0	0	0
300-315	0	0	0	0	0	0	0
315-330	0	0	0	0	0	0	0
330-345	0	0	0	0	0	0	0
345-360	0	0	0	0	0	0	0
total	108	259	119	0	0	0	486

Table A-22
OFFSHORE WAINWRIGHT (BOTTOM) DRIFT CURRENT
1513 12 AUG 1981 - 2013 1 SEPT 1981

Percentages:

Bearing Range	Speed Range (cm/sec) 0.00 15.00	15.00 30.00	30.00 45.00	45.00 60.00	60.00 75.00	> 75.00	total
0 15	0.0	0.0	0.0	0.0	0.0	0.0	0.0
15- 30	0.0	0.0	0.0	0.0	0.0	0.0	0.0
30- 45	0.0	0.0	4.3	0.0	0.0	0.0	4.3
45- 60	0.4	17.9	8.0	0.0	0.0	0.0	26.3
60- 75	1.0	20.4	0.0	0.0	0.0	0.0	21.4
75- 90	1.4	2.7	0.0	0.0	0.0	0.0	4.1
90-105	2.1	0.2	0.0	0.0	0.0	0.0	2.3
105-120	1.6	0.0	0.0	0.0	0.0	0.0	1.6
120-135	1.4	0.0	0.0	0.0	0.0	0.0	1.4
135-150	1.2	0.0	0.0	0.0	0.0	0.0	1.2
150-165	1.2	0.0	0.0	0.0	0.0	0.0	1.2
165-180	1.6	0.0	0.0	0.0	0.0	0.0	1.6
180-195	3.9	0.2	0.0	0.0	0.0	0.0	4.1
195-210	2.7	4.9	1.4	0.0	0.0	0.0	9.1
210-225	3.5	7.0	10.7	0.0	0.0	0.0	21.2
225-240	0.0	0.0	0.0	0.0	0.0	0.0	0.0
240-255	0.0	0.0	0.0	0.0	0.0	0.0	0.0
255-270	0.0	0.0	0.0	0.0	0.0	0.0	0.0
270-285	0.0	0.0	0.0	0.0	0.0	0.0	0.0
285-300	0.0	0.0	0.0	0.0	0.0	0.0	0.0
300-315	0.0	0.0	0.0	0.0	0.0	0.0	0.0
315-330	0.0	0.0	0.0	0.0	0.0	0.0	0.0
330-345	0.0	0.0	0.0	0.0	0.0	0.0	0.0
345-360	0.0	0.0	0.0	0.0	0.0	0.0	0.0
total	22.2	53.3	24.5	0.0	0.0	0.0	100.0

largest screened speed = 43.57 cm/sec
total time period spanned (hours) = 485
sample interval (hours) = 1
total possible observations = 486
actual observations = 486

Table A-23
OFFSHCRE WAINWRIGHT (BOTTOM) DRIFT CURRENT
1513 12 AUG 1981 - 2013 1 SEPT 1981

Row Percents:

Bearing Range	Speed Range (cm/sec) 0.00 15.00	15.00 30.00	30.00 45.00	45.00 60.00	60.00 75.00	> 75.00	total
0 15	0.0	0.0	0.0	0.0	0.0	0.0	0.0
15- 30	0.0	0.0	0.0	0.0	0.0	0.0	0.0
30- 45	0.0	0.0	100.0	0.0	0.0	0.0	100.0
45- 60	1.6	68.0	30.5	0.0	0.0	0.0	100.0
60- 75	4.8	95.2	0.0	0.0	0.0	0.0	100.0
75- 90	35.0	65.0	0.0	0.0	0.0	0.0	100.0
90-105	90.9	9.1	0.0	0.0	0.0	0.0	100.0
105-120	100.0	0.0	0.0	0.0	0.0	0.0	100.0
120-135	100.0	0.0	0.0	0.0	0.0	0.0	100.0
135-150	100.0	0.0	0.0	0.0	0.0	0.0	100.0
150-165	100.0	0.0	0.0	0.0	0.0	0.0	100.0
165-180	100.0	0.0	0.0	0.0	0.0	0.0	100.0
180-195	95.0	5.0	0.0	0.0	0.0	0.0	100.0
195-210	29.5	54.5	15.9	0.0	0.0	0.0	100.0
210-225	16.5	33.0	50.5	0.0	0.0	0.0	100.0
225-240	0.0	0.0	0.0	0.0	0.0	0.0	0.0
240-255	0.0	0.0	0.0	0.0	0.0	0.0	0.0
255-270	0.0	0.0	0.0	0.0	0.0	0.0	0.0
270-285	0.0	0.0	0.0	0.0	0.0	0.0	0.0
285-300	0.0	0.0	0.0	0.0	0.0	0.0	0.0
300-315	0.0	0.0	0.0	0.0	0.0	0.0	0.0
315-330	0.0	0.0	0.0	0.0	0.0	0.0	0.0
330-345	0.0	0.0	0.0	0.0	0.0	0.0	0.0
345-360	0.0	0.0	0.0	0.0	0.0	0.0	0.0
total	22.2	53.3	24.5	0.0	0.0	0.0	100.0

Table A-24
OFFSHORE WAINWRIGHT (BOTTOM) DRIFT CURRENT
1513 12 AUG 1981 - 2013 1 SEPT 1981

Column Percents:

Bearing Range	Speed Range (cm/sec) 0.00 15.00	15.00 30.00	30.00 45.00	45.00 60.00	60.00 75.00	> 75.00	total
0 15	0.0	0.0	0.0	0.0	0.0	0.0	0.0
15- 30	0.0	0.0	0.0	0.0	0.0	0.0	0.0
30- 45	0.0	0.0	17.6	0.0	0.0	0.0	4.3
45- 60	1.9	33.6	32.8	0.0	0.0	0.0	26.3
60- 75	4.6	38.2	0.0	0.0	0.0	0.0	21.4
75- 90	6.5	5.0	0.0	0.0	0.0	0.0	4.1
90-105	9.3	0.4	0.0	0.0	0.0	0.0	2.3
105-120	7.4	0.0	0.0	0.0	0.0	0.0	1.6
120-135	6.5	0.0	0.0	0.0	0.0	0.0	1.4
135-150	5.6	0.0	0.0	0.0	0.0	0.0	1.2
150-165	5.6	0.0	0.0	0.0	0.0	0.0	1.2
165-180	7.4	0.0	0.0	0.0	0.0	0.0	1.6
180-195	17.6	0.4	0.0	0.0	0.0	0.0	4.1
195-210	12.0	9.3	5.9	0.0	0.0	0.0	9.1
210-225	15.7	13.1	43.7	0.0	0.0	0.0	21.2
225-240	0.0	0.0	0.0	0.0	0.0	0.0	0.0
240-255	0.0	0.0	0.0	0.0	0.0	0.0	0.0
255-270	0.0	0.0	0.0	0.0	0.0	0.0	0.0
270-285	0.0	0.0	0.0	0.0	0.0	0.0	0.0
285-300	0.0	0.0	0.0	0.0	0.0	0.0	0.0
300-315	0.0	0.0	0.0	0.0	0.0	0.0	0.0
315-330	0.0	0.0	0.0	0.0	0.0	0.0	0.0
330-345	0.0	0.0	0.0	0.0	0.0	0.0	0.0
345-360	0.0	0.0	0.0	0.0	0.0	0.0	0.0
total	100.0	100.0	100.0	0.0	0.0	0.0	100.0

largest screened speed = 43.57 cm/sec
total time period spanned (hours) = 485
sample interval (hours) = 1
total possible observations = 486
actual observations = 486

APPENDIX B

Meteorological Data

Wind Data

Table B-1 Barrow Wind Data.

Calendar Day	Julian Day	Time (GMT)	Direction (°True)	Speed (knots)
Aug 01	213	0059	290	10
		0359	300	13
		0654	290	10
		0954	300	11
		1257	270	14
		1556	280	11
		1858	290	12
		2154	320	13
Aug 02	214	0054	320	13
		0353	320	12
		0655	340	11
		0955	280	06
		1258	290	09
		1553	280	09
		1856	240	06
		2156	230	06
Aug 03	215	0054	220	06
		0353	180	07
		0652	200	13
		0954	230	11
		1255	220	08
		1557	210	13
		1857	200	11
		2159	180	09
Aug 04	216	0053	200	08
		0354	240	08
		0651	250	10
		0958	230	10
		1257	250	08
		1559	240	09
		1853	250	09
		2156	180	06
Aug 05	217	0057	180	03
		0353	180	08
		0651	230	06
		0955	310	07
		1258	290	03
		1559	320	06
		1857	340	07
		2158	360	08

Table B-2 (Continued)

Calendar Day	Julian Day	Time (GMT)	Direction (°True)	Speed (knots)
Aug 06	218	0057	360	13
		0353	360	12
		0652	360	11
		0953	360	08
		1258	340	10
		1558	340	08
		1853	340	08
		2155	330	06
Aug 07	219	0055	330	08
		0353	350	07
		0652	340	04
		0957	310	06
		1258	320	04
		1554	320	08
		1854	040	05
		2152	020	05
Aug 08	220	0055	050	07
		0354	070	10
		0650	060	08
		0956	070	10
		1258	060	12
		1552	080	10
		1852	080	11
		2154	050	12
Aug 09	221	0054	060	11
		0358	050	11
		0650	060	12
		0953	050	11
		1258	050	08
		1554	060	10
		1852	070	14
		2153	070	12
Aug 10	222	0057	070	09
		0357	090	07
		0650	070	06
		0954	020	07
		1258	010	07
		1553	360	06
		1852	060	07
		2153	050	06

Table B-3 (Continued)

Calendar Day	Julian Day	Time (GMT)	Direction (°True)	Speed (knots)
Aug 11	223	0056	080	07
		0354	080	06
		0651	080	10
		0958	080	10
		1252	080	11
		1553	090	13
		1852	100	14
		2153	090	12
Aug 12	224	0055	080	12
		0356	060	12
		0653	090	12
		0955	060	13
		1251	060	10
		1554	050	10
		1851	020	08
		2156	360	11
Aug 13	225	0057	010	06
		0356	320	05
		0652	250	09
		0954	240	11
		1253	230	08
		1556	270	07
		1850	300	06
		2156	350	03
Aug 14	226	0058	350	05
		0358	320	03
		0656	290	06
		0954	280	05
		1255	310	05
		1551	290	07
		1858	300	06
		2155	330	03
Aug 15	227	0057	140	03
		0357	330	04
		0653	360	04
		0953	010	05
		1252	035	08
		1557	330	06
		1857	020	07
		2156	020	08

Table B-4 (Continued)

Calendar Day	Julian Day	Time (GMT)	Direction (°True)	Speed (knots)
Aug 16	228	0056	350	09
		0354	340	10
		0653	330	10
		0953	300	13
		1257	270	13
		1553	270	11
		1800	260	14
		2151	250	12
Aug 17	229	0055	250	16
		0352	240	13
		0651	260	14
		0953	240	13
		1256	240	14
		1557	230	14
		1858	330	23
		2158	240	14
Aug 18	230	0058	250	14
		0353	250	13
		0651	240	13
		0953	250	13
		1256	250	14
		1555	250	14
		1854	270	11
		2156	250	12
Aug 19	231	0058	270	10
		0334	250	09
		0652	290	06
		0957	300	07
		1257	340	07
		1558	350	10
		1857	350	08
		2157	350	08
Aug 20	232	0057	360	08
		0352	340	08
		0650	010	07
		0954	350	05
		1257	330	07
		1558	040	07
		1856	060	07
		2153	070	07

Table B-5 (Continued)

Calendar Day	Julian Day	Time (GMT)	Direction (°True)	Speed (knots)
Aug 21	233	0053	100	06
		0353	120	08
		0653	120	07
		0951	120	06
		1258	170	08
		1554	350	04
		1854	350	03
		2154	160	09
Aug 22	234	0057	200	08
		0351	210	12
		0657	230	10
		0955	250	11
		1258	260	15
		1554	240	14
		1853	250	15
		2158	250	14
Aug 23	235	0058	240	10
		0357	240	08
		0652	240	08
		0957	230	15
		1255	240	13
		1553	250	14
		1853	310	06
		2153	350	05
Aug 24	236	0055	090	03
		0358	120	06
		0653	120	09
		0955	130	10
		1258	060	06
		1554	230	05
		1854	270	05
		2153	230	05
Aug 25	237	0057	250	09
		0357	300	10
		0657	350	13
		0957	010	09
		1253	020	09
		1554	020	08
		1854	070	10
		2153	050	10

Table B-6 (Continued)

Calendar Day	Julian Day	Time (GMT)	Direction (°True)	Speed (knots)
Aug 26	238	0058	080	09
		0359	070	09
		0655	050	10
		0958	070	14
		1254	080	10
		1554	060	09
		1853	040	10
		2154	060	12
Aug 27	239	0058	060	07
		0357	070	09
		0654	060	08
		0952	070	08
		1254	040	10
		1557	050	09
		1857	050	11
		2158	040	08
Aug 28	240	0056	070	09
		0358	080	08
		0657	070	08
		0953	060	11
		1254	040	08
		1553	040	08
		1858	070	09
		2157	070	07
Aug 29	241	0057	100	08
		0354	100	08
		0654	100	09
		0957	090	08
		1252	090	07
		1557	080	06
		1858	070	06
		2157	340	08
Aug 30	242	0056	340	05
		0357	320	10
		0653	280	12
		0953	280	17
		1257	320	14
		1555	340	13
		1858	330	10
		2156	350	13

Table B-7 (Continued)

Calendar Day	Julian Day	Time (GMT)	Direction (°True)	Speed (knots)
Aug 31	243	0052	320	06
		0356	310	08
		0651	310	11
		0955	310	11
		1251	310	12
		1553	330	08
		1857	320	09
		2156	330	10
Sep 01	244	0058	350	07
		0353	010	08
		0651	020	07
		0951	040	06
		1255	010	10
		1555	350	07
		1854	020	06
		2154	060	05
Sep 02	245	0058	040	03
		0352	040	04
		0652	---	00
		0950	290	05
		1256	320	04
		1556	010	07
		1856	360	07
		2154	060	07
Sep 03	246	0056	060	08
		0353	100	08
		0652	090	11
		0954	080	12
		1255	090	16
		1558	070	12
		1857	070	17
		2154	080	13
Sep 04	247	0052	070	15
		0353	070	14
		0654	060	14
		0958	060	13
		1257	070	10
		1558	070	12
		1854	070	12
		2158	060	15

Table B-8 (Continued)

Calendar Day	Julian Day	Time (GMT)	Direction (°True)	Speed (knots)
Sep 05	248	0050	070	15
		0355	050	13
		0651	040	13
		0958	050	15
		1251	040	14
		1553	080	17
		1854	070	15
		2157	070	14
Sep 06	249	0055	070	12
		0350	060	12
		0650	070	15
		0956	070	12
		1257	080	14
		1559	080	12
		1857	080	13
		2156	080	08
Sep 07	250	0052	070	08
		0351	070	10
		0651	070	11
		0958	070	10
		1255	060	13
		1557	050	10
		1857	080	10
		2158	020	10

Table B-9 Wainwright Wind Data

Calendar Day	Julian Day	Time (GMT)	Direction (°True)	Speed (knots)
Aug 04	216	0000	180	10
		0600	170	03
		1200	260	04
		1800	190	04
Aug 05	217	0000	270	10
		0600	250	04
		1200	150	05
		1800	220	02
Aug 06	218	0000	280	08
		0600	330	06
		1200	010	08
		1800	030	10
Aug 07	219	0000	040	10
		0600	020	09
		1200	050	05
		1800	030	04
Aug 08	220	0000	020	05
		0600	050	07
		1200	070	09
		1800	070	10
Aug 09	221	0000	060	10
		0600	060	10
		1200	070	10
		1800	070	10
Aug 10	222	0000	070	10
		0600	060	06
		1200	050	05
		1800	040	03
Aug 11	223	0000	010	04
		0600	050	07
		1200	060	06
		1800	070	05
Aug 12	224	0000	090	05
		0600	100	07
		1200	060	07
		1800	050	10

Table B-10 (Continued)

Calendar Day	Julian Day	Time (GMT)	Direction (°True)	Speed (knots)
Aug 13	225	0000	030	10
		0600	040	10
		1200	010	03
		1800	---	00
Aug 14	226	0000	270	03
		0600	320	02
		1200	---	00
		1800	---	00
Aug 15	227	0000	360	03
		0600	050	05
		1200	040	03
		1800	030	05
Aug 16	228	0000	010	06
		0600	360	04
		1200	010	10
		1800	350	08
Aug 17	229	0000	290	12
		0600	300	08
		1200	300	10
		1800	270	14
Aug 18	230	0000	250	20
		0600	250	20
		1200	280	16
		1800	300	14
Aug 19	231	0000	290	12
		0600	300	10
		1200	---	00
		1800	300	04
Aug 20	232	0000	340	06
		0600	030	06
		1200	020	06
		1800	060	02
Aug 21	233	0000	---	00
		0600	---	00
		1200	100	02
		1800	140	03

Table B-11 (Continued)

Calendar Day	Julian Day	Time (GMT)	Direction (°True)	Speed (knots)
Aug 22	234	0000	190	07
		0600	180	06
		1200	240	07
		1800	280	06
Aug 23	235	0000	270	14
		0600	250	10
		1200	240	10
		1800	250	08
Aug 24	236	0000	260	06
		0600	350	04
		1200	070	04
		1800	090	05
Aug 25	237	0000	---	00
		0600	320	04
		1200	290	05
		1800	020	07
Aug 26	238	0000	060	12
		0600	060	10
		1200	070	10
		1800	070	08
Aug 27	239	0000	070	10
		0600	060	12
		1200	070	12
		1800	080	12
Aug 28	240	0000	070	10
		0600	060	12
		1200	090	10
		1800	100	12
Aug 29	241	0000	090	10
		0600	080	14
		1200	110	10
		1800	090	10
Aug 30	242	0000	090	12
		0600	070	08
		1200	050	04
		1800	360	03

Table B12 (Continued)

Calendar Day	Julian Day	Time (GMT)	Direction (°True)	Speed (knots)
Aug 31	243	0000	300	10
		0600	020	07
		1200	010	02
		1800	---	00
Sep 01	244	0000	360	05
		0600	030	06
		1200	090	03
		1800	060	04
Sep 02	245	0000	070	07
		0600	070	08
		1200	080	05
		1800	120	04
Sep 03	246	0000	070	06
		0600	060	05
		1200	090	06
		1800	100	08
Sep 04	247	0000	090	13
		0600	090	15
		1200	090	16
		1800	090	10

Table B13 Point Lay Wind Data

Calendar Day	Julian Day	Time (GMT)	Direction (°True)	Speed (knots)
Aug 08	220	0000	020	15
		0600	030	16
		1200	020	12
		1800	030	15
Aug 09	221	0000	020	18
		0600	050	14
		1200	040	05
		1800	030	12
Aug 10	222	0000	030	12
		0600	360	08
		1200	020	04
		1800	010	03
Aug 11	223	0000	360	03
		0600	360	05
		1200	---	00
		1800	350	04
Aug 12	224	0000	340	05
		0600	350	04
		1200	330	14
		1800	300	04
Aug 13	225	0000	---	00
		0600	240	04
		1200	240	02
		1800	240	06
Aug 14	226	0000	240	04
		0600	010	02
		1200	040	04
		1800	090	05
Aug 15	227	0000	340	04
		0600	010	08
		1200	030	05
		1800	020	03
Aug 16	228	0000	330	10
		0600	300	05
		1200	---	00
		1800	330	05

Table B14 (Continued)

Calendar Day	Julian Day	Time (GMT)	Direction (°True)	Speed (knots)
Aug 17	229	0000	300	05
		0600	250	13
		1200	240	12
		1800	240	12
Aug 18	230	0000	230	20
		0600	220	25
		1200	240	24
		1800	250	20
Aug 19	231	0000	270	12
		0600	270	20
		1200	260	17
		1800	360	16
Aug 20	232	0000	330	10
		0600	360	10
		1200	---	00
		1800	---	00
Aug 21	233	0000	---	00
		0600	050	03
		1200	---	00
		1800	090	04
Aug 22	234	0000	---	00
		0600	200	04
		1200	250	07
		1800	250	12
Aug 23	235	0000	250	10
		0600	220	03
		1200	240	03
		1800	---	00
Aug 24	236	0000	---	00
		0600	030	02
		1200	---	00
		1800	---	00
Aug 25	237	0000	---	00
		0600	330	02
		1200	---	00
		1800	---	00

Table B15 (Continued)

Calendar Day	Julian Day	Time (GMT)	Direction (°True)	Speed (knots)
Aug 26	238	0000	020	10
		0600	030	16
		1200	030	06
		1800	030	15
Aug 27	239	0000	060	15
		0600	040	16
		1200	050	16
		1800	040	15
Aug 28	240	0000	040	15
		0600	040	20
		1200	050	20
		1800	050	20
Aug 29	241	0000	050	20
		0600	050	20
		1200	050	15
		1800	050	20
Aug 30	242	0000	050	20
		0600	040	18
		1200	---	00
		1800	020	10
Aug 31	243	0000	360	08
		0600	010	03
		1200	---	00
		1800	---	00
Sep 01	244	0000	---	00
		0600	020	10
		1200	---	00
		1800	030	05
Sep 02	245	0000	050	14
		0600	040	18
		1200	030	10
		1800	030	15
Sep 03	246	0000	060	18
		0600	050	18
		1200	030	15
		1800	030	15

Table B16 (Continued)

Calendar Day	Julian Day	Time (GMT)	Direction (°True)	Speed (knots)
Sep 04	247	0000	050	18
		0600	050	15
		1200	050	05
		1800	060	20

Table B17 Cape Lisburne Wind Data

Calendar Day	Julian Day	Time (GMT)	Direction (°True)	Speed (knots)
Aug 01	213	0055	350	11
		0355	360	11
		0655	340	10
		0957	340	12
		1255	330	11
		1559	340	09
		1856	350	09
		2157	360	06
Aug 02	214	0056	010	03
		0355	---	00
		0655	090	07
		0955	090	07
		1255	100	09
		1557	110	08
		1855	140	03
		2156	130	03
Aug 03	215	0057	---	00
		0355	---	00
		0656	350	05
		0956	240	17
		1257	230	17
		1558	230	16
		1856	220	10
		2157	230	19
Aug 04	216	0056	220	23
		0355	220	19
		0656	220	12
		0958	240	27
		1258	230	26
		1555	230	22
		1856	190	10
		2155	220	10
Aug 05	217	0055	---	00
		0356	---	00
		0657	080	04
		0955	090	05
		1255	080	02
		1555	---	00
		1855	050	04
		2155	080	11

Table B18 (Continued)

Calendar Day	Julian Day	Time (GMT)	Direction (°True)	Speed (knots)
Aug 06	218	0056	060	12
		0355	050	14
		0656	060	14
		0956	060	13
		1255	060	11
		1556	060	13
		1855	070	15
		2156	060	12
Aug 07	219	0056	070	13
		0357	070	12
		0655	060	10
		0958	070	10
		1256	060	10
		1555	060	13
		1855	060	15
		2155	070	18
Aug 08	220	0056	060	17
		0356	060	16
		0658	070	15
		0955	070	14
		1259	060	16
		1555	060	17
		1855	060	15
		2155	070	14
Aug 09	221	0055	070	14
		0355	070	17
		0655	070	13
		0956	070	14
		1257	070	13
		1555	050	10
		1855	040	11
		2155	040	12
Aug 10	222	0055	050	11
		0357	030	12
		0655	030	09
		0955	030	06
		1255	040	06
		1556	030	06
		1855	050	04
		2156	020	05

Table B19 (Continued)

Calendar Day	Julian Day	Time (GMT)	Direction (°True)	Speed (knots)
Aug 11	223	0055	040	02
		0356	010	05
		0656	040	06
		0955	010	04
		1255	060	07
		1556	050	09
		1855	040	08
		2155	020	05
Aug 12	224	0055	010	04
		0358	030	05
		0656	010	03
		0956	330	06
		1255	350	04
		1555	320	03
		1856	320	08
		2157	290	04
Aug 13	225	0055	260	03
		0357	300	05
		0658	230	10
		0958	210	09
		1255	230	06
		1555	130	05
		1855	150	02
		2155	120	04
Aug 14	226	0055	160	08
		0355	111	12
		0655	120	09
		0956	100	10
		1255	080	10
		1555	100	04
		1855	180	03
		2158	050	06
Aug 15	227	0055	---	00
		0359	---	00
		0656	050	08
		0959	030	04
		1258	360	09
		1555	350	06
		1855	350	03
		2155	020	07

Table B20 (Continued)

Calendar Day	Julian Day	Time (GMT)	Direction (°True)	Speed (knots)
Aug 16	228	0055	020	04
		0355	030	08
		0655	040	05
		0955	030	03
		1255	360	05
		1555	330	08
		1855	280	02
		2155	260	02
Aug 17	229	0055	280	05
		0356	310	10
		0655	300	06
		0955	300	15
		1255	300	15
		1555	300	18
		1856	300	19
		2155	300	17
Aug 18	230	0055	290	13
		0358	290	10
		0657	300	09
		0957	310	10
		1255	310	09
		1555	320	10
		1855	270	07
		2155	320	11
Aug 19	231	0055	330	07
		0358	350	06
		0657	340	09
		0955	030	11
		1255	360	12
		1555	360	13
		1855	020	14
		2155	040	09
Aug 20	232	0057	050	09
		0357	040	08
		0655	050	09
		0955	070	08
		1255	090	08
		1555	080	07
		1856	100	06
		2155	150	03

Table B21 (Continued)

Calendar Day	Julian Day	Time (GMT)	Direction (°True)	Speed (knots)
Aug 21	233	0055	160	04
		0355	150	03
		0655	080	02
		0957	070	03
		1255	---	00
		1555	230	18
		1855	230	22
		2155	290	07
Aug 22	234	0055	310	08
		0355	290	12
		0655	340	06
		0955	140	02
		1255	360	04
		1555	---	00
		1855	180	03
		2155	---	00
Aug 23	235	0055	200	02
		0355	110	03
		0655	100	05
		0955	090	06
		1255	100	07
		1555	100	06
		1855	130	03
		2155	150	03
Aug 24	236	0055	---	00
		0356	090	03
		0655	090	05
		0955	090	05
		1255	090	04
		1555	090	03
		1855	---	00
		2155	100	04
Aug 25	237	0055	100	02
		0357	100	03
		0655	100	06
		0955	080	11
		1255	090	11
		1555	090	11
		1855	080	12
		2155	080	10

Table B22 (Continued)

Calendar Day	Julian Day	Time (GMT)	Direction (°True)	Speed (knots)
Aug 26	238	0055	090	10
		0358	090	10
		0655	100	09
		0955	100	08
		1255	100	09
		1555	100	09
		1855	090	11
		2155	090	10
Aug 27	239	0055	090	13
		0356	090	12
		0655	100	16
		0956	100	20
		1255	100	17
		1555	100	17
		1855	100	20
		2155	100	20
Aug 28	240	0055	100	20
		0355	100	18
		0655	100	20
		0956	110	15
		1255	120	10
		1555	120	14
		1855	100	17
		2155	100	15
Aug 29	241	0055	100	13
		0356	090	13
		0655	090	13
		0955	100	09
		1255	100	11
		1555	100	11
		1855	100	12
		2155	090	11
Aug 30	242	0056	100	11
		0355	100	14
		0655	080	14
		0955	080	13
		1255	090	13
		1555	100	11
		1855	100	10
		2155	090	09

Table B23 (Continued)

Calendar Day	Julian Day	Time (GMT)	Direction (°True)	Speed (knots)
Aug 31	243	0055	090	12
		0356	100	11
		0656	100	10
		0955	100	10
		1255	100	10
		1555	100	11
		1855	090	14
		2155	090	12
Sep 01	244	0055	110	10
		0355	090	12
		0655	100	09
		0956	110	14
		1255	100	12
		1555	100	13
		1855	100	12
		2155	100	11
Sep 02	245	0055	140	06
		0355	150	06
		0655	090	08
		0957	090	06
		1255	090	05
		1555	140	03
		1855	140	04
		2155	100	11
Sep 03	246	0055	100	10
		0355	100	11
		0655	100	08
		0955	090	07
		1255	120	04
		1555	100	08
		1855	090	11
		2155	090	12
Sep 04	247	0055	090	16
		0355	100	17
		0655	090	20
		0956	090	20
		1255	080	24
		1555	090	24
		1855	090	23

Atmospheric Pressure Data

Table B24 Atmospheric Pressure

Day	Pressure (mb-Hg) Nome	Barrow
Aug 5	1006.1	1008.1
6	1005.8	1014.6
7	1011.8	1021.2
8	1001.6	1015.2
9	999.8	1011.2
10	1000.9	1011.2
11	1009.9	1013.9
12	1007.3	1008.7
13	999.7	998.9
14	1001.4	997.3
15	1003.5	1004.6
16	1012.9	1009.7
17	1016.8	1012.7
18	1012.4	1000.0
19	1008.0	1000.7
20	1006.1	1009.0
21	1005.1	1010.2
22	1008.9	1003.2
23	1008.5	1009.8
24	1003.6	1013.4
25	1006.6	1017.8
26	1012.6	1023.6
27	1011.6	1030.5
28	1013.6	1033.4
29	1009.2	1028.3
30	1006.8	1019.6
31	1010.6	1018.5

APPENDIX C

Hydrographic Data

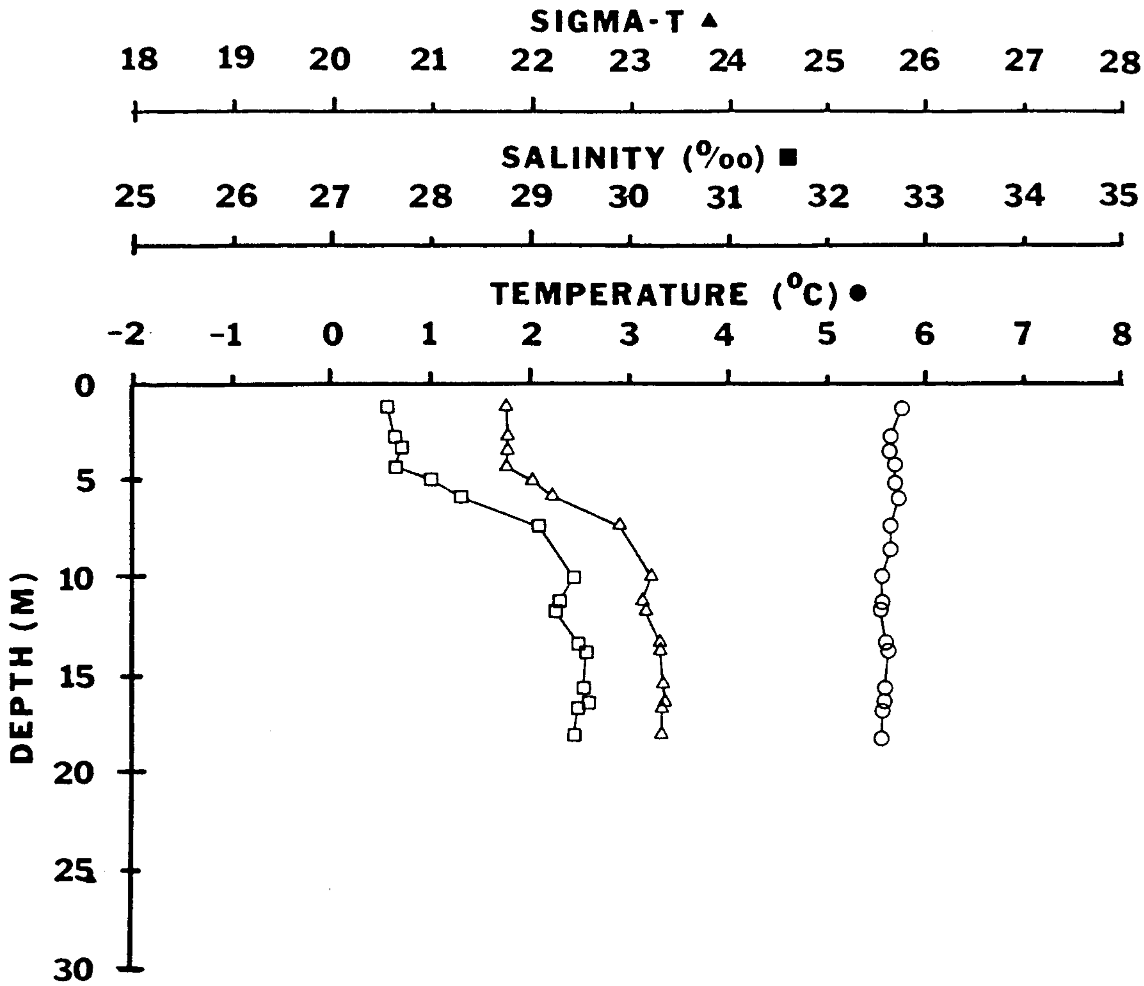

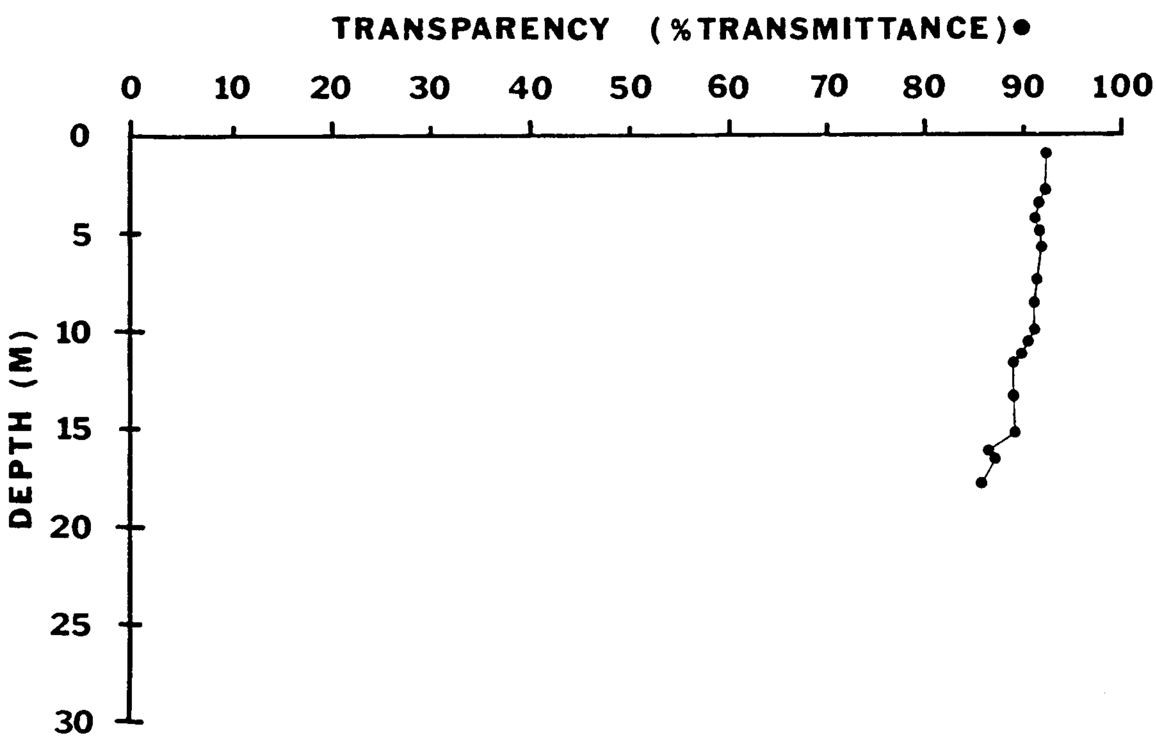

Figure C-1. Hydrographic Profiles for Station Barrow-1

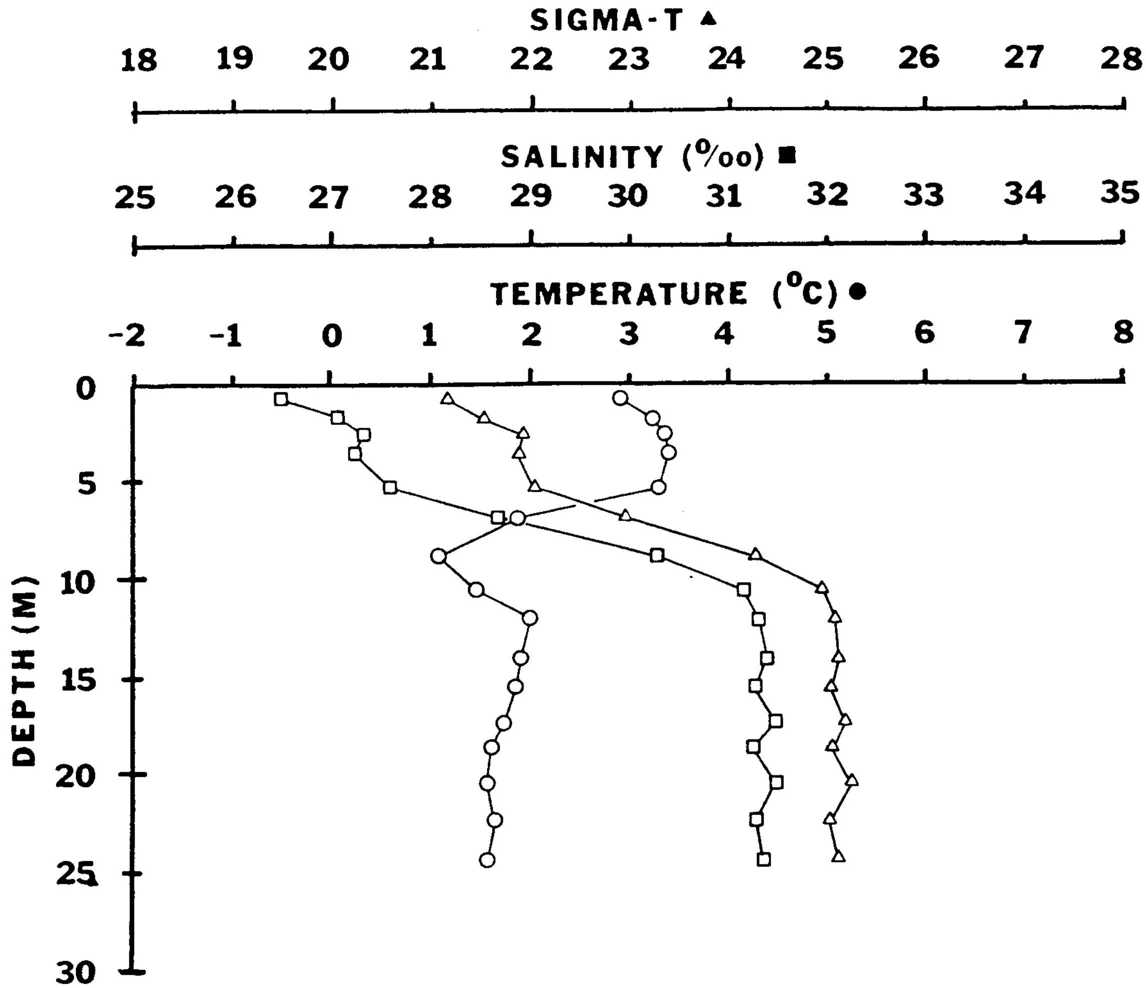

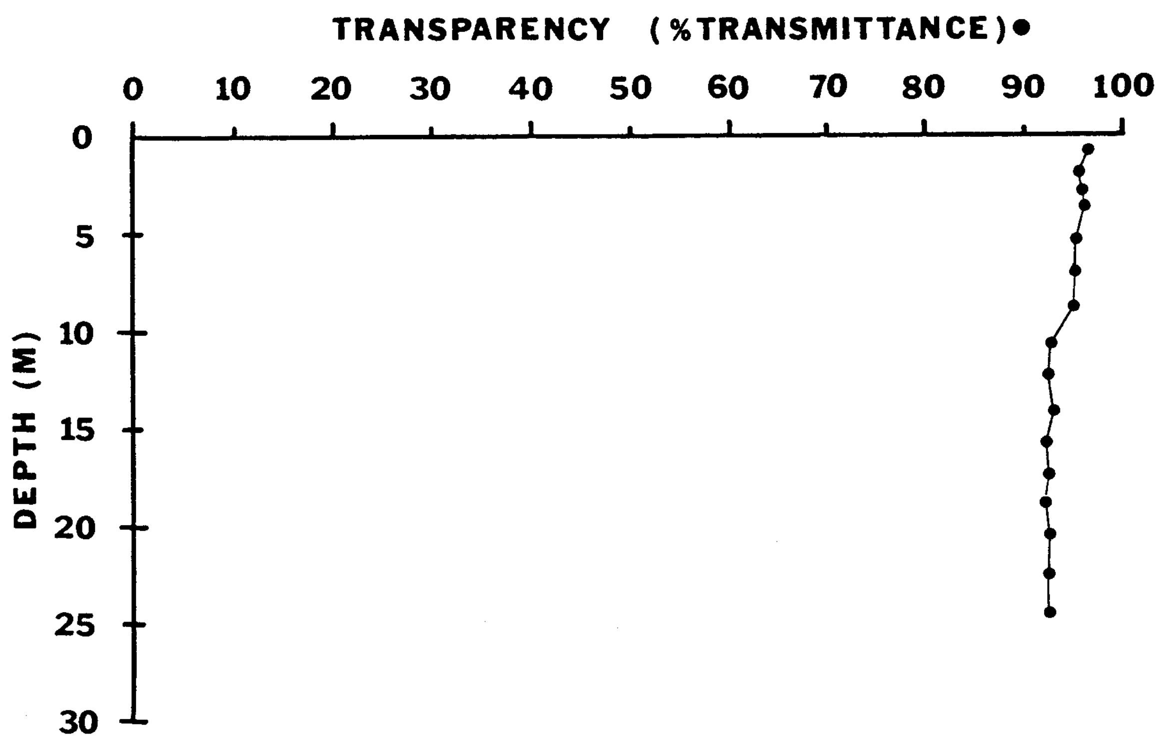

Figure C-2. Hydrographic Profiles for Station Barrow-2

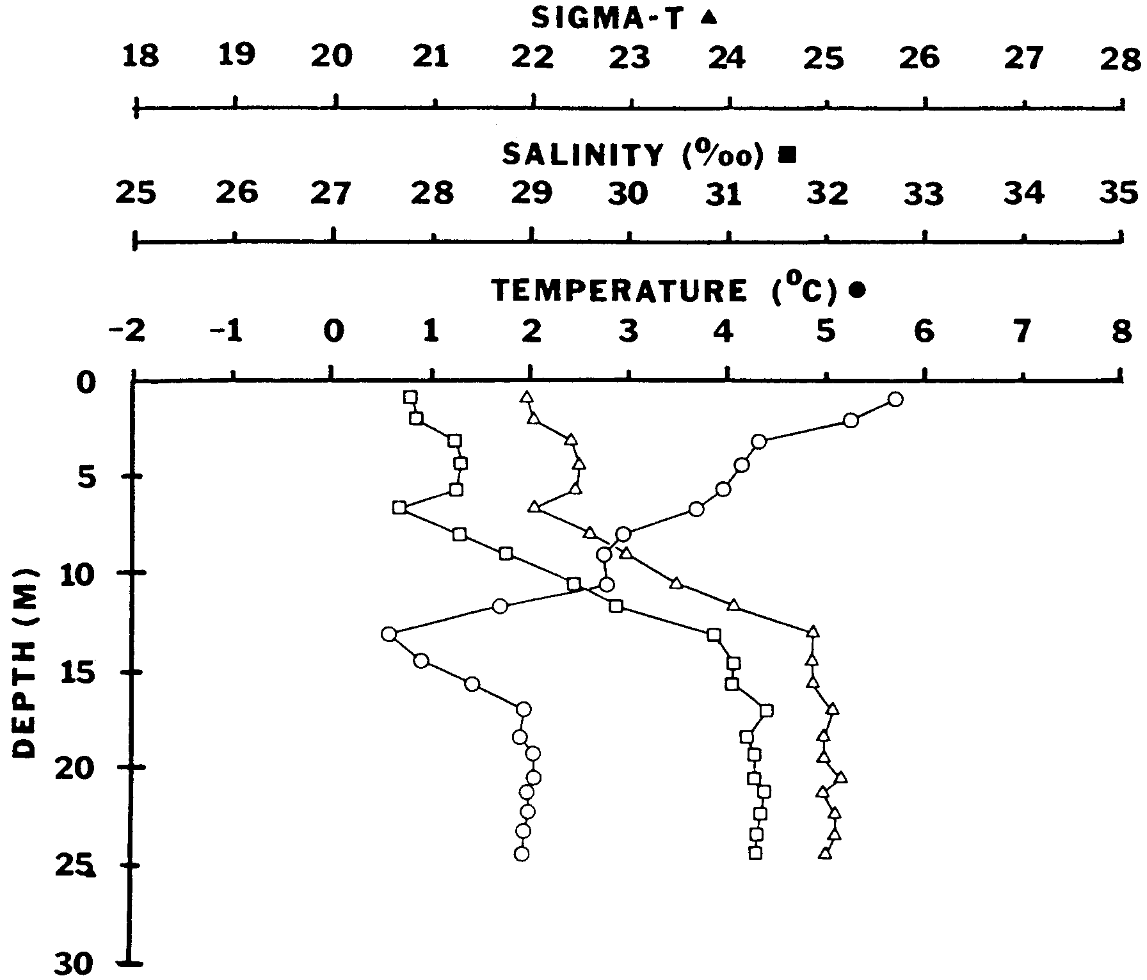

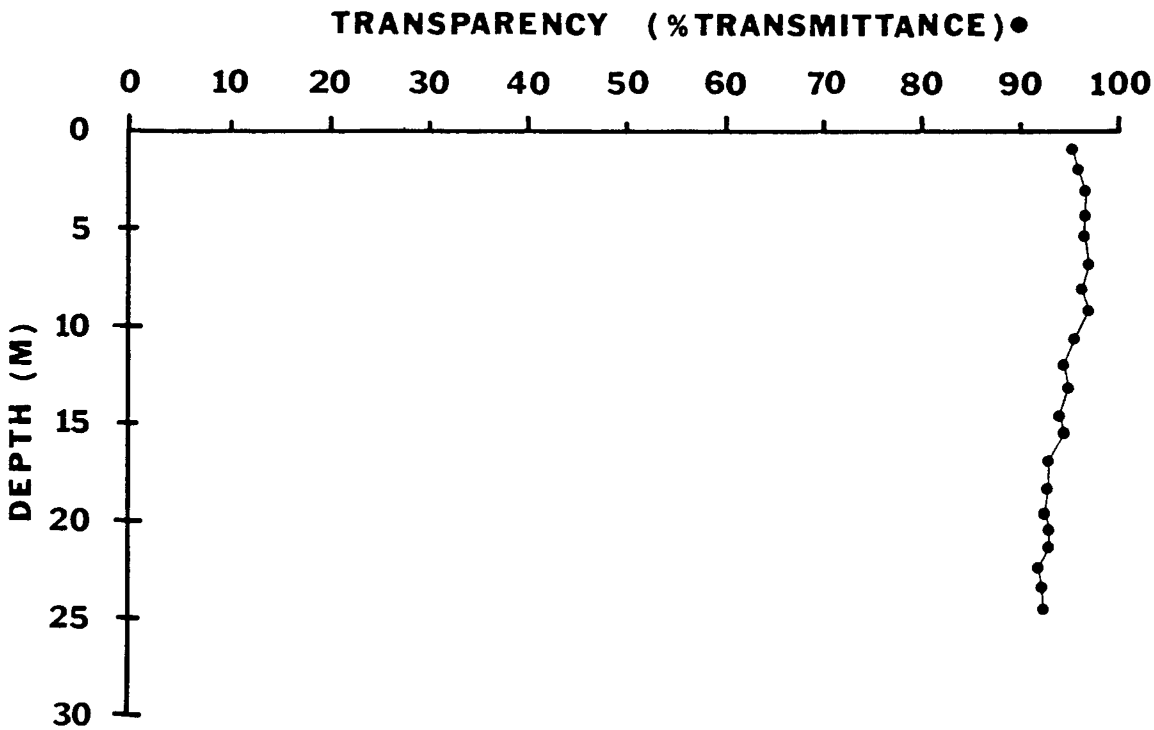

Figure C-3. Hydrographic Profiles for Station Barrow-3

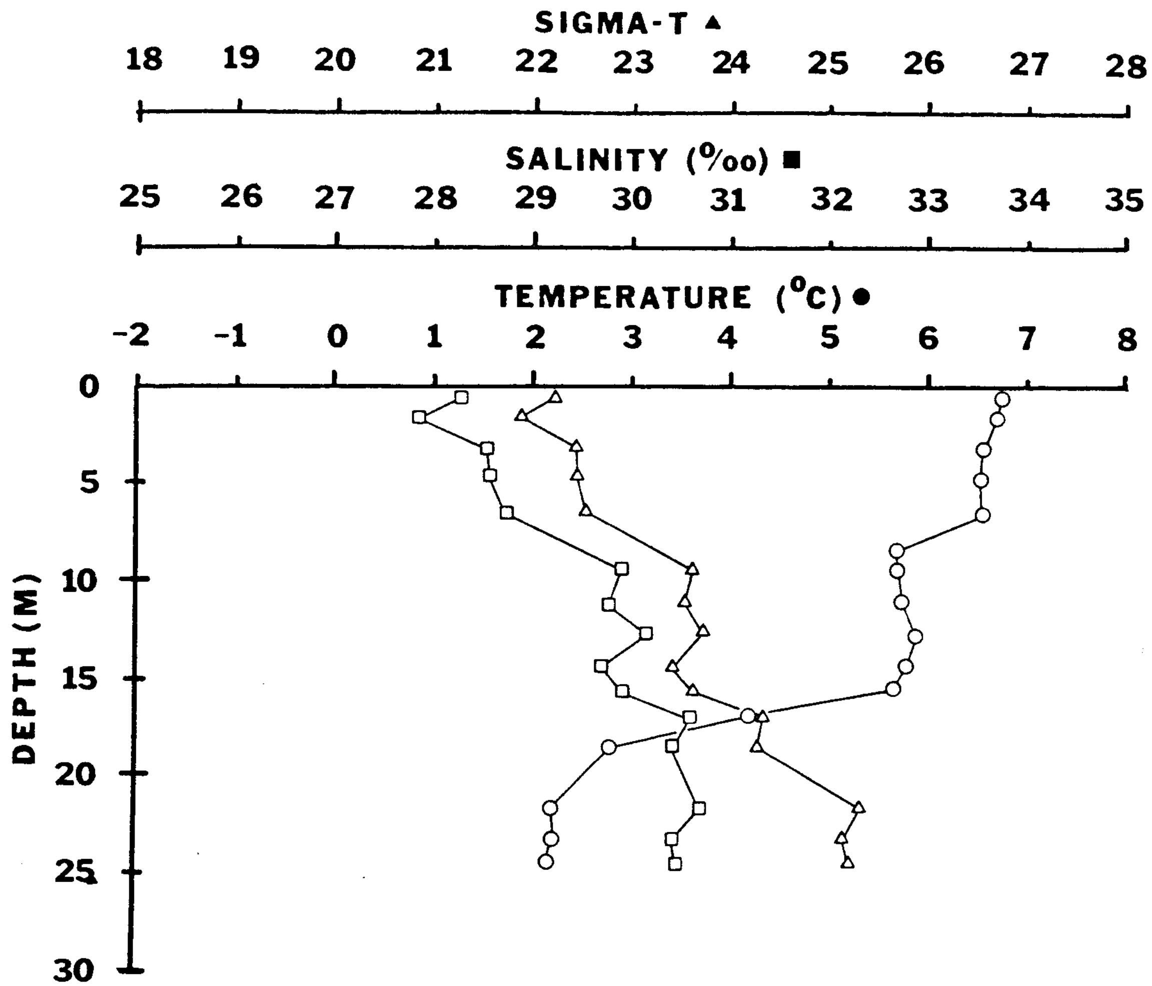

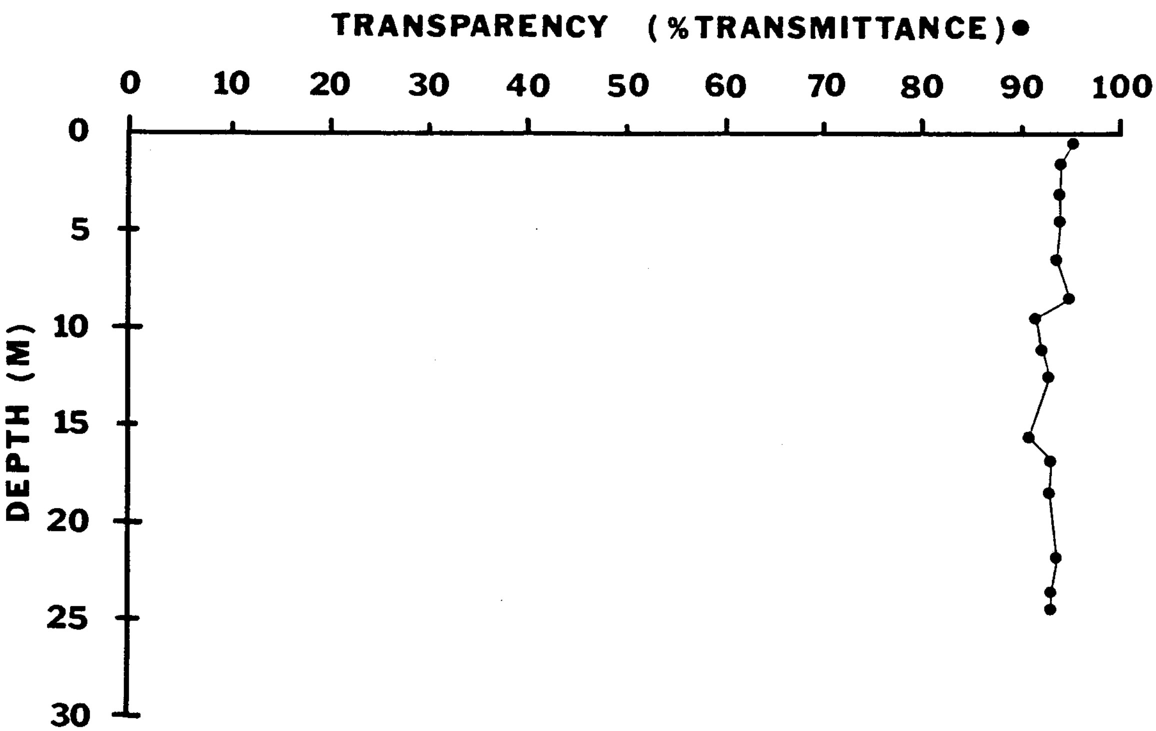

Figure C-4. Hydrographic Profiles for Station Barrow-4

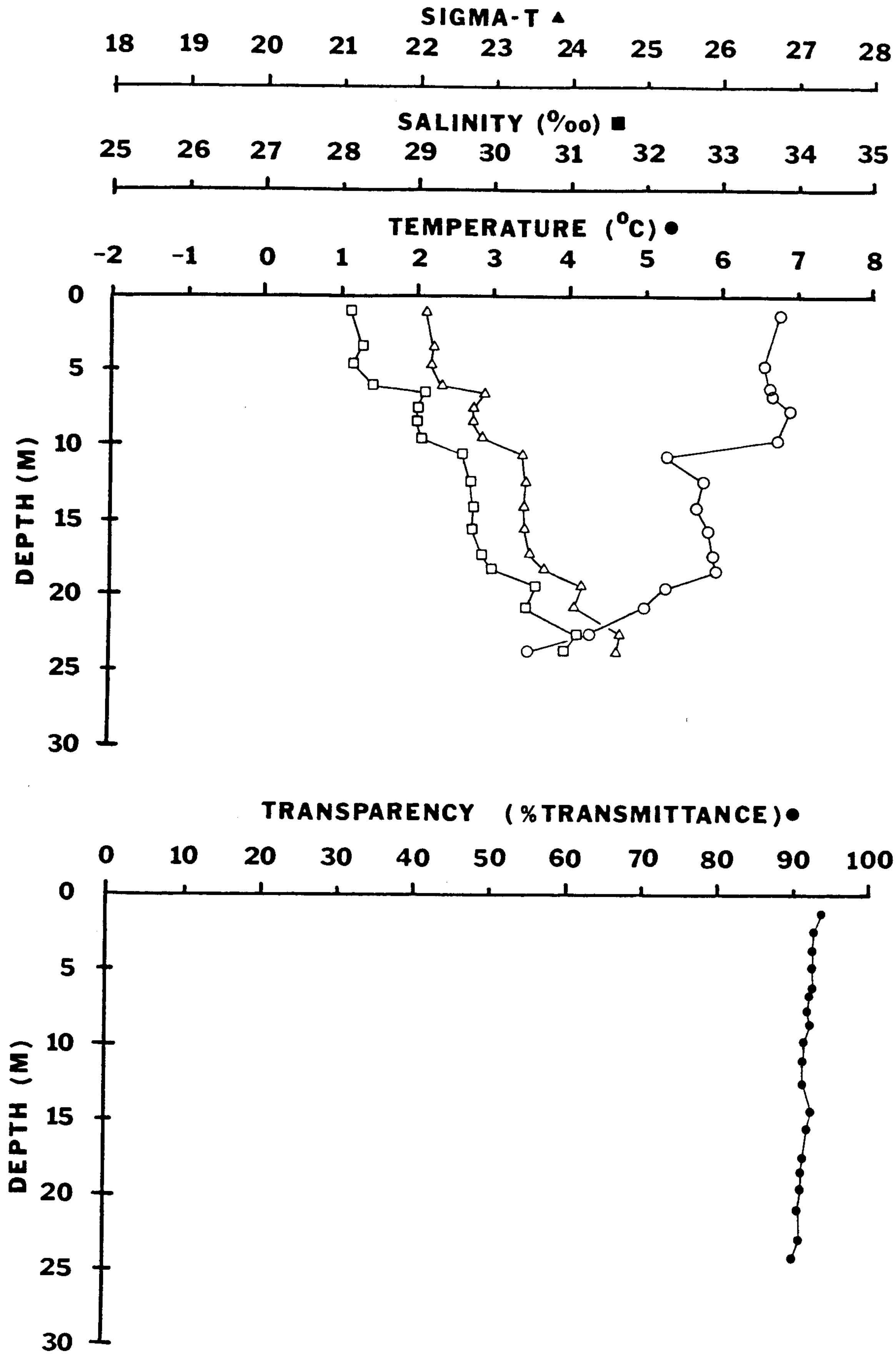

Figure C-5. Hydrographic Profiles for Station Barrow-5

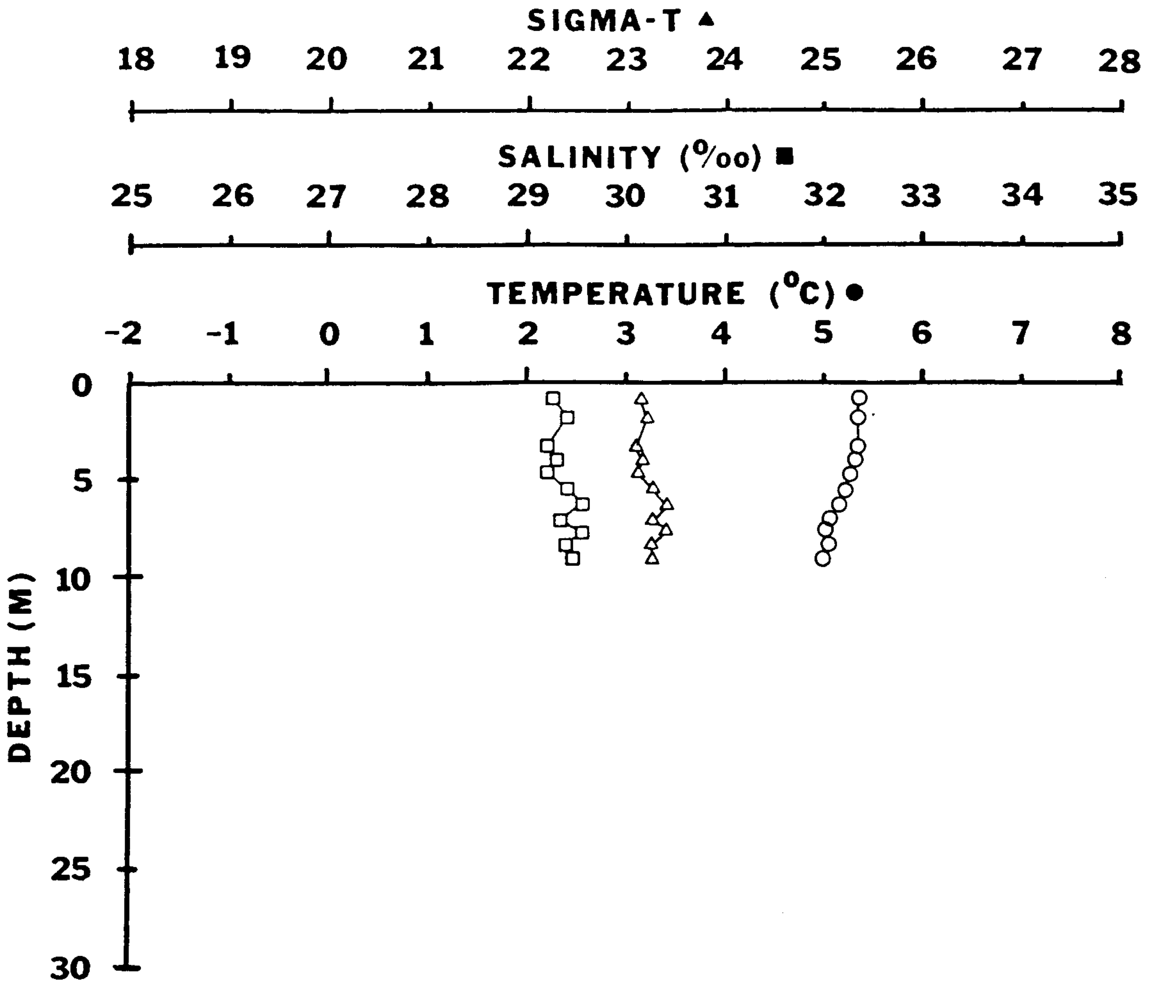

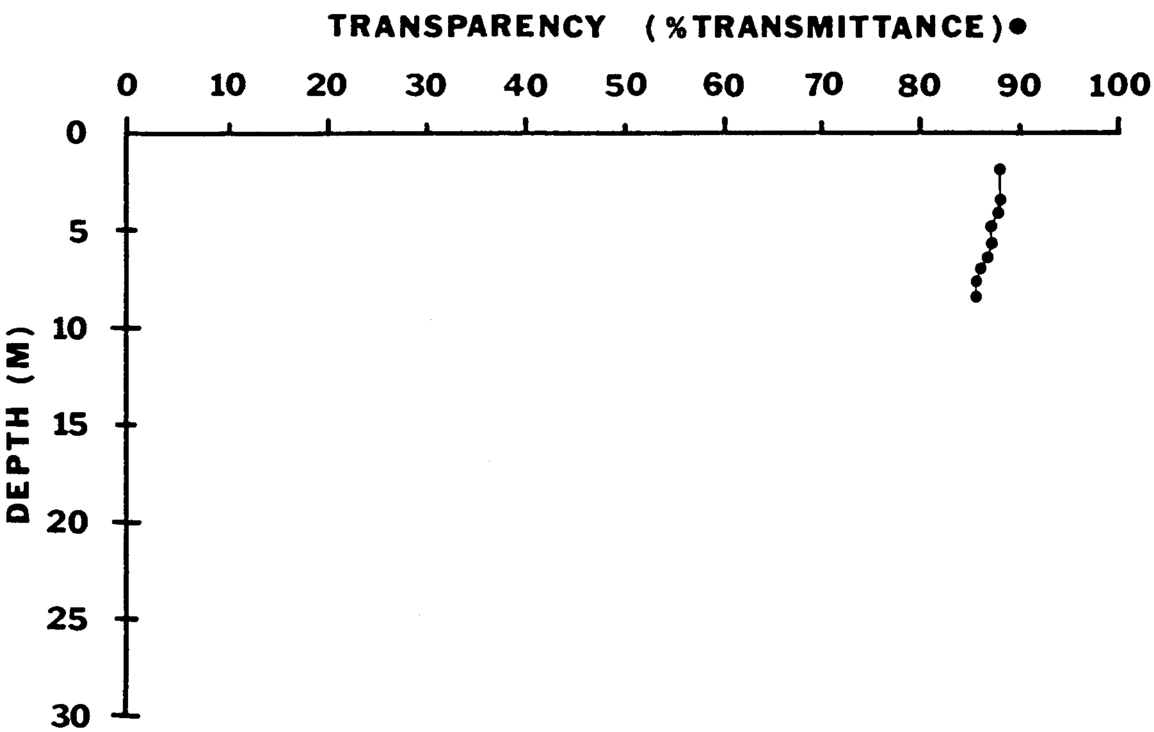

Figure C-6. Hydrographic Profiles for Station Skull Cliffs-6

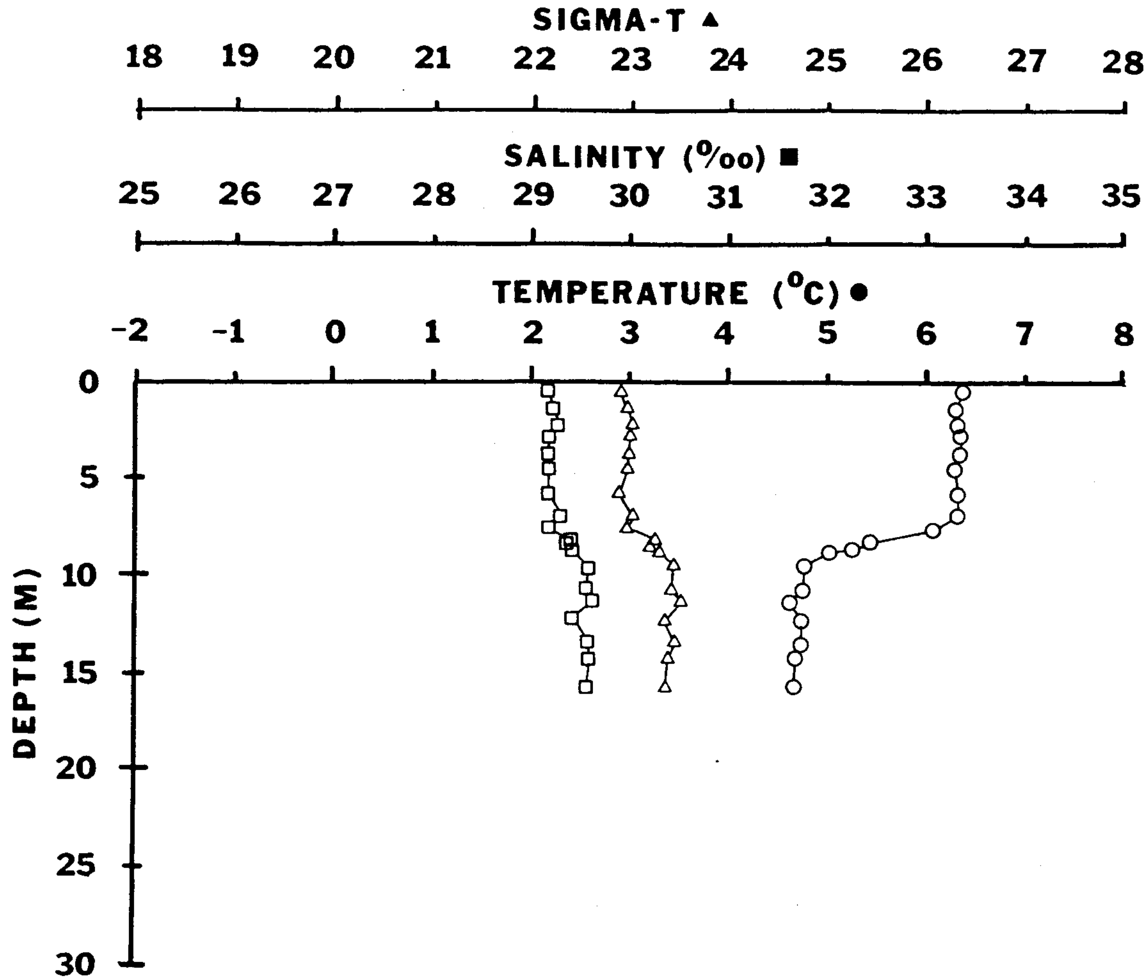

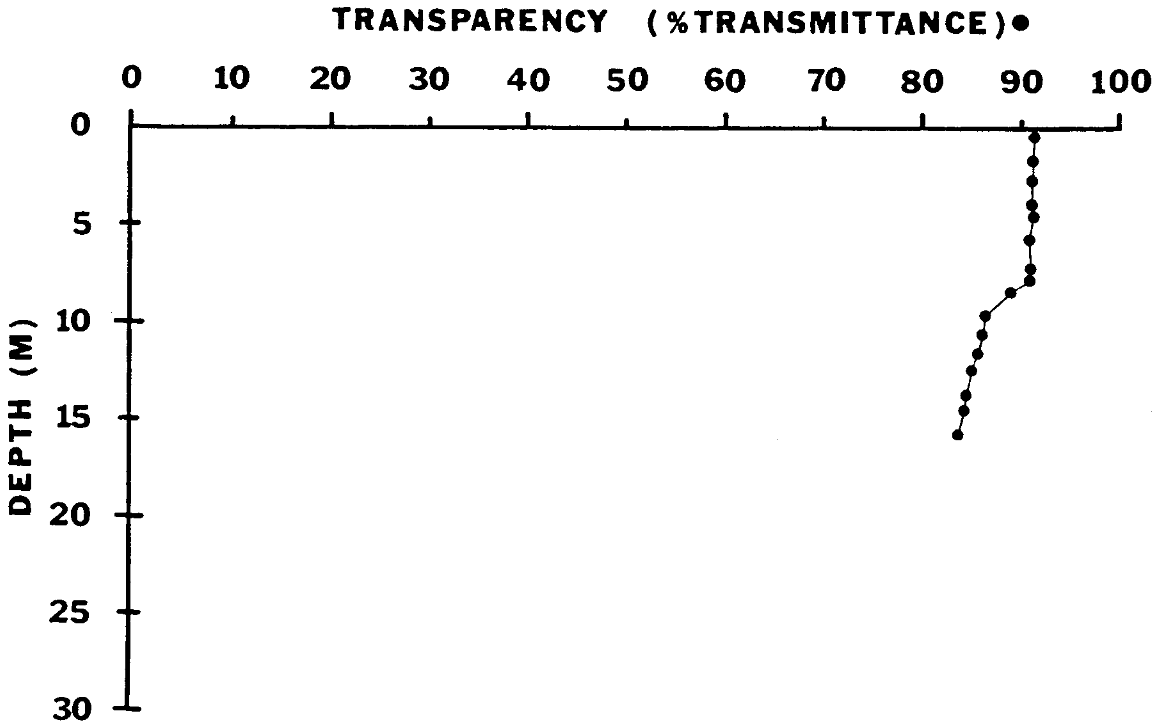

Figure C-7 Hydrophic Profiles for Station Skull Cliffs-7

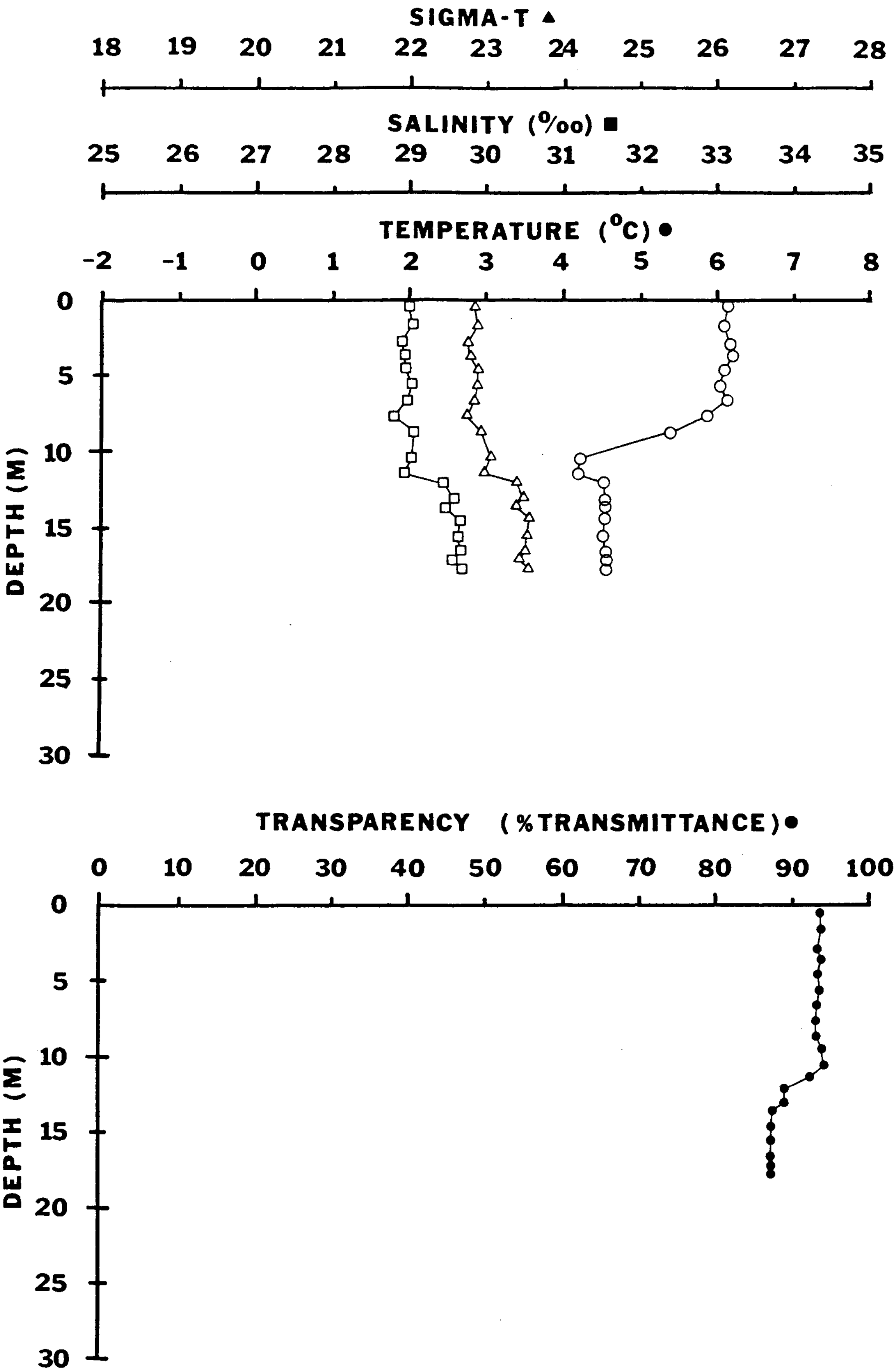

Figure C-8. Hydrographic Profiles for Station Skull Cliffs-8

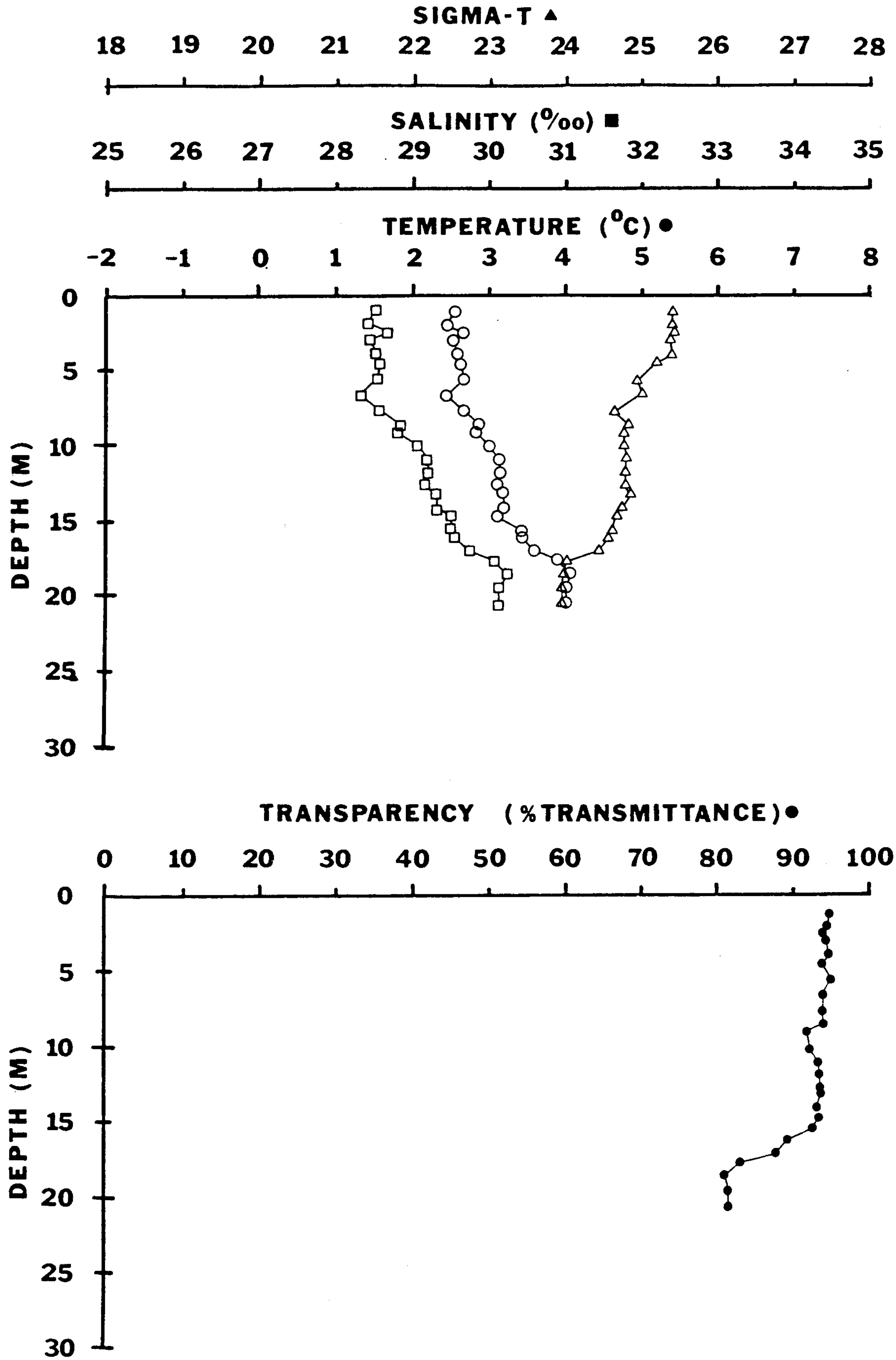

Figure C-9. Hydrographic Profiles for Station Skull Cliffs-9

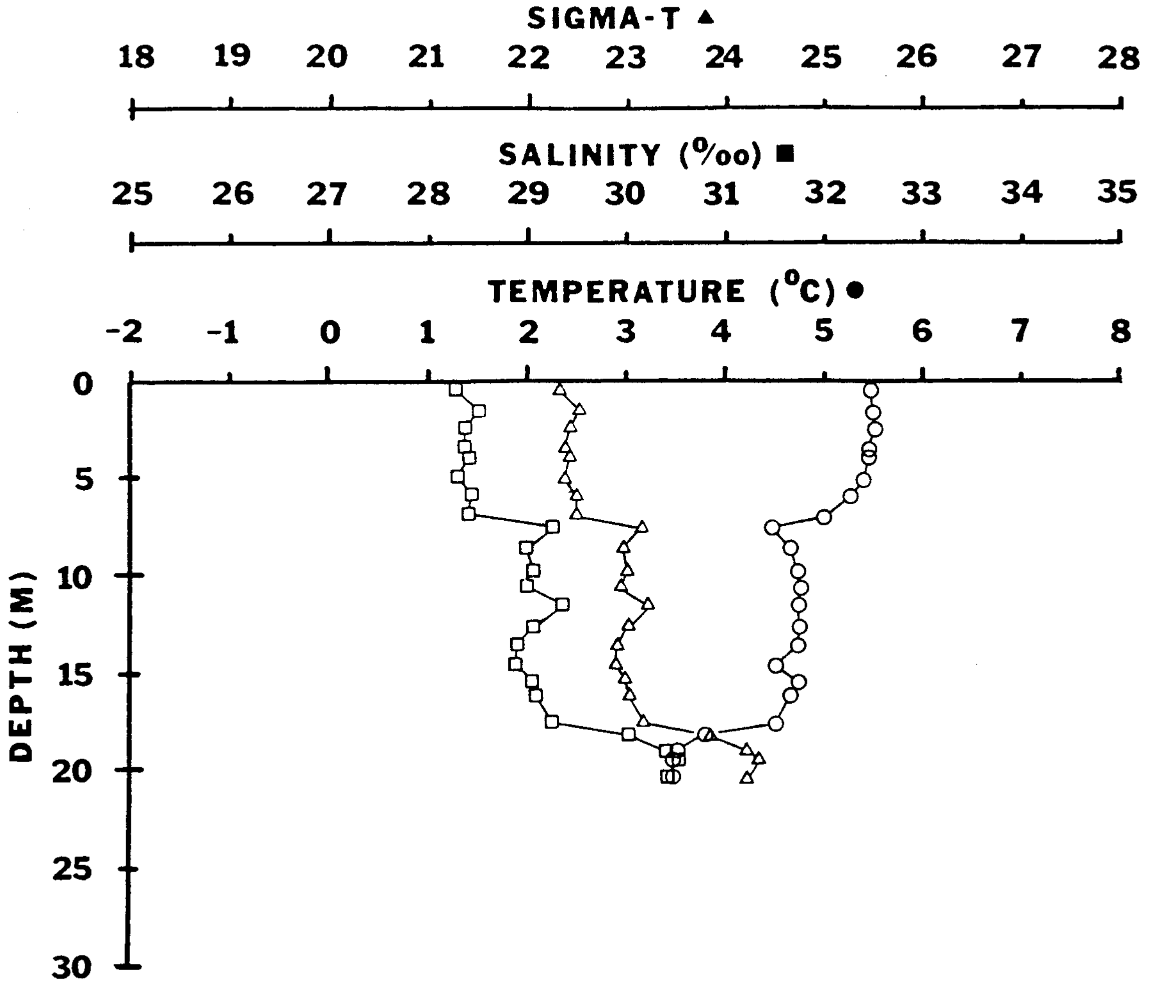

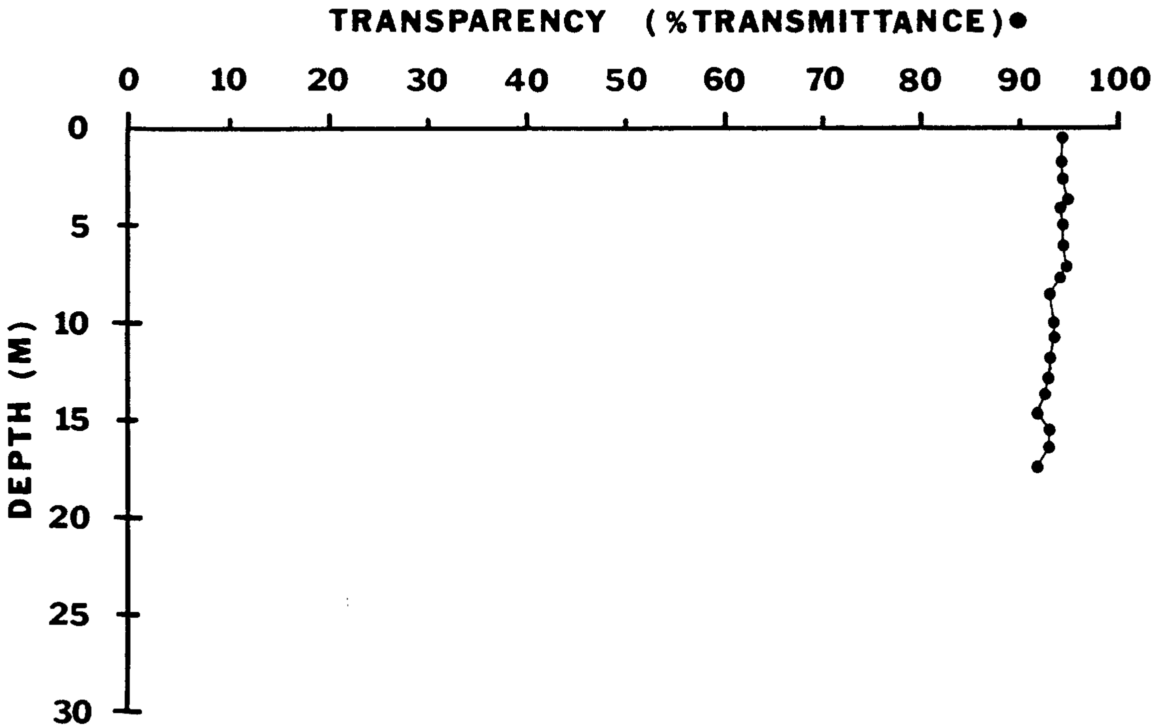

Figure C-10. Hydrographic Profiles for Station Skull Cliffs-10

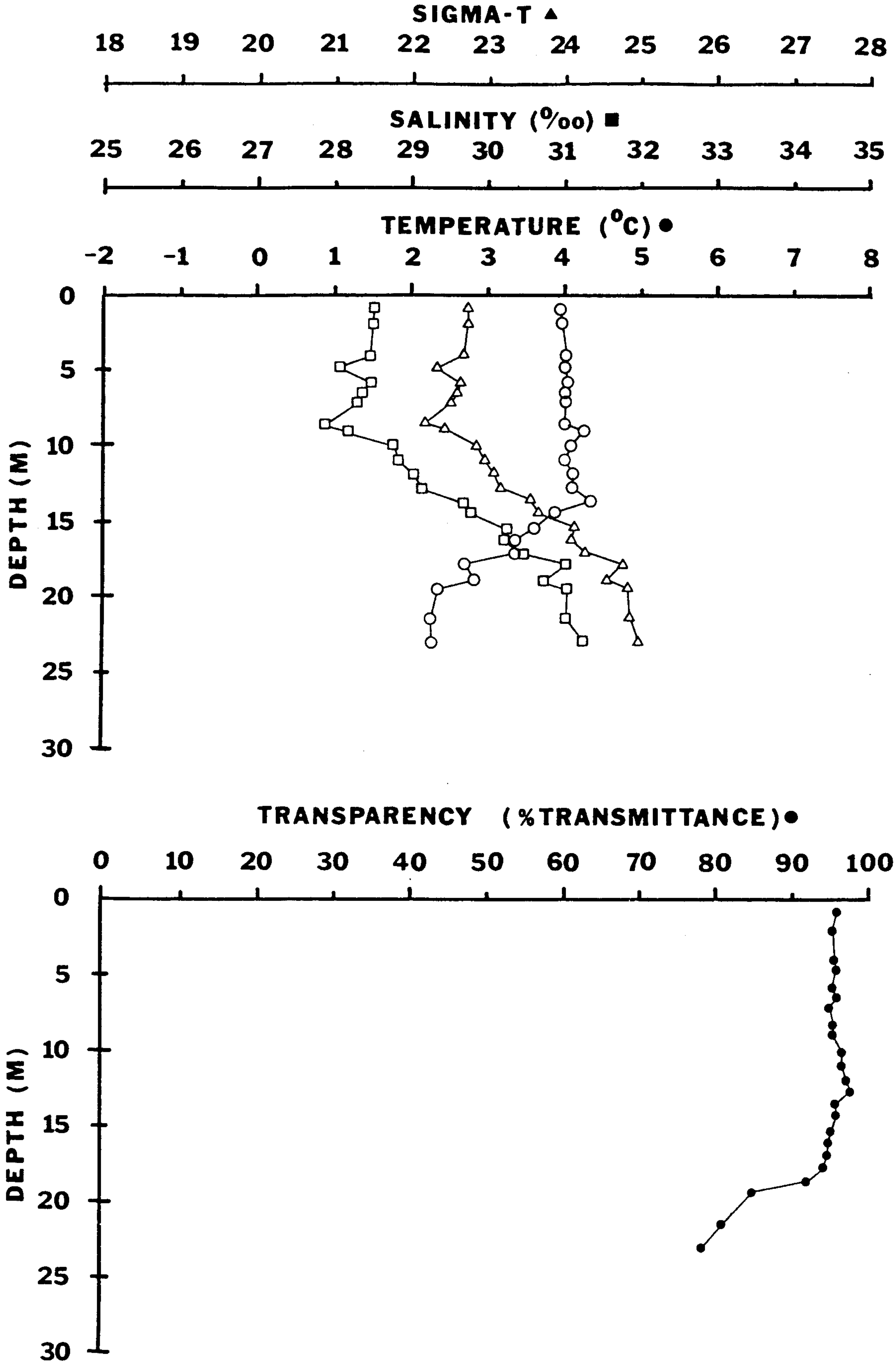

Figure C-11. Hydrographic Profiles for Station Sull Cliffs-11

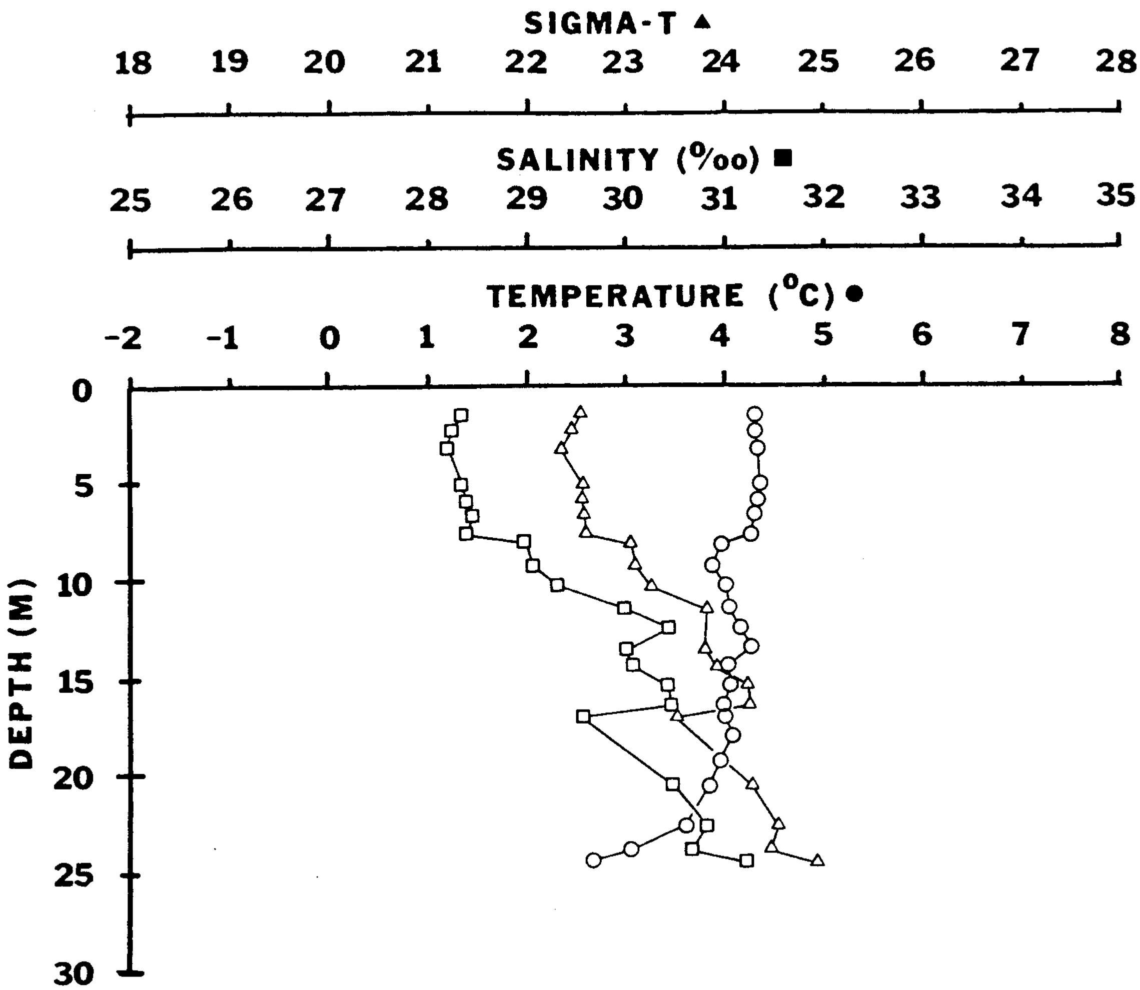

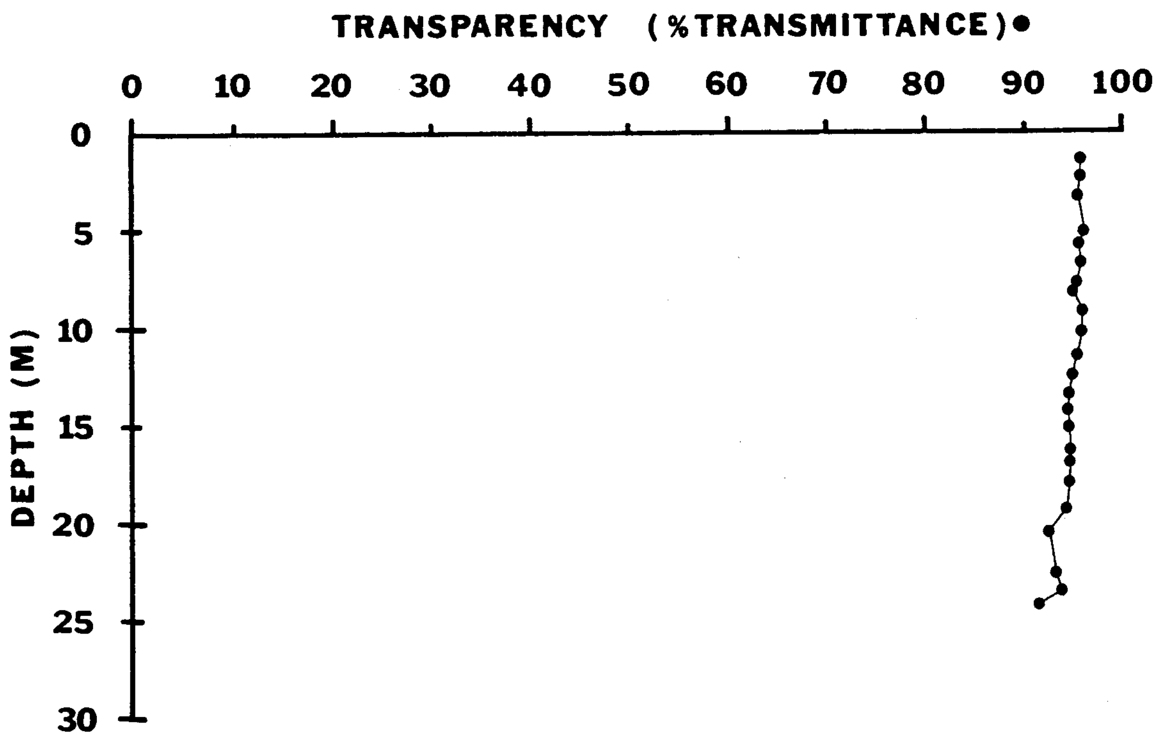

Figure C-12. Hydrographic Profiles for Station Skull Cliffs-12

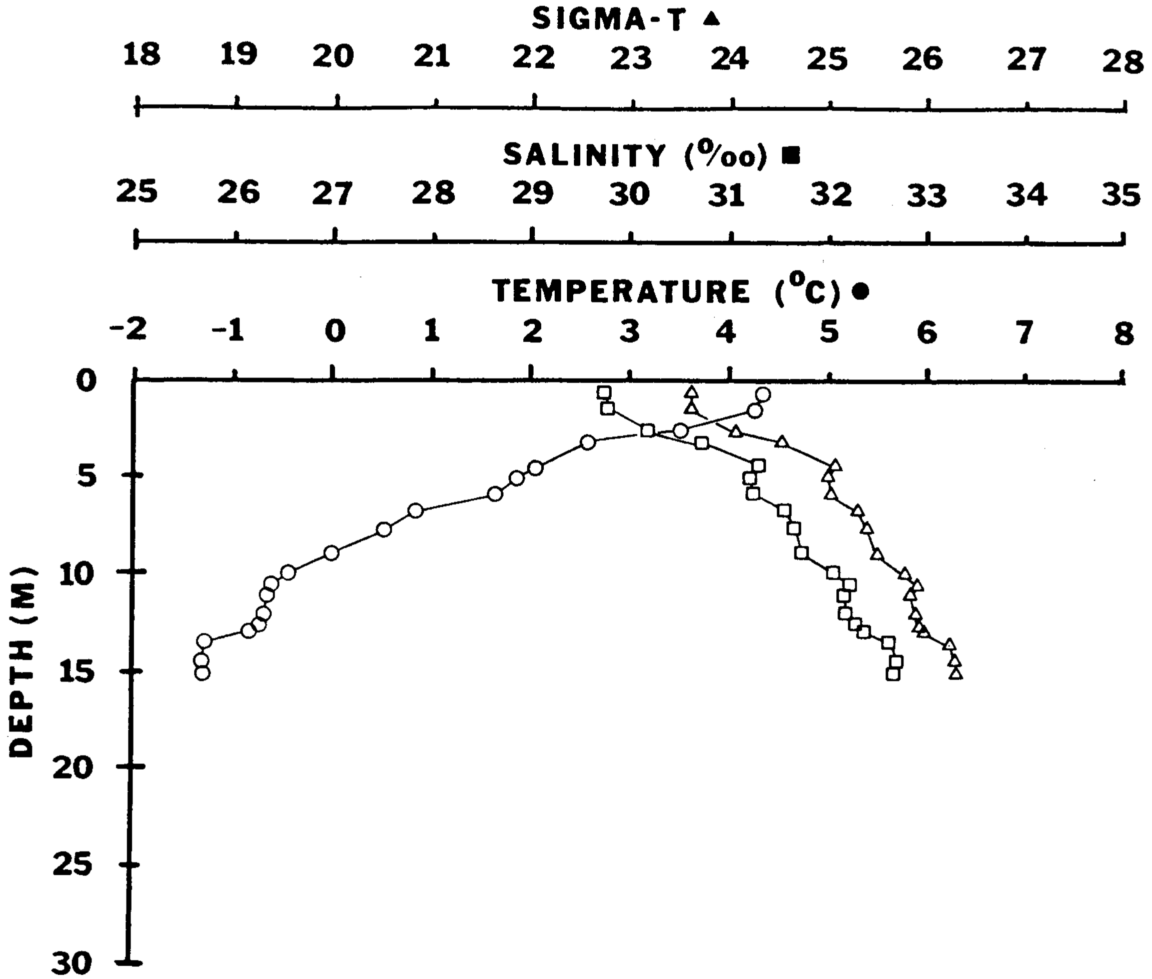

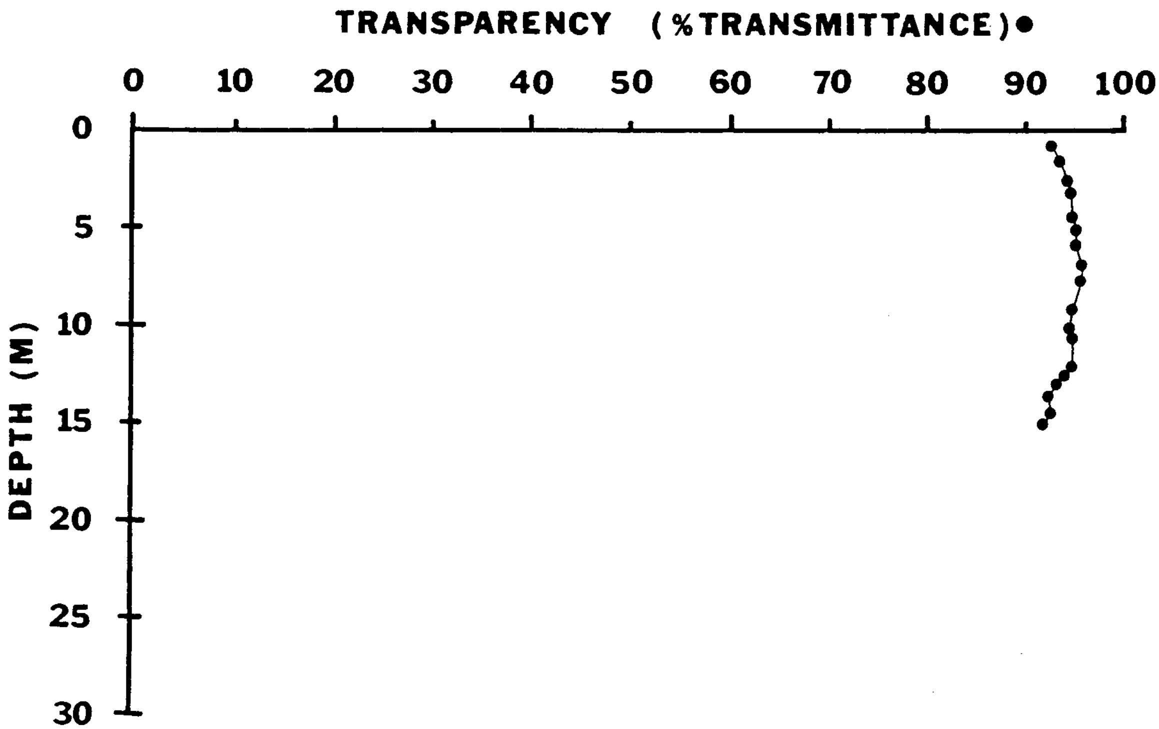

Figure C-13. Hydrographic Profiles for Station Point Belcher-13

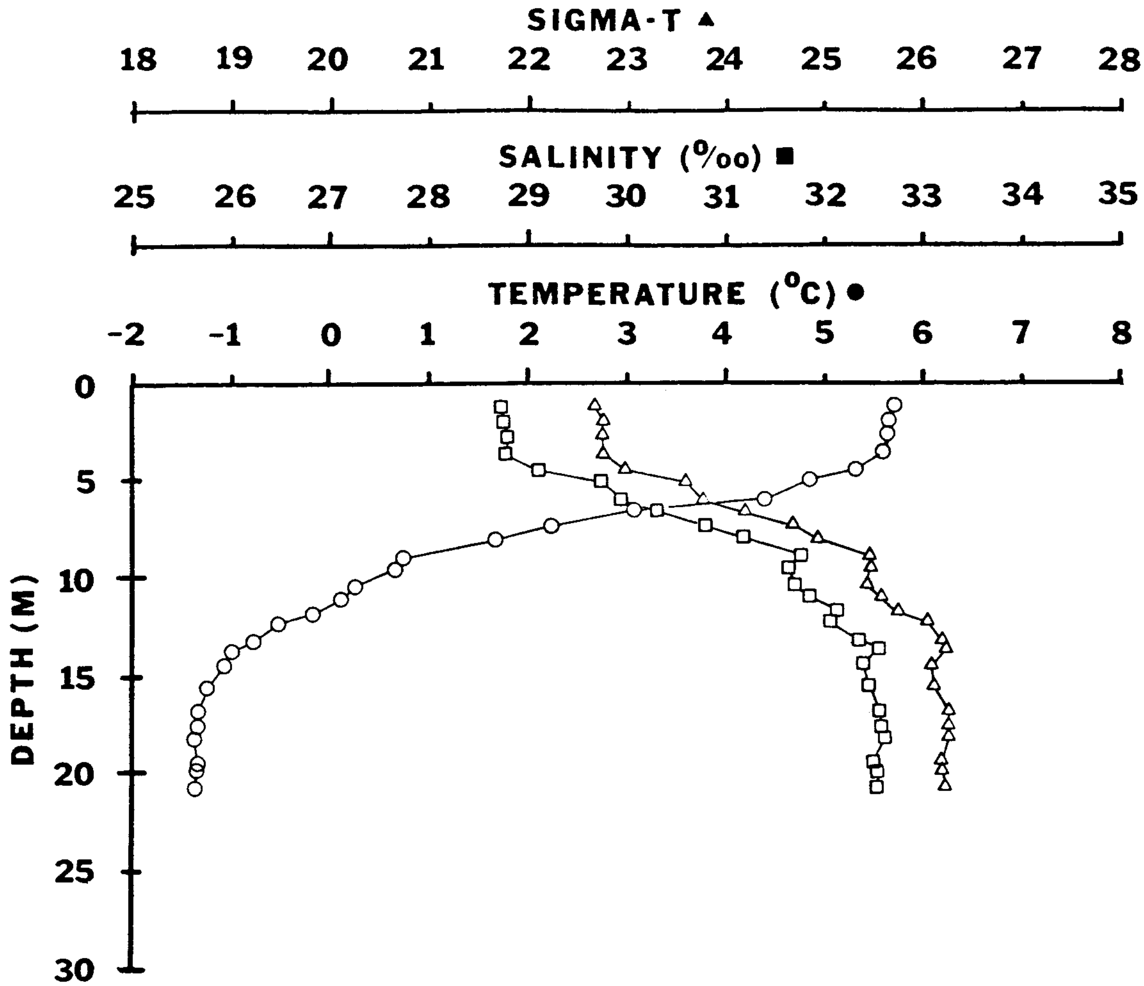

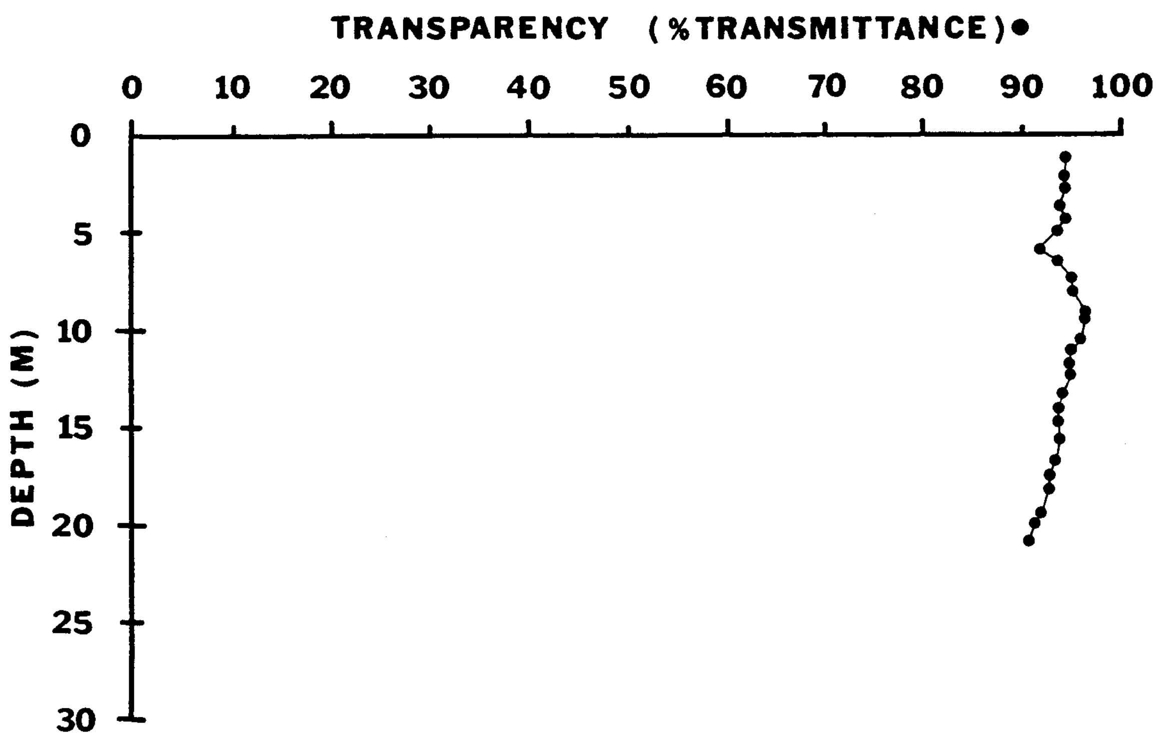

Figure C-14 Hydrographic Profiles for Station Pt. Belcher-14

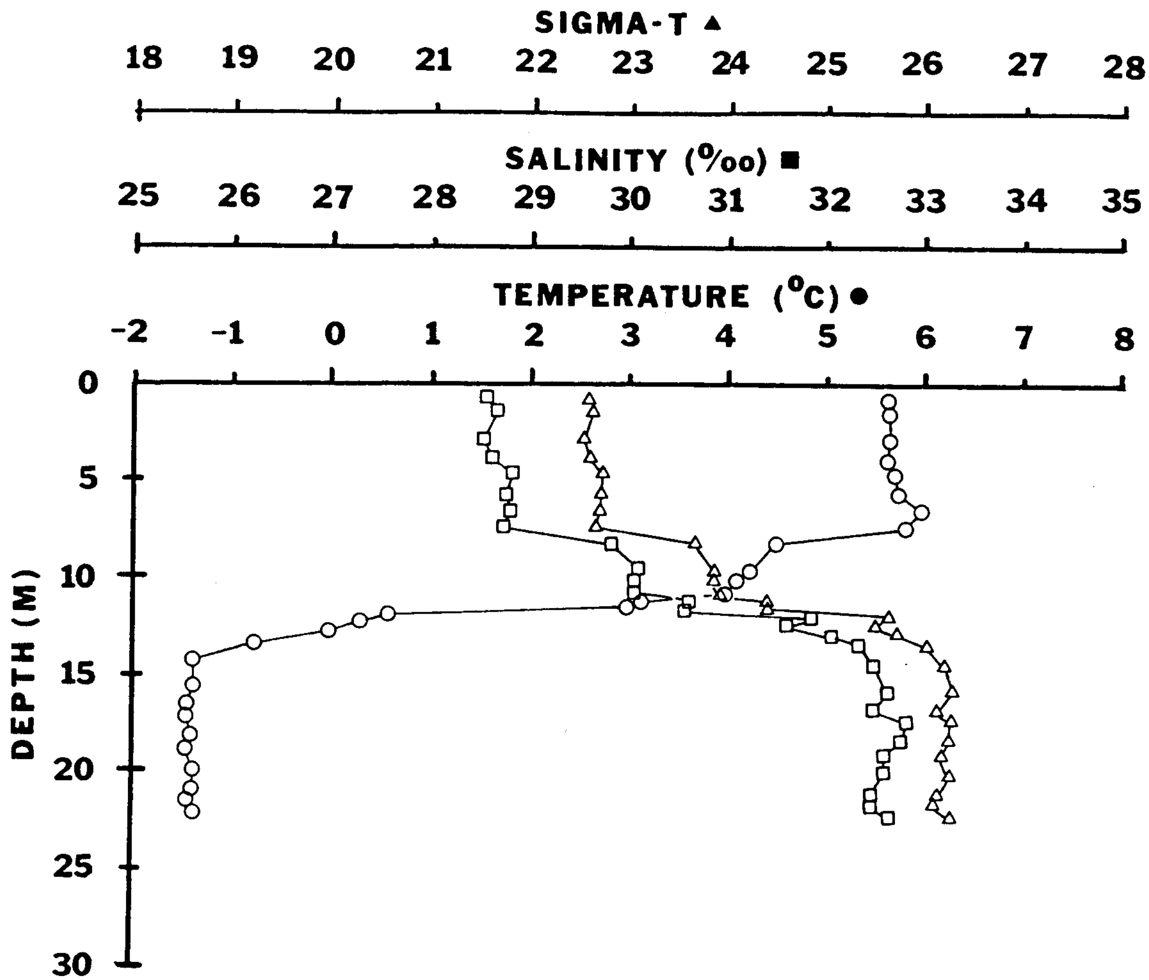

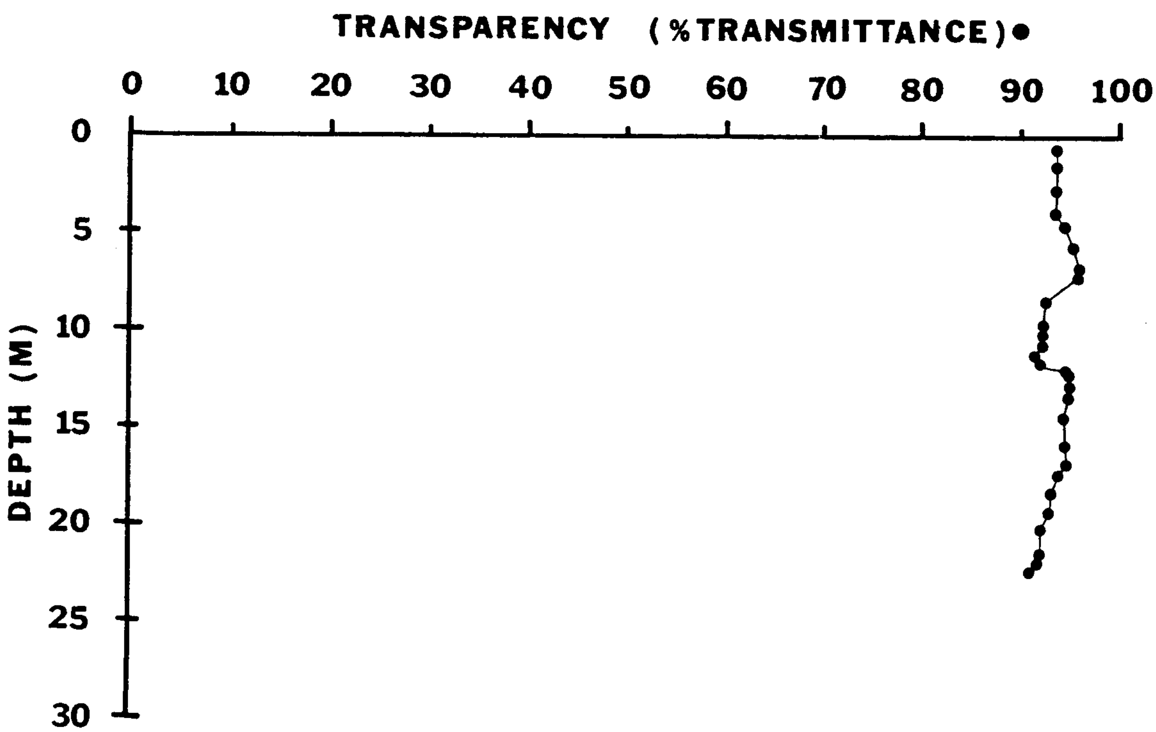

Figure C-15. Hydrographic Profiles for Station Pt. Belcher-15

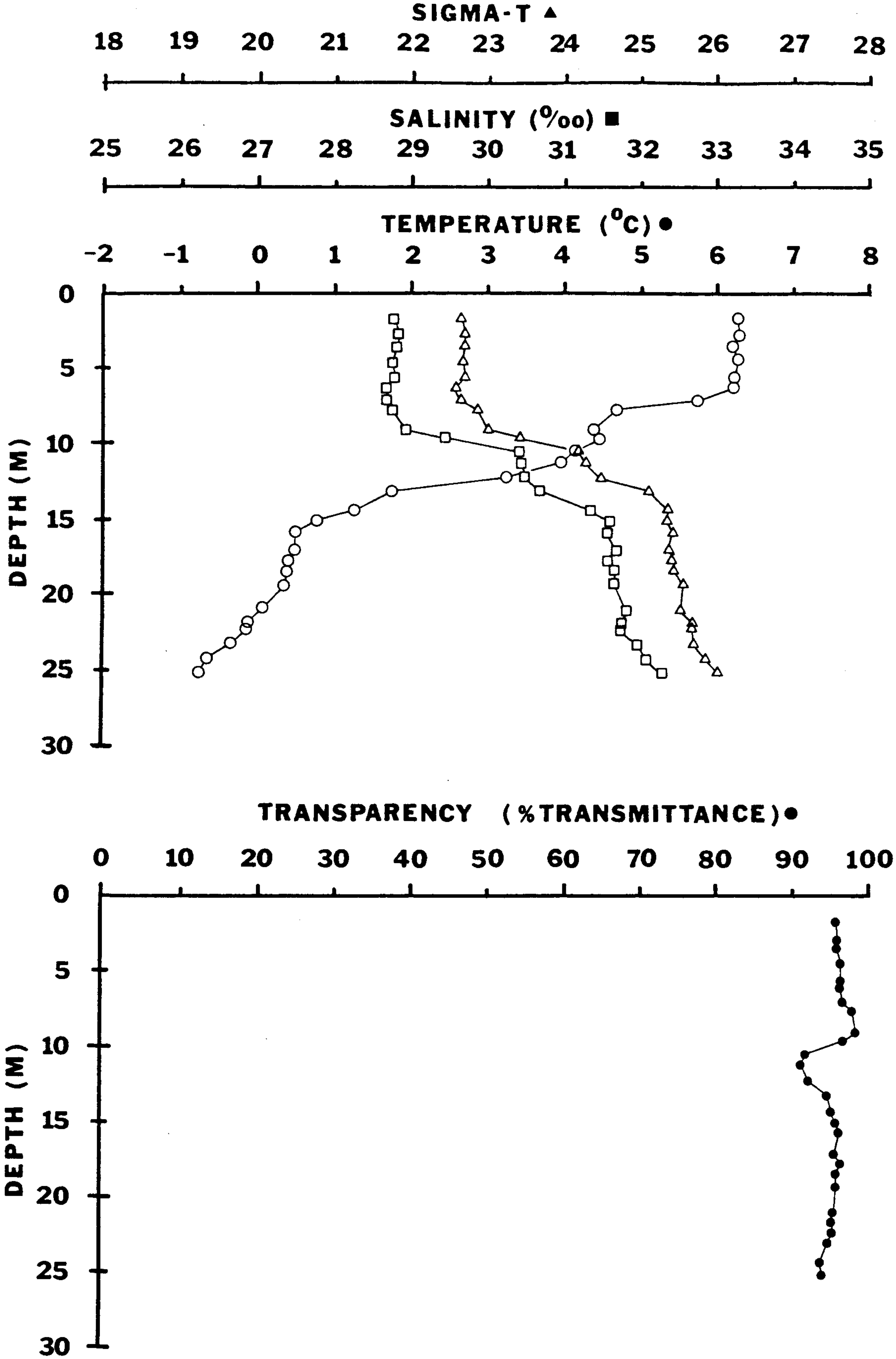

Figure C-16. Hydrographic Profiles for Station Pt. Belcher-16

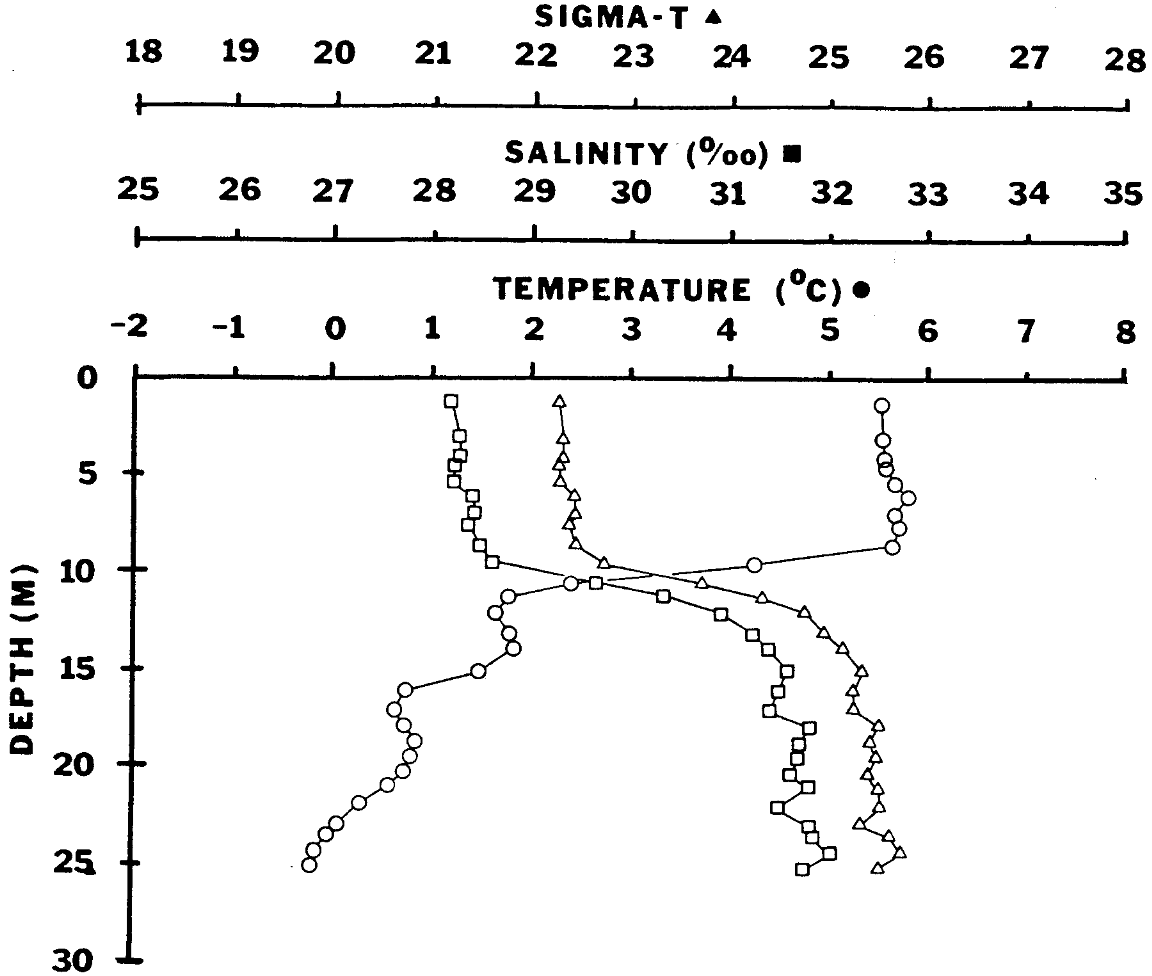

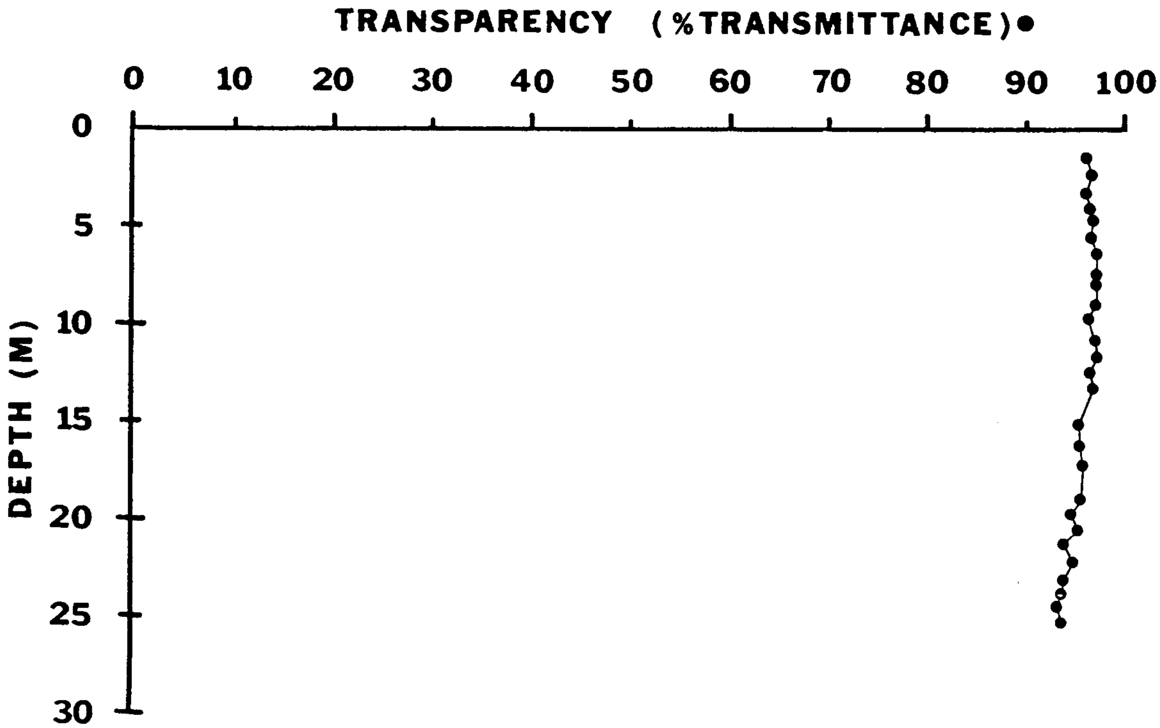

Figure C-17. Hydrographic Profiles for Station Pt. Belcher-17

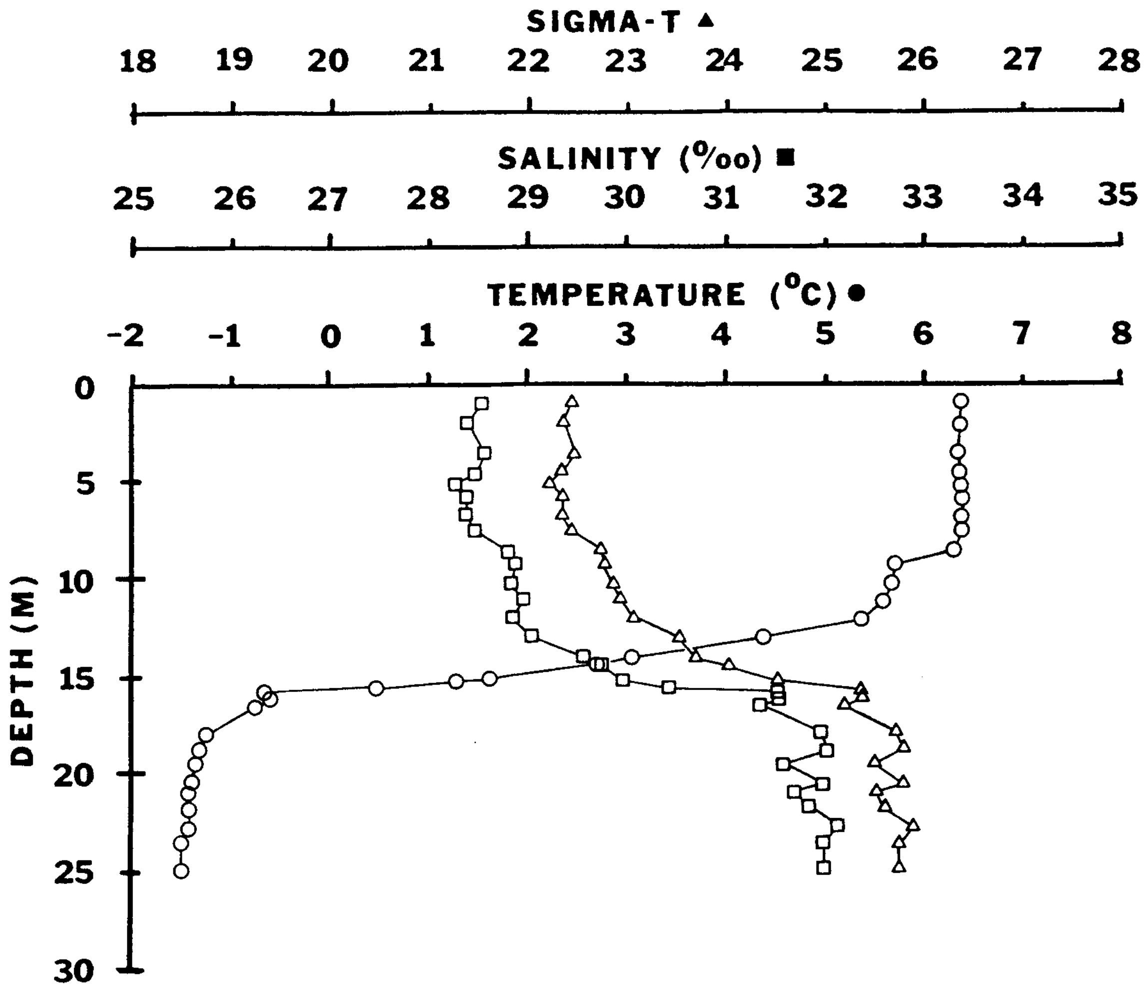

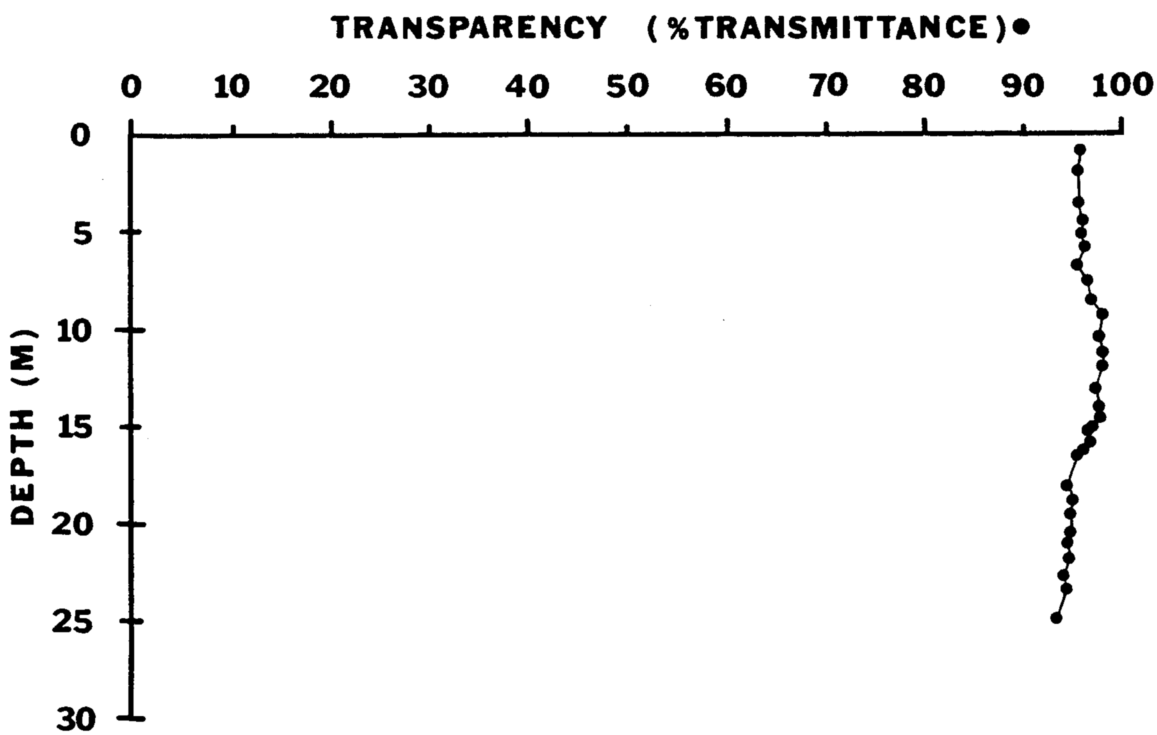

Figure C-18. Hydrographic Profiles for Station Pt. Belcher-18

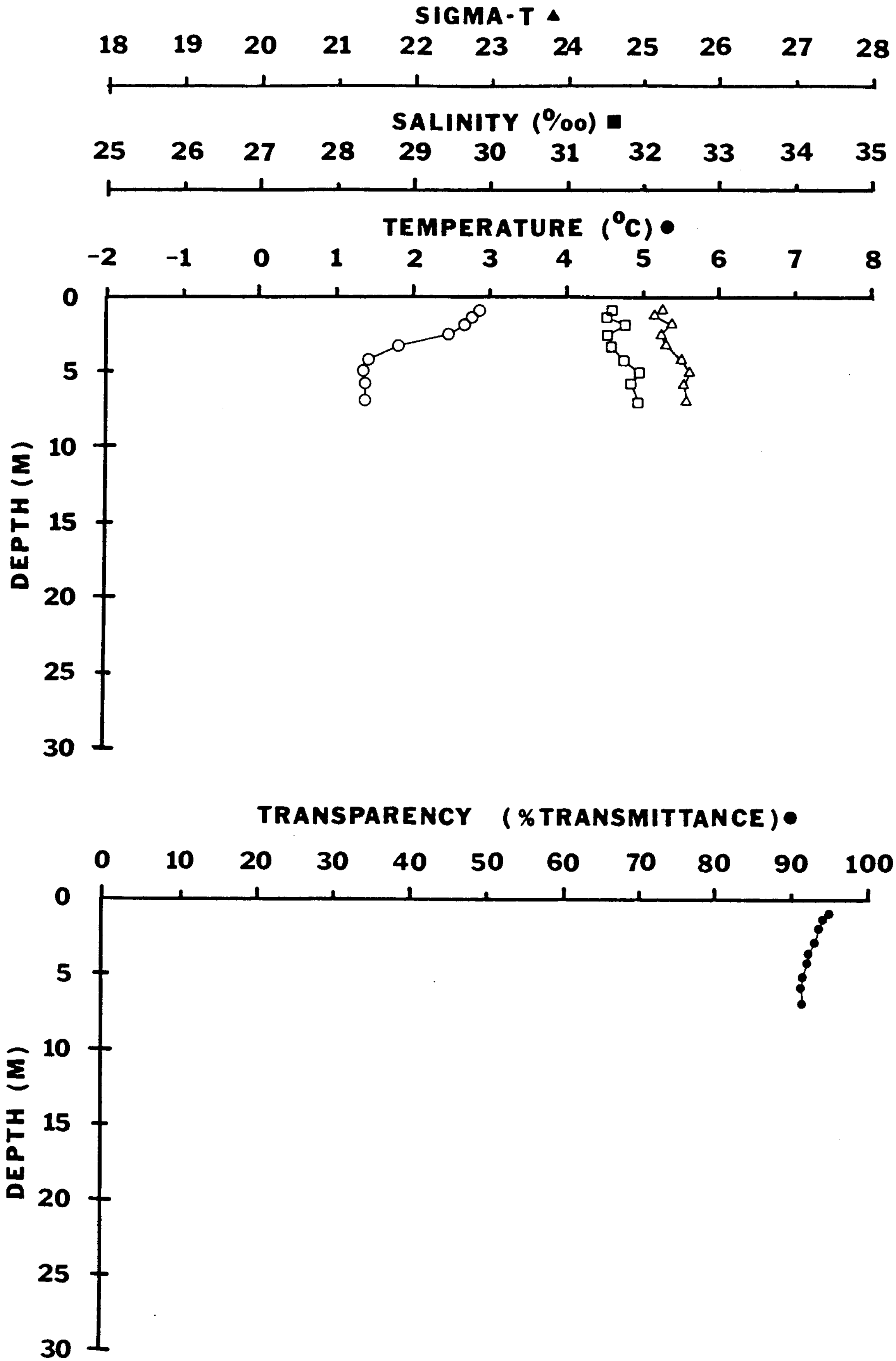

Figure C-19. Hydrographic Profiles for Station Pingorarok Pass-19

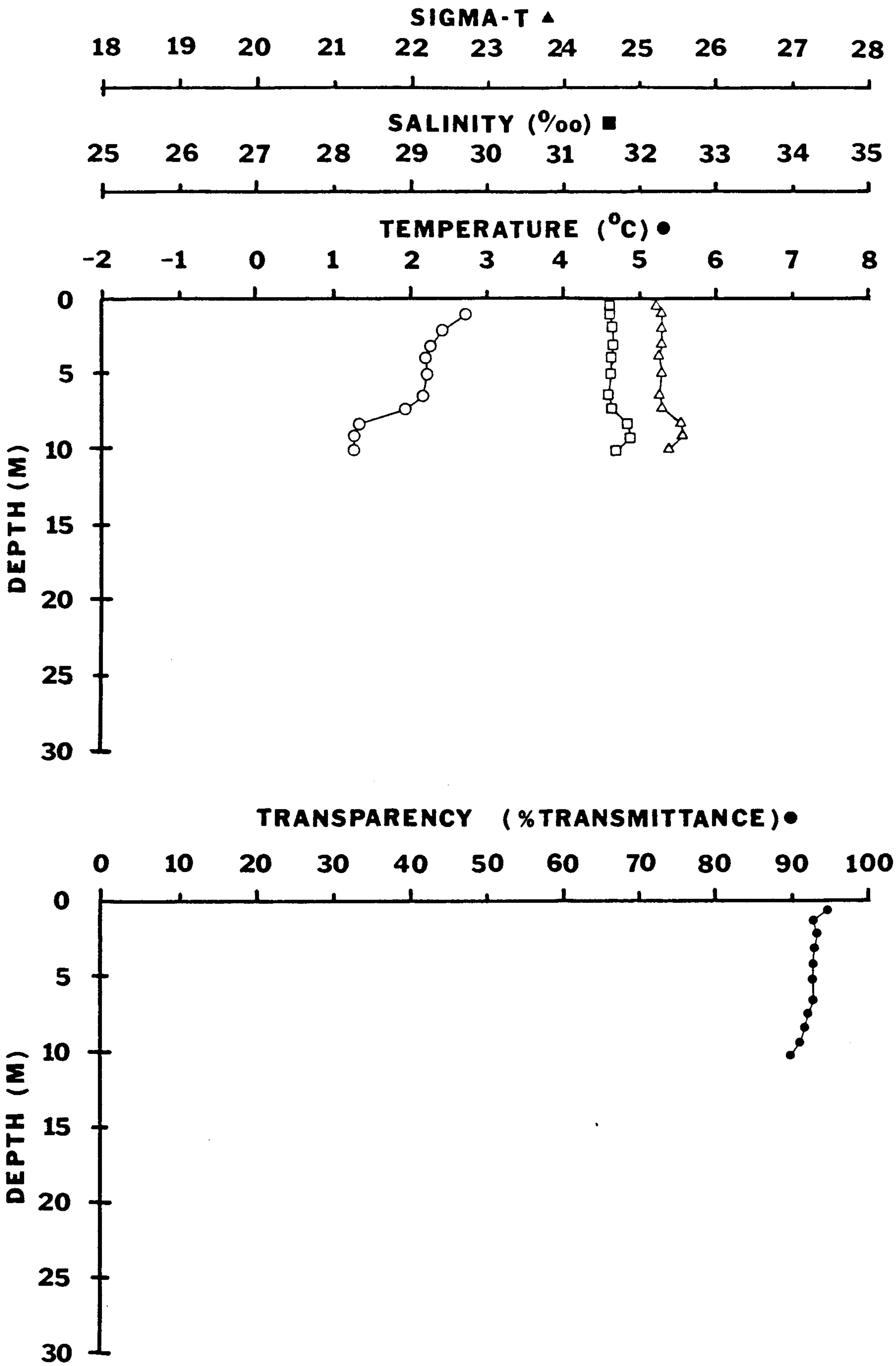

Figure C-20. Hydrographic Profiles for Station Pingorarok Pass-20

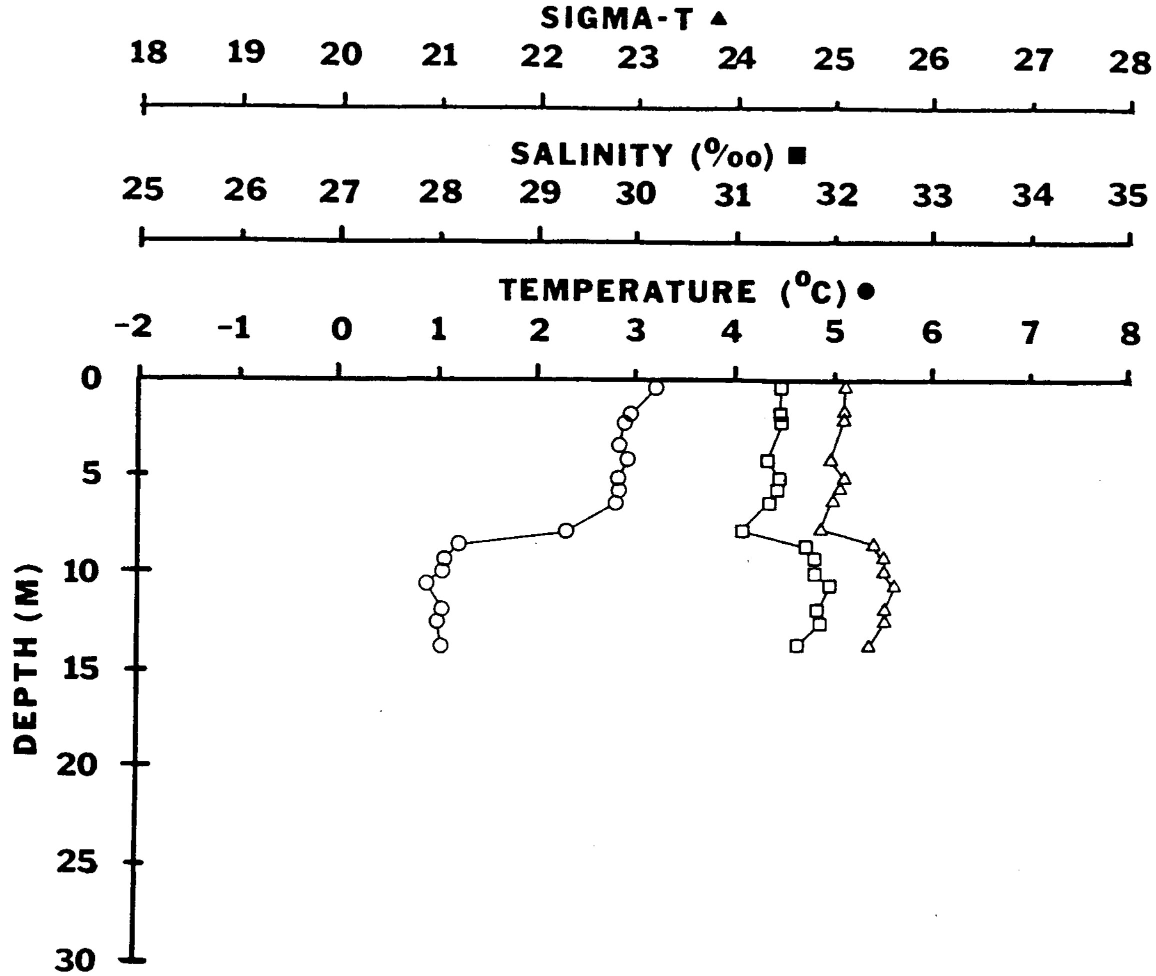

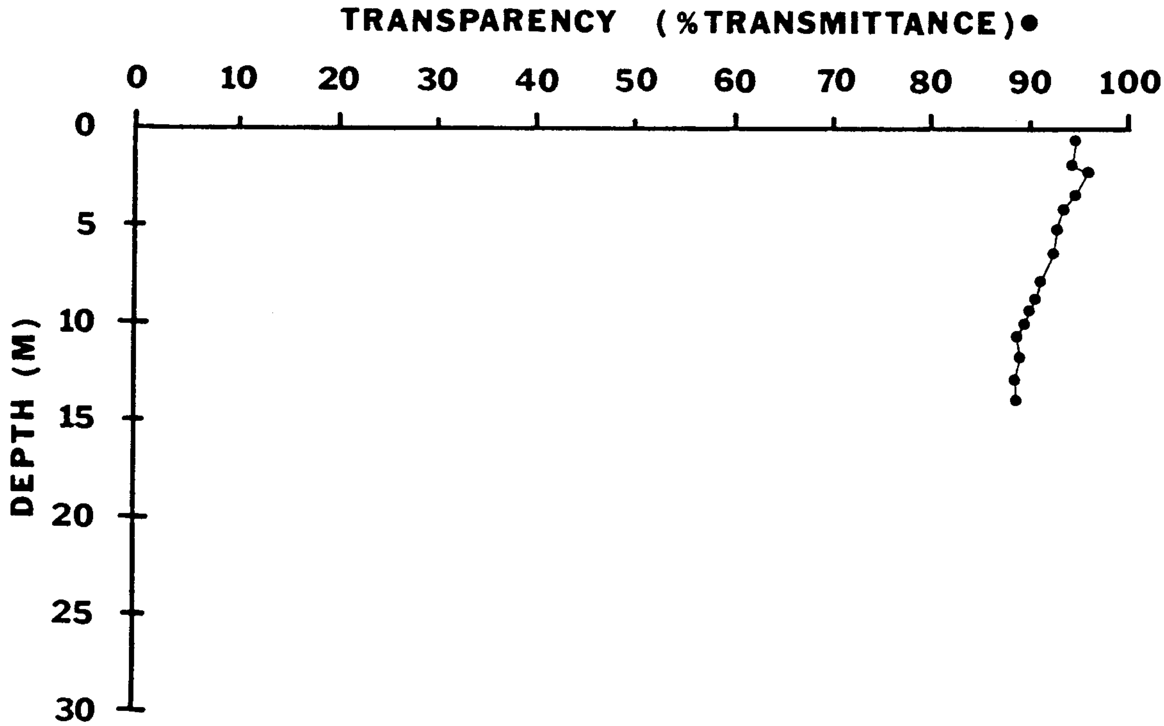

Figure C-21. Hydrographic Profiles for Station Pingorarok Pass-21

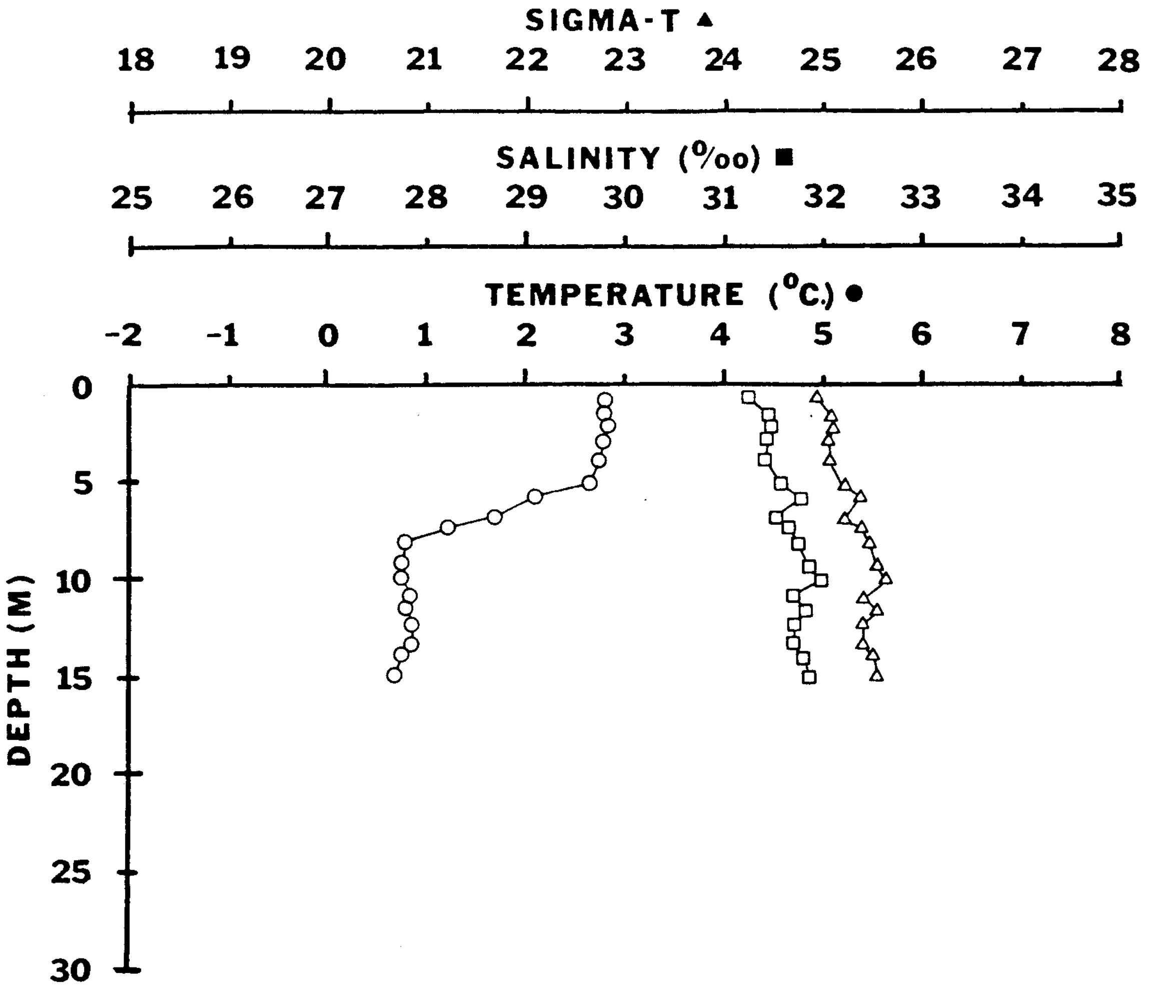

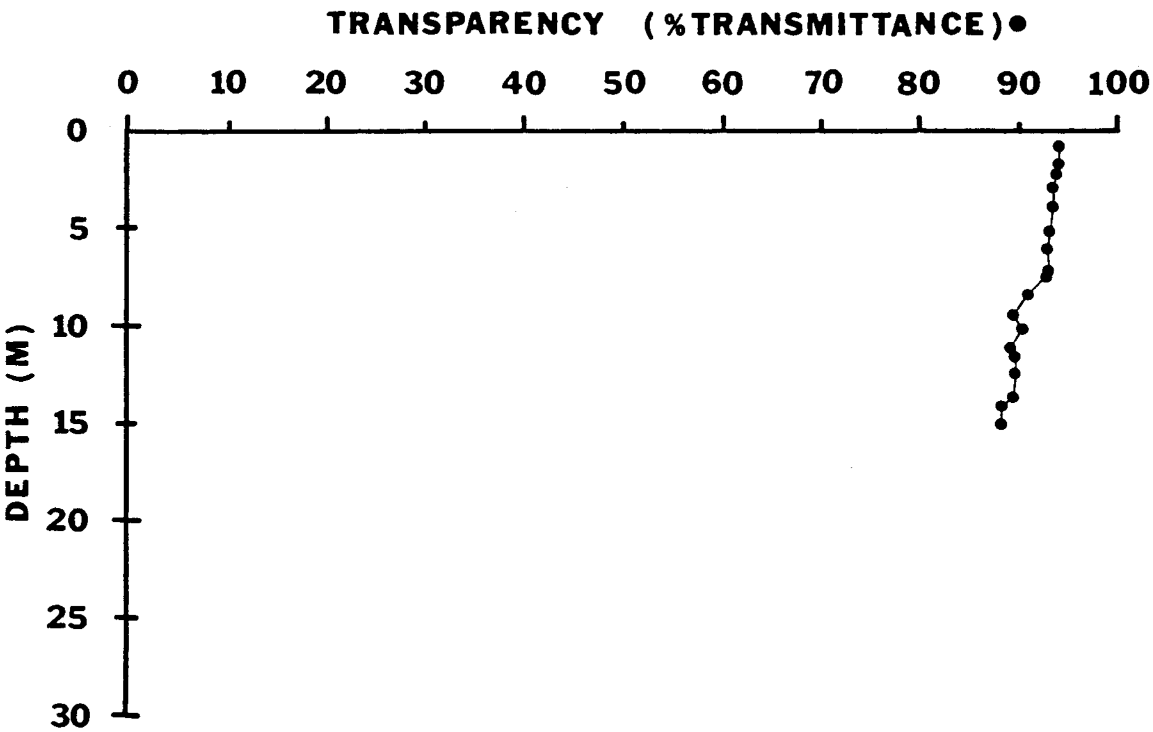

Figure C-22. Hydrographic Profiles for Station Pingorarok Pass-22

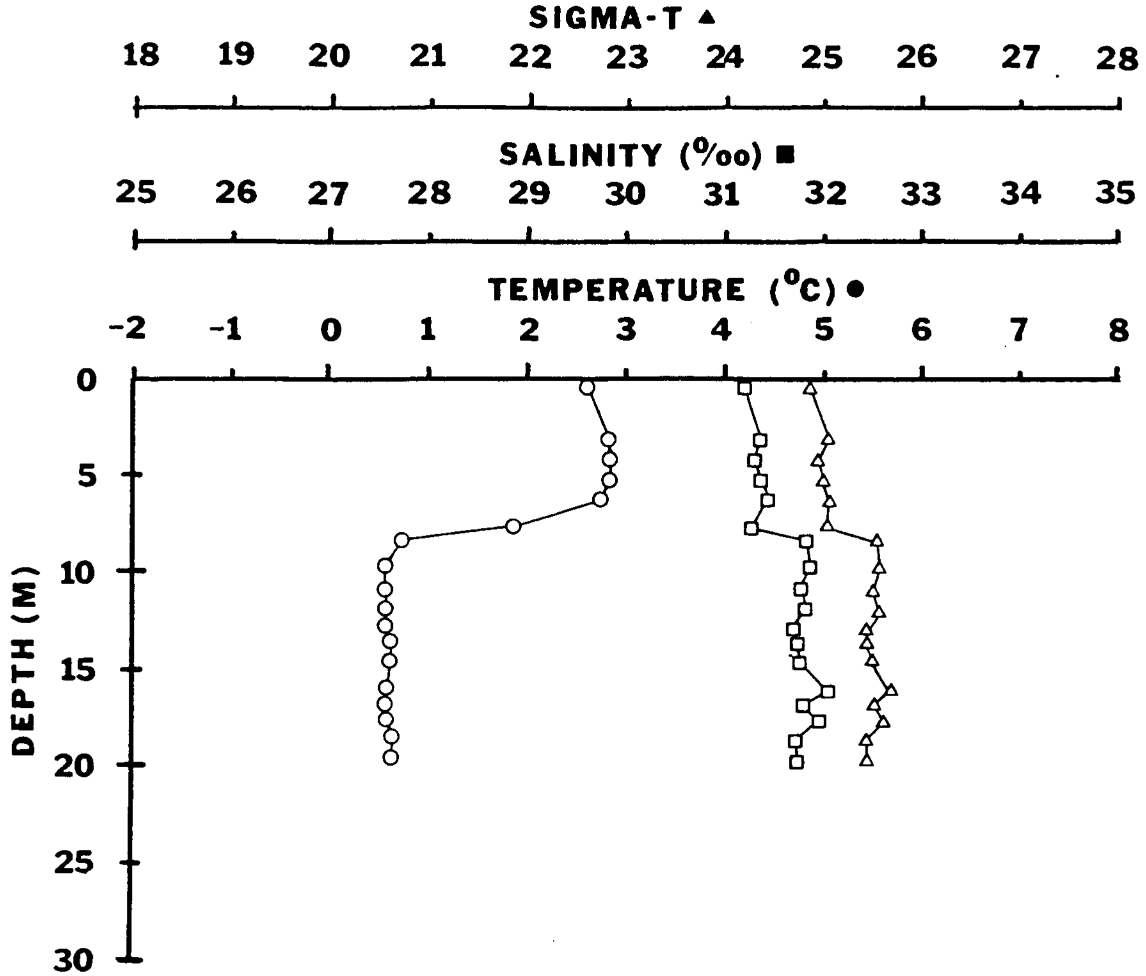

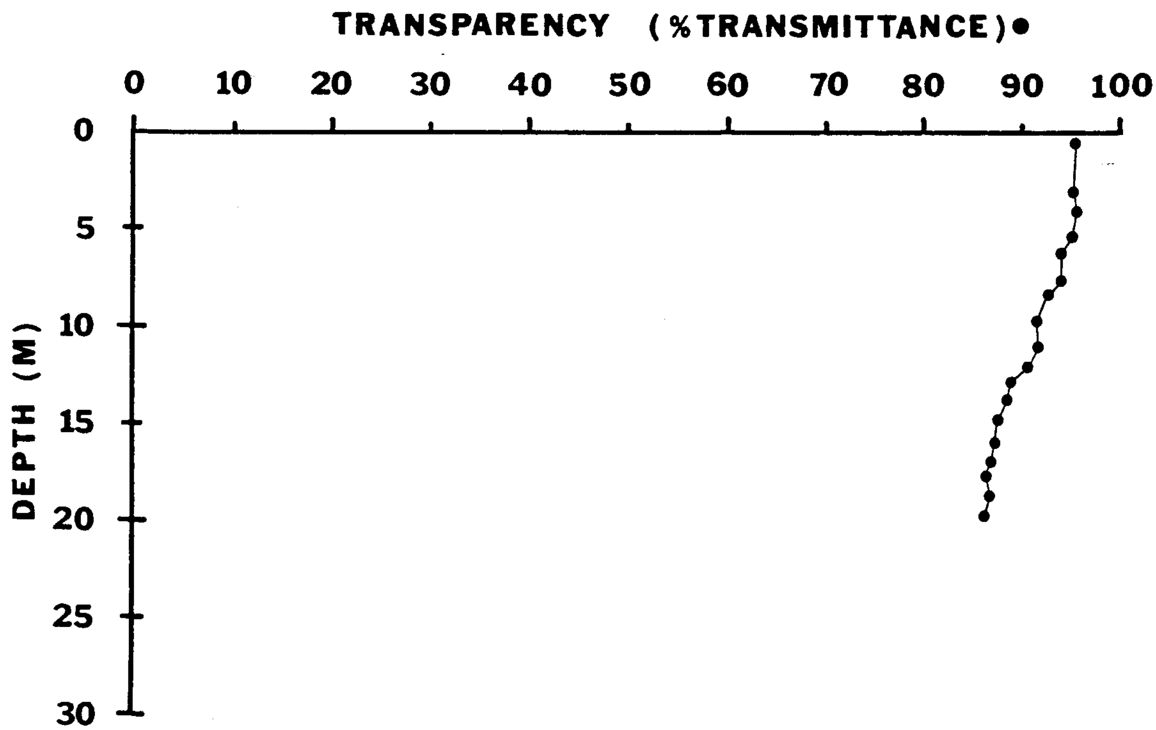

Figure C-23. Hydrographic Profiles for Station Pingorarok Pass-23

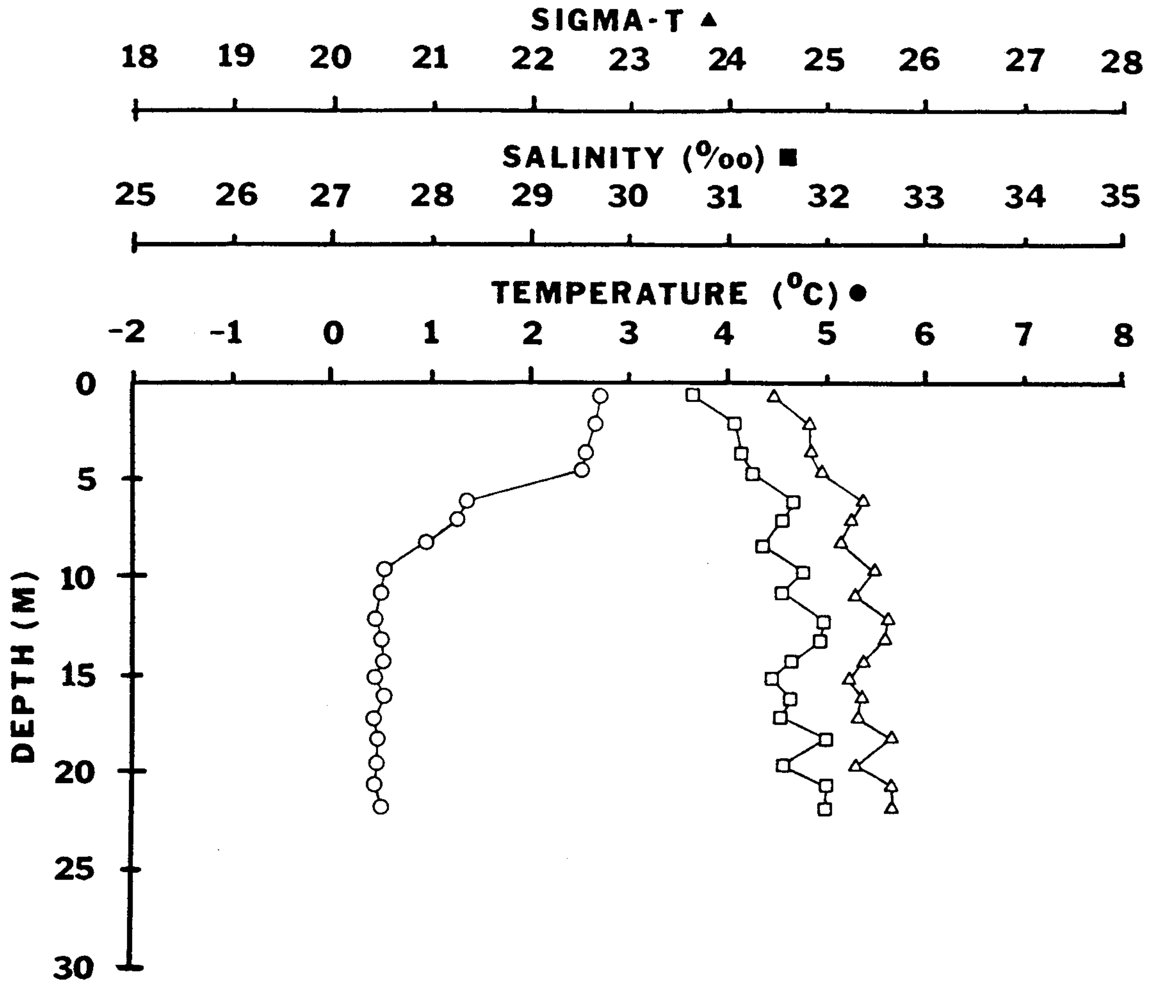

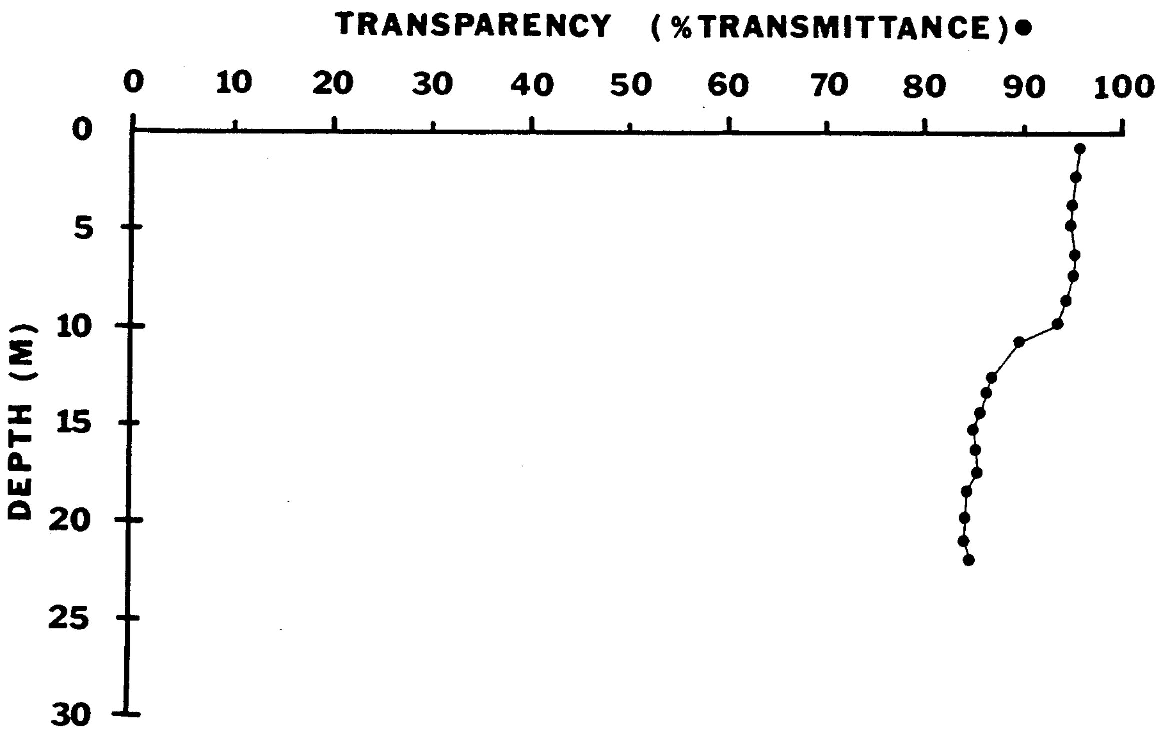

Figure C-24. Hydrographic Profiles for Station Pingorarok Pass-24

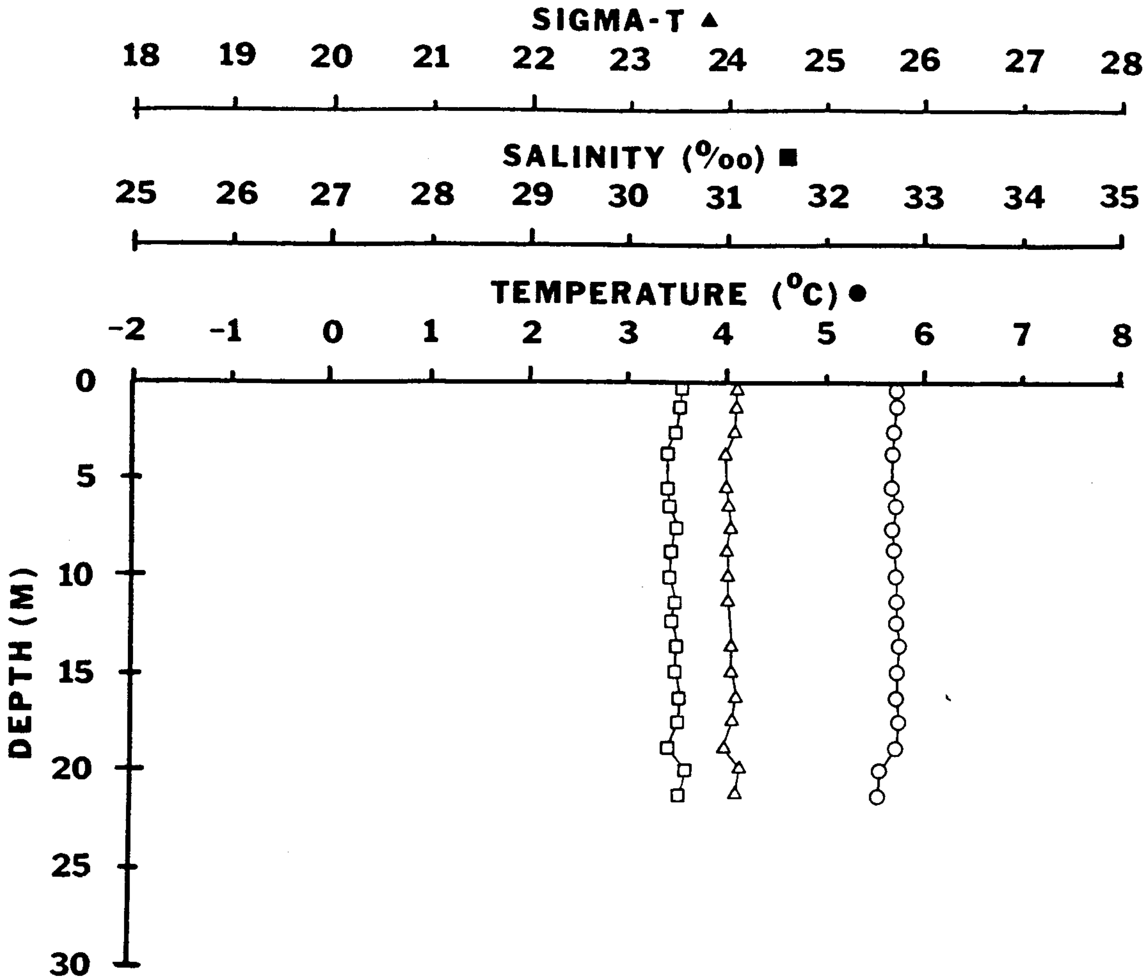

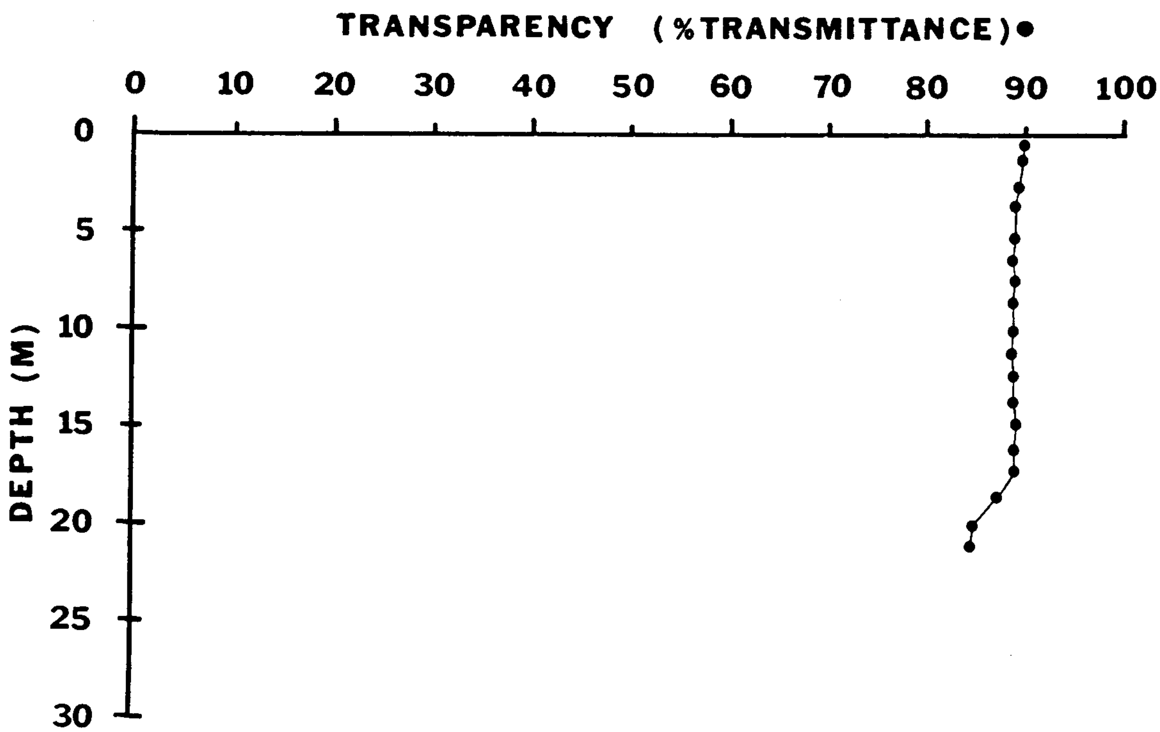

Figure C-25. Hydrographic Profile for Station Wainwright-36

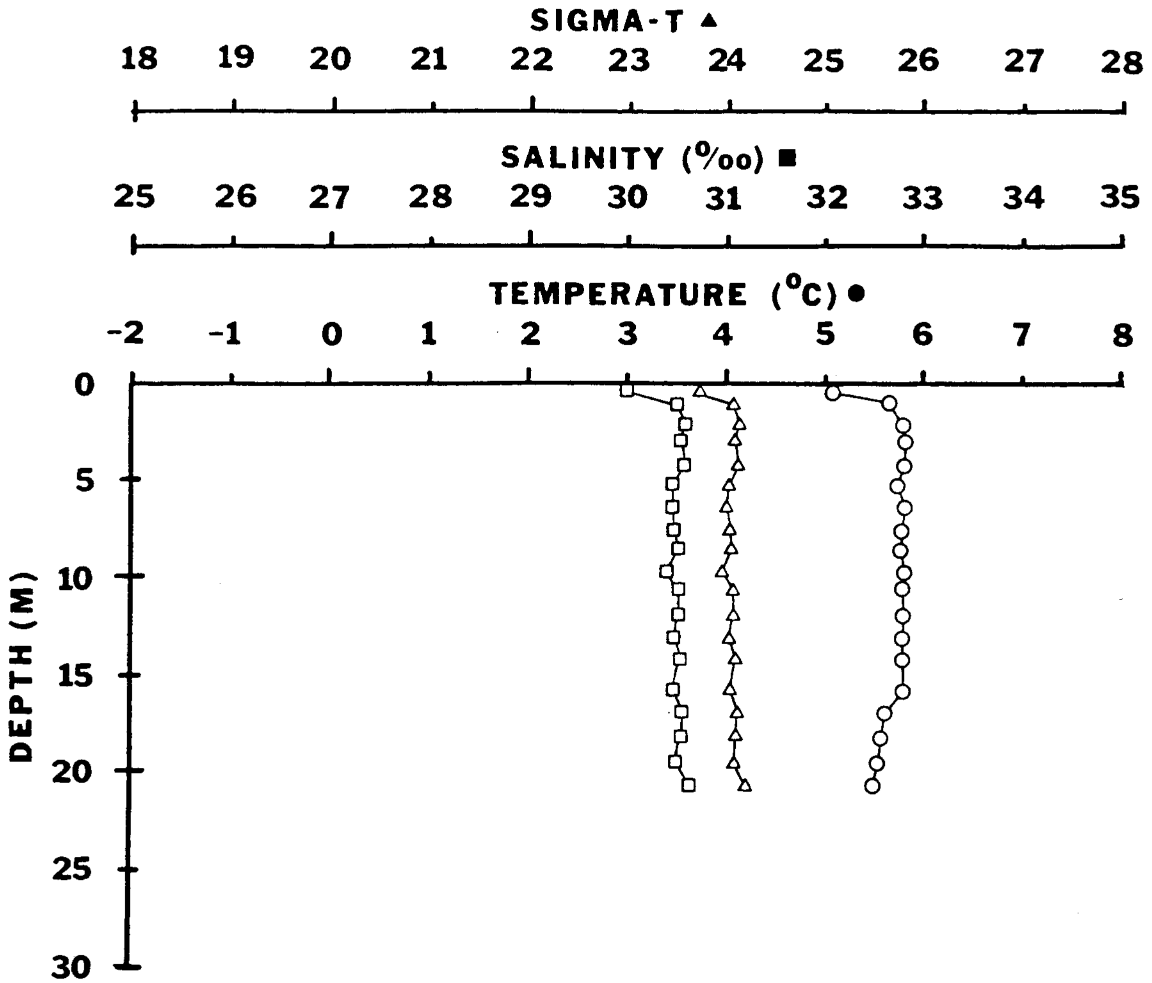

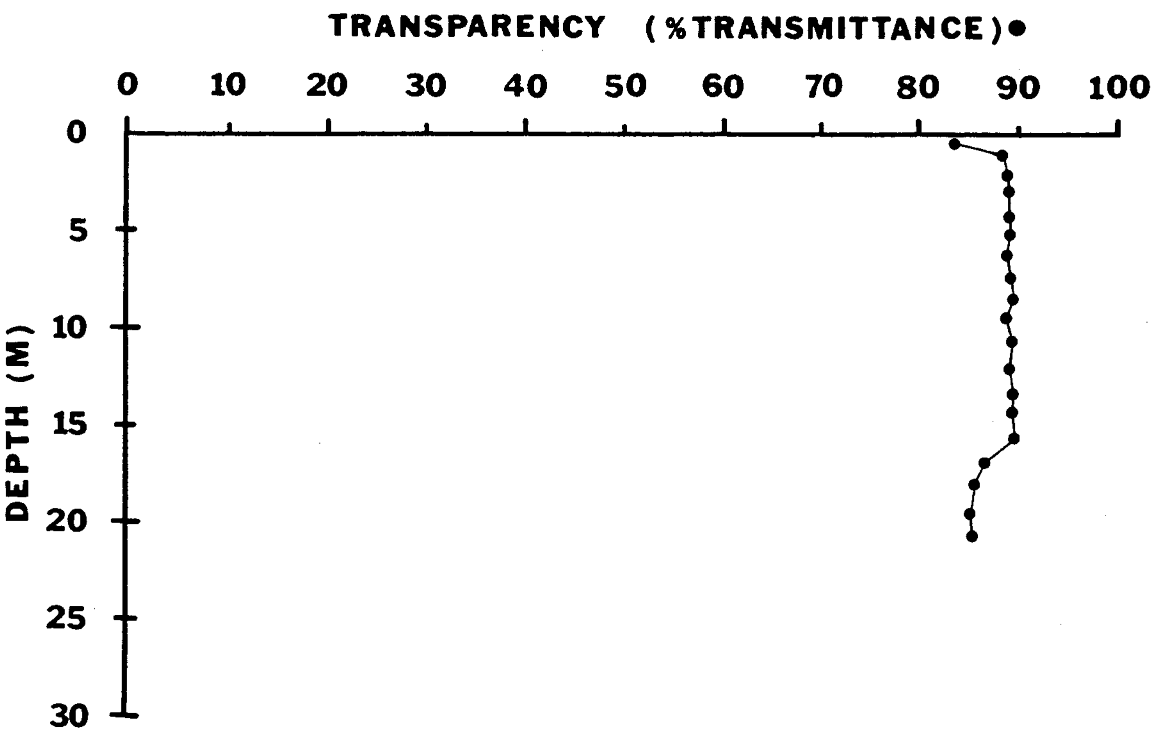

Figure C-26. Hydrographic Profiles for Station Wainwright-37

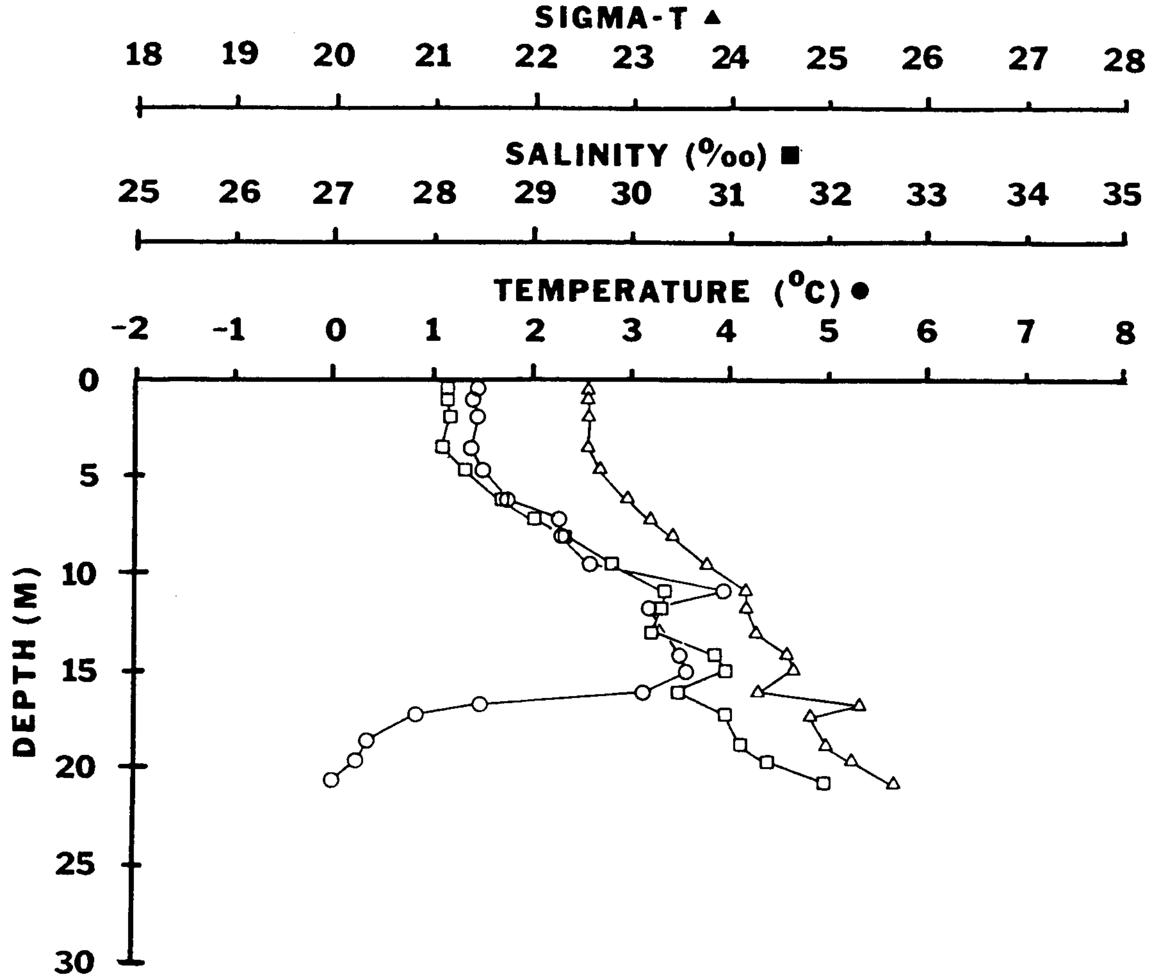

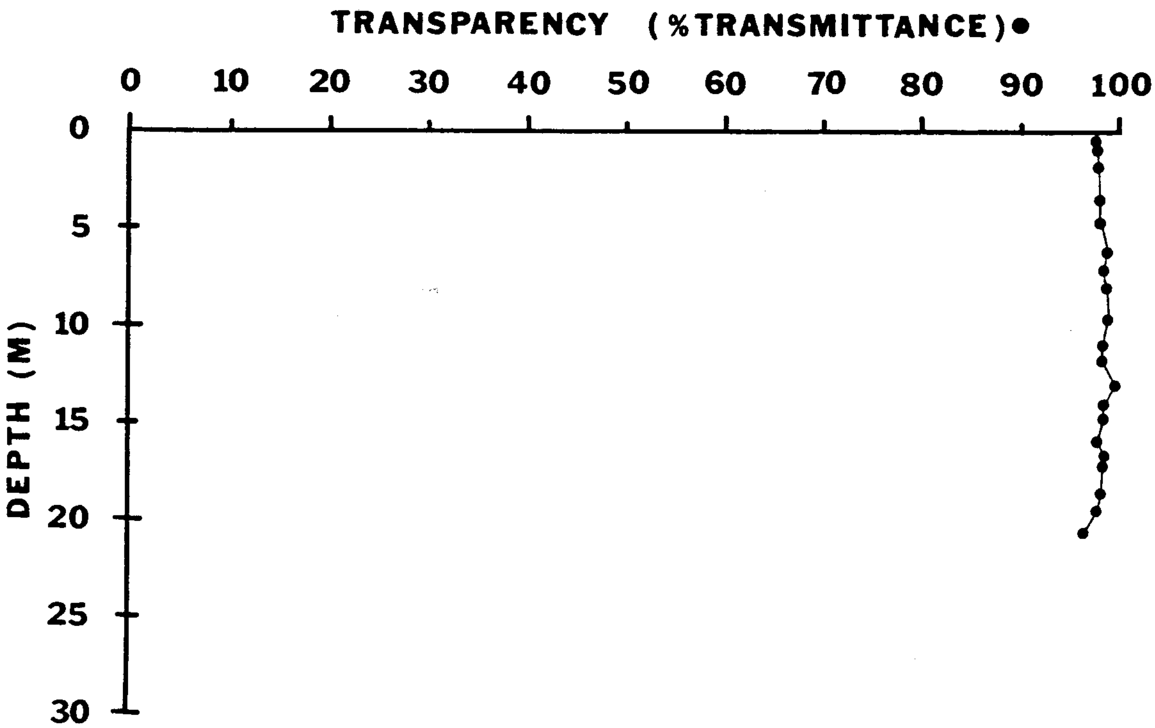

Figure C-27. Hydrographic Profiles for Station Wainwright-39

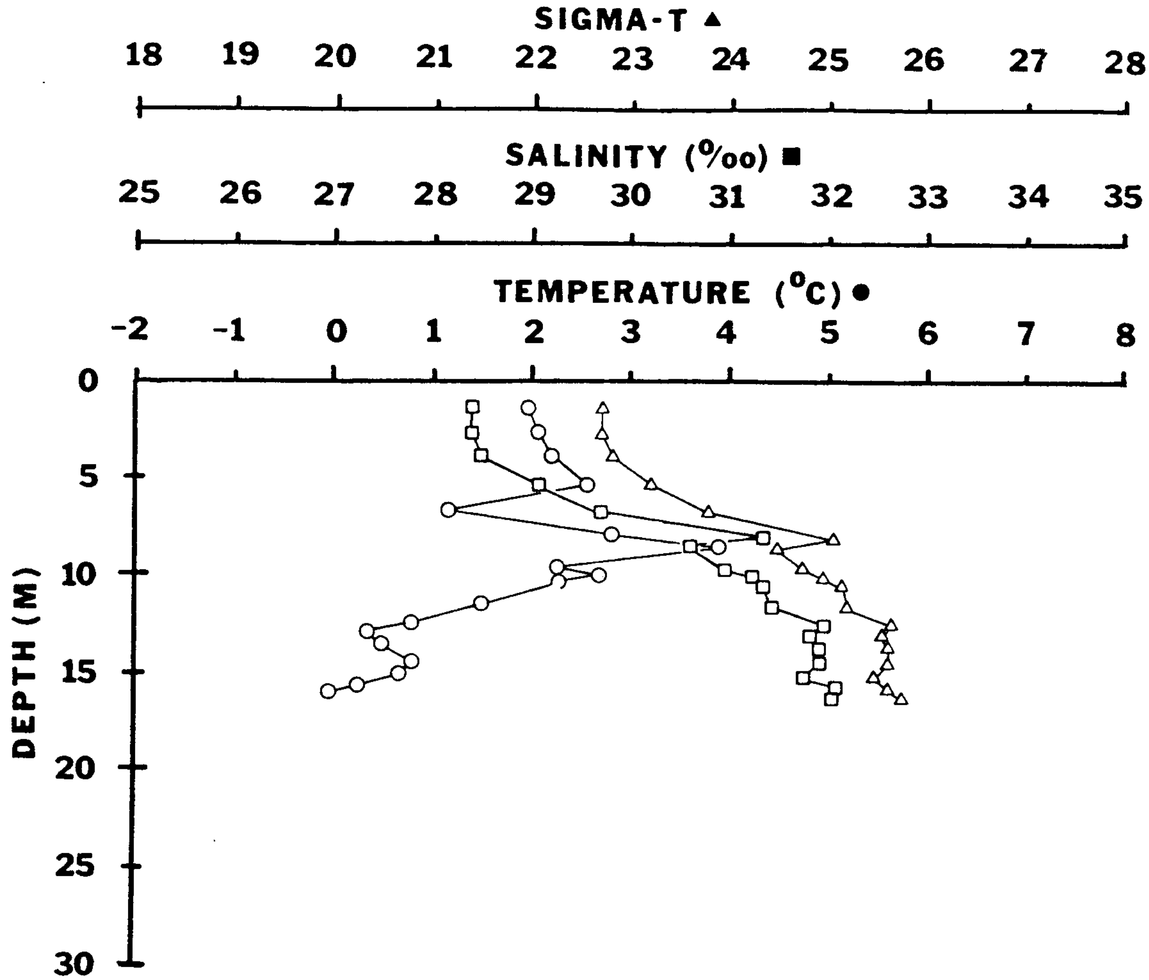

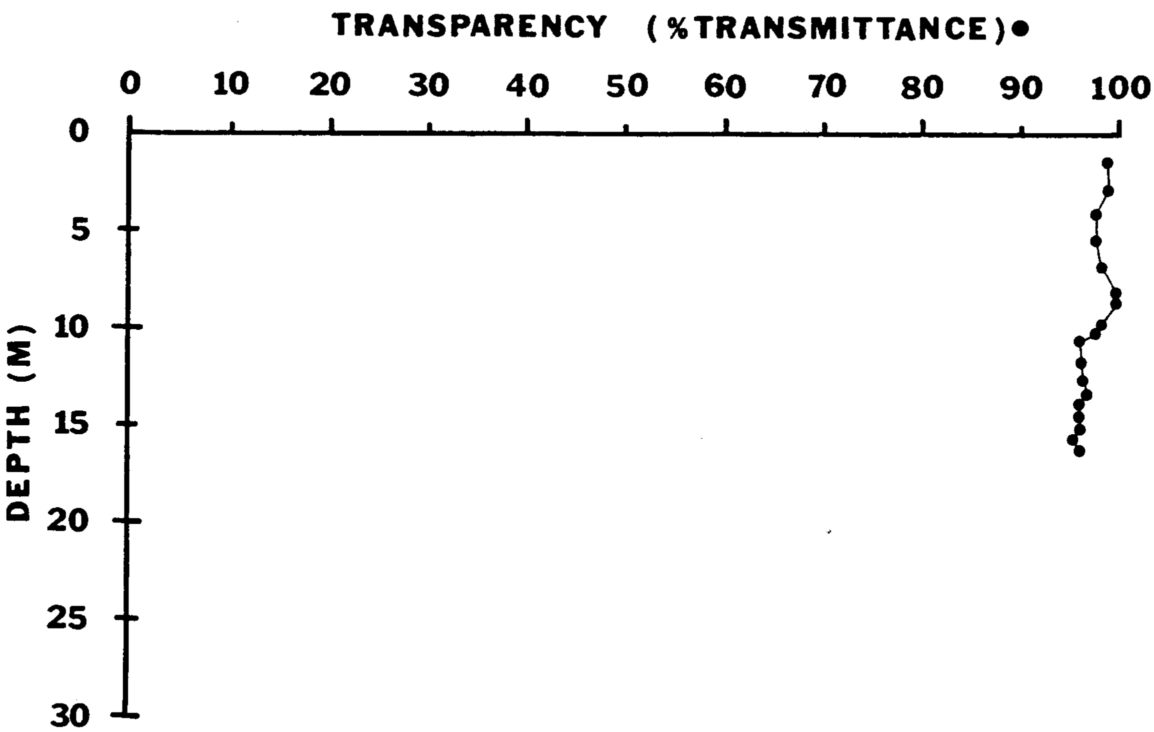

Figure C-28. Hydrographic Profiles for Station Wainwright-40

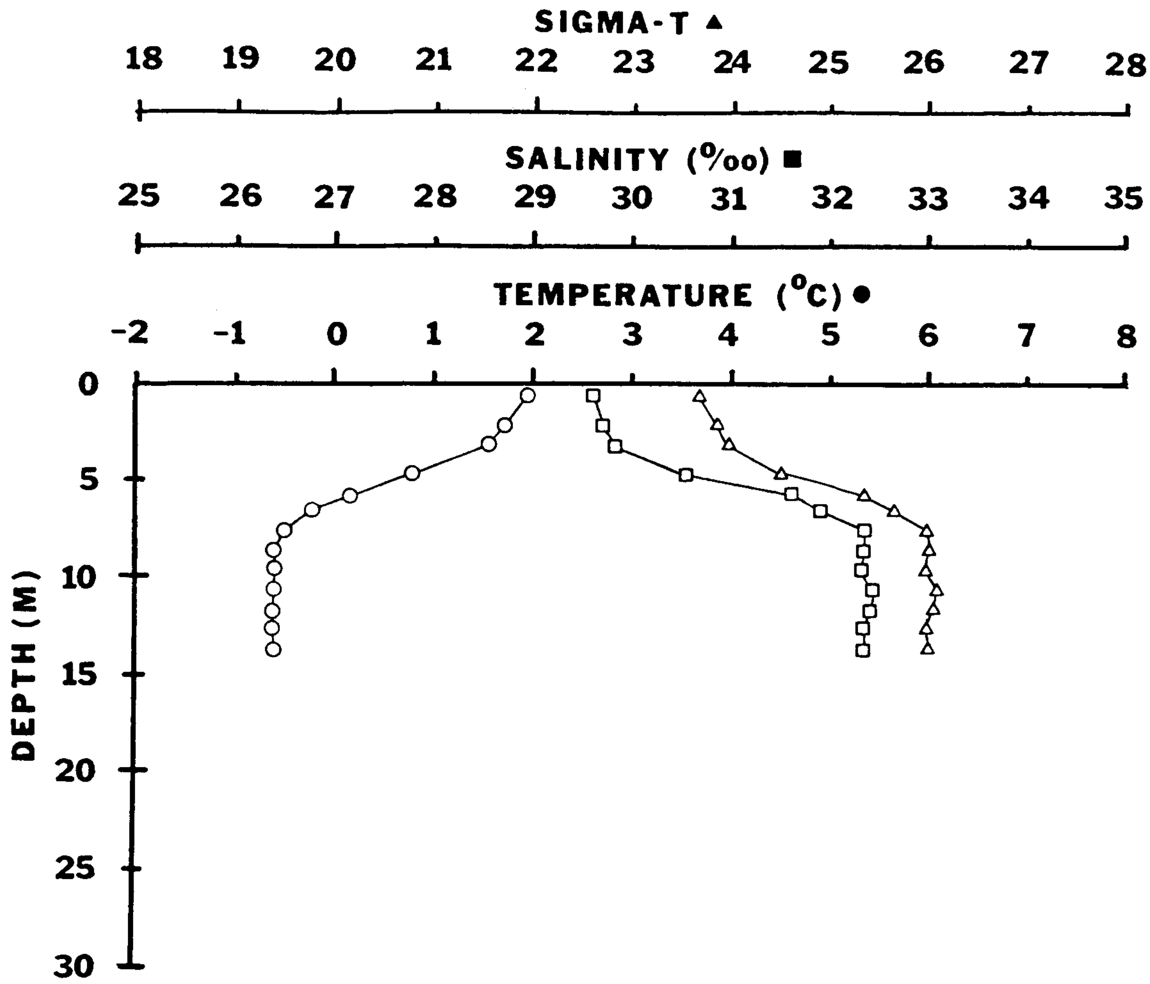

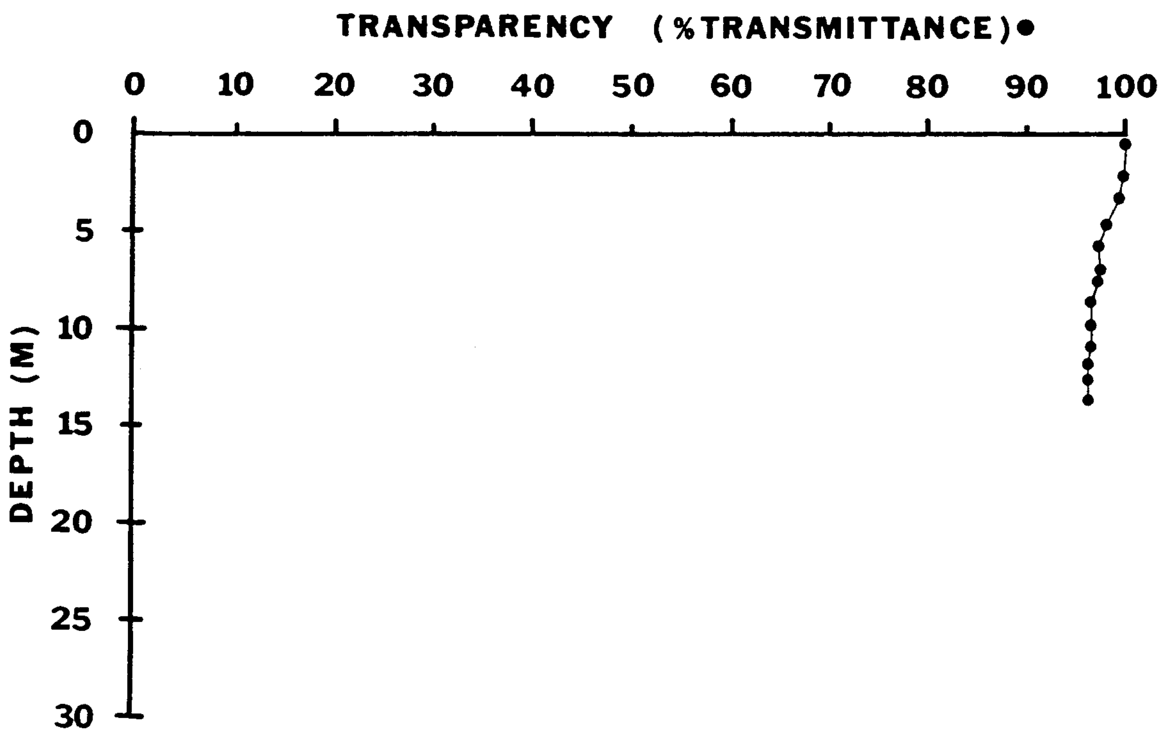

Figure C-29. Hydrographic Profiles for Station Wainwright-41

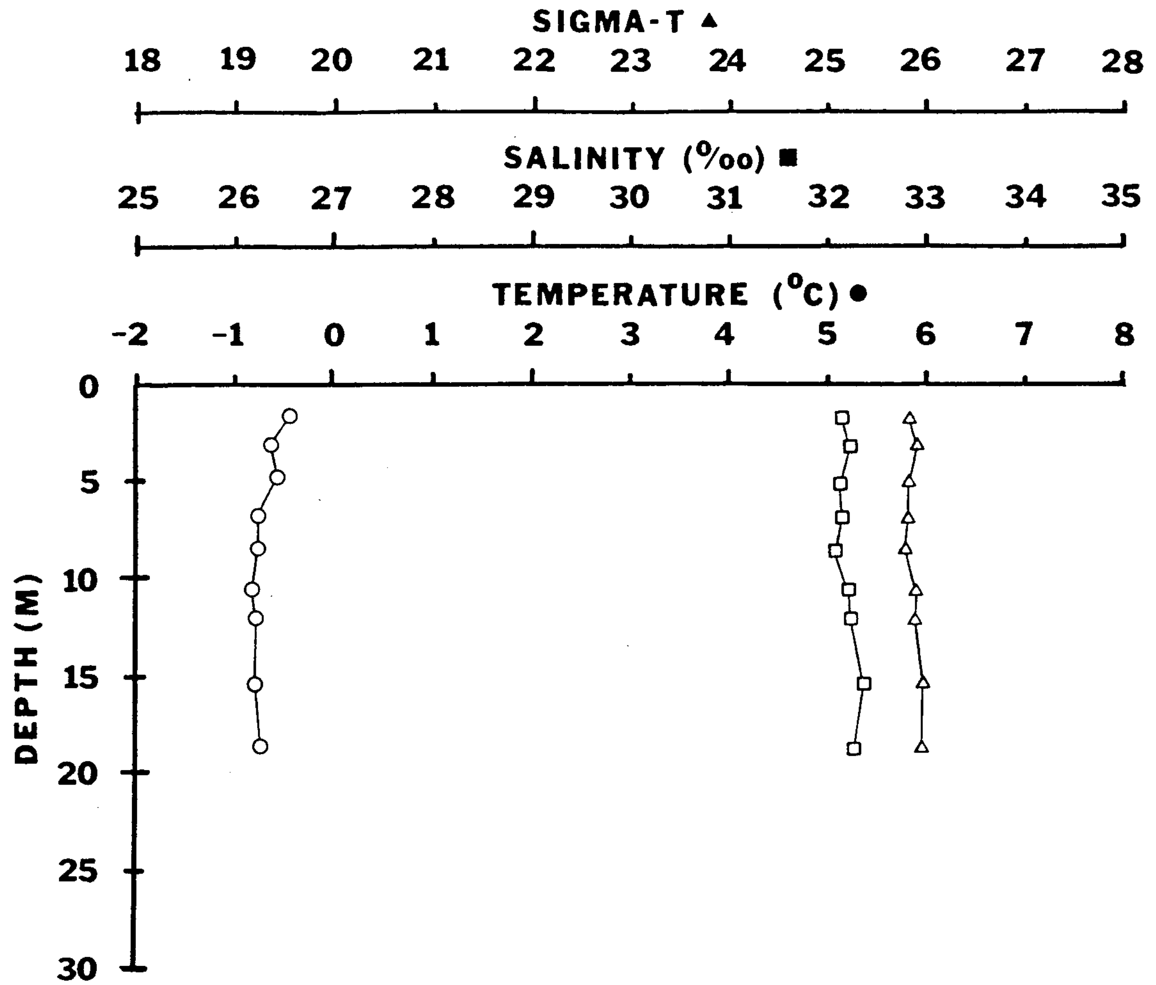

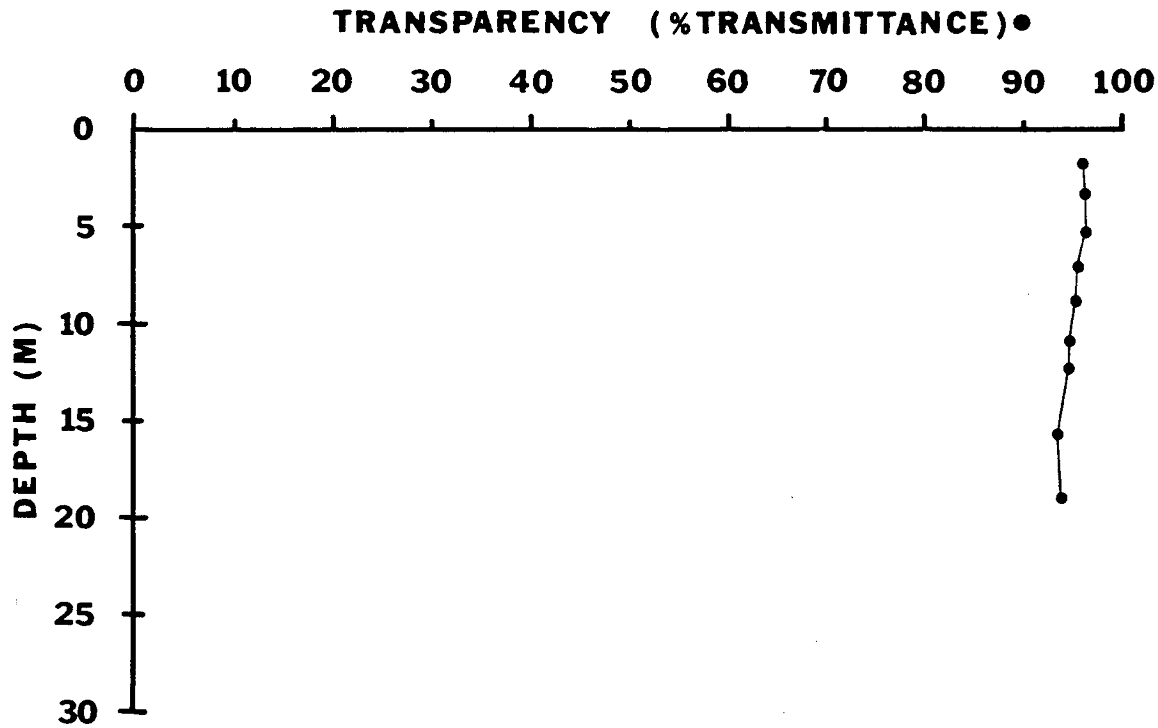

Figure C-30. Hydrographics Profiles for Station Wainwright-42

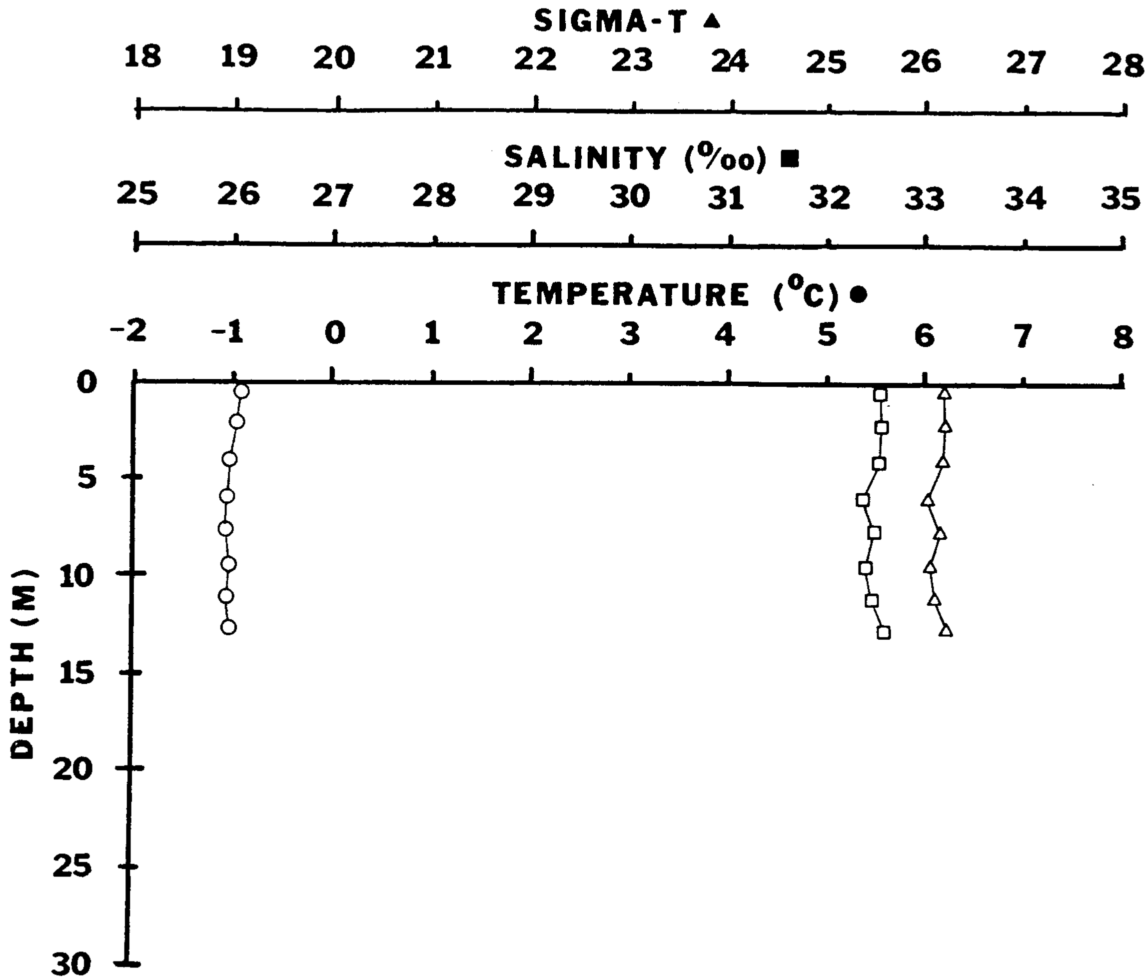

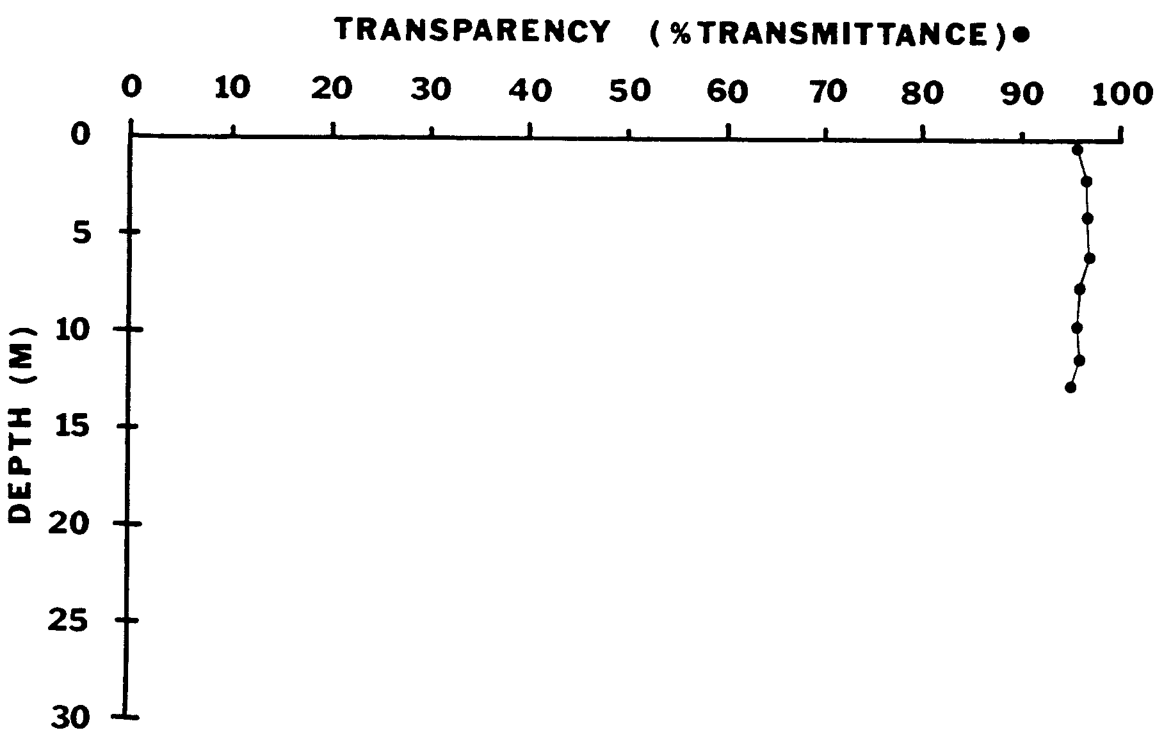

Figure C-31. Hydrographic Profiles for Station Wainwright-43

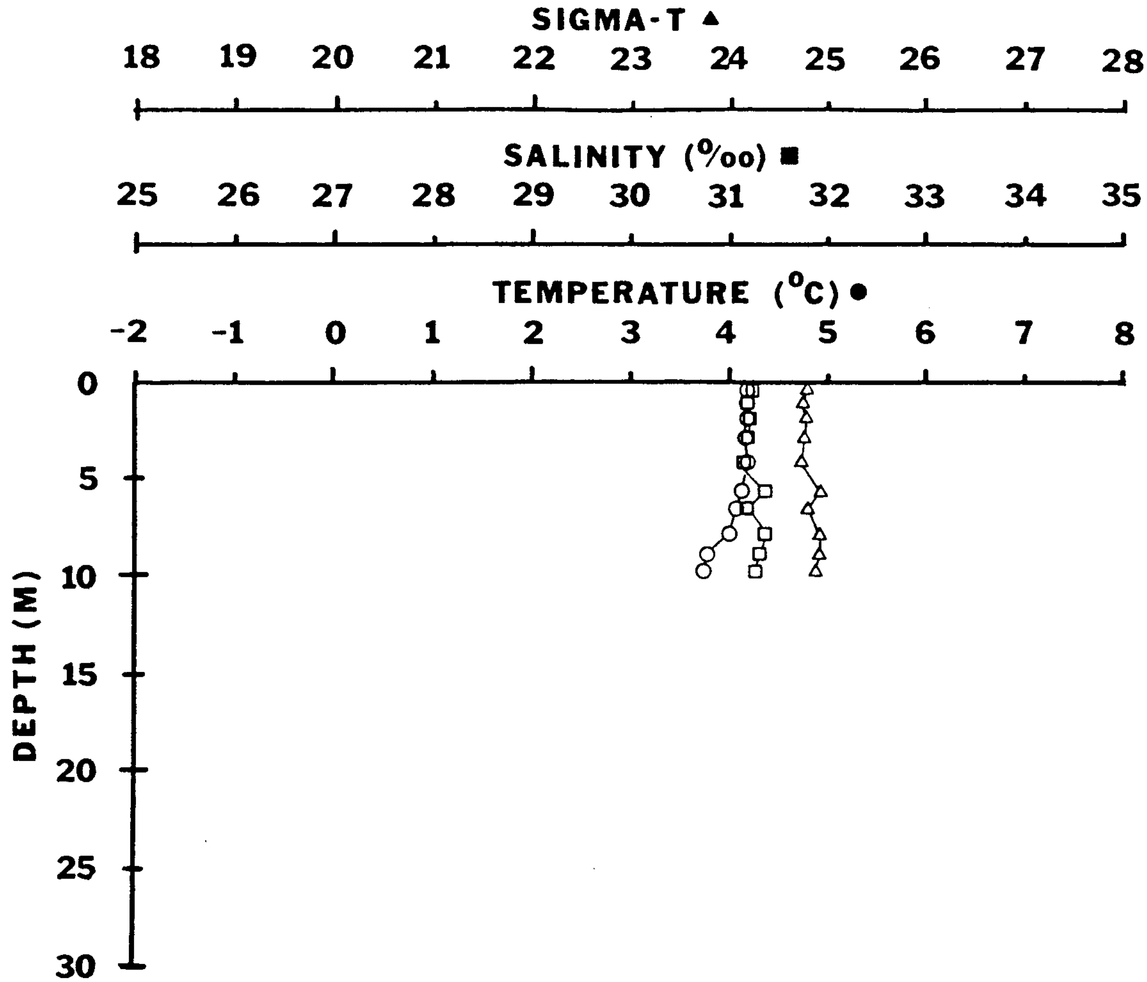

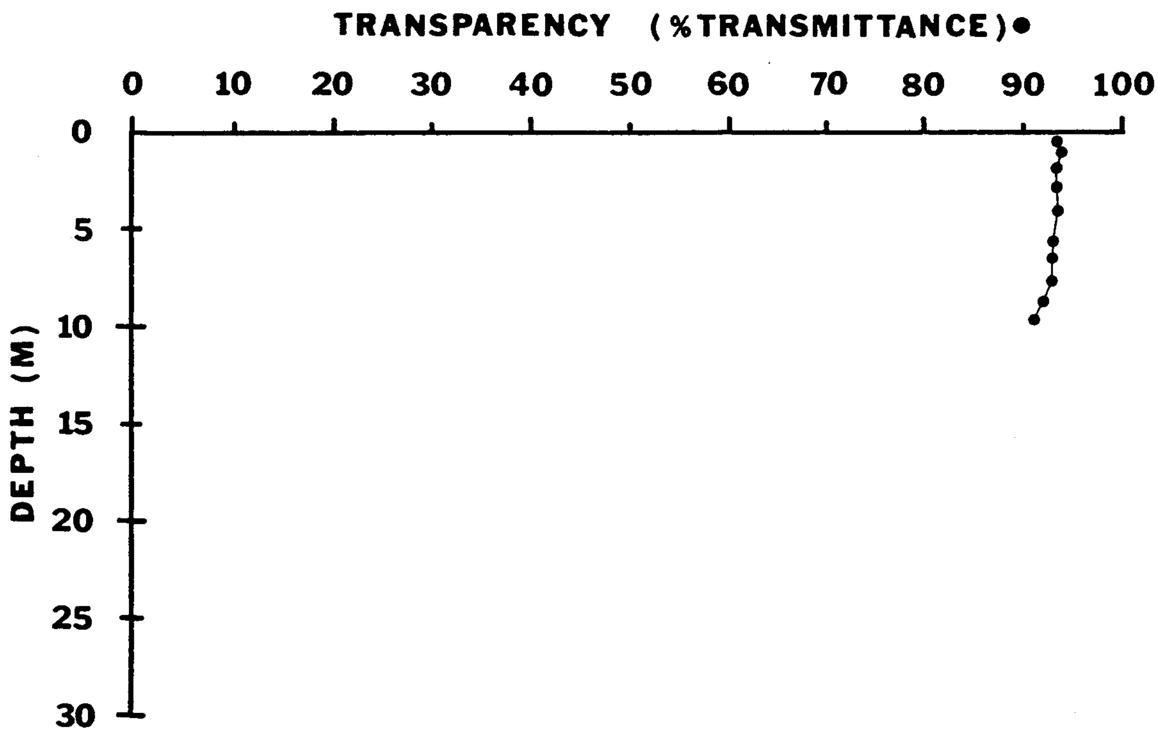

Figure C-32. Hydrographic Profiles for Station Icy Cape-30

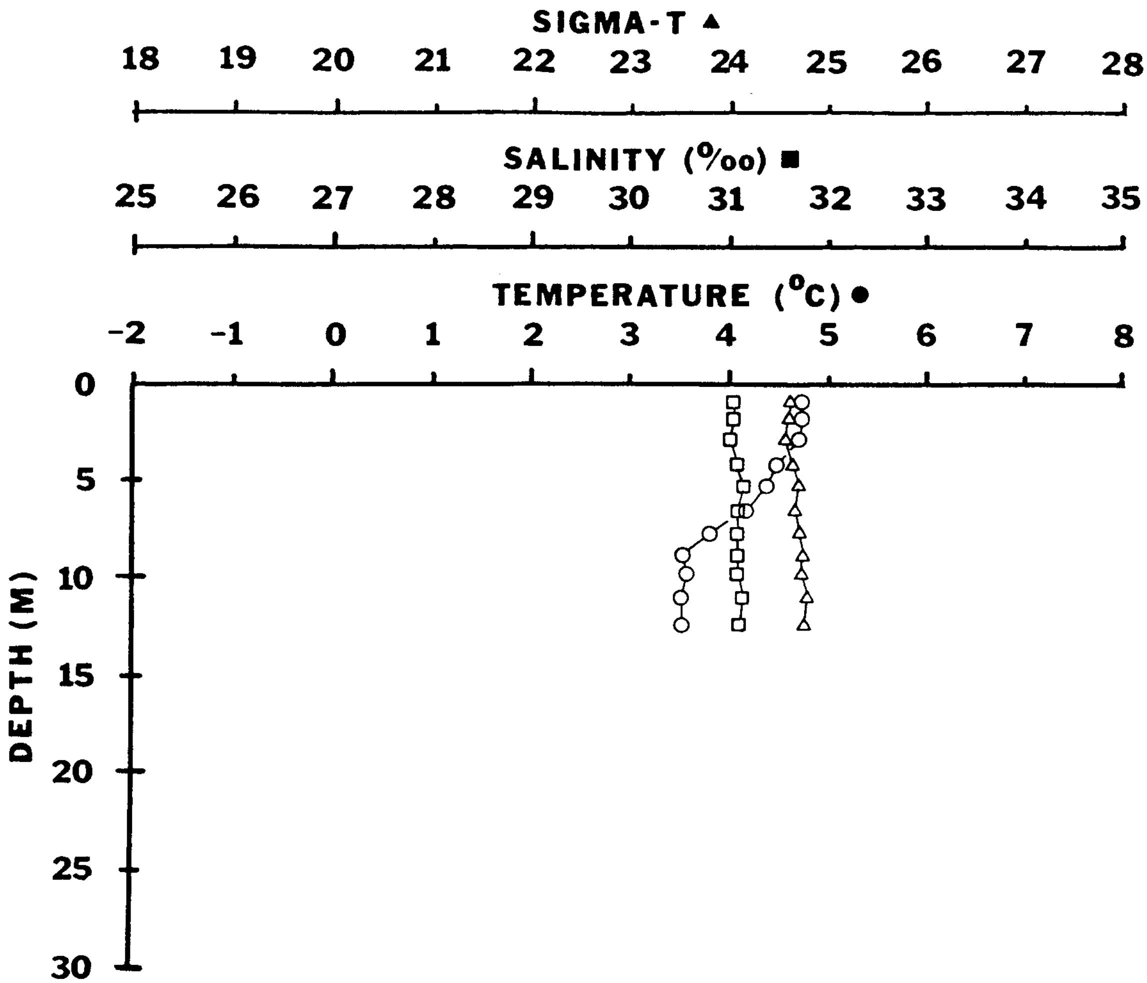

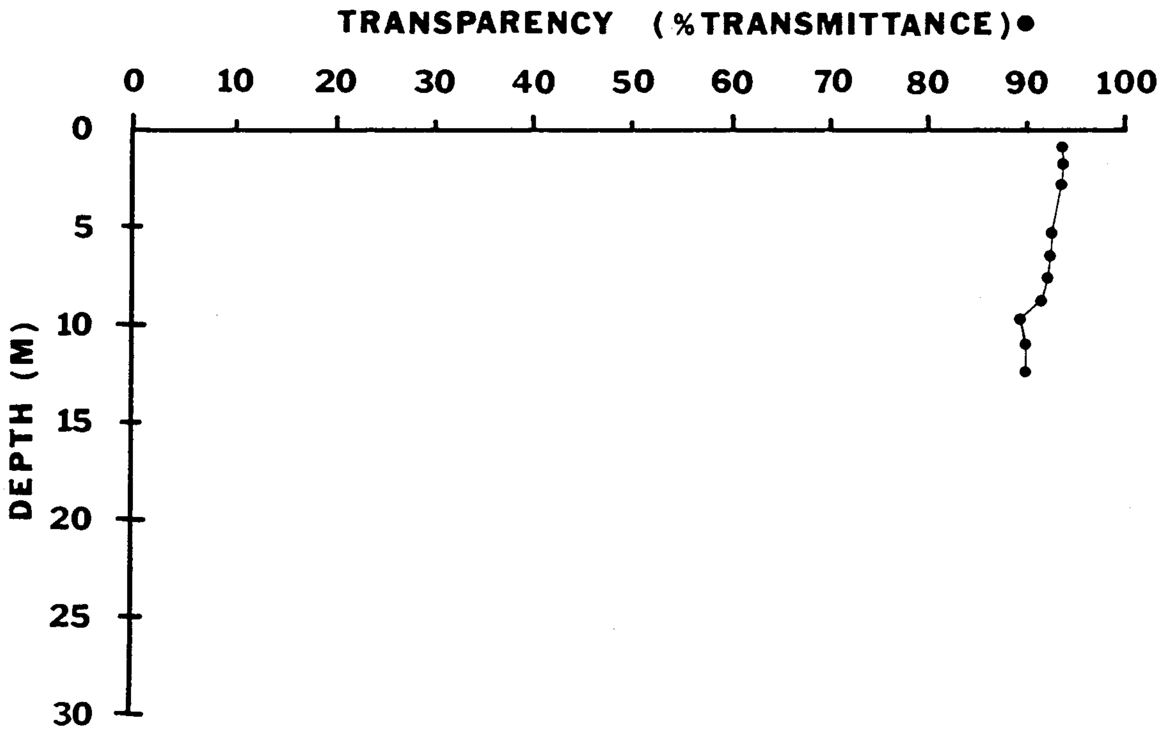

Figure C-33. Hydrographic Profiles for Station Icy Cape-31

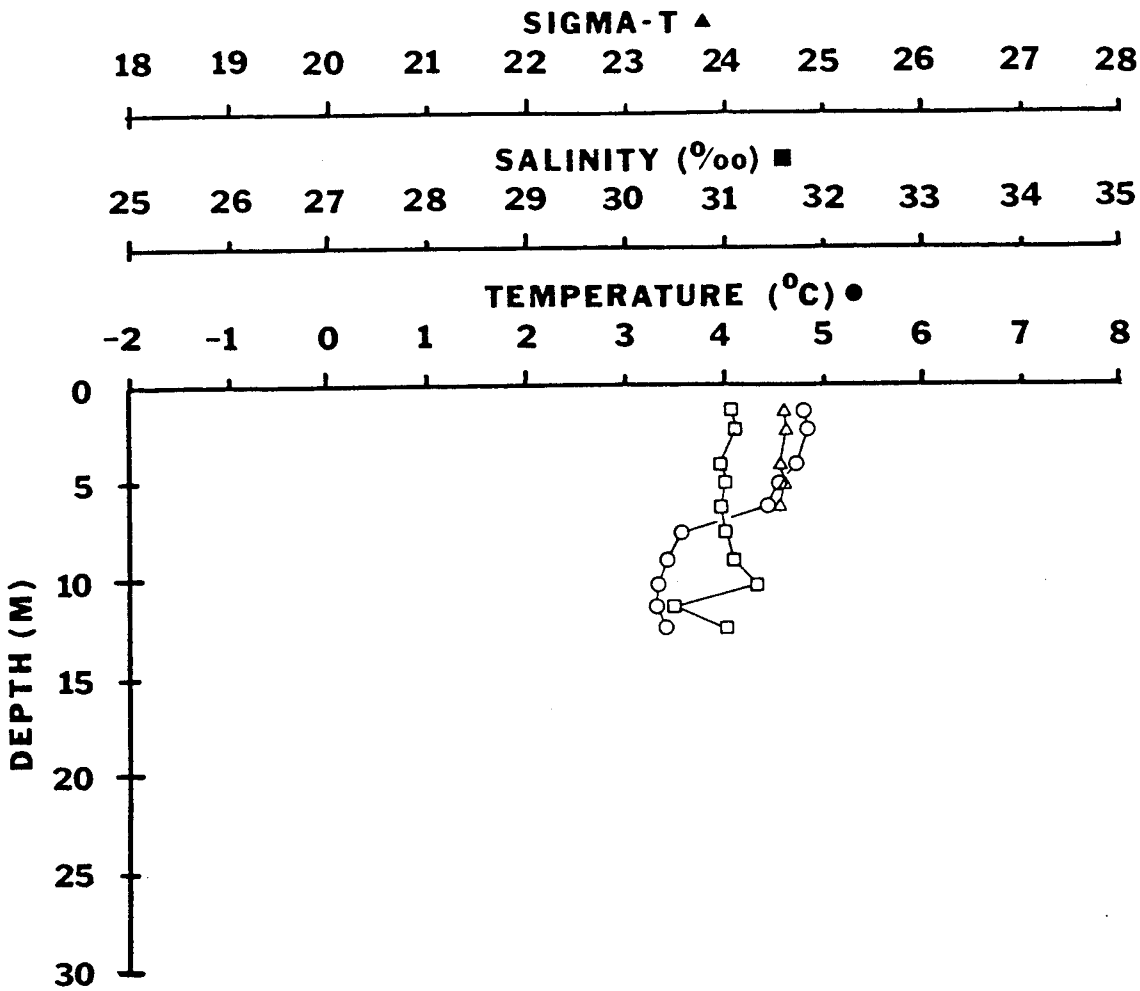

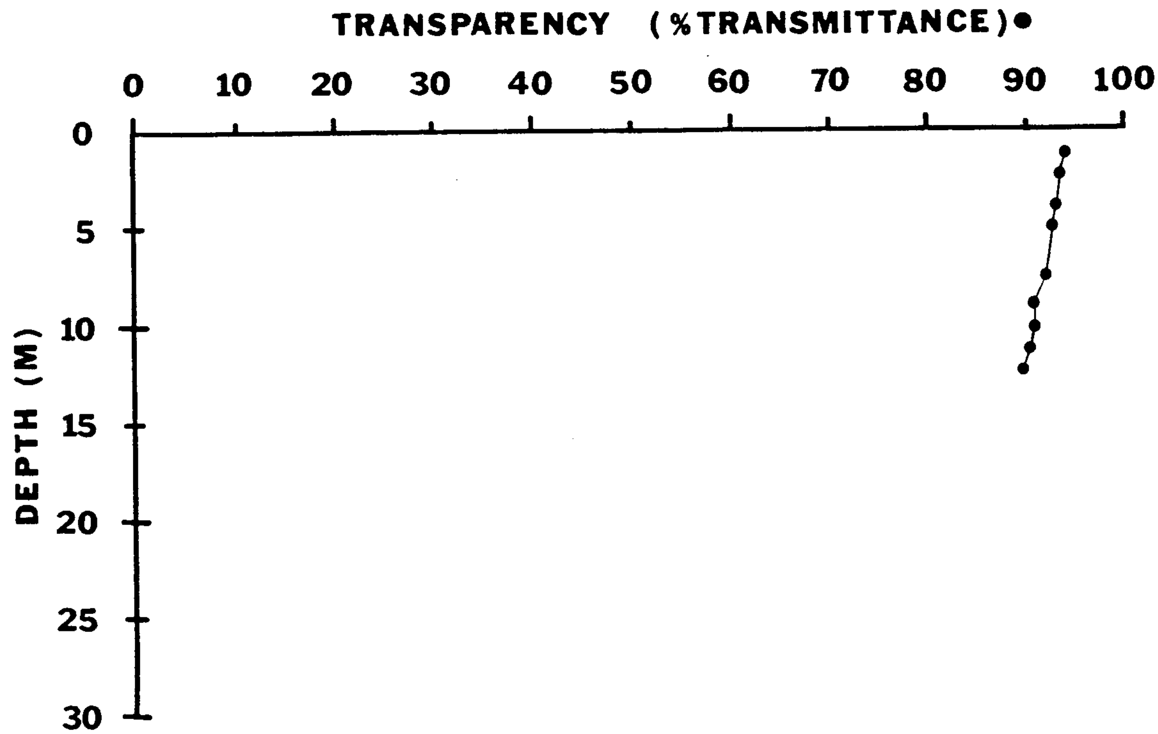

Figure C-34. Hydrographic Profiles for Station Icy Cape-32

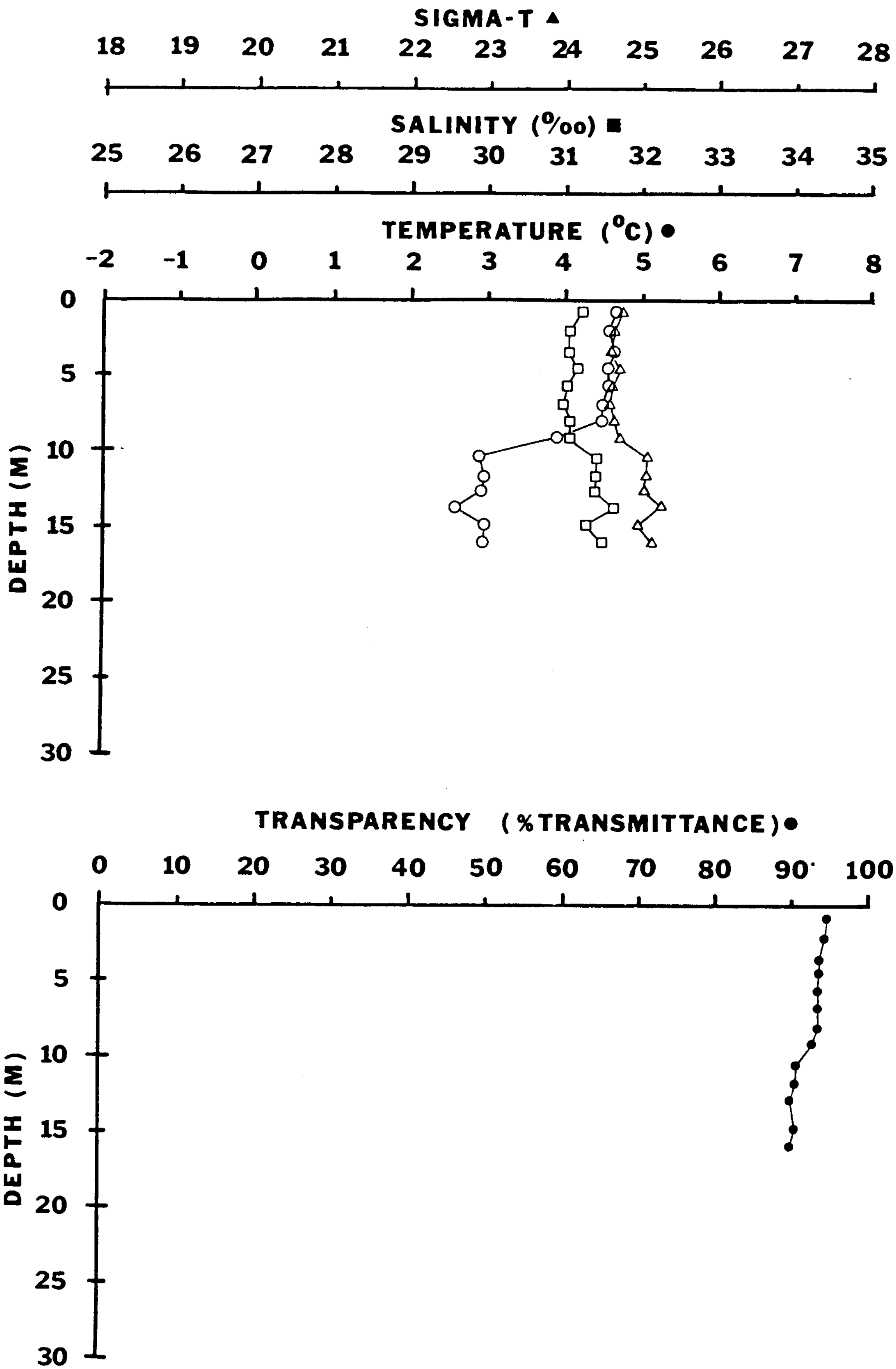

Figure C-35. Hydrographic Profiles for Station Icy Cape-33

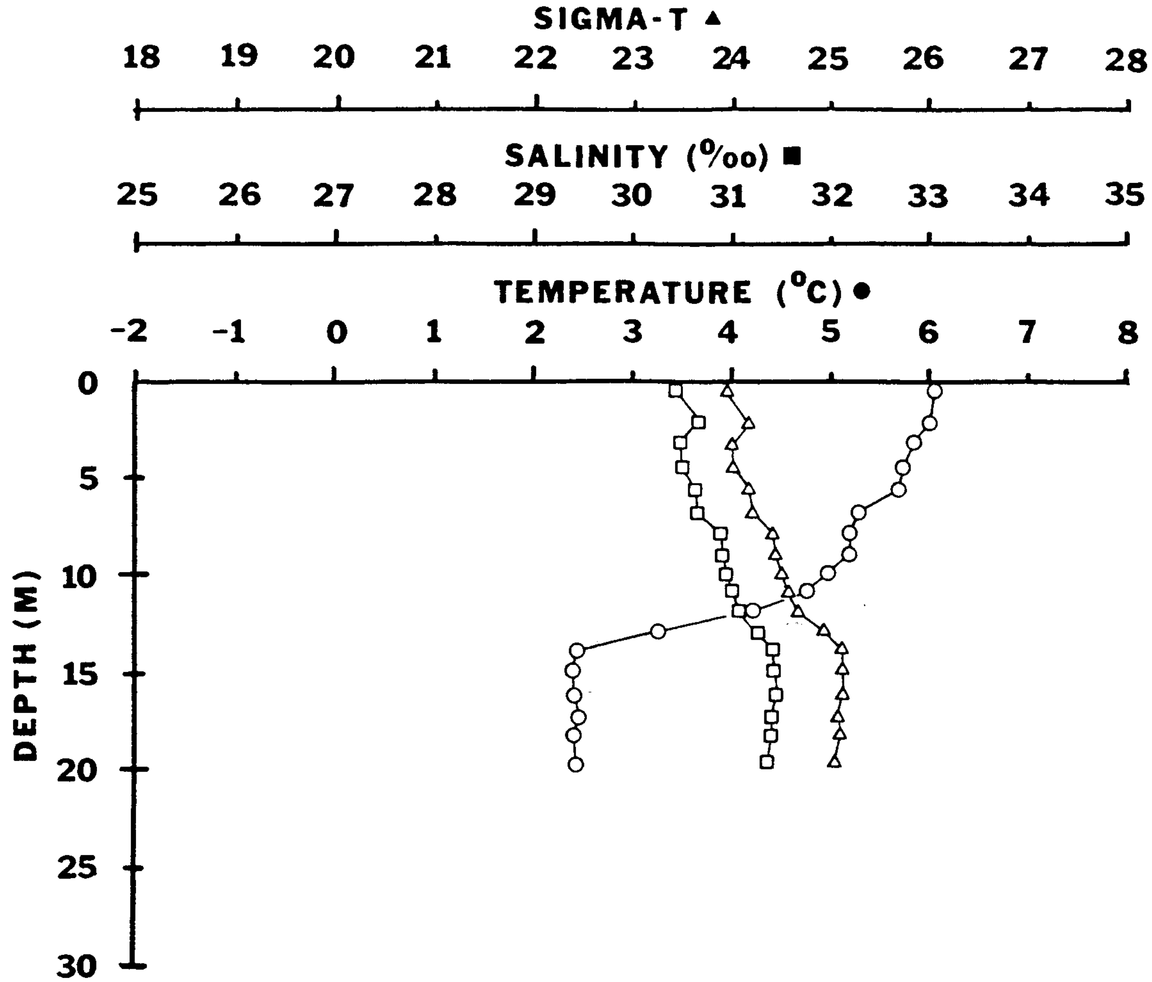

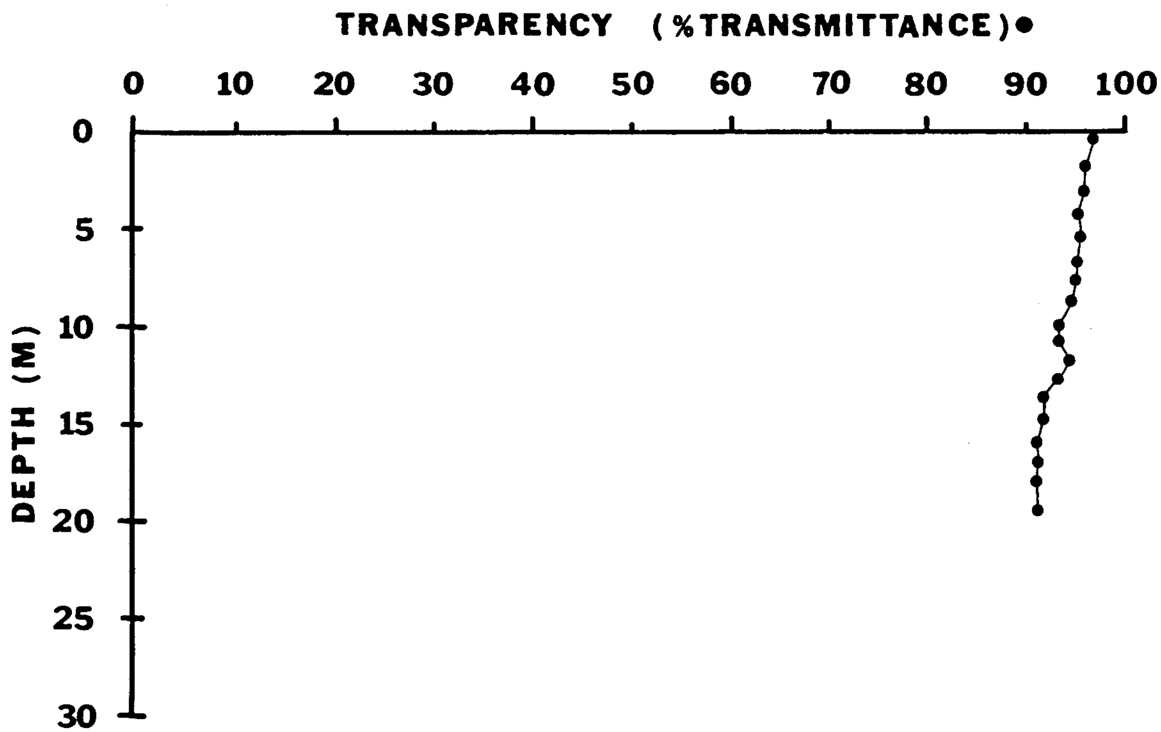

Figure C-36. Hydrographic Profiles for Station Icy Cape-34

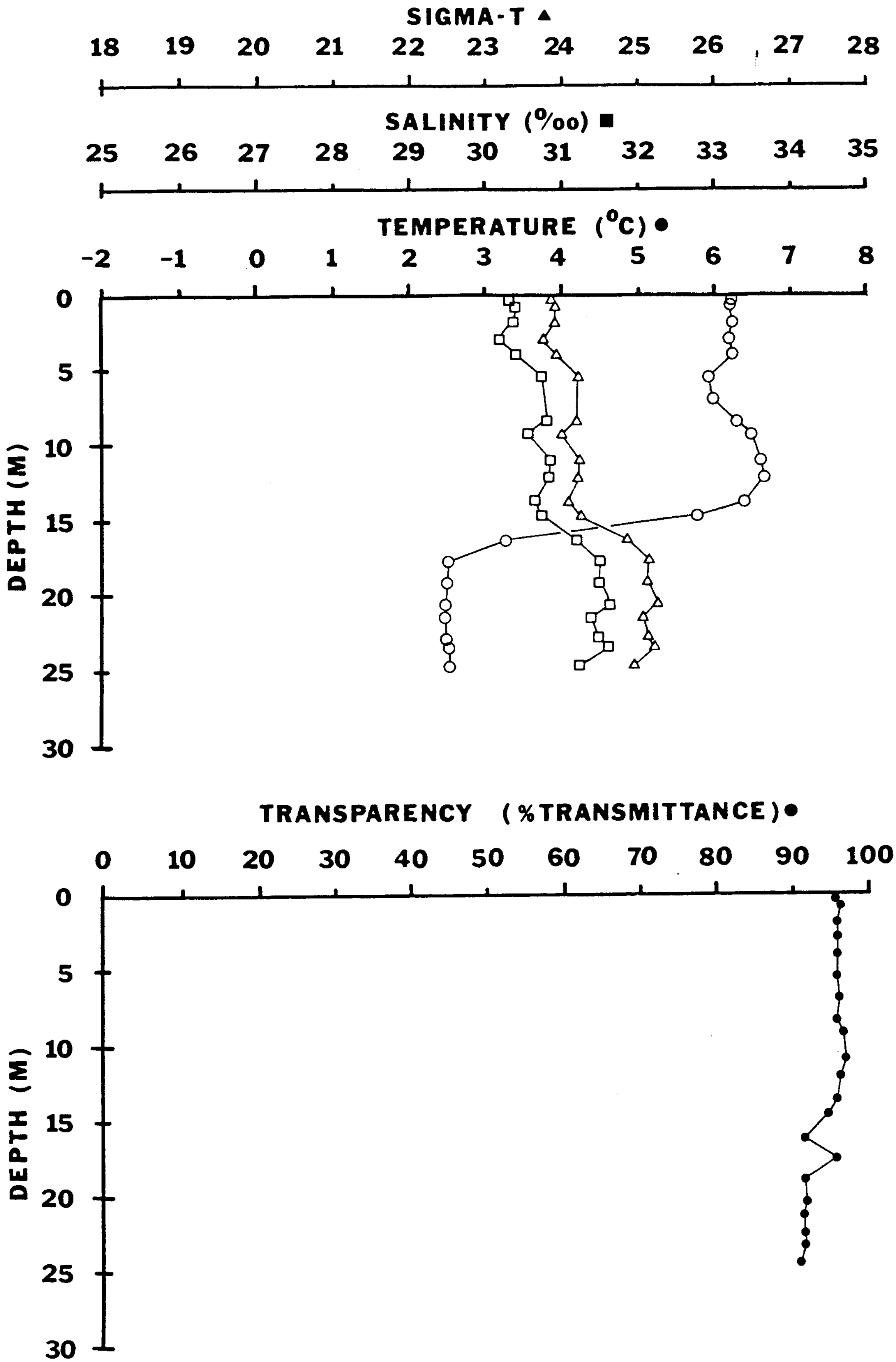

Figure C-37. Hydrographic Prophiles for Station Icy Cape-35

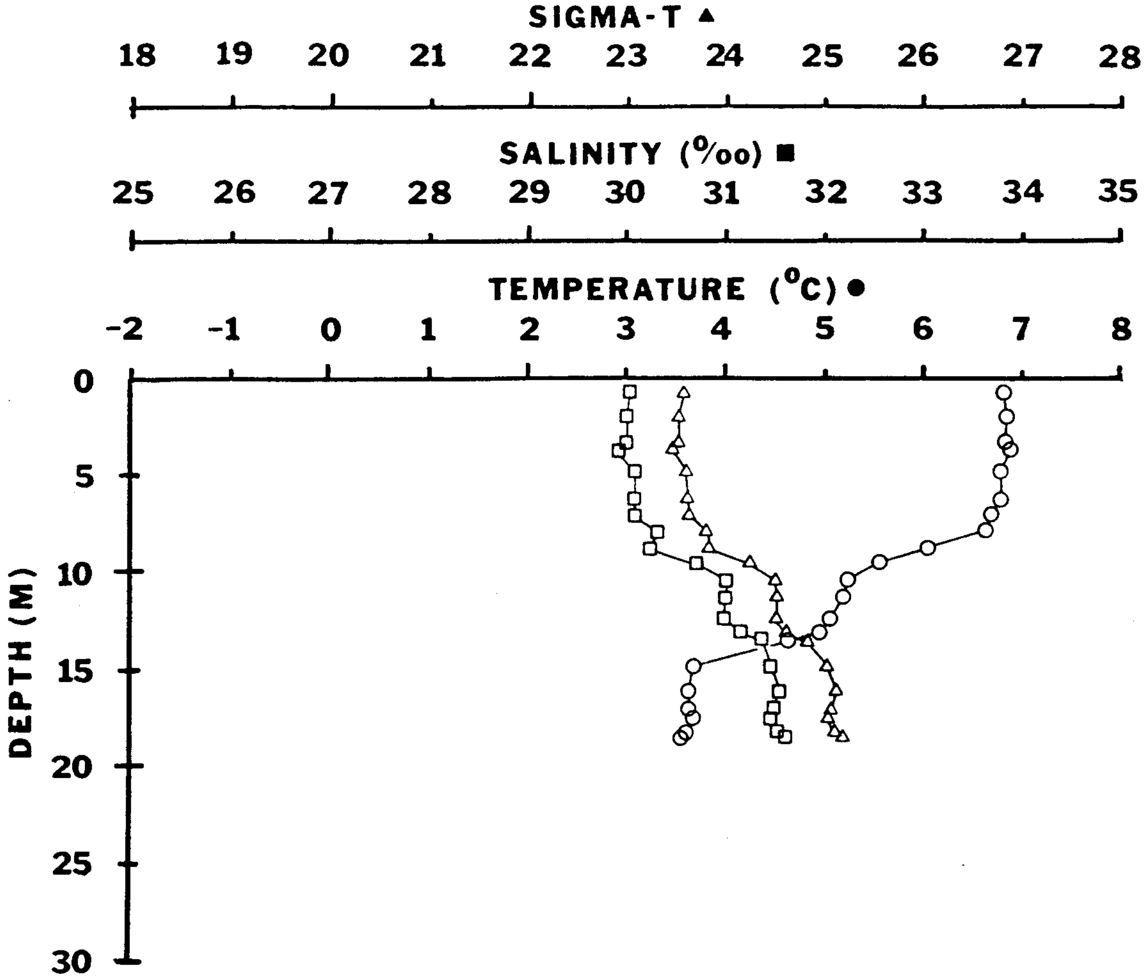

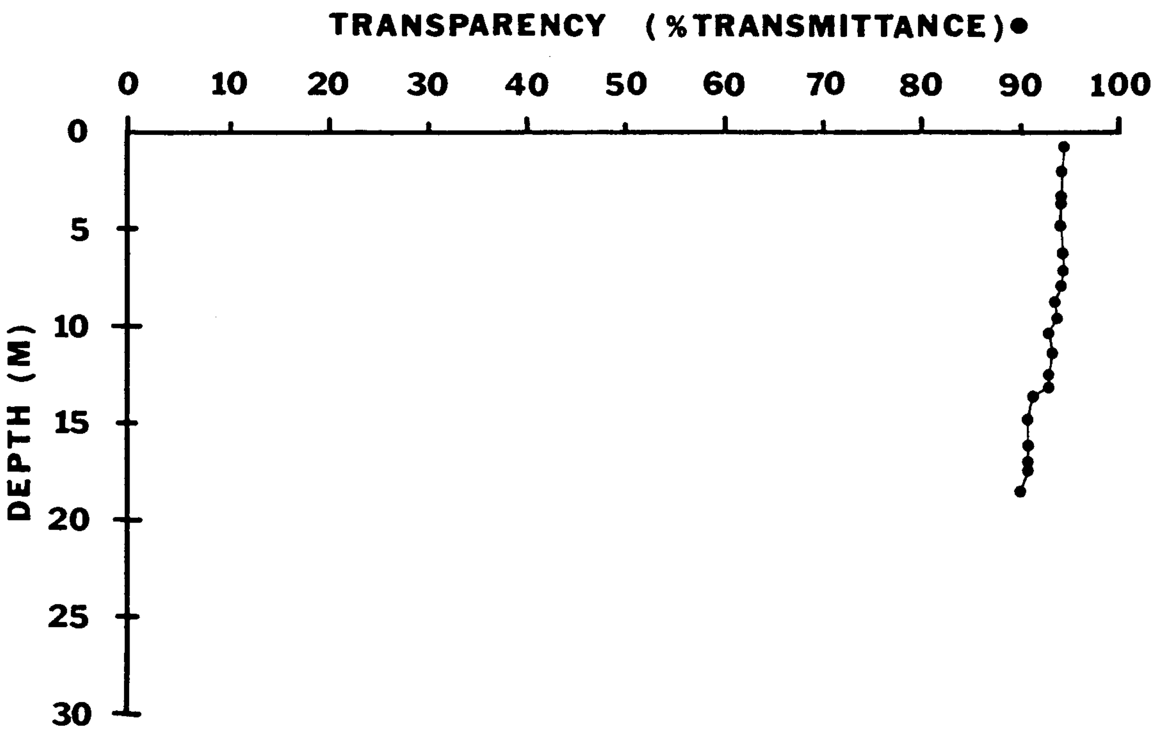

Figure C-38. Hydrographic Profiles for Station Akunik-25

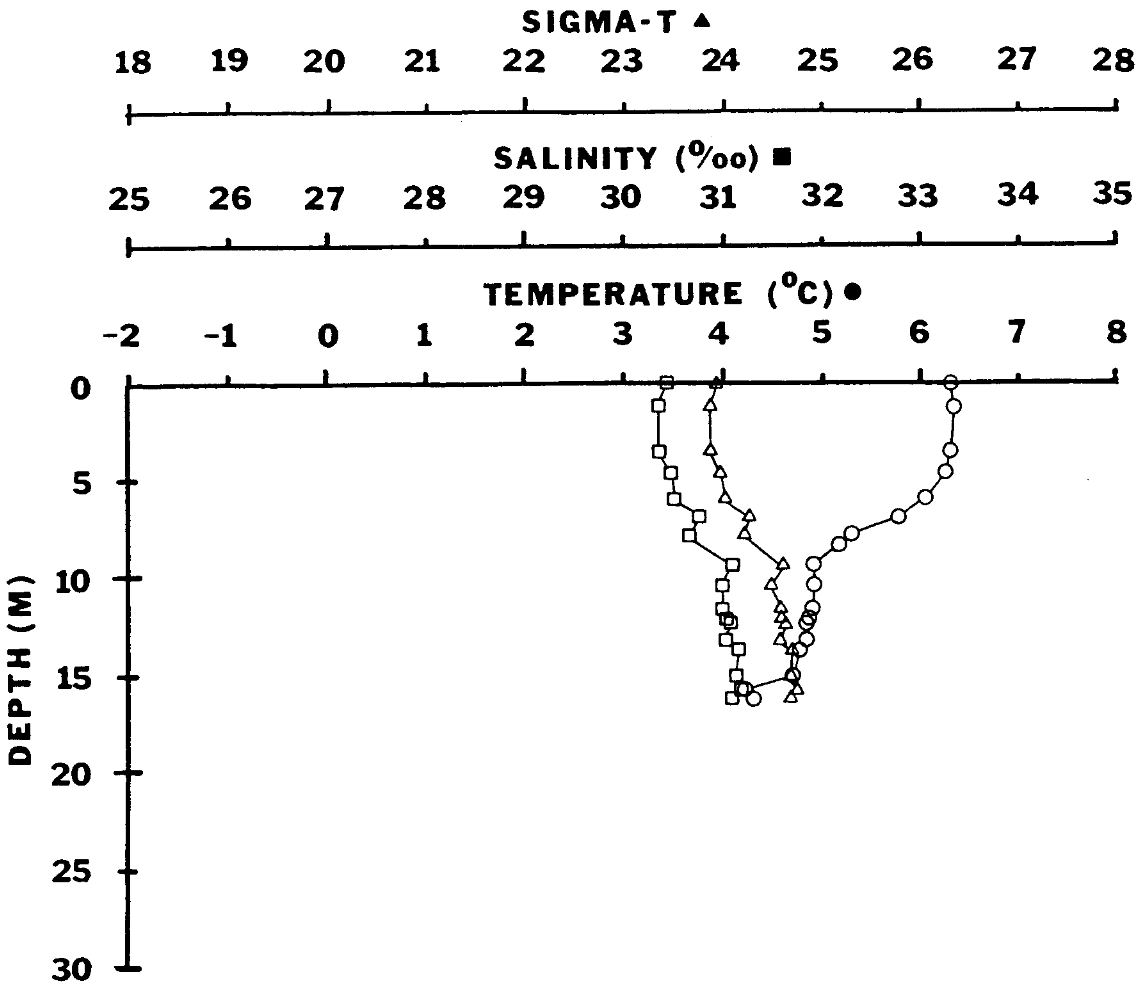

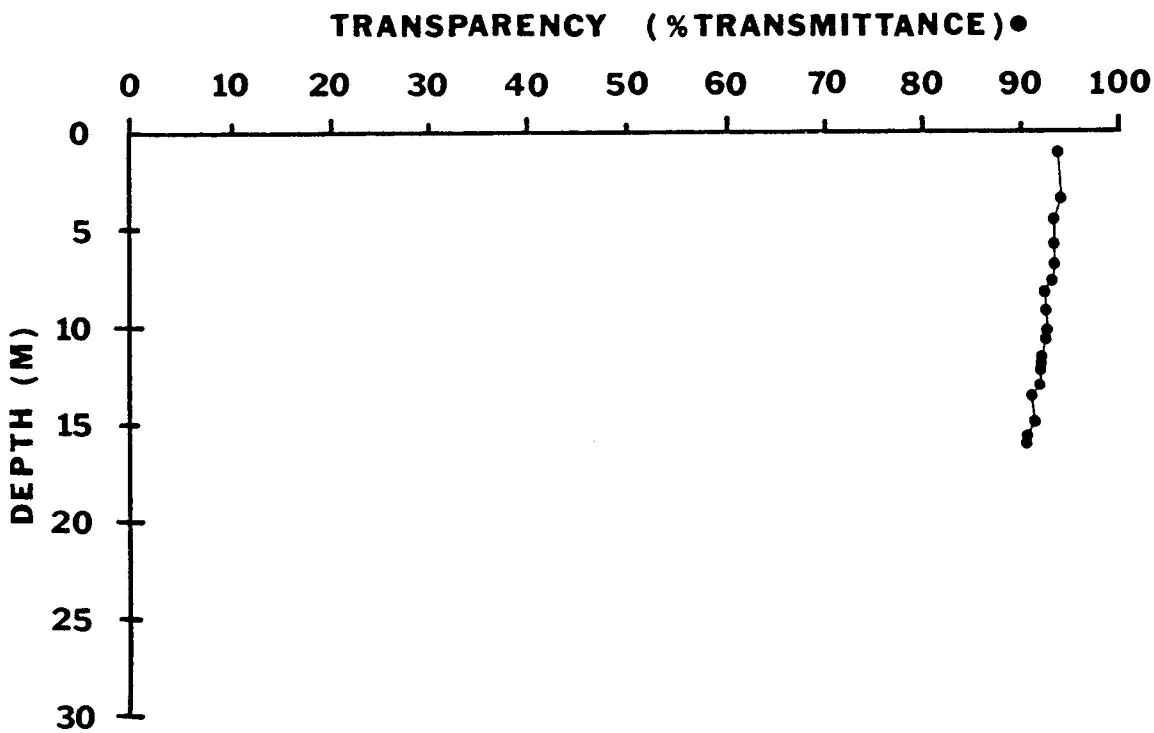

Figure C-39. Hydrografic Profiles for Station Akunik-26

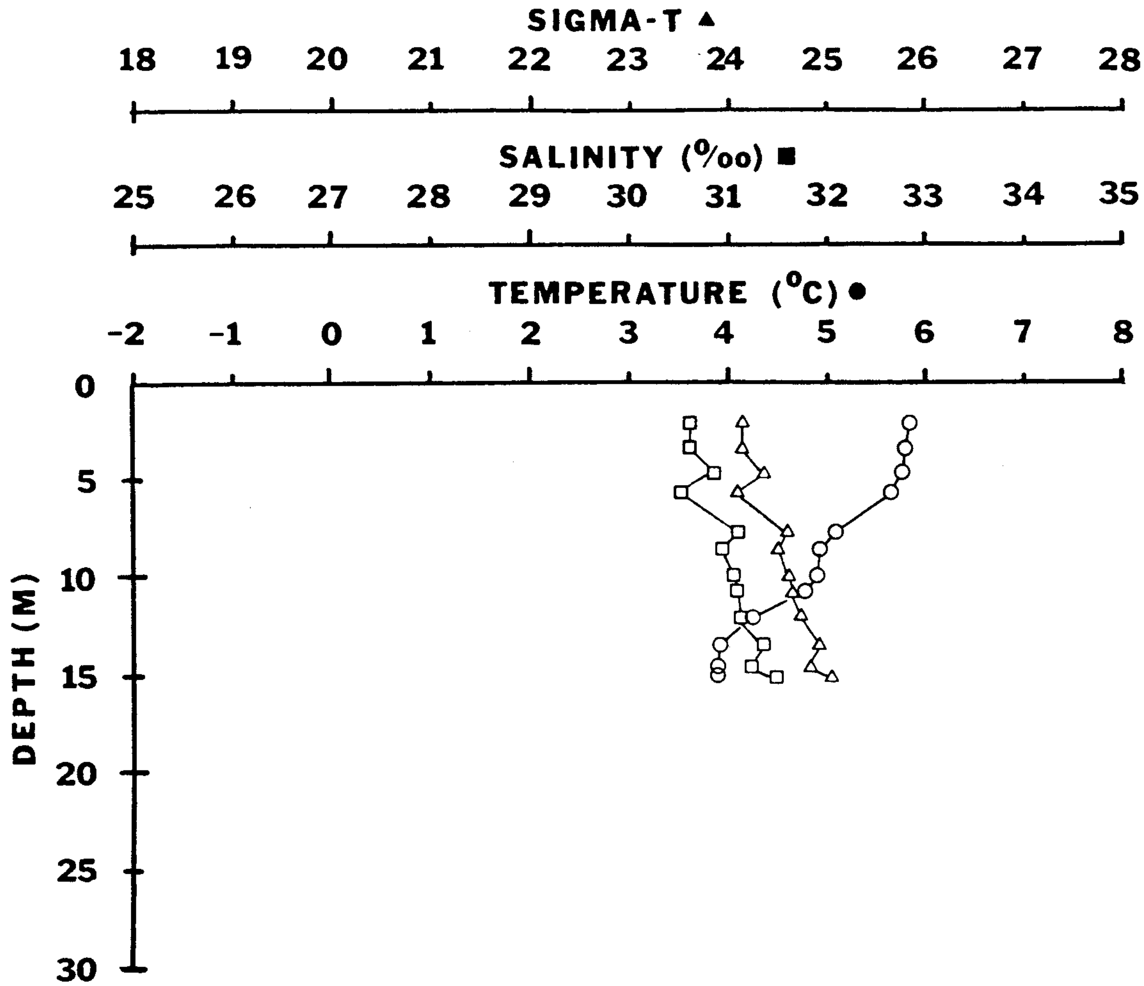

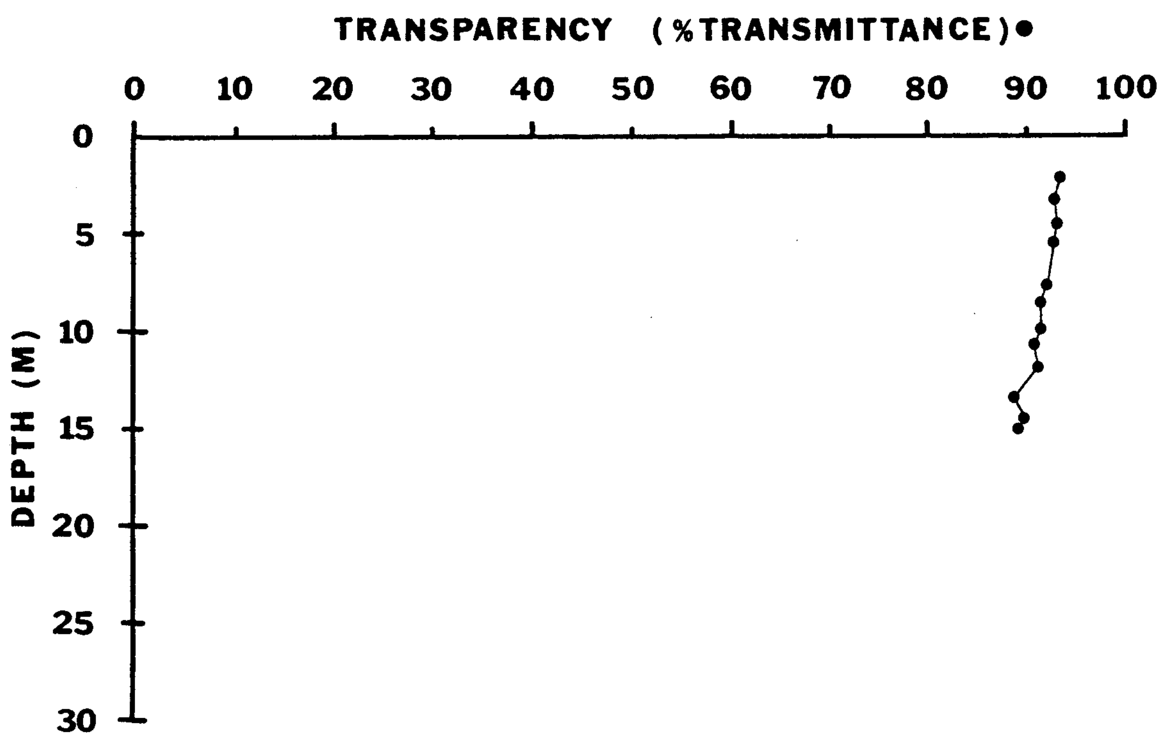

Figure C-40. Hydrographic Profiles for Station Akunik-27

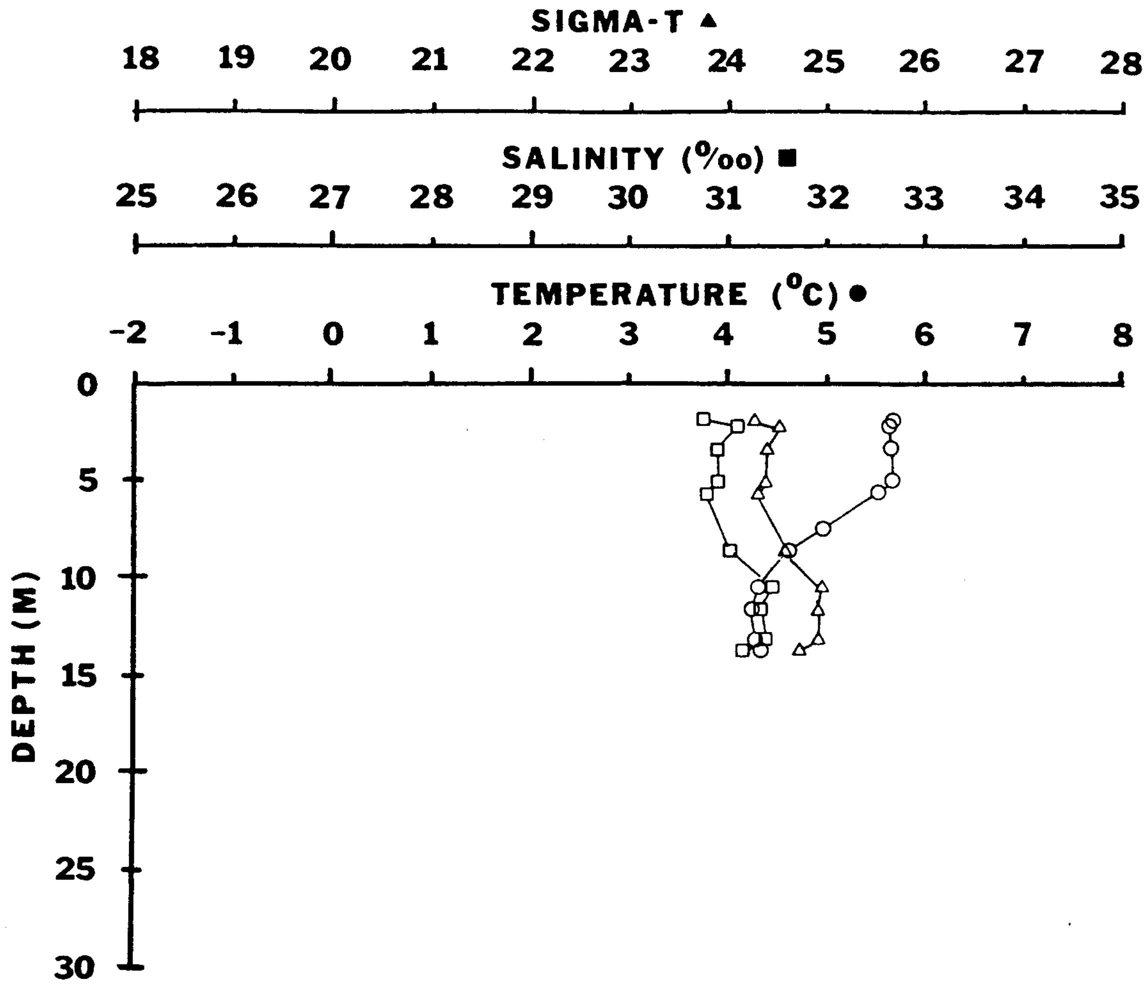

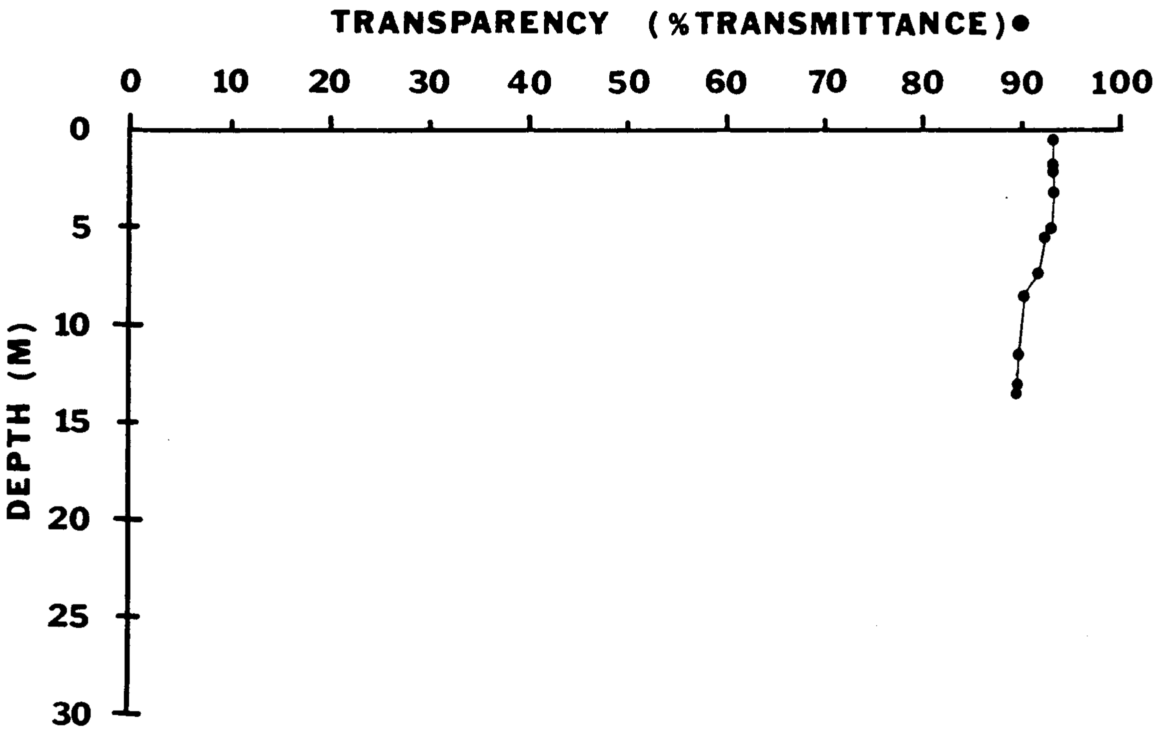

Figure C-41. Hydrographic Profiles for Station Akunik-28

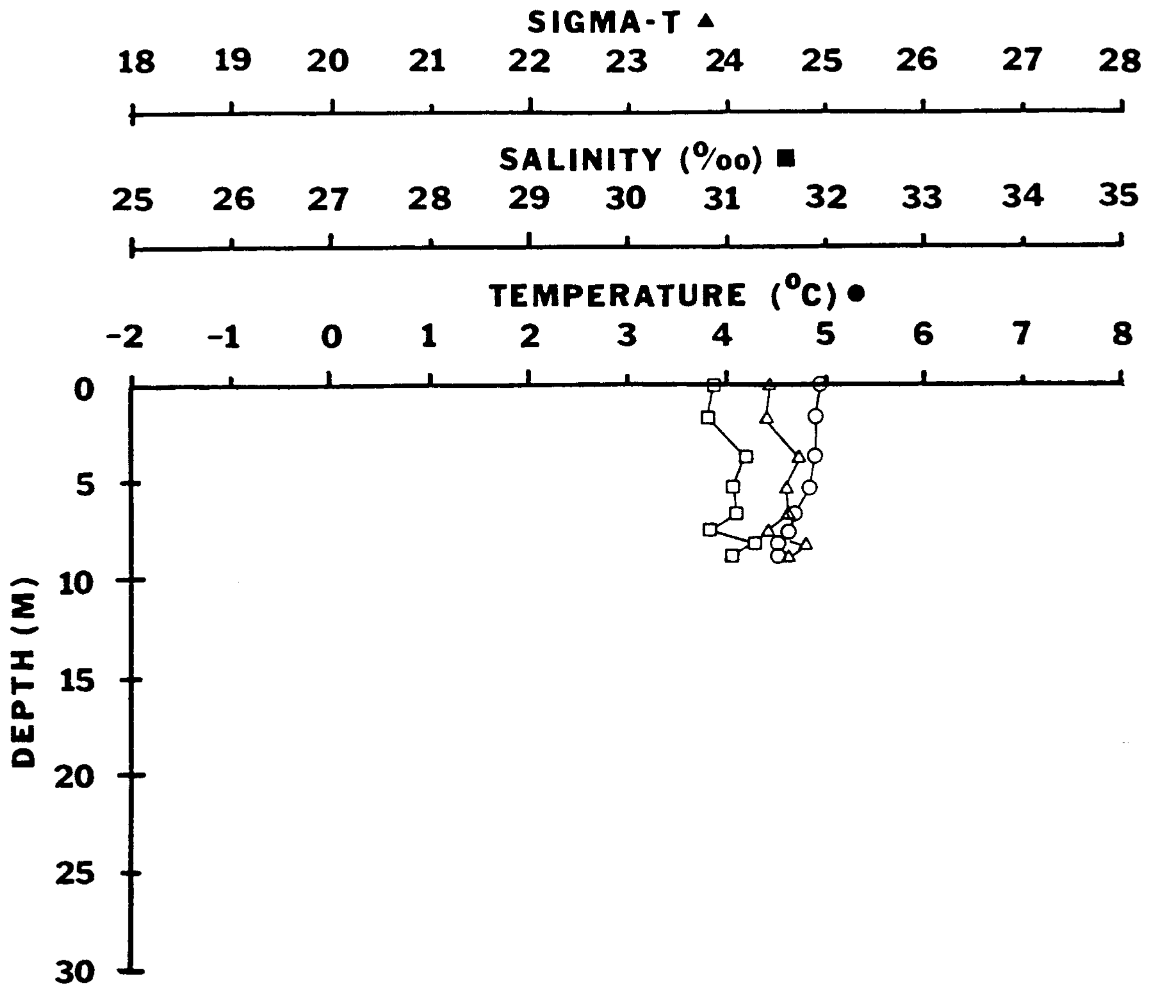

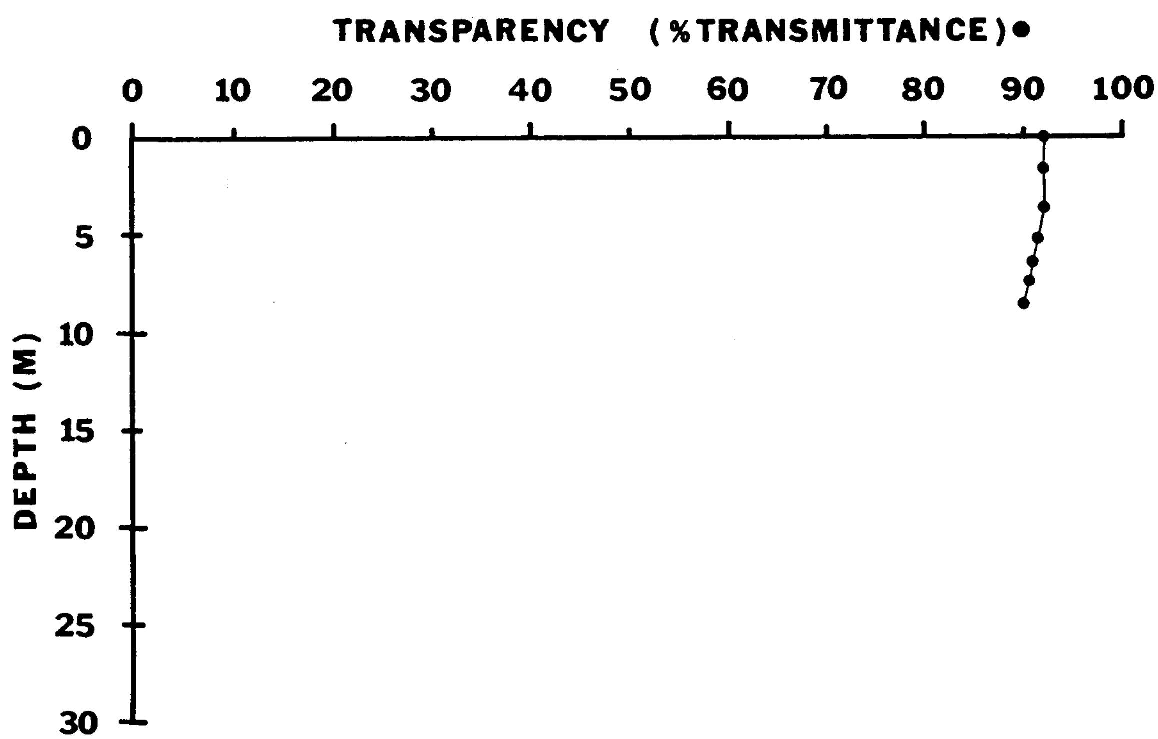

Figure C-42. Hydrographic Profiles for Station Akunik-29

Table: C-1
Study: NOAA 1981

Station: Barrow-1

Date: 7 Aug 81 Time: 1140 CAT Depth: 17m

Latitude: 71°19'27"N Longitude: 156°45'25"W

Depth (m)	Temperature (°C)	Salinity (°/oo)	Sigma-t	Transparency (%)
1.0	5.77	27.59	21.76	92.7
2.7	6.43	27.65	21.74	92.4
3.3	6.53	27.71	21.78	92.5
4.3	6.60	27.63	21.71	92.2
5.0	6.71	28.05	22.02	91.7
5.8	6.84	28.33	22.23	91.0
7.6	6.60	29.13	22.88	91.5
8.7	6.52	-	-	91.7
10.0	5.78	29.44	23.22	91.2
11.3	5.75	29.31	23.12	90.8
11.7	5.78	29.52	23.28	90.8
13.5	6.01	29.55	23.28	89.5
13.7	6.03	29.53	23.27	89.0
15.4	5.96	29.63	23.35	89.4
16.3	5.90	29.65	23.37	89.3
16.6	5.89	29.55	23.29	86.5
16.6	5.94	29.49	23.24	87.3
18.1	5.94	29.52	23.27	86.0

Table: C-2
Study: NOAA 1981

Station: Barrow-2

Date: 7 Aug 81 Time: 1445 CAT Depth: 76m

Latitude: 71°23'28"N Longitude: 156°50'54"W

Depth (m)	Temperature (°C)	Salinity ($^o/_{oo}$)	Sigma-t	Transparency (%)
0.1	2.80	26.55	21.20	96.5
0.2	2.54	22.81	18.24	96.4
0.2	2.65	25.17	20.11	96.9
0.8	2.89	26.50	21.15	96.3
1.8	3.26	27.03	21.55	96.0
2.6	3.33	27.37	21.82	95.7
3.8	3.48	27.27	21.72	95.8
5.3	3.22	27.59	22.00	95.7
7.0	1.87	28.65	22.93	95.2
8.9	1.11	30.25	24.26	95.1
10.7	1.45	31.18	24.98	92.6
12.2	1.99	31.33	25.07	92.2
14.1	1.91	31.43	25.14	92.6
15.5	1.79	31.27	25.03	92.2
17.3	1.69	31.48	25.20	92.3
18.8	1.59	31.31	25.07	92.1
20.6	1.53	31.55	25.27	92.4
22.3	1.57	31.26	25.04	92.6
24.3	1.53	31.63	25.33	92.0
24.3	1.55	31.37	25.13	93.1

Table: C-3
Study: NOAA 1981

Station: Barrow-3

Date: 7 Aug 81 Time: 1520 CAT Depth: 51m

Latitude: 71°22'35"N Longitude: 156°48'54"W

Depth (m)	Temperature (°C)	Salinity (°/oo)	Sigma-t	Transparency (%)
0.9	5.71	27.81	21.95	95.6
2.0	5.26	27.89	22.05	96.0
3.1	4.35	28.24	22.42	96.7
4.4	4.16	28.30	22.48	96.8
5.5	4.00	28.26	22.46	96.8
6.8	3.76	27.73	22.07	97.1
7.9	3.03	28.23	22.52	96.9
7.9	3.00	28.55	22.77	96.4
9.1	2.86	28.82	23.00	96.8
9.2	2.84	28.76	22.96	96.7
10.6	2.90	29.60	23.61	95.7
10.6	2.84	29.40	23.46	95.4
11.8	2.36	29.77	23.79	94.8
11.8	1.75	30.13	24.12	94.9
13.1	0.70	30.85	24.75	95.2
13.1	0.48	31.13	24.99	95.0
14.6	0.94	31.01	24.87	94.3
14.6	0.95	31.10	24.94	94.4
15.7	1.43	31.09	24.91	94.3
16.9	1.96	31.34	25.07	93.6
17.0	2.00	31.58	25.27	93.4
18.4	1.97	31.24	24.99	93.3
19.5	2.13	31.28	25.01	92.9
20.6	2.16	31.70	25.34	93.1
20.7	2.13	31.32	25.04	93.1
21.2	2.12	31.35	25.07	93.1
22.3	2.10	31.36	25.08	92.5
22.3	2.04	31.46	25.16	92.2
23.3	2.00	31.30	25.04	92.1
23.3	2.02	31.48	25.18	92.8
24.4	1.95	31.37	25.10	92.6
24.4	2.02	31.25	25.00	92.1

Table: C-4
Study: NOAA 1981

Station: Barrow-4

Date: 7 Aug 81 Time: 1540 CAT Depth: 55m

Latitude: 71°21'44"N Longitude: 156°47'37"W

Depth (m)	Temperature (°C)	Salinity (°/oo)	Sigma-t	Transparency (%)
0.3	6.76	28.27	22.19	94.8
1.7	6.71	27.81	21.84	93.6
3.0	6.58	28.53	22.41	93.5
4.8	6.56	28.58	22.45	93.6
6.5	6.57	28.72	22.56	93.2
8.3	5.72	-	-	94.0
9.5	5.72	29.89	23.58	91.2
10.9	5.79	29.78	23.49	91.7
12.6	5.91	30.12	23.74	92.7
14.3	5.84	29.67	23.39	-
15.6	5.65	29.89	23.59	90.2
16.9	4.16	30.62	24.32	92.6
18.4	2.78	30.43	24.29	92.5
21.6	2.21	31.68	25.33	93.1
23.1	2.21	31.47	25.16	92.6
24.2	2.17	31.55	25.23	92.5

Table: C-5
Study: NOAA 1981

Station: Barrow-5

Date: 7 Aug 81 Time: 1610 CAT Depth: 40m

Latitude: 71°20'47"N Longitude: 156°45'54"W

Depth (m)	Temperature (°C)	Salinity ($^{o}/_{oo}$)	Sigma-t	Transparency (%)
1.0	6.72	28.11	22.07	93.4
2.2	-	-	-	92.7
3.4	6.56	28.25	22.20	92.8
4.7	6.48	28.15	22.13	92.4
5.9	6.66	28.43	22.32	92.6
6.5	6.76	29.11	22.85	92.3
7.4	6.88	29.02	22.76	92.2
8.3	6.85	29.02	22.76	92.2
9.7	6.81	29.20	22.91	91.8
9.7	6.56	28.97	22.76	91.7
10.7	5.27	29.60	23.40	91.5
12.3	5.78	29.78	23.48	90.4
13.9	5.76	29.75	23.47	90.7
14.0	5.72	29.74	23.46	91.0
15.2	5.84	29.78	23.48	92.7
15.6	5.85	29.68	23.40	92.7
16.9	5.93	30.00	23.64	92.1
17.0	5.95	29.71	23.42	92.2
17.1	5.88	29.83	23.52	91.6
17.9	5.85	30.10	23.74	91.3
19.2	5.28	30.59	24.18	91.1
20.7	5.09	30.47	24.11	91.1
20.8	4.98	30.42	24.08	90.8
22.4	4.17	31.13	24.73	90.3
23.7	3.47	30.92	24.62	90.7

Table: C-6
Study: NOAA 1981

Station: Skull Cliffs-6

Date: 8 Aug 81 Time: 1400 CAT Depth: 9m

Latitude: 70°55'36"N Longitude: 157°39'36"W

Depth (m)	Temperature (°C)	Salinity (‰)	Sigma-t	Transparency (%)
0.7	5.34	29.27	23.13	-
1.7	5.35	29.40	23.24	87.9
1.8	5.35	29.48	23.30	87.9
1.9	5.34	29.27	23.13	87.8
2.1	5.34	29.45	23.27	88.0
-	5.34	29.30	23.16	87.3
3.3	5.37	29.22	23.09	87.8
4.1	5.30	29.29	23.15	87.4
4.7	5.27	29.24	23.12	87.0
5.6	5.21	29.41	23.26	87.0
6.2	5.14	29.57	23.39	86.4
6.9	5.06	29.38	23.25	-
7.6	5.02	29.58	23.41	86.0
8.3	5.07	29.40	23.27	85.5
9.1	5.00	29.55	23.39	85.6
9.2	4.98	29.41	23.29	85.4

Table: C-7
Study: NOAA 1981

Station: Skull Cliffs-7

Date: 8 Aug 81 Time: 1425 CAT Depth: 15m

Latitude: 70°56'23"N Longitude: 157°41'18"W

Depth (m)	Temperature (°C)	Salinity (°/oo)	Sigma-t	Transparency (%)
0.3	6.33	29.13	22.91	91.2
1.4	6.28	29.19	22.96	91.2
2.2	6.29	29.22	22.99	91.1
2.8	6.31	29.17	22.95	91.0
3.7	6.30	29.16	22.94	91.1
4.5	6.31	29.15	22.93	91.0
4.7	6.24	29.15	22.94	91.2
5.6	6.29	29.03	22.84	91.3
5.9	6.30	29.22	22.99	91.3
6.9	6.27	29.27	23.03	90.8
7.7	6.04	29.13	22.95	90.6
8.3	5.39	29.39	23.22	89.1
8.5	5.22	29.35	23.21	88.5
8.6	4.97	29.39	23.27	87.3
9.3	4.73	29.54	23.41	86.5
9.8	4.76	29.59	23.44	86.0
10.8	4.73	29.54	23.41	85.5
11.5	4.61	29.63	23.49	85.4
12.1	4.71	29.40	23.30	-
12.4	4.74	29.41	23.31	85.5
12.6	4.69	29.53	23.41	84.7
13.6	4.70	29.55	23.42	83.8
14.2	4.66	29.61	23.47	83.9
14.5	4.71	29.44	23.33	83.8
15.4	4.66	29.48	23.37	83.5

Table: C-8

Study: NOAA 1981

Station: Skull Cliffs-8

Date: 8 Aug 81 Time: 1445 CAT Depth: 18m

Latitude: 70°57'09"N Longitude: 157°43'06"W

Depth (m)	Temperature (°C)	Salinity (°/oo)	Sigma-t	Transparency (%)
0.2	6.12	29.00	22.84	93.5
1.3	6.10	29.05	22.88	93.6
2.8	6.16	28.91	22.76	93.3
3.5	6.17	28.94	22.78	93.6
4.5	6.16	29.01	22.84	93.3
4.5	6.05	29.14	22.95	93.4
5.6	6.03	29.06	22.89	93.4
6.5	6.14	29.00	22.83	93.2
7.6	5.89	28.83	22.72	93.1
8.7	5.39	29.04	22.95	93.0
9.6	-	-	-	93.5
10.4	4.21	29.04	23.06	93.6
11.3	4.20	28.95	23.00	92.2
11.4	4.18	28.94	22.99	92.1
11.9	4.52	29.48	23.38	88.9
13.0	4.55	29.60	23.48	88.7
13.6	4.56	29.51	23.40	87.7
14.5	4.56	29.72	23.57	87.4
15.4	4.53	29.69	23.55	87.6
16.5	4.57	29.66	23.52	87.2
17.0	4.56	29.57	23.45	87.2
17.6	4.54	29.69	23.55	87.0

Table: C-9

Study: NOAA 1981

Station: Skull Cliffs-9

Date: 8 Aug 81 Time: 1505 CAT Depth: 20m

Latitude: 70°58'00"N Longitude: 157°44'53"W

Depth (m)	Temperature (°C)	Salinity ($^o/_{oo}$)	Sigma-t	Transparency (%)
1.0	5.41	28.49	22.51	94.2
1.8	5.41	28.40	22.44	94.0
2.3	5.42	28.65	22.64	93.3
3.0	5.38	28.45	22.48	93.9
3.9	5.38	28.49	22.52	94.1
4.5	5.19	28.57	22.60	93.6
5.4	4.94	28.56	22.62	94.5
6.7	4.99	28.36	22.45	93.6
7.8	4.67	28.56	22.64	93.7
8.5	4.81	28.86	22.86	93.0
9.2	4.78	28.83	22.84	91.5
10.1	4.78	29.05	23.02	91.9
10.8	4.81	29.17	23.11	92.9
11.7	4.82	29.18	23.12	93.1
12.5	4.81	29.14	23.09	93.1
13.0	4.84	29.25	23.17	93.3
13.9	4.74	29.36	23.27	92.7
14.1	4.78	29.25	23.17	93.1
14.7	4.72	29.15	23.10	92.2
15.4	4.66	29.54	23.42	-
16.0	4.57	29.53	23.42	89.3
16.9	4.43	29.73	23.59	87.3
17.6	4.03	30.11	23.93	82.7
18.4	3.98	30.25	24.04	80.7
19.5	3.98	30.17	23.98	81.1
20.5	3.98	30.18	23.99	81.0

Table: C-10
Study: NOAA 1981

Station: Skull Cliffs-10

Date: 8 Aug 81 Time: 1525 CAT Depth: 20m

Latitude: 70°58'46"N Longitude: 157°46'44"W

Depth (m)	Temperature (°C)	Salinity ($^o/_{oo}$)	Sigma-t	Transparency (%)
0.3	5.44	28.27	22.34	94.6
1.3	5.46	28.51	22.52	94.5
2.3	5.48	28.40	22.43	94.6
3.3	5.45	28.33	22.38	94.9
3.8	5.45	28.39	22.43	94.3
4.9	5.38	28.30	22.37	94.2
5.9	5.26	28.47	22.51	94.2
6.8	5.00	28.43	22.51	94.7
7.6	4.50	29.23	23.19	94.1
8.8	4.67	28.98	22.97	92.8
9.8	4.76	29.07	23.04	93.3
10.4	4.79	28.99	22.97	93.5
11.5	4.78	29.36	23.26	93.2
12.6	4.79	29.08	23.04	93.6
13.5	4.74	28.95	22.94	93.2
14.3	4.52	28.93	22.95	92.0
15.2	4.72	29.04	23.01	93.1
15.9	4.69	29.09	23.06	92.9
17.4	4.55	29.26	23.20	91.8
17.8	3.82	30.06	23.90	85.0
18.7	3.54	30.47	24.26	82.7
19.1	3.51	30.57	24.34	81.9
20.2	3.51	30.47	24.26	82.2

Table: C-11
Study: NOAA 1981

Station: Skull Cliffs-11

Date: 8 Aug 81 Time: 1600 CAT Depth: 23m

Latitude: 71°00'26"N Longitude: 157°50'12"W

Depth (m)	Temperature (°C)	Salinity ($^{o}/_{oo}$)	Sigma-t	Transparency (%)
0.8	3.94	28.52	22.68	95.6
1.8	3.98	28.53	22.68	95.0
3.1	-	-	-	95.2
4.0	3.98	28.45	22.62	95.4
4.7	3.98	28.03	22.29	95.1
5.8	4.02	28.44	22.61	95.3
6.5	3.96	28.35	22.54	94.4
7.2	3.97	28.25	22.46	95.2
8.4	4.05	27.82	22.12	94.9
8.9	4.23	28.18	22.38	95.0
10.0	4.08	28.74	22.83	96.2
11.0	4.00	28.82	22.91	96.2
12.0	4.08	29.00	23.05	96.3
12.8	4.10	29.11	23.13	96.4
13.7	4.34	29.66	23.55	95.2
14.4	3.88	29.74	23.65	95.5
15.3	3.59	30.26	24.08	94.9
16.1	3.36	30.19	24.05	94.4
16.9	3.35	30.43	24.24	94.1
17.8	2.71	31.05	24.78	93.8
18.8	2.81	30.73	24.52	91.2
19.4	2.32	31.05	24.81	82.5
19.5	2.40	31.09	24.84	86.8
21.4	2.20	30.98	24.77	80.5
22.9	2.27	31.25	24.98	78.5
22.9	2.26	31.25	24.98	77.0

Table: C-12
Study: NOAA 1981

Station: Skull Cliffs-12

Date: 8 Aug 81 Time: 1620 CAT Depth: 29m

Latitude: 71°01'58"N Longitude: 157°53'55"W

Depth (m)	Temperature (°C)	Salinity (°/oo)	Sigma-t	Transparency (%)
0.1	4.29	28.15	22.35	95.4
1.2	4.28	28.34	22.51	95.5
2.2	4.30	28.27	22.44	95.4
3.1	4.31	28.17	22.36	95.2
3.2	4.33	28.20	22.39	95.4
4.9	4.36	28.38	22.53	95.3
5.7	4.34	28.41	22.55	95.3
6.5	4.32	28.41	22.56	95.2
7.5	4.31	28.41	22.56	95.1
8.0	4.00	28.98	23.04	96.0
9.2	3.89	29.03	23.09	95.8
10.2	4.03	29.30	23.29	96.1
11.3	4.06	29.99	23.83	95.4
12.3	4.17	30.47	24.20	95.0
13.3	4.26	30.00	23.82	94.8
14.1	4.04	30.10	23.92	94.4
15.1	4.06	30.47	24.21	94.5
16.1	4.02	30.50	24.24	94.5
16.7	4.03	29.61	23.53	94.4
17.8	4.08	-	-	94.5
19.0	3.97	-	-	94.1
20.3	3.84	30.52	24.27	92.7
-	3.78	31.01	24.67	92.9
22.4	3.61	30.85	24.56	93.1
23.4	3.06	30.70	24.48	93.4
24.1	2.70	31.25	24.95	91.2

Table: C-13
Study: NOAA 1981

Station: Pt. Belcher-13

Date: 10 Aug 81 Time: 1330 CAT Depth: 20m

Latitude: 71°49'10"N Longitude: 159°38'00"W

Depth (m)	Temperature (°C)	Salinity ($^o/_{oo}$)	Sigma-t	Transparency (%)
0.8	4.33	29.74	23.61	92.9
1.5	4.23	29.76	23.63	92.7
2.5	3.50	30.16	24.02	94.2
3.2	2.60	30.70	24.52	94.2
4.4	2.03	31.28	25.02	95.0
5.0	1.87	31.19	24.96	95.2
5.8	1.58	31.34	25.10	95.5
5.9	1.68	31.20	24.98	95.1
6.8	0.83	31.54	25.30	96.0
7.6	0.55	31.64	25.40	96.1
8.9	0.03	31.76	25.52	95.5
9.0	0.00	31.70	25.47	95.5
9.8	-0.43	32.10	25.81	95.0
10.4	-0.61	32.19	25.89	94.6
10.4	-0.57	32.24	25.93	95.0
10.9	-0.67	32.14	25.85	94.8
11.8	-0.68	32.19	25.89	94.6
12.0	-0.74	32.18	25.88	94.8
12.3	-0.76	32.25	25.94	94.9
12.4	-0.77	32.25	25.94	94.1
12.7	-0.81	32.30	25.99	94.4
12.8	-0.88	32.39	26.06	93.7
12.9	-0.79	32.32	26.00	94.4
13.5	-1.23	32.60	26.24	92.3
14.3	-1.27	32.68	26.31	92.3
14.7	-1.25	32.59	26.23	91.9
14.8	-1.29	32.73	26.35	92.2

Table::C-14

Study: NOAA 1981

Station: Pt. Belcher-14

Date: 10 Aug 81 Time: 1410 CAT Depth: 30m

Latitude: 70°50'00"N Longitude: 159°39'20"W

Depth (m)	Temperature (°C)	Salinity (°/oo)	Sigma-t	Transparency (%)
1.2	5.71	28.72	22.66	94.1
2.0	5.68	28.77	22.71	94.1
2.6	5.67	28.80	22.73	94.1
3.6	5.61	28.79	22.72	93.9
4.4	5.32	29.08	22.99	94.4
4.9	4.84	29.77	23.58	93.6
5.9	4.40	29.93	23.75	91.7
6.5	3.17	30.39	24.22	93.2
6.5	3.00	30.27	24.14	93.9
7.3	2.22	30.87	24.68	94.9
7.4	2.30	30.84	24.65	95.0
8.1	1.70	31.15	24.94	94.9
8.9	0.77	31.71	25.45	96.3
9.5	0.69	31.80	25.52	96.2
9.6	0.67	31.55	25.32	96.1
10.4	0.29	31.64	25.41	95.8
11.0	0.12	31.84	25.58	95.1
11.7	-0.18	31.84	25.59	94.8
11.8	-0.17	32.07	25.77	94.7
11.9	-0.21	32.13	25.83	94.6
12.2	-0.52	32.04	25.76	94.0
13.3	-0.79	32.35	26.03	93.8
13.8	-0.98	32.54	26.19	-
14.4	-1.09	32.40	26.08	93.3
15.6	-1.22	32.53	26.18	93.2
15.6	-1.30	32.43	25.98	93.0
16.6	-1.35	32.53	26.19	92.4
16.8	-1.34	32.67	26.30	92.3
17.1	-1.35	32.58	26.23	92.4
17.6	-1.37	32.73	26.35	92.1
18.1	-1.33	32.68	26.31	91.7
18.4	-1.37	32.63	26.27	91.4
19.4	-1.34	32.48	26.15	91.2
19.8	-1.35	32.52	26.18	90.8
20.7	-1.38	32.55	26.21	90.3
20.9	-1.36	32.53	26.19	90.1

Table: C-15
Study: NOAA 1981

Station: Pt. Belcher-15

Date: 10 Aug 81 Time: 1432 CAT Depth: 32m

Latitude: 70°50'55"N Longitude: 159°40'15"W

Depth (m)	Temperature (°C)	Salinity (°/oo)	Sigma-t	Transparency (%)
0.4	5.61	28.57	22.56	93.2
1.3	5.63	28.65	22.61	93.3
2.7	5.62	28.51	22.51	93.3
3.7	5.59	28.60	22.58	93.4
4.4	5.70	28.80	22.72	94.2
5.5	5.73	28.76	22.69	95.4
6.5	5.97	28.78	22.68	96.0
7.3	5.87	28.72	22.64	96.0
7.4	5.73	28.82	22.74	96.2
8.2	4.50	29.81	23.64	92.5
9.4	4.21	30.08	23.89	91.3
9.4	4.23	30.03	23.85	92.2
9.9	4.08	30.05	23.88	91.4
10.1	4.10	30.11	23.92	90.8
10.5	3.99	30.09	23.91	91.2
11.0	3.11	30.60	24.40	90.6
11.3	2.99	30.58	24.39	91.6
11.8	0.44	31.97	25.66	94.4
11.8	0.74	31.67	25.41	94.5
12.2	0.56	31.62	25.38	-
12.3	-0.07	32.00	25.72	94.5
12.6	0.22	31.66	25.43	94.9
12.6	0.00	32.01	25.72	94.5
13.2	-0.72	32.29	25.97	94.5
13.2	-0.82	32.38	26.05	94.5
13.4	-0.77	32.38	26.05	94.8
14.2	-1.39	32.47	26.14	94.1
14.3	-1.39	32.58	26.23	94.6
15.3	-1.40	32.71	26.34	95.4
15.4	-1.38	32.61	26.25	94.2
16.5	-1.41	32.49	26.16	94.3
17.2	-1.45	32.85	26.45	93.2
18.2	-1.42	32.80	26.41	93.5
18.9	-1.42	32.63	26.27	93.3
19.3	-1.45	32.59	26.24	92.6
19.8	-1.39	32.52	26.18	92.9
20.2	-1.42	32.64	26.28	92.3
20.9	-1.39	32.47	26.14	92.3
21.4	-1.44	32.45	26.13	91.8
22.0	-1.41	32.64	26.28	90.8
22.2	-1.39	32.62	26.26	91.8
22.2	-1.40	32.80	26.40	90.8

Table: C-16
Study: NOAA 1981

Station: Pt. Belcher-16

Date: 10 Aug 81 Time: 1500 CAT Depth: 44m

Latitude: 70°52'20"N Longitude: 159°43'20"W

Depth (m)	Temperature (°C)	Salinity (°/oo)	Sigma-t	Transparency (%)
0.1	6.18	-	-	96.0
1.6	6.22	28.73	22.61	95.8
2.8	6.23	28.78	22.65	95.9
3.5	6.18	28.77	22.64	95.9
4.5	6.23	28.75	22.62	96.1
5.4	6.21	28.77	22.65	96.2
6.1	6.20	28.60	22.51	96.1
6.1	6.17	28.68	22.57	95.7
6.9	5.71	28.63	22.59	96.4
7.7	4.68	28.78	22.81	97.8
9.0	4.38	28.96	22.98	97.9
9.5	4.42	29.42	23.34	96.1
10.3	4.10	30.41	24.16	91.2
10.4	4.12	30.45	24.19	91.3
11.1	3.93	30.48	24.23	90.9
12.2	3.24	30.69	24.46	92.1
13.1	1.71	31.32	25.08	94.5
14.3	1.23	31.58	25.31	94.9
14.8	0.73	31.52	25.30	95.6
15.7	0.48	31.65	25.41	95.9
16.9	0.44	31.56	25.34	95.5
17.4	0.39	31.61	25.38	95.9
18.2	0.39	31.63	25.40	95.7
18.3	0.36	-	-	95.6
19.2	0.26	31.79	25.53	95.4
19.2	0.36	31.83	25.56	95.7
19.3	0.34	31.89	25.61	95.7
20.9	0.05	31.74	25.50	95.2
21.6	-0.13	31.93	25.66	94.9
22.2	-0.14	31.94	25.67	94.7
22.9	-0.46	31.97	25.71	94.0
22.9	-0.29	31.91	25.66	94.5
24.1	-0.77	-	-	92.7
24.2	-0.69	32.03	25.76	93.6
24.5	-0.82	32.14	25.86	93.1
24.8	-0.79	32.30	25.98	93.1

Table: C-17
Study: NOAA 1981

Station: Pt. Belcher-17

Date: 10 Aug 81 Time: 1530 CAT Depth: 51m

Latitude: 70°54'30"N Longitude: 159°46'00"W

Depth (m)	Temperature (°C)	Salinity (°/oo)	Sigma-t	Transparency (%)
0.1	5.49	28.16	22.25	96.2
1.3	5.51	28.18	22.26	96.0
2.2	-	-	-	96.3
2.9	5.56	28.24	22.30	96.2
3.9	5.57	28.23	22.29	96.4
4.4	5.56	28.21	22.27	96.7
5.2	5.63	28.21	22.27	96.8
6.1	5.76	28.39	22.40	97.0
7.0	5.68	28.39	22.41	97.2
7.6	5.70	28.34	22.37	97.0
8.6	5.65	28.45	22.46	96.9
9.5	4.24	28.59	22.70	96.5
10.4	2.39	29.67	23.71	97.1
11.2	1.77	30.37	24.31	97.2
12.0	1.67	30.91	24.75	96.3
12.9	1.73	31.22	24.99	-
12.9	1.77	31.31	25.07	96.3
13.8	1.80	31.42	25.15	95.5
15.0	1.47	31.61	25.33	95.3
16.0	0.73	31.46	25.24	95.4
16.9	0.67	31.46	25.24	95.9
17.7	0.71	31.80	25.52	-
18.8	0.88	31.73	25.45	95.2
19.4	0.80	31.77	25.49	94.6
20.3	0.73	31.67	25.41	95.0
20.9	0.57	31.82	25.54	94.5
21.7	0.29	31.52	25.31	94.0
22.6	0.08	31.70	25.47	93.9
22.7	0.08	31.83	25.57	93.6
22.7	0.09	31.89	25.62	94.3
23.5	0.00	31.89	25.62	93.4
24.2	-0.12	32.03	25.74	93.4
24.7	-0.14	31.78	25.54	93.6

Table: C-18
Study: NOAA 1981

Station: Pt. Belcher-18

Date: 10 Aug 81 Time: 1605 CAT Depth: 56m

Latitude: 70°56'20"N Longitude: 159°48'40"W

Depth (m)	Temperature (°C)	Salinity (°/oo)	Sigma-t	Transparency (%)
0.1	6.33	28.56	22.47	95.6
0.9	6.37	28.53	22.44	95.6
2.0	6.35	28.45	22.37	95.6
2.6	-	-	-	95.8
3.4	6.32	28.40	22.34	96.0
4.4	6.33	28.54	22.45	96.0
5.2	6.35	28.43	22.36	96.3
5.8	6.36	28.23	22.20	95.7
6.7	6.35	28.36	22.31	96.4
7.4	6.32	28.33	22.29	96.6
7.6	6.34	28.38	22.32	96.8
8.3	6.09	28.50	22.45	97.3
8.4	6.24	28.47	22.41	97.1
9.2	5.70	28.80	22.72	97.8
10.2	5.65	28.84	22.76	97.5
10.9	5.58	28.96	22.86	97.9
12.0	5.33	28.86	22.81	97.8
13.0	4.33	29.04	23.05	97.5
13.9	3.08	29.56	23.57	97.3
14.4	2.64	29.83	23.82	97.4
14.6	2.79	29.65	23.67	98.4
14.6	2.85	28.96	23.11	98.0
15.0	1.28	30.10	24.12	96.4
15.0	1.92	29.86	23.90	96.7
15.1	1.25	29.98	24.03	96.4
15.2	1.81	29.63	23.72	96.9
15.6	0.47	30.41	24.41	96.3
15.8	-0.64	31.49	25.33	97.5
15.8	-0.62	31.55	25.38	96.8
16.0	-0.60	31.53	25.36	96.8
16.4	-0.78	31.32	25.19	96.0
17.9	-1.28	31.97	25.73	95.6
18.7	-1.32	31.50	25.36	94.3
19.5	-1.35	31.38	25.26	95.0
20.3	-1.38	32.02	25.77	94.7
20.4	-1.42	31.66	25.49	94.6
21.0	-1.42	31.97	25.73	94.2
21.8	-1.41	31.67	25.49	94.1
22.6	-1.42	31.80	25.60	94.0
23.5	-1.50	32.16	25.89	94.3
24.2	-1.45	-	-	93.3
24.8	-1.50	31.97	25.74	93.7
24.9	-1.47	-	-	93.6
25.0	-1.50	31.95	25.73	93.0

Table: C-19
Study: NOAA 1981

Station: Pingorarok Pass-19

Date: 13 Aug 81 Time: 1150 CAT Depth: 7m

Latitude: 70°23'30"N Longitude: 160°48'00"W

Depth (m)	Temperature (°C)	Salinity (°/oo)	Sigma-t	Transparency (%)
0.1	2.81	31.51	25.14	94.3
0.7	2.82	31.61	25.22	94.9
0.9	2.73	31.51	25.15	93.8
0.9	2.75	31.51	25.15	94.1
1.5	2.66	31.73	25.33	93.4
2.3	2.44	31.55	25.21	92.9
3.1	1.79	31.58	25.28	92.2
4.0	1.39	31.82	25.50	92.1
4.8	1.34	31.94	25.59	91.3
5.6	1.36	31.83	25.50	90.8
5.6	1.38	31.88	25.55	91.2
6.7	1.37	31.97	25.62	91.1
6.7	1.38	31.88	25.55	91.0

Table: C-20
Study: NOAA 1981

Station: Pingorarok Pass-20

Date: 13 Aug 81 Time: 1210 CAT Depth: 11m

Latitude: 70°24'20"N Longitude: 160°49'40"W

Depth (m)	Temperature (°C)	Salinity (°/oo)	Sigma-t	Transparency (%)
0.2	2.64	31.59	25.22	93.6
0.6	2.86	31.53	25.16	94.3
0.6	2.72	31.62	25.24	94.2
1.1	2.38	-	-	92.7
2.1	2.23	31.63	25.28	93.1
3.1	2.19	31.63	25.29	92.7
4.1	2.20	31.59	25.26	92.7
5.2	2.18	31.61	25.28	92.4
6.4	2.13	31.59	25.26	92.2
7.3	2.01	31.60	25.28	91.8
7.3	1.81	31.60	25.29	91.7
8.3	1.31	31.83	25.51	91.4
9.2	1.24	31.89	25.56	90.8
10.2	1.24	31.68	25.39	90.0
10.2	1.23	31.68	25.39	89.8

Table: C-21
Study: NOAA 1981

Station: Pingorarok Pass-21

Date: 13 Aug 81 Time: 1305 CAT Depth: 14m

Latitude: 70°25'12"N Longitude: 160°51'00"W

Depth (m)	Temperature (°C)	Salinity (°/oo)	Sigma-t	Transparency (%)
0.1	3.11	31.48	25.10	94.5
0.2	3.30	31.57	25.15	94.5
1.5	2.97	31.47	25.10	94.2
2.0	2.91	31.47	25.10	95.9
3.2	2.88	-	-	94.5
3.9	2.92	31.33	24.99	94.0
4.9	2.88	31.46	25.10	93.6
5.7	2.86	31.42	25.07	92.8
6.3	2.82	31.33	25.00	92.2
7.6	2.32	31.08	24.84	91.0
8.5	1.22	31.70	25.41	90.6
9.1	1.09	31.81	25.51	90.0
9.8	1.09	31.82	25.52	89.6
10.5	0.90	31.97	25.64	88.2
11.6	1.04	31.81	25.51	89.0
12.6	1.01	31.87	25.56	88.4
13.6	1.04	31.68	25.41	87.9
13.7	1.06	31.60	25.34	88.6

Table: C-22
Study: NOAA 1981

Station: Pingorarok Pass-22

Date: 13 Aug 81 Time: 1325 CAT Depth: 17m

Latitude: 70°27'00"N Longitude: 160°54'00"W

Depth (m)	Temperature (°C)	Salinity (°/oo)	Sigma-t	Transparency (%)
0.1	2.76	31.48	25.13	94.5
0.5	2.80	31.26	24.95	94.1
1.5	2.82	31.45	25.10	94.0
2.1	2.83	31.47	25.12	94.1
2.7	2.81	31.45	25.09	93.5
3.7	2.74	31.43	25.09	93.4
4.9	2.66	31.62	25.24	93.1
5.6	2.11	31.80	25.43	92.7
6.6	1.70	31.53	25.25	93.1
7.1	1.19	31.71	25.42	92.8
8.1	0.79	31.79	25.50	90.8
9.3	0.76	31.89	25.59	89.6
9.8	0.77	32.00	25.67	90.2
10.7	0.85	31.75	25.47	89.4
11.4	0.83	31.87	25.57	89.8
12.2	0.87	31.74	25.46	89.8
13.1	0.85	31.72	25.45	89.7
13.7	0.75	31.90	25.60	88.6
13.8	0.74	31.77	25.49	88.6
14.6	0.66	31.91	25.61	88.6
14.7	0.71	31.85	25.56	88.6

Table: C-23
Study: NOAA 1981

Station: Pingorarok Pass-23

Date: 13 Aug 81 Time: 1350 CAT Depth: 20m

Latitude: 70°38'40"N Longitude: 160°56'40"W

Depth (m)	Temperature (°C)	Salinity (°/oo)	Sigma-t	Transparency (%)
0.3	2.89	31.17	24.87	95.6
0.3	2.83	31.31	24.98	95.5
0.3	3.12	31.11	24.80	95.4
2.0	-	-	-	95.2
3.0	2.83	31.35	25.02	95.4
4.2	2.85	31.29	24.96	95.6
5.2	2.85	31.33	25.00	95.0
6.2	2.78	31.41	25.07	94.1
7.4	1.86	31.27	25.03	94.0
8.3	0.71	31.85	25.56	92.8
9.6	0.55	31.86	25.58	91.7
10.7	0.56	31.79	25.52	91.5
11.8	0.56	31.85	25.57	90.4
12.7	0.59	31.69	25.44	88.9
13.5	0.58	31.72	25.46	88.5
14.5	0.61	31.78	25.50	87.7
15.8	0.57	32.03	25.71	87.2
16.7	0.57	31.82	25.54	87.0
17.5	0.57	31.93	25.63	87.1
18.5	0.61	31.73	25.46	86.9
19.3	0.61	31.74	25.47	86.3

Table: C-24
Study: NOAA 1981

Station: Pingorarok Pass-24

Date: 13 Aug 81 Time: 1410 CAT Depth: 23m

Latitude: 70°30'30"N Longitude: 160°59'30"W

Depth (m)	Temperature (°C)	Salinity ($^{o}/_{oo}$)	Sigma-t	Transparency (%)
0.1	2.70	30.65	24.47	95.7
2.0	2.67	31.07	24.81	95.3
3.4	2.54	31.13	24.86	95.0
4.6	2.51	31.25	24.96	94.9
5.9	1.32	31.67	25.38	95.1
7.0	1.23	31.53	25.27	95.0
8.3	0.93	31.36	25.15	94.5
9.5	0.54	31.78	25.51	93.6
10.6	0.50	31.55	25.33	89.4
11.9	0.46	31.97	25.67	86.9
12.9	0.50	31.93	25.63	86.3
14.0	0.51	31.65	25.40	85.5
15.0	0.46	31.45	25.25	85.0
15.9	0.52	31.62	25.39	85.2
16.9	0.45	31.58	25.35	85.1
18.1	0.45	31.93	25.63	84.4
18.2	0.45	32.07	25.75	84.3
19.4	0.46	31.57	25.34	83.9
20.6	0.46	32.00	25.69	83.8
21.6	0.47	31.83	25.55	84.2
21.6	0.48	32.18	25.84	84.4

Table: C-25
Study: NOAA 1981

Station: Icy Cape-30

Date: 15 Aug 81 Time: 1428 CAT Depth: 11m

Latitude: 70°18'40"N Longitude: 162°00'40"W

Depth (m)	Temperature (°C)	Salinity (°/oo)	Sigma-t	Transparency (%)
0.1	4.17	31.22	24.79	93.4
0.8	4.17	31.17	24.75	94.0
1.7	4.18	31.20	24.77	93.5
2.8	4.15	31.18	24.76	93.4
4.0	4.20	31.15	24.74	93.5
5.5	4.12	31.39	24.94	93.2
6.4	4.07	31.21	24.79	93.1
7.7	4.00	31.36	24.92	92.9
8.8	3.76	31.33	24.92	92.0
8.9	3.76	31.27	24.87	91.1
9.6	3.73	31.23	24.84	91.1
9.7	3.72	31.34	24.93	91.1
9.7	3.74	31.26	24.87	91.2
9.8	3.74	31.25	24.86	91.3
10.0	3.78	31.28	24.88	91.4

Table: C-26
Study: NOAA 1981

Station: Icy Cape-31

Date: 15 Aug 81 Time: 1445 CAT Depth: 13m

Latitude: 70°19'35"N Longitude: 162°02'20"W

Depth (m)	Temperature (°C)	Salinity (‰)	Sigma-t	Transparency (%)
0.8	4.73	31.05	24.60	93.6
1.7	4.73	31.05	24.60	93.9
2.8	4.69	31.02	24.58	93.6
4.1	4.47	31.07	24.65	-
5.2	4.38	31.16	24.72	92.7
6.5	4.18	31.09	24.69	92.6
7.7	3.82	31.09	24.73	92.2
8.9	3.55	31.10	24.76	91.7
9.8	3.58	31.10	24.75	89.3
11.0	3.51	31.15	24.80	90.8
11.0	3.54	31.22	24.85	90.0
12.2	3.55	30.97	24.65	90.2
12.4	3.54	31.11	24.77	89.9

Table: C-27

Study: NOAA 1981

Station: Icy Cape-32

Date: 15 Aug 81 Time: 1510 CAT Depth: 14m

Latitude: 70°21'12"N Longitude: 162°06'00"W

Depth (m)	Temperature (°C)	Salinity (°/oo)	Sigma-t	Transparency (%)
1.2	4.80	31.05	24.60	94.1
2.2	4.82	31.09	24.63	93.6
4.0	4.72	30.97	24.54	93.1
5.0	4.57	31.00	24.58	92.7
6.2	4.44	30.96	24.56	-
7.6	3.56	31.01	23.89	91.9
9.0	3.42	31.08	24.75	90.7
10.2	3.35	31.32	24.95	90.8
10.2	3.35	31.32	24.95	90.8
11.4	3.35	30.45	24.25	90.4
12.5	3.41	31.02	24.71	89.7

Table: C-28
Study: NOAA 1981

Station: Icy Cape-33

Date: 15 Aug 81 Time: 1537 CAT Depth: 16m

Latitude: 70°22'50"N Longitude: 162°09'30"W

Depth (m)	Temperature (°C)	Salinity (‰)	Sigma-t	Transparency (%)
0.7	4.65	31.20	24.73	94.5
2.0	4.56	31.05	24.62	94.3
3.3	4.63	31.04	24.60	93.7
4.4	4.53	31.15	24.71	93.6
5.6	4.54	31.02	24.60	93.5
6.8	4.46	30.97	24.56	93.5
8.0	4.45	31.03	24.62	93.4
9.1	3.89	31.05	24.69	92.5
10.4	2.88	31.40	25.05	90.6
11.7	2.95	31.38	25.03	90.4
12.7	2.91	31.36	25.02	89.8
13.7	2.55	31.62	25.25	-
14.7	2.95	31.25	24.93	90.3
15.8	2.94	31.46	25.10	89.9

Table: C-29
Study: NOAA 1981

Station: Icy Cape-34

Date: 15 Aug 81 Time: 1600 CAT Depth: 21m

Latitude: 70°24'24"N Longitude: 162°13'20"W

Depth (m)	Temperature (°C)	Salinity ($^o/_{oo}$)	Sigma-t	Transparency (%)
0.3	6.05	29.14	22.95	96.9
0.3	6.06	30.44	23.97	-
2.0	6.01	30.67	24.16	96.1
3.1	5.85	30.47	24.02	96.0
4.4	5.73	30.47	24.04	95.5
5.5	5.70	30.63	24.17	95.7
6.8	5.28	30.64	24.22	95.2
7.8	5.18	30.88	24.42	95.0
8.9	5.18	30.89	24.43	94.6
10.0	4.96	30.94	24.49	93.4
10.9	4.74	30.99	24.56	94.5
11.0	4.70	30.80	24.41	93.4
11.9	4.19	31.07	24.67	93.2
13.0	3.25	31.26	24.91	-
13.9	2.43	31.42	25.10	91.6
14.9	2.41	31.42	25.11	91.6
16.1	2.42	31.44	25.12	91.1
17.1	2.36	31.34	25.04	91.1
17.2	2.46	31.37	25.07	91.1
18.1	2.41	31.39	25.08	91.0
19.6	2.42	31.34	25.04	91.2

Table: C-30
Study: NOAA 1981

Station: Icy Cape-35

Date: 15 Aug 81 Time: 1625 CAT Depth: 27m

Latitude: 70°25'30"N Longitude: 162°17'00"W

Depth (m)	Temperature (°C)	Salinity (°/oo)	Sigma-t	Transparency (%)
0.1	6.24	30.32	23.86	95.5
0.5	6.21	30.39	23.92	96.4
1.7	6.22	30.37	23.90	95.6
2.8	6.19	30.19	23.76	95.7
3.9	6.22	30.42	23.94	95.7
5.4	5.91	30.73	24.22	95.6
7.0	5.98	-	-	95.9
8.4	6.32	30.77	24.20	95.6
9.3	6.51	30.55	24.01	96.4
11.0	6.61	30.84	24.22	96.6
12.2	6.67	30.81	24.20	96.1
13.8	6.40	30.63	24.08	95.5
14.8	5.75	30.73	24.24	94.4
16.3	3.26	31.19	24.85	91.3
17.6	2.53	31.48	25.14	95.5
19.1	2.49	31.44	25.12	91.2
20.6	2.48	31.59	25.23	91.4
21.5	2.48	31.34	25.04	91.0
22.8	2.49	31.44	25.12	91.1
23.5	2.53	31.56	25.21	91.1
24.7	2.53	31.20	24.92	90.3

Table: C-31

Study: NOAA 1981

Station: Wainwright-36

Date: 20 Aug 81 Time: 1351 CAT Depth: 23m

Latitude: 70°39'24"N Longitude: 160°17'15"W

Depth (m)	Temperature (°C)	Salinity (°/oo)	Sigma-t	Transparency (%)
0.3	5.71	30.55	24.10	89.9
1.2	5.73	30.52	24.08	89.8
2.5	5.70	30.49	24.06	89.4
3.6	5.69	30.40	23.99	88.9
5.3	5.69	30.40	23.99	89.0
6.4	5.72	30.45	24.03	88.9
7.5	5.68	30.49	24.06	89.0
8.6	5.71	30.44	24.02	88.9
8.7	5.73	30.40	23.98	89.4
10.0	5.75	30.44	24.01	89.0
10.0	5.72	30.54	24.10	89.2
11.2	5.74	30.49	24.05	88.9
12.4	5.74	30.47	24.04	88.9
13.6	5.76	30.51	24.06	89.0
13.6	5.76	30.49	24.05	88.9
14.9	5.74	30.49	24.05	89.3
16.1	5.74	30.55	24.10	88.8
16.2	5.75	30.54	24.09	89.1
17.4	5.77	30.52	24.07	89.0
18.6	5.74	30.43	24.00	87.3
20.0	5.56	30.60	24.16	84.7
21.1	5.55	30.52	24.10	84.6
21.2	5.60	30.63	24.18	84.9

Table: C-32
Study: NOAA 1981

Station: Wainwright-37

Date: 20 Aug 81 Time: 2109 CAT Depth: 22m

Latitude: 70°38'13"N Longitude: 160°19'19"W

Depth (m)	Temperature (°C)	Salinity (°/oo)	Sigma-t	Transparency (%)
0.4	5.06	29.98	23.72	83.7
0.9	5.66	30.49	24.06	88.4
2.0	5.79	30.58	24.12	88.9
2.9	5.82	30.53	24.08	89.1
4.2	5.81	30.59	24.12	89.2
5.2	5.74	30.45	24.02	89.3
6.4	5.81	30.45	24.01	89.0
7.5	5.78	30.47	24.03	89.3
8.6	5.78	30.50	24.06	89.5
8.7	5.80	30.49	24.05	88.9
9.7	5.82	30.40	23.97	89.0
10.6	5.79	30.53	24.07	89.8
10.7	5.81	30.49	24.04	89.4
12.0	5.79	30.51	24.07	89.3
13.2	5.80	30.47	24.03	89.7
14.2	5.80	30.55	24.09	89.4
15.6	5.81	30.47	24.03	89.6
16.9	5.62	30.56	24.12	86.5
18.1	5.57	30.53	24.11	85.6
19.5	5.55	30.50	24.08	85.1
20.7	5.50	30.64	24.20	85.2
-	5.52	30.52	24.10	85.1

Table: C-33
Study: NOAA 1981

Station: Wainwright---

Date: 2 Sep 81 Time: 1720 CAT Depth: 37m

Latitude: ---------N Longitude: ----------W

Depth (m)	Temperature (°C)	Salinity (°/oo)	Sigma-t	Transparency (%)

Missing data tape

Table: C-34
Study: NOAA 1981

Station: Wainwright-39

Date: 2 Sep 81 Time: 1750 CAT Depth: 29m

Latitude: 70°39'57"N Longitude: 160°23'33"W

Depth (m)	Temperature (°C)	Salinity (°/oo)	Sigma-t	Transparency (%)
0.4	1.42	28.13	22.54	97.5
0.8	1.39	28.12	22.53	97.7
1.7	1.40	28.13	22.54	97.8
3.4	1.36	28.11	22.53	97.9
4.6	1.48	28.31	22.68	97.9
6.1	1.73	28.69	22.97	98.8
7.1	2.25	29.01	23.19	98.3
8.0	2.29	29.30	23.42	98.7
9.3	2.52	30.05	24.00	99.3
9.6	2.73	29.58	23.62	98.8
10.8	3.94	30.34	24.12	98.3
11.6	3.19	30.31	24.16	98.2
12.9	-	-	-	99.5
14.0	3.49	30.87	24.58	98.5
14.7	3.57	30.96	24.65	98.3
15.9	3.11	30.47	24.29	97.7
16.6	1.48	31.61	25.32	98.5
17.0	0.83	30.96	24.84	98.3
18.6	0.32	31.10	24.97	98.1
19.5	0.24	31.42	25.23	97.5
20.5	0.00	31.95	25.68	96.4
20.6	0.01	32.05	25.75	96.4
20.7	0.03	31.87	25.61	96.2

Table: C-35

Study: NOAA 1981

Station: Wainwright-40

Date: 2 Sep 81 Time: 1820 CAT Depth: 23m

Latitude: 70°38'22"N Longitude: 160°19'36"W

Depth (m)	Temperature (°C)	Salinity (°/oo)	Sigma-t	Transparency (%)
0.1	1.94	28.43	22.75	98.3
1.0	1.94	28.38	22.71	98.3
2.5	2.01	28.38	22.71	98.3
3.8	2.19	28.47	22.77	97.4
5.2	2.60	29.04	23.19	97.4
6.4	1.10	29.78	23.88	97.9
6.4	1.13	29.65	23.77	99.3
7.8	2.83	31.38	25.04	100.0
8.3	3.89	30.61	24.34	98.9
9.4	2.29	30.66	24.50	98.1
9.9	2.71	30.97	24.72	97.4
10.1	2.29	31.25	24.98	96.1
10.3	1.56	31.36	25.12	96.3
11.3	1.40	31.45	25.19	96.2
12.3	0.79	31.98	25.66	96.1
12.8	0.34	31.85	25.58	96.4
13.4	0.50	31.93	25.63	96.4
14.3	0.80	31.92	25.61	95.8
14.9	0.67	31.78	25.50	96.2
15.4	0.22	31.95	25.66	95.9
15.5	0.03	32.12	25.81	95.6
15.9	0.02	32.09	25.78	95.9

Table: C-36
Study: NOAA 1981

Station: Wainwright-41

Date: 2 Sep 81 Time: 1840 CAT Depth: 21m

Latitude: 70°37'39"N Longitude: 160°17'23"W

Depth (m)	Temperature (°C)	Salinity (‰)	Sigma-t	Transparency (%)
0.4	1.91	29.60	23.69	99.8
2.0	1.70	29.77	23.84	100.0
3.1	1.52	29.88	23.94	99.7
4.3	0.79	30.54	24.50	97.8
5.7	0.17	31.59	25.38	97.1
6.7	-0.21	31.89	25.64	97.3
7.7	-0.50	32.33	26.00	97.1
8.8	-0.58	32.37	26.03	96.6
9.8	-0.56	32.32	25.99	96.6
10.6	-0.57	32.44	26.09	96.4
11.5	-0.63	32.39	26.06	96.1
12.4	-0.63	32.35	26.02	96.1
13.5	-0.61	32.36	26.03	96.1

Table: C-37

Study: NOAA 1981

Station: Wainwright-42

Date: 2 Sep 81 Time: 1930 CAT Depth: 18m

Latitude: 70°36'51"N Longitude: 160°15'09"W

Depth (m)	Temperature (°C)	Salinity (°/oo)	Sigma-t	Transparency (%)
0.1	-0.36	32.08	25.79	96.8
1.4	-0.43	32.10	25.81	95.9
3.1	-0.61	32.20	25.90	96.1
4.9	-0.58	32.09	25.81	96.1
6.7	-0.76	32.08	25.80	95.6
8.6	-0.76	32.03	25.77	95.1
10.4	-0.83	32.22	25.92	94.7
12.1	-0.79	32.26	25.95	94.4
15.2	-0.80	32.35	26.02	93.6
18.6	-0.72	32.27	25.96	93.8

Table: C-38

Study: NOAA 1981

Station: Wainwright-43

Date: 2 Sep 81 Time: 1950 CAT Depth: 14m

Latitude: 70°35'39"N Longitude: 160°12'16"W

Depth (m)	Temperature (°C)	Salinity ($^o/_{oo}$)	Sigma-t	Transparency (%)
0.3	-0.94	32.55	26.19	95.8
2.1	-0.98	32.56	26.20	96.3
4.2	-1.04	32.53	26.18	96.3
5.9	-1.05	32.39	26.06	96.5
7.5	-1.06	32.48	26.14	96.1
9.6	-1.03	32.41	26.08	95.5
11.1	-1.04	32.44	26.11	95.6
12.6	-1.03	32.58	26.22	95.0

Table: C-39

Study: NOAA 1981

Station: Akunik Pass-25

Date: 14 Aug 81 Time: 1440 CAT Depth: 18m

Latitude: 70°00'26"N Longitude: 163°08'08"W

Depth (m)	Temperature (°C)	Salinity (°/oo)	Sigma-t	Transparency (%)
0.6	6.84	30.04	23.57	94.3
1.9	6.87	29.99	23.53	94.1
3.3	6.84	29.98	23.52	94.2
3.6	6.89	29.91	23.46	94.1
4.9	6.79	30.08	23.60	94.1
6.2	6.80	30.08	23.60	94.2
7.1	6.69	30.09	23.62	94.3
7.9	6.63	30.31	23.81	94.1
8.8	6.04	30.25	23.82	93.4
9.6	5.56	30.72	24.26	93.6
10.4	5.23	31.01	24.51	92.7
11.4	5.18	30.99	24.51	92.9
12.5	5.05	30.98	24.51	92.7
13.2	4.95	31.15	24.66	92.7
13.5	4.62	31.37	24.87	91.2
14.9	3.67	31.45	25.02	90.5
16.1	3.63	31.56	25.11	90.6
17.0	3.63	31.50	25.07	90.5
17.4	3.66	31.46	25.03	90.5
18.2	3.60	31.54	25.10	90.3
18.4	3.54	31.62	25.17	-

Table: C-40

Study: NOAA 1981

Station: Akunik Pass-26

Date: 14 Aug 81 Time: 1710 CAT Depth: 18m

Latitude: 69°58'09"N Longitude: 163°05'54"W

Depth (m)	Temperature (°C)	Salinity (°/oo)	Sigma-t	Transparency (%)
0.0	6.34	30.46	23.96	-
1.1	6.36	30.36	23.87	93.9
-	6.37	30.38	23.89	93.8
3.5	6.31	30.35	23.87	94.1
4.6	6.27	30.48	23.98	93.6
5.9	6.05	30.51	24.03	93.6
6.9	5.78	30.78	24.28	93.6
7.8	5.31	30.67	24.24	93.2
8.3	5.16	-	-	92.5
9.4	4.91	31.12	24.64	92.6
9.5	4.92	31.02	24.56	92.6
10.4	4.93	31.00	24.54	92.7
10.8	-	-	-	92.6
11.6	4.90	31.02	24.56	92.0
12.0	4.87	31.04	24.58	92.1
-	4.91	31.13	24.65	92.6
12.2	4.84	31.07	24.61	92.0
13.1	4.83	31.03	24.57	92.0
13.6	4.77	31.17	24.70	90.9
15.0	4.69	31.14	24.68	91.5
15.8	4.24	31.17	24.75	90.4
16.1	4.34	31.09	24.68	90.3

Table: C-41

Study: NOAA 1981

Station: Akunik Pass-27

Date: 14 Aug 81 Time: 1742 CAT Depth: 16m

Latitude: 69°56'12"N Longitude: 163°02'38"W

Depth (m)	Temperature (°C)	Salinity (°/oo)	Sigma-t	Transparency (%)
2.1	5.84	30.63	24.15	93.1
3.3	5.79	30.59	24.13	92.7
4.5	5.76	30.87	24.35	93.1
5.5	5.64	30.51	24.07	92.7
-	5.24	30.84	24.38	92.3
7.7	5.08	31.08	24.59	91.9
8.6	4.91	30.94	24.50	91.4
10.0	4.89	31.05	24.59	91.3
10.7	4.75	31.09	24.63	90.8
10.8	4.76	30.93	24.50	91.0
12.0	4.25	31.14	24.72	91.2
13.5	3.91	31.35	24.92	88.5
14.7	3.87	31.25	24.84	89.7
15.0	3.88	31.47	25.02	89.1

Table: C-42
Study: NOAA 1981

Station: Akunik Pass-28

Date: 14 Aug 81 Time: 1808 CAT Depth: 14m

Latitude: 69°54'16"N Longitude: 162°53'30"W

Depth (m)	Temperature (°C)	Salinity (°/oo)	Sigma-t	Transparency (%)
0.2	-	-	-	93.3
1.7	5.69	30.75	24.26	93.2
1.9	5.62	31.10	24.54	93.2
3.1	5.65	30.90	24.39	93.3
-	5.64	30.93	24.41	93.3
5.0	5.66	30.91	24.39	93.1
5.4	5.52	30.78	24.31	92.5
7.4	4.97	-	-	91.7
8.5	4.61	31.02	24.59	90.2
10.4	4.33	31.46	24.97	-
11.5	4.26	31.37	24.90	89.8
13.1	4.31	31.40	24.92	89.8
13.5	4.33	31.15	24.72	89.6

Table: C-43
Study: NOAA 1981

Station: Akunik Pass-29

Date: 14 Aug 81 Time: 1830 CAT Depth: 9m

Latitude: 69°53'03"N Longitude: 162°56'10"W

Depth (m)	Temperature (°C)	Salinity (°/oo)	Sigma-t	Transparency (%)
0.0	4.94	30.87	24.44	92.0
1.6	4.91	30.81	24.40	92.0
-	4.95	31.17	24.68	91.8
3.6	4.87	31.20	24.71	91.9
5.2	4.82	31.06	24.60	91.4
6.5	4.66	31.08	24.63	90.7
7.5	4.61	30.81	24.43	90.3
8.2	4.52	31.28	24.81	-
8.7	4.52	31.05	24.62	90.0

APPENDIX D

Drogue Data

Table: D-1
Wainwright Drogue Dispersion Study, 20 Aug 81

Time (LST)	Drogue #	Distance (m) Site A	Site B
1213	10	10037	10655
1218	1	10105	10710
1222	2	10198	10770
1228	6	10327	10852
1235	7	10417	10925
1241	11	10501	11001
1256	4	10262	10792
1300	12	10257	10856
1305	5	10257	10943
1312	3	10345	10616
1317	9	10377	10530
1325	8	10419	10451
1329	10	10073	10410
1331	1	10155	10511
1332	2	10288	10612
1333	6	10405	10710
1333	7	10518	10835
1334	11	10612	10921
1336	4	10355	10736
1336	12	10310	10793
1337	5	10285	10869
1340	3	10422	10602
1341	9	10438	10509
1342	8	10468	10436
1431	10	10184	10276
1433	1	10255	10400
1434	2	10394	10526
1435	6	10540	10646
1436	7	10626	10768
1437	11	10745	10841
1438	4	10475	10679
1439	12	10416	10720
1440	5	10432	10801
1442	3	10566	10557
1443	9	10575	10480
1444	8	10578	10416
1529	10	10306	10175
1530	1	10402	10323
1531	2	10537	10472
1532	6	10661	10592
1533	7	10745	10709

Table: D-2
Wainwright Drogue Dispersion Study (Continued)

Time (LST)	Drogue #	Distance (m) Site A	Site B
1534	11	10873	10845
1536	4	10619	10607
1537	12	10560	10651
1538	5	10575	10730
1540	3	10675	10529
1541	9	10654	10451
1542	8	10646	10387
1630	10	10376	10043
1631	1	10428	10203
1632	2	10540	10375
1634	7	10807	10586
1635	11	10944	10797
1636	5	10713	10649
1637	12	10653	10550
1638	4	10669	10474
1639	6	10736	10457
1640	3	10748	10423
1641	9	10730	10347
1642	8	10718	10261
1730	10	10390	9751
1731	1	10488	9974
1732	2	10643	10165
1733	6	10786	10286
1734	7	10894	10425
1735	11	11050	10632
1736	5	10888	10517
1737	12	10777	10368
1738	4	10798	10317
1738	3	10759	10242
1739	9	10715	10137
1740	8	10641	10012
1829	10	10504	9432
1832	1	10499	9661
1833	2	10609	9839
1834	6	10850	9980
1836	7	10968	10186
1837	11	10999	10366
1838	5	10920	10288
1839	12	10824	10140
1840	4	10893	10077
1840	3	10853	9968
1841	9	10870	9871
1842	8	10806	9671

Table: D-3
Wainwright Drogue Dispersion Study (Continued)

Time (LST)	Drogue #	Distance (m) Site A	Site B
1931	10	10943	9189
1934	1	10764	9358
1935	2	10883	9547
1938	12	11088	9912
1939	11	11246	10121
1940	5	11245	10073
1941	7	11340	10013
1942	4	11255	9894
1942	3	11230	9776
1943	6	11277	9758
1944	9	11295	9704
1945	8	11285	9495
2031	10	11601	9101
2034	1	11282	9207
2035	2	11394	9390
2037	12	11567	9750
2039	11	11741	9989
2040	5	11778	9968
2041	7	11879	9949
2042	4	11802	9823
2043	3	11789	9691
2043	6	11848	9694
2044	9	11872	9640
2045	8	11923	9446
2200	1	12326	9318
2201	2	12375	9441
2203	12	12471	9723
2204	11	12623	9996
2205	5	12717	10008
2206	7	12816	10029
2207	4	12745	9901
2207	3	12745	9972
2208	6	12837	9823
2209	9	12842	9735
2210	8	12880	9616
2211	10	12829	9419
2247	8	13309	9819
2252	1	12979	9641
2253	2	13039	9710
2254	12	13125	9873
2256	11	13277	10209
2258	7	13423	10280
2258	5	13360	10242
2259	4	13339	10163
2259	6	13379	10091

Table: D-4
Wainwright Drogue Dispersion Study (Continued)

Time (LST)	Drogue #	Distance (m) Site A	Site B
2300	3	13270	10034
2303	9	13443	9990
2306	10	13453	9697
2311	1	13124	9741
2313	2	13238	9832
2316	12	13297	9954
2320	11	13498	10332
2321	5	13592	10362
2322	7	13692	10405
2325	5	13617	10383
2325	4	13603	10305
2326	3	13541	10173
2328	6	13703	10246
2331	9	13779	10116
2335	8	13890	10055

Table: D-5

wainwright drogues
dispersion statistics for wind-corrected drogue data

grp no.	mean time (hrs)	relative mean time (t*) (hrs)	log(t*)	centroid position latitude (degrees)	centroid position longitude (degrees)	principal axes major axis (δ_x) (meters)	principal axes minor axis (δ_y) (meters)	bearing of major axis (θ) (deg. true)
1	12.794	0.0000	0.0000	70.6586	-160.2801	375.7	244.9	175.95
2	13.589	0.7945	-0.0999	70.6571	-160.2815	368.9	294.1	177.52
3	14.628	1.8334	0.2633	70.6553	-160.2836	364.9	295.1	158.72
4	15.588	2.7931	0.4461	70.6540	-160.2868	363.9	215.8	142.93
5	16.604	3.8098	0.5809	70.6524	-160.2875	420.4	205.5	140.02
6	17.588	4.7931	0.6806	70.6497	-160.2887	509.6	89.6	135.08
7	18.613	5.8181	0.7648	70.6460	-160.2895	577.2	188.7	148.11
8	19.658	6.8639	0.8366	70.6410	-160.2967	623.9	275.7	156.01
9	20.658	7.8639	0.8956	70.6351	-160.3094	652.5	323.0	161.88
10	22.099	9.3042	0.9687	70.6269	-160.3320	591.7	307.5	165.15
11	22.951	10.1570	1.0068	70.6229	-160.3474	531.0	257.6	161.61
12	23.379	10.5848	1.0247	70.6223	-160.3551	585.8	324.2	155.66

diffusion statistics - wind-corrected drogue data

no.	relative time (s)	centroid velocity X (m/s)	centroid velocity Y (m/s)	speed (m/s)	direction (d. true)	horizontal divergence (10-5 s-1)	relative vorticity (10-5 s-1)	stretching deformation rate (10-5 s-1)	shearing deformation rate (10-5 s-1)
2	2860.20	-0.0177	-0.0611	0.0636	196.1681	0.00000	0.00000	0.00000	0.00000
3	6600.24	-0.0208	-0.0512	0.0552	202.1232	-1.23292	-14.39336	9.15968	-11.17090
4	10055.16	-0.0348	-0.0442	0.0563	218.2107	7.06533	-14.96743	16.20787	3.35382
5	13715.28	-0.0070	-0.0484	0.0489	186.1784	-106.83603	32.34707	-111.62153	0.95107
6	17255.16	-0.0125	-0.0854	0.0863	188.3160	24.72574	81.83278	0.26883	85.48622
7	20945.16	-0.0080	-0.1103	0.1105	184.1265	-9.32969	85.74384	-21.54109	83.51665
8	24710.04	-0.0708	-0.1481	0.1642	205.5581	30.36982	2.92501	16.78757	25.47663
9	28310.04	-0.1310	-0.1842	0.2261	215.4209	18.20386	-1.42129	7.31665	16.72924
10	33495.12	-0.1610	-0.1767	0.2390	222.3425	2.76153	-4.17805	4.41589	2.36264
11	36565.20	-0.1859	-0.1441	0.2352	232.2251	-2.99439	-11.34366	11.73202	-0.06897
12	38105.28	-0.1858	-0.0468	0.1916	255.8576	-134.89640	-33.86603	134.83771	-34.09893

variance vs. relative time regression results:

statistic	variance X**2	variance Y**2	variance X*Y
slope	1.71612	0.18970	0.67737
intercept	31684.58647	13245.90275	18606.52748
correlation	0.82725	0.32992	0.69696
F ratio	21.68050	1.22145	9.44571
diffusivity	0.85806	0.09485	0.33868

error degrees of freedom = 10

note: diffusivities measured in square meters per second

Table: D-6

wainwright drogues
dispersion statistics for raw drogue data

grp. no.	mean time (hrs)	relative mean time (t*) (hrs)	log(t*)	centroid position latitude (degrees)	longitude (degrees)	principal axes major axis (δ_x) (meters)	minor axis (δ_y) (meters)	bearing of major axis (θ) (deg. true)
1	12.794	0.0000	0.0000	70.6587	-160.2805	451.5	248.2	199.02
2	13.589	0.7945	-0.0999	70.6572	-160.2826	375.7	300.5	186.21
3	14.628	1.8333	0.2632	70.6557	-160.2861	359.4	307.0	159.85
4	15.588	2.7931	0.4461	70.6544	-160.2896	378.8	223.6	141.69
5	16.604	3.8097	0.5809	70.6527	-160.2915	411.9	221.7	140.13
6	17.588	4.7931	0.6806	70.6502	-160.2932	498.8	102.1	133.95
7	18.613	5.8181	0.7648	70.6467	-160.2945	556.3	221.6	146.52
8	19.658	6.8639	0.8366	70.6418	-160.3029	598.7	338.3	153.82
9	20.658	7.8639	0.8956	70.6363	-160.3158	628.5	393.9	159.52
10	22.099	9.3042	0.9687	70.6289	-160.3387	600.9	381.9	171.39
11	22.951	10.1569	1.0068	70.6257	-160.3531	532.2	308.7	162.52
12	23.379	10.5847	1.0247	70.6251	-160.3600	505.7	439.1	191.38

diffusion statistics - raw drogue data

no.	relative time (s)	centroid velocity X (m/s)	Y (m/s)	speed (m/s)	direction (d. true)	horizontal divergence (10-5 s-1)	relative vorticity (10-5 s-1)	stretching deformation rate (10-5 s-1)	shearing deformation rate (10-5 s-1)
2	2860.20	-0.0281	-0.0573	0.0638	206.1284	0.00000	0.00000	0.00000	0.00000
3	6600.24	-0.0347	-0.0447	0.0566	217.8114	-2.37131	-13.60342	12.58857	-5.67485
4	10055.16	-0.0369	-0.0435	0.0570	220.3368	0.84778	-2.46334	2.56817	0.43737
5	13715.28	-0.0192	-0.0498	0.0534	201.0933	-21.61134	18.76800	-28.61677	-0.60666
6	17255.16	-0.0176	-0.0809	0.0828	192.2620	8.26331	50.38790	-13.43124	49.26281
7	20945.16	-0.0131	-0.1055	0.1064	187.0974	-2.90497	51.93344	-15.55140	49.63543
8	24710.04	-0.0828	-0.1462	0.1680	209.5277	29.72554	0.37408	14.96428	25.68693
9	28310.04	-0.1333	-0.1675	0.2140	218.5080	14.05576	-3.92718	6.98483	12.81402
10	33495.12	-0.1630	-0.1598	0.2283	225.5759	2.59118	-4.50407	4.45107	2.68120
11	36565.20	-0.1745	-0.1177	0.2105	235.9898	-9.50217	-11.01698	13.77267	-4.68811
12	38105.28	-0.1665	-0.0445	0.1723	255.0190	-109.75113	-16.91623	103.53203	-40.15705

variance vs. relative time regression results:

statistic	variance X**2	Y**2	X*Y
slope	1.30873	0.62354	0.90328
intercept	37111.68292	11002.70123	18976.61367
correlation	0.73407	0.62013	0.72932
F ratio	11.68546	6.24854	11.36354
diffusivity	0.65436	0.31177	0.45164

error degrees of freedom = 10

note: diffusivities measured in square meters per second

APPENDIX E

Index of Digital Data Tapes

INDEX - Digital Data Tapes (Tape File Documentation bound separately)

Files on tape RU531:

Sequence/Name	NODC File Type	Description
01) INBRWB	015	Current meter data from Inshore Point Barrow, bottom meter.
02) OFBRWB	015	Current meter data from Offshore Point Barrow, bottom meter.
03) OFBRWT	015	Current meter data from Offshore Point Barrow, top meter.
04) INWNTB	015	Current meter data from Inshore Wainwright, bottom meter.
05) OFWNTB	015	Current meter data from Offshore Wainwright, bottom meter.
06) OFWNTT	015	Current meter data from Offshore Wainwright, top meter.
07) PEARDB	015	Current meter data from Peard Bay. (salinity and temperature only.)
08) AKUNIK	022	STD data from Akunik Pass.
09) BARROW	022	STD data from Point Barrow.
10) ICYCAP	022	STD data from Icy Cape.
11) PINGOR	022	STD data from Pingora Pass.
12) PTBELC	022	STD data from Point Belcher.
13) SKULLCL	022	STD data from Skull Cliffs.
14) WAINWR	022	STD data from Wainwright.
15) BEAUD1	056	Drogue experiment data from the Beaufort Sea (#1).
16) BEAUD2	056	Drogue experiment data from the Beaufort Sea (#2).
17) BEAUD3	056	Drogue experiment data from the Beaufort Sea (#3).
18) PRDDRG	056	Drogue experiment data from Prudhoe Bay.
19) HARDRG	056	Drogue experiment data from Harrison Bay.
20) WNTDRG	056	Drogue experiment data from Wainwright.

File type is in columns 1-3 of each record of each file.

File name is in columns 4-9 of each record of each file.

133

U.S. DEPARTMENT OF COMMERCE
NATIONAL OCEANIC AND ATMOSPHERIC ADMINISTRATION
NATIONAL OCEAN SERVICE
701 C Street
Box 56
Anchorage, Alaska 99513

OFFICIAL BUSINESS
PENALTY FOR PRIVATE USE $300

POSTAGE AND FEES PAID
U.S. DEPARTMENT OF COMMERCE
COM-210

U.S.MAIL

PRINTED MATTER
CLASS OF POSTAL SERVICE

UNIV OF ALASKA/INFO SERVICES
ARCTIC ENV INFO AND DATA CTR
707 A STREET
ANCHORAGE, AK 99501 *

NOAA FORM 61-13
(9-84)